Dissertation zur Erlangung des Doktorgrades
der Fakultät für Chemie und Pharmazie
der Ludwig-Maximilians-Universität München

Forensic analysis of drugs and explosives:

Novel sampling and analytical methods for complex media

Petra Hehet

aus

Varaždin, Kroatien

2024

Forensic analysis of drugs and explosives:
Novel sampling and analytical methods for complex media

Petra Hehet

Forensic analysis of drugs and explosives: Novel sampling and analytical methods for complex media

PhD thesis, Ludwig Maximilian University of Munich, Germany

Author: Petra Hehet

Disclaimer

The main content of the chapters in this dissertation was published in international scientific journals and the publishing details for individual articles are provided on the cover page of each chapter. The content of the respective chapters is consistent with the articles published, however, the layout has been modified to fit in this dissertation. Additional content apart from the published one is indicated accordingly and can be found at the end of the respective chapter. The numbering of figures, tables and references should be considered in the scope of individual chapters and refers to the respective chapter only. In general, figures and tables without given references are self-designed.

SYnergy of integrated Sensors and Technologies for urban sEcured environment

Dedicated to my parents

My innermost appreciation belongs to my mother,
my greatest example of strength, perseverance and commitment.

A very special dedication is aimed to my father, a police officer,
who conveyed me my great passion for forensics.

Danksagung

„Dankbarkeit ist das Gedächtnis des Herzens." Jean-Baptiste Massillon

Ich bedanke mich bei meinem Doktorvater Herrn **Prof. Dr. Konstantin L. Karaghiosoff** für die universitäre Betreuung meiner Dissertation und die Aufnahme in seinen Arbeitskreis. Begonnen mit meiner Masterarbeit beim Bayerischen Landeskriminalamt (BLKA), haben Sie mich nun auch bei meiner externen Promotion beim BLKA kontinuierlich begleitet, unter anderem mit vielen Anregungen und Diskussionen zur fachlichen Literatur und hatten stets ein offenes Ohr für mich. Herzlichen Dank für das Vertrauen in meine Fähigkeiten und die gegebene Freiheit zur Forschungsarbeit. Insbesondere danke ich Ihnen für die Unterstützung in der Endphase meiner Dissertation.

Beim Herrn **Prof. Dr. Thomas Klapötke** möchte ich mich für die Begutachtung meiner Dissertation bedanken. Den weiteren Mitgliedern meiner **Prüfungskommission** möchte ich ebenfalls einen Dank für die Durchsicht meiner Dissertation sowie für die aktive Teilnahme bei meiner Verteidigung ausrichten.

Ein ganz besonderer Dank geht an **Dr. Natalie Kunert** (BLKA, aktuell Zoll), **Dr. Marc Wende** (BLKA) und **Michael Pütz** (Bundeskriminalamt, BKA), die meine direkten Ansprechpartner vor Ort waren. Ihr habt mir nicht nur den maximalen Freiraum zur Entfaltung meiner Ideen und Interessen gegeben, sondern diese wurden in Kombination mit Eurem Engagement und Eurer Unterstützung noch potenziert. Gleichzeitig standet Ihr mir stets mit Rat und Tat zur Seite. Herrn Pütz danke ich auch als dem SYSTEM-Projektleiter für die organisatorische Unterstützung während meiner Zeit an der Hochschule Fresenius in Idstein in der Vor-Projektphase, den fachlichen Besprechungen zu einzelnen Teilprojekten meiner Dissertation sowie zu projektbezogenen Aspekten bei meinen zahlreichen Aufenthalten beim BKA. Schließlich möchte ich Dr. Wende für seine ersten Kontaktaufnahmen zur Initiierung meiner Promotionsstelle sowie für seine kontinuierliche Begleitung und fachliche Unterstützung, insbesondere im Sprengstoff- und Abwasseranalytikbereich, danken. Dr. Wende stand mir immer mit Rat und Tat als erster Ansprechpartner zur Seite. Eure Begeisterung und innovative Ideen habe ich im Rahmen der gemeinsamen Diskussionen immer sehr genossen. Zusammenfassend möchte ich Euch allen Drei sagen: Abgesehen von Eurer enormen fachlichen Kompetenz schätze ich Euch ganz besonders auch auf der persönlichen Ebene. Bessere Projektleiter und Mentoren hätte ich mir nicht aussuchen können.

Neben der fachlichen Unterstützung gilt der Dank auch allen Beteiligten, die von der administrativen Seite meine Promotionsstelle und Dissertation befürwortet oder verwaltungstechnisch unterstützt haben. In dem Zusammenhang möchte ich mich bei der ehemaligen Leiterin des Kriminaltechnischen Instituts (KTI) im BLKA, **Dr. Christin Hofmann**, sowie bei der aktuellen Leiterin, **Dr. Christina Stoiber**, bedanken. Gleichermaßen danke ich dem ehemaligen Leiter des Sachgebiets Chemie, **Dr. Michael Uhl**, und dem aktuellen Leiter, **Dr. Jürgen Bügler**, insbesondere für die kontinuierliche bzw. fortgesetzte Unterstützung meiner Dissertation und anschließender BMBF- bzw. EU-Projekte. Schließlich möchte ich **Frank Strohmeier** von der BLKA-Personalabteilung für seinen administrativen Einsatz bei der

Table of Contents

List of acronyms and abbreviations

^{13}C-TATP	^{13}C isotopically labelled TATP
ACN	Acetonitrile
ACST	Activated Carbon Sampling Tubes
AF2	Excitation Energy
AF3	Auxiliary Frequence
BKA	"Bundeskriminalamt" = Federal State Criminal Police Office
BLKA	"Bayerisches Landeskriminalamt" = Bavarian State Criminal Police Office
BtMG	"Betäubungsmittelgesetz" = German Narcotic Drugs Act
CB$_1$	Cannabinoid receptor type one
CB$_2$	Cannabinoid receptor type two
CBD	Cannabidiol
CBN	Cannabinol
CE	Collision Energy
CI	Chemical Ionization
CID	Collision Induced Dissociation
CXP	Collision Exit Potential
DADP	Diacetone Diperoxide
DP	Declustering Potential
EDDP	2-Ethylidene-1,5-dimethyl-3,3-diphenylpyrrolidine
EI	Electron Ionization
EMCDDA	European Monitoring Centre for Drugs and Drug Addiction
EP	Entrance Potential
ESI	Electrospray Ionization
EtOAc	Ethyl acetate
EU	European Union
EWS	Early Warning System
EXB	Exit Barrier
GC-PCI-MS/MS	Gas Chromatography-Positive Chemical Ionization-tandem Mass Spectrometry
GTFCh	"Gesellschaft für Toxikologische und Forensische Chemie" = Society of Toxicological and Forensic Chemistry
HME	Homemade Explosive
HMTD	Hexamethylene triperoxide diamine
HRMS	High-Resolution Mass Spectrometry
IED	Improvised Explosive Device
IS	IonSpray Voltage
ISTD	Internal Standard
IUPAC	International Union of Pure and Applied Chemistry
LC-MS/MS	Liquid Chromatography-tandem Mass Spectrometry
LEA	Law Enforcement Agency
LIT	Linear Ion Trap
LLE	Liquid-Liquid Extraction
LOD	Limit of Detection
LOQ	Limit of Quantification
m/z	Mass-to-charge ratio
MDMA	3,4-Methylenedioxymethamphetamine

MeOH	Methanol
MRM	Multiple Reaction Monitoring
MW	Molecular Weight
NPS	New Psychoactive Substance
NpSG	"Neue-Psychoactive-Stoffe-Gesetz" = New Psychoactive Substances Act
PDMS	Polydimethylsiloxane
QC	Quality Control
QqQ	Triple quadrupole
Rel. StDev	Relative Standard Deviation
RF	Radio Frequency
rpm	rounds per minute
RT	Room Temperature
S/N	Signal-to-Noise
SCORE	Sewage analysis CORe group - Europe
SCRA	Synthetic Cannabinoid Receptor Agonist
SIM	Selected Ion Monitoring
sMRM	scheduled Multiple Reaction Monitoring
SoHT	Society of Hair Testing
SPE	Solid-Phase Extraction
SPME	Solid-Phase Microextraction
StDev	Standard Deviation
TATP	Triacetone Triperoxide
THC	Tetrahydrocannabinol
THC-COOH	11-Nor-9-carboxy-Δ^9-tetrahydrocannabinol
TNT	2,4,6-Trinitrotoluene
TP	Transformation Product
UHPLC	Ultra High Performance Liquid Chromatography
UNODC	United Nations Office on Drugs and Crime
V	Voltage
WBE	Wastewater-Based Epidemiology
WWTP	Wastewater Treatment Plant

IUPAC names of the SCRAs used in this work are given in Chapters 4-5 (Supplementary Material).

Aim
and
Concept

I. State of the Art and Motivation

"Everywhere, Everything, Everyone"

European Monitoring Centre for Drugs and Drug Addiction (EMCDDA),
European Drug Report 2022[1]

Recent major global events such as the COVID-19 pandemic (March 2020), the Russian invasion of Ukraine (February 2022) and the armed conflict between Palestinian militant groups and Israel (October 2023) additionally led to a challenging and deteriorated security situation on the global level. These events have impacted all areas of our life and next to the societal impacts they will continue to have a lasting impact on the European Union's (EUs) security. Especially the threat of terrorism does not have respect to borders: The global situation and events happening elsewhere directly affect the security of Europe. The state of permanent risk from potential terror attacks is evident from the recent Europol report, stating that 1560 people were arrested in EU member states on suspicion of terrorism-related offences between 2019 and 2021 [2]. A total of 29 jihadist or extreme right-wing plots were foiled across the EU in this period [3]. In the years before, the incidence of terrorist attacks using improvised explosive devices (IEDs) has risen across Europe. Reports from Europol confirmed that the use of home-made explosives (HMEs), synthesized from easily available chemicals, prevailed as the most common type of explosive used in terrorist IED attacks [4]. Triacetone triperoxide (TATP) was used in the majority of the recent attacks, such as in the Paris attacks 2015, the Brussels airport attack 2016, the Manchester concert bombing 2017 or the Surabaya (Indonesia) attacks 2018 [4,5], remaining the explosive of choice for terrorists. The recent EU regulation on explosives precursors (2019/1148) [6] was published in July 2019 as a result of investigations into the Paris and Brussels terrorist attacks, coming to the conclusion that the chemicals used for illicit explosive production require harsher restrictions and controls. The regulation came into force in February 2021 in the EU and included mandatory verification of legitimate use prior to sale and supply, improved regulations of suspicious transactions, disappearances and thefts of explosives precursors, and a reduction of licenses for members of the general public [6]. Another general challenge regarding terrorism is the globalization which does not only support and facilitate our everyday life but also terrorist operations. Nowadays, as new technologies become available for wide use, extremist groups unfortunately also take advantage of them and exploit them for their illegal use. The online platforms play an important role in this process, not only due to easier spread of violent terrorist propaganda and content but also due to facilitated access to bomb-making knowledge and information. Internet websites, forums, social networks and the darknet are important sources for lone actor terrorists to gain bomb-making knowledge [4]. Social isolation and increased time spent online during COVID-19 pandemic have amplified all these risks, especially among younger people and minors [2]. Additionally, Russia's war of aggression against Ukraine attracts and sparks violent extremist reactions, especially on online platforms [7]. Currently, the strained global geopolitical situation is felt on national territory and in neighboring countries as well, as exemplified on the one hand by the recent increased rate of violent antisemitic incidents [8,9], and on the other hand by general bomb threats against different public institutions, e.g. in Germany and France, resulting in evacuations of numerous

schools and airports [10,11]. Conclusively, events on the national but also international territory, i.e. occurring **everywhere** on the world, might incite **terrorist threats**, which may be fulfilled with almost **everything** considering the progressing digitalization and everyday chemicals available for **HMEs** production, so that **everyone** might be affected by the negative impacts.

A similar phenomenon can be observed for drugs, which are a great legal, health and social problem. A key message of the European Drug Report 2022 [1] was that **illicit drugs** are infiltrated into our society in such an extent that their use is encountered almost **everywhere** and almost **everything** with psychoactive properties is a potential drug so that **everyone** might be affected, either directly or indirectly. A concerning magnitude and severity of the drug problem on public health was estimated by 'The Global Burden of Disease Study 2017: mortality and morbidity attributable to the use of drugs', reported in World Drug Report 2020 [12], stating that 585,000 lives and 42 million years of 'healthy' life were lost globally in 2017 due to the use of drugs. Moreover, drugs are often linked to greater levels of violence and are frequently associated with different other offences. They aggravate some general social problems such as homelessness, youth criminality, failed rehabilitation of imprisoners or lacking therapeutic capabilities, leading to impaired public health in general. Therefore, the negative impacts of drugs can be directly observed in individuals developing addiction and relying on treatment, or are indirectly manifested in increased crime rates as well as in the strain on health and social costs. A concerning fact is that next to the high drug availability, particularly due to increasing online trade, a greater diversity of the psychoactive substances has continuously developed in the past years on the drug market, leading to new health and policy challenges. This diversity is mainly driven by new synthetic drugs (new psychoactive substances, NPS), which are associated with severe risks of intoxications and deaths due to their often higher potency or polydrug mixtures. These risks are even enhanced by the unawareness of consumers of the product composition, regarding the active ingredients contained, their concentration and their toxicological profiles. Even during the social isolation and strict border controls during the COVID-19 pandemic, the European market has shown its resilience in drug supply and use. The increasing digitalization took progress, with social media applications and encrypted services facilitating drug purchase [1]. An overarching conclusion that can be drawn is that law enforcement agencies (LEAs) are facing an increase of complex drug problems, expressed by high availability of drugs on the illicit drug market and great variability of drug consumption patterns. The high availability and use of illicit drugs across the EU can be exemplified by the fact that up to 2022 approx. 83.4 million or 29% of adults (aged 15 - 64) were estimated to have ever used an illicit drug, distributed over males (50.5 million) and in some lesser extent over females [1]. The complexity and dynamics NPS add to the drug market is illustrated by around 930 substances of this class monitored by the EMCDDA at the end of 2022, 41 of which first occurred on the European market in 2022 [13]. For comparison, the total number of NPS monitored by the end of 2013 was around 350 [14], showing at which pace the NPS market develops. In general, consumption patterns and illicit drug market fluctuations are not only influenced by national policies but also by some global events such as legislations regarding NPS in their most important source countries (China and India). A more recent development were illicit cannabis products adulterated with synthetic cannabinoid receptor agonists (SCRAs), the most prominent sub-group of NPS in the EU. This phenomenon was reported by 8 EU Member States since July 2020 [1]. Moreover, SCRAs are

particularly widespread among certain populations, e.g. young people [15] and in vulnerable and marginalized populations, such as homeless and prisoners [16-18].

All the above-mentioned situations and challenges Europe is facing today only reiterate the role of the security systems to ensure security and safety. It needs numerous different stakeholders to address these challenges, including public stakeholders, policymakers and various security authorities. As a citizen of a democratic and constitutionally governed EU country relying on justice and equality principles on the one hand, and as a scientist on the other hand, I would like to assert my expertise aiming to sustain these goals. Science and technology play a key role in combating crime, and forensic science represents a mainstay of the justice system. Contribution to further developments of this important scientific field represents the motivation for the selection of the area of investigation to perform this dissertation thesis.

II. Aim of the Work and General Concept

"Forensic science is a case-based (or multi case-based) research-oriented, science-based endeavour to study traces – the remnants of past activities (such as an individual's presence and actions) – through their detection, recognition, recovery, examination and interpretation to understand anomalous events of public interest (e.g., crimes, security incidents)." Sydney Declaration[19]

The above definition of forensic science by the recently published Sydney Declaration revisits its essence, indicating that forensic science is not predictive but retrodictive, yielding reconstructions of (often past) events or circumstances. The forensic analyses of traces of drugs and explosives feed investigation and intelligence efforts and answer justice- or litigation-based questions in the criminal justice system framework. When considering the perspective of illicit drugs and explosives as holistic problems, their relevance even extends to potential contributions to policing and security matters. Better understanding of the broader drug problem and deciphering the illicit drug market, or intelligence gathering on explosives production for a preventive function represent such potential contributions. All these aspects must reach compliance with legal requirements by basing the forensic evidence on a sound scientific methodology, analysis and evaluation. In this context, the motto **'Science meets practice'** has driven the work performed in this thesis, which combined scientific methodologies with applications in police practice. The overarching goal of the thesis was the development of novel methods and approaches for forensic detection and identification of illicit drugs and explosives in complex matrices. The focus was set on NPS, more precisely on SCRAs (Synthetic Cannabinoid Receptor Agonists) often referred to shortly as synthetic cannabinoids, and the home-made explosive triacetone triperoxide (TATP). The matrices investigated were biological (hair) and environmental (sewage) for drugs analysis and extended to different forensic evidence samples in context of pre-blast and post-blast explosive examinations.

One important aspect for practical implications was to elaborate robust, simple and efficient on-site sampling methods that can be employed by untrained personal, and develop optimized analytical methods to be used for sewage analysis in forensic work, especially to study the prevalence of synthetic cannabinoids. This objective comprised stability assessment of synthetic cannabinoids in sewage, the development and optimization of sampling as well as the implementation of analytical methods for the detection and quantification of synthetic cannabinoids, and finally the method application to real sewage networks.

An additional method developed for the main human cannabis metabolite was aimed to be applied to authentic hair samples from cannabis users or individuals suspected of cannabis use to determine the metabolite's concentration distribution in forensic hair samples and estimate the frequency of cannabis use for the particular cases (occasional, frequent or regular use). The data gained from authentic case samples were used for statistical evaluation to derive trends of drug use, or to assess the method performance.

For illicit drugs, the main goal was a statistic evaluation and triangulation of authentic data from different sources (hair samples, sewage water and police seizures) to draw conclusions about the prevalence of synthetic cannabinoids.

For TATP, a method for liquid and gas phase sampling and subsequent trace analysis had to be developed, allowing for the identification of TATP from production sites (chemical waste, air, clothes, etc.), as well as from post-blast residues after an explosion.

Results of forensic analysis of drugs and explosives are used in court proceedings for legal purposes, so that the validity of the results gained by the examination of forensic samples must be ensured. This is achieved by handling the criminal evidences in a careful manner and chronological documentation during the processing of the evidence, from collection until analysis. The process is designated as 'chain of custody' and aims to prevent contamination and manipulation of the criminal evidences used in court [20]. Therefore, the main goal for the development and establishment of methods in the scope of this work was to minimize and rule out possible pitfalls and establish valid methodologies.

Chromatographic techniques coupled with mass spectrometry are well established forensic analytical tools for the identification of illicit drugs and explosives in forensic analysis. This can be attributed to the high sensitivity, specificity and selectivity of these analytical methods. Analysis of evidence samples using these methods encompasses two basic steps. The first step is the sample preparation procedure to extract target analytes from the matrix of an evidence sample and the second step entails the analytical detection part with gas-chromatography (GC) or liquid-chromatography (LC) in combination with mass spectrometry (MS) or multistage mass-spectrometry (MS^n). This apparently simple process implies many factors that impact the analysis. The first important factor is of general nature and involves sample collection and sample availability aspects. The time point of sample collection relative to an event might strongly impact the loss of information. Moreover, forensic evidence samples cannot be regarded as reproducible experiments. Often only a limited amount of sample is available and after the extraction process the sample cannot be recovered. The second important factor is that the evidence sample may include a broad spectrum of different complex matrices, which obstruct the analytical process. Therefore, the approach is rendered ineffective, if sample preparation is not satisfying. This step is crucial not only due to the importance of effective and efficient extraction of target analytes, but also serves as a cleaning step to exclude matrix interferences from the sample, while preventing any external contamination. Great efforts must be made in method validation and quality management to ensure the validity of the analysis results and avoid false positive or false negative results (third important factor). Finally, the interpretation of the results as the last factor must be made with precaution and take into account quality control (QC) parameters (blank samples, internal and external quality control samples) to account for possible pitfalls during both the sample preparation and the analytical detection.

In the following, short background information, objectives and concept of individual sub-topics, treated in individual chapters (**Chapters 1 – 6**), will be provided. A compiled scheme of the general concept is given in **Figure I**.
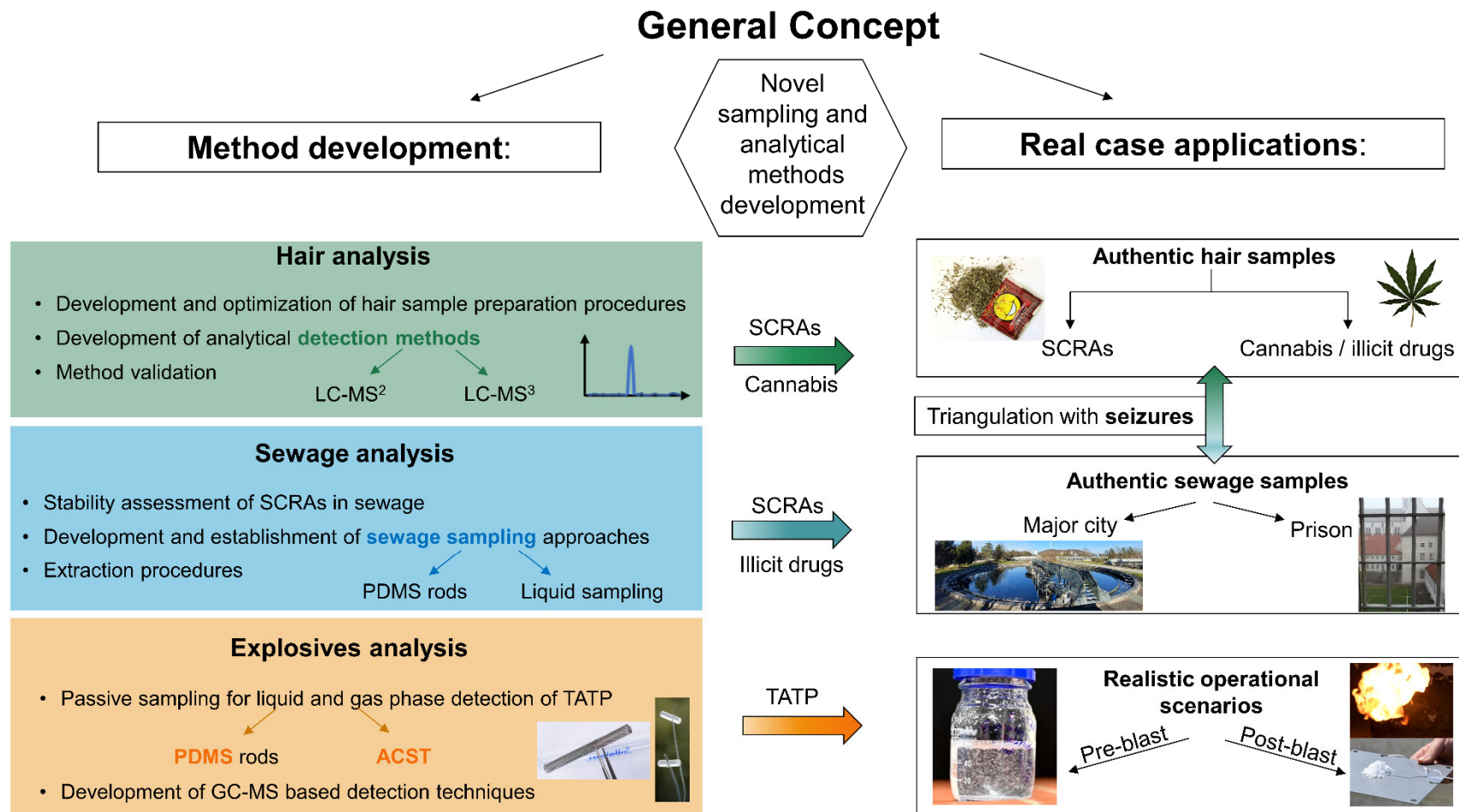
Figure I. Scheme of the general concept together with individual objectives of the dissertation.

Chapter 1:	General Introduction

This chapter deals with theoretical backgrounds of forensic hair, wastewater and explosives analysis. Key features are cannabis and SCRAs as illicit drugs, as well as the explosive TATP, which were all discussed in more detail.

Chapter 2:	Hair analysis

'Human performance toxicology', a sub-discipline of forensic toxicology, is often applied in cases of driving ability examinations, diagnosis of chronic exposure to drugs, diagnosis of drug addiction and criminal liability, or in drug facilitated crimes. The most commonly used biological matrices are blood, urine and hair. Identification of illicit substances and/or their metabolites in these biological matrices is considered as an unambiguous proof of active drug consumption. In comparison to blood or urine, hair acts as a long-term storage medium of different xenobiotics and thus offers the ability of a longer detection window (months to years, depending on the length of the hair) to monitor retrospective illicit drug consumption, establishing it as an important forensic tool.

The aim of the work in this section was to develop and establish efficient, fast, non-laborious and sensitive LC-MS routine method for the determination of 11-nor-9-carboxy-Δ^9-tetrahydrocannabinol (THC-COOH), one of the major endogenously formed metabolites of cannabis, in hair samples. Since dealing with very low target concentrations in a complex matrix, an optimized sample preparation procedure and a sensitive instrumental analysis are essential. Therefore, different sample preparation procedures as well as analysis approaches were tested. With the aim of a quantitative determination of cannabis use, the method set-up for THC-COOH was extensively validated in compliance to the established guidelines. Finally, the method developed was applied to authentic case samples and statistical analysis of the results was performed.

Chapters 3 - 4:	Sewage analysis

Consumption of illicit drugs remains a widespread and challenging problem worldwide. Cannabis continues to be the most widespread used substance with over 22 million EU adults (aged 15 - 64) accounting to the European Drug Report 2022 [1], followed by millions of users of stimulants and opioids [1]. However, an increasing diversity in drug consumption patterns can be observed, especially due to the continuously evolving NPS market. SCRAs have an important role in the NPS market in the EU, and the continuous emergence of new relevant substances poses a great challenge to monitor NPS use.

Health and social policy issues of drug abuse can only be addressed by a profound knowledge of the situation and analysis of the trends. A promising tool to estimate community prevalence and consumption of illicit drugs is wastewater-based epidemiology (WBE). The approach

relies on detection of target residues of illicit drugs in municipal wastewater and even allows to gain quantitative data on drug loads normalized to the catchment population by a back-calculation. The methodology is well established for the most common illicit drugs, i.e. cannabis, cocaine, amphetamine, methamphetamine and MDMA. However, there is a gap for the NPS. The aim of the work in this section was to bridge this gap and develop, optimize and establish sampling protocols, extraction procedures and an analytical detection method for the determination of SCRAs in wastewater. The first step was the selection of appropriate SCRA biomarkers in sewage and encompassed stability assessment of chemically diverse SCRAs and selected human metabolites under sewage conditions. The investigation included elucidation of processes, i.e. microbial degradation or physico-chemical processes, which control the in-sewer stability of SCRAs. After successful determination of SCRA biomarkers for wastewater analysis, two wastewater sampling protocols were evaluated. A very convenient and easy-to-use solid phase extraction method gave time averaged samples for several days, while a technically more demanding liquid sampling approach allowed for time resolved analysis. Another key aspect of the study was the application of both methods to real sewage networks. In the first step, the examination was aimed to the small and very specific population of a German prison, and was then extended to multiple points in sewer network of a larger and more general population covered by a city district of Munich, representing a catchment area of about 25,000 inhabitants. Data from a computational sewer network model were used for the selection of suitable sampling sites in the complex sewage system, with the benefit either to allow for higher local geographical resolution or to cover wider areas.

For the analytical detection of SCRAs, a targeted LC-MS/MS method was developed and continuously updated in order to keep pace with the fluctuations of the dynamic SCRA market.

Chapter 5: **Triangulation of police seizures, wastewater and toxicological hair analysis to assess SCRA use**

After establishing the analytical method for the determination of the cannabis metabolite THC-COOH in hair samples, as described in Chapter 2, another important aspect of this work was the development of a methodology for SCRA detection via hair analysis. With the protocol established, data collected from authentic hair samples were analyzed, evaluated and correlated to estimate the prevalence of synthetic cannabinoids use. The toxicological and the environmental data (see Chapters 3 and 4) were triangulated with police seizures to obtain a comprehensive picture on SCRA use.

Wastewater analysis was extended to sampling in a wastewater treatment plant, collecting sewage pollution load corresponding to

approximately 1.4 million inhabitants. Additionally, cannabis and other conventional drugs were included in the data analyses to enable a comprehensive SCRA user profiling via toxicological analysis and to estimate the extent of SCRA abuse in the general population as derived from sewage analysis data. The user profiles not only covered age and gender, but also the degree of co-use of SCRAs and various conventional illicit drugs. The different types of samples were secured over the course of 1.5 years (2021-2022) or selected periods therein, and the SCRAs detected were correlated to changes in German drugs legislation.

Chapter 6:	Explosives analysis – Triacetone triperoxide (TATP)

Organic peroxides are often produced as homemade explosives (HMEs) by terrorists due to inexpensive precursor chemicals, simple synthesis procedures and widely available instructions. TATP is one of the most notable peroxide explosives, having been used in improvised explosive devices (IEDs) for several terrorist attacks in the last years [21]. Therefore, the importance of TATP in forensic investigations prompts law enforcement agencies (LEAs) to continuously develop and improve analytical tools and methodologies for detection of TATP. Forensic identification of TATP in pre-blast and post-blast residues, including on-field investigations of possible production sites, demands for practicable and simultaneously sensitive diagnostic methods. This work seeks to address this demand and presents a concept suitable for laboratory as well as on-site sampling and trace amount detection of TATP residues in liquid (aqueous TATP synthesis waste) and gas phase. It features TATP enrichment from the aqueous or gas phase by exploring and establishing different passive samplers (polydimethylsiloxane (PDMS) sampling rods and activated carbon sampling tubes (ACST)), followed by identification of the explosive with GC-MS or GC-PCI-MS/MS analytical techniques. Analytical developments were aimed at a quantitative GC-MS/MS analysis with ^{13}C-TATP as internal standard and a qualitative analysis that was based on a field-portable GC-MS system. Stability of TATP in aqueous solution, retention behaviour of TATP on passive samplers under different storage conditions, re-extraction procedures of TATP from passive samplers, and preliminary uptake kinetics experiments in gas phase were main objectives to be assayed in the course of the study. The practical suitability and performance of the methodology was demonstrated during a TATP synthesis performed (pre-blast scenario), by analysing synthesis waste and trace amounts in ambient air and on clothing. A second application concept focused on the investigation of post-blast residues after controlled blasting experiments (post-blast scenarios), probing the influence of surface, time delay and sampling conditions on the amount of TATP recovered.

A compiled scheme of the structure of the dissertation is depicted in **Figure II.**

Structure of the Dissertation

State of the Art and Motivation
Aim of the Work and General Concept

Chapter 1.

General Introduction

Chapter 2. Hair analysis	**Chapters 3-4.** Sewage analysis	**Chapter 5.** Triangulation study	**Chapter 6.** Explosives analysis
Determination of the major cannabis metabolite in hair using LC-MS^3 • Method development and optimization • Authentic casework	i) Stability assessment of SCRAs in sewage system ii) Novel sampling approach based on passive samplers to investigate SCRA prevalence in a prison and a major city	Hair ⇄ Sewage Police seizures Comparative study of hair, sewage and police seizure data to assess illicit drug use • SCRAs • Conventional drugs	Triacetone triperoxide (TATP) • Sampling and analytical method development • Applications: • Pre-blast • Post-blast

Summary and Conclusion

Figure II. Structure of the dissertation that was compiled in individual chapters.

10

References

[1]   European Monitoring Centre for Drugs and Drug Addiction (EMCDDA), European Drug Report 2022: Trends and Developments. 2022; Luxembourg: Publications Office of the European Union.

[2]   Europol. European Union Terrorism Situation and Trend Report. 2022; Luxembourg: Publications Office of the European Union.

[3]   Council of the EU and the European Council. The EU's work to tackle terrorism. 2022. https://www.consilium.europa.eu/en/eu-response-to-terrorism/. Date accessed: October 25, 2023.

[4]   Europol, European Union Terrorism Situation and Trend Report. 2017; Luxembourg: Publications Office of the European Union.

[5]   Joint Counterterrorism Assessment Team - National Counterterrorism Center (NCTC), Department of Homeland Security (DHS), and the Federal Bureau of Investigation (FBI). Triacetone triperoxide (TATP): Indicators of acquisition and manufacture, and considerations for response. 2019. https://www.dni.gov/files/NCTC/documents/jcat/firstresponderstoolbox/78--NCTC-DHS-FBI---Triacetone-Triperoxide-%28TATP%29-.pdf. Date accessed: October 30, 2023.

[6]   Regulation (EU) 2019/1148 of the European Parliament and of the Council of 20 June 2019 on the marketing and use of explosives precursors, amending Regulation (EC) No 1907/2006 and repealing Regulation (EU) No 98/2013 (Text with EEA relevance). *OJ L*. 2019;186:1-20. http://data.europa.eu/eli/reg/2019/1148/oj.

[7]   Europol. European Union Terrorism Situation and Trend Report. 2023; Luxembourg: Publications Office of the European Union.

[8]   European Commission. European Commission Statement on antisemitic incidents in Europe. 2023. https://ec.europa.eu/commission/presscorner/detail/en/statement_23_5527. Date accessed: November 06, 2023.

[9]   The Federal Association of Departments for Research and Information on Antisemitism (Bundesverband RIAS). Antisemitic reactions in Germany to the Hamas massacres in Israel. 2023. https://report-antisemitism.de/monitoring/. Date accessed: November 06, 2023.

[10]   Spiegel. Bundesweite Welle von Bombendrohungen an Schulen. 2023. https://www.spiegel.de/panorama/justiz/schulen-bundesweite-welle-von-bombendrohungen-a-1b9e8f8e-39f8-4bbe-81ec-990b293aeb1b. Date accessed: November 01, 2023.

[11]   Spiegel. Mehrere Flughäfen nach Anschlagsdrohungen geräumt. 2023. https://www.spiegel.de/panorama/justiz/frankreich-mehrere-flughaefen-nach-anschlagsdrohungen-geraeumt-a-ff0a2776-3546-48a0-b0b1-0e71284a0ac3.
Date accessed: November 01, 2023.

[12]   United Nations Office on Drugs and Crime (UNODC). World Drug Report 2020. 2020; Vienna: United Nations publication, Sales No. E.20.XI.6.

[13]   European Monitoring Centre for Drugs and Drug Addiction. New psychoactive substances - the current situation in Europe (European Drug Report 2023). 2023. https://www.emcdda.europa.eu/publications/european-drug-report/ 2023/new-psychoactive-substances_en. Date accessed: October 28, 2023.

[14]   European Monitoring Centre for Drugs and Drug Addiction. European Drug Report 2014: Trends and Developments. 2014; Luxembourg: Publications Office of the European Union.

[15]   European School Survey Project on Alcohol and Other Drug (ESPAD) Group. ESPAD Report 2019: Results from the European School Survey Project on Alcohol and Other Drugs. 2020; Luxembourg: Publications Office of the European Union.

[16]   Van Hout MC, Benschop A, Bujalski M, et al. Health and Social Problems Associated with Recent Novel Psychoactive Substance (NPS) Use Amongst Marginalised, Nightlife and Online Users in Six European Countries. *Int J Ment Health Addiction.* 2018;16:480-495. DOI: 10.1007/s11469-017-9824-1.

[17]   Csák R, Szécsi J, Kassai S, Márványkövi F, Rácz J. New psychoactive substance use as a survival strategy in rural marginalised communities in Hungary. *Int J Drug Policy*. 2020;85:102639. DOI: 10.1016/j.drugpo.2019.102639.

[18]   European Monitoring Centre for Drugs and Drug Addiction (EMCDDA). New psychoactive substances in prison: Results from an EMCDDA trendspotter study. 2018; Luxembourg: Publications Office of the European Union.

[19]   Roux C, Bucht R, Crispino F, et al. The Sydney declaration – Revisiting the essence of forensic science through its fundamental principles. *Forensic Sci. Int.* 2022;332:1111 82. DOI: 10.1016/j.forsciint.2022.111182.

[20]   Evans MM, Stagner PA, Rooms R. Maintaining the chain of custody - evidence handling in forensic cases. *AORN J.* 2003;78(4):563-569. DOI: 10.1016/S0001-2092(06)60664-9.

[21]   Bergen P, Sterman D, Salyk-Virk M. Terrorism in America 18 Years After 9/11. 2019. https://www.newamerica.org/future-security/reports/terrorism-america-18-years-after-911/. Date accessed: November 01, 2023.

Chapter 1

General Introduction

1.1 Conventional drugs of abuse: Cannabis

The most common classes of conventional drugs of abuse involve stimulants, opioids, hallucinogens and phytocannabinoids (active ingredients of cannabis). Few typical examples of commonly abused drugs, graded into the aforementioned classes, include:

- Stimulants: amphetamine, methamphetamine, 3,4-methylenedioxyamphetamine (MDA), 3,4-methylenedioxymethamphetamine (MDMA) and cocaine

- Opioids: heroin, fentanyl, oxycodone and methadone

- Hallucinogens: lysergic acid diethylamide (LSD) and *N,N*-dimethyltryptamine (DMT)

- Phytocannabinoids: mainly (−)-*trans*-Δ^9-tetrahydrocannabinol (Δ^9-THC) and tetrahydrocannabinolic acid (THCA), but also non psychoactive substances including cannabinol (CBN) and cannabidiol (CBD)

In general, cannabis is part of the cannabinoids family which divides into three main groups:

- Endocannabinoids: The endogenously produced cannabinoid receptor agonists of human origin

- Phytocannabinoids: Δ^9-THC and related compounds of cannabis plant origin

- Synthetic cannabinoids or synthetic cannabinoid receptor agonists (SCRAs): Artificially made substances belonging to the new psychoactive substances (NPS), a novel class of drugs of abuse, that act pharmacologically similar as Δ^9-THC

Since the focus of the methodological developments in this work is related to cannabis (Chapter 2) and SCRAs (Chapters 3-5), these drug classes will be discussed in more detail in the following sections. Conventional drugs of abuse are covered by Chapter 4 (section 4.7) and Chapter 5, providing data on sewage and/or hair analysis of common illicit drugs. Detailed background information on these drugs is beyond the scope of this introduction.

1.1.1 Components of cannabis

Cannabis (*Cannabis sativa*), also known as Indian hemp, was originally cultivated in Central Asia (India and China) and has been used for centuries as fiber, food and oil source as well as for therapeutic, cultural and recreational purposes. The latter use ows to the psychoactive effects of cannabis, which can be traced back to the first century A.D. with the first known documented reference in the Chinese pharmacopoeia [1-3]. The medicinal reports of this pharmacopoeia alerted of excessive ingestion of cannabis seeds, which "will produce hallucinations (literally 'seeing devils'). If taken over a long term, makes one communicate with spirits and lightens one's body "will produce visions of devils … over a long term, it makes one communicate with spirits and lightens one's body… [3].
The cannabis plant (Figure 1) contains 483 different chemical compounds known so far, such as phytocannabinoids, terpenoids, hydrocarbons, nitrogenous compounds, carbohydrates, flavonoids, fatty acids, phenols, phytosterols, simple alcohols, aldehydes, ketones, acids, esters and lactones [4]. Phytocannabinoids are terpenophenolic compounds being unique to the cannabis plant, which was found to synthesize at least 144 such compounds [5]. The two main phytocannabinoids are the primary psychoactive component of cannabis *trans*-Δ^9-tetrahydrocannabinol (Δ^9-THC) and the non-psychoactive cannabidiol (CBD), which has been

found to mitigate some of the effects of THC[1] [6-9]. Other main phytocannabinoid constituent of cannabis is cannabichromene (CBC) [10], while important minor phytocannabinoids encompass Δ^8-THC and cannabinol (CBN), the degradation product of THC. Whereas Δ^8-THC is approximately 20% less active than Δ^9-THC [4], CBN is a much less potent cannabinoid that derives from the oxidation of THC during prolonged storage. In fresh plants, 95% of the three main constituents exist in their cannabinoid acid forms [10]: tetrahydrocannabinolic acid (THCA), cannabidiolic acid (CBDA) and cannabichromenic acid (CBCA). These cannabinoid acids are biosynthesized from a common precursor, cannabigerolic acid (CBGA), via distinct biosynthesis routes mediated through specific enzymes [5]. Upon prolonged storage or heating including smoking or baking, the acids readily decarboxylate to the corresponding phytocannabinoids. Therefore, the active compounds are partly formed during smoking of cannabis, a process that might release more than 2,000 compounds by pyrolysis [11]. The distinct biosynthesis routes of THCA and CBDA indicate that THC production acts limiting on the CBD quantities and vice versa. The composition is mainly affected by botanic characteristics (cannabis strain type), but also growing conditions have significant effects on the cannabinoid production.

Figure 1. Female cannabis plant throughout different growth phases. Source: Forensic Science Institute, Bavarian State Criminal Police Office.

The cannabinoids are produced and sequestered by the plant in small, resinous and sticky structures called glandular trichomes (Figure 2). These structures play a key role in the defense of the plant against herbivores and environmental stress. The highest concentration of the trichomes is located around the female flowers, therefore having the highest quantity of cannabinoids on the inflorescences. The distinctive odor of cannabis originates from 140 different terpenoids, which represent acyclic, monocyclic, or polycyclic hydrocarbons including substituted functional groups of alcohols, ethers, aldehydes, ketones, and esters [4]. Variations of the terpenoide profile influences cannabis use from the olfactory and gustatory perception and may influence the pharmacological effects [12].

---

[1] Unless stated otherwise, THC always refers to the Δ^9-THC in this work

Figure 2. Small, resinous and sticky structures called glandular trichomes distributed around the female flowers represent the main cannabinoid production sites. Source: Forensic Science Institute, Bavarian State Criminal Police Office.

1.1.2 Cannabis pharmacokinetics

Pharmacokinetics comprises of drug absorption, distribution, metabolism, and excretion. Drug formulation and the route of administration dictate the rate of drug absorption, its distribution and metabolism.

a) Absorption

The principal routes of cannabis administration are either smoking/inhalation or oral ingestion. Inhalation represents a rapid and efficient drug delivery from the lungs to the brain, with THC detectable in plasma immediately after the first puff of a cannabis cigarette [13] and peak plasma concentrations achieved 3 to 10 minutes after onset of smoking [14]. The level of the THC metabolite 11-OH-THC was found to be substantially lower than THC level and reached peak plasma concentration approximately 13 min after starting to smoke [15], whereas THC-COOH concentrations gradually increased and exceeded THC concentrations 30-45 min after the end of smoking [16]. After oral ingestion, the absorption is delayed and erratic, yielding maximum plasma concentrations of THC usually after 60-120 minutes up to 6 h [14]. Due to assumed degradation under acidic conditions in stomach as well as due to an extensive first-pass liver metabolism, the bioavailability of THC after oral consumption is reduced and amounts to 4-12% [17] as opposed to a greater bioavailability after inhalational cannabis use (2-56%), with intra- and inter-subject variability in smoking dynamics contributing to uncertainty in dose delivery [17-19]. In general, inhalation produces stronger psychoactive effects and thus greater abuse potential when compared to oral ingestion [20] due to nearly immediate drug exposure to the central nervous system (CNS).

b) Distribution

THC features high lipophilicity and high affinity to lipoproteins in blood, with 90% distributed in the blood plasma and the residual 10% in the erythrocytes [21]. Plasma concentrations of THC decline rapidly after the completion of smoking due to its rapid distribution into highly perfused tissues, such as the lung, heart, brain, and liver [11], as well as due to the onset of the hepatic metabolism in the liver. After absorption, the highly lipophilic THC is preferentially stored in adipose tissues of the body, the major long-term deposit site, yielding concentration

17

ratios between fat and plasma of up to 10,000:1 [22]. From the fat tissue, THC slowly diffuses back into the bloodstream. This effect was especially observed for chronic cannabis users, where substantial THC concentrations in blood persisted weeks after last cannabis intake [23]. Similarly, Johansson et al. [24] determined an elimination half-life of THC in plasma of 4.1 d for subjects smoking four cigarettes during a two-day period, each containing 15 mg THC.

c) Metabolism

THC is metabolized into more than 100 metabolites that have been identified, including di- and trihydroxy compounds, ketones, aldehydes, and carboxylic acids [11,14]. The biotransformation of THC occurs mainly in the liver (hepatic metabolism) by catalysis of the cytochrome P450 (CYP) enzyme system [25,26]. Phase I metabolic reactions encompass allylic and aliphatic hydroxylations, oxidation of alcohols to ketones and acids, β-oxidation, and degradation of the pentyl side chain, whereas Phase II reaction includes conjugation with glucuronic acid [11]. The glucuronide conjugate enhances water solubility and hence excretion. The primary metabolite 11-hydroxy-THC (11-OH-THC) is formed by hydroxylation of THC and further oxidized to the 11-oxo-THC before final oxidation to 11-nor-9-carboxy-THC (THC-COOH). THC-COOH together with its glucuronide conjugate represent the major final products of THC metabolism in most species, including humans [27]. Whereas 11-OH-THC generates equipotent psychoactive effect as THC [28], THC-COOH is a non psychoactive metabolite [27,29]. THC metabolism might also take place at extrahepatic metabolic sites in tissues such as brain, lung, and intestine [11].

d) Elimination

The majority of THC (80-90%) is excreted within 5 d, mostly in the form of its major metabolites [11]. The elimination is established mainly by biliary excretion via feces (> 65%), with 11-OH-THC found as predominant fecal cannabinoid, and to a lesser extent via urinary excretion (about 20%), with THC-COOH glucuronide conjugate as the major urinary metabolite [11,30,31]. Contrary to urine, neutral cannabinoids such as THC are preferably incorporated in alternative biological matrices including oral fluid and hair when compared to their acidic metabolites such as THC-COOH.

1.1.3 Cannabis pharmacodynamics: Mechanism of action and pharmacological effects of cannabis

Cannabinoid receptor type one (CB$_1$) and cannabinoid receptor type two (CB$_2$) constitute together with endogenous ligands (endocannabinoids) the endocannabinoid system. The most relevant endocannabinoids are arachidonylethanolamide (anandamide) and 2-arachidonylglycerol, each of which can activate both CB$_1$ and CB$_2$ receptors, and are believed to act as neurotransmitters or neuromodulators [14,32]. The CB$_1$ receptor is widely distributed in several brain regions, with the highest densities found in the frontal cortex, hippocampus, basal ganglia, hypothalamus, cerebellum, as well as in spinal cord and peripheral nervous system [14,33]. CB$_2$ receptors are encountered primarily in immune cells (leucocytes), spleen and tonsils [34]. The most effects of phytocannabinoids are associated with their agonistic or antagonistic actions on the cannabinoid receptors. Agonists are substances that activate a receptor to generate a biological response, while antagonists block or dampen the action of the agonists. The ability of a drug to bind to and act as an agonist or antagonist at a receptor

is expressed as its receptor binding activity (Ki), with lower values indicating stronger binding. Besides the receptor binding affinity, efficacy and potency are further important indicators for the characterization of a drug activity profile. Efficacy is the maximum biological effect a drug can elicit based on its receptor binding, while potency is the amount of drug needed for a predefined biological effect, often fixed as 50% of the maximum effect. THC shares the ability of the endocannabinoids to activate both cannabinoid receptors, however the CB_1 and CB_2 affinity is lower than for many synthetic agonists, for example HU-210 or CP-55,940 [32]. Moreover, THC features lower CB_1 and CB_2 efficacy than these synthetic compounds, indicating that THC acts as a partial (low-efficacy) agonist for both cannabinoid receptors [32], while many synthetic compounds are full agonists. Finally, the efficacy of THC is lower at CB_2 than at CB_1 receptors [14]. In general, the psychoactive effects derive from the drug activity at CB_1 receptors, while the anti-inflammatory and analgesic properties involve drug interaction with CB_2 receptors [35,36]. The stereoselectivity of THC plays an important role in its pharmacological activity, since the natural (-)-*trans* isomer exhibits 6-100 times higher potency relative to the (+)-*trans* isomer, depending on the assay [14].

After consumption, cannabis induces euphoria, relaxation, intensification of sensory experiences, stimulation of appetite, and antiemesis, but it is also associated with acute and chronic adverse effects, including anxiety, panic attacks, acute and chronic cardiovascular and respiratory side effects, impaired memory, learning and motor coordination, schizophrenia/psychosis, depression, and dependency [14,37]. These effects can be particularly pronounced and irreversible for young consumers. Psychological effects of THC have been classified into four categories: affective (euphoria and easy laughter), sensory (intensification of external stimuli and perception of the own body), somatic (feeling of the body floating or sinking in the bed) and cognitive (distorted time perception, memory impairment, difficulty in concentration) [14]. The increased potency of cannabis products, as suggested by the recent data for the US [38] and EU [39], has been observed to have important implications for adverse health effects, such as symptoms of cannabis use disorder [40-42] or elevated risks of psychosis [43,44]. Furthermore, the increased THC concentrations were observed to be accompanied by increased incidence of first-time admissions to drug treatment due to cannabis-associated problems [45]. In the EU, the increase in average potency of herbal cannabis and cannabis resin equaled to about 60% and nearly 200%, respectively, between 2011 and 2021 [39].

Besides the aforementioned physical, cognitive, and psychological effects, cannabis use implies concerns on public health and safety as well. Adversely affected psychomotor and cognitive performance impairs driving ability in a dose-dependent manner [46-48] and the likelihood of fatal and nonfatal motor vehicle collisions increases by 2-7 times [47,48]. Cannabis use can progress to addiction, with 9-10% of individuals who start using cannabis becoming addicted, and the risk is even higher when the use is initiated in adolescent age (16-17%) or among daily cannabis users (25-50%) [37]. First after the age of 25 years the addiction risk decreases [49]. Especially early exposure to cannabis also increases vulnerability to abuse of and addiction to other psychoactive substances due to alteration of the reactivity of brain dopamine reward centers [50]. Conclusively, cannabis use might have pronounced negative and long-term impacts on vulnerable populations, including young people under the age of 25 years, individuals with substance use disorders, individuals with pre-existing personal or

family history of mental illness, persons with compromised cardiovascular or respiratory systems, and women during gestation [51-53].

1.2 New psychoactive substances (NPS)

1.2.1 NPS phenomenon and major classes of NPS

New psychoactive substances consist of chemically diverse groups of substances that have been synthesized to mimic the pharmacological effect of illicit drugs and simultaneously to circumvent the legislative measures established for the conventional illicit drugs. The definition of NPS as adopted into European law by the EU is:

"*a substance in pure form or in a preparation that is not covered by the 1961 United Nations Single Convention on Narcotic Drugs, as amended by the 1972 Protocol, or by the 1971 United Nations Convention on Psychotropic Substances but may pose health or social risks similar to those posed by the substances covered by those Conventions*" [54].
(Article 1 of Council Framework Decision 2004/757/JHA of 25 October 2004, as amended by Directive (EU) 2017/2103 of the European Parliament and of the Council of 15 November 2017)

Besides their perceived legal status, the main driving factors for NPS use include their easy availability via online shops, often low price, their limited detectability with conventional drug screening tests, perception of higher purity, and exciting user experience [55-58]. The popularity of NPS is confirmed by the data published in the recent report of the UNODC, revealing a cumulative number of 1,184 substances over the last 15 years [59]. In the EU, the number of monitored NPS has risen to 930 substances at the end of 2022, 41 of which were first reported in Europe 2022 [60]. The rapid information exchange to detect and assess the threats posed by NPS is achieved between the EU member states, Norway, Turkey and UK by the EU Early Warning System (EU EWS) [61]. Key data on monitoring of the NPS phenomenon in Europe over the last 25 years are summarized in Table 1.

Table 1. Monitoring of NPS by the EU EWS from 1997 to 2021 [61].

EU EWS monitoring of NPS		
	1997 to 2021	2020 or 2021
Number of NPS being formally notified for the first time	884 NPS	52 NPS in 2021
Seizures	283 500 seizures (since 2005)	21 200 in 2020
	31.6 tonnes (since 2005)	5.1 tonnes in 2020
Public health risk communications	168	7 in 2021
Risk assessment	37 NPS	2 NPS in 2021
NPS legislative ban	27 NPS under EU control; 26 NPS subsequently controlled internationally	2 NPS in 2021

Based on their toxicologic profiles, NPS can be categorized into six different classes: synthetic cannabinoid receptor agonists (synthetic cannabinoids), stimulants, synthetic opioids,

benzodiazepines (and other sedative-hypnotics), hallucinogens and dissociatives. A short overview of the different NPS classes and their sub-classes will be given, and the class of synthetic cannabinoids will be discussed in more detail in section 1.2.2.

1. Stimulants

The class of stimulants represents a large and chemically diverse group with synthetic cathinones, which account for largest quantities of NPS seized in EU countries [60]. The class of NPS stimulants can be further divided into following sub-classes:

- Cathinones: Synthetic cathinones are β-keto phenethylamines that are derived from cathinone (*S*-(-)-2-amino-1-phenylpropan-1-one), the psychoactive compound present in the khat plant (*Catha edulis*). Synthetical analogues include NPS such as 4-methylmethcathinone (mephedrone), and analogues of pyrovalerone (e.g. 3,4-methylenedioxypyrovalerone, MDPV) or 3,4-methylenedioxy substituted cathinones (methylone, ethylone, and butylone), the latter being structurally related to MDMA. Synthetic cathinones have been identified in numerous NPS products marketed as 'bath salts', 'plant food' or 'research chemicals'.

- Phenethylamines: This group mainly includes derivatives of amphetamine (e.g. 4-fluoroamphetamine, *para*-methoxymethamphetamine). According to structural analogy, 2,5-dimethoxyphenethylamines, colloquially known as "2C" or "2C-X" series, as well as their associated derivatives of *N*-(2-methoxybenzyl) or "25X-NBOMe" series are also included, although they rather act as hallucinogens than as stimulants [62,63].

- Piperazines: Initially researched as potential therapeutic agents, but never brought to market maturity, piperazines became the designation of 'failed pharmaceuticals' [64]. The most common piperazine, 1-benzylpiperazine (BZP), was developed as a potential antidepressant drug [65], but showed psychoactive properties similar to amphetamine and hence implied liability for abuse. Some other common piperazines used as NPS are 1-(3-chlorophenyl) piperazine (*m*CPP) and 1-(3-trifluoromethylphenyl) piperazine (TFMPP). They are most frequently encountered in "party pills" as a substitute for ecstasy tablets.

- Aminoindanes: Compounds are derived from aminoindane (2-amonoindane, 2-AI), a cyclic analogue of amphetamine. The aminoindane structure was modified to generate derivatives such as 5,6-methylenedioxy-2-aminoindane (MDAI) [66], which act predominantly as central nervous system (CNS) stimulants and mimic the effects of the conventional drugs such as cocaine, amphetamine, methamphetamine, MDMA, and cocaine.

2. Hallucinogens

Most hallucinogenic NPS belong to the "2C" class (see above), the ergoline class or the tryptamine class. The latter are indolealkylamines, some of which occurring naturally, such as the neurotransmitter serotonin, the hormone melatonin, and a variety of psychoactive hallucinogens found in plants, fungi, and animals, e.g. *N,N*-dimethyltryptamine (DMT), psilocybin, and 5-methoxy-*N,N*-dimethyltryptamine (5-MeO-DMT). The psychoactivity seems to be highly affected by the substitution at the indole ring (positions 4 and 5) and the alkylation of the sidechains (N-sidechain and C-sidechain). [67], leading to a variety of synthetic derivatives of the natural compounds. Hallucinogens act primarily as agonists of the serotonin

5-HT$_{2A}$ receptor and induce profound changes in sensory perception, mood and thoughts, resulting in users experiencing severe hallucinatory effects [68]. The popularity of hallucinogens raised after the discovery of lysergic acid diethylamide (LSD) and its hallucinogenic properties in the mid-1900s, when recreational use spread among young people [68]. New synthetically produced hallucinogens appeared on the illicit drug market throughout the 1990s and in the last years, with representatives such as alpha-methyltryptamine (AMT), 5-methoxy-*N,N*-diisopropyltryptamine (5-MeO-DIPT) [69] or 1-cyclopropionyl-LSD (1cp-LSD) as 'legal' alternatives to LSD.

3. Synthetic Opioids

Synthetic opioids are narcotic analgesics that have recently become popular on the drug market, however many of these substances are highly potent with life-threatening risk of poisoning. A particularly potent sub-class of synthetic opioids are fentanils. Although many of these substances are used in human and veterinary medicine, fentanils are often synthesized in clandestine laboratories and sold on the illegal drug market as 'synthetic heroin' or as mixtures with heroin, methamphetamine, and cocaine, and even as counterfeit or fake medicines [70,71]. These clandestine productions include established fentanyl derivatives as well as novel substances, developed for the illicit drug market. All these formulations increase the likelihood of a fatal outcome due to significant risks of an inadvertent exposure. Drug trafficking organizations typically distribute fentanyl by the kilogram, and one kilogram of fentanyl has the potency to intoxicate and induce death of 500,000 people [70]. Deaths involving illicitly manufactured fentanyl and its derivatives are of special concern in the US, with nearly 74,000 drug overdose deaths in 2022 due to synthetic opioids other than methadone, including fentanyl, fentanyl derivatives, and tramadol [72]. The most potent fentanyl derivative on the drug market is carfentanil, with a lethal dose of only 20 µg, corresponding to a clinical potency 10,000 times greater than that of morphine and 100 times greater than fentanyl. [73,74]. In case of an opioid overdose, naloxone can be used as an antidote due to its property as a short-acting competitive opioid receptor antagonist [75].
A new generation of synthetic opioids emerged on the drug market in 2010, such as MT-45 (piperazine analogue), AH-7921 (benzamide analogue), isotonitazene, and U-47700 (structural isomer of AH-7921) [67].

4. Others

Benzodiazepines are the most widely prescribed class of medicines in the world and used in the therapy of neurological and psychiatric disorders such as panic attacks, anxiety, insomnia, epilepsy, muscle spasms, and alcohol withdrawal [61,76]. As these are typically subject to prescription, an increasing number of new benzodiazepines has entered the recreational drug market, including pharmaceutical drugs never approved for medical use or derivatives of registered drugs. These substances are commonly referred to as designer benzodiazepines within the NPS group, and their abuse has become of increasing concern. The first designer benzodiazepine identified on the illicit market in Europe was phenazepam in 2007, followed by the benzodiazepine analogue etizolam in 2011 [77]. Co-use of benzodiazepines with other central nervous system depressants, such as alcohol or opioids, increases the risk of poisonings [78,79], which might be even more amplified by the uncertain doses and largely unknown toxicology of designer benzodiazepines.

Arylcyclohexylamines include ketamine, phencyclidine (PCP) and methoxetamine, summarized in the class of dissociatives. Ketamine is widely used in human and veterinary medicine as an anesthetic agent, however its abuse is a long-lasting issue dating back to the 1980s [80]. Especially for the experience of 'k-hole' with near-death and out-of-body experiences [81], ketamine established itself among club drugs [82].

1.2.2 Synthetic cannabinoid receptor agonists (SCRAs): Evolution, properties, structural classification, modifications and pharmacology

Evolution of SCRAs

The first synthetic cannabinoids were derived from THC and similar phytocannabinoids. The design of these compounds was aimed to investigate the endocannabinoid system and its mechanism in order to develop novel therapeutics. The earliest compounds were bicyclic synthetic cannabinoids including HU-210 (dibenzopyran) and CP-47,497 (cyclohexylphenol), which both show greater affinity for CB_1 and CB_2 receptors when compared to THC [83-85]. HU-210 acts as a highly potent CB_1 and CB_2 agonist, with a potency of at least 100 times that of THC [86]. The development of additional classes of cannabimimetic compounds dissimilar to THC diversified the landscape of synthetic cannabinoids. Pravadoline (WIN-48,098) belonged to the chemical class of aminoalkylindoles and research revealed that pravadoline and many compounds of this class act as cannabinoid receptor agonists [87-90]. Moreover, many aminoalkylindoles are characterized as full agonists [91], meaning that they exhibit maximum efficacy at cannabinoid receptors as opposed to THC, which is a partial agonist that does not reach the same extent of receptors activation regardless of concentration. This fact suggests that synthetic cannabinoids of the aminoalkylindole class might result in effects beyond or entirely different to that of THC. The aminoalkylindoles were extensively developed in 1990s, when John W. Huffman at Clemson University discovered the most extensive SCRAs series (JWHs), that elicited potent cannabimimetic effects in animals [89]. In many of these early SCRAs, the prefixes of the substances denote the initials of the researchers who developed and studied these substance series. Other SCRAs developed were of the AM series [92] and indazole-carboxamide derivatives, such as AB-FUBINACA and ADB-FUBINACA which were both described by the pharmaceutical company *Pfizer* in a 2009 patent [93] claiming both compounds to be potent CB_1 agonists and potential therapeutic agents. Interestingly, the stereocenters of the isopropyl and *tert*-butyl linked groups of the last two compounds show activity exclusively for the (*S*)-enantiomers [93].

All this research led to the first generation of SCRAs encountered on the illicit drug market between 2008 and 2014, starting in 2008, when CP-47,497, CP-47,497-C8 homolog (cannabicyclohexanol), and JWH-018 were identified as psychoactive substances in herbal incenses in Germany and Japan [94,95], marketed under the brand names 'Spice' (Figure 3, top) and 'K2', described as 'air fresheners' or 'herbal smoking blends'. Hundreds of similar products (Figure 3, top) were found on the drug market within few years, mostly produced by mixing one or several dissolved powders of SCRAs and dried plant material, e.g. Damiana (*Turnera diffusa*) (Figure 3, bottom). Flavoured with artificial flavors and sealed in colorful packages (Figure 3), mostly containing 1 – 5 g, these products were typically sold via Internet shops. Alternatively, tobacco was also observed to be used instead of herbal material, especially in prisons. Other forms of SCRA products include powders ('research chemicals'), liquids for electronic cigarettes ('cannabinoid liquids'), and synthetic hashish imitations. All

these formulations can be consumed in the same way, as conventional cannabis or nicotine products. A very recent phenomenon, mainly encountered in prisons due to their inconspicuous appearance, is pieces of paper (i.e. letters, greeting cards, paper trips) infused with SCRAs (Figure 3, bottom).

Besides physical forms, the chemical variety of SCRA compounds also evolved. After legal restriction of CP-47,497 along with its dimethylhexyl, dimethyloctyl and dimethylnonyl homologues, and JWH-018 in many states, new structurally diverse indole SCRAs emerged on the drug market [96-99]. Besides precedent substances from the scientific literature and patents, an increasing number of SCRAs with clandestine origin have been found in forensic samples in the last years. SCRAs have become the largest group of NPS being monitored in the EU, with 245 substances that have appeared on the drug market up to 2022 since 2008, including 24 new compounds notified to the EU EWS in 2022 [60].
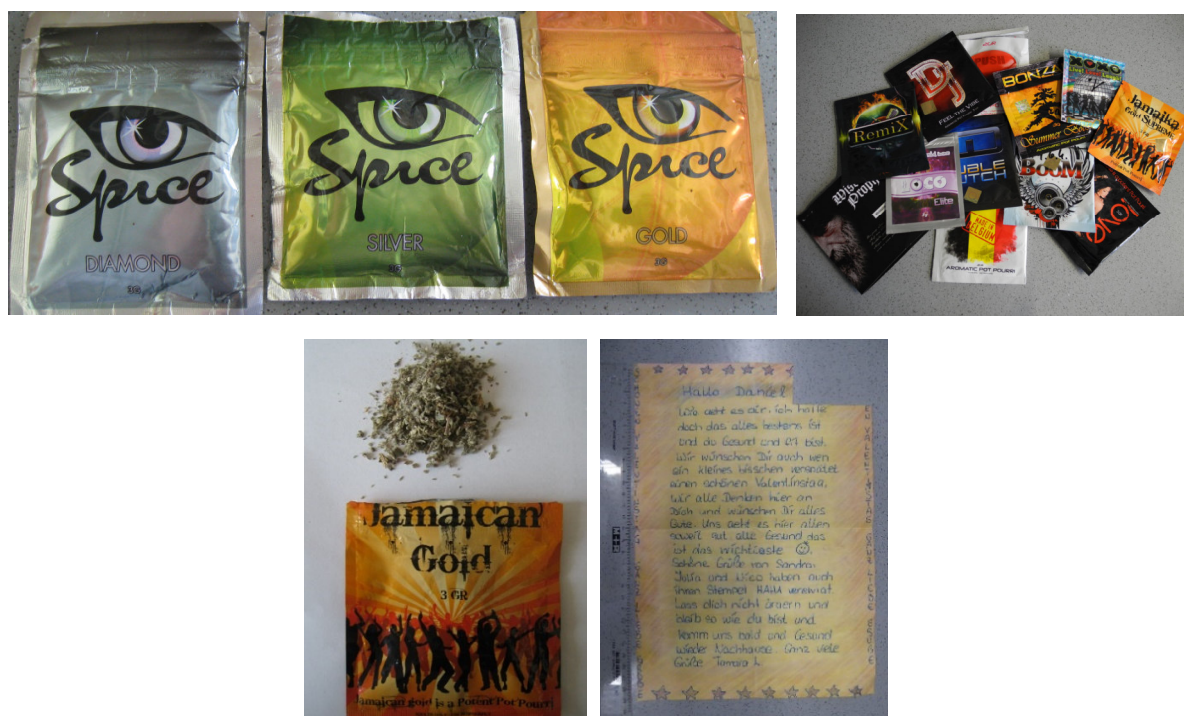
Figure 3. Initial SCRA products marketed under the brand name 'Spice' in colorful packages, followed by hundreds of similar products (top); A representative herbal mixture containing SCRAs deposited on a plant material, and a paper letter impregnated with SCRAs (bottom). Source: Forensic Science Institute, Bavarian State Criminal Police Office.

Physical and chemical properties

In their pure form, SCRAs appear as white or yellowish crystalline powders, sometimes featuring brownish discoloration or an unpleasant odor. Substances of this drug class are usually highly lipophilic and hence little soluble in water, with octanol-water partition coefficients ranging from log K_{ow} = 4.5 (MDMB-CHMINACA) to log K_{ow} = 7 (JWH-018) [100]. Good solubility can be achieved in aliphatic alcohols and other organic solvents such as methanol, ethanol, acetonitrile, ethyl acetate, acetone or isooctane [101]. However, dissolution in alcohols might lead to transesterification of quinolinyl carboxylates (PB-22, 5F-PB-22 and FUB-PB-22) [101]. Another important aspect regarding chemical stability of SCRAs is their thermal degradation. The quinolinyl ester SCRAs (e.g. 5F-PB-22) are thermally labile

and degrade to a certain extent [102], while others (e.g. UR-144 or FUB-144) undergo opening of a sterically constrained cyclopropyl ring upon heating [103,104]. This might occur during smoking and can be observed during GC-MS analysis. Interestingly, pyrolysis products might retain affinity to cannabinoid receptors and hence play a role in the pharmacological effect [105], similar as this is the case for some psychoactive metabolites. Thermal instability of esters and amides might even lead to potential misinterpretation of toxicological hair analysis results, if metabolites used as consumption markers resemble thermal degradation products. This was shown for thermally cleaved terminal ester and amide groups in 5F-PB-22 and AB-CHMINACA, respectively, during smoking [106]. Regarding SCRA toxicity, various SCRAs with carboxamide linker have found to yield a range of potentially toxic pyrolysis degradants (naphthalene, 1-naphthylamine, toluene and cyanide) at temperatures typically reached during smoking herbal material [107]. The temperature routinely reached during smoking of a cigarette or joint amounts to 700°C up to 900°C at some hot spots [108].

Structural classification

Although an enourmous variety of substances are known, the chemical structures are often related. Most clandestine producers induce only minor changes to the structure of an established SCRA, e.g. changing an indole to an indazole core structure or modification of the common tail structure element (*N*-pentyl group) by terminal fluorination. Hence, the large and diverse group of SCRAs can be classified into fourteen relevant subgroups. An overview of the different subgroups together with chemical structures of representative substances is given in Figure 4. The subgroups of indole and indazole carboxamides can be further divided in accordance to different linked groups, as depicted in Figure 5, with representative SCRAs shown. Some of the most frequently encountered and toxicologically relevant SCRAs, such as MDMB-4en-PINACA, 4F-MDMB-BICA, 4F-MDMB-BINACA, 5F-MDMB-PICA, 5F-MDMB-PINACA (5F-ADB), AMB-FUBINACA and MDMB-CHMICA, belong to the indole and indazole carboxamide subgroups.
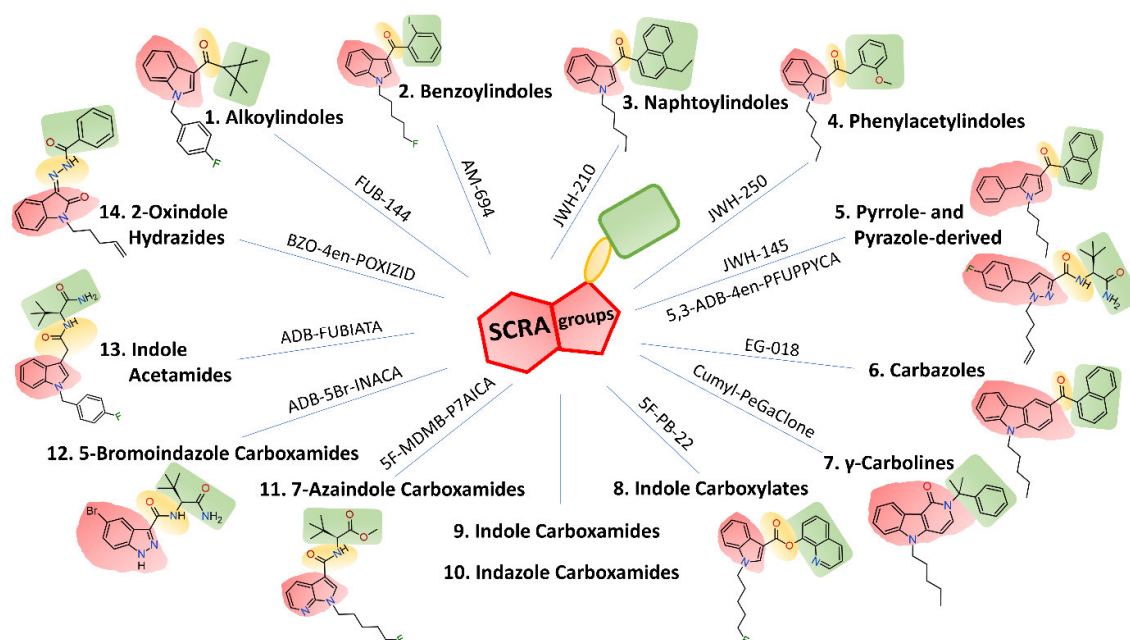
Figure 4. Fourteen relevant SCRA subgroups, together with chemical structures of representative substances. Source: Self-designed.
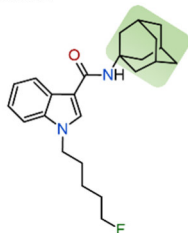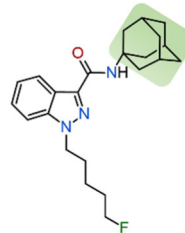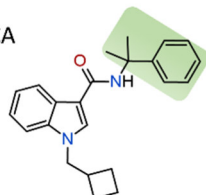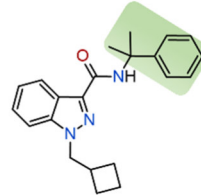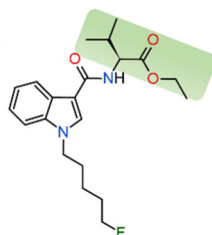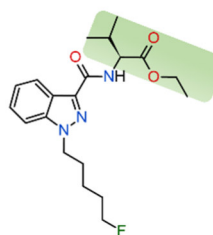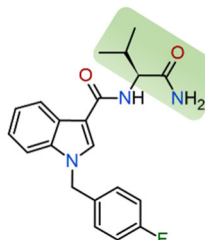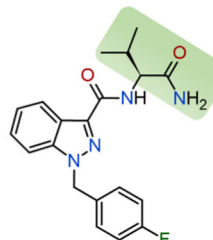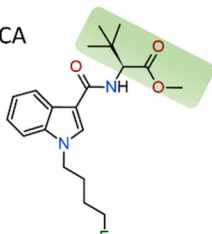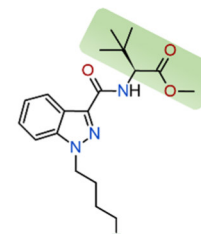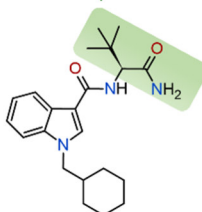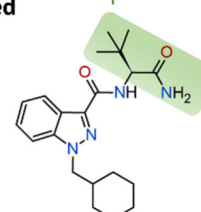
Figure 5. Subdivision of the indole and indazole carboxamides in accordance to the common variations of the linked group, with a representative SCRA for each linked group category. Source: Self-designed.

Nomenclature and common modifications of SCRAs

The non-harmonized alphanumeric codes used throughout the pharmaceutical industry and research groups to abbreviate the early synthetic cannabinoids, such as CP-47,497, JWH-018 or AM-2201, and the often non-systematic naming of SCRA vendors (i.e. AKB-48, likely named after a pop music group), ultimately lead to ambiguous names without the possibility to

deduce information on the chemical structure. Hence, EMCDDA introduced a semi-systematic nomenclature in 2013 based on the abbreviation of structural features through a selection of letter codes, which has recently been revised and expanded [109]. The naming convention considers division of a SCRA into four fundamental building blocks and the generic compound composition is shown in Figure 6, together with the most common chemical moieties for each building block abbreviated by letter codes. IUPAC names and structural moieties assigned to the particular letter code are given in Table A1 at the end of this chapter (Appendix). These illustrations depict the structural variations and the chemical diversity of SCRAs. Letter codes act as acronyms for the chemical name indicating structural features of each building block, joined via the basic syntax **"Linked group-TailCoreLinker"**. This naming convention is demonstrated below for few SCRAs resulting in semi-systematic names which were used throughout this work. It should be noted that the semi-systematic names in this work rely on the initial version of the EMCDDA nomenclature, however the majority of the formerly assigned SCRA names remained the same within the new EMCDDA naming framework.

<u>Cumyl-BC[2.2.1]HpMeGaClone</u>: **Cumyl**-**Bic**yclo[2.2.1]-**Hep**tyl**Me**thyl-**Ga**mma-**C**arbo**lin**one

<u>MDMB-4en-PINACA</u>: **M**ethyl 3,3,-**dim**ethyl**b**utanoate-1-(**P**ent-**4**-**en**-1-yl)-1*H*-**in**d**a**zole-3-**c**arbox**a**mide

<u>AB-FUBINACA</u>: 1-**A**mino-3-methyl-1-oxo**b**utane-1-(4-**F**l**u**oro**b**enzyl)-1*H*-**in**d**a**zole-3-**c**arbox**a**mide
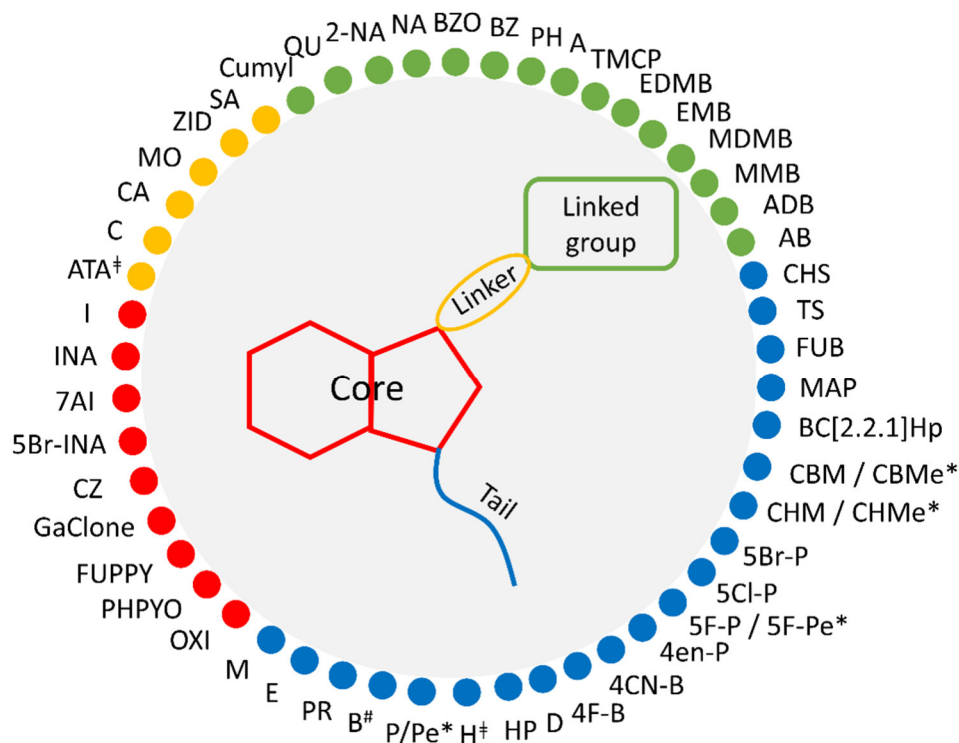
Figure 6. Generic composition of a SCRA with four fundamental building blocks (core, tail, linker, and linked group), together with the most common chemical moieties for each building block abbreviated by letter codes. *In combination with γ-carbolinones; ‡ ATA abbreviated in some sources as ACA; BUT used for butyl moiety in the case of ADB-BUTINACA; H abbreviated sometimes as HEX. Source: Self-designed.

The four main building blocks can be combined into different configurations and result in thousands of potential combinations. For example, MDMB-5F-PINACA (5F-MDMB-PINACA) is composed of an indazole core 'INA', a carboxamide linker 'CA', an *N*-fluoropentyl tail '5F-P', and methyl 3,3-dimethylbutanoate linked group 'MDMB'. The indazole core replaced with a 7-azaindole or an indole ring yields 5F-MDMB-P7AICA or 5F-MDMB-PICA, respectively. In total, 30 different linked groups, 27 tails, 14 cores, and 8 linkers were monitored across 224 SCRAs notified to the EU EWS between December 2008 and December 2021, considering SCRAs that structurally comply with the four-block model (core, linker, linked group, and tail) [110]. The most frequent structural elements of the four building blocks and their modifications over the time in the EU are summarized by Andrews et al. [110].

SCRA pharmacokinetics

a) Absorption and distribution

The most common consumption route for SCRAs is smoking of plant material, soaked or laced with one or multiple SCRA compounds. Alternative administration route involves inhalation using a vaporizer or e-liquids vaporized in electronic cigarettes. These administration routes lead to a rapid absorption via pulmonary alveoli and maximum blood concentrations (C_{max}) within few minutes [111]. After oral administration, C_{max} can be expected between 30 minutes and several hours post-dose [112]. As for cannabis, oral intake results in a reduced bioavailability of SCRAs due to the first-pass effect in the liver, so that an increased dose is required to achieve the desired effects when compared to the inhaling route.
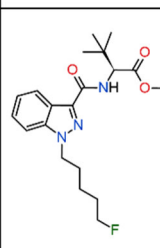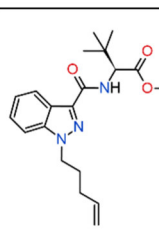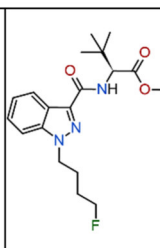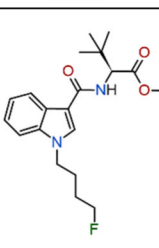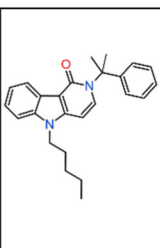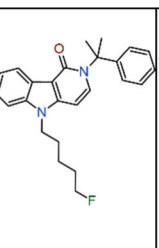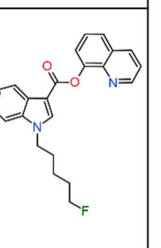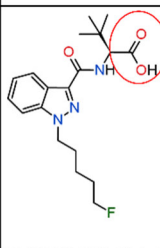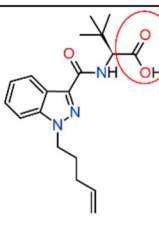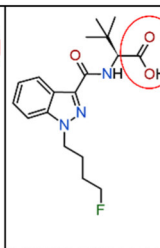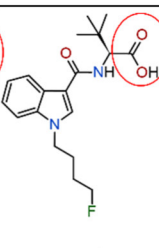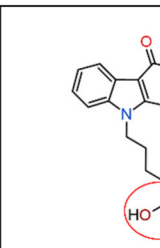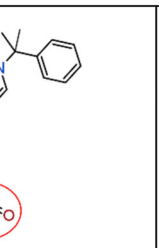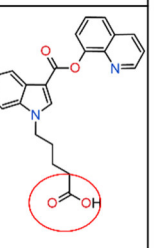
Being among the first SCRAs on the recreational drug market, the JWH-series were studied particularly well. The toxicological detection of several SCRAs, mainly of the JWH series, has been reported in oral fluid, serum, and urine after controlled administration via inhalation. For JWH-018, systematic studies for all the three biological fluids were reported by Toennes et al. [113-115] recently. The authors concluded that the pharmacokinetic properties of inhaled JWH-018 are similar to that of THC. Remarkable was the detection of the predominant metabolite, JWH-018 *N*-pentanoic acid, in urine over several weeks after single dosing (2-3 mg JWH-018) [114]. In blood, the detection window of JWH-018 was limited to early periods directly after consumption, however a slow terminal elimination of the drug and metabolites may lead to accumulation in chronic users [115]. Like THC, the deposition of lipophilic SCRAs in adipose tissue appears to be common as well. JWH-122 and JWH-210 were detected in the rodent adipose tissue four weeks after a single dose [116]. Extremely high levels in human adipose tissue were observed for MAM-2201 (124-fold higher than blood concentration) at a post-mortem interval of 4 days [117].

b) Metabolism and elimination

Due to their high lipophilicity, SCRAs are usually extensively metabolized prior to renal excretion. Hence, urinary metabolites often play an important role for SCRAs detection in biological fluids. SCRAs are metabolized on different routes according to their chemical structures and this aspect will be illustrated with few examples. Wohlfarth et al. [118] demonstrated that the predominant metabolic pathway for 5F-PB-22, the first marketed SCRA with an ester linkage, among with its non-fluorinated analog, was ester hydrolysis. In total, 22

phase I and II 5F-PB-22 metabolites were detected after incubation with human hepatocytes, deriving from ester hydrolysis, hydroxylation and dihydroxylation, oxidative defluorination, carboxylation, epoxide hydrolysis, conjugation with glucuronic acid or cysteine, or a combination of these reactions. Besides the ester hydrolysis product, PB-22 *N*-pentanoic acid was the most abundant metabolite detected. The *tert*-leucinate methyl ester (MDMB-type) indole-3-carboxamide MDMB-PICA, yielded 12 phase I metabolites that originated from 9 different biotransformation reactions (mono-hydroxylation, hydrolytic defluorination, dehydrogenation, amide, and ester hydrolysis, and combinations of these reactions) in an *in vitro* assay using pooled human liver microsomes (pHLM) [119]. Following hepatocyte incubations, another study [120] identified 22 metabolites and methyl ester hydrolysis product was the most abundant metabolite in both studies [119,120]. A total of 32 metabolites were detected for a related SCRA, MDMB-4en-PINACA, with ester hydrolysis and/or dihydrodiol formation at the terminal alkene group with further hydroxylation and/or dehydrogenation being the most frequent metabolic pathways [121]. The analysis of authentic urine samples suggested the ester hydrolysis product and ester hydrolysis product combined with the terminal alkene oxidation as two suitable urinary markers [121,122], but confirmed the presence of the parent compound in urine as well [121-123]. For example, 10 out of 22 authentic urine samples screened positive for MDMB-4en-PINACA in its unchanged form [122]. The most pronounced metabolic phase I pathways for SCRAs with terminal amide functionality rather comprise mono- and di-hydroxylations than hydrolysis of the terminal amide [124]. Similarly, the main *in vivo* phase I metabolite of the γ-carbolinone derived SCRA Cumyl-PeGaClone was the mono-hydroxylated compound at the γ-carbolinone core [125]. In contrast, its fluorinated analog 5F-Cumyl-PeGaClone mainly underwent gradual 5-fluoropentyl chain degradation over pentanoic acid to the propionic acid metabolite, which were the two most abundant metabolites in all urine samples [126]. In accordance with the phase I / phase II biotransformation studies, the most common metabolites, all of them terminal carboxylic acid derivatives, formed by hydrolysis or oxidation reactions, were chosen for selected SCRAs in this work, as depicted in Table 2.

Table 2. Selected SCRAs and their metabolites, as used in this work.

29

Glucuronidation is the most common phase II metabolic pathway for SCRAs, as observed in several studies [118,124,127-132]. Hence, cleavage of glucuronic acid conjugates is recommended for analysis of human urine samples in routine practice. In sewage, the hydrolysis/deconjugation to the parent metabolite can be assumed to occur analogous to the glucuronide conjugate of the cannabis metabolite THC-COOH with β-glucuronidases of fecal bacteria [133]. Hence, glucuronide conjugates of SCRAs can be neglected in wastewater analysis.

Pharmacodynamics

<u>Mechanism of action</u>

SCRAs used as recreational drugs typically feature increased affinity for and efficacy at cannabinoid CB_1 receptors [134], which play an important role in the mediation of psychoactive effects [35,36,134]. In contrast, SCRAs with a higher affinity to the CB_2 receptors rather cause anti-inflammatory and analgesic effects than psychoactive effects [36], making them non suitable as drugs of abuse.

Many SCRAs are designated as full agonists at CB_1, and sometimes CB_2 receptors, and can therefore produce more pronounced effects than those experienced with cannabis. SCRAs are typically fast-acting and reach maximum blood concentrations in less than few minutes during smoking [111]. A rapid onset of effects was reported by users on Internet forums, e.g. after consumption of MDMB-CHMICA the desired effects were noted 0.5-5 min after smoking and ended after approximately 2-4 h, while negative effects persisted for up to 15 h (cf. Adamowicz [135]). Functional activities of several SCRAs in comparison to THC and CP-55,490 are exemplarily given in Table 3 [136], with half maximal effective concentrations (EC_{50}, indicative of potency) and efficacies relative to the full agonist CP-55,940 (E_{max}). For example, 5F-MDMB-PINACA (5F-ADB) acts as a highly potent agonist at both CB_1 and CB_2 receptors, with 290 times greater potency in comparison to THC and 17 times higher potency than MDMB-CHMICA [136] (cf. Table 3). This was reflected in high prevalence of 5F-ADB among SCRA-related fatalities in different countries [137,138] and description as one of the most dangerous SCRAs on the drug market [139]. Its indole counterpart, 5F-MDMB-PICA is a similarly potent SCRA (cf. Table 3), linked to serious intoxications and deaths [140,141]. Other SCRAs as Cumyl-PeGaClone exert rather lower toxicity [142]. In general, structure modifications have shown to affect the pharmacological activity of a compound. For example, indazole cores increased the potency of some compounds by stabilization of cannabinoid receptor interactions with specific G-proteins [143-145]. Different linked moieties also impacted the potency, which seemed to drive the prevalence of certain compounds: SCRAs with L-*tert*-leucinamide (ADB) linked groups are more frequent in Europe than their counterparts with L-valinamide (AB) and L-phenylalaninamide (APP) groups, probably relying on a higher binding affinity of ADB-linked groups to cannabinoid receptors (ADB > AB > APP) [145]. Halogenation of alkyl tail elements with fluorine as a common strategy of drug producers to circumvent the law appeared to have beneficial pharmacological properties (higher potency) as well [92,146].

Table 3. Functional activity of THC (Δ^9-THC), CP-55,490, and several selected SCRAs. Half maximal effective concentrations (EC_{50}, indicative of potency) and efficacies of different SCRAs relative to the full agonist CP-55,940 (E_{max}), assessed in a fluorometric assay of membrane potential [136]. The ratio EC_{50} (CB_2)/EC_{50}(CB_1) denotes the CB_1 selectivity of the drug, with a high ratio indicating preference for the CB_1 receptor.

Substance	EC_{50} [nM] (CB_1)	E_{max} (CB_1) (% CP-55,940)	EC_{50} [nM] (CB_2)	E_{max} (CB_2) (% CP-55,940)	EC_{50} (CB_2) / EC_{50} (CB_1)
Δ^9-THC	171	50%	Inactive	20% (10 μM)	NA
CP-55,490	42	100%	68	100%	1.6
5F-MDMB-PICA	0.45	110%	7.4	94%	16.4
5F-MDMB-PINACA	0.59	108%	7.5	94%	12.7
MDMB-CHMICA	10	112%	71	103%	7.1
AMB-FUBINACA	2.0	103%	18	92%	9.0

Similar to 11-OH-THC, some mono-hydroxylated SCRA metabolites retain the pharmacological activity at the CB_1 receptor and contribute to the pharmacological profile, for example JWH-018 and JWH-073 [147,148]. However, the carboxylic acids formed as main metabolites of many SCRA compounds can be assumed to be inactive at the CB_1 receptor. This was experimentally confirmed by the ester hydrolysis product of (*S*)-MDMB-4en-PINACA (MDMB-4en-PINACA 3,3-dimethylbutanoic acid), which showed 233-fold lower potency regarding CB_1 receptor activation in comparison to the parent compound [123]. In general, stereochemistry plays an essential role for the drug potency of SCRAs, as evidenced by a 206-fold reduction in potency observed for (*R*)-MDMB-4en-PINACA relative to (*S*)-MDMB-4en-PINACA [149]. Due to the high potency and health risk of SCRAs arising from case reports, (*S*)-enantiomers of many different SCRAs are assumed to be dominant on the illicit drug market.

Pharmacological effects

Many highly potent SCRAs such as 5F-MDMB-PINACA (5F-ADB), MDMB-4en-PINACA, 4F-MDMB-BICA, ADB-BUTINACA or MDMB-CHMICA are assumed to be active at doses less than 1 mg [150-154], producing cannabis-like effects. According to user experiences summarized by Adamowicz [135] for MDMB-CHMICA, starting doses reported were as low as 0.05 mg and typical recreational doses ranged between 0.1 and 0.3 mg. Analysis of some SCRA products revealed that one gram of herbal material might contain more than 100 mg of an active compound [151], thus leading to a great number of effective doses. Typical doses of less potent compounds are higher, for example 2-4 mg for JWH-018 [111,155]. As 100 – 300 mg herbal material are considered a regular dose by many users [156], many of the intoxications reported can be attributed to unintentional overdosing. For comparison, typical cannabis doses amount to 10 – 15 mg THC.

When consuming herbal smoking mixtures, users typically don't know the purity, amount and/or composition of SCRA products consumed. For example, two packages of the same brand were often found to contain entirely different active ingredients [156]. Many of the products were found to be inhomogeneous regarding the content of active compounds, with both high intra- as well as inter-package variability [157], often caused by the existence of particles of the pure SCRAs, so called 'hot-spots' [157-159]. The results suggested that two cigarettes (joints) of herbal mixture prepared from the same package could significantly differ

in the amount of the active substance [157]. Similar was also observed on papers (blotters, letters and cards) impregnated with SCRAs [160]. In combination with the high potency of SCRAs, all these effects contribute to an elevated risk of unintentional and serious poisoning, especially because smoking or vaping as the most common administration route leads to a rapid absorption of SCRAs into the blood to reach central nervous system. Reports from hospitalized users and people witnessing SCRA poisonings indicated that only a small number of cigarette puffs might be sufficient for a toxic dose and lead to severe and fatal acute poisoning [151]. Several outbreaks of mass poisonings ranging from 4 or 5 to over 800 victims were caused by SCRAs smoking mixtures [151,161-163].

The severe toxicity of SCRAs has been evidenced by case reports in literature for numerous SCRAs, including some relevant compounds in this work, such as JWH-210 [164], 5F-ADB [165,166], 5F-MDMB-PICA [140,167], MDMB-4en-PINACA [123,168,169], 4F-MDMB-BINACA [167,170], 4F-MDMB-BICA [171] and ADB-BUTINACA [124,172]. Common health harms include increased heart rate, agitation, delirium, nausea and vomiting as well as more severe adverse clinical effects, such as cardiac complications (e.g. myocardial infarction), stroke, psychosis, seizures and kidney injuries [173-176]. Seizures are a common and severe adverse effect linked to SCRA consumption [174], but rarely reported with cannabis use. Furthermore, the considerably greater potency of SCRAs often leads to more pronounced neuropsychiatric effects in comparison to THC [174]. Psychosis appears to be a frequent condition resulting from SCRA abuse, however, similar to seizures, has been rarely reported with cannabis use [177].

Among others, demand for medical care due to SCRA intoxications is frequently encountered in prison settings [173]. A short report from an UK prisoner provides the best impression of negative SCRA effects [178]:

"I've seen someone do a Spice bong, come running out their cells, running as fast as they can along the landing and running into the bars. Knocked himself clean out. And then he got back up, he ran down the other side and done it again."

1.2.3 Legislation

The German Narcotics Act (Betäubungsmittelgesetz, BtMG) is a law to control possession and handling of certain drugs, defined by a list of named substances. The Act sets out three different categories (Annex I – III), and the placement of a substance into one of the categories is based upon the substance's commercial or therapeutic relevance, defined as follows:

- Annex I controlled substances are non-tradable and underly strictest controls (e.g. lysergic acid diethylamide, LSD), with exception of an authorized scientific use or for other purposes of public interest
- Annex II controlled substances are tradable with an authorized permission, however not prescribable as a medicine (e.g. aminorex)
- Annex III controlled substances can be both traded and prescribed in accordance to the prescription regulations for narcotics (e.g. morphine)

Following the identification of the first SCRAs in herbal blends, CP-47,497 with its homologs and JWH-018 were placed into Annex II of the BtMG. Further amendments of the Narcotics Act successively scheduled new SCRAs under the BtMG, with a total of 70 SCRAs being controlled to date [179-195]. A detailed list of the amendments and SCRAs included is given in Table A2 as appendix to this section. However, only a portion of SCRAs circulating on the drug market is covered by the BtMG. On average, 1-3 new SCRAs have been placed on the European drug market every month since 2011 according to the reports of the EU EWS [100]. Although the trend of an average of 2-3 substances emerging monthly between 2011 and 2015 has dropped to max. 1 substance per month since 2016, diversity and dynamics of the market remain significant with a tremendous chemical variety and extent of possible SCRA compounds. Several thousand potential cannabimimetics have already been published - the patents of the pharmaceutical company *Pfizer* from 2009 alone describe around 1,300 cannabimimetics, all of which belong to one of many structural groups of synthetic cannabinoids [93,196]. These dimensions exceed the legal framework of the BtMG for many reasons. The inclusion of a new substance into the BtMG requires proof of an increased prevalence and risk of the substance for public health, implying that a certain time period must elapse, before these data can be collected. Based on these data, the scheduling of new substances must then be advised by the expert committee of the Federal Institute for Drugs and Medical Devices (Bundesinstitut für Arzneimittel und Medizinprodukte, BfArM) during two annual meetings. Upon recommendation of the expert committee, the government can start a legislative process to change the current law. Balancing the long time period of this legislation process against the commercial lifetime of SCRAs on the drug market often as low as one year shows that the BtMG always lags behind and it has become difficult to regulate SCRAs in a timely manner. In addition, the drug market has shown very rapid adaptions to the control measures by the introduction of small chemical changes to regulated SCRAs, which led to new substances not covered by the law. Until 2014, trading with NPS not yet listed in the BtMG was prosecuted for violation of the German Medicinal Products Act (Arzneimittelgesetz), however a decision of the European Court of Justice in July 2014 annuled this practice. In order to close this legal loophole and end the race between the ever-changing variations of regulated substances and the continuous need to adapt the Narcotics Act, the NPS Act (German: Neue-psychoaktive-Stoffe-Gesetz, NpSG) came into force on November 26, 2016.

NPS Act

In contrast to the enumerative approach of the BtMG, the NPS Act (NpSG) follows a generic approach, containing substance group regulations to complement the BtMG. At the moment, the following substance groups are covered: compounds derived from 2-phenethylamine, cannabimimetics/synthetic cannabinoids, benzodiazepines, *N*-(2-aminocyclohexyl)amide derived compounds, tryptamine derived compounds, arylcyclohexylamine derived compounds, and benzimidazole derived compounds [197]. The substance group definitions contain chemical structures in the annex of the Act, where individual structural elements and their substitutions are clearly defined, similar to many patent specifications. The structural definitions have been adjusted over time in order to keep pace with the ever-changing market, while single substances with a high extent of abuse and particularly hazardous to health continue to be placed under the BtMG. In these cases, the stricter regulations of the BtMG

take precedence over those of the NpSG. The NpSG ban covers trafficking, placing on the market, manufacturing, import, export and transit through the territory to which the Act applies, acquisition, possession, and the administration of NPS to others. As these group definitions can be expected to include substances without psychoactive effects and hence little potential of abuse, acquisition and possession of NPS are prohibited, but not sanctioned, which is the main difference to stricter BtMG regulations. As for the BtMG, the penalties for NpSG violations depend on the amount – more precise: the number of single doses for consumption - of the individual substances. However, penalty frameworks are generally lower for the NpSG in comparison to the BtMG. Possession for commercial, industrial or scientific use, i.e. in an analytical laboratory, is excluded from the regulations of the NpSG.

Similar legislative controls on NPS were introduced in other countries as well. In the United Kingdom (UK), the national Narcotics Law (Misuse of Drugs Act 1971, MDA) classifies controlled substances based on their harms into three classes, A, B, or C, with Class A drugs being most harmful and attracting the highest penalties [198]. SCRAs are classified as Class B drugs in form of structural analog controls. A blanket ban on substances with psychoactive effects, with few exceptions like alcohol, tobacco and similar, was enacted in the UK in May 2016 (Psychoactive Substances Act 2016) and covered any new SCRAs behind the analog controls [199]. Similarly, the NPS definition in the Austrian NPS legislation (Neue-Psychoaktive-Substanzen-Gesetz and Neue-Psychoaktive-Substanzen-Verordnung), enacted in 2012, demands a psychoactive effect for the inclusion of a substance into NpSG [200].

Regulation of SCRAs in the NpSG

The generic definitions for SCRAS in the NpSG include two subgroups: indole-, pyrazole- and 4-quinolone-derived compounds, and compounds derived from 3-sulfonylamido benzoic acid. The vast majority of SCRAs belong to the first group and show a modular composition with four building blocks (core, tail, linked group and linker), as described in more detail in section 1.2.2. Using the structural example of 1-fluoro-JWH-018 (Figure 7), the law defines chemical groups and moieties for each of the four building blocks, as well as possible substitutions of the core structures. For example, core elements covered so far are illustrated in Figure 8.
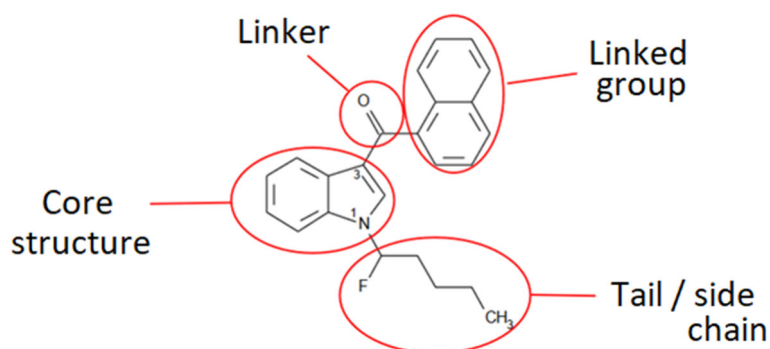
Figure 7. Generic definition of SCRA compounds by the NpSG using a structural example of 1-fluoro-JWH-018. Chemical elements constituting of core, linker, linked group and tail/side chain are defined by the law with their possible substituted residues.
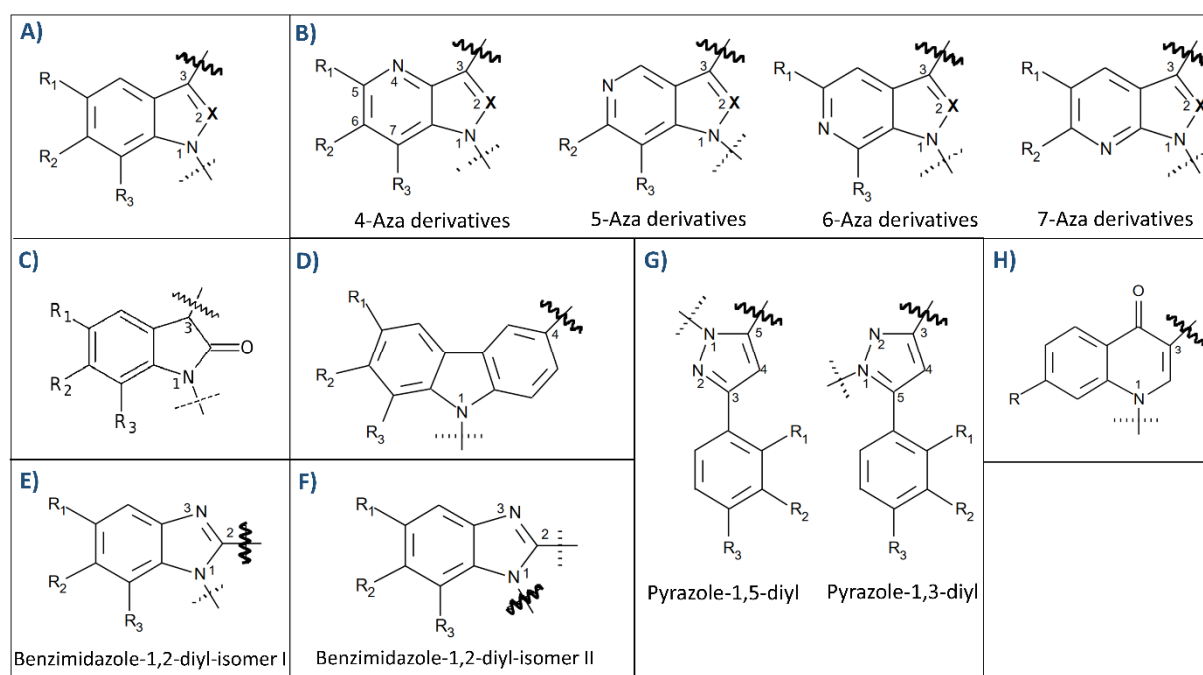
Figure 8. Compiled depiction of SCRA cores covered so far by the NpSG, according to their definitions in the annex of the Act [197]. The wavy line indicates the binding site for the linker and the broken line indicates the binding site for the tail.

1.3 Hair analysis

Finding arsenic in hair of the Emperor Napoleon Bonaparte [201] or cocaine in the hair of Peruvian mummies [202] centuries after their deaths are some famous examples of the toxicological hair analysis. The first case of poison identification in human hair was arsenic determined in the hair of a body exhumed after 11 years, published by Hoppe in "Practical Guide to Legal Medicine" in 1858 [203]. Nearly 100 years later, in 1954, the first analysis of organic compounds in hair was carried out by Goldblum [204], when he determined barbiturates in the hair of a guinea pig. The breakthrough for a modern use of hair analysis as a detection tool for drugs of abuse was achieved by Baumgartner in 1979 [205], who extracted hair of opiate addicts using methanol and detected the presence of opiates via radioimmunoassay screening. In 1980, Klug [206] confirmed radioimmunological results by a chromatographic method and quantified morphine in scalp hair using fluorescence detection following thin-layer chromatography. In the following years, other chromatographic methods and optimized preparation procedures were implemented for hair analysis and the attention to hair analysis has amplified substantially with the advancing detection techniques. State of the art methodology includes chromatographic methods coupled with mass spectrometry (MS) detectors, often as tandem MS, time-of-flight MS (TOF-MS) or ion trap MS (IT-MS). The sensitive detection methods enable proof of consumption even after a single dose [207] or by analyzing a single hair [208]. Cut-off values for quantification, together with recommendations on sample collection, storage, preparation, and analysis methods, are recommended by the Society of Hair Testing (SoHT), a worldwide network of members established in 1995 [209]. In order to understand basic principles of hair analysis, the following sections will elucidate the morphology and chemical composition of hair, hair growth cycle and growth rate, and mechanisms of drug incorporation into hair. Details regarding hair analysis of cannabinoids relevant for this work, i.e. cannabis (THC-COOH) and synthetic cannabinoids, are given in Chapter 2 and Chapter 5, respectively, with focus on hair sample preparation procedures and analytical detection methods.

1.3.1 Morphology and chemical composition of hair

Morphology

Hair is a protein filament that is synthesized in the hair follicle that is placed 3-5 mm below the skin surface, where the rich capillary system supplies the growing hair fiber with metabolic nutrients. There are about 5 million hair follicles in human skin, of which around 100,000 are prominently displayed as scalp hair [210]. Each hair follicle consists of three main structures: the outer rooth sheath (ORS), the inner rooth sheath (IRS), and the follicle bulb [207]. The ORS is a part of the epidermis and encloses the other layers. In the region near the sebum gland, the ORS is assumed to be the origin of stem cells for follicle development and pigmentation [211] The IRS encases and directs the growing fiber upward [207]. At the base of the hair follicle is the hair bulb papilla which is connected to the capillary system responsible for hair growth. The matrix cells around the papilla include keratinocytes and melanocytes present on the basement membrane and the formation of a mature hair fiber from the matrix cells is described in the following according to Pragst and Balikova [212], cf. Figure 9A. The extensive mitotic activity of the matrix cells gives rise to their migration in the next upper zones, where the pigment incorporation and keratinization, i.e. gene experession for keratine formation,

takes place. Cortex cells change to a spindle-like form and protein filaments are synthesized in the cell. Cuticle cells are drawn from the outer sphere of the papilla and change to a shingle-like form containing amorphous protein. In the course of hardening, disulfide bonding, resorption and dehydration in the next zone, the cells dissociate and cytoplasmic organelles disappear. The remaining protein-containing cellular residues fuse together and these keratinized cells are coupled by the cell membrane complex (CMC). The CMC consists of proteins and a protein-lipid complex of the remaining cell membranes from previously dissociated cells. In the course of keratinization, the inner rooth sheath degrades and a mature hair fiber is formed (Figure 9A). Near hair follicle are sebaceous glands which produce the oily substance sebum and lubricate the hair shaft before reaching the skin surface [213]. The eccrine sweat glands are in the surrounding area of the follicle, however do not secrete directly into follicle but exit on the surface of the skin [213].
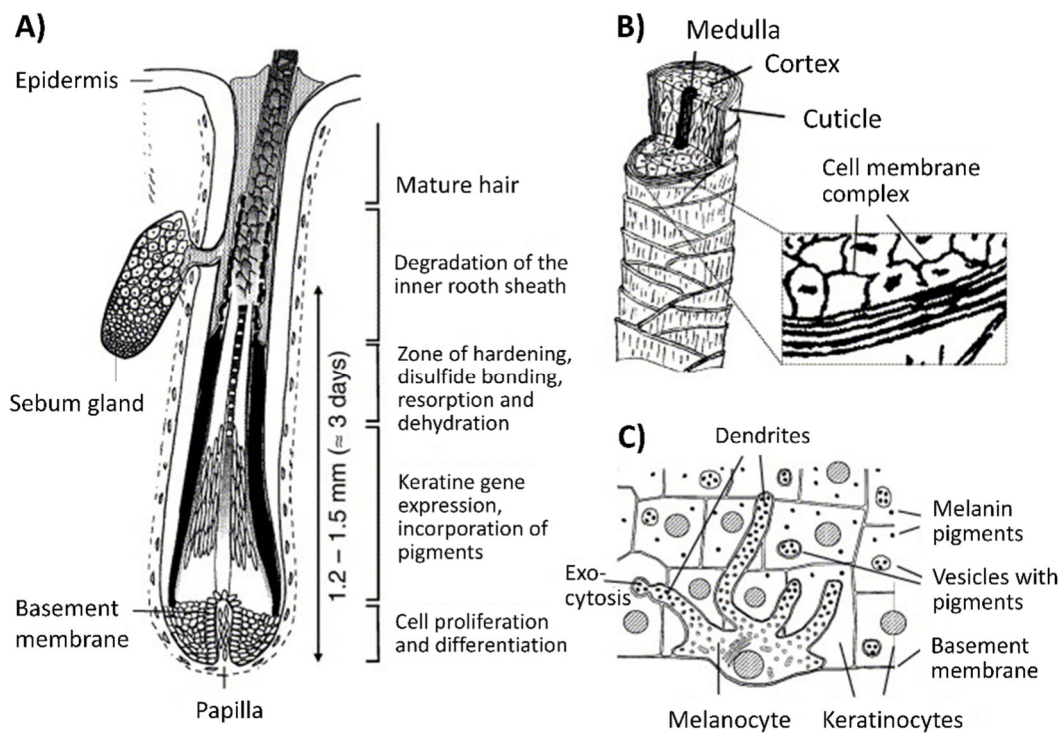
Figure 9. Structure of a hair follicle and depiction of the hair formation process (A); Morphological structure of a mature hair fiber (B); Melanin production by melanocytes in the basal layer of the cortex, followed by discharge of melanin pigments in the neighbouring keratinocytes by exocytosis. After phagocytosis, the pigment remains embedded in the keratonocytes (C). Slightly adapted (minor reformatting) and reprinted with permission from [212]. Copyright (2006) Elsevier.

Hair fiber does not have a homogeneous structure, but consists of three concentric structures, cuticle, cortex and medulla (Figure 9B). Cuticle cells are overlapping scale cells of approximately 0.35-0.45 µm thickness, 28-38 µm width and 40-48 µm length [214]. The 5-10 layers of cuticle cells form a cuticle layer which has protective function against physical and chemical influences [212] (Figure 10). Cortex is composed of spindle-shaped cortical cells of approximately 3-5 µm thickness and 60-110 µm length [214], that compose the bulk of the hair shaft. The cortical cells are mainly constituted of macrofibrils (90%), nuclear remnants and pigment granules (10%) [215]. One macrofibril (0.1 to 0.4 µm in width or diameter) is

further composed of a few hundred filament proteins densely packed in a less-ordered matrix. (215,216) The pigment granules (0.2 to 0.8 µm in diameter) are dispersed over cortical cells and do not occur in the cuticle of scalp hair [216]. The CMC is placed both between cuticula and cortex cells fixing them together and forms the major pathway for diffusion and elimination of drugs [212]. Medulla is composed of loosely packed porous channels located near the center of the fiber, and is often contained in thicker hair only [216].

Hair pigment is produced within melanosomes, cytoplasmic organelles of melanocytes located on the basement membrane of the follicle in the hair bulb (Figure 9C). The pigment formation occurs exclusively within hair follicle (follicular melanogenesis) and involves enzymes, receptors, transporters, and structural and regulatory proteins during the anagen phase of hair growth cycle [207]. Melanocytes penetrate with their long dendrites the neighbouring keratinocytes and discharge melanosomes within vesicles by exocytosis. After phagocytosis, the pigment accumulates in the keratonocytes and forms the pigmented hair shaft (Figure 9C). The melanin pigment is mainly transferred to the cortical keratinocytes, in lesser content to the medulla, and only rarely to the cuticle [207].
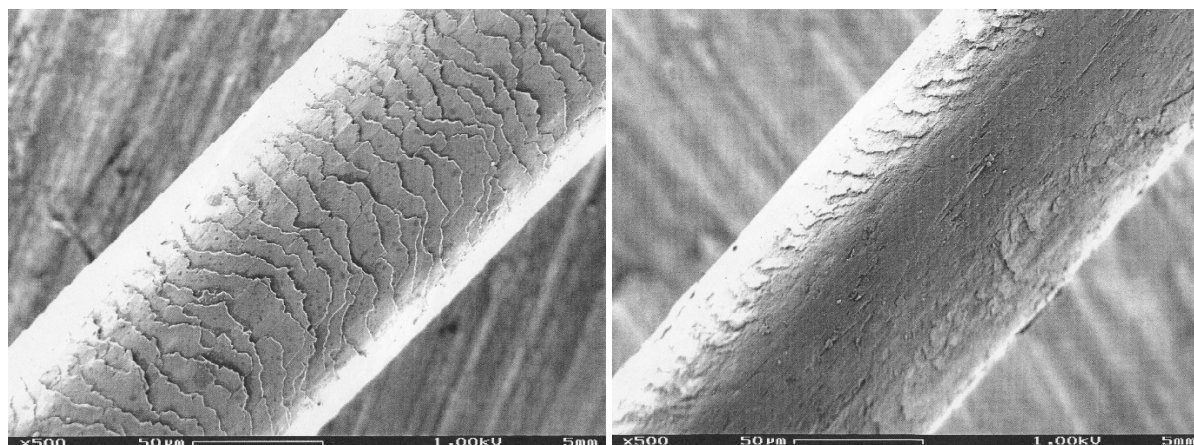
Figure 10. Scanning electron microscopy image of human hair (500-fold magnification) with intact (left) and damaged, more specifically missing, cuticle (right). Source: Forensic Science Institute, Bavarian State Criminal Police Office.

Chemical composition

Hair fibers are mainly composed of 65-95% proteins, 1-9% lipids, 0.1-5% melanin, and remaining constituents comprise small amounts of trace elements, polysaccharides, and water [217]. Interestingly, the hair fiber can absorb up to 30% water by radial swelling [212]. Hair color differences depend on the type and quantity of melanin pigment. Four types of melanin presumably play a role: eumelanin, pheomelanin, together with their oxidation products, oxyeumelanin and oxypheomelanin [218]. Brown to black eumelanin contributes to darker colors, whereas the pheomelanin results in red pigmentation. Increasing amounts of oxidative products contribute to lighter shades in both cases, e.g. large amounts of oxyeumelanin lead to blond hair [213]. While the eumelanins are heterogeneous polymers with 5,6-dihydroxyindole (DHI) and 5,6-dihydroxyindole-2-carboxylic acid (DHICA) structural elements, pheomelanins contain benzothiazine, benzothiazole, and isoquinoline units [207].

1.3.2 Hair growth cycle and growth rate

Hair growth cycle can be divided in three stages: anagen (growing stage), catagen (transition stage) and telogen (resting stage). The processes in the growing stage have been described in the previous section (cf. Figure 9A). The cells in the follicle bulb undergo mitosis every 23 to 72 hours, inducing hair shaft growth, and thus exceed in velocity every other cell type in the body [219]. During the catagen stage, the follicle bulb undergoes apoptosis-driven regression, reduces its size and migrates upwards in the skin. A specialized structure, the club hair, is formed and the follicle approaches the telogen stage. The combined catagen and telogen stage lasts 2-6 months for scalp hair [212]. Afterwards, another growth cycle commences. It is estimated that at any given time 85% of scalp hair is in the growing phase and the remaining 15% in the resting phase [212].

Different anatomical sites exhibit different growth rates, different duration of anagen stage, and varying percentage of non-growing hair (Table 4). These factors determine the maximum hair length at various anatomical sites.

Table 4. Growth rate, duration of growing stage, and portion of catagen and telogen human hair from different anatomical sites [212].

Anatomical site	Growth rate [mm/day]	Duration of anagen stage	Catagen + telogen hair [%]
Scalp	0.32 - 0.46	2 – 6 y	6-18
Beard	0.25 - 0.29	14 – 22 m	40
Axillary	0.29 – 0.33	44 – 72 w	50
Pubis	0.30	47 – 77 w	50

Scalp hair is preferred for toxicological analyses, with posterior vertex region of the head as the recommended sampling site due to the minimum variation in growth rate. The SoHT recommends use of an average growth rate of 1 cm/month for scalp hair [220] and general recommendation of the United Nations Office on Drugs and Crime (UNODC) [221] for segmental analysis is division of hair sample into 1 - 3 cm segment lengths to obtain a retrospective toxicological calendar of the subject. When alternative anatomical sites are sampled (beard, pubic or axillary hair), the different growth cycles and proportion of catagen/telogen hair must be taken into account for proper interpretation of the analytical results, e.g. catagen/telogen hair from a previous consumption period can result in positive findings despite drug abstinence.

1.3.3 Mechanisms of drug incorporation into hair

The understanding of mechanisms and factors influencing drug incorporation into growing hair is essential for correct interpretation of the results obtained by hair analysis. The generally proposed mechanism for drug incorporation into hair includes passive diffusion of drugs from the bloodstream into the growing hair cells of the follicle. During the following keratogenesis the drugs become trapped in the stable hair protein structure. It is assumed that the process of passive diffusion from blood occurs over a length of 1.2 – 1.5 mm between the hair follicle base and the keratinization zone, which corresponds to a drug exposure period of about three days [212] (cf. Figure 9A). Drug concentration in hair depends on its concentration in blood, which again correlates with the consumed dose. Due to a constant hair growth rate, the position of drugs incorporated along the hair shaft can depict a toxicological chronology of

drug exposures. This assumption provides the fundamental basis for segmental hair analysis which uses successive hair segments to correlate drug use with a specific time period. However, experimental findings indicated that various other mechanisms play a role, as demonstrated by a multi-compartment model of Henderson [222]. Albeit with some time delay, intradermal transfer of drugs from deep skin compartments might be another possible incorporation route during hair shaft formation, especially for lipophilic drugs such as tetrahydrocannabinol (THC) trapped in the skin [223]. However, the most important alternative route to the passive diffusion from blood is diffusion from sweat or sebum secretions into the formed hair shaft. Several drugs of abuse have been evidenced in sweat, e.g. amphetamine [224], cocaine [225], phencyclidine [226] and methadone [227], supporting the contribution of this route to drug deposition into hair. And finally, due to high surface-to-volume ratio of hair, external contamination is also a possible source for drug entry in hair, especially for smoked drugs such as amphetamine, cocaine, heroin, and marijuana. Next to the exposure to smoke, direct contact with fine powders might also induce external contaminations. In order to remove such external impurities and avoid false positive results, but also to reduce possible analytical interferences from residues of hair care products (wax, shampoo and hair sprays), sweat, sebum and dust, applying of a suitable decontamination procedure is essential. However, washing procedures cannot always ensure a complete removal of drugs from external sources so that the detection of metabolites has been established for judicial evidence. The metabolites are breakdown products during metabolic reactions in body and prove in this way an active uptake of the drug.

Next to external deposition of drugs, elimination of incorporated drugs in hair might occur as well. Mechanical stress, cosmetic treatments (oxidative dyeing, perming or bleaching) and long-term effects of weather (sunlight, rain and wind) can damage the hair shaft and hence provide routes for elimination of drugs, mainly due to a damaged or destroyed cuticle. Nevertheless, daily shampooing does not significantly affect drug concentrations [212,228] so that the retention and stability of drugs in hair is generally considered good. The overview of incorporation and elimination routes of drugs in hair is displayed in Figure 11.
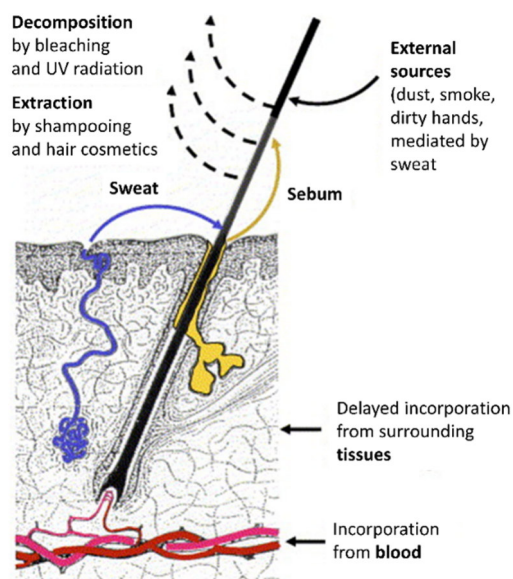
Figure 11. Possible incorporation and elimination routes of drugs in hair. The incorporation of drugs is proposed to occur by various mechanisms, in multiple sites and at various periods during the hair growth. Slightly adapted (minor reformatting) and reprinted with permission from [212]. Copyright (2006) Elsevier.

The dominating mechanism influencing incorporation of drugs into a growing hair is mainly governed by the chemical characteristics of the incorporated drug and the individual physiological characteristics. From the physiological aspect, individual variability in secretions (sweat and sebum) and differences in metabolism might favor specific incorporation routes. From the physicochemical aspect, lipophilicity and basicity of the substance and melanin content of hair play crucial role [212]. The incorporation of drugs from bloodstream into hair cells is controlled by drug permeability of lipid membranes. Lipophilic substances can more easily pass the lipid membranes of hair matrix cells than hydrophilic or charged drugs, and diffuse according to the concentration gradient in the intracellular matrix. Nakahara et al. [229] evidenced this by a high correlation coefficient (0.770) between lipophilicity and the incorporation rate for nineteen common drugs of abuse. However, THC-COOH did not fit in these trends: Despite its highest lipophilicity, the incorporation rate of THC-COOH into hair was the lowest with 3600-fold difference to cocaine, the most efficiently incorporated drug [229]. Since all drugs investigated except THC-COOH were basic or amphoteric substances with amino functional groups, this suggested that the incorporation of acidic and neutral compounds is controlled by membrane permeability due to the pH gradient between blood (pH 7.4) and acidic hair matrix cells. The intracellular pH of melanocytes amounts to 3-5 [230] and keratinocytes were determined to be acidic as well [231]. Under physiological conditions in blood (pH = 7.4) both basic cocaine (pKa = 8.85)[2] and acidic THC-COOH (pKa = 4.02)[2] exist in their ionized forms as the protonated amine and carboxylate anion, respectively. Following deprotonation of cocaine or protonation of THC-COOH to a neutral state, the molecules reach hair matrix cells. Lower intracellular pH in hair matrix cells favors the protonated form of cocaine so that the distribution equilibrium is clearly shifted towards hair matrix cells (cf. Figure 12). In addition, binding of basic drugs to melanin amplifies this effect with clear preference for pigmented hair [212]. On the contrary, acidic drugs like THC-COOH are only poorly incorporated due to the efflux of the neutral species existing at the acidic pH of matrix cells, i.e. distribution equilibrium is shifted towards the extracellular blood plasma (cf. Figure 12). Moreover, melanin affinity for THC-COOH was determined to be low [229], thus preventing its retention by melanin in the matrix cells. The binding of certain chemicals by melanin is one of the most pronounced retention mechanisms of the body [232]. Several studies demonstrated a significant correlation of basic drugs with high melanin affinity. For example, Borges et al. [233] investigated effects of melanin type for cocaine, benzoylecgonine, amphetamine and its non-basic analogue *N*-acetylamphetamine *in vitro*. The basic drugs cocaine and amphetamine exhibited clear tendency for eumelanins, whereas their net neutral analogues benzoylecgonine and *N*-acetylamphetamine did not bind to any melanin type. Melanin might be considered a weak cationic exchanger so that it binds and interacts with basic drugs [221]. The binding relies on multiple chemical interactions: Electrostatic interactions of positively charged cationic groups of basic drugs with the anionic carboxylic groups of melanin, van der Waals forces between aromatic rings of the drugs and the aromatic indole cores in melanin, and hydrophobic interactions [207].

Besides the aforementioned THC-COOH, metabolites are in general encountered in lesser extent in hair than their parent substances, which can be derived from increased hydrophilicity introduced by drug metabolism. For example, benzoylecgonine and morphine

---

[2] pKa values predicted by Chemicalize, calculation module developed by ChemAxon, https://chemicalize.com/.

enter hair to a lesser extent than their lipophilic parent compounds cocaine and 6-monoacetylmorphine, respectively [229]. The incorporation rate differences might be high, e.g. 10-fold more cocaine than benzoylecgonine was found in hair, although the metabolite prevailed in blood plasma (4-fold higher plasma concentration of benzoylecgonine compared to cocaine) [234]. In addition to the low lipophilicity and low melanin affinity of benzoyl-ecgonine [229], the membrane permeability based on the pH gradient between blood and hair matrix (cf. Figure 12) affects the low incorporation rate of benzoylecgonine in hair matrix as well.
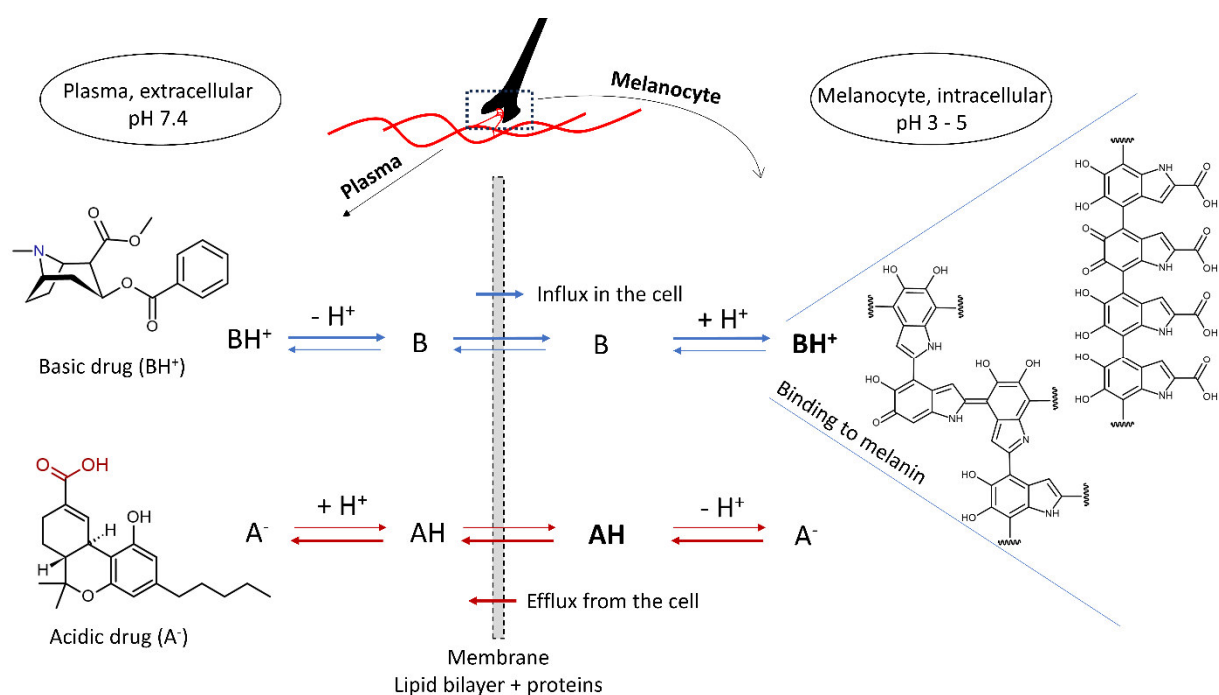
Figure 12. Incorporation of basic (cocaine) and acidic drugs (THC-COOH) in hair, showing their distribution equilibrium between the blood plasma and hair matrix cells. Source: Self-designed.

1.4 Sewage analysis

Sewage analysis was originally used in the 1990s to monitor the footprint of liquid household waste in the environment, and Daughton [235] first proposed the method to measure illicit drugs in 2001. Few years later, in 2005, Zuccato et al. [236] analyzed cocaine and its main urinary metabolite benzoylecgonine in surface water and wastewater to estimate the community level of drug abuse, thus introducing the wastewater-based epidemiology (WBE) approach. The premise of the approach is that drugs and/or their metabolites are excreted through urine and feces into the sewer network, thus enabling their identification in wastewater and allowing for the estimation of the illicit drug loads of the population served by the sewer network or wastewater treatment plant (WWTP) investigated. Although the main wastewater sampling point for such studies is usually influent wastewater in a WWTP before the treatment processes, it was shown that the drugs persist even in treated wastewater [237,238]. One of the decisive steps for the successful detection of target substances is the selection of an appropriate wastewater biomarker. The key markers used for the detection of the main illicit drugs in sewage, e.g. amphetamine, methamphetamine, 3,4-methylenedioxymethamphetamine (MDMA), cocaine, cannabis and meanwhile ketamine, are well established [239,240]. Next to the monitoring of illicit drugs, nicotine and alcohol markers were also evaluated and implemented in the scope of wastewater monitoring programs [240]. Moreover, several other studies successfully applied WBE in recent years to assess health and illness indicators within a community, especially during the COVID-19 pandemic [241].

In the past 20 years, WBE has grown exponentially and is nowadays established as an important tool for illicit drug use monitoring, acknowledged both by the EMCDDA [239,242] and the UNODC [59]. In order to obtain a comprehensive picture on drug use trends, EMCDDA implemented a multi-faceted approach, combining traditional tools for data collection and WBE. The latter has been accomplished under the auspices of the Sewage analysis CORE group – Europe (SCORE) that was established in 2010 in order to standardize the analytical approach for wastewater analysis and coordinate international studies to estimate the extent of illicit drug consumption across Europe [243]. The first study was performed in 2011 in 19 European cities, demonstrating a first WBE based approach to disclose geographical differences in illicit drug use in Europe [244]. Further comparable studies were conducted during the consecutive years, with increasing number of cities and countries participating each year. The last study in 2023 covered 88 cities and 24 countries in the EU and Turkey [239]. Raw 24-hour wastewater composite samples were collected at WWTPs in the participating cities during a one-week period and analyzed by chemical analysis for parent drugs and their selected metabolites. Wastewater biomarkers for cocaine and cannabis were their metabolites benzoylecgonine and THC-COOH, respectively, and for the residual illicit drugs investigated the parent compounds, i.e. amphetamine, methamphetamine, MDMA and ketamine. Data from all wastewater studies since 2011 are available on the EMCDDA website [239] via an interactive tool that enables to explore individual sites, study years, target drugs, and average daily, weekday and weekend sewer loads expressed as mg/1,000 persons/day (Figure 13). In addition, data from outside Europe has been included in the interactive tool since 2023.
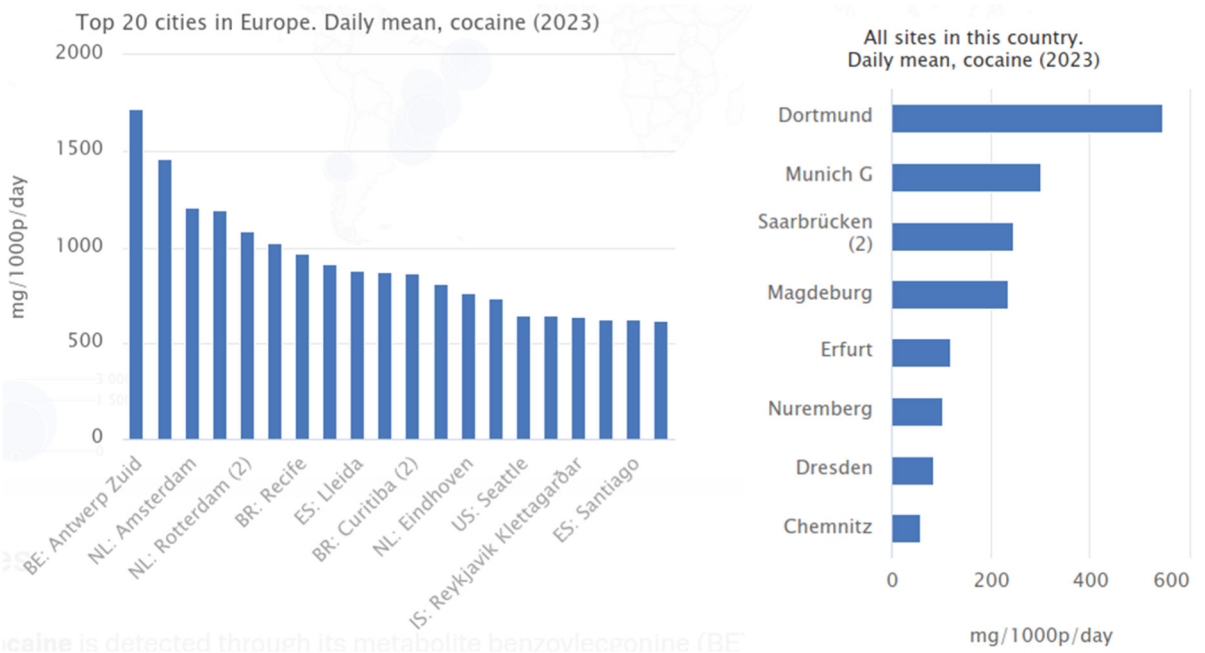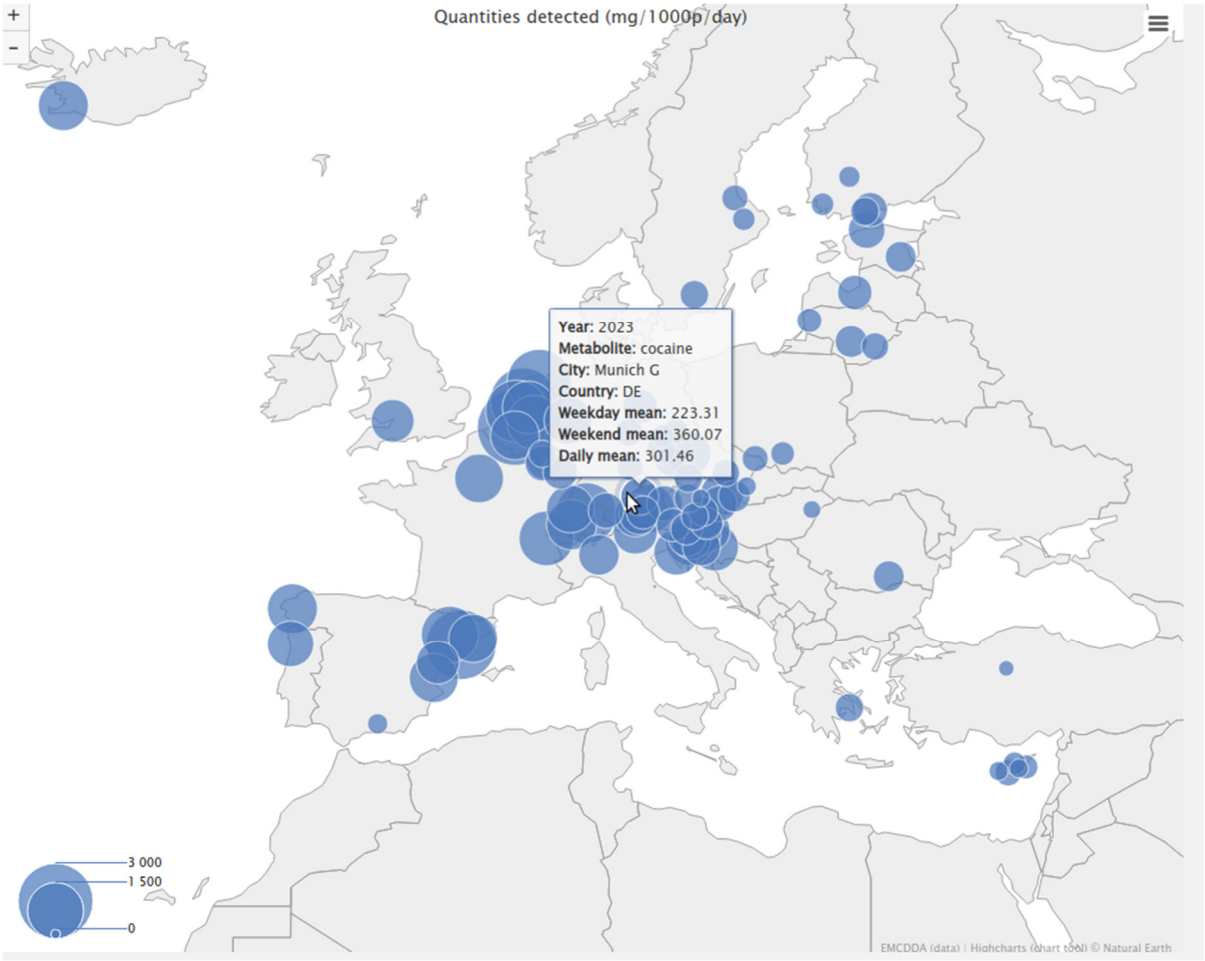
Figure 13. Data representation by the interactive tool at the EMCDDA website [239], showing results of WBE analyses across Europe. The data shown illustrate cocaine loads across Europe in 2023 (top), with average daily loads across top twenty cities and German cities participating in the study (below).

A few key findings of the SCORE study in 2023 as the most recent study, and other similar wastewater monitoring programs will be presented in the following section in order to recognize the potential but also limitations of wastewater analysis as a monitoring tool for illicit drug use. The SCORE study revealed that all illicit drugs investigated were detected in almost every European city participating in the study, however distinct geographical patterns of drug use were observed. Similar to previous years, the highest cocaine levels were reported in western and southern European cities (cf. Figure 13, top), whereas amphetamine use peaked in the north and east of Europe. Geographical differences were also shown for MDMA and methamphetamine: The highest mass loads of MDMA were located around Belgium, the Netherlands, France and the western of Germany, while methamphetamine use remained generally low with highest loads historically concentrated in Czechia, Slovakia and the east of Germany. The most pronounced cannabis use was situated in western and southern European cities. Temporal fluctuations in weekly patterns were disclosed as well. Amphetamine, cocaine, ketamine and MDMA use appeared to be higher during weekend (Friday to Monday) than during weekdays in most cities, as opposed to cannabis and methamphetamine use, which did not show any remarkable differences over the whole week. The use of WBE to measure geographical and temporal variations of drug use patterns within national populations was recognized beyond European borders as well. The Australian Criminal Intelligence Commission has implemented a National Wastewater Drug Monitoring Program across the country since 2016 [240]. The monitoring program includes 12 licit and illicit drugs, and 62 WWTPs covering 57% of the Australian population (14.5 million people), as of August 2023 [245]. The data obtained through WBE assist the Australian government in identifying differences between capital cities and regional areas, across different Australian jurisdictions, and finally in assessing the effectiveness of intervention strategies for licit and illicit drugs. Moreover, the WBE studies even allowed for the estimation of illicit drug retail market size, with valuable insights: More than 16.5 tonnes of methamphetamine, cocaine, MDMA and heroin were consumed between August 2022 and August 2023 in Australia, with their estimated street value amounting to 12.4 billion dollars. Addition of cannabis estimates resulted in more than 30 tonnes of the five illicit drugs consumed on the nationwide level over the one-year period in 2022-2023. In addition to the large-scale monitoring, wastewater analysis has been used worldwide on a smaller scale among high-risk populations or populations that might demand special drug reduction strategies, such as schools [246], colleges [247], prisons [248] or music festival populations [249]. Monitoring of illicit drugs in small communities requires social and ethical aspects to be considered in order to avoid stigmatization and adverse policy responses towards the entire community, regardless of the individual drug use. While all the examples in this section demonstrate a great potential of wastewater analysis for drug monitoring agencies, law enforcement, policymakers and other public stakeholders, certain limitations are associated with the approach as well. For instance, it cannot provide information on the number and main classes of users or patterns of drug use, such as administration routes, number of doses and their purity, and frequency of use. Hence, calculating the number of average doses consumed from the sewage loads is rather challenging. Other uncertainties arise from the selection of target biomarkers, the fate of the biomarkers in the sewer, different back-calculation approaches and estimation of the catchment population size [250,251]. Special challenges and a lack of data are associated with the detection of NPS, particularly SCRAs, as described in more detail in Chapter 3 (section 3.1

Introduction) and Chapter 4 (section 4.1 Introduction), not least due to the lack of excretion rates and in-sewer stability data for this substance class.

1.5 Explosives analysis

1.5.1 Explosives: General properties and their occurrence in forensic casework

The German Explosives Act (German: Sprengstoffgesetz) describes explosive materials as solid or liquid compounds and formulations, *"which could explode due to a not extraordinary thermal, mechanical or other stress"* and *"show explosive behavior during test methods such as thermal sensitivity and mechanical sensitivity with respect to either shock or friction"* [252]. According to their typical use, these materials can be attributed to several categories, including high explosives, pyrotechnics, propellants and others. Due to their outstanding detonation characteristics and hence particular military, civil and forensic relevance, only high explosives are covered within this thesis.

According to their sensitivity and energetic properties, high explosives can be classified into primary and secondary explosives. **Primary explosives** are substances highly sensitive towards heat, impact or friction and undergo a fast transition from combustion (or deflagration) to detonation [253]. Their higher sensitivity in comparison to secondary explosives is reflected in typical values of ≤ 4 J for impact, ≤ 10 N for friction and ≤ 20 mJ for electrostatic discharge [253-255]. Upon these external stimuli they produce either a large amount of heat or a shockwave, which can initiate less sensitive secondary explosives, so that they are used as initiators for secondary booster charges (e.g. in detonators), main charges or propellants [253]. Usually, they are used in relatively small quantities to initiate a secondary or main explosive charge. Although they are considerably more sensitive than secondary explosives, the performance (detonation velocities, detonation pressures and heat of explosions) of primary explosives is generally lower than that of secondary explosives. For example, detonation velocities for typical primary explosives are in the range of 3500 - 5500 m/s, while typical secondary explosives reach 6500 - 9000 m/s. [253]. Some common primary explosives are lead azide, lead styphnate, diazadinitrophenole (DDNP), and in former times also mercury fulminate.

Secondary explosives are characterized by a higher structural stability, implying that they cannot be initiated as easily as primary explosives through heat or shock. Their lower sensitivity toward external stimuli, when compared to primary explosives, is mirrored in values of ≥ 4 J for impact, ≥ 50 N for friction and ≥ 100 mJ for electrostatic discharge [253]. Typical secondary explosives are trinitrotoluol (TNT), hexogen (RDX), octogen (HMX) and pentaerythriol tetranitrate (PETN).

Explosives can also be categorized depending on their use as military, civil and homemade (HME) explosives. For example, typical explosives for military applications are TNT, RDX, HMX and PETN, and for civil applications ammonium nitrate composite explosives, such as ammonium nitrate / fuel oil (ANFO). Nitroglycerine (NG) is a powerful and highly sensitive explosive and hence never used in pure form, but as a compound in ammonium nitrate explosives and in nitrocellulose propellants. From a chemical point of view, the most powerful explosives are organic compounds that can be categorized as nitroamines, nitroaromatics or

nitroesters, all containing the nitro functional group, and the peroxides. Some of the most representative compounds are depicted in Figure 14, with their full names and classification according to their use in Table 5.
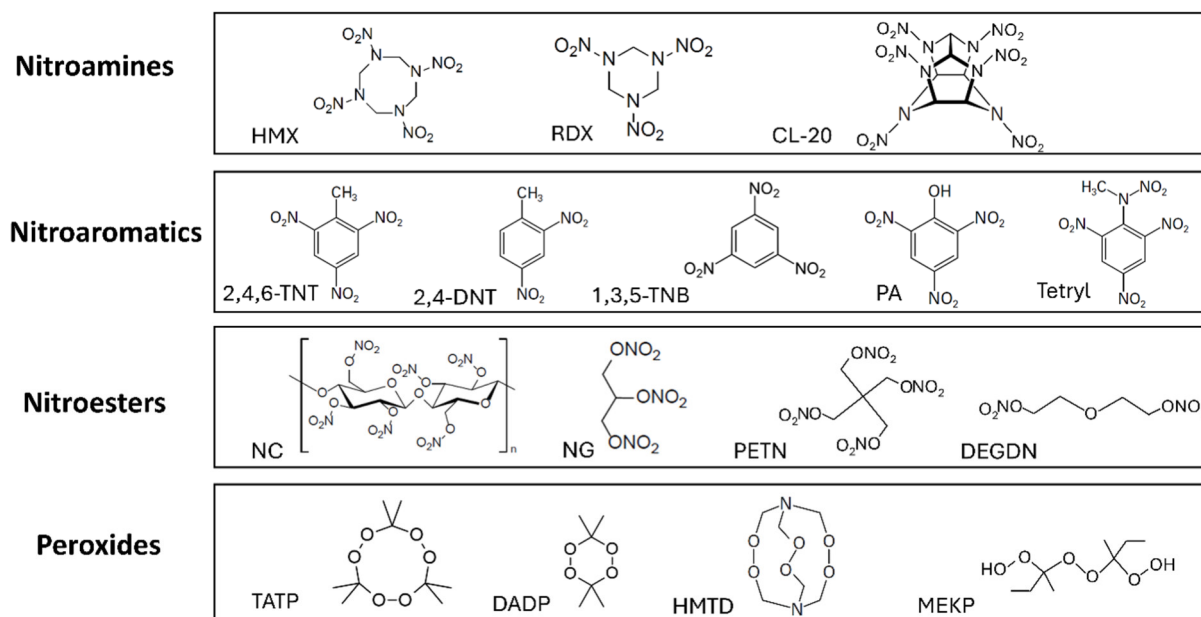
Figure 14. Organic explosives categorized as nitroamines, nitroaromatics, nitroesters and peroxides, with relevant representative compounds. Source: Self-designed.

Table 5. Some of the most prominent organic and inorganic (ammonium nitrate) explosives, categorized by their use. Many of these compounds play an important role in the forensic casework.

Explosive (Abbreviation)	Full name	Category
HMX	Cyclotetramethylene tetranitramine; Octogen	Military
RDX	Cyclotrimethylene trinitramine; Hexogen; 'Research Development Explosive'	Military
CL-20	Hexanitrohexaazaisowurtzitane	Military
TNT	Trinitrotoluene	Military, civil[1]
PA	Picric acid	Military
PETN	Pentaerythritol tetranitrate; Penthrite; Nitropenta	Military, civil
ETN	Erythritol tetranitrate	Homemade
NC	Nitrocellulose	Military, civil
NG	Nitroglycerin	Military, civil[1]
NQ	Nitroguanidine	Military, civil[1]
EGDN	Ethylene glycol dinitrate	Military, civil[1]
DEGDN	Diethylene glycol dinitrate	Military, civil[1]
AN[2]	Ammonium nitrate	Civil, homemade
UN	Urea nitrate	Civil, homemade
TATP	Triacetone triperoxide	Homemade
DADP	Diacetone diperoxide	Homemade
HMTD	Hexymethylene triperoxide diamine	Homemade
MEKP	Methyl ethyl ketone peroxide	Homemade

[1] In mixtures with other explosives
[2] Inorganic explosive

In accordance with their usage that demands safe handling and storage, military and civil bulk explosives comply with the characteristics of secondary explosives. Due to the restricted access to these explosives, criminals and terrorists move to improvised, homemade explosives (HMEs), clandestinely synthesized from commercially available materials, to manufacture improvised explosive devices (IEDs). HMEs range from peroxide explosives, fertilizer-based explosives to pyrotechnics (e.g. chlorates, and perchlorates mixed with various fuels). Even PETN, ETN or RDX are occasionally encountered as HME, since the precursor chemicals can be purchased in bulk amounts. An example of a terrorist plot with a fertilizer-based explosive is the attack on the government district of Oslo in 2011, with ammonium nitrate, aluminium and fuel oil (ANALFO) used as the main charge [256]. The most common peroxide explosives are triacetone triperoxide (TATP) and hexamethylene triperoxide diamine (HMTD), synthesized from easily available chemicals, such as hydrogen peroxide, acetone and acid. The forensic casework encompasses a wide spectrum of explosives, from the HME clandestine laboratories with raw materials and intact explosives, over military explosives encountered as shells, grenades, plastic explosives or IEDs made from these, to post-blast scenarios (Figure 15).

Figure 15. Few examples of the typical forensic casework regarding explosives: Synthesis of a HME with the produced explosive (TATP, A); Military explosives encountered as grenades (B); Post-blast scenario (C). Source: Forensic Science Institute, Bavarian State Criminal Police Office.

Forensic explosives analysis

While the analysis of bulk explosives can be complex, the identification of trace amounts of explosives and their products in a post-blast scenario surely is. An overview of the latest developments in the analysis and detection of explosives and explosives residues is provided by several Interpol reviews from 2013, 2016, 2019 and 2023 [257-260]. In general, the selection of an analytical method for analysis of explosives depends on the type of explosive (organic or inorganic) and the type of investigation (pre-blast or post-blast). Pre-blast analysis includes intact bulk explosives and precursors, while post-blast analysis deals with explosives residues after a blasting event. Bulk analysis of both inorganic and organic explosives can be performed with spectroscopic techniques like infrared and Raman spectroscopy, often as portable instruments for on-site detection, but also with X-ray diffraction (XRD) for crystalline substances, and X-ray fluorescence (XRF) for the elemental composition of inorganic explosives. Analysis of post-blast explosives residues requires more sensitive and selective analytical methods. For example, LC and GC separation techniques in combination with MS detection fulfill these requirements and represent the preferred methodology for identification of trace amounts of organic explosives. For post-blast residues of inorganic explosives, ion chromatography (IC) or capillary electrophoresis (CE) are often deployed in routine casework.

1.5.2 TATP: Properties, formation and degradation

Among HMEs used in terrorist and other criminal activity within the last decade, TATP reached the top position. Several attacks with TATP based IEDs were carried out worldwide, often by suicide bombers, and gained worldwide attendance. Therefore, the explosives part of this thesis (Chapter 6), will focus on TATP.

Properties

Like HMTD and other peroxide-based explosives, TATP (chemical nomenclature: 3,3,6,6,9,9-hexamethyl-1,2,4,5,7,8-hexaoxonane or 3,3,6,6,9,9-hexamethyl-1,2,4,5,7,8-hexaoxacyclo-nonane, generally known as acetone peroxide (APEX) or TATP) does not find use as civil or military explosive due to its high volatility as well as high impact, friction and thermal sensitivity. It became known almost exclusively as a terrorist explosive, both as initiating and main charge. However, not only terrorist attacks with TATP, but also accidental cases of TATP formation are well known. Already in 1943 it was noted that the explosions of isopropyl ether that had been stored for a long time originate from the formation of peroxides, and the isolation and characterization of the formed crystals revealed TATP [261]. Recently, a cautionary tale for hazmat teams and laboratory stuff was reported on TATP formation in a 2-propanol bottle after a dozen years past the expiration date of the chemical [262]. TATP can be even produced during the disposal of chemical waste, as this happened in 2001 in Germany, requiring a large-scale deployment of special police and fire department units [263].

When handling or disposing of TATP, all the great caution is needed due to the fact that TATP is a highly sensitive and quite powerful primary explosive with high initiating efficiency. It reacts extremely sensitive to impact (impact sensitivity: 0.3 J), comparable to nitroglycerine (impact sensitivity: 0.2 J), and even more sensitive to friction (reaction at 0.1 N pistil load) [264]. For comparison, nitroglycerine shows no critical reaction up to 353 N pistil load [264]. Next to the impact and friction, TATP explodes violently on heating and might generally be detonated under water [265]. Even static electricity could trigger an explosion of TATP and spontaneous explosions can occur as well. Wet TATP is considerably less sensitive but might still result in a detonation at a moisture content of up to 25% [265]. The potential use of TATP as a primary explosive is illustrated by very low quantities (0.05 g) sufficient to initiate PETN [266]. The explosive power of TATP has been reported up to 88% the power of TNT, depending on the type of method used [267-269]. Some key chemical and physical properties, together with sensitivity and performance data of TATP, compared to those of TNT, are given in Table 6.

Table 6. Chemical and physical properties, together with sensitivity and performance data of TNT and TATP.

		TNT	TATP
Explosive type		Secondary explosive	Primary explosive
Physical appearance		Pale yellow crystals	Colorless crystals
Molecular formula		$C_7H_5N_3O_6$	$C_9H_{18}O_6$
Molecular weight		227.1 g/mol	222.2 g/mol
Density		1.65 g/cm^3 (crystals) 1.47 g/cm^3 (molten)	1.22 g/cm^3
Melting point		80.8°C	95-98.8°C [254]
Vapor pressure		5 x 10^{-4} Pa (25°C) [270]	7 Pa (25°C) [270] 6.7 Pa (25°C) [271]
Solubility in organic solvents	Good	Benzene, toluene, acetone, chloroform [272]	Acetone, hexane, benzene, carbon disulfide, chloroform, carbon tetrachloride, pyridine, toluene [273]
	Poor	Ethanol, carbon tetrachloride [272]	Methanol, ethanol [273]
Solubility in water		100.5 mg/L (25°C, pH 6.8) [274]	177 mg/L (22°C) [275]
Impact sensitivity		15 J	0.3 J
Friction sensitivity		up to 353 N no reaction	0.1 N
Lead block test		300 cm^3 / 10 g	250 cm^3 / 10 g
Decomposition point		250°C	150-160°C [254]
Detonation velocity (V$_D$)		6900 m/s at 1.6 g/cm^3, 6950 m/s [276]	5300 m/s at 1.18 g/cm^3, 6107 m/s [277]
Detonation heat (Q)		5418 kJ/kg [276]	3843 kJ/kg [277]
Detonation pressure (p$_{cj}$)		19.0 GPa [276]	10.0 GPa [277]

Reference: [264], unless stated otherwise.

Formation

TATP was first synthesized by Wolffenstein [278] in 1895, who observed formation of small quantities of TATP crystals after leaving a mixture of acetone and 10% hydrogen peroxide solution at room temperature for several days. Higher concentrations of hydrogen peroxide (50%) and longer reaction periods of 4 weeks led to even higher quantities of TATP formed. An interesting observation of Wolffenstein was the missing reaction when using purified acetone and distilled hydrogen peroxide, however immediate formation could be introduced by addition of a droplet of phosphoric acid. Thus, the reaction of acetone and hydrogen peroxide is driven by an acid-based catalysis. Besides the trimeric cyclic peroxide (TATP), a dimeric (diacetone diperoxide, DADP) and more seldom a tetrameric form (tetraacetone tetraperoxide, TrATrP) [279] were also observed in more recent experiments. Several other peroxides are formed in the reaction, such as linear peroxide intermediates, but only TATP and DADP are encountered as the main precipitates, not least due to their low solubility in aqueous solutions. The overall reaction yield and amount of the two main cyclic peroxides, TATP and DADP, seemed to be affected by varying reaction conditions, including reaction temperature, the molar ratio of acid to hydrogen peroxide/acetone, initial concentrations of reactants, and duration of reaction [280]. In a follow-up study, Oxley et al. [281] postulated a

mechanistic pathway for the formation of TATP and DADP (Figure 16), and revealed that water has a profound effect on their formation and distribution. In this context, the importance of acid concentration and equivalents on the product composition had been discussed previously in the literature [282], often being interpreted via the lens of the acid type (sulphuric acid vs. hydrochloric acid) [279]. Although the essential importance of an acid catalyst for the overall reaction is well known, the oxidation reaction of acetone by hydrogen peroxide takes place even without acid catalysis, however at significantly slower formation rate lasting weeks and months for TATP and DADP formation and precipitation [283].
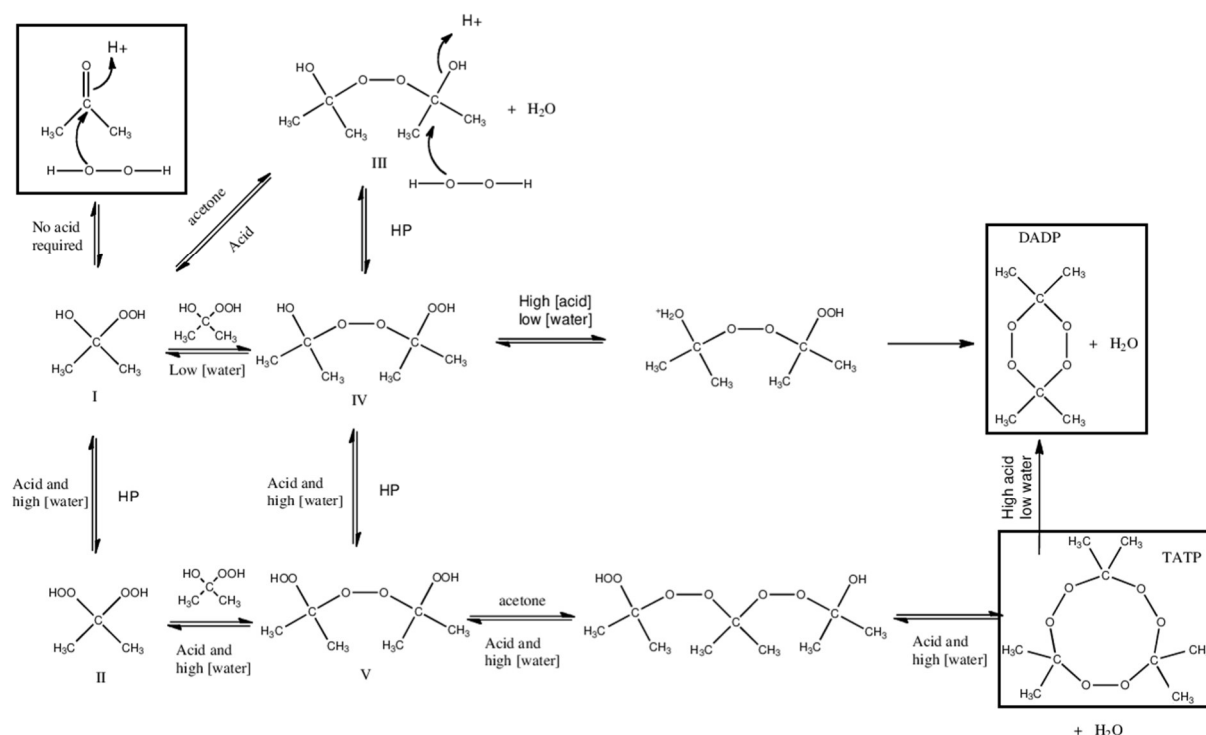
Figure 16. Mechanism for the formation of TATP and DADP, as proposed by Oxley et al. [281]. HP = hydrogen peroxide. Slightly adapted (minor reformatting) and reprinted with permission from [281]. Copyright (2013) John Wiley and Sons.

Decomposition

The explosive properties and mechanism of thermal decomposition of TATP were studied by Dubnikova et al. [284] using X-ray crystallography and electronic structure calculations. The calculated pathway of TATP was found to be a complex multistep process with many intermediates and transition states that lead to the main final products, acetone and ozone. Along with the main products, dioxygen, methyl acetate, ethane, and carbon dioxide were predicted to be formed as well. The results led authors to conclude that the explosion of TATP is not a thermochemically highly favored event, but is rather driven entropically. The entropy burst is the result of formation of four gaseous molecules, one ozone and three acetone molecules, from every TATP molecule in the solid state. This implies an enormous volume expansion and hence entropy increase of the gaseous state. Therefore, the explosion of TATP is rather a decomposition reaction than an oxidation process driven by excessive heat of

formation, as opposed to most other explosive materials. Correspondingly, the three isopropylidene units and the oxygen atoms in TATP do not account for fuel and oxidant, respectively. Instead of releasing thermal energy during the explosion, the isopropylidene units act only as molecular scaffolds for the peroxide bonds that undergo a decomposition chain reaction, as postulated by Dubnikova et al. [284]. Furthermore, the authors concluded that the formation of the dimeric acetone peroxide, DADP, is not likely in the course of TATP decomposition. This was in accordance with experimental data from Eyler [285] and Oxley [286], who did not report DADP as a thermal decomposition product of TATP in the gas phase.

1.6 References

[1]   Touw M. The religious and medicinal uses of Cannabis in China, India and Tibet. *J Psychoactive Drugs*. 1981;13:23-34.

[2]   Zuardi AW. History of cannabis as a medicine: a review. *Braz J Psychiatry*. 2006;28:153-157.

[3]   Li HL. Hallucinogenic plants in Chinese herbals. *J Psychodelic Drugs*. 1978;10:17-26.

[4]   Brenneisen R. Chemistry and Analysis of Phytocannabinoids and Other Cannabis Constituents. In: ElSohly MA, ed. *Marijuana and the Cannabinoids*. Humana Press; 2007.

[5]   Hanuš LO, Meyer SM, Muñoz E, Taglialatela-Scafati O, Appendino G. Phytocannabinoids: a unified critical inventory. *Nat Prod Rep.* 2016;33:1357-1392.

[6]   Bhattacharyya S, Morrison PD, Fusar-Poli P, et al. Opposite Effects of Δ-9-Tetrahydrocannabinol and Cannabidiol on Human Brain Function and Psychopathology. *Neuropsychopharmacology*. 2010;35:764-774.

[7]   Englund A, Morrison PD, Nottage J, et al. Cannabidiol inhibits THC-elicited paranoid symptoms and hippocampal-dependent memory impairment. *J Psychopharmacol.* 2013;27:19-27.

[8]   Morgan CJA, Freeman TP, Schafer GL, Curran HV. Cannabidiol Attenuates the Appetitive Effects of Δ^9-Tetrahydrocannabinol in Humans Smoking Their Chosen Cannabis. *Neuropsycho-pharmacology*. 2010;35:1879-1885.

[9]   Bergamaschi MM, Queiroz RH, Zuardi AW, Crippa JA. Safety and Side Effects of Cannabidiol, a Cannabis sativa Constituent. *Curr Drug Saf.* 2011;6:237-249.

[10]   United Nations Office on Drugs and Crime. Recommended Methods for the Identification and Analysis of Cannabis and Cannabis Products. 2022; Vienna, United Nations publication, ST/NAR/40/REV.1.

[11]   Huestis MA. Human cannabinoid pharmacokinetics. *Chem Biodivers*. 2007;4:1770-1804.

[12]   Russo EB. Taming THC: potential cannabis synergy and phytocannabinoid-terpenoid entourage effects. *Br J Pharmacol*. 2011;163:1344-1364.

[13]   Huestis MA, Sampson AH, Holicky BJ, Henningfield JE, Cone EJ. Characterization of the absorption phase of marijuana smoking. *Clin Pharmacol Ther.* 1992;52:31-41.

[14]   Grotenhermen F. Pharmacokinetics and pharmacodynamics of cannabinoids. *Clin Pharmaco-kinet.* 2003;42:327-360.

[15]   Huestis MA, Henningfield JE, Cone EJ. Blood Cannabinoids. I. Absorption of THC and Formation of 11-OH-THC and THCCOOH During and After Smoking Marijuana. *J Anal Toxicol.* 1992;16:276-282.

[16]   Mason AP, McBay AJ. Cannabis: pharmacology and interpretation of effects. *J Forensic Sci*. 1985;30:615-631.

[17]   Ohlsson A, Lindgren JE, Wahlen A, Agurell S, Hollister LE, Gillespie HK. Plasma delta-9 tetrahydrocannabinol concentrations and clinical effects after oral and intravenous administration and smoking. *Clin Pharmacol Ther*. 1980;28:409-416.

[18]   Lindgren JE, Ohlsson A, Agurell S, Hollister L, Gillespie H. Clinical effects and plasma levels of Δ^9-Tetrahydrocannabinol (Δ^9-THC) in heavy and light users of cannabis. *Psychopharmacology.* 1981; 74:208-212.

[19]   Ohlsson A, Lindgren JE, Wahlén A, Agurell S, Hollister LE, Gillespie HK. Single dose kinetics of deuterium labelled Δ^1-tetrahydrocannabinol in heavy and light cannabis users. *Biomed Mass Spectrom*. 1982;9:6-10.

[20]   Fischer B, Robinson T, Bullen C, et al. Lower-Risk Cannabis Use Guidelines (LRCUG) for reducing health harms from non-medical cannabis use: A comprehensive evidence and recommendations update. *Int J Drug Policy*. 2022;99:103381. DOI: 10.1016/j.drugpo.2021.103381.

[21]   Widman M, Agurell S, Ehrnebo M, Jones G. Binding of (+)- and (-)- Δ^1-tetrahydrocannabinols and (-)-7-hydroxy-Δ^1-tetrahydrocannabinol to blood cells and plasma proteins in man. *J Pharm Pharmacol.* 1974;26:914-916.

[22]   Harvey DJ, Leuschner JTA, Paton WDM. Gas chromatographic and mass spectrometric studies on the metabolism and pharmacokinetics of Δ^1-tetrahydrocannabinol in the rabbit. *J Chromatogr A.* 1982;239:243-250.

[23]   Karschner EL, Swortwood MJ, Hirvonen J, Goodwin RS, Bosker WM, Ramaekers JG, Huestis MA. Extended plasma cannabinoid excretion in chronic frequent cannabis smokers during sustained abstinence and correlation with psychomotor performance. *Drug Test Anal.* 2016;8:682-689.

[24]   Johansson E, Agurell S, Hollister LE, Halldin MM. Prolonged apparent half-life of Δ^1-tetra-hydrocannabinol in plasma of chronic marijuana users. *J Pharm Pharmacol.* 1988;40:374-375.

[25]   Matsunaga T, Iwawaki Y, Watanabe K, Yamamoto I, Kageyama T, Yoshimura H. Metabolism of Δ^9-tetrahydrocannabinol by cytochrome P450 isozymes purified from hepatic microsomes of monkeys. *Life Sci.* 1995;56:2089-2095.

[26]   Narimatsu S, Watanabe K, Matsunaga T, et al. Cytochrome P-450 isozymes involved in the oxidative metabolism of Δ^9-tetrahydrocannabinol by liver microsomes of adult female rats. *Drug Metab Dispos.* 1992;20:79-83.

[27]   Wall ME, Perez-Reyes M. The Metabolism of Δ^9-Tetrahydrocannabinol and Related Cannabinoids in Man. *J Clin Pharmacol.* 1981;21:178S-189S.

[28]   Perez-Reyes M, Timmons MC, Lipton MA, Davis KH, Wall ME. Intravenous Injection in Man of Δ^9-Tetrahydrocannabinol and 11-OH-Δ^9-Tetrahydrocannabinol. *Science.* 1972;177(4049):633-635.

[29]   Burstein SH. The cannabinoid acids: nonpsychoactive derivatives with therapeutic potential. *Pharmacol Ther.* 1999;82:87-96.

[30]   Wall ME, Sadler BM, Brine D, Taylor H, Perez-Reyes M. Metabolism, disposition, and kinetics of delta-9-tetrahydrocannabinol in men and women. *Clin Pharmacol Ther*. 1983;34:352-363.

[31]   Williams PL, Moffat AC. Identification in human urine of Δ^9-tetrahydrocannabinol-11-oic acid glucuronide: a tetrahydrocannabinol metabolite. *J Pharm Pharmacol.* 1980;32:445-448.

[32]   Pertwee RG. The diverse CB_1 and CB_2 receptor pharmacology of three plant cannabinoids: Δ^9-tetrahydrocannabinol, cannabidiol and Δ^9-tetrahydrocannabivarin. *Br J Pharmacol.* 2008;153: 199-215.

[33]   Iversen L. Cannabis and the brain. *Brain.* 2003;126:1252-1270.

[34]   Pertwee RG. Sites and Mechanisms of Action. In: Grotenhermen F, Russo E, ed. *Cannabis and Cannabinoids: Pharmacology Toxicology and Therapeutic Potential.* Haworth Press; 2002.

[35]   Huestis MA, Gorelick DA, Heishman SJ, et al. Blockade of Effects of Smoked Marijuana by the CB1-Selective Cannabinoid Receptor Antagonist SR141716. *Arch Gen Psychiatry.* 2001;58:322-328.

[36]   Hess C, Schoeder CT, Pillaiyar T, Madea B, Müller CE. Pharmacological evaluation of synthetic cannabinoids identified as constituents of spice. *Forensic Toxicol.* 2016;34:329-343.

[37]   Sachs J, McGlade E, Yurgelun-Todd D. Safety and Toxicology of Cannabinoids. *Neurotherapeutics.* 2015;12:735-746.

[38]   Chandra S, Radwan MM, Majumdar CG, Church JC, Freeman TP, ElSohly MA. New trends in cannabis potency in USA and Europe during the last decade (2008-2017). *Eur Arch Psychiatry Clin Neurosci.* 2019;269:5-15.

[39]   European Monitoring Centre for Drugs and Drug Addiction and Europol. EU Drug Market: Cannabis — In-depth analysis. 2022. https://www.emcdda.europa.eu/publications/eu-drug-markets/cannabis_en. Date accessed: March 04, 2024.

[40]   Cinnamon Bidwell L, YorkWilliams SL, Mueller RL, Bryan AD, Hutchison KE. Exploring cannabis concentrates on the legal market: User profiles, product strength, and health-related outcomes. *Addict Behav Rep*. 2018;8:102-106.

[41]   Freeman TP, Winstock AR. Examining the profile of high-potency cannabis and its association with severity of cannabis dependence. *Psychol Med.* 2015;45:3181-3189.

[42]   Meier MH. Associations between butane hash oil use and cannabis-related problems. *Drug Alcohol Depend*. 2017;179:25-31.

[43]   Di Forti M, Marconi A, Carra E, et al. Proportion of patients in south London with first-episode psychosis attributable to use of high potency cannabis: a case-control study. *Lancet Psychiatry.* 2015;2:233-238.

[44]   Schoeler T, Petros N, Di Forti M, et al. Effects of continuation, frequency, and type of cannabis use on relapse in the first 2 years after onset of psychosis: an observational study. *Lancet Psychiatry.* 2016;3:947-953.

[45]   Freeman TP, van der Pol P, Kuijpers W, et al. Changes in cannabis potency and first-time admissions to drug treatment: a 16-year study in the Netherlands. *Psychol Med.* 2018;48: 2346-2352.

[46]   Lenné MG, Dietze PM, Triggs TJ, Walmsley S, Murphy B, Redman JR. The effects of cannabis and alcohol on simulated arterial driving: Influences of driving experience and task demand. *Accid Anal Prev.* 2010;42:859-866.

[47]   Hartman RL, Huestis MA. Cannabis effects on driving skills. *Clin Chem.* 2013;59:478-492.

[48]   Ramaekers JG, Berghaus G, van Laar M, Drummer OH. Dose related risk of motor vehicle crashes after cannabis use. *Drug Alcohol Depend.* 2004;73:109-119.

[49]   McCormick MA, Shekhar A. Review of Marijuana Use in the Adolescent Population and Implications of its Legalization in the United States. *J Drug Metab Toxicol.* 2014;5:1000165. DOI: 10.4172/2157-7609.1000165

[50]   Volkow ND, Baler RD, Compton WM, Weiss SR. Adverse Health Effects of Marijuana Use. *N Engl J Med*. 2014;370:2219-2227.

[51]   Kahan M, Srivastava A, Spithoff S, Bromley L. Prescribing smoked cannabis for chronic noncancer pain, Preliminary recommendations. *Can Fam Physician*. 2014;60:1083-1090.

[52]   Lawn W, Mokrysz C, Lees R, et al. The CannTeen Study: Cannabis use disorder, depression, anxiety, and psychotic-like symptoms in adolescent and adult cannabis users and age-matched controls. *J Psychopharmacol.* 2022;36:1350-1361.

[53]   Carlier J, Huestis MA, Zaami S, Pichini S, Busardò FP. Monitoring Perinatal Exposure to Cannabis and Synthetic Cannabinoids. *Ther Drug Monit.* 2020;42:194-204.

[54]   Directive (EU) 2017/2103 of the European Parliament and of the Council of 15 November 2017 amending Council Framework Decision 2004/757/JHA in order to include new psychoactive substances in the definition of 'drug' and repealing Council Decision 2005/387/JHA. *OJ* L 305, 21.11.2017, p. 12–18. Date accessed: March 19, 2024.
Available online: http://data.europa.eu/eli/dir/2017/2103/oj.

[55]   Simonis S, Canfyn M, Van Dijck A, *et al.* Awareness of users and motivational factors for using new psychoactive substances in Belgium. *Harm Reduct J*. 2020;17:1-11 (article number 52). DOI: 10.1186/s12954-020-00393-0.

[56]   Sutherland R, Bruno R, Peacock A, et al. Motivations for new psychoactive substance use among regular psychostimulant users in Australia. *Int J Drug Policy*. 2017;43:23-32.

[57]   Soussan C, Kjellgren A. The users of Novel Psychoactive Substances: Online survey about their characteristics, attitudes and motivations. *Int J Drug Policy.* 2016;32:77-84.

[58]   European Monitoring Centre for Drugs and Drug Addiction. New psychoactive substances in prison. Results from an EMCDDA trendspotter study. 2018; Luxembourg: Publications Office of the European Union.

[59] United Nations Office on Drugs and Crime. World Drug Report 2023. 2023; Vienna: United Nations publication, Sales No. E.23.XI.7.

[60] European Monitoring Centre for Drugs and Drug Addiction. European Drug Report 2023: Trends and Developments. 2023; Luxembourg: Publications Office of the European Union.

[61] European Monitoring Centre for Drugs and Drug Addiction. New psychoactive substances: 25 years of early warning and response in Europe. An update from the EU Early Warning System. 2022; Luxembourg: Publications Office of the European Union.

[62] Dean BV, Stellpflug SJ, Burnett AM, Engebretsen KM. 2C or not 2C: phenethylamine designer drug review. *J Med Toxicol.* 2013;9:172-178.

[63] Wood DM, Sedefov R, Cunningham A, Dargan PI. Prevalence of use and acute toxicity associated with the use of NBOMe drugs. *Clin Toxicol (Phila).* 2015;53:85-92.

[64] King LA, Kicman AT. A brief history of 'new psychoactive substances'. *Drug Test Anal.* 2011;3:401-403.

[65] Barrett PA, Caldwell AG, Walls LP. Treatment of depression with benzylpiperazine. United States Patent. 1968;3(401):224.

[66] Sainsbury PD, Kicman AT, Archer RP, King LA, Braithwaite RA. Aminoindanes - the next wave of 'legal highs'? *Drug Test Anal.* 2011;3:479-482.

[67] Lukić V, Micić R, Arsić B, Nedović B, Radosavljević Ž. Overview of the major classes of new psychoactive substances, psychoactive effects, analytical determination and conformational analysis of selected illegal drugs. *Open Chemistry*. 2021;19: 60-106.

[68] Araújo AM, Carvalho F, de Lourdes Bastos M, Guedes de Pinho P, Carvalho M. The hallucinogenic world of tryptamines: an updated review. *Arch Toxicol.* 2015;89:1151-1173.

[69] United Nations Office on Drugs and Crime. Tryptamines. Available at: https://www.unodc.org/LSS/SubstanceGroup/Details/68c027b6-0ed9-4c07-a139-7f1ca7ffce84. Date accessed: March 28, 2024.

[70] United States Drug Enforcement Administration (DEA). Facts About Fentanyl. Available at: https://www.dea.gov/resources/facts-about-fentanyl. Date accessed: March 30, 2024.

[71] European Monitoring Centre for Drugs and Drug Addiction. Spotlight on… Fentanils and other new opioids. Available at: https://www.emcdda.europa.eu/spotlights/fentanils-and-other-new-opioids_en. Date accessed: March 30, 2024.

[72] Spencer MR, Garnett MF, Miniño AM. Drug overdose deaths in the United States, 2002–2022. National Center for Health Statistics (NCHS) Data Brief, No 491. Hyattsville, Maryland: National Center for Health Statistics. 2024. DOI: 10.15620/cdc:135849.

[73] Casale JF, Mallette JR, Guest EM. Analysis of illicit carfentanil: Emergence of the death dragon. *Forensic Chem*. 2017;3:74-80.

[74] George AV, Lu JJ, Pisano MV, Metz J, Erickson TB. Carfentanil - an ultra potent opioid. *Am J Emerg Med*. 2010;28:530-532.

[75] Rzasa Lynn R, Galinkin JL. Naloxone dosage for opioid reversal: current evidence and clinical implications. *Ther Adv Drug Saf*. 2018;9:63-88.

[76] Zawilska JB, Wojcieszak J. An expanding world of new psychoactive substances-designer benzodiazepines. *Neurotoxicology*. 2019;73:8-16.

[77] European Monitoring Centre for Drugs and Drug Addiction. New benzodiazepines in Europe – a review. 2021; Luxembourg: Publications Office of the European Union.

[78] Gudin JA, Mogali S, Jones JD, Comer SD. Risks, management, and monitoring of combination opioid, benzodiazepines, and/or alcohol use. *Postgrad Med*. 2013;125:115-130.

[79] McAuley A, Matheson C, Robertson JR. From the clinic to the street: the changing role of benzodiazepines in the Scottish overdose epidemic. *Int J Drug Policy*. 2022;100:103512. DOI: 10.1016/j.drugpo.2021.103512.

[80] United Nations Office on Drugs and Crime. Phencyclidine-type substances. Available at: https://www.unodc.org/LSS/SubstanceGroup/Details/6bf165ed-82e7-47e0-9eaa-daacc42d99cd. Date accessed: March 25, 2024.

[81] Dillon P, Copeland J, Jansen K. Patterns of use and harms associated with non-medical ketamine use. *Drug Alcohol Depend.* 2003;69:23-28.

[82] Senn Ch, Bücheli A, Schaub M, Stohler R. Partydrogen [Club drugs]. *Ther Umsch.* 2007;64:109-13. In German.

[83] Stern E, Lambert DM. Medicinal chemistry endeavors around the phytocannabinoids. *Chem Biodivers*. 2007;4:1707-1728.

[84] Titishov N, Mechoulam R, Zimmerman AM. Stereospecific Effects of (-)- and (+)-7-Hydroxy-Delta-6-Tetrahydrocannabinol-Dimethylheptyl on the Immune System of Mice. *Pharmacology.* 1989;39:337-349.

[85] Weissman A, Milne GM, Melvin LS Jr. Cannabimimetic activity from CP-47,497, a derivative of 3-phenylcyclohexanol. *J Pharmacol Exp Ther*. 1982;223:516-523.

[86] United Nations Office on Drugs and Crime. Synthetic cannabinoids. 2024. Available at: https://www.unodc.org/LSS/SubstanceGroup/Details/ae45ce06-6d33-4f5f-916a-e873f07bde02. Date accessed: March 25, 2024.

[87] D'Ambra TE, Estep KG, Bell MR, et al. Conformationally restrained analogues of pravadoline: nanomolar potent, enantioselective, (aminoalkyl)indole agonists of the cannabinoid receptor. *J Med Chem.* 1992;35:124-135.

[88] Kuster JE, Stevenson JI, Ward SJ, D'Ambra TE, Haycock DA. Aminoalkylindole binding in rat cerebellum: selective displacement by natural and synthetic cannabinoids. *J Pharmacol Exp Ther.* 1993;264:1352-1363.

[89] Huffman JW, Dai D, Martin B, Compton DR. Design, synthesis and pharmacology of cannabi-mimetic indoles. *Bioorg. Med. Chem. Lett.* 1994;4:563-566.

[90] Aung MM, Griffin G, Huffman JW, et al. Influence of the N-1 alkyl chain length of cannabimimetic indoles upon CB_1 and CB_2 receptor binding. *Drug Alcohol Depend.* 2000;60:133-140.

[91] Fantegrossi WE, Moran JH, Radominska-Pandya A, Prather PL. Distinct pharmacology and metabolism of K2 synthetic cannabinoids compared to Δ^9-THC: Mechanism underlying greater toxicity? *Life Sci.* 2014;97:45-54.

[92] Makriyannis A, Deng, H. Cannabimimetic Indole Derivatives. 2001. Patent WO 01/28557 A1.

[93] Buchler IP, Hayes MJ, Hedge SG, et al. Indazole Derivatives. 2009. Patent WO 2009/106982 A1.

[94] Auwärter V, Dresen S, Weinmann W, Müller M, Pütz M, Ferreirós N. 'Spice' and other herbal blends: harmless incense or cannabinoid designer drugs? *J Mass Spectrom.* 2009;44:832-837.

[95] Uchiyama N, Kikura-Hanajiri R, Kawahara N, Haishima Y, Goda Y. Identification of a Cannabinoid Analog as a New Type of Designer Drug in a Herbal Product. *Chem Pharm Bull.* 2009;57:439-441.

[96] Seely KA, Patton AL, Moran CL, et al. Forensic investigation of K2, Spice, and "bath salt" commercial preparations: A three-year study of new designer drug products containing synthetic cannabinoid, stimulant, and hallucinogenic compounds. *Forensic Sci Int*. 2013;233:416-422.

[97] Zuba D, Byrska B. Analysis of the prevalence and coexistence of synthetic cannabinoids in "herbal high" products in Poland. *Forensic Toxicol.* 2013;31:21–30.

[98] Chung H, Choi H, Heo S, Kim E, Lee J. Synthetic cannabinoids abused in South Korea: drug identifications by the National Forensic Service from 2009 to June 2013. *Forensic Toxicol.* 2014;32:82-88.

[99] Langer N, Lindigkeit R, Schiebel HM, Ernst L, Beuerle T. Identification and quantification of synthetic cannabinoids in 'spice-like' herbal mixtures: A snapshot of the German situation in the autumn of 2012. *Drug Test Anal.* 2014;6:59-71.

[100] European Monitoring Centre for Drugs and Drug Addiction. Synthetic cannabinoids in Europe – a review. 2021; Luxembourg: Publications Office of the European Union.

[101] Tettey JNA, Crean C, Rodrigues J, et al. United Nations Office on Drugs and Crime: Recommended methods for the Identification and Analysis of Synthetic Cannabinoid Receptor Agonists in Seized Materials. *Forensic Sci Int Synerg.* 2021;3:100129. DOI: 10.1016/j.fsisyn.2020.11.003.

[102] Uchiyama N, Matsuda S, Kawamura M, et al. Two new-type cannabimimetic quinolinyl carboxylates, QUPIC and QUCHIC, two new cannabimimetic carboxamide derivatives, ADB-FUBINACA and ADBICA, and five synthetic cannabinoids detected with a thiophene derivative α-PVT and an opioid receptor agonist AH-7921 identified in illegal products. *Forensic Toxicol.* 2013;31:223–240.

[103]   Grigoryev A, Kavanagh P, Melnik A, Savchuk S, Simonov A. Gas and liquid chromatography-mass spectrometry detection of the urinary metabolites of UR-144 and its major pyrolysis product. *J Anal Toxicol.* 2013;37:265-276.

[104]   Adamowicz P, Zuba D, Sekuła K. Analysis of UR-144 and its pyrolysis product in blood and their metabolites in urine. *Forensic Sci Int.* 2013;233:320-327.

[105]   Thomas BF, Lefever TW, Cortes RA, et al. Thermolytic Degradation of Synthetic Cannabinoids: Chemical Exposures and Pharmacological Consequences. *J Pharmacol Exp Ther.* 2017;361:162-171.

[106]   Franz F, Angerer V, Hermanns-Clausen M, Auwärter V, Moosmann B. Metabolites of synthetic cannabinoids in hair - proof of consumption or false friends for interpretation? *Anal Bioanal Chem*. 2016;408:3445-3452.

[107]   Kevin RC, Kovach AL, Lefever TW, Gamage TF, Wiley JL, McGregor IS, Thomas BF. Toxic by design? Formation of thermal degradants and cyanide from carboxamide-type synthetic cannabinoids CUMYL-PICA, 5F-CUMYL-PICA, AMB-FUBINACA, MDMB-FUBINACA, NNEI, and MN-18 during exposure to high temperatures. *Forensic Toxicol.* 2019;37:17-26.

[108]   Baker R. Temperature distribution inside a burning cigarette. *Nature.* 1974;247:405–406.

[109]   Pulver B, Fischmann S, Gallegos A, Christie R. EMCDDA framework and practical guidance for naming synthetic cannabinoids. *Drug Test Anal.* 2023;15:255-276.

[110]   Andrews R, Jorge R, Christie R, Gallegos A. From JWH-018 to OXIZIDS: Structural evolution of synthetic cannabinoids in the European Union from 2008 to present day. *Drug Test Anal.* 2023;15:378-387.

[111]   Teske J, Weller JP, Fieguth A, Rothämel T, Schulz Y, Tröger HD. Sensitive and rapid quantification of the cannabinoid receptor agonist naphthalen-1-yl-(1-pentylindol-3-yl)methanone (JWH-018) in human serum by liquid chromatography-tandem mass spectrometry. *J Chromatogr B*. 2010; 878:2659-2663.

[112]   Castaneto MS, Wohlfarth A, Desrosiers NA, Hartman RL, Gorelick DA, Huestis MA. Synthetic cannabinoids pharmacokinetics and detection methods in biological matrices. *Drug Metab Rev.* 2015;47:124-174.

[113]   Toennes SW, Geraths A, Pogoda W, et al. Pharmacokinetic properties of the synthetic cannabinoid JWH-018 in oral fluid after inhalation. *Drug Test Anal*. 2018;10:644-650.

[114]   Toennes SW, Geraths A, Pogoda W, et al. Excretion of metabolites of the synthetic cannabinoid JWH-018 in urine after controlled inhalation. *J Pharm Biomed Anal.* 2018;150:162-168.

[115]   Toennes SW, Geraths A, Pogoda W, et al. Pharmacokinetic properties of the synthetic cannabinoid JWH-018 and of its metabolites in serum after inhalation. *J Pharm Biomed Anal.* 2017;140:215-222.

[116]   Schaefer N, Peters B, Bregel D, Maurer HH, Schmidt PH, Ewald AH. Can JWH-210 and JWH-122 be detected in adipose tissue four weeks after single oral drug administration to rats? *Biomed Chromatogr.* 2014;28:1043-1047.

[117]   Saito T, Namera A, Miura N, *et al.* A fatal case of MAM-2201 poisoning. *Forensic Toxicol.* 2013; 31:333–337.

[118]   Wohlfarth A, Gandhi AS, Pang S, Zhu M, Scheidweiler KB, Huestis MA. Metabolism of synthetic cannabinoids PB-22 and its 5-fluoro analog, 5F-PB-22, by human hepatocyte incubation and high-resolution mass spectrometry. *Anal Bioanal Chem*. 2014;406:1763-1780.

[119]   Mogler L, Franz F, Rentsch D, et al. Detection of the recently emerged synthetic cannabinoid 5F-MDMB-PICA in 'legal high' products and human urine samples. *Drug Test Anal*. 2018;10:196-205.

[120]   Truver MT, Watanabe S, Åstrand A, et al. 5F-MDMB-PICA metabolite identification and cannabinoid receptor activity. *Drug Test Anal.* 2020;12:127-135.

[121]   Watanabe S, Vikingsson S, Åstrand A, Gréen H, Kronstrand R. Biotransformation of the New Synthetic Cannabinoid with an Alkene, MDMB-4en-PINACA, by Human Hepatocytes, Human Liver Microsomes, and Human Urine and Blood. *AAPS J.* 2019;22:13. DOI: 10.1208/s12248-019-0381-3.

[122]   Erol Ozturk Y, Yeter O. In Vitro Phase I Metabolism of the Recently Emerged Synthetic MDMB-4en-PINACA and Its Detection in Human Urine Samples. J Anal Toxicol. 2021;44:976-984.

[123] Krotulski AJ, Cannaert A, Stove C, Logan BK. The next generation of synthetic cannabinoids: Detection, activity, and potential toxicity of pent-4en and but-3en analogues including MDMB-4en-PINACA. *Drug Test Anal.* 2021;13:427-438.

[124] Kronstrand R, Norman C, Vikingsson S, et al. The metabolism of the synthetic cannabinoids ADB-BUTINACA and ADB-4en-PINACA and their detection in forensic toxicology casework and infused papers seized in prisons. *Drug Test Anal.* 2022;14:634-652.

[125] Mogler L, Wilde M, Huppertz LM, Weinfurtner G, Franz F, Auwärter V. Phase I metabolism of the recently emerged synthetic cannabinoid CUMYL-PEGACLONE and detection in human urine samples. *Drug Test Anal.* 2018;10:886-891.

[126] Mogler L, Halter S, Wilde M, Franz F, Auwärter V. Human phase I metabolism of the novel synthetic cannabinoid 5F-CUMYL-PEGACLONE. *Forensic Toxicol.* 2019;37:154-163.

[127] Sobolevskii TG, Prasolov IS, Rodchenkov GM. Application of mass spectrometry to the structural identification of the metabolites of the synthetic cannabinoid JWH-018 and the determination of them in human urine. *J Anal Chem*. 2011;66:1314–1323.

[128] Chimalakonda KC, Bratton SM, Le VH, et al. Conjugation of synthetic cannabinoids JWH-018 and JWH-073, metabolites by human UDP-glucuronosyltransferases. *Drug Metab Dispos.* 2011; 39:1967-1976.

[129] Erratico C, Negreira N, Norouzizadeh H, et al. In vitro and in vivo human metabolism of the synthetic cannabinoid AB-CHMINACA. *Drug Test Anal.* 2015;7:866-876.

[130] Carlier J, Diao X, Wohlfarth A, Scheidweiler K, Huestis MA. *In Vitro* Metabolite Profiling of ADB-FUBINACA, A New Synthetic Cannabinoid. *Curr Neuropharmacol.* 2017;15:682-691.

[131] Kavanagh P, Grigoryev A, Krupina N. Detection of metabolites of two synthetic cannabimimetics, MDMB-FUBINACA and ADB-FUBINACA, in authentic human urine specimens by accurate mass LC–MS: a comparison of intersecting metabolic patterns. *Forensic Toxicol.* 2017;35:284–300.

[132] Grigoryev A, Kavanagh P, Pechnikov A. Human urinary metabolite pattern of a new synthetic cannabimimetic, methyl 2-(1-(cyclohexylmethyl)-1*H*-indole-3-carboxamido)-3,3-dimethyl-butanoate. *Forensic Toxicol.* 2016;34:316-328.

[133] Castiglioni S, Zuccato E, Chiabrando C, Fanelli R, Bagnati R. Mass spectrometric analysis of illicit drugs in wastewater and surface water. *Mass Spectrom Rev.* 2008;27:378-394.

[134] Tai S, Fantegrossi WE. Synthetic Cannabinoids: Pharmacology, Behavioral Effects, and Abuse Potential. *Curr Addict Rep*. 2014;1:129-136.

[135] Adamowicz P. Fatal intoxication with synthetic cannabinoid MDMB-CHMICA. *Forensic Sci Int.* 2016;261:e5-e10. DOI: 10.1016/j.forsciint.2016.02.024.

[136] Banister SD, Longworth M, Kevin R, et al. Pharmacology of Valinate and tert-Leucinate Synthetic Cannabinoids 5F-AMBICA, 5F-AMB, 5F-ADB, AMB-FUBINACA, MDMB-FUBINACA, MDMB-CHMICA, and Their Analogues. *ACS Chem Neurosci.* 2016;7:1241-1254.

[137] Groth O, Roider G, Angerer V, et al. "Spice"-related deaths in and around Munich, Germany: A retrospective look at the role of synthetic cannabinoid receptor agonists in our post-mortem cases over a seven-year period (2014-2020). *Int J Legal Med.* 2023;137:1059-1069.

[138] Yoganathan P, Claridge H, Chester L, Englund A, Kalk NJ, Copeland CS. Synthetic Cannabinoid-Related Deaths in England, 2012-2019. *Cannabis Cannabinoid Res*. 2022;7:516-525.

[139] Hasegawa K, Wurita A, Minakata K, et al. Identification and quantitation of 5-fluoro-ADB, one of the most dangerous synthetic cannabinoids, in the stomach contents and solid tissues of a human cadaver and in some herbal products. *Forensic Toxicol.* 2015;33:112–121.

[140] Kleis J, Germerott T, Halter S, et al. The synthetic cannabinoid 5F-MDMB-PICA: A case series. *Forensic Sci Int.* 2020;314:110410. DOI: 10.1016/j.forsciint.2020.110410.

[141] World Health Organization (WHO). Critical Review Report: 5F-MDMB-PICA. Expert Committee on Drug Dependence, Forty-second Meeting. 2019; Geneva. Available at: https://researchonline.ljmu.ac.uk/id/eprint/11446/1/ECDD42_5F-MDMB-PICA.pdf. Date accessed: January 25, 2024.

[142] Halter S, Angerer V, Röhrich J, et al. Cumyl-PEGACLONE: A comparatively safe new synthetic cannabinoid receptor agonist entering the NPS market? *Drug Test Anal.* 2019;11:347-349.

[143] Zagzoog A, Brandt AL, Black T, et al. Assessment of select synthetic cannabinoid receptor agonist bias and selectivity between the type 1 and type 2 cannabinoid receptor. *Sci Rep*. 2021;11:10611. DOI: 10.1038/s41598-021-90167-w.

[144] Patel M, Manning JJ, Finlay DB, et al. Signalling profiles of a structurally diverse panel of synthetic cannabinoid receptor agonists. *Biochem Pharmacol.* 2020;175:113871. DOI: 10.1016/j.bcp. 2020.113871.

[145] Sparkes E, Cairns EA, Kevin RC, et al. Structure-activity relationships of valine, *tert*-leucine, and phenylalanine amino acid-derived synthetic cannabinoid receptor agonists related to ADB-BUTINACA, APP-BUTINACA, and ADB-P7AICA. *RSC Med Chem*. 2021;13:156-174.

[146] Wilkinson SM, Banister SD, Kassiou M. Bioisosteric Fluorine in the Clandestine Design of Synthetic Cannabinoids. *Aust J Chem.* 2015;68:4-8.

[147] Brents LK, Reichard EE, Zimmerman SM, Moran JH, Fantegrossi WE, Prather PL. Phase I Hydroxylated Metabolites of the K2 Synthetic Cannabinoid JWH-018 Retain *In Vitro* and *In Vivo* Cannabinoid 1 Receptor Affinity and Activity. *PLoS ONE*. 2011;6:e21917. DOI: 0.1371/journal. pone.0021917.

[148] Brents LK, Gallus-Zawada A, Radominska-Pandya A, et al. Monohydroxylated metabolites of the K2 synthetic cannabinoid JWH-073 retain intermediate to high cannabinoid 1 receptor (CB1R) affinity and exhibit neutral antagonist to partial agonist activity. *Biochem Pharmacol.* 2012; 83:952-961.

[149] Antonides LH, Cannaert A, Norman C, et al. Shape matters: The application of activity-based in vitro bioassays and chiral profiling to the pharmacological evaluation of synthetic cannabinoid receptor agonists in drug-infused papers seized in prisons. *Drug Test Anal.* 2021;13:628-643.

[150] EMCDDA. Report on the risk assessment of methyl 2-[[1-(cyclohexylmethyl)-1*H*-indole-3-carbonyl]amino]-3,3-dimethylbutanoate (MDMB-CHMICA) in the framework of the Council Decision on new psychoactive substances. 2016; Luxembourg: Publications Office of the European Union. DOI: 10.2810/964776.

[151] EMCDDA. Report on the risk assessment of methyl 2-{[1-(5-fluoropentyl)-1*H*-indazole-3-carbonyl]amino}-3,3-dimethylbutanoate (5F-MDMB-PINACA) in the framework of the Council Decision on new psychoactive substances. 2018; Luxembourg: Publications Office of the European Union. DOI: 10.2810/868403.

[152] EMCDDA. Report on the risk assessment of methyl 3,3-dimethyl-2-{[1-(pent-4-en-1-yl)-1*H*-indazole-3-carbonyl]amino}butanoate (MDMB-4en-PINACA) in accordance with Article 5c of Regulation (EC) No 1920/2006 (as amended). 2022; Luxembourg: Publications Office of the European Union. DOI: 10.2810/007489.

[153] EMCDDA. Report on the risk assessment of methyl 2-{[1-(4-fluorobutyl)-1*H*-indole-3-carbonyl]amino}-3,3-dimethylbutanoate (4F-MDMB-BICA) in accordance with Article 5c of Regulation (EC) No 1920/2006 (as amended). 2022; Luxembourg: Publications Office of the European Union. DOI: 10.2810/398973.

[154] World Health Organization (WHO). Critical review report: ADB-BUTINACA. Expert Committee on Drug Dependence, Forty-fifth Meeting. 2022; Geneva. Available at: https://cdn.who.int/media/docs/default-source/controlled-substances/45th-ecdd/adb-butinaca_draft.pdf?sfvrsn=89c83ba5_1. Date accessed: January 25, 2024.

[155] Theunissen EL, Hutten NRPW, Mason NL, et al. Neurocognition and subjective experience following acute doses of the synthetic cannabinoid JWH-018: a phase 1, placebo-controlled, pilot study. *Br J Pharmacol.* 2018;175:18-28.

[156] Bavarian State Criminal Police Office, Forensic Science Institute. Internal data from the casework.

[157] Moosmann B, Angerer V, Auwärter V. Inhomogeneities in herbal mixtures: a serious risk for consumers. *Forensic Toxicol.* 2015;33:54-60.

[158] Schäper J. Wirkstoffgehalte und inhomogene Verteilung des Wirkstoffs MDMB-CHMICA in Kräutermischungen. *Toxichem Krimtech.* 2016;83:112–114.

[159] Frinculescu A, Lyall CL, Ramsey J, Miserez B. Variation in commercial smoking mixtures containing third-generation synthetic cannabinoids. *Drug Test Anal.* 2017;9:327-333.

Chapter 1

[160]   Norman C, Walker G, McKirdy B, et al. Detection and quantitation of synthetic cannabinoid receptor agonists in infused papers from prisons in a constantly evolving illicit market. *Drug Test Anal*. 2020;12:538-554.

[161]   Adams AJ, Banister SD, Irizarry L, Trecki J, Schwartz M, Gerona R. "Zombie" Outbreak Caused by the Synthetic Cannabinoid AMB-FUBINACA in New York. *N Engl J Med.* 2017;376:235-242.

[162]   Monte AA, Bronstein AC, Cao DJ, et al. An outbreak of exposure to a novel synthetic cannabinoid. *N Engl J Med*. 2014;370:389-390.

[163]   Note on outbreak of intoxications suspected to be caused by legal high product name „Mocarz" in Poland. 2015. Available at: https://legal-high-inhaltsstoffe.de/sites/default/files/uploads/information_mocarz.pdf.   Date accessed: January 25, 2024.

[164]   Hermanns-Clausen M, Kithinji J, Spehl M, et al. Adverse effects after the use of JWH-210 - a case series from the EU Spice II plus project. *Drug Test Anal.* 2016;8:1030-1038.

[165]   Kraemer M, Fels H, Dame T, et al. Mono-/polyintoxication with 5F-ADB: A case series. *Forensic Sci Int*. 2019;301:e29-e37.

[166]   Neukamm MA, Halter S, Auwärter V, Schmitt G, Giorgetti A, Bartel M. Death after smoking of fentanyl, 5F-ADB, 5F-MDMB-P7AICA and other synthetic cannabinoids with a bucket bong. *Forensic Toxicol*. 2024;42:82-92.

[167]   Tokarczyk B, Jurczyk A, Krupińska J, Adamowicz P. Fatal intoxication with new synthetic cannabinoids 5F-MDMB-PICA and 4F-MDMB-BINACA - parent compounds and metabolite identification in blood, urine and cerebrospinal fluid. *Forensic Sci Med Pathol.* 2022;18:393-402.

[168]   Goncalves R, Labadie M, Chouraqui S, et al. Involuntary MDMB-4en-PINACA intoxications following cannabis consumption: clinical and analytical findings. *Clin Toxicol*. 2022;60:458-463.

[169]   Simon G, Kuzma M, Mayer M, Petrus K, Tóth D. Fatal Overdose with the Cannabinoid Receptor Agonists MDMB-4en-PINACA and 4F-ABUTINACA: A Case Report and Review of the Literature. *Toxics.* 2023;11:673. DOI: 10.3390/toxics11080673.

[170]   Simon G, Tóth D, Heckmann V, Mayer M, Kuzma M. Simultaneous fatal poisoning of two victims with 4F-MDMB-BINACA and ethanol. *Forensic Toxicol.* 2023;41:151-157.

[171]   Doerr AA, Walle N, Heinbuch S, Potente S, Schmidt PH, Schaefer N. Deadly mono-intoxication after ingestion of 4F-MDMB-BICA. *Ann Toxicol Anal.* 2022;34:S46-S47.

[172]   Tokarczyk B, Suchan M, Adamowicz P. New Synthetic Cannabinoid ADB-BUTINACA-Related Death of a Police Dog. *J Anal Toxicol.* 2023;47:e23-e28.

[173]   European Monitoring Centre for Drugs and Drug Addiction (EMCDDA). New psychoactive substances in prison. Results from an EMCDDA trendspotter study. 2018; Luxembourg: Publications Office of the European Union. DOI: 10.2810/7247.

[174]   Alipour A, Patel PB, Shabbir Z, Gabrielson S. Review of the many faces of synthetic cannabinoid toxicities. *Ment Health Clin.* 2019;9:93-99.

[175]   Gurney SM, Scott KS, Kacinko SL, Presley BC, Logan BK. Pharmacology, Toxicology, and Adverse Effects of Synthetic Cannabinoid Drugs. *Forensic Sci Rev*. 2014;26:53-78.

[176]   Seely KA, Lapoint J, Moran JH, Fattore L. Spice drugs are more than harmless herbal blends: A review of the pharmacology and toxicology of synthetic cannabinoids. *Prog Neuropsychopharmacol Biol Psychiatry.* 2012;39:234-243.

[177]   Henquet C, Krabbendam L, Spauwen J, et al. Prospective cohort study of cannabis use, predisposition for psychosis, and psychotic symptoms in young people. BMJ. 2004;330:11. DOI: 10.1136/bmj.38267.664086.63.

[178]   The Centre for Social Justice. Drugs in Prison. 2015. Available at: https://www.centreforsocialjustice.org.uk/wp-content/uploads/2015/03/CSJJ3090_Drugs_in_Prison.pdf. Date accessed: January 21, 2024.

[179]   Bundesgesetzblatt. 22. Verordnung zur Änderung betäubungsmittelrechtlicher Vorschriften. BGBl. 2009 Jahrgang 2009 Teil I Nr. 3, 49-50.

[180]   Bundesgesetzblatt. 24. Verordnung zur Änderung betäubungsmittelrechtlicher Vorschriften. BGBl. 2009 Jahrgang 2009 Teil I Nr. 80, 3944-3945.

[181] Bundesgesetzblatt. 26. Verordnung zur Änderung betäubungsmittelrechtlicher Vorschriften. BGBl. 2012 Jahrgang 2012 Teil I Nr. 35, 1639-1641.

[182] Bundesgesetzblatt. 27. Verordnung zur Änderung betäubungsmittelrechtlicher Vorschriften. BGBl. 2013 Teil I Nr. 37, 2274-2275.

[183] Bundesgesetzblatt. 28. Verordnung zur Änderung betäubungsmittelrechtlicher Vorschriften. BGBl. 2014 Jahrgang 2014 Teil I Nr. 57, 1999-2002.

[184] Bundesgesetzblatt. 29. Verordnung zur Änderung betäubungsmittelrechtlicher Vorschriften. BGBl. 2015 Teil I Nr. 19, 723-724.

[185] Bundesgesetzblatt. 30. Verordnung zur Änderung betäubungsmittelrechtlicher Vorschriften. BGBl. 2015 Teil I Nr. 45, 1992-1993.

[186] Bundesgesetzblatt. 31. Verordnung zur Änderung betäubungsmittelrechtlicher Vorschriften. BGBl. 2016 Jahrgang 2016 Teil I Nr. 26, 1282-1283.

[187] Bundesgesetzblatt. 18. Verordnung zur Änderung von Anlagen des Betäubungsmittelgesetzes. BGBl. 2017 Teil I Nr. 38, 1670-1671.

[189] Bundesgesetzblatt. Verordnung zur Änderung betäubungsmittelrechtlicher und anderer Vorschriften. BGBl. 2018 Teil I Nr. 24, 1078-1079.

[190] Bundesgesetzblatt. Verordnung zur Änderung der Anlage des Neue-psychoaktive-Stoffe-Gesetzes und von Anlagen des Betäubungsmittelgesetzes. BGBl. 2019 Teil I Nr. 27, 1083-1094.

[191] Bundesgesetzblatt. 20. Verordnung zur Änderung von Anlagen des Betäubungsmittelgesetzes. BGBl. 2020 Teil I Nr. 35, 1691.

[192] Bundesgesetzblatt. 21. Verordnung zur Änderung von Anlagen des Betäubungsmittelgesetzes. BGBl. 2021, Teil I Nr. 2, 70.

[193] Bundesgesetzblatt. 32. Verordnung zur Änderung betäubungsmittelrechtlicher Vorschriften. BGBl. 2021 Teil I Nr. 24, 1096-1097.

[194] Bundesgesetzblatt. 22. Verordnung zur Änderung von Anlagen des Betäubungsmittelgesetzes. BGBl. 2021 Teil I Nr. 77, 4791.

[196] Buchler IP, Hayes MJ, Hedge SG, et al. Indazole Derivatives. 2009. Patent WO 2009/106980 A2.

[197] Bundesgesetzblatt. Vierte Verordnung zur Änderung der Anlage des Neue-psychoaktive-Stoffe-Gesetzes (4. NpSGAnlÄndV). BGBl. 2023 Teil I Nr. 69, Geltung ab 16.03.2023.

[198] United Kingdom's Government. 001/2024: The Misuse of Drugs Act 1971 (Amendment) Order 2024 and The Misuse of Drugs and Misuse of Drugs (Designation) (England and Wales and Scotland) (Amendment and Revocation) Regulations 2024. Published March 20, 2024. Available at: https://www.gov.uk/government/publications/circular-0012024-control-of-20-new-drugs/0012024-the-misuse-of-drugs-act-1971-amendment-order-2024-and-the-misuse-of-drugs-and-misuse-of-drugs-designation-england-and-wales-and-scotlan.

[199] United Kingdom's Government. Psychoactive Substances Act 2016. Available at: https://www.gov.uk/government/collections/psychoactive-substances-bill-2015. Date accessed: April 25, 2024.

[200] Bundesgesetz über den Schutz vor Gesundheitsgefahren im Zusammenhang mit Neuen Psychoaktiven Substanzen (Neue-Psychoaktive-Substanzen-Gesetz, NPSG). Available at: https://www.ris.bka.gv.at/GeltendeFassung.wxe?Abfrage=Bundesnormen&Gesetzesnummer=20007605. Date accessed: April 25, 2024.

[201] Smith H, Forshufvud S, Wassén A. Distribution of Arsenic in Napoleon's Hair. *Nature* 1962; 194:725-726.

[202] Springfield AC, Cartmell LW, Aufderheide AC, Buikstra J, Ho J. Cocaine and metabolites in the hair of ancient Peruvian coca leaf chewers. *Forensic Sci Int.* 1993;63:269-275.

[203] Casper JL. *Practisches Handbuch der Gerichtlichen Medicin.* 2 Band. Berlin, August Hirschwald; 1860: 440-441.

[204] Goldblum RW, Goldbaum LR, Piper WN. Barbiturate concentrations in the skin and hair of guinea pigs. *J Invest Dermatol*. 1954;22:121-128.

[205] Baumgartner AM, Jones PF, Baumgartner WA, Black CT. Radioimmunoassay of hair for determining opiate-abuse histories. *J Nucl Med.* 1979;20:748-752.

[206] Klug, E. Zur Morphinbestimmung in Kopfhaaren. *Z Rechtsmed* 1980;84:189-193.

[207]   Kintz P. *Analytical and Practical Aspects of Drug Testing in Hair.* Boca Raton: Taylor & Francis Group, CRC Press; 2007.

[208]   Wiedfeld C, Skopp G, Musshoff F. Single hair analysis: Validation of a screening method for over 150 analytes and application on documented single-dose cases. *Drug Test Anal.* 2021;13:817-832.

[209]   Society of Hair Testing Website: http://www.soht.org.

[210]   Paus R, Foitzik K. In search of the "hair cycle clock": a guided tour. *Differentiation*. 2004;72:489-511.

[211]   Paus R, Arck P, Tiede S. (Neuro-)endocrinology of epithelial hair follicle stem cells. *Mol Cell Endocrinol*. 2008;288:38-51.

[212]   Pragst F, Balikova MA. State of the art in hair analysis for detection of drug and alcohol abuse. *Clin Chim Acta.* 2006;370:17-49.

[213]   Kintz P, Salomone A, Vincenti M. *Hair Analysis in Clinical and Forensic Toxicology*. 1st ed. Amsterdam: Academic Press (Elsevier Inc.); 2015.

[214]   Madea B, Mußhoff F. *Haaranalytik. Technik und Interpretation in Medizin und Recht.* Köln: Dt. Ärzte-Verl.; 2004.

[215]   Buffoli B, Rinaldi F, Labanca M, et al. The human hair: from anatomy to physiology. *Int J Dermatol.* 2014;53:331-341.

[216]   Robbins CR. *Chemical and Physical Behavior of Human Hair.* 4th ed. New York: Springer-Verlag; 2002.

[217]   Harkey MR. Anatomy and physiology of hair. *Forensic Sci Int.* 1993;63:9-18.

[218]   Prota G. Melanins, melanogenesis and melanocytes: looking at their functional significance from the chemist's viewpoint. *Pigment Cell Res*. 2000;13:283-293.

[219]   Boumba VA, Ziavrou KS, Vougiouklakis T. Hair as a biological indicator of drug use, drug abuse or chronic exposure to environmental toxicants. *Int J Toxicol.* 2006;25:143-163.

[220]   Favretto D, Cooper G, Andraus M, et al. The Society of Hair Testing consensus on general recommendations for hair testing and drugs of abuse testing in hair. *Drug Test Anal.* 2023; 15:1042-1046.

[221]   United Nations Office on Drugs and Crime. Guidelines for Testing Drugs under International Control in Hair, Sweat and Oral Fluid. 2014; Vienna, United Nations publication, ST/NAR/30/Rev.3.

[222]   Henderson GL. Mechanisms of drug incorporation into hair. *Forensic Sci Int*. 1993;63:19-29.

[223]   Touitou E, Fabin B, Dany S, Almog S. Transdermal delivery of tetrahydrocannabinol. *Int J Pharm.* 1988;43:9-15.

[224]   Vree TB, Muskens AT, van Rossum JM. Excretion of Amphetamines in Human Sweat. *Arch Int Pharmacodyn Ther.* 1972;199:311-317.

[225]   Smith FP, Liu RH. Detection of Cocaine Metabolite in Perspiration Stain, Menstrual Bloodstain, and Hair. *J Forensic Sci.* 1986;31:1269-1273.

[226]   Perez-Reyes M, Di Guiseppi S, Brine DR, Smith H, Cook CE. Urine pH and phencylidine excretion. *Clin Pharmacol Ther.* 1982;32:635-641.

[227]   Henderson GL, Wilson BK. Excretion of methadone and metabolites in human sweat. *Res Commun Chem Pathol Pharmacol.* 1973;5:1-8.

[228]   Röhrich J, Zörntlein S, Pötsch L, Skopp G, Becker J. Effect of the shampoo Ultra Clean on drug concentrations in human hair. *Int J Legal Med.* 2000;113:102-106.

[229]   Nakahara Y, Takahashi K, Kikura R. Hair analysis for drugs of abuse. X. Effect of physicochemical properties of drugs on the incorporation rates into hair. *Biol Pharm Bull*. 1995;18:1223-1227.

[230]   Pötsch L, Skopp G, Moeller MR. Influence of pigmentation on the codeine content of hair fibers in guinea pigs. *J Forensic Sci*. 1997;42:1095-1098.

[231]   van Erp PEJ, Jansen MJJM, de Jongh GJ, Boezeman JBM, Schalkwijk J. Ratiometric measurement of intracellular pH in cultured human keratinocytes using carboxy-SNARF-1 and flow cytometry. *Cytometry.* 1991;12:127-132.

[232]   Larsson BS. Interaction between chemicals and melanin. *Pigment Cell Res*. 1993;6:127-133.
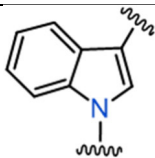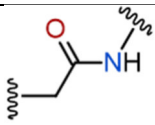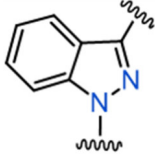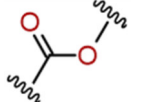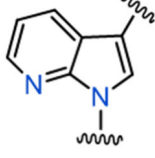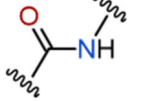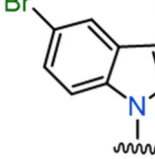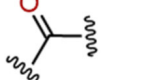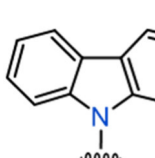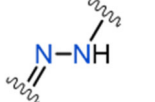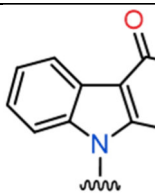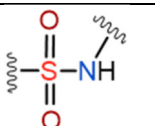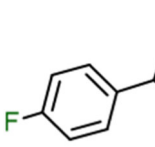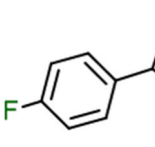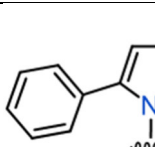
[233] Borges CR, Roberts JC, Wilkins DG, Rollins DE. Cocaine, Benzoylecgonine, Amphetamine, and *N*-Acetylamphetamine Binding to Melanin Subtypes. *J Anal Toxicol*. 2003;27:125-134.

[234] Nakahara Y, Ochiai T, Kikura R. Hair analysis for drugs of abuse. V. The facility in incorporation of cocaine into hair over its major metabolites, benzoylecgonine and ecgonine methyl ester. *Arch Toxicol.* 1992;66:446-449.

[235] Daughton CG. Illicit Drugs in Municipal Sewage, Proposed New Nonintrusive Tool to Heighten Public Awareness of Societal Use of Illicit-Abused Drugs and Their Potential for Ecological Consequences. In: Daughton CG, Jones-Lepp TL, ed. *Pharmaceuticals and Care Products in the Environment: Scientific and Regulatory Issues.* Washington, American Chemical Society; 2001.

[236] Zuccato E, Chiabrando C, Castiglioni S, et al. Cocaine in surface waters: a new evidence-based tool to monitor community drug abuse. *Environ Health*. 2005;4:14. DOI: 10.1186/1476-069X-4-14.

[237] Bijlsma L, Serrano R, Ferrer C, Tormos I, Hernández F. Occurrence and behavior of illicit drugs and metabolites in sewage water from the Spanish Mediterranean coast (Valencia region). *Sci Total Environ*. 2014;487:703-709.

[238] Haalck I, Löffler P, Baduel C, Wiberg K, Ahrens L, Lai FY. Mining chemical information in Swedish wastewaters for simultaneous assessment of population consumption, treatment efficiency and environmental discharge of illicit drugs. *Sci Rep*. 2021;11:13510. DOI: 10.1038/s41598-021-92915-4.

[239] EMCDDA. Wastewater analysis and drugs - a European multi-city study. Available at: https://www.emcdda.europa.eu/publications/html/pods/waste-water-analysis_en. Date accessed: March 11, 2024.

[240] Australian Criminal Intelligence Commission (ACIC). National Wastewater Drug Monitoring Program reports. Available at: https://www.acic.gov.au/publications/national-wastewater-drug-monitoring-program-reports. Date accessed: March 11, 2024.

[241] Rubio-Acero R, Beyerl J, Muenchhoff M, et al. Spatially resolved qualified sewage spot sampling to track SARS-CoV-2 dynamics in Munich - One year of experience. *Sci Total Environ.* 2021;797:149031. DOI: 10.1016/j.scitotenv.2021.149031.

[242] EMCDDA. Assessing illicit drugs in wastewater. Advances in wastewater-based drug epidemiology. 2016; Luxembourg: Publications Office of the European Union.

[243] SCORE network. https://score-network.eu/. Date accessed: March 11, 2024.

[244] Thomas KV, Bijlsma L, Castiglioni S, et al. Comparing illicit drug use in 19 European cities through sewage analysis. *Sci Total Environ*. 2012;432:432-439.

[245] Australian Criminal Intelligence Commission (ACIC). National Wastewater Drug Monitoring Program, Report 21. Published March 13, 2024. Available at: https://www.acic.gov.au/sites/default/files/2024-03/Wastewater%2021%20FOR%20WEB2.PDF. Date accessed: May 14, 2024.

[246] Zuccato E, Gracia-Lor E, Rousis NI, et al. Illicit drug consumption in school populations measured by wastewater analysis. *Drug Alcohol Depend*. 2017;178:285-290.

[247] Gushgari AJ, Driver EM, Steele JC, Halden RU. Tracking narcotics consumption at a Southwestern US university campus by wastewater-based epidemiology. *J Hazard Mater.* 2018;359:437-444.

[248] Postigo C, de Alda ML, Barceló D. Evaluation of drugs of abuse use and trends in a prison through wastewater analysis. *Environ Int*. 2011;37:49-55.

[249] Benaglia L, Udrisard R, Bannwarth A, et al. Testing wastewater from a music festival in Switzerland to assess illicit drug use. *Forensic Sci Int.* 2020;309:110148. DOI: 10.1016/j.forsciint.2020.110148.

[250] Castiglioni S, Bijlsma L, Covaci A, et al. Evaluation of uncertainties associated with the determination of community drug use through the measurement of sewage drug biomarkers. *Environ Sci Technol*. 2013;47:1452-1460.

[251] Lai FY, Anuj S, Bruno R, et al. Systematic and day-to-day effects of chemical-derived population estimates on wastewater-based drug epidemiology. *Environ Sci Technol.* 2015;49:999-1008.
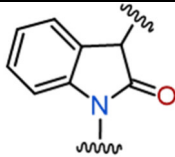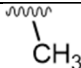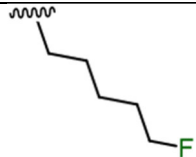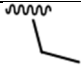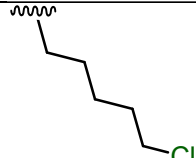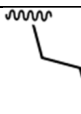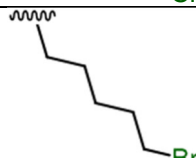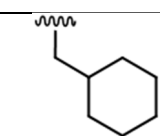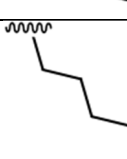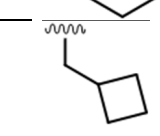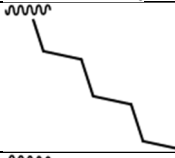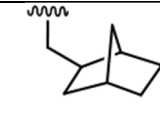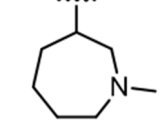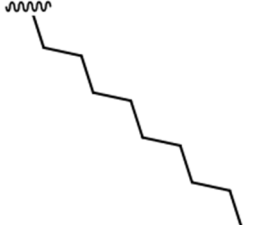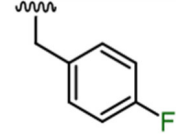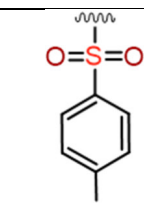
[252] Papsthart C. Waffenrecht: Waffengesetz, Beschussgesetz, Sprengstoffgesetz, Gesetz über die Kontrolle von Kriegswaffen und Durchführungsvorschriften; Textausgabe mit Sachverzeichnis und einer Einführung. 20. Auflage. München: Dt. Taschenbuch-Verl.; 2023.

[253] Klapötke TM. *Chemistry of High-Energy Materials*. 6th ed. Berlin: De Gruyter; 2022.

[254] Matyáš R, Pachman J. *Primary Explosives.* Heidelberg: Springer-Verlag; 2013.

[255] Mehta N, Oyler K, Cheng G, Shah A, Marin J, Yee K. Primary explosives. *Z Anorg Allg Chem*. 2014;640:1309-1313.

[256] Collett G. An examination of the precursor chemicals used in the manufacture of explosive compositions found within Improvised Explosive Devices (IEDs). 2021. Available at: https://aoav.org.uk/wp-content/uploads/2021/08/Precursor-chemicals_IEDs-v5.pdf. Date accessed: January 05,2024.

[257] Klapec DJ, Czarnopys G. Analysis and detection of explosives and explosives residues review: 2010 to 2013. In: *17th Interpol International Forensic Science Managers Symposium,* Lyon 8th-10th October 2013, Review Papers. 2013;280-435.

[258] Klapec DJ, Czarnopys G. Analysis and detection of explosives and explosives residues review: 2013 to 2016. In: *18th Interpol International Forensic Science Managers Symposium,* Lyon 11th-13th October 2016, Review Papers. 2016;194-261.

[259] Klapec DJ, Czarnopys G. Analysis and detection of explosives and explosives residues review: 2016 to 2019. In: *19th Interpol International Forensic Science Managers Symposium*, Lyon 8th-10th October 2019, Review Papers. 2019;194–283.

[260] Klapec DJ, Czarnopys G, Pannuto J. Interpol review of the analysis and detection of explosives and explosives residues. *Forensic Sci Int Synerg*. 2023;6:100298.
DOI: 10.1016/j.fsisyn.2022.100298.

[261] Acree F, Haller HL. Trimolecular Acetone Peroxide in Isopropyl Ether. *J Am Chem Soc.* 1943;65:1652-1652.

[262] Pye CC. Chemical safety: TATP formation in 2-Propanol. *ACS Chem Health Saf*. 2020:27;279-279.

[263] Himmelrath A. Die GSG9 und das blaue Fass. 2001, Spiegel Online. Available at: https://www.spiegel.de/lebenundlernen/uni/explosive-universitaet-bonn-die-gsg-9-und-das-blaue-fass-a-155383.html. Date accessed: March 10, 2024.

[264] Meyer R, Köhler J, Homburg A. *Explosives*. 7th ed. Weinheim: Wiley-VCH Verlag; 2016.

[265] Fedoroff BT, Aaronson HA, Resse EF, Sheffield OE, Clift GD. *Encyclopedia of Explosives and Related Items*. Volume 1. New Jersey, USA: U.S. Army Research and Development Command, TACOM, ARDEC, Warheads, Energetics and Combat Support Center, Picatinny Arsenal (U.S. Army); 1960:A42-A45.

[266] Rohrlich M, Sauermilch W. Sprengtechnische Eigenschaften von Trizykloazetonperoxyd. *Z. Gesamte Schiess Sprengstoffwes*. 1943;38:97-99.

[267] Brown ME, Gallagher PK. *Handbook of Thermal Analysis and Calorimetry. Volume 2: Applications to Inorganic and Miscellaneous Materials*. 1st ed. Amsterdam: Elsevier B.V.; 2003.

[268] Oxley J, Smith J. Peroxide explosives. In: Schubert H, Kuznetsov A, ed. *Detection and disposal of improvised explosives.* Dordbrecht: Springer; 2006:113-121.

[269] Balachandar KG, Thangamani A. Studies on some of the Improvised Energetic Materials (IEMs): Detonation, Blast Impulse and TNT Equivalence Parameters. *Orient J Chem.* 2019;35:1813-1823.

[270] Oxley JC, Smith JL, Shinde K, Moran J. Determination of the vapor density of triacetone triperoxide (TATP) using a gas chromatography headspace technique. *Propellants Explos Pyrotech*. 2005;30:127-130.

[271] Härtel MAC, Klapötke TM, Stiasny B, Stierstorfer J. Gas-phase Concentration of Triacetone Triperoxide (TATP) and Diacetone Diperoxide (DADP). *Propellants Explos Pyrotech.* 2017;42:623-634.

[272] Yinon J. Classification of explosives and basic terms. In: *Forensic and Environmental Detection of Explosives.* Chichester: John Wiley & Sons Ltd; 1999:1-28.

[273] Kende A, Lebics F, Eke Z, Torkos K. Trace level triacetone-triperoxide identification with SPME–GC-MS in model systems. *Microchimica Acta.* 2008;163:335-338.
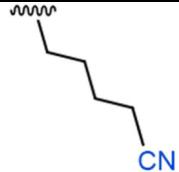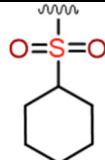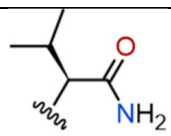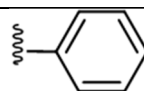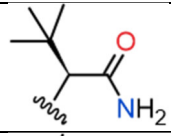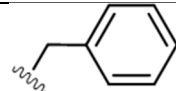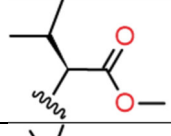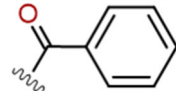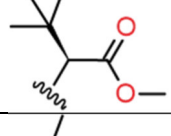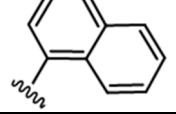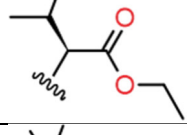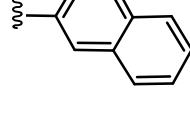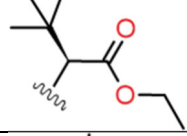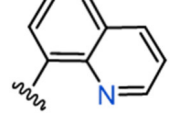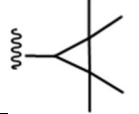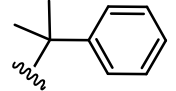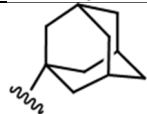
[274]   Ro KS, Venugopal A, Adrian DD, et al. Solubility of 2,4,6-trinitrotoluene (TNT) in water. *J Chem Eng Data*. 1996;41:758-761.

[275]   Walter MA. Dissertation: Herstellung und Charakterisierung von Antikörpern gegen Triacetontriperoxid (TATP). Humboldt-Universität zu Berlin; 2014.

[276]   Politzer P, Murray JS. Some Perspectives on Estimating Detonation Properties of C, H, N, O Compounds. *Cent Eur J Energy Mater*. 2011;8:209-220.

[277]   Miao Z, Li F, Luan Y. Theoretical studies on triacetonetriperoxide (TATP) derivatives to improve their performance. *Quim Nova*. 2019;42:22-27.

[278]   Wolffenstein R. Über die Einwirkung von Wasserstoffsuperoxyd auf Aceton und Mesityloxyd. *Ber Dtsch Chem Ges* (in German). 1985;28:2265-2269.

[279]   Schulte-Ladbeck R, Kolla P, Karst U. Trace analysis of peroxide-based explosives. *Anal Chem*. 2003;75:731-735.

[280]   Oxley JC, Smith JL, Bowden PR, Rettinger RC. Factors influencing triacetone triperoxide (TATP) and diacetone diperoxide (DADP) formation: Part I. *Propellants Explos Pyrotech*. 2013;38:244-254.

[281]   Oxley JC, Smith JL, Steinkamp L, Zhang G. Factors influencing triacetone triperoxide (TATP) and diacetone diperoxide (DADP) formation: Part 2. *Propellants Explos Pyrotech*. 2013;38:841-851.

[282]   Matyáš R, Pachman J. Study of TATP: Influence of Reaction Conditions on Product Composition. *Propellants Explos Pyrotech*. 2010;35:31-37.

[283]   Wilson SA, Brady JE, Smith JL, Oxley JC. The Risk of Mixing Dilute Hydrogen Peroxide and Acetone Solutions. *J Chem Health Safety*. 2012;19:27-33.

[284]   Dubnikova F, Kosloff R, Almog J, Zeiri Y, Boese R, Itzhaky H, Alt A, Keinan E. Decomposition of triacetone triperoxide is an entropic explosion. *J Am Chem Soc.* 2005;127:1146-1159.

[285]   Eyler GN, Mateo CM, Alvarez EE, Canizo AI. Thermal decomposition reaction of acetone triperoxide in toluene solution. *J Org Chem.* 2000;65:2319-2321.

[286]   Oxley JC, Smith JL, Chen H. Decomposition of a Multi-Peroxidic Compound: Triacetone Triperoxide (TATP). *Propellants Explos Pyrotech*. 2002;27:209-216.

Appendix

Table A1. IUPAC names and structural moieties assigned to letter codes used for the semi-systematic SCRA nomenclature.

Letter code	Systematic name	Structure element	Letter code	Systematic name	Structure element
Core			**Linker**		
I	1*H*-indole		ATA	acetamide	
INA	1*H*-indazole		C	carboxylate	
7AI	1*H*-7-azaindole		CA	carboxamide	
5Br-INA	5-bromo-1*H*-indazole		MO	methanone	
CZ	9*H*-carbazole		ZID	hydrazide	
GaClone	gamma-carboline-1-one		SA	sulfonamide	
5,3-FUPPY	5-(4-fluorophenyl)-1*H*-pyrazol-3-yl				
3,5-FUPPY	3-(4-fluorophenyl)-1*H*-pyrazol-5-yl				
PHPYO	5-phenyl-1*H*-pyrrole				

OXI	2-oxindole				
		Tail			
M	methyl	CH₃	5F-P	5-fluoropentyl	F
E	ethyl		5Cl-P	5-chloropentyl	Cl
PR	propyl		5-Br-P	5-bromopentyl	Br
B	butyl		CHM / CHMe*	cyclohexylmethyl	
P / Pe*	pentyl		CBM / CBMe*	cyclobutylmethyl	
H	hexyl		BC[2.2.1] Hp	Bicyclo[2.2.1] Heptyl	
HP	heptyl		MAP	1-methyl-azepan-3-yl	
D	decyl		FUB	4-fluorobenzyl	
4F-B	4-fluoro-butyl		TS	tosyl	

4CN-B	4-cyano-butyl		CHS	cyclohexylsulfonyl	
4en-P	pent-4-en				
Linked Group					
AB	1-amino-3-methyl-1-oxobutane		PH	phenyl	
ADB	1-amino-3,3-dimethyl-1-oxobutane		BZ	benzyl	
MMB / AMB	methyl 3-methyl-butanoate		BZO	benzoyl	
MDMB	methyl 3,3-dimethyl-butanoate		NA	1-naphthyl	
EMB	ethyl 3-methyl-butanoate		2-NA	2-naphthyl	
EDMB	ethyl 3,3-dimethyl-butanoate		QU	8-quinolinyl	
TMCP	tetramethyl-cyclopropane		Cumyl	2-phenylpropan-2-yl	
A	adamantyl				

Table A2. Amendment Ordinances of the German Narcotics Act (German: Betäubungsmitteländerungs-verordnung (BtMÄndV) and Betäungungsmittelanlagenänderungsverordnung (BtMGAnlÄndV)), regarding SCRAs since their first inclusion in 2009. Shown are all substances scheduled with the particular amendment, with SCRAs highlighted in bold.

	Annex I	Annex II	Annex III
22nd 'BtMÄndV' (January 22, 2009)		**CP 47,497, CP 47,497-C6-homolog, CP 47,497-C8-homolog, CP 47,497-C9-homolog, JWH-018** (temporarily scheduled)	
24th 'BtMÄndV' (January 22, 2010)	Mephedrone (4-Methylmeth-cathinone)	**CP 47,497, CP 47,497-C6-homolog, CP 47,497-C8-homolog, CP 47,497-C9-homolog, JWH-018** (permanently scheduled) **JWH-019, JWH-073**	Tapentadol
26th 'BtMÄndV' (July 26, 2012)	4-Fluoroamphetamine	**1-Adamantyl(1-pentyl-1*H*-indol-3-yl) ethanone**, **AM-694**, Butylone, Ethcathinone, Flephedrone (4-FMC), 4-Fluorometh-amphetamine, *p*-Fluoro-phenylpiperazine, 4-Fluorotropacocaine, **JWH-007, JWH-015, JWH-081, JWH-122, JWH-200, JWH-203, JWH-210, JWH-250, JWH-251**, Methedrone, *p*-Methoxyethylamphetamine, 4-Methylamphetamine, Methylbenzylpiperazine, 3,4-Methylenedioxy-pyrovalerone (MDPV), 4-Methylethcathinone, Methylone, Naphyrone, **RCS-4**, 3-Trifluoromethyl-phenylpiperazine	
27th 'BtMÄndV' (July 17, 2013)	Dimethoxymeth-amphetamine, Methiopropamine, Methoxetamine	**AKB-48, AKB-48F, AM-1220, AM-1220-Azepane, AM-2201, AM-2232, AM-2233**, 5-APB, 6-APB, Buphedrone, 3,4-Dimethylmethcathinone, Ethylphenidate, 3-Fluoro-methcathinone, **MAM-2201, XLR-11, JWH-307**, Pentedrone, α-Pyrrolidino-valerophenone (α-PVP), **RCS-4 *ortho*-isomer, UR-144**	Etizolam, Lisdexamfet-amine, Phenazepam
28th 'BtMÄndV' (December 13, 2014)	5-(2-Aminopropyl) indole, 25B-NBOMe,	**AB-FUBINACA, AB-PINACA**, AH-7921, **APICA, BB-22**,	

	2C-C, 2C-D, 2C-E, 25C-NBOMe, 2C-P, N-Ethyl-buphedrone, 4-Ethyl-methcathinone, Ethylone, 2-Fluoro-methamphetamine, 3-Fluoromethamphet-amine, 25I-NBOMe, 4-Methylbuphedrone, 3-Methylmethcathinone (3-MMC), Pentylone, Thienoamphetamine	Desoxypipradrol, Dimethocaine, 2,5-Dimethoxy-4-iodo-amphetamine, **EAM-2201**, **FDU-PB-22**, **5F-PB-22**, **FUB-PB-22**, **PB-22**, **STS-135**, **THJ-2201**	
29th 'BtMÄndV' (May 23, 2015)		**AB-CHMINACA**, 4,4'-DMAR (*para*-Methyl-4-methyl-aminorex), **5F-ABICA**, **5F-AB-PINACA**, **5F-AMB**, **5F-SDB-006**, MT-45, **SDB-006**, **THJ-018**	
30th 'BtMÄndV' (November 21, 2015)	Clephedrone (4-Chloromethcathinone)	Diclazepam, Flubromazepam, **MDMB-CHMICA**, 3-Methoxyphencyclidine, **NM-2201**	
31st 'BtMÄndV' (June 09, 2016)	25N-NBOMe	**ADB-CHMINACA, ADB-FUBINACA, AMB-FUBINACA, 5F-ADB, 5F-MN-18**	
18th 'BtMGAnlÄndV' (June 21, 2017)		Acetylfentanyl, Acryloylfentanyl, *Alpha*-PVT (*alpha*-Pyrrolidinopentio-thiophenone), **AMB-CHMICA**, Butyrfentanyl, **5Cl-AKB-48**, **5Cl-JWH-018**, Furanylfentanyl, **MDMB-CHMCZCA**, **MMB-2201**, **NE-CHMIMO**, U-47700	
'BtMRÄndV' (July 13, 2018)		**CUMYL-PEGACLONE, CUMYL-5F-P7AICA**	
'NpSGuBtmGAnlÄndV' (July 18, 2019)		**CUMYL-4CN-BINACA, CUMYL-5F-PEGACLONE**, Cyclopropylfentanyl, 4-Fluoroisobutyrfentanyl, Methoxyacetylfentanyl, Ocfentanil, Tetrahydrofuranylfentanyl, U-48800	
20th 'BtMGAnlÄndV' (July 17, 2020)		**5F-MDMB-PICA**	
21st 'BtMGAnlÄndV' (January 21, 2021)		Crotonylfentanyl, *N*-Ethylhexedrone, Flualprazolam,	

		4F-MDMB-BINACA, α-Pyrrolidinohexanophenone (α-PHP), Valerylfentanyl	
32nd 'BtMÄndV' (May 22, 2021)		Isotonitazene, **MDMB-4en-PINACA**, 2-Methyl-AP-237 (2-Methyl-Bucinnazine)	Remimazolam
22nd 'BtMGAnlÄndV' (November 11, 2021)		Clonazolam, Diphenidine, Flubromazolam, **4F-MDMB-BICA**	
23rd 'BtMGAnlÄndV' (June 08, 2023)		**ADB-BINACA**, α-Pyrrolidino-isohexanophenone (α-PiHP), Etazene (Etodesnitazene), Etonitazepyne, Protonitazene	

ADB-BINACA refers to *N*-[1-amino-3,3-dimethyl-1-oxobutan-2-yl]-1-butyl-1*H*-indazole-3-carboxamide. In Chapter 5 referred to as ADB-BUTINACA (cf. Chapter 5, section 5.2.1 for more details).

Chapter 2

Hair analysis:

Cannabis

Fast and highly sensitive determination of tetrahydrocannabinol (THC) metabolites in hair using liquid chromatography-multistage mass spectrometry (LC-MS³)
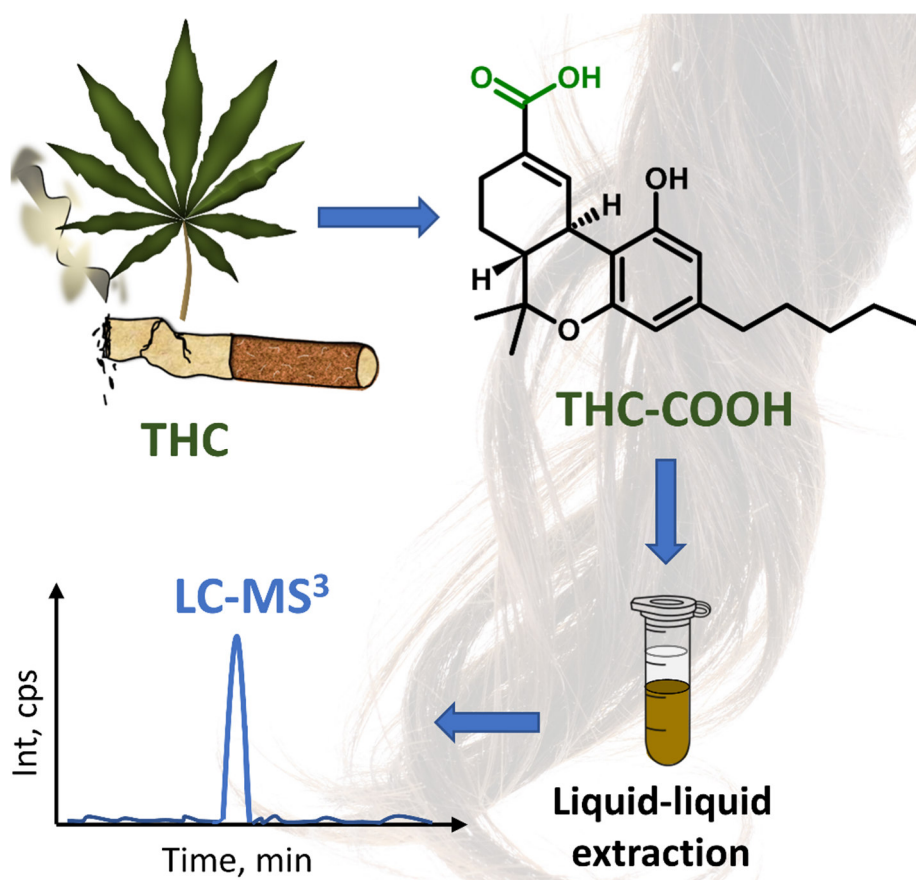
Abstract

In hair analysis, identification of 11-nor-9-carboxy-Δ^9-tetrahydrocannabinol (THC-COOH), one of the major endogenously formed metabolites of the psychoactive cannabinoid tetrahydro-cannabinol (THC), is considered unambiguous proof of cannabis consumption. Due to the complex hair matrix and low target concentrations of THC-COOH in hair, this kind of investigation represents a great analytical challenge. The aim of this work was to establish a fast, simple, and reliable LC-MS³ routine method for sensitive detection of THC-COOH in hair samples. Furthermore, the LC-MS³ method developed also included the detection of derivatized 11-hydroxy-Δ^9-THC (11-OH-THC) as an additional marker of cannabis use. Hair sample preparation prior to detection of the two THC metabolites was based on digestion of the hair matrix under alkaline conditions followed by an optimized liquid-liquid extraction (LLE) procedure. Sample preparation by LLE proved to be more suitable than solid-phase extraction (SPE) due to less laborious and time-consuming steps while still yielding satisfactory results. A significant improvement in analytical detection was introduced by multistage fragmentation (MS³), which led to enhanced sensitivity and selectivity and thus low limits of quantification (0.1 pg/mg hair). The MS³ method included two transitions for THC-COOH (m/z 343 → 299 → 245 and m/z 343 → 299 → 191) encompassing the quantifier (m/z 245) and the qualifier ion (m/z 191). The method was fully validated, and successful application to authentic toxicology case samples was demonstrated by the analysis of more than 2000 hair samples from cannabis users with THC-COOH concentrations determined ranging from 0.1 to >15 pg/mg hair.

2.1 Introduction

According to recent data published by the United Nations Office on Drugs and Crime (UNODC), cannabis remains by far the most commonly used drug with an estimated 192 million consumers worldwide [1]. After typical routes of administration (especially smoking, but also oral intake), the most important psychoactive natural constituent of *Cannabis sativa*, tetrahydrocannabinol (THC), undergoes a hepatic metabolic pathway relying on oxidation and subsequent glucuronidation as described in detail in literature [2,3]. The first oxidative step of THC yields the pharmacologically active metabolite 11-hydroxy-Δ^9-tetrahydrocannabinol (11-OH-THC) followed by further oxidation to the inactive metabolite 11-nor-9-carboxy-Δ^9-tetrahydrocannabinol (THC-COOH, Figure 1). Glucuronidation occurs in the last step, resulting in glucuronide conjugate (THC-COOH-GLcA) which is then urinary excreted. Oxidatively formed metabolites are often detected in biological matrices with diagnostic relevance in forensic toxicology (blood, urine, hair). Hair analysis provides a valuable complementary tool to conventional matrices due to the possibility of long-term retrospective detection, less invasive sample collection, and greater sample stability in comparison to body fluids, i.e. blood and urine. However, biological cannabinoids pose a special analytical challenge for hair analysis due to several reasons. Only the detection of metabolites provides an unambiguous confirmation of cannabis abuse, as THC and its biogenetic precursor Δ^9-tetrahydro-cannabinolic acid A (THCA-A) can also origin from external contaminations, such as the adsorption of sidestream smoke by hair or cross-contamination via hand contact [4,5]. However, the primary metabolite THC-COOH has a low incorporation rate into the hair matrix due to its acidic nature so that only low target concentrations are present in a complex matrix. The metabolite 11-OH-THC is recommended as a further suitable marker to prove active cannabis use [6,7].

Several analytical methods have been introduced to achieve the required low detection limits of THC-COOH in hair. Most of these methods include gas chromatography (GC)-based methods, including gas chromatography-tandem mass spectrometry (GC-MS/MS) with negative chemical ionization (NCI) [8-11]. Further alternatives to achieve the required specificity imply two-dimensional GC separation [12], large volume GC injection in combination with NCI-MS detection [13], or time-consuming high-performance liquid chromatography (HPLC) clean-up [14]. Alternative methods using liquid chromatography (LC) coupled with a tandem MS for determination of biogenic cannabinoids in hair are represented only in a small number of publications, although LC-based systems have a wide area of application nowadays. The main advantage of LC-based methods encompasses the elimination of the expensive and laborious derivatization step needed for GC-MS. Mercolini et al. developed one of the first LC-MS/MS methods for biogenic cannabinoid monitoring in hair with limits of quantification (LOQs) of 3 pg/mg hair and 1 pg/mg hair for THC and THC-COOH, respectively [15]. Different approaches for the application of LC-based methods have been introduced to achieve lower LOQs. Dulaurent et al. developed an LC-MS/MS method for the detection of THC, cannabinol (CBN), and cannabidiol (CBD) in MS/MS mode, whereas THC-COOH detection was performed in MS^3 mode with the LOQ reaching 0.2 pg/mg hair [16]. Thieme et al. successfully presented the sensitive detection of THC-COOH in hair using selective methylation and the application of LC-multistage MS [17]. Kuwayama et al. used a micro-pulverized extraction pretreatment method on hair samples to reduce the matrix

amount and successfully detected THC-COOH at 0.2 pg/mg hair using LC-MS/MS [18]. An approach based on an automated pressurized liquid extraction (PLE) followed by a solid-phase extraction (SPE) clean-up for sample preparation before detection via HPLC-high resolution MS/MS (HRMS/MS) was described by Montesano et al. [19]. Cho et al. applied LC-MS instrumental analysis improvement by using their previously introduced column switching system with three columns (precolumn, trap column and analytical column) in combination with MS^3 analysis to reduce the matrix interferences and reach 0.1 pg/mg hair as the LOQ [20]. The aim of this work was to establish a fast, simplified, and non-laborious LC-MS routine method for sensitive and quantitative determination of THC-COOH and 11-OH-THC in hair samples. An appropriate combination of hair processing and instrumental analysis is crucial for detection of trace amounts of THC-COOH. Therefore, different sample preparation techniques, including SPE and liquid-liquid extraction (LLE) after alkaline digestion of hair samples, as well as two different analysis approaches (MS^2 vs. MS^3) were compared to achieve this aim. Finally, the method developed using optimized sample preparation and instrumental analysis conditions was fully validated and applied to authentic hair samples from cannabis users.

2.2 Experimental

2.2.1 Chemicals and materials

Methanolic solutions of (±)-11-nor-9-carboxy-Δ⁹-tetrahydrocannabinol (THC-COOH, 100 μg/mL) and (±)-11-nor-9-carboxy-Δ⁹-tetrahydrocannabinol D9 (THC-COOH D9, 100 μg/mL) were purchased from Cerilliant Corporation (Round Rock, TX, USA). Standards of THC-OH and the deuterated (D3) analogue were supplied by LGC Standards GmbH (Wesel, Germany). High-purity solvents, including ultra LC-MS grade methanol and ultra LC-MS grade water, were supplied by scienTEST-bioKEMIX GmbH (Wesel, Germany). Acetic acid (glacial), isohexane, acetone, ethyl acetate, isooctane, potassium hydroxide pellets, and sodium acetate trihydrate were obtained from Merck KGaA (Darmstadt, Germany) and sodium hydroxide (1 M solution) from Carl Roth GmbH + Co. KG (Karlsruhe, Germany), all as analytical reagent grade chemicals.

Safe-lock tubes of various volumes (2 mL, 5 mL) were supplied by Eppendorf AG (Hamburg, Germany) and 300 μL fixed insert glass vials with a screw top by Thermo Scientific (Langerwehe, Germany). Strata Screen-A cartridges (200 mg, 3 mL) for solid-phase extraction were obtained from Phenomenex (Aschaffenburg, Germany).

2.2.2. Hair samples

Blank head hair for the calibration and validation procedure was provided by volunteers and analyzed for the target compounds prior to use. Authentic toxicology case samples were collected from male and female cannabis users preferentially at the vertex posterior region of the head near the scalp using scissors. In a small number of cases, alternative body hair samples (e.g. beard hair, arm hair) were subjected to analysis. Segmental analysis was performed depending on the hair sample length. Hair samples were taken on official order of the prosecutor's office, police, court, driver's license office or upon other request.

2.2.3 Sample preparation

Hair strands were subjected to an external decontamination procedure including sequential washing with isohexane and acetone for 30 sec in ultrasonic bath each step. After drying, the samples were cut into small pieces approximately 1 mm in length and weighed (20 mg) in a safe-lock tube (2 mL, polypropylene). Quality controls and calibrators for the calibration curve were prepared using blank hair provided by volunteers and spiked with known THC-COOH concentrations. Hair sample preparation prior to detection of THC-COOH and 11-OH-THC was based on digestion of the hair matrix under alkaline conditions followed by an extraction procedure. Two different extraction procedures were compared for the main metabolite, THC-COOH, as described below.

2.2.3.1 Solid-phase extraction

Solid-phase extraction (SPE) of THC-COOH was conducted according to our previously established sample preparation procedure for GC-NCI-MS/MS system [4] with slight modifications. A 10 M solution of potassium hydroxide was prepared by dissolving potassium hydroxide pellets (280.5 g) in deionized water (500 mL), and sodium acetate trihydrate crystals (13.6 g) were stirred in deionized water (1000 mL) to obtain a 0.1 M sodium acetate solution. Together with methanol (0.5 mL) and internal standard (0.2 pg/μL THC-COOH-D9, 100 μL) the hair sample (20 mg) was digested using the potassium hydroxide solution (10 M, 0.4 mL) at 80°C for 30 min. The pH was then adjusted to 5–6 by addition of glacial acetic acid (0.5 mL), and afterwards the sodium acetate/methanol mixture (0.1 M sodium acetate/methanol, 95/5; v/v, 0.6 mL) was added. The clean-up of the digested and acidified hair sample was performed by SPE on Strata Screen-A cartridges containing silica-based mixed mode sorbent (C_8 phase and strong anion exchange). After the cartridges were conditioned with methanol (2 x 2 mL) followed by sodium acetate/methanol mixture (2 x 2 mL), the sample was loaded at a slow flow rate. Washing was accomplished with deionized water (2 mL) and a mixture of methanol/deionized water (60/40; v/v, 2 mL). Cartridges were aspirated to dryness, and the analyte was collected in the elution solvent (isohexane/ethyl acetate/glacial acetic acid, 50/50/1; v/v/v, 2 x 0.85mL). Extracts were evaporated to dryness (35°C, gentle nitrogen stream) and reconstituted with methanol (50 μL) and water (50 μL).

2.2.3.2 Liquid-liquid extraction

The following procedure represents optimized conditions for liquid-liquid extraction (LLE) of 11-OH-THC and THC-COOH. The alkaline digestion of the sample occurred after addition of sodium hydroxide (1 M, 1 mL) and methanol (100 μL) in the presence of internal standard (0.2 pg/μL THC-COOH-D9, 100 μL) at 80°C for 1 h. After cooling to ambient temperature, isohexane/ethyl acetate mixture (9/1; v/v, 2 ml) was added to the aqueous phase. The content of the tube was shaken for 5 minutes at 420 rpm, and after centrifugation (4600 g, 5 minutes) the clear organic phase collected was used for the determination of 11-OH-THC. The detailed procedure encompassing derivatization of 11-OH-THC with picolinic acid prior to LC-MS³ analysis was described previously by Franz et al. [21]. After collection of the organic phase for the determination of 11-OH-THC, the remaining interphase containing solid residues and matrix compounds was discarded. The aqueous phase, containing THC-COOH, was transferred to a 5 mL polypropylene safe-lock tube and adjusted to pH 4–4.5 by addition of glacial acetic

acid (0.5 mL). The subsequent washing step included the addition of isooctane (0.5 mL) and twenty-fold inversion of the tube. The following LLE was conducted in an analogous way using isohexane/ethyl acetate mixture (9/1; v/v, 2 mL). After centrifugation at 4600 g for 5 min, the organic phase was collected and subsequently evaporated to dryness at 35°C under a gentle stream of nitrogen. The dry residue was reconstituted with methanol (50 µL) and water (50 µL).

2.2.4 Instrumentation and analytical conditions

LC-MS^2 and LC-MS^3 methods

The analysis of the hair samples was performed using an LC-MS system consisting of an ultra-high-performance LC (UHPLC) Nexera X2 (Shimadzu, Munich, Germany) equipped with a DGU-20A degasser, LC-30AD binary pumps, an SIL-30AC autosampler, a CTO-30A column oven, a CBM-20A controller, and a QTRAP® 6500 triple quadrupole linear ion trap mass spectrometer equipped with a TurboIonSpray® interface (Sciex, Darmstadt, Germany). Chromatographic separation was carried out on a Kinetex® Biphenyl analytical column (100 x 2.1 mm, 1.7 µm particle size, 100 Å pore diameter) provided with a SecurityGuard™ ULTRA Biphenyl guard column (2 x 2.1 mm, both sourced from Phenomenex, Aschaffenburg, Germany). The column temperature was set to 40°C, and the autosampler temperature was maintained at 10°C. Injection volume was set to 20 µL. The mobile phase comprised ultrapure water (A) and methanol (B) delivered at 0.5 mL/min in gradient elution mode as follows: elution started with 30% mobile phase B, which was then linearly increased within 4 min to 75% B and in a second step further increased to 80% B within 5.5 min; a final linear increase to 100% mobile phase B occurred within 0.5 min and the isocratic elution at 100% organic solvent was maintained for 2 min. Starting conditions were restored within 0.1 min and kept for 2.9 min so that the total run time was 15 min including re-equilibration to the initial conditions before each injection. Mass spectrometry included Multiple Reaction Monitoring (MRM) acquisition mode using an electrospray interface operating in negative mode (ESI-) at -4500 V. The source and gas conditions were as follows: curtain gas 40 psi, collision gas 'high', nebulizer gas flow (GS1) and desolvation gas flow (GS2) both 65 psi, and source temperature 550°C. MS^2 analysis comprised detection of first stage fragment ions for THC-COOH (m/z 343.1 → 299.2 and m/z 343.1 → 245.2) and THC-COOH D9 (m/z 352.2 → 308.2 and m/z 352.2 → 254.2). MS^3 analysis was performed using the linear ion trap (LIT) to introduce the second fragmentation stage. The set MRM^3 method included two transitions for THC-COOH (m/z 343.1 → 299.2 → 245.4 and m/z 343.1 → 299.2 → 191.4) encompassing both the quantifier (m/z 245.4) and the qualifier ion (m/z 191.4) detected in the parameter range m/z 170–255 at a scan rate of 10000 Da/sec, with Q0 trapping enabled, Q3 entry barrier of 8 V and LIT resolution of Q3. Tentative chemical structures of the fragmented ions are depicted in Figure 1. Internal standard (THC-COOH D9) was monitored in a second MS^3 experiment by the fragmentation cascade m/z 352.2 → 308.2 → 254.4 where a mass scan was centered at m/z 254.4 with width of ±15 Da. All details regarding the ionization and fragmentation parameters for MS^2 and MS^3 analysis are given in Table 1, together with the MS parameters for the determination of 11-OH-THC, which was analyzed using a separate analytical method. All further details regarding the LC and MS parameters for the 11-OH-THC analytical method have been published previously [21]. The LC-MS operation and data processing were performed using Analyst® Software 1.6.2 and SCIEX OS® 2.0.1 Software, respectively.
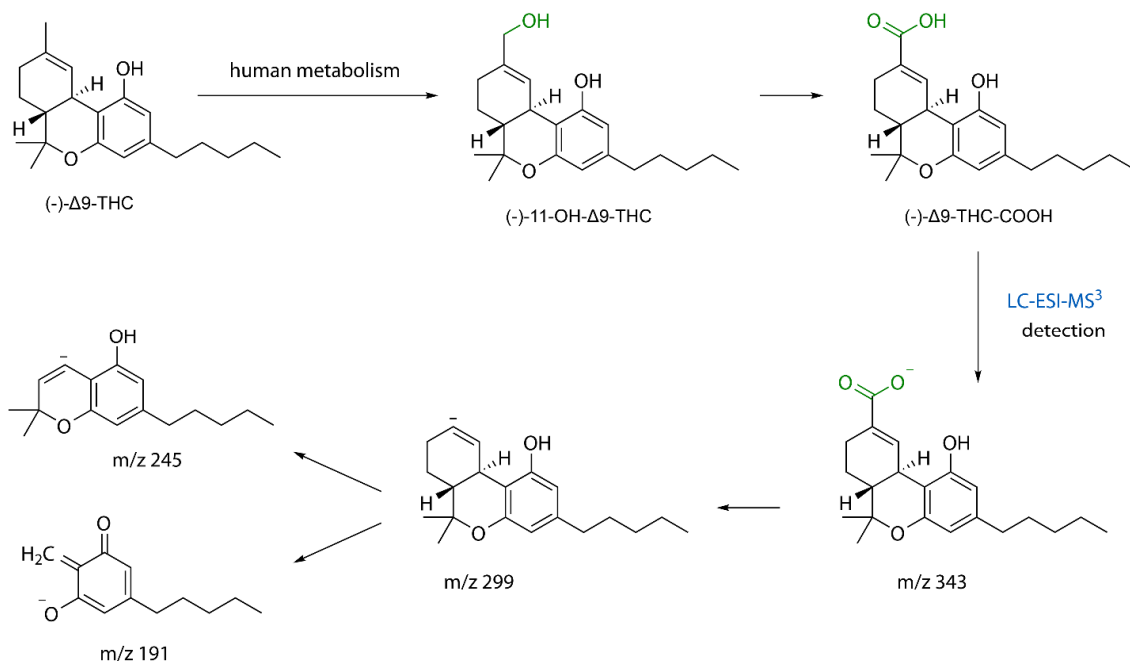
Figure 1. Human hepatic metabolism of tetrahydrocannabinol (THC) yielding the pharmacologically active metabolite 11-hydroxy-Δ^9-tetrahydrocannabinol (11-OH-THC) followed by a further oxidation step to the inactive metabolite 11-nor-9-carboxy-Δ^9-tetrahydrocannabinol (THC-COOH). Detection of THC-COOH via the LC-ESI(-)-MS^3 analytical method with a consecutive fragmentation cascade and tentative chemical structures of the fragmentation ions generated.

Table 1. Precursor and fragment ions including MS parameters used in the applied LC-MS^2 and LC-MS^3 methods for THC-COOH and THC-COOH D9. The second metabolite, 11-OH-THC, and its deuterated analogue were analyzed after picolination using a separate analytical method.

Compound	Precursor Ion	2nd Precursor Ion MS^2				Product Ion MS^3		
		m/z	DP [V]	CE [V]	EP [V]	Mass scan, m/z	AF2 [V]	Fixed Fill Time [msec]
THC-COOH	343.1	299.2	-55	-28	-10	170–255	0.08	250
		245.2	-55	-40	-10			
THC-COOH D9	352.2	308.2	-55	-28	-10	254.4 ±15	0.08	250
		254.2	-55	-36	-10			
11-OH-THC (picolinated)	541.2	374.2	71	31	9	170–370	0.11	100
11-OH-THC D3 (picolinated)	544.2	377.2	71	31	9	170–370	0.11	100

DP declustering potential, CE collision energy, EP entrance potential, AF2 excitation energy

2.2.5 Method validation

Validation of the method developed for determination of THC-COOH and 11-OH-THC in hair was performed in accordance with the guidelines of the Society of Toxicological and Forensic Chemistry (GTFCh) [22,23]. Evaluation of the following parameters was included: selectivity, linearity, limit of detection (LOD), limit of quantification (LOQ), precision, accuracy, processed sample stability, matrix effect, and recovery. Selectivity was examined using six cannabinoid-

free hair samples of different origin, once without the addition of internal standard (blank samples) and once with the fortification with standard and internal standard (fortified samples). Additionally, two cannabinoid-free hair samples were fortified only with internal standard. Calibration standards were prepared at eight concentration levels ranging from the LOQ to 15.0 pg/mg hair using drug-free hair samples fortified with the appropriate amount of standard solution. The eight calibrators included the following concentrations: 0.1, 0.2, 0.5, 1.0, 2.0, 5.0, 10.0 and 15.0 pg/mg hair. Six replicate determinations of the calibration curve were used to assess the linearity. Calibration curves were obtained by plotting the area ratio of THC-COOH to THC-COOH D9 against the expected concentrations. The LOD and LOQ were determined using linear regression of calibrators in the anticipated concentration range (0.05, 0.06, 0.07, 0.08, 0.09, 0.1, 0.2, 0.5 pg/mg hair). After applying linear regression, the analytical limits were calculated using the equations described in the guidelines [22].

Processed sample stability indicated analyte stability during resident time in the autosampler longer than over the anticipated run time of a regular batch size. Therefore, quality control samples prepared at a low (0.5 pg/mg) and high concentration (5.0 pg/mg) were processed, pooled, aliquoted, placed in the autosampler, and injected at regular time intervals within 20 h. Accuracy and precision were evaluated by analyzing spiked samples at a low (0.3 pg/mg), medium (1.0 pg/mg), and high (5 pg/mg) calibration level. Two replicates of each concentration level were analyzed on eight different days. Bias (n = 8) between the nominal and measured concentration was calculated to assess accuracy, whereas intra-day (n = 16) and inter-day (n = 8) precision were expressed as relative standard deviation (RSD) and denoted as RSD_r and $RSD_{(T)}$, respectively.

Matrix effect and extraction recovery were assessed at a low (0.5 pg/mg) and high (5.0 pg/mg) concentration level using hair from five different origins (n = 5). Analyte signal areas of three sample sets were compared: diluted analyte standard and internal standard solution in water/methanol (1/1; v/v) represented neat solution (1); extracts of five different drug-free human hair samples fortified with analyte and internal standard after extraction indicated post-spiked samples (2), whereas the identical set of five different drug-free human hair samples fortified with analyte and its internal standard prior to extraction indicated pre-spiked samples (3). Absolute matrix effects were calculated as a percentage of signal areas in post-spiked samples (2) relative to the signal areas in neat solution (1). Absolute extraction recovery included a comparison of analyte areas response in pre-spiked samples (3) relative to the analyte areas response in post-spiked samples (2).

Software Valistat (Arvecon GmbH, Walldorf, Germany) and MS Excel (Microsoft Corporation, Redmond, WA, USA) were used for statistical analysis.

2.3 Results and Discussion

2.3.1 Comparison of sample preparation procedures (SPE vs. LLE)

For the purpose of sample preparation for THC-COOH analysis, hair specimens predominantly undergo alkaline hair digestion followed by a sample clean-up and extraction procedure using either SPE or LLE. The suitability of both extraction procedures for sample preparation was investigated to ensure the best method for efficient removal of interferences. The initial objective was to keep the extraction procedure fast and simple, so the focus was placed on

LLE. The adequate LLE workup was established after optimization of extraction efficiency and reduction of the interfering matrix by implementation of suitable washing steps. The procedure for SPE relied on our previously validated and established workflow for a GC-NCI-MS/MS system, except for the fact that the derivatization step needed for GC-NCI-MS/MS analysis was omitted. The optimized LLE allowed for a greater signal-to-noise ratio (S/N) due to a reduced interfering background, when compared to the S/N obtained from the SPE procedure established previously for THC-COOH (Figure 2). Due to the fact that SPE workflows are more intricate as compared to an LLE procedure, the optimization of the present SPE procedure for the detection of underivatized THC-COOH by LC-MS^3 was not subjected to a further follow-up. The LLE developed in this study proved to be suitable for efficient separation of THC-COOH from matrix interferences, and in combination with the advantages comprising less laborious and time consuming steps was selected as the sample preparation procedure of choice.
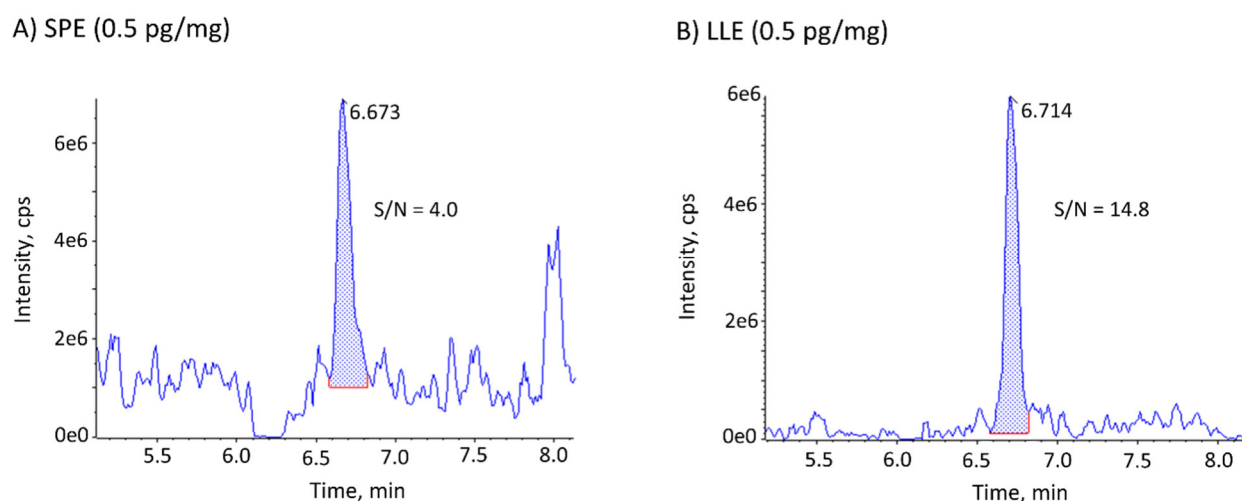
Figure 2. Comparison of the THC-COOH quantifier ion using LC-MS^3 analysis after SPE (A) and LLE (B) clean-up procedures of drug-free hair samples fortified with 0.5 pg THC-COOH/mg hair. Signal-to-noise ratio (S/N) was calculated using Peak-To-Peak algorithm.

2.3.2 Instrumental analysis comparison (MS^2 vs. MS^3)

Direct comparison of the MS^2 and MS^3 acquisition modes is shown in Figure 3, which represents the measured THC-COOH signal response in both modes for diluted standard solution (matrix-free) as well as for hair matrix samples fortified with THC-COOH at a concentration level of 5 pg/mg hair (MS^2 mode) and 0.5 pg/mg hair (MS^3 mode). The ion transitions monitored in the particular acquisition mode are outlined accordingly.

Application of multistage fragmentation (MS^3) yielded a significant improvement in sensitivity as indicated by comparison of matrix-free standard solution in the MS^2 and MS^3 acquisition modes. The improvement in sensitivity was achieved by collection of ions during a prolonged time period, i.e. applying a fixed fill time of 250 msec, using a linear ion trap. The S/N of matrix-free standard solution obtained by MS^3 mode proved to be 6-7 times greater compared to the S/N in MS^2 mode (Figure 3, A). Furthermore, the additional fragmentation step in the MS^3 setup yielded a consecutive fragmentation cascade and thus a significant improvement in

selectivity, as shown by comparison of hair matrix samples for both modes (Figure 3, B). The first fragmentation reaction that was completed in MS^2 mode (m/z 343.1 → 299.2) seemed to be non-specific for THC-COOH since many interfering matrix compounds were observed. Consequently, the S/N was significantly lower as opposed to the results from MS^3, which were additionally disadvantaged by one order of magnitude lower concentration level (cf. 5 pg/mg for MS^2 and 0.5 pg/mg for MS^3 in Figure 3, B). An additional fragmentation step in MS^3 provided a more specific signal, thus clearly differentiating THC-COOH from the reduced matrix background. The signal-to-noise ratio proved to be 2-3 times superior by application of MS^3, while detecting one order of magnitude lower concentration level (Figure 3, B).
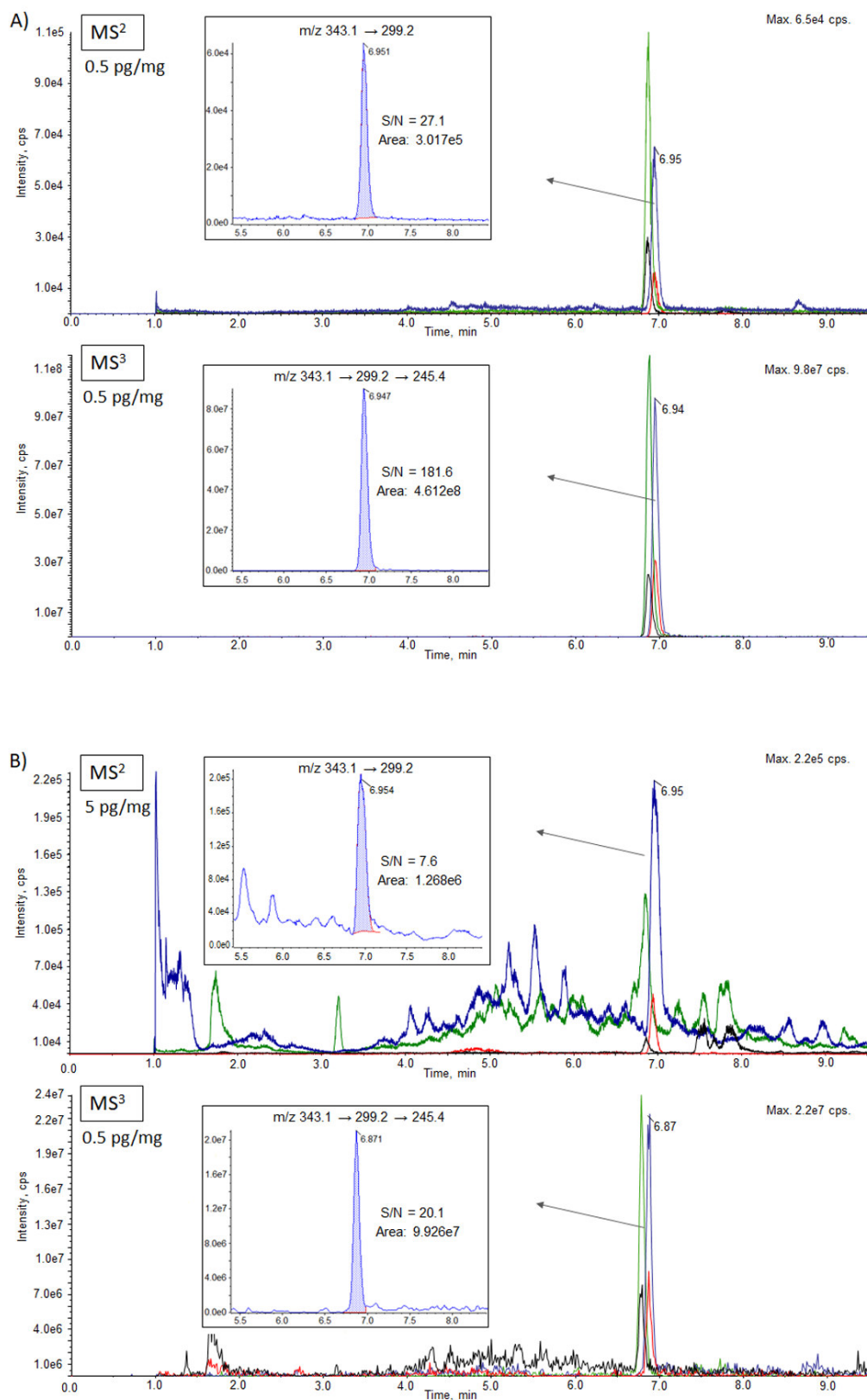
Figure 3. Direct comparison of the MS^2 and MS^3 acquisition modes, once for matrix-free diluted standard solution (A) and once for fortified matrix samples (B). The concentration level comprised 0.5 pg THC-COOH/mg hair, except for the MS^2 analysis of a matrix sample with concentration level of 5 pg THC-COOH/mg hair (B, top). The monitored ion transitions include THC-COOH quantifier (blue, additionally magnified) and qualifier ion (red), together with THC-COOH D9 quantifier (green) and qualifier ion (black). S/N was calculated using Peak-To-Peak algorithm.

85

2.3.3 Method validation for THC-COOH

Blank and fortified hair samples originating from six different sources did not reveal any endogenous or exogenous interferences at the monitored MS^3 transitions of THC-COOH or the corresponding internal standard. The LOD and LOQ of THC-COOH were 0.08 and 0.1 pg/mg hair, respectively. Good linear correlation between the response and concentration in the range between the lower LOQ and highest calibrator (0.1–15.0 pg/mg hair) was shown by correlation coefficients (r) of at least 0.999. For all the assessed calibration curves (n = 6) a 1/x weighting factor was applied. The method developed showed satisfactory precision and accuracy at low, medium, and high concentration levels. From both, the intra-day (n = 16) and inter-day precision (n = 8), the RSD values determined were lower than 9.6% and the accuracy (n = 8) ranged between -5.6 and 1.2% at evaluated concentration levels (0.3, 1.0, and 5.0 pg/mg hair corresponding to low, medium, and high concentration levels, cf. Table 2). The processed sample stability in the autosampler was given over a time period of 20 h since the analyte area response relative to the initial time was within the acceptance criteria (±15%) for both a low (0.5 pg/mg) and high (5.0 pg/mg) concentration level.

The absolute matrix effect amounted to 55.7% and 47.6% at the low and high concentration level, respectively, indicating ion suppression phenomenon. However, the use of deuterated internal standard compensated for this effect as indicated by the relative matrix effect being slightly above 100% (Table 2). Extraction losses depicted by absolute extraction recoveries (40.6% at 0.5 pg/mg and 45.1% at 5.0 pg/mg) were well compensated by the addition of internal standard as shown by relative recoveries reaching approximately 100%.

The validation data for 11-OH-THC have been published previously [21].

Table 2. Validation parameters including intra-day and inter-day precision, accuracy, absolute matrix effect, and extraction recovery, as well as relative matrix effect and extraction recovery.

Intra-day precision RSD$_r$, % (n = 16)			Inter-day precision RSD$_{(T)}$, % (n = 8)			Accuracy Bias, % (n = 8)		
0.3 pg/mg	1 pg/mg	5 pg/mg	0.3 pg/mg	1 pg/mg	5 pg/mg	0.3 pg/mg	1 pg/mg	5 pg/mg
7.1	5.1	9.6	7.2	6.7	9.6	1.2	-5.6	-1.9

	Low concentration (0.5 pg/mg)				High concentration (5 pg/mg)			
	Matrix effect [%]	SD (n=5) [%]	Recovery [%]	SD (n=5) [%]	Matrix effect [%]	SD (n=5) [%]	Recovery [%]	SD (n=5) [%]
Abs.	55.7	15.7	40.6	4.9	47.6	7.3	45.1	4.5
Rel.	101.7	7.1	103.9	7.5	106.8	4.5	102.8	2.8

2.3.4 Application to authentic hair samples

The validated method was applied to 2225 authentic hair samples from cannabis users or individuals suspected of cannabis use who were involved in violations of the narcotics law, traffic offenses, cases of restoration of driver's licenses, abstinence monitoring programs for offenders on probation, or similar cases. In total, 1487 of the hair samples examined represented violations of the narcotics law, with positive identification of THC-COOH in 978 hair samples. The quantitative results of cases associated with violations of the narcotics law are summarized in Figure 4. Concentrations determined from the 978 hair samples positive for THC-COOH ranged from 0.1 to >15 pg THC-COOH/mg hair, whereas 11-OH-THC

concentrations were distributed from 0.2 pg/mg to >5 pg/mg hair. Quantities above the validated linear ranges were extrapolated yielding 50.5 pg/mg and 42.7 pg/mg hair as maximum concentrations for THC-COOH and 11-OH-THC, respectively, in the set of hair samples examined. The median THC-COOH concentration (50th percentile) in the hair segments analyzed amounted to 2.93 pg/mg hair, while the first quartile (Q1, 25th percentile) and the third quartile (Q3, 75th percentile) were equivalent to 0.92 pg/mg and 7.10 pg/mg, respectively. For 11-OH-THC, the median concentration was 3.84 pg/mg with the 25th percentile equaling 1.21 pg/mg and the 75th percentile 9.74 pg/mg. Concentration levels were classified in three different groups indicating low (<Q1), medium (Q1–Q3), and high (>Q3) concentration ranges corresponding to occasional, frequent, and regular cannabis use, respectively. The detectability of the two metabolites and their concentrations were correlated for hair samples depicted in Figure 4. Both metabolites in combination were determined in more than half (65.5%) of the positive samples, whereas 31.4% of the samples represented THC-COOH-positive but 11-OH-THC-negative samples. The determination of 11-OH-THC without the presence of THC-COOH included 3.1% of the samples. In general, 11-OH-THC was present in similar or even higher concentrations compared to THC-COOH (cf. median and mean concentrations in Figure 4) and proved to be a further suitable marker of active cannabis use.

The THC-COOH statistic agrees with our previously published data regarding the concentration distribution of more than 100 drugs and metabolites in forensic hair samples [24] in which the median concentration of THC-COOH determined in 402 case samples amounted to 3.43 pg/mg hair. The method for THC-COOH deployed in the previous study was based on SPE clean-up followed by derivatization of THC-COOH and LC-MS^2 analysis, as described by Franz et al. [21].
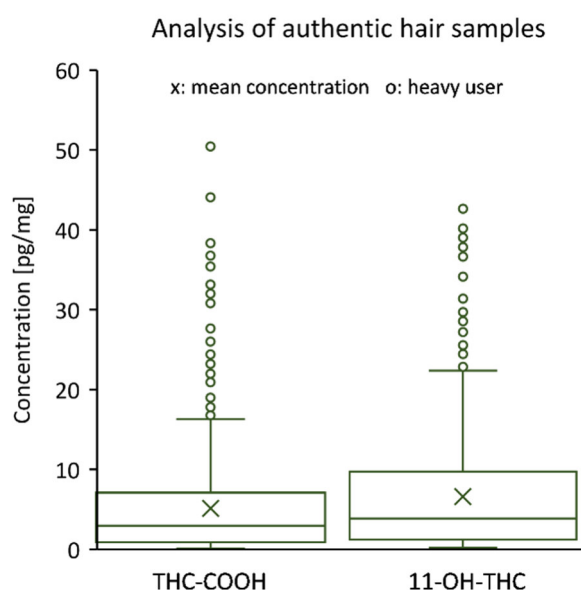
Figure 4. Quantitative distributions of THC-COOH (left) and 11-OH-THC (right) in authentic hair samples, originating from cases of violations of the narcotics law, are depicted as box plots using the classification into quartiles: first quartile (Q1, 25th percentile), second quartile (median, 50th percentile) and third quartile (Q3, 75th percentile). The most extreme data points are indicated by whiskers which are extended from the edges of the boxes. Mean values as well as data points in the high concentration range beyond the whiskers (heavy user cases) are plotted individually and denoted accordingly.

2.4 Conclusion

In the present work, two different extraction procedures (SPE and LLE) for the processing of hair samples as well as application of LC-MS instrumental analysis in two different acquisition modes (MS^2 and MS^3) were compared in order to develop a fast and sensitive method for the determination of major cannabis metabolites. Extraction based on alkaline hair digestion combined with optimized LLE clean-up proved satisfactory for successfully validating the procedure without the need for complex and costly workup as given by SPE or additional derivatization procedures. The main target analyte of our work was represented by the detection of THC-COOH, and the set-up method also allowed for simultaneous detection of 11-OH-THC through a two-step LLE procedure using a single hair sample. The MS^3 acquisition mode showed great advantages in terms of sensitivity and selectivity enhancement when compared to commonly used methods based on MS/MS acquisition. Given the described conditions, the method presented allowed the detection of THC-COOH with an LOQ of 0.1 pg/mg using only a small amount (20 mg) of hair sample.

The validation data and the successful application to 2225 authentic toxicology case samples demonstrated that the present method is suitable for hair analysis of the most important cannabis (THC) consumption markers and can serve as an alternative to the present default methods based on time-consuming derivatization processes and subsequent GC-MS/MS analysis. Since LC-based methods are continuously gaining applicability in forensic and toxicology laboratories, the advantages of the LC-MS^3 methodology presented together with a simple sample preparation procedure without expensive and laborious steps might be appealing for the identification and quantification of THC metabolites via hair analysis for both legal and public health issues.

2.5 References

[1]   United Nations Office on Drugs and Crime (UNODC). World Drug Report 2020. 2020; Vienna: United Nations publication, Sales No. E.20.XI.6. https://wdr.unodc.org/wdr2020/index.html. Accessed September 10, 2021.

[2]   Huestis MA. Human cannabinoid pharmacokinetics. *Chem Biodivers*. 2007;4:1770-1804.

[3]   Maurer HH, Sauer C, Theobald DS. Toxicokinetics of drugs of abuse: current knowledge of the isoenzymes involved in the human metabolism of tetrahydrocannabinol, cocaine, heroin, morphine, and codeine. *Ther Drug Monit.* 2006;28:447-453.

[4]   Uhl M, Sachs H. Cannabinoids in hair: strategy to prove marijuana/hashish consumption. *Forensic Sci Int.* 2004;145:143-147.

[5]   Moosmann B, Roth N, Auwärter V. Hair analysis for THCA-A, THC and CBN after passive in vivo exposure to marijuana smoke. *Drug Test Anal.* 2014;6:119-125.

[6]   Franz T, Skopp G, Schwarz G, Musshoff F. Proof of active cannabis use comparing 11-hydroxy-Δ9-tetrahydrocannabinol with 11-nor-9-carboxy-tetrahydrocannabinol concentrations. *Drug Test Anal.* 2018;10:1573-1578.

[7]   Casati S, Angeli I, Ravelli A, Del Fabbro M, Minoli M, Orioli M. 11-OH-THC in hair as marker of active cannabis consumption: Estimating a reliable cut-off by evaluation of 672 THC-positive hair samples. *Forensic Sci Int.* 2019;304:109951.

[8]   Uhl M. Determination of drugs in hair using GC/MS/MS. *Forensic Sci Int.* 1997; 84:281-294.

[9]   Huestis MA, Gustafson RA, Moolchan ET, et al. Cannabinoid concentrations in hair from documented cannabis users. *Forensic Sci Int.* 2007;169:129-136.

[10]   Minoli M, Angeli I, Ravelli A, Gigli F, Lodi F. Detection and quantification of 11-nor-Δ9-tetrahydrocannabinol-9-carboxylic acid in hair by GC/MS/MS in negative chemical ionization mode (NCI) with a simple and rapid liquid/liquid extraction. *Forensic Sci Int.* 2012;218:49-52.

[11]   Han E, Park Y, Kim E, et al. Simultaneous analysis of Δ^9-tetrahydrocannabinol and 11-nor-9-carboxy-tetrahydrocannabinol in hair without different sample preparation and derivatization by gas chromatography-tandem mass spectrometry. *J Pharm Biomed Anal*. 2011;55:1096-1103.

[12]   Moore C, Rana S, Coulter C, Feyerherm F, Prest H. Application of two-dimensional gas chromatography with electron capture chemical ionization mass spectrometry to the detection of 11-nor-Δ^9-tetrahydrocannabinol-9-carboxylic acid (THC-COOH) in hair. *J Anal Toxicol.* 2006;30:171-177.

[13]   Moore C, Guzaldo F, Donahue T. The determination of 11-nor-Δ^9-tetrahydrocannabinol-9-carboxylic acid (THC-COOH) in hair using negative ion gas chromatography-mass spectrometry and high-volume injection. *J Anal Toxicol*. 2001;25(7):555-558.

[14]   Sachs H, Dressler U. Detection of THCCOOH in hair by MSD-NCI after HPLC clean-up. *Forensic Sci Int.* 2000;107:239-247.

[15]   Mercolini L, Mandrioli L, Protti M, Conti M, Serpelloni G, Raggi MA. Monitoring of chronic Cannabis abuse: An LC–MS/MS method for hair analysis. *J Pharm Biomed Anal*. 2013;76:119-125.

[16]   Dulaurent S, Gaulier JM, Imbert L, Morla A, Lachâtre G. Simultaneous determination of D9-tetrahydrocannabinol, cannabidiol, cannabinol and 11-nor-D9-tetrahydro-cannabinol-9-carboxylic acid in hair using liquid chromatography–tandem mass spectrometry. *Forensic Sci Int.* 2014;236:151-156.

[17]   Thieme D, Sachs H, Uhl M. Proof of cannabis administration by sensitive detection of 11-nor-Delta(9)-tetrahydrocannabinol-9-carboxylic acid in hair using selective methylation and application of liquid chromatography- tandem and multistage mass spectrometry. *Drug Test Anal.* 2014;6:112-118.

[18]   Kuwayama K, Miyaguchi H, Yamamuro T, et al. Micro-pulverized extraction pretreatment for highly sensitive analysis of 11-nor-9-carboxy-Δ^9-tetrahydro-cannabinol in hair by liquid chromatography/tandem mass spectrometry. *Rapid Commun Mass Spectrom*. 2015;29:2158-2166.

[19]   Montesano C, Simeoni MC, Vannutelli G, et al. Pressurized liquid extraction for the

determination of cannabinoids and metabolites in hair: detection of cut-off values by high performance liquid chromatography-high resolution tandem mass spectrometry. *J Chromatogr A*. 2015;1406:192-200.

[20]   Cho HS, Cho B, Sim J, Baeck SK, In S, Kim E. Detection of 11-nor-9-carboxy-tetrahydrocannabinol in the hair of drug abusers by LC–MS/MS analysis. *Forensic Sci Int.* 2019;295:219-225.

[21]   Franz T, Skopp G, Schwarz G, Musshoff F. Proof of active cannabis use comparing 11-hydroxy-Δ9-tetrahydrocannabinol with 11-nor-9-carboxy-tetrahydrocannabinol concentrations. *Drug Test Anal.* 2018;10:1573-1578.

[22]   Peters FT, Hartung M, Herbold M, Schmitt G, Daldrup T, Musshoff F. GTFCh, Appendix B - Requirements for the validation of analytical methods. English translation, available online at https://www.gtfch.org/cms/index.php/en/ guidelines. Accessed September 14, 2021. Original German version published in *Toxichem Krimtech* 2009;76(3):185-208.

[23]   Musshoff F, Skopp G, Pragst F, Sachs H, Thieme D. GTFCh, Appendix C - Quality requirements for the analysis of hair samples. English translation, available online at https://www.gtfch.org/cms/index.php/en/guidelines. Accessed September 14, 2021. Original German version published in *Toxichem Krimtech* 2009;76(3):209-216.

[24]   Musshoff F, Schwarz G, Sachs H, Skopp G, Franz T. Concentration distribution of more than 100 drugs and metabolites in forensic hair samples. *Int J Legal Med*. 2020;134:989-995.

Chapter 2

A fast, simple and sensitive LC-MS³ routine method for the quantitative identification of major endogenously formed cannabis metabolites of the psychoactive cannabinoid tetrahydro-cannabinol (THC) was developed for proof of active cannabis consumption via hair analysis. The method was fully validated and successfully applied to more than 2000 authentic toxicology case samples demonstrating an appealing combination of sensitive analytical detection (LC-MS³) and a simple, non-laborious sample preparation procedure based on liquid-liquid extraction.
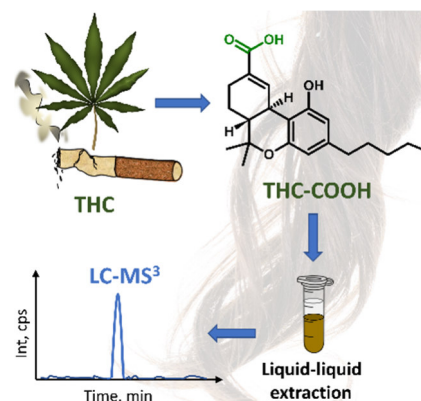
Fast and highly sensitive determination of tetrahydrocannabinol (THC) metabolites in hair using liquid chromatography-multistage mass spectrometry (LC-MS³)

Petra Hehet*, Thomas Franz, Natalie Kunert and Frank Musshoff

Chapter 3

Sewage analysis:
Stability assessment of SCRAs in sewage water

Synthetic cannabinoid receptor agonists and their human metabolites in sewage water: Stability assessment and identification of transformation products
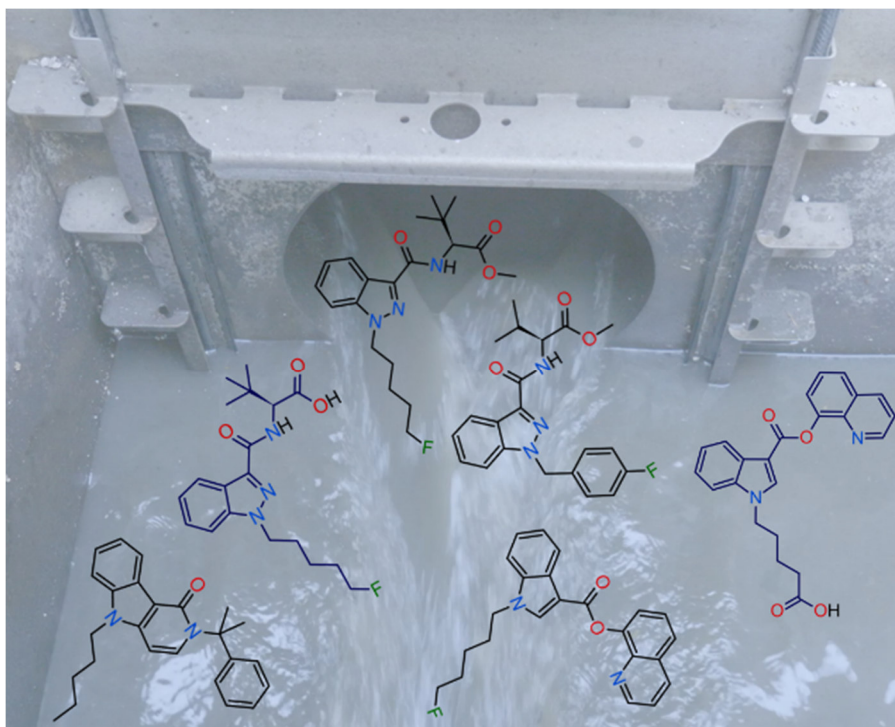
General remark: Significant portions of section 3.6 'Supplementary Material' (Figures S2-S20 and Tables S5-S18) were not elaborated by the author of this dissertation and are not included in this chapter. Available under the DOI indicated above.

Chapter 3

Abstract

Since their first appearance in 2008, synthetic cannabinoid receptor agonists (SCRAs) remain the most popular new psychoactive substances (NPS) in the EU. Following consumption, these drugs and their metabolites are urinary excreted and enter the sewage system enabling the application of wastewater-based epidemiology (WBE). Knowing the fate of target analytes in sewage water is essential for successful application of WBE. This study investigates the stability of several chemically diverse SCRAs and selected human metabolites under sewage conditions utilizing a combination of liquid chromatography-tandem mass spectrometry and high-resolution mass spectrometry (HRMS). Target analytes included SCRAs with indole (5F-PB-22, PB-22 pentanoic acid), indazole (AMB-FUBINACA, 5F-ADB, 5F-ADB dimethylbutanoic acid), carbazole (MDMB-CHMCZCA, EG-018) and γ-carboline (Cumyl-PeGaClone) chemical core structures representing most of the basic core structures that have occurred up to now. Stability tests were performed using wastewater effluent containing 5% activated sludge as inoculum to monitor degradation processes and formation of transformation products (TPs). The majority of investigated SCRAs, excluding the selected human metabolites, was recalcitrant to microbial degradation in sewage systems over a period of 29 days. Their stability was rather controlled by physico-chemical processes like sorption and hydrolysis. Considering a typical hydraulic in-sewer retention time of 24 hours, the concentration of AMB-FUBINACA decreased by 90% thus representing the most unstable SCRA investigated in this study. Among the ten newly identified TPs three could be considered as relevant markers and should be included into future WBE studies to gain further insight into use and prevalence of SCRAs on the drug market.

Keywords: synthetic cannabinoid receptor agonists · new psychoactive substances · sewage · stability profiles · transformation products
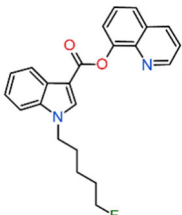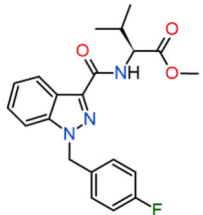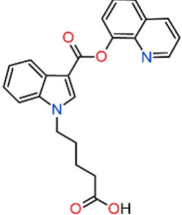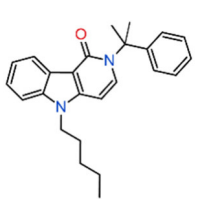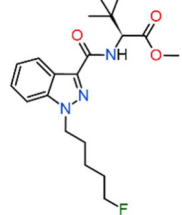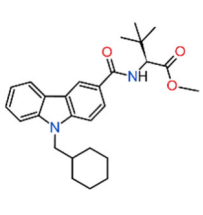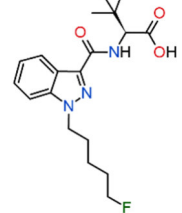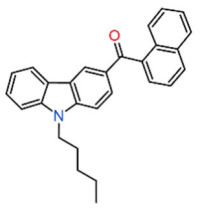
3.1 Introduction

New psychoactive substances (NPS) are compounds designed to mimic effects of established illicit drugs often being traded as 'legal' alternatives, mostly via online shops. Over the last decade, NPS seem to have established their own market increasing the complexity of narcotic products. Although the number of NPS reported to the Early Warning System of the European Monitoring Centre for Drugs and Drug Addiction (EMCDDA) currently decreases (53 newly introduced NPS in 2019) in comparison to the peak times (100 new substances each year in 2014-2015), the availability of products remains high due to the high dynamics in the NPS market [1]. The decrease in the number of newly monitored NPS may reflect the legal response introduced in many countries across Europe to control NPS, including the commencement of the German new psychoactive substance act (NpSG) in 2016, as well as legal changes to restrict production in source countries, such as China. Simulants and synthetic cannabinoid receptor agonists (SCRAs) represent predominant groups of NPS in terms of the vast majority of the substances identified on the global market, whereas continuous and persistent prevalence of SCRAs use was noted in toxicology cases associated with high rates of fatalities worldwide [2,3].

Estimating community prevalence and consumption of NPS poses a great challenge since confiscation data, medical reports, and toxicology data might only capture a smaller portion of the population with a representative spectrum of NPS products. A promising complementary tool to estimate NPS use at population level is wastewater-based epidemiology (WBE). This approach is based on chemical analysis of target residues in urban wastewater, which can be used to calculate corresponding drug loads normalized to the catchment population [4]. This provides objective estimation of market prevalence and consumption trends with potential to detect local and temporal patterns of drug use. Several studies concerning the estimation of NPS in wastewater have been performed at different time and geographical scales [5-19]. The vast majority of reported studies mostly identified synthetic cathinones in urban sewage water, with only few positive findings for SCRAs [5,7,13,16,17]. The determination of NPS in sewage is related to greater challenges in comparison to the established illicit drug groups, since the expected NPS loads are rather low due to the distribution of consumption over higher numbers of individual compounds and due to the typically lower effective single doses consumed in comparison with classic drugs such as cocaine or amphetamine-type-stimulants (ATS). The dynamic nature of NPS market and limited availability of reference standards represent a challenge for analytical methodologies, which must keep pace with the continuous appearance of new substances. There are also some general factors associated with uncertainties which need to be addressed for full application of WBE approach, e.g. human NPS metabolism and pharmacokinetic data, as well as stability of potential drug biomarkers in wastewater [20]. The metabolism of SCRAs has been studied in more detail [21-27], but the stability of parent substances and the corresponding metabolites in wastewater is unknown. Additionally, transformation processes during residence time in sewers need to be examined to address potential target substances for chemical analysis. McCall et al. [28] summarized the current knowledge regarding the in-sample (sample preparation, preservation and storage) and in-sewer (during transport in real sewers) stability of common illicit drugs in urban wastewater, however, lacking any published

data on SCRAs. Recently published data focused on the investigation of biotransformation products of selected synthetic cathinones and phenethylamines in sewage water [29,30].

The present work aims to expand the sewage stability data to a range of SCRAs belonging to different chemical subclasses representing most of the core structures that have occurred up to now: indoles, indazoles, carbazoles and γ-carbolines. Additionally, four different types of side chains at the nitrogen atom of the core structure as well as two different linkers (carboxamide and less stable carboxylate) and five different linked residues are represented in the sample pool. Furthermore, some of the target substances (5F-ADB, Cumyl-PeGaClone, 5F-PB-22, AMB-FUBINACA, Table 1) represent highly prevalent SCRAs in Europe at the time period of the study. Besides the parent compounds, two selected metabolites (5F-ADB dimethylbutanoic acid and PB-22 pentanoic acid, Table 1) have been the objective of this study. Urinary marker metabolites play an essential role as consumption indicators since SCRAs are usually extensively metabolized [31]. However, detection of parent compounds in urine was also demonstrated, either using a sensitive analytical method [32] or comprising certain compounds [33-35], among others 5F-ADB [25].

Table 1. Selected SCRAs and two corresponding human metabolites with their chemical names, abbreviations and chemical structures. AMB-FUBINACA, 5F-ADB and MDMB-CHMCZCA are assumed to be present as (S)-enantiomers [37-39].

Name	Abbreviation	Chemical structure	Name	Abbreviation	Chemical structure
Quinolin-8-yl 1-(5-fluoropentyl)-1*H*-indole-3-carboxylate	5F-PB-22		Methyl (2S)-2-[1-(4-fluorobenzyl)-1*H*-indazole-3-carboxamido]-3-methyl-butanoate	AMB-FUBINACA	
5-(3-((quinolin-8-yloxy)carbonyl)-1*H*-indole-1-yl)pentanoic acid	PB-22 pentanoic acid		2,5-dihydro-2-(1-methyl-1-phenyl-ethyl)-5-pentyl-1*H*-pyrido[4,3-*b*]indol-1-one	Cumyl-PeGaClone	
Methyl (2S)-2-[1-(5-fluoropentyl)-1*H*-indazole-3-carboxamido]-3,3-dimethyl-butanoate	5F-ADB		Methyl (2S)-2-(9-(cyclohexylmethyl)-9*H*-carbazole-3-carboxamido)-3,3-dimethyl-butanoate	MDMB-CHMCZCA	
(2S)-2-[1-(5-fluoropentyl)-1*H*-indazole-3-carboxamido]-3,3-dimethyl-butanoic acid	5F-ADB dimethyl-butanoic acid		Naphthalene-1-yl(9-pentyl-9*H*-carbazol-3-yl)methanone	EG-018	

Besides urinary excretion, disposal of SCRAs in their solid form, or as herbal or liquid incense into the sewage system is also a conceivable input source since illegal designer drug facilities dealing with preparation (e.g. spraying SCRA solutions on herbal material such as *Damiana*) and packaging of herbal blend mixtures containing SCRA are frequently located in Europe. An example for direct disposal of illegal classic drugs into the sewage system by clandestine drug laboratories were the excessively high mass loads of 3,4-methylenedioxymethamphetamine (MDMA) in wastewater of Utrecht in the Netherlands, which was clearly attributable to non-consumed MDMA via enantiomeric profiling [36]. This example confirms that not only human metabolites, but also parent drugs represent relevant target analytes for stability studies in wastewater. In this context, the investigation of transformation reactions of parent SCRA compounds in wastewater and the comparison of identified transformation products (TPs) with known urinary metabolites can address the important question whether the biotransformation conditions in the sewage system promote similar degradation pathways as the human body.

In this manner, the present study demonstrates the first comprehensive stability data for SCRAs and some of their human metabolites in urban wastewater, additionally also providing the information on formed TPs, which can be useful for future WBE applications to gain further insight into use and prevalence of NPS on the drug market.

3.2 Experimental

3.2.1 Chemicals and materials

Synthetic cannabinoids (methyl (2S)-2-[1-(5-fluoropentyl)-1*H*-indazole-3-carboxamido]-3,3-dimethylbutanoate (5F-ADB), 2,5-dihydro-2-(1-methyl-1-phenyl-ethyl)-5-pentyl-1*H*-pyrido [4,3-*b*]indol-1-one (Cumyl-PeGaClone), quinolin-8-yl 1-(5-fluoropentyl)-1*H*-indole-3-carboxylate (5F-PB-22), methyl (2S)-2-[1-(4-fluorobenzyl)-1*H*-indazole-3-carboxamido]-3-methylbutanoate (AMB-FUBINACA), methyl (2S)-2-(9-(cyclohexylmethyl)-9*H*-carbazole-3-carboxamido)-3,3-dimethylbutanoate (MDMB-CHMCZCA) and naphthalene-1-yl(9-pentyl-9*H*-carbazol-3-yl)methanone (EG-018) were provided by the Federal Criminal Police Office (Forensic Science Institute, Wiesbaden, Germany), either dissolved in acetonitrile (5F-ADB, 5F-PB-22, MDMB-CHMCZCA, EG-018, AMB-FUBINACA) or methanol (Cumyl-PeGaClone) at a concentration level of 10 mg/mL. Both metabolites, (2S)-2-[1-(5-fluoropentyl)-1*H*-indazole-3-carboxamido]-3,3-dimethylbutanoic acid (5F-ADB dimethyl- butanoic acid) and 5-(3-((quinolin-8-yloxy)carbonyl)-1*H*-indol-1-yl)pentanoic acid (PB-22 pentanoic acid), were supplied by Cayman Chemicals (Ann Arbor, MI, USA) as 5 mg/mL solution in acetonitrile and as 1 mg powder, respectively. Internal standard (ISTD) included 1'-naphtoyl indole provided by the Federal Criminal Police Office as 1 mg/mL solution in methanol. Ultra LC-MS grade acetonitrile and methanol were purchased from Carl Roth (Karlsruhe, Germany) and Riedel-de Haën (Seelze, Germany), respectively. Formic acid (> 98%, p.a.) and sodium benzoate (≥ 99.0%) were supplied by Carl Roth (Karlsruhe, Germany), whereas ammonium formate (for mass spectrometry, ≥ 99.0%) was provided by Sigma Aldrich (Steinheim, Germany). Ultrapure water was produced by a Simplicity® UV water purifier system (18.2 MΩ) from Merck Millipore (Burlington, USA). If not stated differently, this water was used for preparation of solutions and dilutions. Regenerated cellulose filters (0.2 µm, Spartan®) for wastewater filtration were obtained from Carl Roth (Karlsruhe, Germany), while single-use syringes and disposable

hypodermic needles (0.80 x 40 mm and 0.80 x 120 mm, Sterican®) were purchased from B. Braun (Melsungen, Germany).

3.2.2 Stock and working solutions preparation

PB-22 pentanoic acid stock solution was prepared by dissolving 1 mg of the solid substance in 0.2 mL acetonitrile resulting in the concentration of 5 mg/mL. Working ISTD solution of 1'-naphtoyl indole (10 µg/mL) was obtained by appropriate dilution of the stock solution in methanol. Mixed standard solution comprising all the SCRAs and their metabolites was prepared in acetonitrile at a concentration of 10 µg/mL. All the substance stock and working solutions of SCRAs, their metabolites and ISTD were stored at -26°C.

3.2.3 Biotransformation experiments

Biotransformation experiments were performed with an inoculum consisting of 95% wastewater treatment plant (WWTP) effluent and 5% activated sludge (w/w), both taken from the municipal WWTP Beuerbach (Hesse, Germany). Wastewater samples were collected in amber glass bottles in November 2018. Stability of the selected SCRAs in the investigated wastewater inoculum was assessed using laboratory scale die-away experiments under aerobic conditions, at ambient temperature (20°C-25°C), under exclusion of light, and at the original pH of the wastewater (7.47 at 23.7°C). Analytes were spiked at a concentration of 10 µg/mL or 5 µg/mL and a separate sterile control (sterilized with 5 g/L sodium azide) was prepared for each analyte. The analyte concentration of 5 µg/mL was applied for the two selected SCRA metabolites. Three separate replicates were prepared for each active and non-active assay. The bioactivity of the inoculum was controlled with sodium benzoate (100 mg/L), which was used as a representative substance due to its known transformation rate under microbial activity conditions (100% degradation within six days). Two blanks were prepared without addition of the active test substance to the inoculum, but comprised methanol and acetonitrile, respectively, since these solvents were used in the stock solutions.

Samples were collected over a period of 29 days including frequent sampling intervals at the beginning of the experiment (0 h, 4 h, 18 h, 24 h, 48 h), later every 2 days (4th, 6th, 8th and 10th day), then every 3-4 days (13th and 17th day) and in the last phase every 6 days (23rd and 29th day). Each sampling (600 µL) was followed by addition of the equal amount of acetonitrile (600 µL) in order to suppress the residual bioactivity and inhibit further degradation of the substance. Subsequently, the samples were vortexed and frozen at -26°C until analysis.

Sample preparation for LC-ESI-MS/MS analysis comprised filtration (0.2 µm, regenerated cellulose filters) and dilution of the filtered sample with ultrapure water/methanol at the ratio 80/20 resulting in the end concentration of 800 ng/mL for EG-018 and MDMB-CHMCZCA, and 100 ng/mL for the remaining SCRAs and the metabolites. Prior to the LC-ESI-MS/MS analysis, ISTD was added resulting in the end concentration of 100 ng/mL in each sample. For 5F-ADB, 5F-ADB dimethylbutanoic acid, 5F-PB-22 and for PB-22 pentanoic acid (excluding the non-active assay in the last case), analyses including active and non-active assay were performed in triplicate. For the residual selected SCRAs, measurements were performed in single determination.

3.2.4 Instrumentation and analytical conditions

3.2.4.1 LC method

The chromatographic separation was achieved on a XSelect HSS T3 (50 x 2.1 mm, 3.5 μm, 100 Å pore size, Waters) analytical column equipped with a guard column (XSelect HSS T3 VanGuard Cartridge, 5 x 2.1 mm, 3.5 μm, 100 Å) at a constant flow of 0.3 mL/min. The mobile phase consisted of ultrapure water with 5 mmol ammonium formate, pH3 (A) and methanol with 5% ultrapure water and 5 mmol ammonium formate, pH 3 (B). The applied gradients are shown in Table S1. The autosampler and column temperatures were not controlled and the injection volume was set to 20 μL.

3.2.4.2 LC-ESI-MS/MS method

The chromatograph, a PerkinElmer Series 200 (PerkinElmer, Waltham, Massachusetts) equipped with an autosampler, two pump modules and a vacuum degasser, was coupled to a 3200 QTrap (Sciex, Darmstadt, Germany) triple quadrupole linear ion trap mass spectrometer equipped with an electrospray interface (Turbo Spray) operating in positive ESI polarity (ESI+). For chromatographic separation, the liquid chromatography method described above was used. Quantification of target compounds was carried out in multiple reaction monitoring (MRM) mode using two MRM transitions per compound. The temperature of the TurboIonSpray® probe was set to 500°C, curtain gas to 25 psi, "ion source gas 1" to 55 psi, "ion source gas 2" to 65 psi, and the ion spray voltage was set to +5500 V. Detailed settings and parameters are given in the Supplementary Material (Table S2). Operation and data acquisition mode was carried out with the Analyst Software, version 1.5.1 and data evaluation was performed with MultiQuant 3.0.2 (both Sciex, Darmstadt, Germany).

3.2.4.3 LC-ESI-HRMS method

LC-ESI-HRMS analysis was performed with a 1200 Agilent Series HPLC (Agilent Technologies, Waldbronn, Germany) coupled with an Orbitrap Velos Pro that was equipped with a Heated Electrospray Ionization (H-ESI II) ion source (both Thermo Scientific, Bremen, Germany). Chromatographic separation was achieved with the liquid chromatography method described previously, however the flow rate and injection volume were changed to 0.2 mL/min and 50 μL, respectively. The HRMS method consisted of two alternating scan events: a survey scan in a range of m/z 100 to 1000 with a nominal resolution of 100000 at m/z 400 and a data-dependent HCD (higher collisional energy dissociation) MS/HRMS scan (nominal resolution 7500 at m/z 400) of the three most intense ions. The signal of protonated dibutyl phthalate (*m/z* 279.1591) was used as lock mass to enhance mass accuracy. Additional details about the Orbitrap method are shown in Table S3. Peak picking was either performed manually with Thermo Xcalibur (Version 4.0.27.21, Thermo Scientific, Bremen, Germany) or automatically with enviMass [40] (Version 3.5, enviBee, Switzerland).

3.2.4.4 Method validation

The LC-MS/MS method was validated by determination of the linearity of calibration, instrumental limit of detection (ILOD), instrumental limit of quantification (ILOQ), filtration recovery, matrix effect and precision. Matrix effects and filtration recoveries were evaluated in inoculum at 100 ng/mL, which represented the concentration level for LC-MS/MS stability

profile analysis for most of the targeted substances. More details on the determination of the validation parameters are shown in the Supplementary Material.

3.3 Results and Discussion

3.3.1 Method validation

The validation parameters for each substance are reported in Table S4 in the Supplementary Material, with linear correlation coefficients of the obtained eight-point calibration curves being higher than 0.997 for all compounds. The calculated matrix effects (n = 4) ranged between -2.7% and 8.3%, whereas positive values indicate ion enhancement and negative values ion suppression. Filtration recoveries (n = 4) in inoculum were satisfactory for almost all compounds, varying between 72% and 100%, except for EG-018 and MDMB-CHMCZCA, the two most non-polar substances, with recoveries of 11% and 26%, respectively. Since similar recoveries were also observed after filtration in ultrapure water (Table S4), the observed analyte loss can be attributed to the interaction with the filter material and not to sorption to the particulate fraction of inoculum. Overall method intra-day precision (n = 6) was evaluated in the examined inoculum (WWTP effluent/activated sludge, 95/5, v/v) at two different concentration levels (20 ng/mL and 100 ng/mL) as relative standard deviations (RSDs), which were lower than 19.9% for all analytes.

3.3.2 Stability profiles of SCRAs and selected human metabolites

3.3.2.1 5F-PB-22 and PB-22 pentanoic acid

5F-PB-22 and its non-fluorinated analogue, PB-22, represent the first marketed SCRAs containing an ester linkage group instead of the common carbonyl and carboxamide linkages. This structural feature was particularly interesting for the stability assessment under sewage conditions since ester bonds are unstable and hydrolysis-susceptible. Wohlfarth et al. [29] have shown an extensive ester hydrolysis of 5F-PB-22 in human hepatic metabolic profiles and identified ester hydrolysis as well as oxidative defluorination as the predominant metabolic transformation pathways for 5F-PB-22 in humans. In sewage environment, 5F-PB-22 was equally transformed by approx. 50% after 29 days both in the active and non-active assay (Figure 1, left) ruling out most likely biodegradation.

3.3.2.2 5F-ADB, 5F-ADB dimethylbutanoic acid, and AMB-FUBINACA

Figure 2 shows the stability profiles of 5F-ADB, its human metabolite 5F-ADB dimethylbutanoic acid, and AMB-FUBINACA. 5F-ADB showed transformation in both assays, however the degradation in the active assay was increased in comparison to the non-active assay. As from the chemical structure, ester or amide hydrolysis and ß-oxidation after oxidative defluorination are likely to occur.

The relative concentration of AMB-FUBINACA decreased in both assays rapidly by 90% within the first 24 h (Figure 2, below).
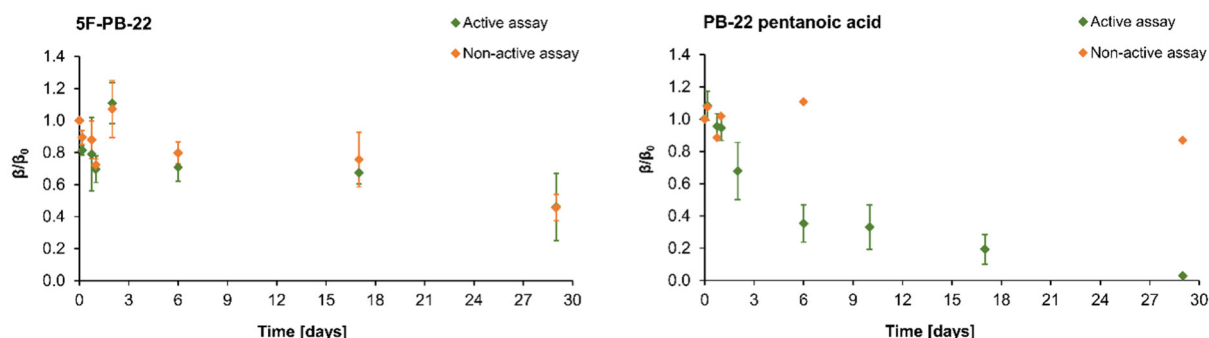
Figure 1. Stability profiles of 5F-PB-22 (left) and its human metabolite PB-22 pentanoic acid (right) showing concentrations relative to t_0 (β/β_0) during 29 days. LC-MS/MS analysis including active assay (indicated in green) and non-active assay (indicated in orange) in this experiment was performed in triplicate (n = 3), besides the non-active assay of PB-22 pentanoic acid (n = 1); error bars indicate the standard deviation.
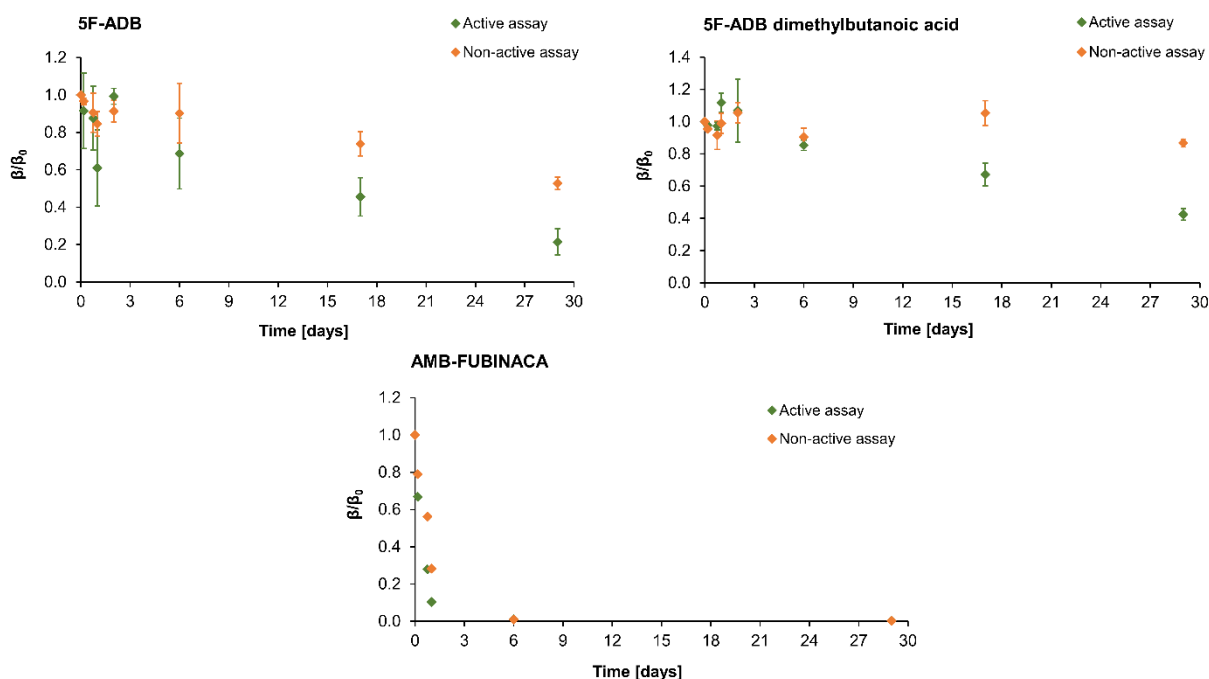
Figure 2. Stability profiles of 5F-ADB (left), its human metabolite, 5F-ADB dimethylbutanoic acid (right), and AMB-FUBINACA (below) showing concentrations relative to t_0 (β/β_0) during 29 days. LC-MS/MS analysis including active assay (indicated in green) and non-active assay (indicated in orange) in this experiment was performed in triplicate (n = 3); error bars indicate the standard deviation.

3.3.2.3 Cumyl-PeGaClone, MDMB-CHMCZCA and EG-018

The stability profiles of Cumyl-PeGaClone (γ-carboline core structure), MDMB-CHMCZCA and EG-018 (carbazole core structure) are shown in Figure S1. Cumyl-PeGaClone and EG-018 showed minor primary degradation and can be regarded as stable. The stability of both substances might be related to their comparatively lipophilic chemical structures characterized by low susceptibility to hydrolysis or biological degradation. MDMB-CHMCZCA showed a fast primary degradation in the first 24 hours in the active assay and the substance

was stable afterwards. In the non-active assay, a constant decrease of MDMB-CHMCZCA was observed during 29 days.

3.3.2.4 Identification of transformation products (TPs)

5F-PB-22, PB-22 pentanoic acid, 5F-ADB, 5F-ADB dimethylbutanoic acid and AMB-FUBINACA showed primary transformation in their stability tests. Thus, identification of their TPs was attempted with HPLC-(ESI+)-HRMS. The identification strategy utilized for all TPs is exemplarily discussed for PB-22 pentanoic acid.

The Xcalibur and EnviMass software were used to search for the calculated masses of predicted PB-22 pentanoic acid TPs (Table S5) and additional signals that were neither present in an inoculum blank nor in a sterile control. This led to the detection of *m/z* 361.1184 ($C_{21}H_{17}O_4N_2^+$, Δ 1.24 ppm, isotopic pattern (Table S6) fitting), which was consistent with an oxidation of PB-22 pentanoic acid. The isotopic pattern fitting of *m/z* 361.1184 as well as the proposed fragmentation pathway obtained from MS/HRMS data (Figure S2) with comparison to the MS/HRMS data of PB-22 pentanoic acid (Figure S3 and Table S7), resulted in the proposed structure of TP 361 in Figure 3. PB-22 pentanoic acid and TP 361 had a neutral loss of 8-hydroxychinolin to *m/z* 244.0974 and *m/z* 216.0659, respectively. Both fragments were further fragmented to *m/z* 144.0447 by losing either the pentanoic or propanoic side chain, confirming the proposed structure of TP 361. TP 361 was formed by ß-oxidation of the pentanoic acid side chain to a propanoic acid side chain and only observed in the active assay. The identification of TP 361 was fulfilled at identification level 2 according to the classification scheme proposed by Schymanski et al. [41], since the probable structure could be proposed by diagnostic evidence and experimental data. A reference standard for this TP was not commercially available and thus, neither a final confirmation of the structure nor accurate quantification was possible. Thus, the TP formation was assessed under the assumption of a similar ESI response of the TP and its precursor. During the evaluation of TP 361, in-source fragmentation was observed. EnviMass showed a formation process of *m/z* 216.0658 that possessed an identical retention time and peak shape and a similar fragmentation pathway to TP 361 (*m/z* 216.0658 is part of the proposed fragmentation pathway of TP 361). Hence, the sum of both signals was used to assess the TP formation (Figure S4). TP 361 reached its maximum concentration after eight days where it was estimated at 55% of the initial PB-22 pentanoic acid concentration (Figure S5).

Following this procedure, ten TPs were tentatively identified and are shown in Figure 3 with their apex concentration, the time when this concentration is reached, stability and identification confidence level. The degradation and formation curves, the proposed fragmentation pathways and additional HRMS data (mass accuracy ≤ 2 ppm, isotopic pattern fitting, proposed fragmentation pathway) are shown in Figures S6 – S20 and Tables S8 – S18 in Supplementary Material.

5F-PB-22 seemed to be recalcitrant and the identified transformation processes including ester hydrolysis as abiotic process (non-active assay) and oxidative defluorination followed by β-oxidation as biotic process (active assay) were represented only in minor amounts (Figure 3). Contrary, the human metabolite PB-22 pentanoic acid showed primary biodegradation in the active assay, but was stable over the entire test period in the non-active assay. The

ongoing biotic transformation processes could be explained by ß-oxidation of the pentanoic acid chain of PB-22 pentanoic acid (TP 361, 55% formation after 8 days, Figure 3).

The most significant TP found for 5F-ADB was formed abiotically via ester hydrolysis (TP 364, approx. 12% after 29 days, Figure 3). Ester hydrolysis also corresponds to the most abundant metabolic pathway of 5F-ADB in humans [25]. The stability profile of the corresponding metabolite, 5F-ADB dimethylbutanoic acid, showed primary degradation in the active assay, but a constant concentration in the non-active assay. Several TPs of minor formation percentage could be identified (Figure 3). Similarly like for 5F-PB-22 and PB-22 pentanoic acid, the human metabolite was again more prone to biodegradation if compared to its parent compound. Further, by comparison of biotransformation kinetics for the both investigated metabolites in this study (Figure 1 right, and Figure 2 right above), the carboxylic group placed on tert-butylacetic acid moiety of 5F-ADB dimethylbutanoic acid was less prone to the impact of microbial degradation as opposed to the carboxylic group at pentyl chain moiety of PB-22 pentanoic acid. The β-oxidation process in the latter case seems to occur with a high rate in sewage environment.

AMB-FUBINACA yielded two TPs being result of ester hydrolysis (TP 370, approx. 20% formed after 4 days) which was followed by amide hydrolysis (TP 271, approx. 8% formed after 8 days), both occurring as abiotic transformation processes (Figure 3). Ester hydrolysis was also found to be one of the prevailing human metabolic pathways, whereas amide hydrolysis present in sewage was not a metabolic reaction in human liver microsome system [26]. In addition to the two identified TPs, further factors are required to explain the observed concentration decrease of AMB-FUBINACA. Comparing the molecular structures of AMB-FUBINACA and 5F-ADB, its closest analogue among the selected SCRAs, the main difference consists in the fluorobenzyl versus a 5-fluoropentyl side chain. Since no pronounced physico-chemical processes, at least not at such a fast rate as for AMB-FUBINACA, have been observed for 5F-ADB, the fluorobenzyl side chain remains the most probable reason for the concentration decrease either due to strong hydrophobic interactions with the glassware and/or inoculum particles, or due to susceptibility to chemical processes linked to this moiety.
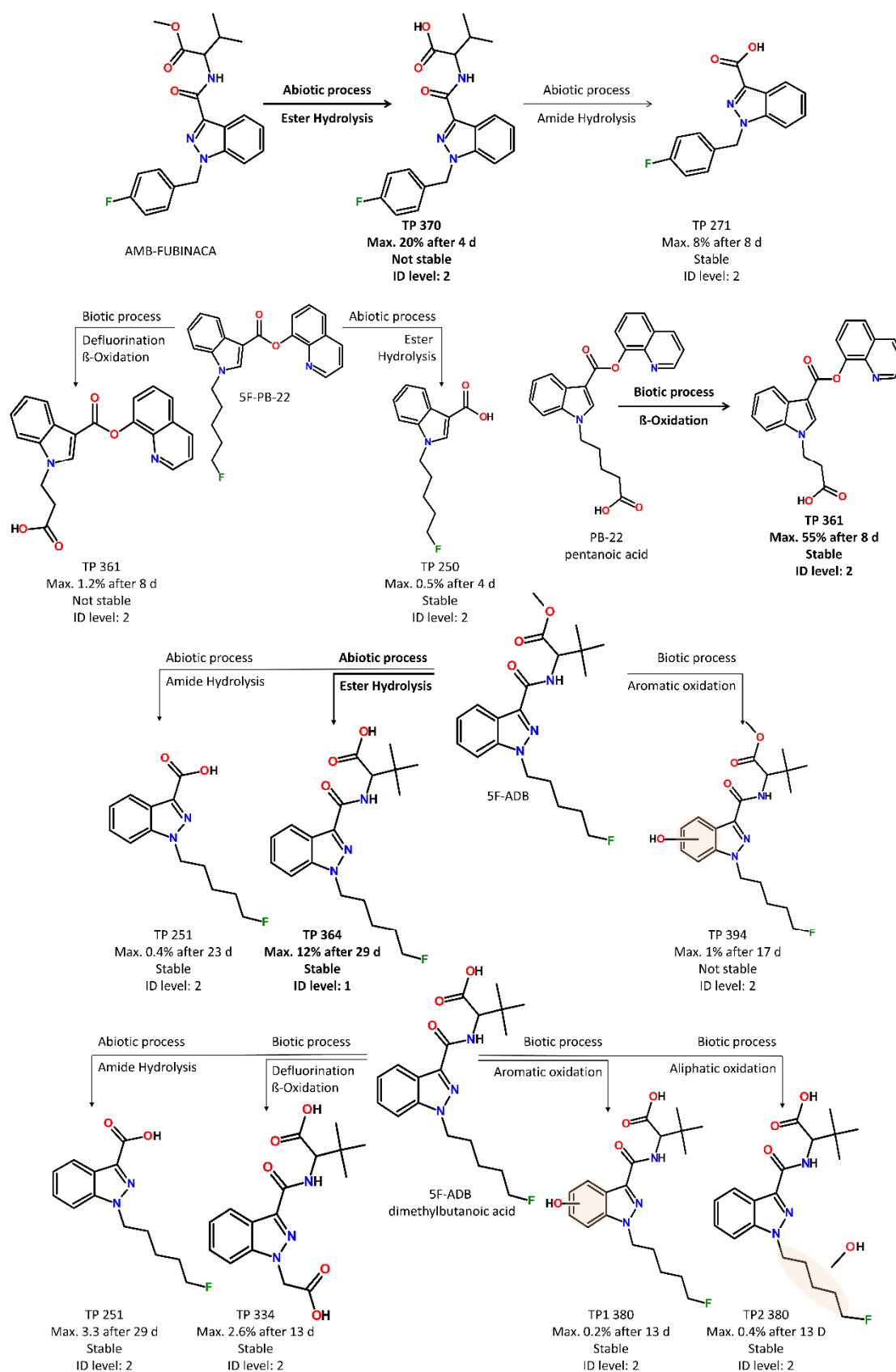
Figure 3. Degradation pathways, transformation processes, maximum formation percentage after certain days and identification confidence levels of TPs originating from 5F-PB-22, PB-22 pentanoic acid, 5F-ADB, 5F-ADB dimethylbutanoic acid and AMB-FUBINACA. Main TPs and their pathways are indicated in bold.

106

3.4 Conclusion

In order to simulate optimal conditions to investigate biodegradation of SCRAs in the sewage system, wastewater effluent and sludge were used for laboratory scale die-away experiments of six selected SCRAs and two of their human metabolites. Analytical methods including LC-MS/MS and LC-(MS/)HRMS were successfully applied for the determination of the corresponding stability profiles and for the identification of potential TPs. The results of the study indicate that the majority of the selected SCRAs (5F-ADB, 5F-PB-22, Cumyl-PeGaClone, MDMB-CHMCZCA and EG-018) are suitable sewage biomarkers, except for AMB-FUBINACA due to its fast transformation rate in sewage. Similar transformation kinetics of active and non-active assay suggest that physico-chemical processes such as hydrolysis or sorption dominate the fate of these SCRAs in wastewater. The investigated metabolites, 5F-ADB dimethylbutanoic acid and PB-22 pentanoic acid, can also be considered as suitable biomarkers for WBE studies, however, they exhibit greater susceptibility to microbial degradation than the respective parent SCRAs. Metabolic processes in humans like oxidative defluorination of 5F-PB-22 to carboxylic acid (PB-22 pentanoic acid) seem to be a decisive point for a pronounced biological degradation in wastewater environment. Hydrolysis of the terminal groups as a common metabolic reaction for SCRAs leads to formation of metabolites having a terminal carboxyl group, e.g. 5F-ADB dimethylbutanoic acid. These compounds were also identified as TPs in wastewater implying no possibility to discriminate between consumption and discharge in the course of clandestine manufacture of related designer drug products as input sources if these biomarkers are used. The presented stability data can serve as a starting point for implementation of a sewage-epidemiologic study on the prevalence of SCRAs abuse and SCRAs replacement timelines. Apart from the parent substances, three TPs were determined that should be included in the target list for WBE studies (TP 361 from PB-22 pentanoic acid, TP 364 from 5F-ADB and TP 370 from AMB-FUBINACA). These TPs will complement results based on their corresponding SCRA analytes.

3.5 References

[1]   European Monitoring Centre for Drugs and Drug Addiction (EMCDDA). European Drug Report 2020: Trends and Developments. 2020; Luxembourg: Publications Office of the European Union. https://www.emcdda.europa.eu/system/files/publications/13236/TDAT2000 1ENN_web.pdf. Accessed April 23, 2021.

[2]   United Nations Office on Drugs and Crime (UNODC). Current NPS Threats – Volume I. 2019; Vienna. https://www.unodc.org/documents/scientific/Current_NPS_Threats_Volume_ I.pdf. Accessed April 23, 2021.

[3]   United Nations Office on Drugs and Crime (UNODC). Current NPS Threats – Volume II. 2020; Vienna. https://www.unodc.org/documents/scientific/Current_NPS_Threats_Volume _II_Web.pdf. Accessed April 23, 2021.

[4]   Zuccato E, Chiabrando C, Castiglioni S, Bagnati R, Fanelli R. Estimating community drug abuse by wastewater analysis. *Environ Health Perspect.* 2008;116:1027-1032. DOI: 10.1289/ehp.11022.

[5]   Reid MJ, Derry L, Thomas KV. Analysis of new classes of recreational drugs in sewage: Synthetic cannabinoids and amphetamine-like substances. *Drug Test Anal*. 2014;6(1-2):72-79. DOI: 10.1002/dta.1461.

[6]   Senta I, Krizman I, Ahel M, Terzic S. Multiresidual analysis of emerging amphetamine-like psychoactive substances in wastewater and river water. *J Chromatogr A*. 2015;1425:204-212. DOI: 10.1016/j.chroma. 2015.11.043.

[7]   Borova VL, Gago-Ferrero P, Pistos C, Thomaidis NS. Multi-residue determination of 10 selected new psychoactive substances in wastewater samples by liquid chromatography–tandem mass spectrometry. *Talanta*. 2015;144:592-603. DOI: 10.1016/j.talanta.2015.06.080.

[8]   Kinyua J, Covaci A, Maho W, McCall AK, Neels H, van Nuijs AL. Sewage-based epidemiology in monitoring the use of new psychoactive substances: Validation and application of an analytical method using LC-MS/MS. *Drug Test Anal*. 2015;7(9):812-818. DOI: 10.1002/dta.1777.

[9]   González-Mariño I, Gracia-Lor E, Bagnati R, Martins CP, Zuccato E, Castiglioni S. Screening new psychoactive substances in urban wastewater using high resolution mass spectrometry. *Anal Bioanal Chem*. 2016;408(16):4297-4309. DOI: 10.1007/ s00216-016-9521-0.

[10]   Bade R, Bijlsma L, Sancho JV, et al. Liquid chromatography-tandem mass spectrometry determination of synthetic cathinones and phenethylamines in influent wastewater of eight European cities. *Chemosphere*. 2017;168:1032-1041. DOI: 10.1016/j.chemosphere. 2016.10.107.

[11]   Gao T, Du P, Xu Z, Li X. Occurrence of new psychoactive substances in wastewater of major Chinese cities. *Sci Total Environ*. 2017;575:963-969. DOI: 10.1016/j.scitotenv. 2016.09.152.

[12]   Causanilles A, Kinyua J, Ruttkies C, et al. Qualitative screening for new psychoactive substances in wastewater collected during a city festival using liquid chromatography coupled to high-resolution mass spectrometry. *Chemosphere*. 2017;184:1186-1193. DOI: 10.1016/j.chemosphere.2017.06.101.

[13]   Lai FY, Wilkins C, Thai P, Mueller JF. An exploratory wastewater analysis study of drug use in Auckland, New Zealand. *Drug Alcohol Rev*. 2017;36:597-601. DOI: 10.1111/dar.12509.

[14]   González-Mariño I, Thomas KV, Reid MJ. Determination of cannabinoid and synthetic cannabinoid metabolites in wastewater by liquid–liquid extraction and ultra-high performance supercritical fluid chromatography-tandem mass spectrometry. *Drug Test Anal*. 2018;10(1):222-228. DOI: 10.1002/dta. 2199.

[15]   Salgueiro-González N, Castiglioni S, Gracia-Lor E, et al. Flexible high resolution-mass spectrometry approach for screening new psychoactive substances in urban wastewater. *Sci Total Environ*. 2019;689:679-690. DOI: 10.1016/j.scitotenv. 2019.06.336.

[16]   Bade R, Tscharke BJ, White JM, et al. LC-HRMS suspect screening to show spatial patterns of New Psychoactive Substances use in Australia. *Sci Total Environ*. 2019;650:2181-2187. DOI: 10.1016/j.scitotenv.2018.09.348.

[17]   Pandopulos AJ, Bade R, O'Brien JW, et al. Towards an efficient method for the extraction and analysis of cannabinoids in wastewater. *Talanta*. 2020;217: 121034. DOI: 10.1016/j.talanta.2020.121034.

[18]   Castiglioni S, Salgueiro-González N, Bijlsma L, et al. New psychoactive substances in several European populations assessed by wastewater-based epidemiology. *Water Res*. 2021;195:116983. DOI: 10.1016/j.watres.2021.116983.

[19]   Bade R, White JM, Chen J, et al. International snapshot of new psychoactive substance use: Case study of eight countries over the 2019/2020 new year period. *Water Res*. 2021;193:116891. DOI: 10.1016/j.watres.2021.116891.

[20]   Bijlsma L, Celma A, López FJ, Hernández F. Monitoring new psychoactive substances use through wastewater analysis: current situation, challenges and limitations. *Curr Opin Environ Sci Health.* 2019;9:1-12. DOI: 10.1016/j.coesh.2019.03.002.

[21]   Mogler L, Wilde M, Huppertz LM, Weinfurtner G, Franz F, Auwärter V. Phase I metabolism of the recently emerged synthetic cannabinoid CUMYL-PEGACLONE and detection in human urine samples. *Drug Test Anal*. 2018;10(5): 886-891. DOI: 10.1002/dta.2352.

[22]   Mogler L, Franz F, Wilde M, et al. Phase I metabolism of the carbazole-derived synthetic cannabinoids EG-018, EG-2201, and MDMB-CHMCZCA and detection in human urine samples. *Drug Test Anal*. 2018;10(9):1417-1429. DOI: 10.1002/ dta.2398.

[23]   Diao X, Carlier J, Zhu M, Huestis MA. Metabolism of the new synthetic cannabinoid EG-018 in human hepatocytes by high-resolution mass spectrometry. *Forensic Toxicol*. 2018;36:304-312. DOI: 10.1007/s11419-018-0404-2.

[24]   Wohlfarth A, Gandhi AS, Pang S, Zhu M, Scheidweiler KB, Huestis MA. Metabolism of synthetic cannabinoids PB-22 and its 5-fluoro analog, 5F-PB-22, by human hepatocyte incubation and high-resolution mass spectrometry. *Anal Bioanal Chem*. 2014;406(6):1763-1780. DOI: 10.1007/s00216-014-7668-0.

[25]   Yeter O, Ozturk YE. Metabolic profiling of synthetic cannabinoid 5F-ADB by human liver microsome incubations and urine samples using high-resolution mass spectrometry. *Drug Test Anal*. 2019;11:847-858. DOI: 10.1002/dta.2566.

[26]   Xu D, Zhang W, Li J, Wang J, Qin S, Lu J. Analysis of AMB-FUBINACA Biotransformation Pathways in Human Liver Microsome and Zebrafish Systems by Liquid Chromatography-High Resolution Mass Spectrometry. *Front. Chem*. 2019;7:240. DOI: 10.3389/fchem.2019.00240.

[27]   Staeheli SN, Poetzsch M, Veloso VP, et al. In vitro metabolism of the synthetic cannabinoids CUMYL-PINACA, 5F-CUMYL-PINACA, CUMYL-4CN-BINACA, 5F-CUMYL-P7AICA and CUMYL-4CN-B7AICA. *Drug Test Anal*. 2018;10(1):148-157. DOI: 10.1002/dta.2298.

[28]   McCall AK, Bade R, Kinyua J, et al. Critical review on the stability of illicit drugs in sewers and wastewater samples. *Water Res*. 2016;88:933-947. DOI: 10.1016/j.watres.2015.10.040.

[29]   Kinyua J, Negreira N, McCall AK, et al. Investigating in-sewer transformation products formed from synthetic cathinones and phenethylamines using liquid chromatography coupled to quadrupole time-of-flight mass spectrometry. *Sci Total Environ*. 2018;634:331-340. DOI: 10.1016/j.scitotenv.2018.03.253.

[30]   Kinyua J, Psoma AK, Rousis NI, et al. Investigation of Biotransformation Products of p-Methoxymethylamphetamine and Dihydromephedrone in Wastewater by High-Resolution Mass Spectrometry. *Metabolites*. 2021;11:66. DOI: 10.3390/metabo 11020066.

[31]   Diao X, Huestis MA. Approaches, Challenges, and Advances in Metabolism of New Synthetic Cannabinoids and Identification of Optimal Urinary Marker Metabolites. *Clin Pharmacol Ther.* 2017;101:239-253. DOI: 10.1002/cpt.534.

[32]   Minakata K, Yamagishi I, Nozawa H, et al. Sensitive identification and quantitation of parent forms of six synthetic cannabinoids in urine samples of human cadavers by liquid chromatography–tandem mass spectrometry. *Forensic Toxicol*. 2017;35:275-283. DOI: 10.1007/s11419-017-0354-0.

[33]   Giorgetti A, Mogler L, Haschimi B, et al. Detection and phase I metabolism of the 7-azaindole-derived synthetic cannabinoid 5F-AB P7AICA including a preliminary pharmacokinetic evaluation. *Drug Test Anal*. 2020;12:78-91. DOI: 10.1002/dta. 2692.

[34]   Vikingsson S, Gréen H, Brinkhagen L, Mukhtar S, Josefsson M. Identification of AB-FUBINACA metabolites in authentic urine samples suitable as urinary markers of drug intake using liquid chromatography quadrupole tandem time of flight mass spectrometry. *Drug Test Anal*. 2016;8:950-956. DOI: 10.1002/dta.1896.

[35]   Blandino V, Wetzel J, Kim J, Haxhi P, Curtis R, Concheiro M. Oral Fluid vs. Urine Analysis to Monitor Synthetic Cannabinoids and Classic Drugs Recent Exposure. *Curr Pharm Biotechnol*. 2017;18:796-805. DOI: 10.2174/1389201018666171122113934.

[36]   Emke E, Evans S, Kasprzyk-Hordern B, de Voogt P. Enantiomer profiling of high loads of amphetamine and MDMA in communal sewage: a Dutch perspective. *Sci Total Environ*. 2014;487:666-672. DOI: 10.1016/j.scitotenv.2013.11.043.

[37]   Antonides LH, Cannaert A, Norman C, et al. Enantiospecific Synthesis, Chiral Separation, and Biological Activity of Four Indazole-3-Carboxamide-Type Synthetic Cannabinoid Receptor Agonists and Their Detection in Seized Drug Samples. *Front Chem*. 2019;7:321. DOI: 10.3389/fchem.2019.00321.

[38]   Weber C, Pusch S, Schollmeyer D, Münster-Müller S, Pütz M, Opatz T. Characterization of the synthetic cannabinoid MDMB-CHMCZCA. *Beilstein J Org Chem*. 2016;12:2808-2815. DOI: 10.3762/bjoc.12.279.

[39]   Andernach L, Pusch S, Weber C, et al. Absolute configuration of the synthetic cannabinoid MDMB-CHMICA with its chemical characteristics in illegal products. *Forensic Toxicol*. 2016;34:344–352. DOI: 10.1007/s11419-016-0321-1.

Chapter 3

[40]   Loos, M. 2019. enviMass version 3.5 LC-HRMS trend detection workflow - R package. Zenodo. DOI: 10.5281/zenodo.1213098.

[41]   Schymanski EL, Jeon J, Gulde R, et al. Identifying Small Molecules via High Resolution Mass Spectrometry: Communicating Confidence. *Environ. Sci. Technol*. 2014;48(4):2097–2098. DOI: 10.1021/es5002105.

3.6 Supplementary Material

Table S1. Gradient of the HPLC-Orbitrap method.

Time	Eluent A (%)	Eluent B (%)
0.0	95	5
0.5	95	5
8.0	0	100
11.0	0	100
11.1	95	5
16.0	95	5

Table S2. MRM parameters including the precursor ion (Q1) and the two most prominent product ions (Q3), declustering potential (DP), entrance potential (EP), collision cell entrance potential (CEP), collision energy (CE) and collision cell exit potential (CXP). Quantifier ion is indicated for each analyte as underlined Q3 ion.

Analyte	Q1 m/z	Q3 m/z	DP in V	EP in V	CEP in V	CE in V	CXP in V
5F-PB-22	377	<u>232</u>	31	4.5	16	21	4
	377	144	31	4.5	16	57	4
PB-22 pentanoic acid	389	<u>244</u>	16	4.0	18	19	4
	389	144	16	4.0	18	45	4
5F-ADB	378	<u>233</u>	41	5.5	18	29	4
	378	318	41	5.5	18	21	4
5F-ADB dimethylbutanoic acid	364	<u>233</u>	41	7.0	14	27	4
	364	318	41	7.0	14	19	4
Cumyl-PeGaClone	373	<u>255</u>	31	9.0	22	17	4
	373	167	31	9.0	22	67	4
AMB-FUBINACA	384	<u>109</u>	46	7.0	14	47	4
	384	253	46	7.0	14	31	4
MDMB-CHMCZCA	435	<u>290</u>	41	6.0	20	25	4
	435	166	41	6.0	20	73	4
EG-018	392	<u>155</u>	51	10.5	16	33	4
	392	127	51	10.5	16	69	4
1`-naphthoyl indole	272	<u>155</u>	41	7.50	16	27	4
	272	127	41	7.50	16	51	4

Table S3. Method parameters for the Orbitrap method.

Parameter	Value
Collision energy	50 (normalized collision energy)
Spray voltage	3.2 kV (ESI+)
Capillary temp.	350°C
Heater temp.	30°C
Sheath gas flow rate	30 arbitrary units
Auxiliary gas flow rate	12 arbitrary units

Method validation

Linearity of calibration was assessed by analyzing standard solution of SCRAs and metabolites in triplicate injection at eight different concentration levels ranging from 1 to 250 ng/mL for all the compounds, except for EG-018 and MDMB-CHMCZCA which showed a linearity range from 20 ng/mL to 1000 ng/mL. Instrumental limit of detection (ILOD) was defined as the lowest quantity of a substance that can be differentiated from the background level accomplishing at least signal-to-noise ratio of 3/1, for both the quantifier and the qualifier ion. Instrumental limit of quantification (ILOQ) was assigned to the calibrator concentration that was at least nine times the average background noise (calculated signal-to-noise corresponding to 9/1) for both ions. The ILOD was calculated to be between 0.3 and 6.7 ng/mL, whereas the ILOQ was in the interval of 1 - 20 ng/mL.

Matrix effects (ME) were expressed as quantifier mean area response ($\bar{A}$) for inoculum spiked with analyte post-filtration relative to the area response in analyte standard solution (80:20, water:MeOH) (Eq. 1, n = 4).

$$ME\ [\%] = \left(\frac{\left(\bar{A} \text{ (post spiked analyte in matrix)} - \bar{A} \text{ (matrix)} \right)}{\bar{A} \text{ (analyte standard)}} \cdot 100 \right) - 100 \qquad (1)$$

Since sample preparation comprised only filtration (0.2 µm, regenerated cellulose filters) and dilution of the filtered sample with ultrapure water/methanol prior to LC-ESI-MS/MS analysis, filtration recovery was determined. Filtration recovery was assessed as quantifier mean area response of analyte ($\bar{A}$) being subjected to filtration in inoculum as percentage of the area response in inoculum spiked with analyte post-filtration, shown in Eq. 2 (n = 4).

$$Recovery\ [\%] = \left(\frac{\left(\bar{A} \text{ (pre spiked analyte in matrix)} - \bar{A} \text{ (matrix)} \right)}{\bar{A} \text{ (post spiked analyte in matrix)}} \cdot 100 \right) - 100 \qquad (2)$$

Table S4. Relevant validation parameters including linear correlation coefficients (R^2), instrumental limit of detection (ILOD), instrumental limit of quantification (ILOQ), recovery, matrix effect, and precision of the method.

Analyte	R^2	ILOD[a] [ng/mL]	ILOQ [ng/mL]	Filtration recovery [%] inoculum	Filtration recovery [%] ultrapure water[b]	Matrix effect [%]	RSD [%] 20 ng/mL	RSD [%] 100 ng/mL
5F-ADB	0.9993	0.3	1	87.7	93.4	8.1	10.3	8.3
5F-ADB dimethylbutanoic acid	0.9998	1.7	5	97.7	93.2	6.6	10.1	8.6
5F-PB-22	0.9994	0.3	1	82.9	85.1	7.0	8.9	9.0
PB-22 pentanoic acid	0.9990	1.7	5	100.0	93.9	-0.3	10.6	10.4
AMB-FUBINACA	0.9995	0.3	1	87.2	95.9	8.3	10.6	9.1
Cumyl-PeGaClone	0.9996	1.7	5	72.5	75.3	8.0	10.1	9.6
EG-018	0.9975	6.7	20	10.9	15.5	-2.7	1.3	19.9
MDMB-CHMCZCA	0.9975	6.7	20	26.0	18.3	5.7	8.0	13.7

a ILOD was determined on the basis of the ILOQ values (1/3 of the ILOQ). ILOQ relied on signal-to-noise (S/N) ratio calculations of lower calibrators

b Filtration recovery in ultrapure water (n = 1)
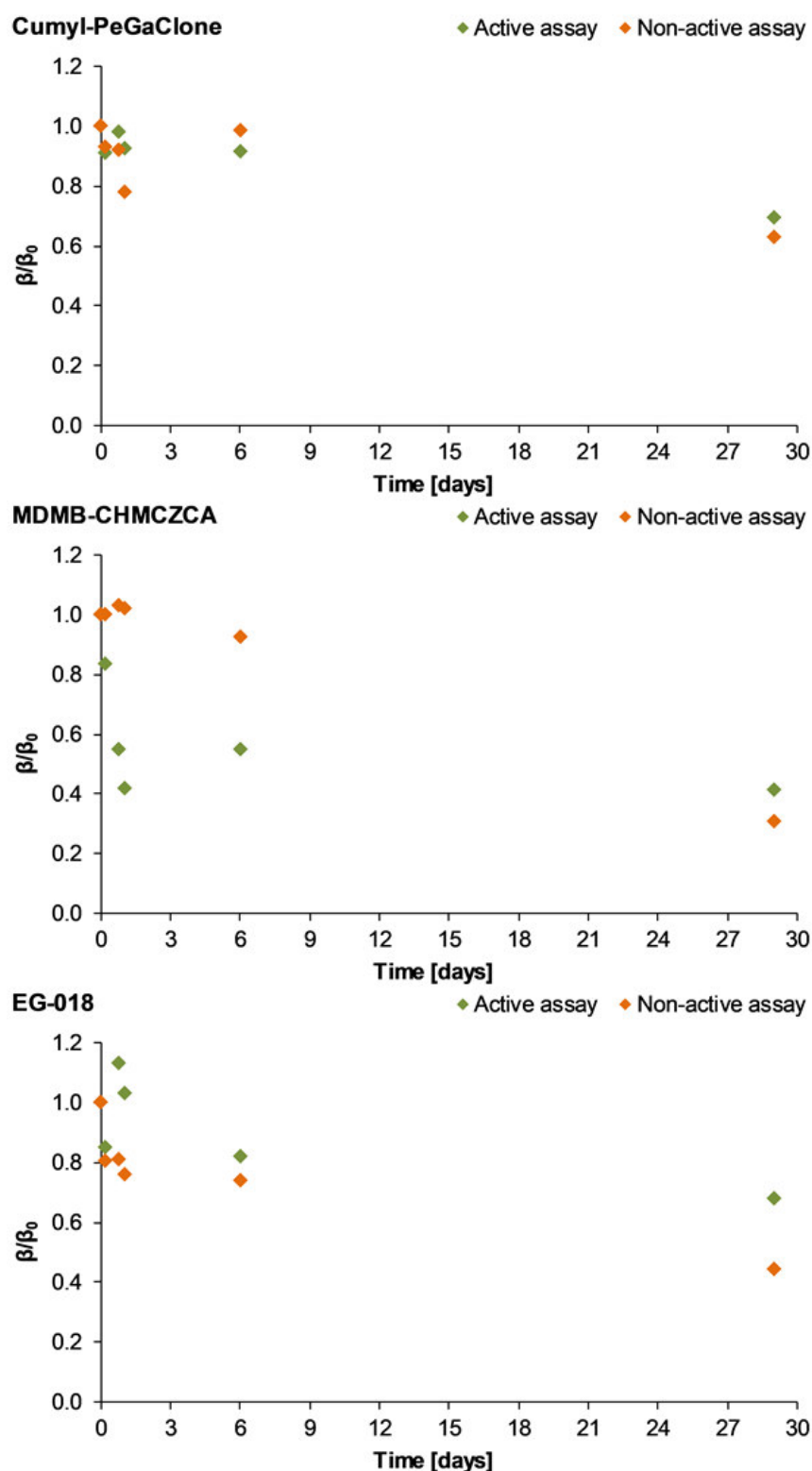
Figure S1. Sewage stability profiles of Cumyl-PeGaClone (top), MDMB-CHMCZCA (middle) and EG-018 (bottom). All measurements were done in single determination.

General remark: Figures **S2-S20** and Tables **S5-S18** were not elaborated by the author of this dissertation and, hence, are not part of this work. These results can be found in the Electronic Supplementary Material of the published article.

Stability of several chemically diverse synthetic cannabinoid receptor agonists (SCRAs) and their selected human metabolites were investigated under sewage conditions utilizing a combination of liquid chromatography-tandem mass spectrometry and high-resolution mass spectrometry (HRMS). The determined stability profiles and transformation reactions of parent SCRA compounds in wastewater enable a valuable inside in use and prevalence of SCRAs via application of wastewater-based epidemiology (WBE).
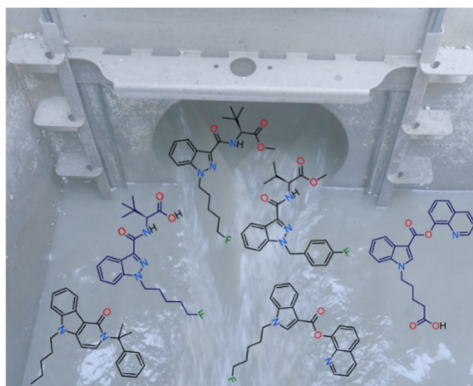
Synthetic cannabinoid receptor agonists and their human metabolites in sewage water: Stability assessment and identification of transformation products

Petra Hehet, Niklas Köke, Daniel Zahn, Tobias Frömel, Thorsten Rößler, Thomas P. Knepper and Michael Pütz*

Chapter 4

Sewage analysis:

Novel wastewater sampling approach applied in a prison and a major city

Prevalence of synthetic cannabinoid receptor agonists use assessed by sewage monitoring via LC-MS/MS, Part A:

Novel wastewater sampling approach applied in a prison and a major city
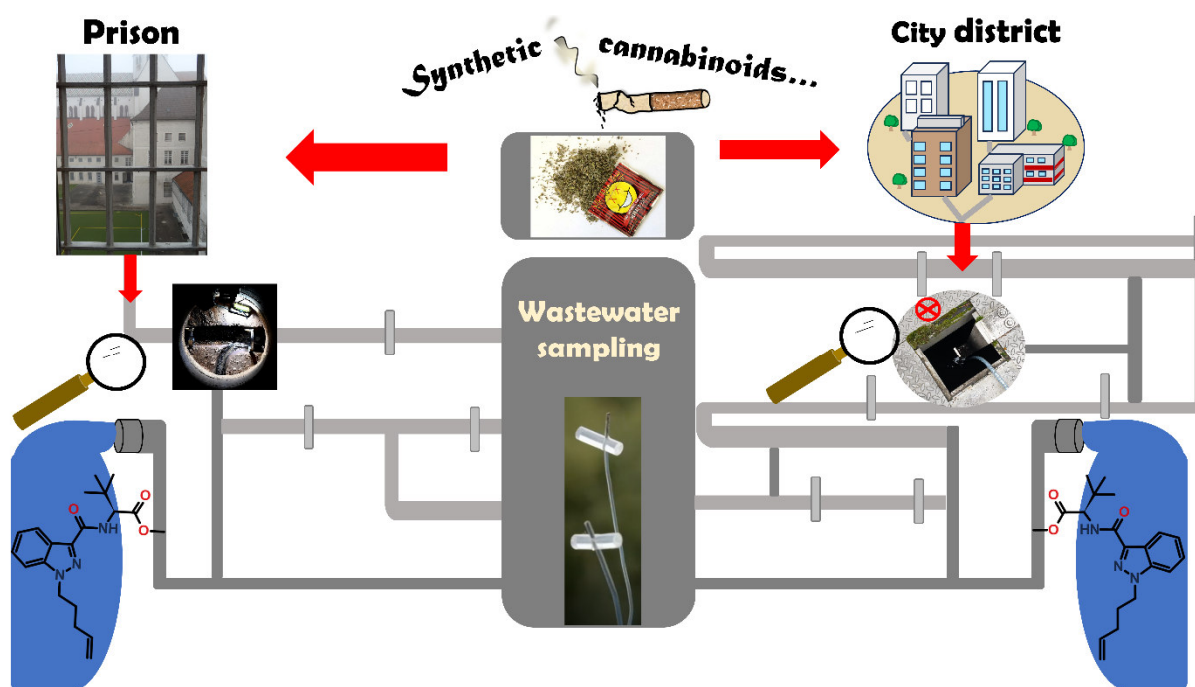
Hehet P, Wende M, Shehata O, Krause S, Pütz M.
Manuscript for submission to *Forensic Chem.* **2024.**

Chapter 4

Abstract

A novel wastewater sampling approach using polydimethylsiloxane (PDMS) rods as solid phase adsorbers was developed and optimized for illicit drug consumption prevalence investigations via wastewater analysis, particularly for synthetic cannabinoid receptor agonists (SCRAs) use assessment. The PDMS rods were deployed directly in the wastewater stream and the methodology was compared to the traditional liquid wastewater collection approach using a time- and event-programmable automated liquid sampling device. Featuring several key advantages, such as cost-effective analyte collection, simple and flexible deployment, as well as small size, the passive sampling methodology represents an appealing approach to monitor drug use. Successful application to a real sewage system was demonstrated by wastewater monitoring of two different populations in Germany: a prison population and a population of a city district in Munich. The selection of suitable sampling locations in a complex sewage system of the city district was based on a sewer network model, enabling either a wider area coverage or a higher local geographical resolution. Both sampling approaches and subsequent LC-MS/MS analysis provided valuable snapshots of the drug consumption patterns in the respective populations over the course of several days in 2021. Several SCRAs, including MDMB-4en-PINACA, 4F-MDMB-BINACA, 4F-MDMB-BICA, 5F-MDMB-PICA / 5F-EMB-PICA, Cumyl-CBMICA, 5F-PB-22, EG-018, MAM-2201 and JWH-210, were detected in sewage water of the selected populations, some of them exhibiting a remarkable time pattern. Prevalence of the most abundant SCRAs in prison correlated with the SCRAs detected in wider population. Thus, the information gained by wastewater analysis on SCRA monitoring of different populations might serve as a multi-approach indicator for the illicit SCRA market. Comparison of the wastewater analyses with seized sample analysis data showed good correlation, highlighting prevalent SCRA use in the prison examined.

Keywords: synthetic cannabinoid receptor agonists (SCRAs) · new psychoactive substances · sewer network model· sewage · prison · polydimethylsiloxane (PDMS) rods · LC-MS/MS

4.1 Introduction

Although the prevalence of use of new psychoactive substances (NPS) in the general population remains to be lower in comparison to conventional illicit drugs, the absolute amounts seized by police and customs authorities have been on the rise for the past few years, reaching apex quantities ever seized in 2021 [1]. Moreover, its specifically prevalent use among particular groups, e.g. young people [2] and some vulnerable and marginalized populations, such as homeless and prisoners, is of particular concern worldwide [3,4]. The most prevalent substance class of NPS being used in this context are synthetic cannabinoid receptor agonists (SCRAs) [2, 5-9], colloquially often referred to as "Spice". SCRA use in prisons has been associated with severe health risks and drug-related problems of such a magnitude, that it became a serious threat to the safety and security of prison systems in some countries. The first report of SCRA use in prisons originates from the United Kingdom (UK) approximately a decade ago (around 2010-2011) [9,10], but it became a Europe-wide phenomenon in the subsequent years [7,11], extending further even to the US [12,13]. Some of the crucial driving factors for SCRA use in prisons seem to be their high potency even in small doses, and the limited detectability of these substances by sniffer dogs as well as in routine urinary drug tests [7,9,14,15]. Numerous routes ensure the supply of NPS into prisons, and the inventive and constantly evolving new smuggling methods pose great challenges for prison services. Recently, the sending of postal packages or letters impregnated with NPS were identified as a routine method for trafficking NPS, especially SCRAs, into prisons [16]. First reported quantitative data on SCRA infused papers revealed typical concentrations of < 0.05 - 1.17 mg/cm^2 paper on papers seized in three Scottish prisons between 2018 and 2019 [17]. The concentration mapping data of the study disclosed high variations of SCRA concentrations (0.47 - 2.38 mg/cm^2 paper) on larger paper sheets, demonstrating a high degree of inhomogeneity that further undermines a safe dosing by users. For consumption, large sheets of infused paper are typically cut into small pieces (often 0.5 x 0.5 cm), included into a cigarette and smoked [18]. The concerning use of NPS requires monitoring tools to elucidate prevalence of these substances and introduce appropriate health and policy measures. The diverse, dynamic and constantly changing nature of the SCRA market requires approaches able to effectively gauge these changes in community drug use. One promising concept addressing these challenges is wastewater-based epidemiology (WBE). Analysis of municipal wastewater has been successfully demonstrated for community-wide assessment of illegal drugs [19,20], including NPS [21,22]. Few recent studies have reported detection of SCRAs via WBE in Australia [23,24], United States [25], Greece [26] and China [27]. However, the detection rate of SCRAs was very low in nearly all studies, e.g. when compared to other NPS such as synthetic cathinone derivatives. These challenges can be derived from the great diversity of SCRAs and the rate at which they are exchanged on the illicit drug market, as well as from their consumption in much lower doses in comparison to the conventional drugs. All this leads to low concentration levels of SCRAs in a complex wastewater matrix, requiring efficient sampling and sensitive analytical methods.

Besides monitoring trends in the general population, wastewater analysis (WWA) might be an effective tool to gain comprehensive insight into drug consumption and hence trafficking within a prison. This approach provides near real-time data on collective use of drugs in a given inmate population and might be used as a practical, fast, objective, inconspicuous and non-

invasive tool to track the consumption patterns and effectiveness of countermeasures adopted as a part of anti-drug strategies in prisons. Compared to random urinalyses (RUA), the results are not affected by prisoners' altered drug use behavior during mandatory drug testing days and represent the entirety of inmates instead a limited number of individuals. To date, only six wastewater studies were performed in prisons worldwide, including a Spanish [28], a Northern Irish [29], a US American [30], three French [31] and two Australian prisons [32,33]. The pilot study in Spain reported levels of heroin, amphetamine, methamphetamine and 3,4-methylenedioxymethamphetamine (MDMA), as well as quantifiable loads, i.e. estimated daily doses, for methadone, alprazolam, ephedrine, cannabis and cocaine. Furthermore, comparison with drug quantities determined via WWA for the general population of a nearby city suggested that the drug consumption in the prison was lower for the most drugs included in the study [28]. Another study conducted in Europe included three French prisons for which the authors reported high cannabis use estimated to an average daily consumption of 0.5 - 3 cannabis joints per person, whereas cocaine quantities were small corresponding to 1 - 4 doses per 1,000 inmates [31]. The wastewater study in the US American prison investigated, whether a statistically significant change of wastewater loads for methamphetamine and cocaine could be observed with respect to RUA testing days. Although the illicit drug loads in wastewater did not show significant statistical differences for RUA and non-RUA testing days, WWA offered additional data showing a high prevalence of methamphetamine consumption in the prison due to its high frequency of detection in sewage (every day and every hour), which could not be obtained by RUA alone (6 out of 243 samples positive) [30]. Similarly, WWA in an Australian prison quantitatively assessed the use of licit and illicit drugs. Comparing these findings with urinalyses, WWA was found to provide more comprehensive data on drug use [32]. Another study in an Australian prison monitored changes in medication and illicit drug consumption during COVID-19 restrictions, showing decreased methamphetamine and buprenorphine levels when access to the prison was restricted [33]. And most recently, the prevalence of NPS, including several SCRAs, was explored for the first time by wastewater analysis in a prison, however without positive detection of substances of this drug class in sewage water samples of a prison in Northern Ireland [29].

One key component of WWA is wastewater sampling, which is traditionally performed either manually or with an automated sampler, resulting in grab or composite wastewater samples. Passive sampling of analytes from wastewater is a convenient, time-saving and cost-effective alternative to the traditional active sampling methods. The ability of passive sampling techniques to capture a time-weighted average amount of analytes over longer periods of time, that may range from days to months [34], makes it appealing for wastewater surveillance. Traditionally, passive sampling has been used for environmental monitoring purposes, but several passive sampler configurations were trialled for wastewater-based illicit drug monitoring. These comprise polar organic compound integrative samplers (POCIS) with Hydrophilic-Lipophilic Balance (HLB) sorbent between two polyethersulfone (PES) hydrophilic membranes [35-38], a Chemcatcher® sampling device containing styrene-divinylbenzene adsorbent bound in a polytetrafluorethylene (PTFE) matrix disk [39], cylindrical microporous polyethylene tubes (MPT) containing polymeric sorbent phases (pure or in agarose) [40] and diffusive gradients in thin films (DGT) consisting of an agarose binding layer (crosslinked polystyrene adsorbent), an agarose diffusive layer and a PES filter membrane [41]. In 2014,

the feasibility of POCIS for the qualitative detection of methamphetamine in a sewage system was demonstrated and they were proposed as a forensic tool for law enforcement agencies to identify areas with illicit drug activities [35]. In recent years, quantification approaches were undertaken for all the described passive samplers to determine their linear uptake kinetics and sampling rates required for calculation of drug loads in sewage [38-41]. Polydimethyl-siloxane (PDMS) rods are traditionally deployed for sampling of organic micropollutants in water samples [42], but have also demonstrated their forensic applicability for aqueous sampling of the homemade explosive triacetone triperoxide (TATP) in our previous study [43]. Therefore, we aimed to examine and extend the application of PDMS passive samplers for sewage monitoring of conventional drugs and SCRAs. This is the first approach utilizing a PDMS sorbent for this aim, thus introducing a novel passive sampler for wastewater sampling and surveillance of illicit drugs, particularly SCRAs. Furthermore, the present work demonstrates a successful application of WWA to a prison facility to monitor NPS (SCRA) use for the first time, and it is one of the few pilot studies worldwide monitoring drug use in a prison setting via WWA. Moreover, data gathered by wastewater analysis of the prison effluent were correlated to confiscations of illicit drug products from this facility. In the second step, the wastewater sampling was performed in a city district of Munich, where a more general population and larger sewer network with significantly higher water flows were encompassed. Sampling sites in the city were selected on the basis of simulations of a sewer network model, representing the first approach of this kind for wastewater-based illicit drug monitoring. Both sewer networks were probed via time-resolved liquid sampling as well as time-averaged passive sampling with PDMS rods. The overall methodological objective of this study was to develop, optimize and establish different wastewater sampling approaches (passive sampling and active automated liquid wastewater sampling), a liquid chromato-graphy-tandem mass spectrometry (LC-MS/MS) based analytical method and a computational simulation model for the assessment of SCRA use by wastewater analysis. Part B of this study will focus on WWA in the city of Munich, including a wastewater treatment plant, and triangulate results from wastewater analysis, toxicological analysis of hair samples and police seizures.

4.2 Experimental

4.2.1 Chemicals and materials

SCRAs were provided by the Bavarian State Criminal Police Office (Forensic Science Institute, Munich, Germany) in cooperation with the EU-funded project ADEBAR *plus* and dissolved in methanol or acetonitrile at a concentration level of 1 mg/mL. Selected metabolites were supplied by Cayman Chemicals (Ann Arbor, MI, USA), either as 1 mg powders (PB-22 N-pentanoic acid, Cumyl-PeGaClone N-pentanoic acid, 5F-MDMB-PICA dimethylbutanoic acid, 4F-MDMB-BICA dimethylbutanoic acid and 4F-MDMB-BINACA dimethylbutanoic acid), a methanolic solution (4F-MDMB-BINACA N-(butanoic acid) dimethylbutanoic acid, 1 mg/mL) or a solution in acetonitrile (5F-ADB dimethylbutanoic acid, 5 mg/mL; MDMB-4en-PINACA dimethylbutanoic acid, 10 mg/mL). A table with a detailed list of all SCRA compounds and their selected metabolites, including their semi-systematic and IUPAC names, molecular formulas, monoisotopic masses and chemical structures is provided in the Supplementary Material (Table S1). Methanolic solutions of the phytocannabinoids cannabinol (CBN, 1 mg/mL), (-)-cannabidiol (CBD, 100 µg/mL) and (-)-*trans*-Δ^9-tetrahydrocannabinol (Δ^9-THC, 1 mg/mL) were

purchased from LGC (Wesel, Germany), while deuterated (-)-*trans*-Δ^9-THC (THC-D$_3$, 100 µg/mL) and the selected metabolite (±)-11-nor-9-carboxy-Δ^9-tetrahydrocannabinol (THC-COOH, 100 µg/ml) originated from Sigma Aldrich (Steinheim, Germany). High-purity solvents, including ultra LC-MS grade acetonitrile, ultra LC-MS grade acetonitrile with 0.1% formic acid, ultra LC-MS grade water and ultra LC-MS grade water with 0.1% formic acid, were supplied by scienTEST-bioKEMIX GmbH (Wesel, Germany). Acetic acid (glacial), isohexane, ethyl acetate, sulfuric acid (95 - 97%) and potassium peroxydisulfate were obtained from Merck KGaA (Darmstadt, Germany) as analytical reagent grade chemicals.

Polyethylene (PE) bottles of various capacities were acquired from VWR International GmbH (Ismaning, Germany) and centrifuge tubes (16 mL) from Sarstedt AG (Nümbrecht, Germany). Screw top glass vials with fixed 300 µL glass insert were sourced from Thermo Scientific (Langerwehe, Germany) and glass vials of 1.5 mL volume capacity from Phenomenex (Aschaffenburg, Germany). Polydimethylsiloxane (PDMS) rods were initially purchased as a long string (25 m, ∅ = 2.5 mm; LUX & CO. Bergwerks- und Industriebedarf GmbH, Cologne, Germany) that was cut into pieces as needed, mostly of 1 or 2 cm length.

4.2.2 Wastewater sampling

Wastewater sampling in one German prison took place in a manhole located on the area of the prison setting, in short distance to the connection to the public sewer system. Thus, a total catchment area of the present prisoner population (> 500 inmates) was covered. The sampling was performed by an automated sampling device (Basic Ex 1 mobil, ORI® Abwassertechnik GmbH & Co, cf. Figure 1A). The sampling period included a prolonged weekend (May 22-24, 2021; Saturday-Sunday-Monday), where Monday was a public holiday. According to prison security officials, higher consumption was expected during weekend and holidays, consequently a prolonged weekend was specifically selected. The sampling device was programmed to collect a 100 mL wastewater sample every 12 minutes over 48 h sampling time, resulting in twelve individual 4-hour composite samples, that were transferred to PE bottles and transported to the laboratory. Details of the sampling parameters are given in Table S2 (Supplementary Material). In parallel to the liquid wastewater sampling, a PDMS rod (approx. 8 cm length) was attached on the hose of the sampling device and remained in the wastewater flow from May 21, 2021 (10 a.m.) until May 25, 2021 (10 a.m.). The length of approx. 8 cm was chosen due to easier handling during the installation. Only a part of the rod (1 cm, Figure 1B) was used for laboratory analysis to extract the drugs enriched, while the residual part was kept as a reserve sample at -20°C.

Wastewater sampling in a city district of Munich (Germany) was performed in a similar way and the corresponding details are described in Part B of this study [44]. Briefly, the above mentioned automated sampling device was installed in a manhole of the sewer network within two different time periods, once during two weekdays and once during an upcoming weekend in September 2021 (48 h sampling each). In parallel, PDMS rods were mounted on the hose of the sampling device during the weekdays and during the upcoming weekend. In addition, two further locations in the city district were selected in accordance to the computational sewer network model to install the PDMS rods for drug consumption monitoring during the weekdays period. All details regarding the installation and deinstallation dates and placement times for the PDMS rods in the sewage network of the city

district can be found in Table S3 (Supplementary Material). A part of each PDMS rod (2 cm) deployed was used for laboratory analysis to extract the target analytes.
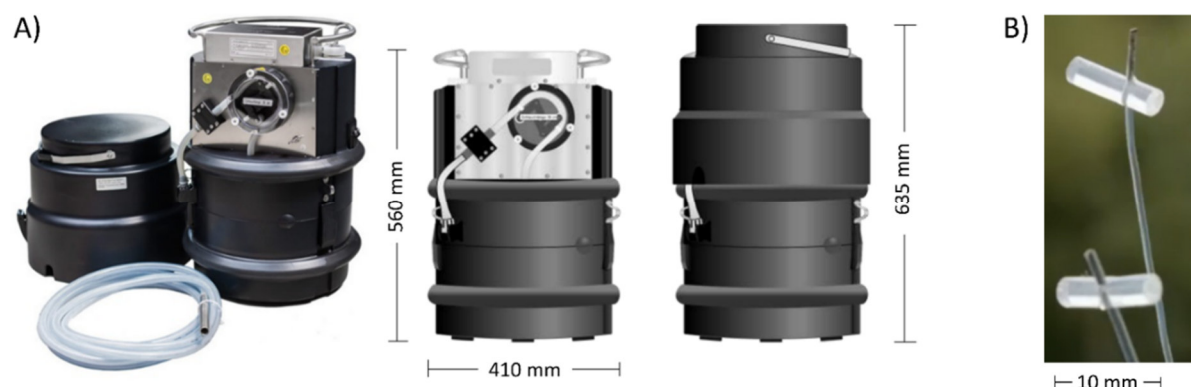
Figure 1. Sampling device for automated wastewater sampling and its dimensions (A, adapted from ORI Abwassertechnik GmbH & Co. KG). The weight of the sampler amounts to 26 kg including battery 10 Ah or 30 kg including battery 22 Ah. Depiction of PDMS rods (1 cm length) deployed for direct sampling in wastewater stream (B).

4.2.3 Wastewater characterization

As an influence of wastewater composition on adsorption or desorption of analytes to/from passive samplers cannot be ruled out, all wastewater samples were analyzed for pH and electric conductivity, using a WTW Multiline® Multi 3630 IDS field meter with a SenTix® pH electrode and a TetraCon® 925 conductivity cell, for general characterization. Based on the measured values for pH and electric conductivity, an influence of rainwater, infiltrating groundwater or industrial discharges to the sewer network would have been detected.

To verify whether the characteristics of the sampled wastewater differed from those of a typical domestic wastewater, the most important nutrients and wastewater constituents (nitrogen, phosphorus, and Chemical Oxygen Demand – COD) were also analyzed. Total phosphorous was analyzed according to DIN EN ISO 15681 using a Seal AutoAnalyzer 3 continuous flow analyzer after digestion with sulfuric acid and potassium peroxydisulfate. Nitrogen was analyzed as Total Kjeldahl Nitrogen (TKN) according to DIN EN 25663, using a BÜCHI K-436 SpeedDigester and a BÜCHI B-324 for steam distillation. COD was analyzed according to DIN ISO 15705 using Spectroquant® cell tests by Merck and a WTW photoLab 7600 UV-VIS photometer.

4.2.4 Sample preparation

Liquid-liquid extraction (LLE)

After sampling, the liquid wastewater samples were kept frozen at -20°C until analysis without further manipulation. For extraction and pre-concentration of the analytes from the wastewater matrix, the 4-hour composite wastewater samples were first thawed and homogenized by multiple inversion of the sampling bottles to ensure a uniform distribution of the particulate and dissolved fraction. As suggested by Pandopulos et al. [24], the particulate fraction was not removed due to substantial SCRA adsorption to the particulates and hence a significant contribution of this fraction to enhanced recoveries. The optimized extraction procedure was as follows, however the acidification step described below was introduced

later in the course of method optimization for SCRA metabolites and was not applied to the wastewater samples from the prison. An aliquot of the wastewater sample (10 mL) was transferred to a conical polypropylene tube (volume capacity of 16 mL) and acidified with acetic acid (glacial, 0.5 mL) to a pH of 2-3. Subsequently, the extraction was carried out with an isohexane/ethyl acetate mixture (2.5 mL, 9/1, v/v) by 20-fold inversion of the tubes and subsequent shaking for five minutes using a vertical shaker (VV3, VWR International GmbH, Ismaning, Germany). The following centrifugation (7000 rpm, 6 min) of the samples facilitated the phase separation and emulsion minimization. Finally, the organic phase (1.9 mL) was transferred to a glass vessel with a pipette. The extraction procedure was repeated with the aqueous phase in an analogous way for one more time, using a slightly smaller volume of the extraction mixture (2 mL). The complete extraction procedure was repeated with additional 10 mL of wastewater sample, and all the organic phases collected were combined. After evaporation to dryness at 35°C under a gentle stream of nitrogen, the dry residue was reconstituted with acetonitrile (50 µL) and diluted with water (50 µL). Finally, the reconstituted extracts were transferred to 300 µL insert glass vials and analyzed by an LC-MS/MS system (cf. section 4.2.6).

Passive samplers (PDMS rods)

After wastewater sampling in sewers, the PDMS rods deployed (approximately 8 - 10 cm length) were stored at -20°C and later cut to small pieces of the desired length (1 cm or 2 cm) for the analysis. The cutting occurred with a scalpel and a digital caliper gauge in order to achieve a constant and reproducible size of each piece (Figure 2A). The extraction of sampled analytes from PDMS rods was performed by addition of an isohexane/ethyl acetate mixture (9/1, v/v; 1 mL) to a PDMS rod (1 cm length) in a glass vial (1.5 mL volume capacity) and agitation in a vertical shaker (VV3, VWR International GmbH, Ismaning, Germany) at medium intensity level for 20 minutes. Afterwards, the liquid phase was transferred to a separate vial, and the extraction was repeated. The collected organic phases were combined and subsequently evaporated to dryness at 35°C under a gentle stream of nitrogen. The dry residue was dissolved with acetonitrile (50 µL) and subsequently diluted with water (50 µL). For longer PDMS rods (2 cm length) larger extraction solvent mixture volumes (1.5 mL) were used.

4.2.5 Assay of the desorption of SCRAs from PDMS material under sewage water flow

In order to elucidate possible desorption effects of target analytes from PDMS rods under sewage water flow, a systematic study was conducted. PDMS rods (4 x 3.5 cm length) were placed in a beaker containing a solution of three different SCRAs (100 µL, 1 µg/mL) in distilled water (5 mL). The SCRAs included 4F-MDMB-BINACA, MDMB-4en-PINACA and Cumyl-CBMICA. The mixture was left at room temperature for 30 minutes to ensure the adsorption of the dissolved target analytes onto the PDMS material. Afterwards, the PDMS rods were removed from the solution and one rod was kept as a reference (t = 0). The residual three PDMS rods were placed under sewage water flow for 1 h, 3 h, and 21 h, respectively, using the assembly shown in Figure 2B. Subsequently, three pieces of 1 cm length each were cut from the rods to allow for analyses in three-fold replications (n = 3). Re-extraction of SCRAs from PDMS rods was carried out according to the procedure described in the previous section after addition of an internal standard (THC-D3, 100 µL, 0.01 µg/mL) to the collected organic

phases for quantitative analysis. In the second part of the study, a further experiment with extended periods of time for desorption (1 h, 74 h, and 95 h) was repeated in an analogous way, except for using twice as low SCRAs concentration in distilled water (60 µL of 1 µg/mL SCRAs solution in 6 mL distilled water).

Figure 2. PDMS rod after wastewater sampling in sewer, prepared to be cut in small rods of the desired length (2 cm in the particular case) for the analysis. The cutting occurred with a scalpel and a digital caliper gauge (A). Assembly of PDMS rods mounted on a thin metal sheet by a cable tie and attached to metallic weights on a line. The set-up was immersed in a grit chamber (sedimentation tank) in the WWTP to assay the desorption of pre-loaded SCRAs from PDMS material under sewage water flow (B).

4.2.6 Instrumentation and analytical conditions

LC-MS/MS method

Analysis of wastewater samples was performed using an LC-MS/MS system consisting of an ultra-high-performance LC (UHPLC) Nexera X2 (Shimadzu Corporation, Duisburg, Germany) equipped with a DGU-20A degasser, LC-30AD binary pumps, an SIL-30AC autosampler, a CTO-30A column oven, a CBM-20A controller, and a SCIEX QTRAP® 6500 triple quadrupole linear ion trap mass spectrometer assembled with an IonDrive™ Turbo V ion source (SCIEX, Darmstadt, Germany).

Chromatographic separation was performed on a Kinetex® Biphenyl analytical column (100 x 2.1 mm, 1.7 µm particle size, 100 Å pore size) provided with a SecurityGuard™ ULTRA Biphenyl guard column (2 x 2.1 mm, both from Phenomenex, Aschaffenburg, Germany). The column temperature was set to 40°C and the autosampler temperature was maintained at 10°C. The LC mobile phase consisted of water with 0.1% formic acid (UHPLC grade, mobile phase A) and acetonitrile with 0. 1% formic acid (UHPLC grade, mobile phase B) which eluted the analytes from the analytical column at a flow rate of 0.5 mL/min in high pressure gradient mode. The optimized gradient program was as follows: elution started with 40% mobile phase B (isocratic for 1 minute), then increased linearly to 65% mobile phase B within 6.5 min, followed by a further linear increase to 100% mobile phase B within 3.5 min. Initial conditions were restored within 0.1 min and maintained for 2.9 min to ensure sufficient re-equilibration prior to each injection. The graphical representation of the described gradient program is given in Figure S1, Supplementary Material. The injection volume was set to 5 µL (wastewater samples from the prison) or 20 µL (wastewater samples from the city).

Mass spectrometric data acquisition was based on the Multiple Reaction Monitoring (MRM) acquisition mode, where the precursor ions were isolated in the first quadrupole and multiple fragment ions by the subsequent second detection quadrupole. In total, four ion transitions were detected per substance. For the required ionization of the analytes, an electrospray interface operating in positive mode (ESI+) at 4.5 kV was used. The source and gas parameters were set as follows: curtain gas 40 psi, collision gas (CAD) "medium", nebulizer gas (GS1) and heater gas (GS2) both 65 psi, and TurboIonSpray® probe temperature 550°C. All further details regarding the ionization and fragmentation parameters are given in Table S4 in the Supplementary Material. The LC-MS/MS operation and data processing were performed using Analyst® Software 1.6.2 and SCIEX OS® 2.0.1 Software, respectively.

Target analytes

Several chemically diverse substances from the SCRAs class were selected as target analytes for the analytical method used (Table S5, Supplementary Material). The selection was based on prevalence data from police seizures of herbal mixtures ("Spice" products) and SCRA-containing powders. Based on these data, eight human metabolites of selected SCRAs were chosen as target analytes as well. The analytical method also included phytocannabinoids as target substances, namely Δ^9-THC and its major human metabolite THC-COOH, CBN as well as CBD. Details regarding all target analytes including their chemical structures are provided in Table S1.

4.3 Results and Discussion

4.3.1 Wastewater characterization

As can be seen from Figure 3, the wastewater samples from the prison exhibit slightly higher pH values than those from the city district. In addition, the pH varies somewhat more in those samples. This can be attributed to the lower number of people contributing and an upstream sewer network with a shorter flow time. Therefore, individual discharges (shower, toilet, kitchen, etc.) have a higher impact on the wastewater sampled. Overall, the observed range of pH values in both groups of wastewater samples can be considered normal, and no effects on adsorption to or desorption from passive samplers are to be expected.
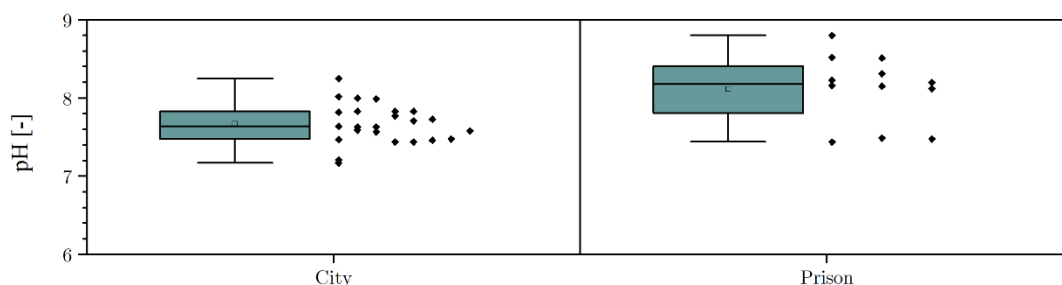
Figure 3. pH-values of wastewater samples from city district (left) and prison (right).

The same overall findings apply to the electric conductivity measured in the samples. Again, the characteristics of the catchment area led to a greater fluctuation of the measured values for the prison wastewater samples (ref. Figure 4). Overall, the absolute values of pH and EC do not indicate any unusual discharges of salts, acids, or alkaline compounds in both groups of samples.
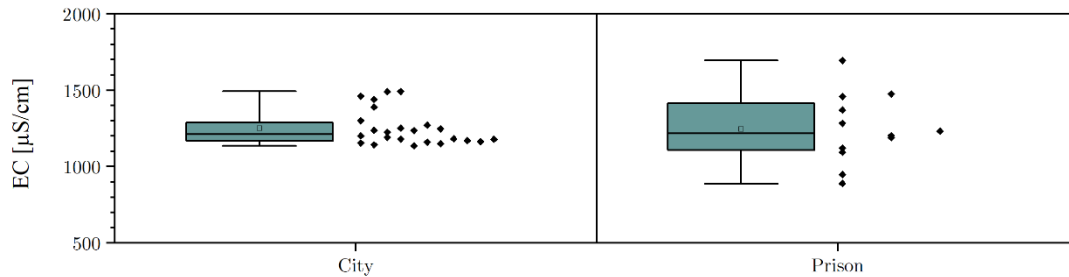
Figure 4. Electric conductivity of wastewater samples from city district (left) and prison (right).

The analytical results for the main nutrients (C, N, P) are shown in Figure 5. To classify the results, the expected concentrations according to DWA A 198 and a wastewater amount of 150 L/(cap·d) are indicated.
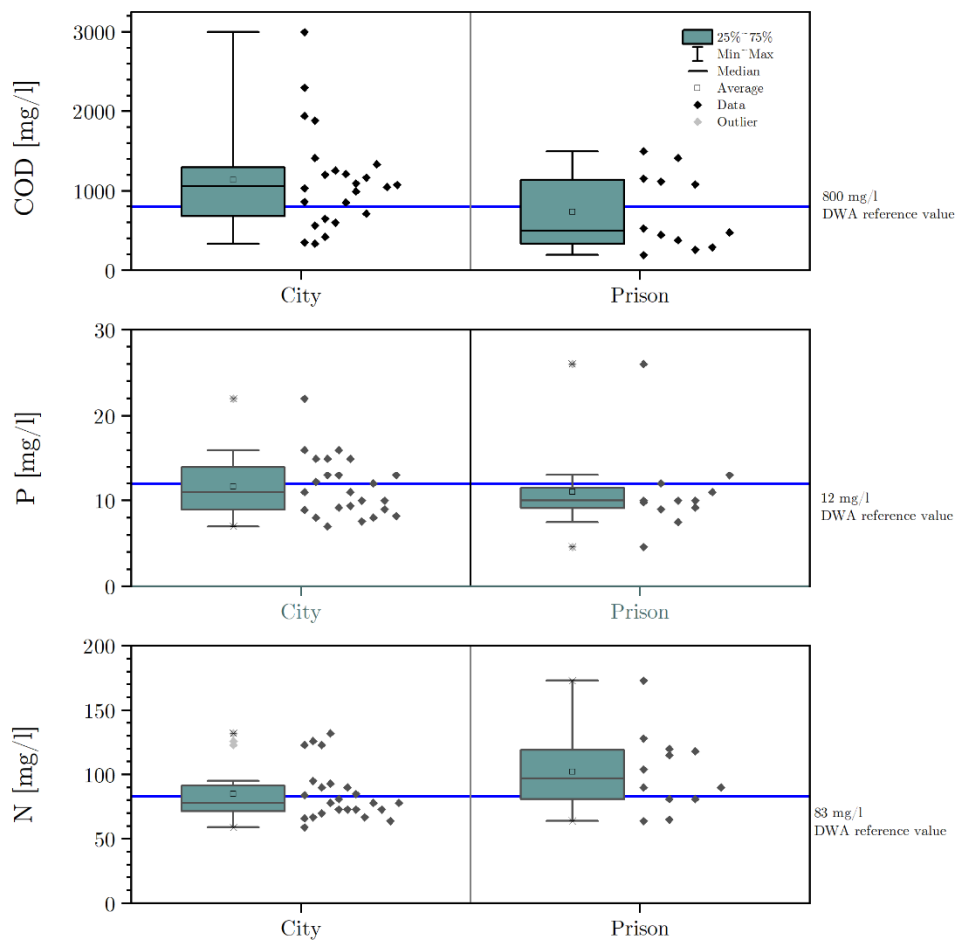
Figure 5. C, N and P concentrations of wastewater samples from city district (left) and prison (right).

4.3.2 Optimization of the sample preparation procedure for PDMS

The authentic PDMS sample collected in the wastewater of the prison was used for the optimization of the sample preparation procedure for PDMS rods, with six different analytes recovered from the PDMS matrix. As these experiments were only comparative studies, not designed to deliver absolute concentrations, only signal areas of the analytes were compared without quantitation against an internal standard. The comparability was assured by using the same extraction conditions with equal amounts of PDMS material and equal extraction volumes. Two parameters were investigated in order to determine the most efficient re-extraction procedure for SCRAs from PDMS material. Firstly, isohexane/ethyl acetate (9/1, v/v) and methanol as two different extractants were compared, then the extraction efficiency was probed by performing a second extraction step. As shown in Table S6 (Supplementary Material), the isohexane/ethyl acetate mixture yielded a superior extraction efficiency compared to methanol for all the six SCRAs, with at least 50% greater signal areas for the majority of the substances. Furthermore, the second extraction step offered a potential to improve the recovery of target analytes from the PDMS rod by approximately 30%. Based on these results, the extraction procedure was set as described in section 4.2.4. Comparison of the PDMS and the LLE extraction protocols showed no general trend. While LLE gave higher yields for two analytes, PDMS proved superior for four analytes. Remarkably, two of the six SCRAs could only be detected using the PDMS method (cf. Table S6).

4.3.3 Assay of the desorption of SCRAs from PDMS material under sewage water flow

The experiments described above clearly demonstrate the suitability of PDMS rods for the extraction of SCRAs from authentic wastewater. However, their practical use strongly depends on the degree of desorption of initially adsorbed analytes after prolonged exposure to a wastewater flow. A high degree of desorption would considerably limit the time interval that can be covered by the use of a rod. To assay the desorption effect, PDMS rods were first laced with three different model SCRAs by placing the rods in an aqueous solution of the analytes for 30 minutes. Of these loaded PDMS rods, one was analyzed without desorption as a reference, and the residual three were placed under sewage water flow for 1 h, 3 h, and 21 h, respectively. As these periods of time only led to moderate losses of analytes, a second set of experiments was conducted with extended durations up to 95 h. An internal standard (THC-D3, 100 µL, 0.01 µg/mL) was added during re-extraction as an internal control.

Desorption kinetics for three currently prevalent and chemically diverse SCRAs, 4F-MDMB-BINACA, MDMB-4en-PINACA and Cumyl-CBMICA, are presented in Figure 6. The SCRAs selected feature indole or indazole cores and vary regarding linked residues and side chains. The structural differences between the targeted SCRAs seem to influence the desorption rate of individual SCRAs from PDMS material. Whereas 42% and 23% loss relative to the initial values occurred after 95 h in sewage water flow for 4F-MDMB-BINACA and MDMB-4en-PINACA, respectively, the Cumyl-CBMICA amount decreased by 71% during the same time period (Figure 6). Interestingly, for all three SCRAs a desorption equilibrium is reached latest after 74 h, since no differences between 74 h and 95 h were observed.

As the SCRAs generally exhibit low polarities and hence low solubilities in water, which facilitates their enrichment in the unpolar PDMS matrix, rather low desorption rates from the PDMS matrix would be expected in water. Additionally, a decomposition of SCRAs in PDMS

during wastewater sampling is unlikely, since the results of our previous study indicated SCRAs as recalcitrant under sewage conditions [45]. Nevertheless, interactions with unpolar sewage matrix components or detergents might stimulate SCRA desorption from PDMS. While the present results prove that PDMS rods can successfully be employed for qualitative wastewater sampling over several days to monitor SCRAs such as MDMB-4en-PINACA and 4F-MDMB-BINACA, the advantage of longer sampling intervals must be carefully balanced against notable substance losses due to desorption effects (cf. Cumyl-CBMICA in Figure 6). Therefore, a quantitative approach using PDMS rods for calculation of drug loads in wastewater for a longer period of time might be difficult due to opposing adsorption and desorption effects. Also, further experiments would be needed to establish general correlations between the key structural elements and desorption trends.
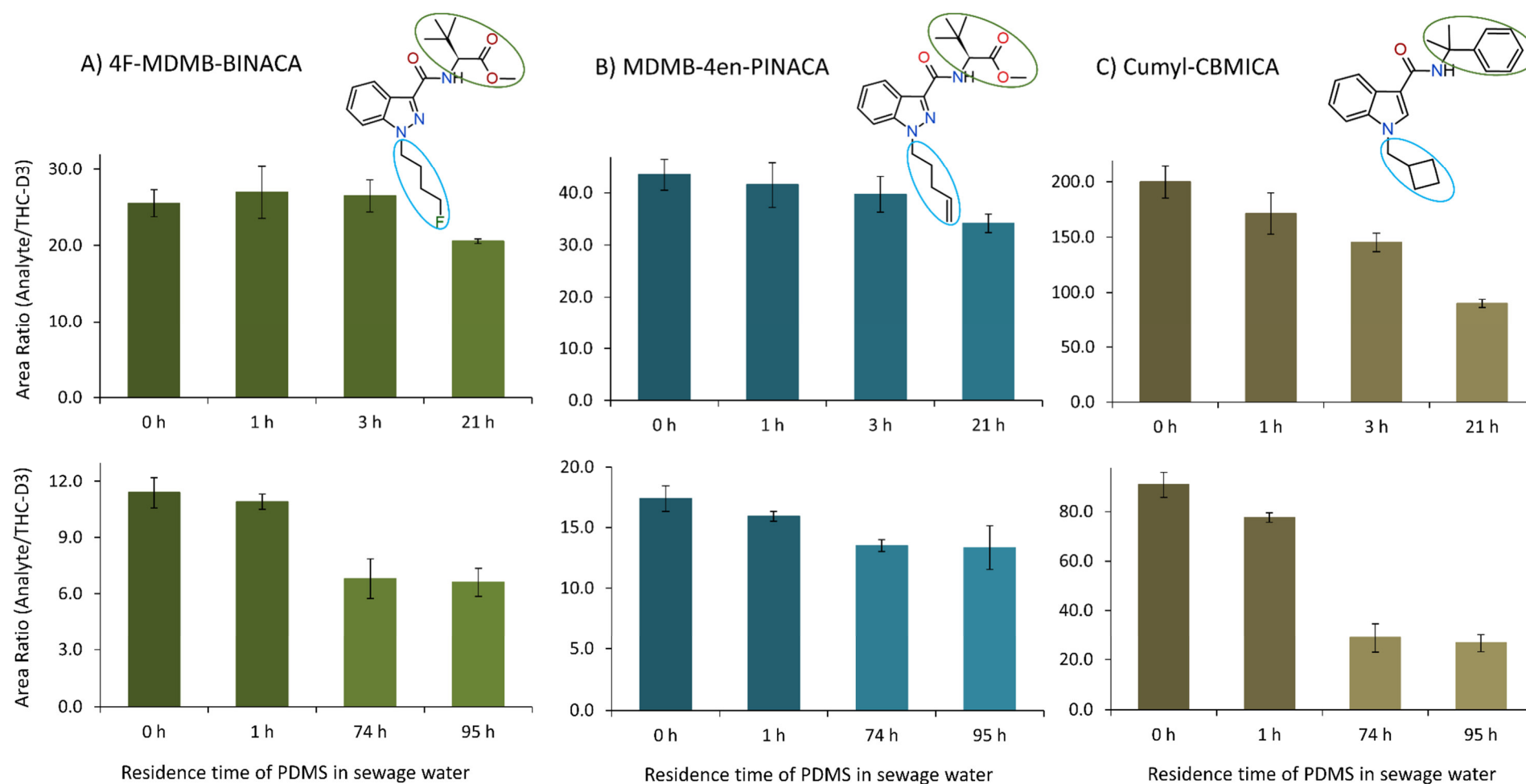
Figure 6. Time profiles for 4F-MDMB-BINACA (left), MDMB-4en-PINACA (middle) and Cumyl-CBMICA (right) recovered from pre-loaded PDMS rods, which were subjected to sewage water flow for up to 21 h (top) and 95 h (below). The analysis was performed in three-fold determination (n=3) and the resulting standard deviation is indicated by the error bars for each time point in the diagrams. Area ratios of the analyte signal relative to the internal standard (THC-D3) are depicted. Chemical structures of SCRAs are depicted as well, with N-side chains (blue) and linked residues (green) indicated accordingly.

4.3.4 Assessment of SCRA use in a prison

To test the established sampling and analytical methods in an authentic environment, wastewater from a German prison was investigated by liquid sampling and by PDMS extraction directly from the wastewater stream. A prison seemed an ideal starting point, since the prevalence of SCRAs in correctional establishments is expected to be higher than in general population. Moreover, the prison selected for this study is specifically known for the pronounced SCRA use as confirmed by seizures in this facility. Due to ethical issues, the prison name, location and further details are not given here.

Liquid wastewater samples

The collected 4 h composite wastewater samples were extracted via the LLE workup and analyzed by LC-MS/MS, as detailed in the experimental section. The interpretation of absolute drug concentrations in wastewater depends on many parameters (sewage water levels and flow rate, drug excretion rate, etc.), most of which can be expected to be extremely fluctuating, hence requiring more sophisticated models beyond the scope of this work. Particularly for SCRAs, an additional challenge is the dynamic NPS market with continuously emerging new substances implying that parameters such as excretion rates are mostly unknown. As this study emphasizes the development and field test of analytical methodologies, only qualitative or semi-quantitative data for SCRAs detected are given. Nevertheless, time-resolved and semi-quantitative prevalence profiles could be established based on the measured data. Therefore, the signal intensities for each substance were compared at different time points. The diagrams below (Figure 7) show signal intensities (peak areas) relative to the maximum signal intensity in percent for the respective substance. Since the metabolism or excretion rate remain unknown for many of these substances, the detection time point does not allow reliable conclusions about the exact time of consumption. However, extensive metabolism is assumed for SCRAs [46] so that low concentrations of the SCRAs can be expected. The red line in the figures is an indicator of the analytical detection limit, and values above this line can be regarded as positive identifications of the respective substance. The detection limit was determined by a signal-to-noise (S/N) ratio, whereby an S/N of at least 9/1 was required for the most intense ion transition in these samples. A further ion transition had to be present to unequivocally identify the substance (S/N of at least 3/1). Further criteria required for a positive identification were a compliant retention time and ion ratio with the reference standard. Ion ratio denotes the area ratio of the less intense ion transition in the MS/MS acquisition mode relative to the most intense one. In accordance with the criteria for positive substance identification, several SCRAs were detected in the collected wastewater samples of the prison during the period of May 22-24, 2021. These SCRAs comprised 4F-MDMB-BINACA, MDMB-4en-PINACA, 4F-MDMB-BICA, 5F-MDMB-PICA / 5F-EMB-PICA and Cumyl-CBMICA. 5F-MDMB-PICA and 5F-EMB-PICA are isomers, varying only in the position of one methyl group, and can thus not be discriminated with the method used. It should be noted that a targeted analysis, including only the selected SCRAs and a limited number of their metabolites (ref. Table S5), was carried out. The presence of further substances, which were not included in the analytical method, cannot be excluded in the analyzed wastewater samples.

The time profiles generated for individual substances allow for several trends to be identified. MDMB-4en-PINACA and 4F-MDMB-BINACA appear to be the most prevalent SCRAs in the prison examined, since the two substances were detected in each wastewater sample of the time period investigated. Interestingly, as depicted in Figure 7, the time points of the maximum signal areas differed significantly: while the highest amount for 4F-MDMB-BINACA was detected on Monday (May 24, 2021; the maximum from 2 - 6 a.m., and the second highest from 6 - 10 a.m.), the greatest signal for MDMB-4en-PINACA was detected on Saturday (May 22, 2021; the maximum from 2 - 6 p.m., and the second highest from 6 - 10 p.m.). The signal areas are directly proportional to concentrations/amounts present, so an increasing signal area correlates with increasing concentration. The mentioned temporal differences could indicate different consumer groups, different products consumed, different consumption times, or different supply sources for the SCRAs. Although substance-specific metabolic pathways and durations could also contribute to the effect, the observed temporal discrepancies (32 hours between the maxima of the two substances) seem to be too large for two structurally related drugs, so that different consumption time points can indeed be assumed.

Another prevalent SCRA was 4F-MDMB-BICA, identified in nearly all wastewater samples as well (Figure S2A, Supplementary Material), but showing a distinct maximum in one sample (Sunday: 6 - 10 p.m.). Other SCRAs detected included 5F-MDMB-PICA / 5F-EMB-PICA and Cumyl-CBMICA, both less prevalent and present in rather lower amounts in the wastewater samples (Figures S2B and S2C, Supplementary Material). While low amounts of 5F-MDMB-PICA / 5F-EMB-PICA were detected over all three days (Saturday: 10 a.m. - 2 p.m., 2 - 6 p.m., 6 - 10 p.m., 10 p.m. - 2 a.m.; Sunday: 10 a.m. - 2 p.m., 2 - 6 p.m., 6 - 10 p.m., and Monday: 2 - 6 a.m. and 6 - 10 a.m.), Cumyl-CBMICA was detected only during two time intervals (Sunday: 2 - 6 p.m. and Monday: 2 - 6 a.m.).
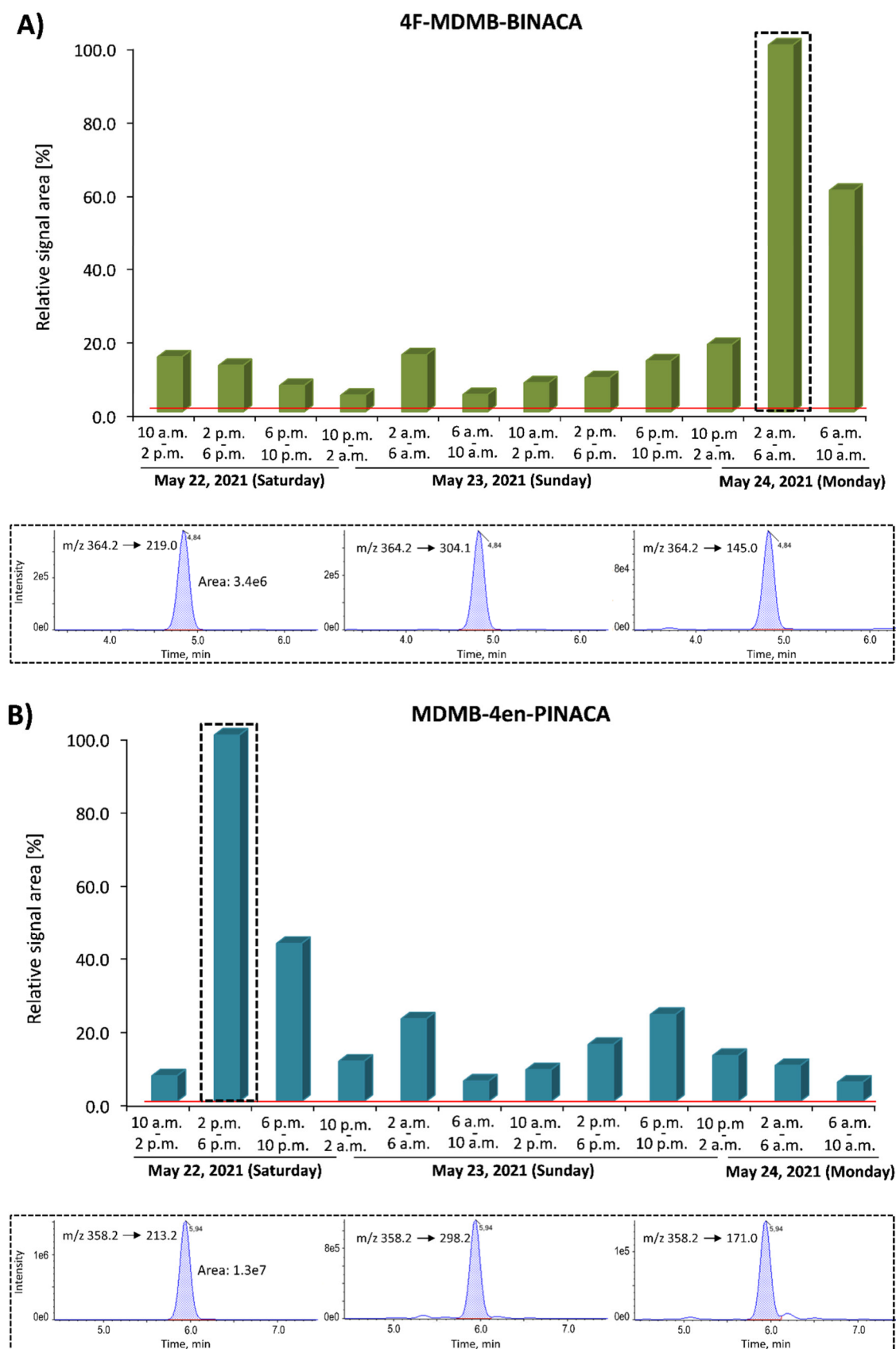
Figure 7. Time profiles for MDMB-BINACA (A) and MDMB-4en-PINACA (B) detected in prison wastewater from May 22-24, 2021, represented in relation to the most concentrated samples. For these, chromatograms of the three most intense ion transitions are depicted accordingly (4F-MDMB-BINACA: May 24, 2021, 2 - 6 a.m.; MDMB-4en-PINACA: May 22, 2021, 2 - 6 p.m.). The red line denotes the S/N ratio corresponding to 9/1 for the most intense ion transition, with S/N values calculated using Peak-To-Peak algorithm (Analyst® Software 1.6.2).

In all liquid samples analyzed, only one metabolite (MDMB-4en-PINACA dimethylbutanoic acid) was detected in one of the authentic wastewater samples. This sample (Saturday: 6 - 10 p.m.) represents the one subsequent to the sample with the highest concentration of the parent compound MDMB-4en-PINACA (Saturday: 2 - 6 p.m.), as can be expected from pharmacokinetics. The absence of further metabolites detected can partly be explained by lower analytical sensitivities for them or their lower expected concentrations due to the formation of multiple different metabolites after SCRA consumption. A second relevant factor was observed during further fine-tuning of the LLE workup after the preliminary experiments in prison. The detection of SCRA metabolites turned out to be strongly dependent on pH, and acidification of wastewater samples was vital for the effectiveness of their detection. However, the sensitivity of the method was still lower for the metabolites than for the parent SCRAs. For the SCRAs themselves and the phytocannabinoids, pH value did not play any role, since the extraction yields did not differ significantly for pH 7 and pH 2. In addition to the adjustment of the pH of wastewater samples (pH of 2-3), the use of a more polar extraction solvent or different extraction procedures might result in an improved recovery of SCRA metabolites. The detection of parent SCRAs as the most relevant compounds in authentic wastewater, as shown in this work, was observed in other related studies as well [23-27]. This trend was confirmed in Part B of our study [44], where none of the metabolites included was detected, despite the application of the optimized method with the acidification step.

Passive samplers (PDMS rods)

In parallel to the pump-based liquid wastewater sampling, a passive sampling approach based on PDMS rods was used for direct sampling in the sewer as well. For an equal sampling period, lower signal intensities might be expected for PDMS rods than for wastewater samples because of the relatively small surface area and hence low sampling capacity of PDMS rods as well as due to a certain degree of desorption of target analytes from PDMS matrix in wastewater. On the other hand, liquid samples contained only the SCRAs from a 4 h period of time, with a "blind spot" of 12 minutes between the individual sampling steps, whereas PDMS rods continuously collect analytes over a much longer time frame. In fact, several SCRAs were detected via PDMS rod (1 cm analyzed) in the wastewater of the prison during the period of May 21-25, 2021 (96 h), including 4F-MDMB-BINACA, MDMB-4en-PINACA, 4F-MDMB-BICA, 5F-MDMB-PICA / 5F-EMB-PICA, MAM-2201 and EG-018. The corresponding chromatograms for three representative SCRAs with their two most intense ion transitions are depicted in Figure 8A-C. When comparing the substance identifications obtained by PDMS rod sampling with the results obtained by analysis of liquid wastewater samples, two further SCRAs, MAM-2201 and EG-018, were detected only by PDMS sampling. The presence of EG-018 is notable, as it is structurally differentiated from other SCRAs by its carbazole core in place of an indole or indazole core. The observed difference between LLE and PDMS in the substances detected can most probably be attributed to the different sampling periods. Whereas the wastewater sampling covered the time period from May 22, 2021 (10 a.m.) until May 24, 2021 (10 a.m.), the PDMS rod remained in the wastewater for additional 48 h, from May 21, 2021 (10 a.m.) until May 25, 2021 (10 a.m.) for technical reasons. Another reason might be the low polarity of the naphthyl moiety in MAM-2201 and EG-018 (cf. chemical structures in Figure 8D) that facilitates their enrichment in the unpolar resin of the PDMS matrix. Cumyl-CBMICA was not adsorbed on the PDMS rod in sufficient amounts to be detected. This is not surprising, since

the amounts of this compound in the wastewater stream were rather low, with a distinct signal only in one sample, as indicated by the liquid sample analysis (see Figure S2C). For low amounts of SCRAs or short release time windows into wastewater, the short contact time to the PDMS rod during the dynamic sewage water flow can be expected to result in concentrations being below the limit of detection. Therefore, the liquid sampling approach would be more advisable for such cases. Nevertheless, PDMS rods might still be used as solid phase adsorbents for analyte extraction from the liquid samples, as shown in our previous study for the organic explosive triacetone triperoxide (TATP) in liquid synthesis waste samples [43].

Although a quantitative comparison of the two wastewater sampling approaches (liquid wastewater samples vs. direct PDMS sampling) is possible with limitations only due to slightly different sampling intervals, certain tendencies can be derived from the assessment of absolute areas. As summarized in Table S6, higher amounts of MDMB-4en-PINACA and 5F-MDMB-PICA / 5F-EMB-PICA were recovered from PDMS rods, compared to the most concentrated liquid samples. For 4F-MDMB-BINACA and 4F-MDMB-BICA the opposite was observed. The differences were notable, but not drastic, proving the technically much easier sampling with PDMS rods to be equally suited as liquid sampling, if time resolution is not relevant.
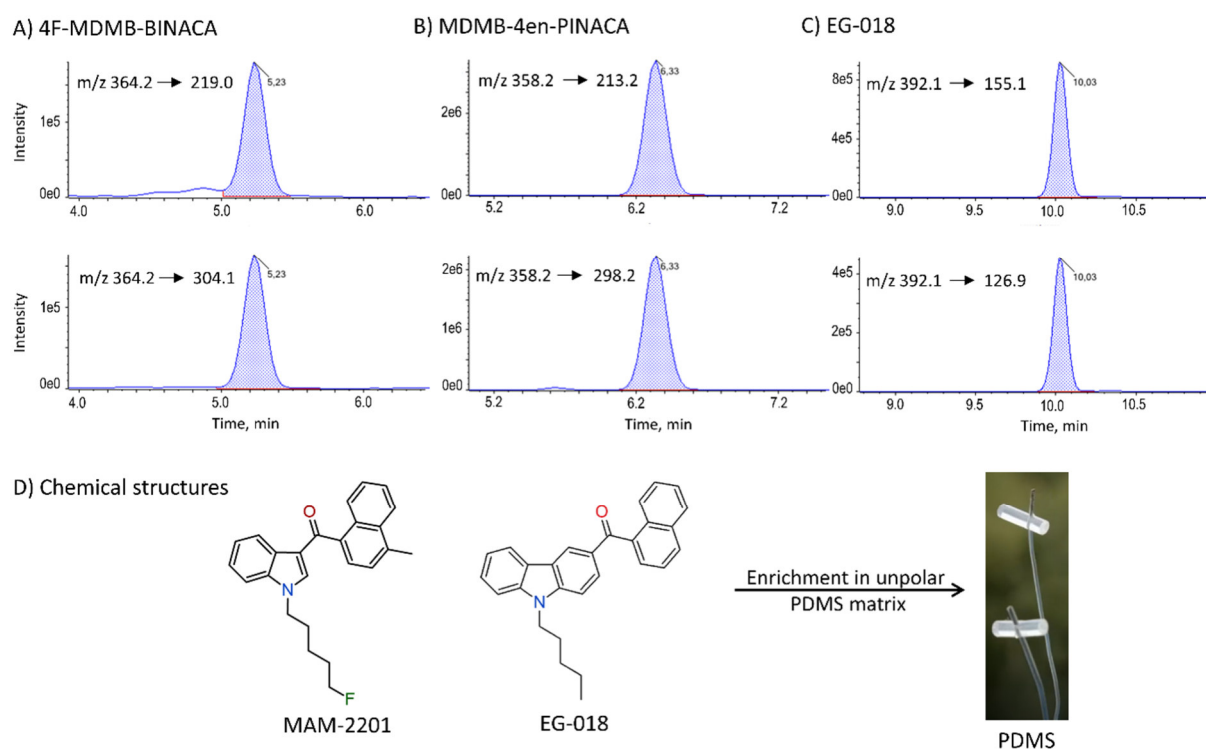
Figure 8. Chromatograms representing the two most intense ion transitions for three representative SCRAs sampled by PDMS rod in the wastewater of the prison from May 21-25, 2021 (A-C); Chemical structures of the two additional SCRAs detected by PDMS rod (D), when compared to liquid wastewater sampling.

Correlations of drug confiscations with wastewater analysis results for a prison

As illustrated in Table 1, various items such as letters/infused papers, herbal mixtures and powders were seized in the period from January to June 2021 in the prison subjected to wastewater analysis in this study, hence including the period of the wastewater sampling (May 2021). Analysis of the seized samples yielded several SCRAs as toxicologically relevant components: MDMB-4en-PINACA, 5F-Cumyl-PeGaClone, 4CN-Cumyl-BINACA, MAM-2201, Cumyl-BC[2.2.1]HpMINACA, ADB-BUTINACA and 4F-MDMB-BICA [47]. Furthermore, larger amounts of the semisynthetic opioid buprenorphine were identified in a seizure. The remaining seizures (Table 1) clearly indicated a prevalent use of SCRAs. Based on the high frequency of its positive identification in the seized items, MDMB-4en-PINACA seemed to be the most prevalent SCRA in this prison. This is in good agreement with the results obtained by wastewater analysis. Furthermore, 4F-MDMB-BICA was seized together with MDMB-4en-PINACA in larger amounts in powder form. This seizure also correlates well with the results of wastewater analysis, as 4F-MDMB-BICA was detected in nearly all wastewater samples. MAM-2201 was another prevalent SCRA encountered frequently in the seizures, which matches its positive identification in the sewage system of the prison. However, the remaining SCRAs identified by the seized sample analysis, such as Cumyl-BC[2.2.1]HpMINACA, 4CN-Cumyl-BINACA or 5F-Cumyl-PeGaClone, did not show up in the wastewater analysis. On the other hand, the SCRAs 4F-MDMB-BINACA, 5F-MDMB-PICA / 5F-EMB-PICA and Cumyl-CBMICA were found in the wastewater samples collected in May 2021, but not in the seizures. The differences between the seized drugs and the prevalent drugs according to the wastewater analysis can be explained by the short wastewater monitoring period and a presumed significant amount of non-seized evidence items. The wastewater analysis referred to a limited and short time frame (May 21-25, 2021), while the seizures occurred over a longer time period of six months. None of the listed seizures originated from the exact wastewater sampling period. Although the wastewater analysis presented here covered only a specific and relatively short period of 96 hours, a diverse and comprehensive picture of the drug situation in the prison investigated was obtained. Moreover, complementary insights were gained to those obtained from the seizures in terms of additional SCRAs identified. In summary, wastewater analysis represents a promising monitoring tool for drug use in prison settings, especially considering the passive sampling approach based on PDMS rods, which features simple use with low time and cost efforts.

Table 1. Seized items of evidence including letters/infused papers, herbal mixtures, and powders in the period from January to June 2021 in the prison investigated in this study.

Item of evidence	Number of items	Identified SCRAs/drugs
Unknown herbal blend	2	MDMB-4en-PINACA
Herbal blend 'Nexus Weed Blueberry'	1	MDMB-4en-PINACA
Unknown herbal blend	1	5F-Cumyl-PeGaClone
Infused paper/letter	1	MDMB-4en-PINACA 4CN-Cumyl-BINACA
Infused paper/letter	2	MDMB-4en-PINACA 4CN-Cumyl-BINACA MAM-2201 Unknown substance
Infused paper/letter	9	MDMB-4en-PINACA 4CN-Cumyl-BINACA MAM-2201
Infused paper/letter	1	MDMB-4en-PINACA Cumyl-BC[2.2.1]HpMINACA
Infused paper/letter	4	MDMB-4en-PINACA Cumyl-BC[2.2.1]HpMINACA 4CN-Cumyl-BINACA MAM-2201
Infused paper/letter	4	MDMB-4en-PINACA
Infused paper/letter	2	ADB-BUTINACA*
Powder	1	Buprenorphine/Mannite
Powder in „bubbles"	43 25	MDMB-4en-PINACA 4F-MDMB-BICA

*ADB-BUTINACA refers to *N*-[1-amino-3,3-dimethyl-1-oxobutan-2-yl]-1-butyl-1*H*-indazole-3-carboxamide

4.3.5 Assessment of SCRA use in a city district

4.3.5.1 Sewer network model-based planning of sampling sites

After the initial experiments with wastewater samples from a prison had served as a proof-of-principle and as a base for method development, further experiments were conducted in a larger sewer network, encompassing a district of the city of Munich. Moving from a prison population to a major city population entails a more complex sewer system, larger water flows and larger catchment areas. To ensure effective coverage of multiple subcatchment areas by deploying a limited number of sampling devices and/or passive samplers in a sewer network, a computational sewer network model was established. This model provides essential

structural information about the sewage system of the area of interest, encompassing the geo-referenced locations of manholes as potential sampling sites and a hydraulically directed graph relationship that describes interconnections among buildings, sewers and manholes. The hydraulic model supplies data pertaining to wastewater flow, velocity profiles, flow directions and the catchment areas contributing to wastewater discharge at each manhole.

To demonstrate the practical application of this approach for sampling site planning, a simplified example is given below. The hydraulic model in Figure 9A shows seven possible sampling sites, i.e. manholes (M), within the sewer subnetwork investigated. The corresponding catchment areas are indicated in green for each sampling location (Figures 9B-F). Based on these data, Locations 1-3 (M1 – M3, Figures 9B-D) comprise the largest catchment areas and hence fulfill an important criterion for the selection area for a prevalence study.

Figure 9. Sewer subnetwork in the city: overview of manholes (**A**), catchment areas of single manholes (**B-E**) or a set of three manholes (**F**). The sampling points for Locations 1-7 are indicated with differently colored circles.

As depicted in Figure 9A, M1 (orange circle) is positioned downstream relative to M2 (blue circle) and M3 (yellow circle) in the sewer system, resulting in higher wastewater flows and greater dilution. Relative to the catchment areas corresponding to M2 and M3, the additional catchment area covered by the location of the M1 was not significantly large. Large catchment areas are usually preferred for prevalence studies to capture a high number of possible drug consumers. However, specifically for the SCRAs, rather low wastewater loads are expected due to low single doses and their diversion over a variety of individual compounds. Therefore, a compromise was required between large catchment areas and a non-extensive dilution in this initial phase of the method development and optimization to assess general detectability of SCRAs in the sewage system of a larger city district. This criterion led to the selection of M2 and M3. Additionally, Location 4 (M4, green circle, Figure 9E) positioned upstream relative to M3 was selected to investigate possible differences and geographical resolution of the sampling concept. Moreover, all the selected sampling sites (manholes) were preferrable due to their accessibility, traffic load or similar. While Munich is a city with slightly more than 1.5 million inhabitants [48], the district investigated corresponded to significantly smaller catchment areas at the selected locations.

In the next step, the sampling techniques were chosen for each sampling site. As sampling with PDMS is technically much easier than automated pump-based liquid wastewater sampling, PDMS rods were placed in the three selected manholes within one branch of the municipal sewer network. One of the manholes (M2) was additionally equipped with an ORI device for active automated liquid sampling. The sampling activities at the different locations were performed during September 21-24, 2021. An additional time interval (September 24-27, 2021) was chosen for the location of M2, addressing not only the general detectability of SCRAs use but also possible differences of consumption patterns between weekdays and weekend alike.

Liquid sampling (4-hour composite liquid wastewater samples) and use of PDMS rods were basically the same as described for the prison sampling campaign. As before, the time intervals for the exposure of the PDMS rods exceeded the sampling periods of liquid wastewater samples for technical reasons. As installation and deinstallation of PDMS rods in the different manholes had to be conducted consecutively, slightly different time periods with max. 3 h delay between the three sampling locations were covered as well (cf. Table S7, Supplementary Material). It is important to note that the delay period was significantly extended due to mounting/demounting of additional sensors not being part of this study. The installation/ deinstallation times of PDMS rods would otherwise have been significantly reduced. Since rather lower amounts of SCRAs were expected in the city district compared to the prison, not least due to higher sewage flow rates and thus higher dilution, analytical conditions were adjusted to further improve the method sensitivity. A promising way to optimize the limits of detection was to increase the injection volume for LC-MS/MS analysis. In Figure S3 in the Supplementary Material, chromatograms for two SCRAs (MDMB-4en-PINACA and Cumyl-CBMICA) are depicted, detected in an authentic wastewater sample collected on September 21, 2021 in Munich. The linear correlation of the signal intensity with the increasing injection volume from 5 µL to 20 µL can be observed. The two most intense ion transitions are displayed per substance. Since adverse effects of increased background matrix were observed for none of the ion transitions, a 20 µL injection volume was selected for subsequent experiments. Besides the increased injection volume for the LC-MS/MS system, longer cuts of PDMS rods

(2 cm length) were analyzed as well. The correlation of the increased analyte quantities with increasing lengths of the PDMS rods was assumed due to larger adsorption surface, as proven in our previous study [43]. The criteria for analyte identification via LC-MS/MS matched the previously specified ones (cf. section 4.3.4, Liquid wastewater samples), except for lowering the detection limit to S/N ratio of at least 3/1 for both ion transitions. All samples from both liquid and PDMS sampling were analyzed for conventional illicit drugs as well, which is discussed in detail in Part B of this study [44].

4.3.5.2 Geographical and temporal correlations of consumption patterns

Different SCRAs were successfully detected by the use of PDMS rods, comprising MDMB-4en-PINACA, 4F-MDMB-BINACA, 4F-MDMB-BICA, 5F-MDMB-PICA / 5F-EMB-PICA, 5F-PB-22, EG-018 and JWH-210. The phytocannabinoid THC and its metabolite THC-COOH were detected as well. Although not directly comparable with the wastewater samples due to slightly different sampling periods, the findings were in good correlation.

The presence of different SCRAs varied between locations, as summarized in Table S7. Whereas all the substances were identified at the location of M2, the residual locations lacked for at least two of these SCRAs. For the locations of M3 and M4 4F-MDMB-BINACA and 5F-PB-22 were missing, for M4 additionally 4F-MDMB-BICA. These findings can easily be explained by different catchment areas encompassed by individual manholes. Maps of the city district showing the three PDMS sampling positions, the corresponding catchment areas (indicated in green) and the SCRAs/phytocannabinoids identified at the locations of M2 and M3 are depicted below (Figure 10). Chromatograms with denoted absolute areas for particular SCRAs at the two different locations are given in Table S8 in the Supplementary Material. The greatest variations were observed for absolute areas of MDMB-4en-PINACA, when comparing the two locations. Besides the geographical correlations, the PDMS approach seems to be a promising monitoring tool to track temporal correlations (although with lower time resolution compared to liquid sampling) of consumption patterns as well. In the particular case, no essential differences in SCRAs identified during the selected weekdays and the following weekend were found at the location of M2, merely variations in their signal areas were recognizable. Conclusively, PDMS rods demonstrated their suitability for SCRAs sampling in a more complex sewer network of a big city over longer periods of time (three days), offering an easy way to monitor geographical and temporal patterns of NPS consumption. The crucial advantages for practical use include an uncomplicated and inconspicuous setup that uses cheap, disposable equipment on site, and can be deployed and recovered fast and easily at several locations in parallel, even by untrained personal.
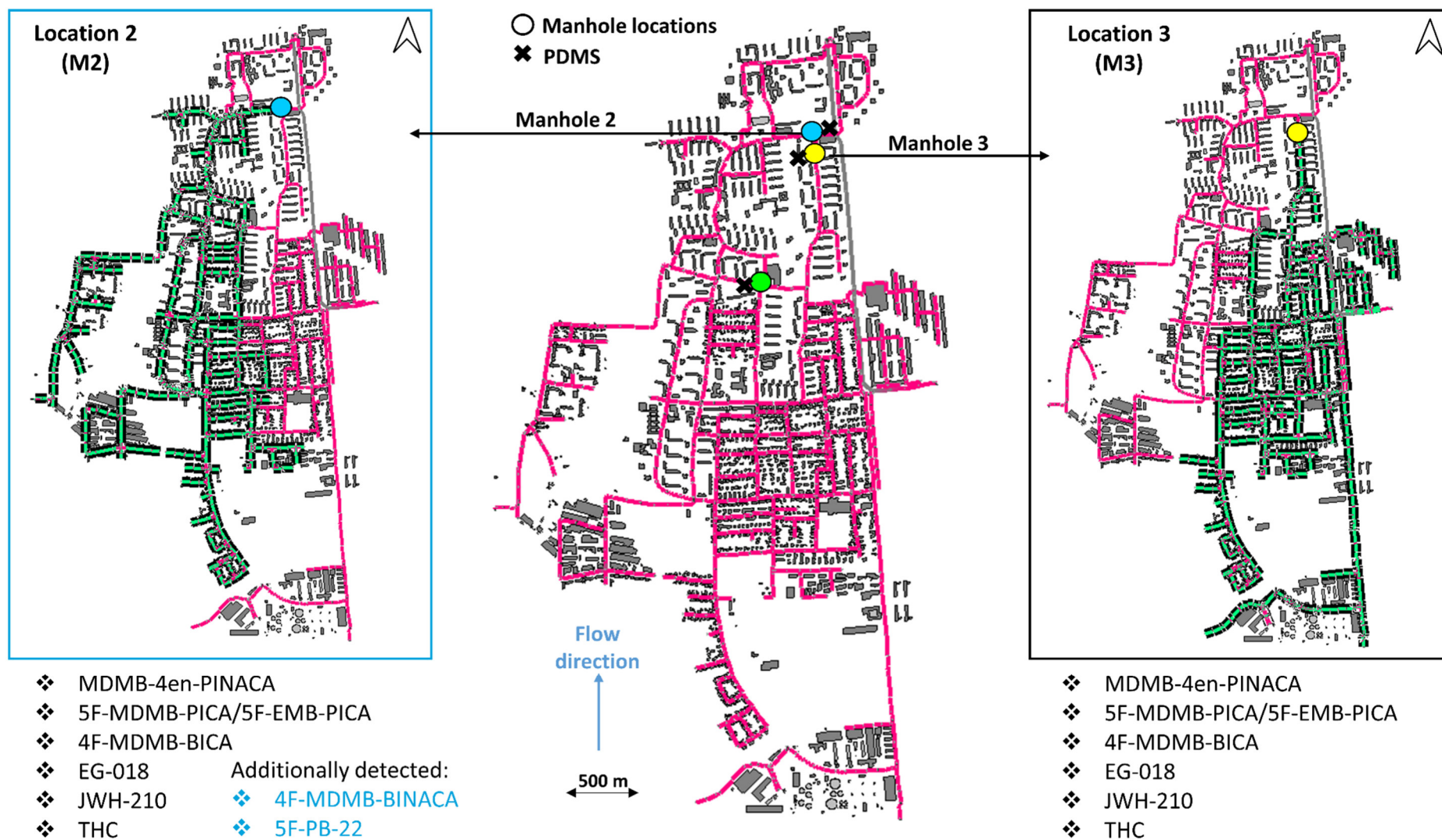
Figure 10. Maps of the city district showing the three PDMS sampling positions (middle) and the catchment areas (indicated in green) covered by the location of M2 (left) and M3 (right). SCRAs/phytocannabinoids identified at the corresponding locations during September 21-24, 2021 are indicated accordingly

4.4 Conclusion

This study focused on the development and application of different analytical tools for monitoring of synthetic cannabinoid receptor agonists (SCRAs) consumption prevalence by wastewater analysis. Sampling protocols, analytical procedures and detection methods were developed, optimized and compared in terms of their advantages and disadvantages. Conventional liquid wastewater sampling with an automated pump-based sampling device was performed as a starting point, posing a technically more demanding, but highly time resolved concept. Polydimethylsiloxane (PDMS) rods as passive solid phase adsorbers were directly deployed in wastewater for SCRAs enrichment, representing a novel and promising wastewater sampling approach for drug prevalence investigations. This methodology is cheap and easy to use, delivering summarized parameters for several days. The practical application of both sampling protocols was probed by analysis of real sewage samples of two different populations: a prison population and a population of a city district. Several SCRAs, including MDMB-4en-PINACA, 4F-MDMB-BINACA, 4F-MDMB-BICA, 5F-MDMB-PICA / 5F-EMB-PICA, Cumyl-CBMICA, 5F-PB-22, EG-018, MAM-2201 and JWH-210, were detected in sewage water of the selected populations in 2021. Wastewater analysis indicated a significant use of SCRAs in the prison investigated, exhibiting a distinct time profile for several analytes. The analytical results were in good agreement with those of seized drugs from the corresponding prison in a correlated time frame. Moreover, when regarding the short wastewater sampling time window (max. 96 h), a comprehensive information on drug use was gained, even with some complementary insights to the seizures. The SCRA consumption prevalence in the investigated prison correlated well with the prevalence of SCRAs detected in the sewage system of a city district reflecting a larger population, where the number of SCRAs identified indicates a considerable presence and availability of NPS products on the illicit drug market. The data retrieved by both sampling concepts, active and passive, yielded comparable results, suggesting that passive sampling with PDMS rods can be equally suited as active liquid sampling, if time resolution is less relevant. The newly introduced PDMS rod sampling approach is especially appealing due to numerous advantages concerning practical use, such as simple and straightforward handling, low consumables costs and fast installation/ deinstallation, even by not technically educated staff and without requirements for more complex sampling devices. Therefore, it represents a very promising monitoring tool for illicit drug use via wastewater-based epidemiology. The practical advantages allow for a more frequent sampling, providing time-averaged data, instead of single snapshots. This study evaluated time-weighted average data over max. 4 days for continuous wastewater monitoring, however, even longer sampling periods are conceivable. The longer sampling intervals need to be balanced against possible desorption effects, although the first experiments in this study suggested rather moderate desorption of SCRAs from PDMS material in sewage water matrices. Furthermore, sampling events using the passive sampling concept based on PDMS rods can be easily conducted at several wastewater sample points simultaneously, allowing for a wider area coverage or higher local resolution. The selection of suitable sampling locations in the city district was based on a sewer network model, enabling geographical differences in drug consumption patterns to be easily revealed. Conclusively, a sampling and detection strategy for SCRAs monitoring in a complex sewer network was developed, based on the interaction of the sewer network model prediction data and the

chemical analysis. While this novel approach requires a research follow-up regarding its standardization, robustness and reproducibility, particularly concerning a quantitative assay, it has proven to be a suitable and convenient assay for trends of drug use at a qualitative level in current stage. The application of this concept for the assessment of prevalence of consumption of conventional drugs of abuse will be detailed in Part B of this study, along with triangulation with data from toxicological analyses and seizures for SCRAs.

4.5 References

[1]   European Monitoring Centre for Drugs and Drug Addiction (EMCDDA). European Drug Report 2023: Trends and Developments. 2023; Luxembourg: Publications Office of the European Union. https://www.emcdda.europa.eu/publications/european-drug-report/2023_en. Accessed December 13, 2023. DOI: 10.2810/161905.

[2]   European School Survey Project on Alcohol and Other Drug (ESPAD) Group. ESPAD Report 2019: Results from the European School Survey Project on Alcohol and Other Drugs. 2020; Luxembourg: Publications Office of the European Union. https://www.emcdda.europa.eu/publications/joint-publications/espad-report-2019_en. Accessed December 13, 2023. DOI: 10.2810/877033.

[3]   United Nations Office for Drugs and Crime (UNODC). World Drug Report 2022. 2022; Vienna: United Nations publication. https://www.unodc.org/unodc/en/data-and-analysis/wdr-2022_booklet-4.html. Accessed December 12, 2023.

[4]   United Nations Office for Drugs and Crime (UNODC). World Drug Report 2023. 2023; Vienna: United Nations publication. https://www.unodc.org/unodc/en/data-and-analysis/Exsum_wdr2023.html. Accessed December 12, 2023.

[5]   Van Hout MC, Benschop A, Bujalski M, et al. Health and Social Problems Associated with Recent Novel Psychoactive Substance (NPS) Use Amongst Marginalised, Nightlife and Online Users in Six European Countries. *Int J Ment Health Addict*. 2018; 16(2):480-495. DOI: 10.1007/s11469-017-9824-1.

[6]   Csák R, Szécsi J, Kassai S, Márványkövi F, Rácz J. New psychoactive substance use as a survival strategy in rural marginalised communities in Hungary. *Int J Drug Policy*. 2020;85:102639. doi: 10.1016/j.drugpo.2019.102639.

[7]   European Monitoring Centre for Drugs and Drug Addiction (EMCDDA). New psychoactive substances in prison: Results from an EMCDDA trendspotter study. 2018; Luxembourg: Publications Office of the European Union. https://www.emcdda.europa.eu/publications/rapid-communications/nps-in-prison_en. Accessed December 02, 2023. DOI: 10.2810/7247.

[8]   Vaccaro G, Massariol A, Guirguis A, Kirton SB, Stair JL. NPS detection in prison: A systematic literature review of use, drug form, and analytical approaches. *Drug Test Anal.* 2022;14(8):1350-1367. DOI: 10.1002/dta.3263.

[9]   User Voice. Spice: the bird killer. What prisoners think about the use of spice and other legal highs in prison. 2016; London: User Voice. https://www.uservoice.org/wp-content/uploads/2020/07/User-Voice-Spice-The-Bird-Killer-Report-compressed.pdf. Accessed December 02, 2023.

[10]   Her Majesty's (HM) Inspectorate of Prisons. HM Chief Inspector of Prisons for England and Wales Annual Report 2013–14. 2014; UK government. https://www.justiceinspectorates.gov.uk/hmiprisons/wp-content/uploads/sites/4/2014/10/HMIP-AR_2013-141.pdf. Accessed December 14, 2023.

[11]   European Monitoring Centre for Drugs and Drug Addiction (EMCDDA). Prison and drugs in Europe: Current and future challenges. 2021; Luxembourg: Publications Office of the European Union. https://www.emcdda.europa.eu/publications/insights/prison-and-drugs-in-europe_en. Accessed December 02, 2023. DOI: 10.2810/420042.

[12]   Hvozdovich JA, Chronister CW, Logan BK, Goldberger BA. Case Report: Synthetic Cannabinoid Deaths in State of Florida Prisoners. *J Anal Toxicol*. 2020;44(3):298-300. DOI: 10.1093/jat/bkz092.

[13]   McMann TJ, Calac A, Nali M, Cuomo R, Maroulis J, Mackey TK. Synthetic Cannabinoids in Prisons: Content Analysis of TikToks. *JMIR Infodemiology*. 2022; 2(1):e37632. DOI: 10.2196/37632.

[14]   Ralphs R, Williams L, Askew R, Norton A. Adding Spice to the Porridge: The development of a synthetic cannabinoid market in an English prison. *Int J Drug Policy*. 2017;40:57-69. DOI: 10.1016/j.drugpo.2016.10.003.

[15]   Reuter P, Pardo B. Can new psychoactive substances be regulated effectively? An assessment of the British Psychoactive Substances Bill. *Addiction*. 2017;112(1):25-31. DOI: 10.1111/add.13439.

[16]   Ford LT, Berg JD. Analytical evidence to show letters impregnated with novel psychoactive substances are a means of getting drugs to inmates within the UK prison service. *Ann Clin Biochem*. 2018;55(6):673-678. DOI: 10.1177/0004563218767462.

[17]   Norman C, Walker G, McKirdy B, et al. Detection and quantitation of synthetic cannabinoid receptor agonists in infused papers from prisons in a constantly evolving illicit market. *Drug Test Anal*. 2020;12(4):538-554. DOI: 10.1002/dta.2767.

[18]   Personal communication with prison staff.

[19]   Thomas KV, Bijlsma L, Castiglioni S, et al. Comparing illicit drug use in 19 European cities through sewage analysis. *Sci Total Environ*. 2012;432: 432-439. DOI: 10.1016/j.scitotenv.2012.06.069.

[20]   Australian Criminal Intelligence Commission. National Wastewater Drug Monitoring Program, Report 14. 2021.

https://www.acic.gov.au/publications/national-wastewater-drug-monitoring-program-reports/report-14-national-wastewater-drug-monitoring-program. Accessed December 07, 2023.

[21]   Castiglioni S, Salgueiro-González N, Bijlsma L, et al. New psychoactive substances in several European populations assessed by wastewater-based epidemiology. *Water Res.* 2021;195:116983. DOI: 10.1016/j.watres.2021.116983.

[22]   Bade R, White JM, Chen J, et al. International snapshot of new psychoactive substance use: Case study of eight countries over the 2019/2020 new year period. *Water Res.* 2021;193:116891. DOI: 10.1016/j.watres.2021.116891.

[23]   Bade R, Tscharke BJ, White JM, et al. LC-HRMS suspect screening to show spatial patterns of New Psychoactive Substances use in Australia. *Sci Total Environ.* 2019;650:2181-2187. DOI: 10.1016/j.scitotenv.2018.09.348.

[24]   Pandopulos AJ, Bade R, O'Brien JW, et al. Towards an efficient method for the extraction and analysis of cannabinoids in wastewater. *Talanta*. 2020;217:121034. DOI: 10.1016/j.talanta.2020.121034.

[25]   O'Rourke CE, Subedi B. Occurrence and Mass Loading of Synthetic Opioids, Synthetic Cathinones, and Synthetic Cannabinoids in Wastewater Treatment Plants in Four U.S. Communities. *Environ Sci Technol*. 2020;54(11):6661-6670. DOI: 10.1021/acs.est.0c00250.

[26]   Diamanti K, Aalizadeh R, Alygizakis N, Galani A, Mardal M, Thomaidis NS. Wide-scope target and suspect screening methodologies to investigate the occurrence of new psychoactive substances in influent wastewater from Athens. *Sci Total Environ.* 2019;685:1058-1065. DOI: 10.1016/j.scitotenv.2019.06.173.

[27]   Fan X, Zhang J, Fu X, et al. Analysis of synthetic cannabinoids in wastewater of major cities in China. *Sci Total Environ*. 2022;827:154267. DOI: 10.1016/j.scitotenv.2022.154267.

[28]   Postigo C, López de Alda M, Barceló D. Evaluation of drugs of abuse use and trends in a prison through wastewater analysis. *Environ Int*. 2011;37(1):49-55. DOI: 10.1016/j.envint.2010.06.012.

[29]   Davies B, Paul R, Osselton D. Wastewater analysis for new psychoactive substances and cocaine and cannabis in a Northern Ireland Prison. *Sci Rep.* 2023;13(1):18634. DOI: 10.1038/s41598-023-44453-4.

[30]   Brewer AJ, Banta-Green CJ, Ort C, Robel AE, Field J. Wastewater testing compared with random urinalyses for the surveillance of illicit drug use in prisons. *Drug Alcohol Rev*. 2016;35(2):133-137. DOI: 10.1111/dar.12185.

[31]   Néfau T, Sannier O, Hubert C, Karolak S, Lévi L. Analysis of drugs in sewage: an approach to assess substance use, applied to a prison setting. *Memo 2017-01*, French Monitoring Centre for Drugs and Drug Addiction (OFDT). 2017. https://en.ofdt.fr/publications/memo-posters-maps/analysis-drugs-sewage-approach-assess-substance-use-applied-prison-setting/. Accessed December 10, 2023.
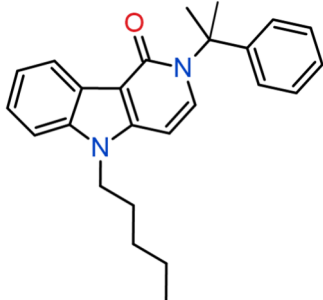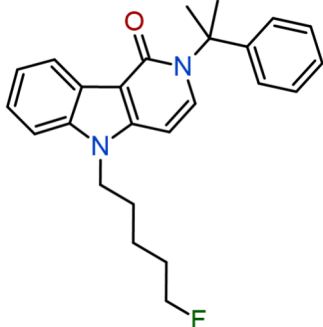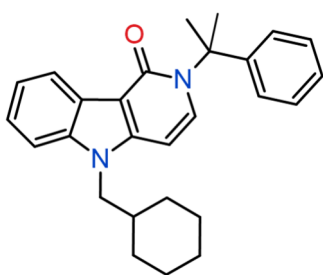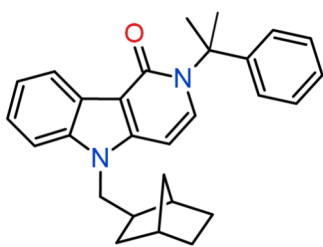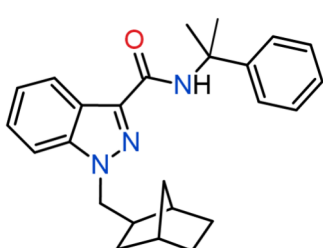
[32] van Dyken E, Lai FY, Thai PK, et al. Challenges and opportunities in using wastewater analysis to measure drug use in a small prison facility. *Drug Alcohol Rev*. 2016;35(2):138-147. DOI: 10.1111/dar.12156.

[33] Wang Z, Mueller JF, O'Brien JW, et al. Monitoring medication and illicit drug consumption in a prison by wastewater-based epidemiology: Impact of COVID-19 restrictions. *Water Res.* 2023;244:120452. DOI: 10.1016/j.watres.2023.120452.

[34] Vrana B, Allan IJ, Greenwood R, et al. Passive sampling techniques for monitoring pollutants in water. *Trends Analyt Chem.* 2005;24:845-868. DOI: 10.1016/j.trac.2005.06.006.

[35] Boles TH, Wells MJ. Pilot survey of methamphetamine in sewers using a Polar Organic Chemical Integrative Sampler. *Sci Total Environ.* 2014;472:9-12. DOI: 10.1016/j.scitotenv.2013.10.122.

[36] Bishop N, Jones-Lepp T, Margetts M, Sykes J, Alvarez D, Keil DE. Wastewater-based epidemiology pilot study to examine drug use in the Western United States. *Sci Total Environ.* 2020;745:140697. DOI: 10.1016/j.scitotenv.2020.140697.

[37] Zilles Hahn R, Augusto do Nascimento C, Linden R. Evaluation of Illicit Drug Consumption by Wastewater Analysis Using Polar Organic Chemical Integrative Sampler as a Monitoring Tool. *Front Chem.* 2021;9:596875. DOI: 10.3389/fchem.2021.596875.

[38] Baz-Lomba JA, Harman C, Reid M, Thomas KV. Passive sampling of wastewater as a tool for the long-term monitoring of community exposure: Illicit and prescription drug trends as a proof of concept. *Water Res*. 2017;121:221-230. DOI: 10.1016/j.watres.2017.05.041.

[39] Petrie B, Gravell A, Mills GA, Youdan J, Barden R, Kasprzyk-Hordern B. In Situ Calibration of a New Chemcatcher Configuration for the Determination of Polar Organic Micropollutants in Wastewater Effluent. *Environ Sci Technol*. 2016;50(17):9469-9478. DOI: 10.1021/acs.est.6b02216.

[40] Verhagen R, Tscharke BJ, Clokey J, et al. Multisite Calibration of a Microporous Polyethylene Tube Passive Sampler for Quantifying Drugs in Wastewater. *Environ Sci Technol*. 2021;55(19):12922-12929. DOI: 10.1021/acs.est.1c02900.

[41] Guo C, Zhang T, Hou S, et al. Investigation and Application of a New Passive Sampling Technique for in Situ Monitoring of Illicit Drugs in Waste Waters and Rivers. *Environ Sci Technol*. 2017;51(16):9101-9108. DOI: 10.1021/acs.est.7b00731.

[42] Montero L, Popp P, Paschke A, Pawliszyn J. Polydimethylsiloxane rod extraction, a novel technique for the determination of organic micropollutants in water samples by thermal desorption-capillary gas chromatography-mass spectrometry. *J Chromatogr A*. 2004;1025(1):17-26. DOI: 10.1016/j.chroma.2003.08.058.

[43] Hehet P, Pütz M, Kämmerer B, et al. Determination of triacetone triperoxide (TATP) traces using passive samplers in combination with GC-MS and GC-PCI-MS/MS methods. *Forensic Sci Int.* 2023;348:111673. DOI: 10.1016/j.forsciint.2023.111673.
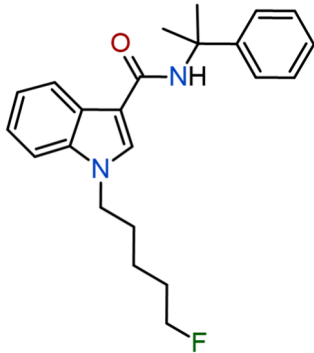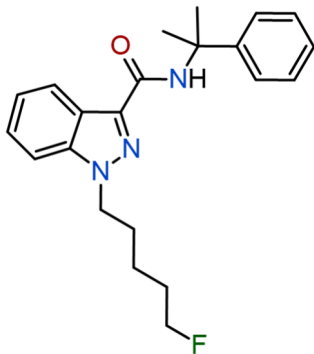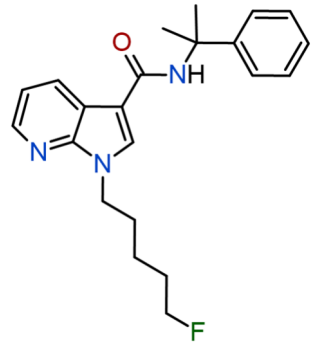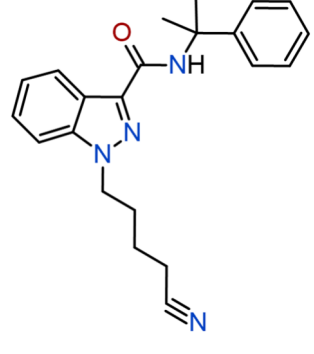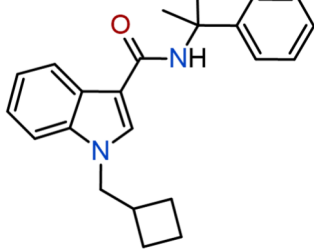
[44]   Hehet P, Scheufler F, Kunert N, et al. Prevalence of synthetic cannabinoid receptor agonists use assessed by sewage monitoring via LC-MS/MS, Part B: Triangulation of police seizures, wastewater and toxicological hair analysis. To be submitted to *Forensic Chem*.

[45]   Hehet P, Köke N, Zahn D, et al. Synthetic cannabinoid receptor agonists and their human metabolites in sewage water: Stability assessment and identification of transformation products. *Drug Test Anal.* 2021;13(10):1758-1767. DOI: 10.1002/ dta.3129.

[46]   Diao X, Huestis MA. Approaches, Challenges, and Advances in Metabolism of New Synthetic Cannabinoids and Identification of Optimal Urinary Marker Metabolites. *Clin Pharmacol Ther*. 2017;101:239-253. DOI: 10.1002/cpt.534.

[47]   Bavarian State Criminal Police Office, Forensic Science Institute. Seized sample analysis data based on GC-MS analytical method. 2021.

[48]   The official city portal of Munich. https://stadt.muenchen.de/infos/statistik-bevoelkerung.html. Accessed December 16, 2023.
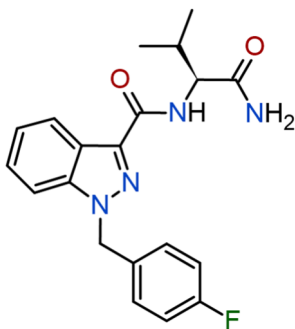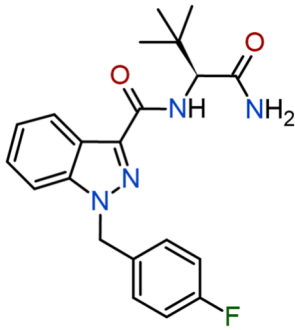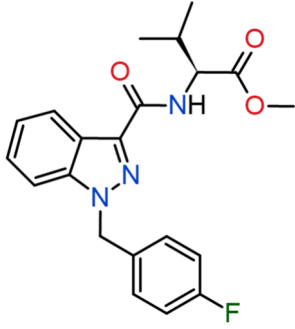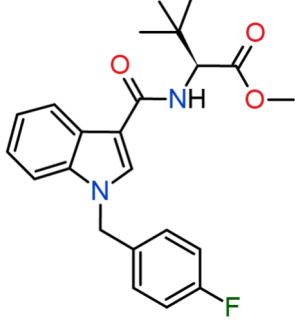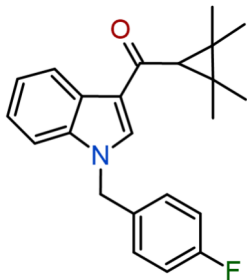
4.6 Supplementary Material
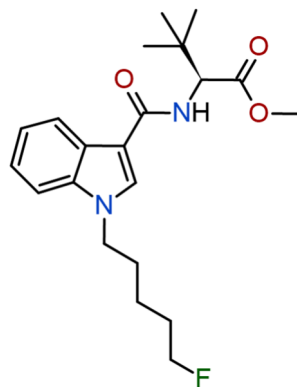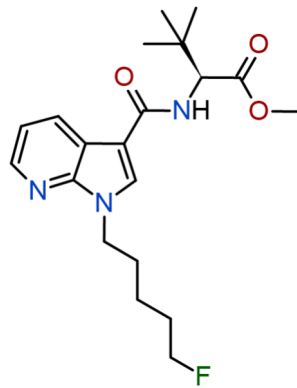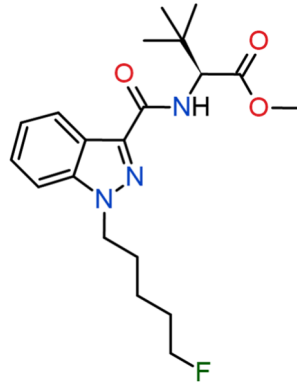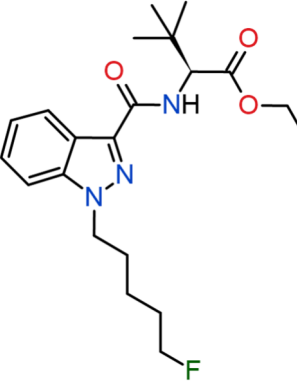
Table S1. Semi-systematic and IUPAC names, common synonyms, molecular formulas, monoisotopic masses and chemical structures listed for the target analytes.
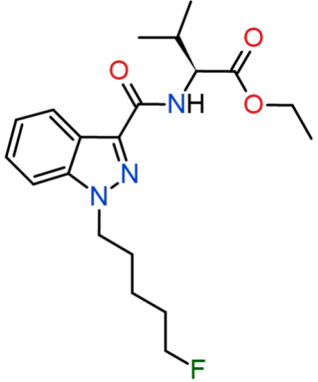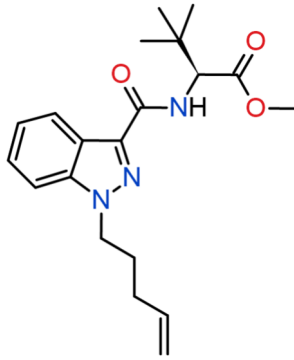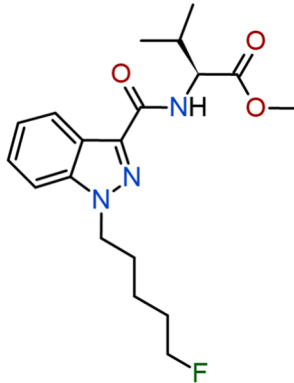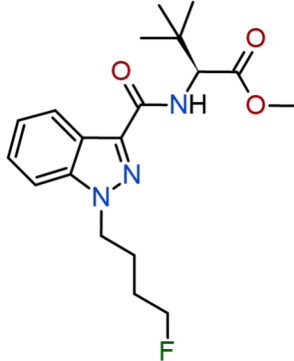
Semi-systematic substance name / Synonyms / IUPAC name	Molecular formula	Monoisotopic mass [Da]	Chemical structure
Cumyl-PeGaClone 5-Pentyl-2-(2-phenylpropan-2-yl)-2,5-dihydro-1*H*-pyrido[4,3-b]indol-1-one	$C_{25}H_{28}N_2O$	372.2202	
5F-Cumyl-PeGaClone 5F-SGT-151 5-(5-Fluoropentyl)-2-(2-phenylpropan-2-yl)-2,5-dihydro-1*H*-pyrido[4,3-b]indol-1-one	$C_{25}H_{27}FN_2O$	390.2107	
Cumyl-CH-MeGaClone SGT-270 5-Cyclohexylmethyl-2-(2-phenylpropan-2-yl)-2,5-dihydro-1*H*-pyrido[4,3-*b*]indol-1-one	$C_{27}H_{30}N_2O$	398.2358	
Cumyl-BC[2.2.1]HpMeGaClone Cumyl-NBMeGaClone SGT-271 5-[(Bicyclo[2.2.1]heptan-2-yl)methyl]-2-(2-phenylpropan-2-yl)-2,5-dihydro-1*H*-pyrido[4,3-b]indol-1-one	$C_{28}H_{30}N_2O$	410.2358	
Cumyl-BC[2.2.1]HpMINACA Cumyl-NBMINACA SGT-152 1-(Bicyclo[2.2.1]heptan-2-yl)methyl)-*N*-(2-phenylpropan-2-yl)-1*H*-indazole-3-carboxamide	$C_{25}H_{29}N_3O$	387.2311	
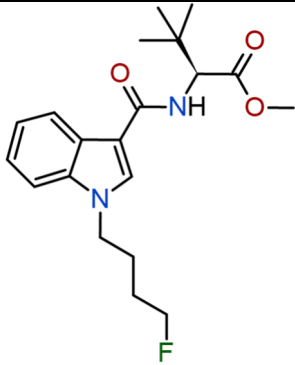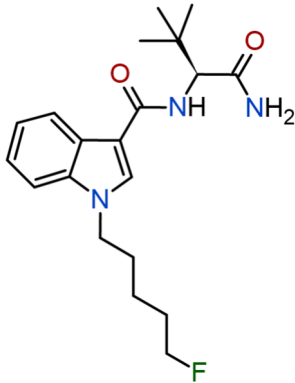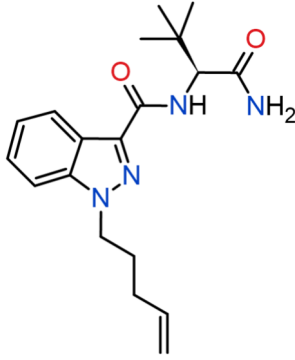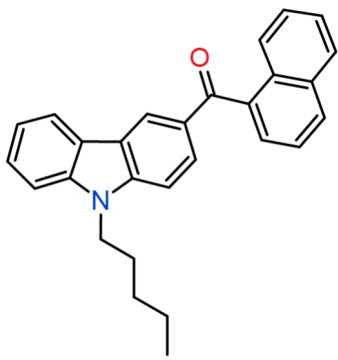
5F-Cumyl-PICA SGT-67 1-(5-Fluoropentyl)-*N*-(2-phenylpropan-2-yl)-1*H*-indole-3-carboxamide	$C_{23}H_{27}FN_2O$	366.2107	
5F-Cumyl-PINACA SGT-25 1-(5-Fluoropentyl)-*N*-(2-phenylpropan-2-yl)-1*H*-indazole-3-carboxamide	$C_{22}H_{26}FN_3O$	367.2060	
5F-Cumyl-P7AICA SGT-263 1-(5-Fluoropentyl)-*N*-(2-phenylpropan-2-yl)-1*H*-pyrrolo[2,3-b]pyridine-3-carboxamide	$C_{22}H_{26}FN_3O$	367.2060	
Cumyl-4CN-BINACA 4CN-Cumyl-BUTINACA SGT-78 1-(4-Cyanobutyl)-*N*-(2-phenylpropan-2-yl)-1*H*-indazole-3-carboxamide	$C_{22}H_{24}N_4O$	360.1950	
Cumyl-CBMICA 1-(Cyclobutylmethyl)-*N*-(2-phenylpropan-2-yl)-1*H*-indole-3-carboxamide	$C_{23}H_{26}N_2O$	346.2045	

AB-FUBINACA *N*-(1-Amino-3-methyl-1-oxobutan-2-yl)-1-[(4-fluorophenyl)methyl]-1*H*-indazole-3-carboxamide	$C_{20}H_{21}FN_4O_2$	368.1649	
ADB-FUBINACA *N*-(1-Amino-3,3-dimethyl-1-oxobutan-2-yl)-1-[(4-fluorophenyl)methyl]-1*H*-indazole-3-carboxamide	$C_{21}H_{23}FN_4O_2$	382.1805	
AMB-FUBINACA MMB-FUBINACA FUB-AMB Methyl 2-[[1-[(4-fluoro-phenyl)methyl]-1*H*-indazole-3-carbonyl]amino]-3-methylbutanoate	$C_{21}H_{22}FN_3O_3$	383.1645	
MDMB-FUBICA Methyl 2-[[1-[(4-fluoro phenyl)methyl]-1*H*-indole-3-carbonyl]amino]-3,3-dimethylbutanoate	$C_{23}H_{25}FN_2O_3$	396.1849	
FUB-144 FUB-UR-144 [1-[(4-Fluorophenyl)methyl]-1*H*-indol-3-yl]-(2,2,3,3-tetramethyl cyclopropyl)methanone	$C_{23}H_{24}FNO$	349.1842	

AB-CHMINACA *N*-(1-Amino-3-methyl-1-oxobutan-2-yl)-1-(cyclohexyl-methyl)-1*H*-indazole-3-carboxamide	$C_{20}H_{28}N_4O_2$	356.2212	
ADB-CHMINACA MAB-CHMINACA *N*-(1-Amino-3,3-dimethyl-1-oxobutan-2-yl)-1-(cyclohexyl-methyl)-1*H*-indazole-3-carboxamide	$C_{21}H_{30}N_4O_2$	370.2369	
MDMB-CHMICA Methyl 2-[[1-(cyclohexyl-methyl)-1*H*-indole-3-carbonyl]amino]-3,3-dimethylbutanoate	$C_{23}H_{32}N_2O_3$	384.2413	
MDMB-CHMCZCA Methyl 2-[[9-(cyclohexyl-methyl)-9*H*-carbazole-3-carbonyl]amino]-3,3-dimethylbutanoate	$C_{27}H_{34}N_2O_3$	434.2569	
5F-EMB-PICA Ethyl 2-[[1-(5-fluoropentyl)-1*H*-indole-3-carbonyl]amino]-3-methylbutanoate	$C_{21}H_{29}FN_2O_3$	376.2162	
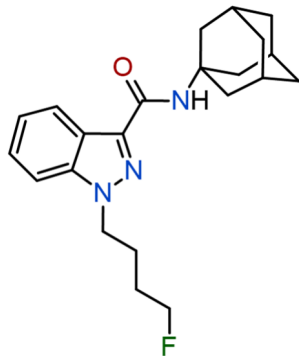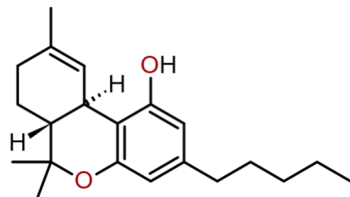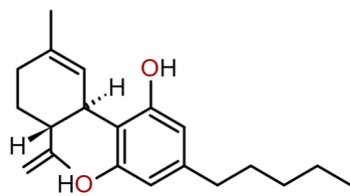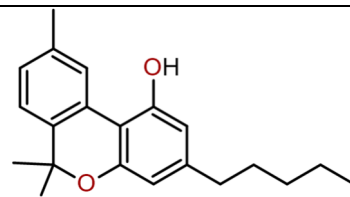
5F-MDMB-PICA 5F-MDMB-2201 Methyl 2-[[1-(5-fluoropentyl)-1*H*-indole-3-carbonyl] amino]-3,3-dimethylbutanoate	$C_{21}H_{29}FN_2O_3$	376.2162	
5F-MDMB-P7AICA 5F-MDMB-7-PAICA 7'N-5F-ADB Methyl 2-[[1-(5-fluoropentyl)-1*H*-pyrrolo[2,3-b]pyridine-3-carbonyl]amino]-3,3-dimethylbutanoate	$C_{20}H_{28}FN_3O_3$	377.2115	
5F-ADB 5F-MDMB-PINACA Methyl 2-[[1-(5-fluoropentyl)-1*H*-indazole-3-carbonyl]amino]-3,3-dimethylbutanoate	$C_{20}H_{28}FN_3O_3$	377.2115	
5F-EDMB-PINACA Ethyl 2-[[1-(5-fluoropentyl)-1*H*-indazole-3-carbonyl]amino]-3,3-dimethylbutanoate	$C_{21}H_{30}FN_3O_3$	391.2271	

5F-EMB-PINACA 5F-AEB Ethyl 2-[[1-(5-fluoropentyl)-1*H*-indazole-3-carbonyl]amino]-3-methylbutanoate	$C_{20}H_{28}FN_3O_3$	377.2115	
MDMB-4en-PINACA Methyl 2-[[1-(pent-4-en-1-yl)-1*H*-indazole-3-carbonyl]amino]-3,3-dimethylbutanoate	$C_{20}H_{27}N_3O_3$	357.2052	
5F-AMB 5F-MMB-PINACA 5F-AMB-PINACA Methyl 2-[[1-(5-fluoropentyl)-1*H*-indazole-3-carbonyl]amino]-3-methylbutanoate	$C_{19}H_{26}FN_3O_3$	363.1958	
4F-MDMB-BINACA Methyl 2-[[1-(4-fluorobutyl)-1*H*-indazole-3-carbonyl]amino]-3,3-dimethylbutanoate	$C_{19}H_{26}FN_3O_3$	363.1958	

Chapter 4
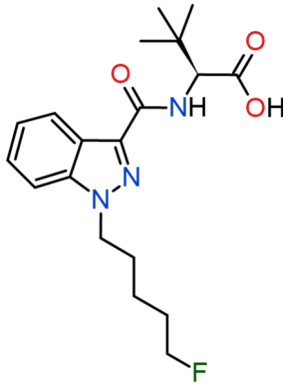
4F-MDMB-BICA Methyl 2-[[1-(4-fluorobutyl)-1*H*-indole-3-carbonyl]amino]-3,3-dimethylbutanoate	$C_{20}H_{27}FN_2O_3$	362.2006	
5F-ADBICA 5F-ADB-PICA *N*-(1-Amino-3,3-dimethyl-1-oxobutan-2-yl)-1-(5-fluoropentyl)-1*H*-indole-3-carboxamide	$C_{20}H_{28}FN_3O_2$	361.2166	
ADB-4en-PINACA *N*-(1-Amino-3,3-dimethyl-1-oxobutan-2-yl)-1-(pent-4-en-1-yl)-1*H*-indazole-3-carboxamide	$C_{19}H_{26}N_4O_2$	342.2056	
EG-018 Naphthalen-1-yl(9-pentyl-9*H*-carbazol-3-yl)methanone	$C_{28}H_{25}NO$	391.1936	

Chapter 4
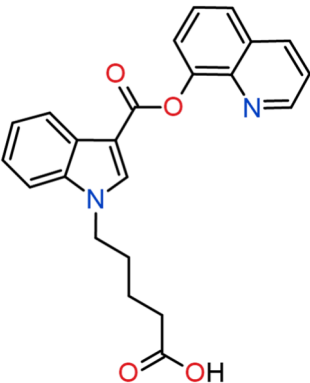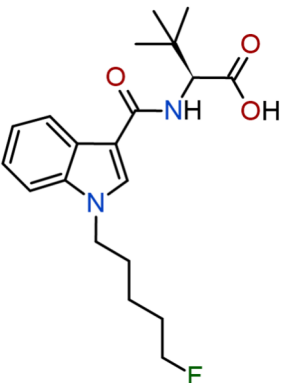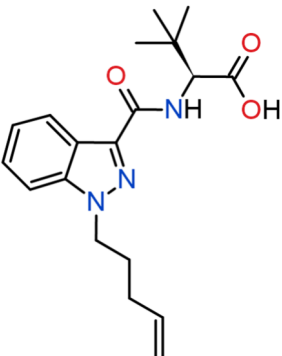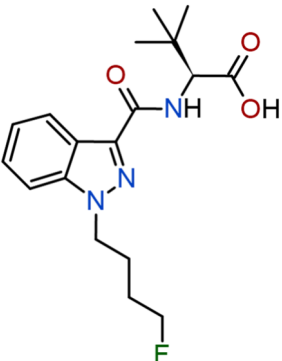
JWH-018 Naphthalen-1-yl(1-pentyl-1*H*-indol-3-yl)methanone	$C_{24}H_{23}NO$	341.1780	
JWH-210 (4-Ethylnaphthalen-1-yl)(1-pentyl-1*H*-indol-3-yl)methanone	$C_{26}H_{27}NO$	369.2093	
MAM-2201 JWH-122 5-fluoropentyl analog, AM-2201 4-methylnaphthyl analog (4-Methylnaphthalen-1-yl)[1-(5-fluoropentyl)-1*H*-indol-3-yl]methanone	$C_{25}H_{24}FNO$	373.1842	
5F-PB-22 5F-QUPIC Quinolin-8-yl 1-(5-fluoropentyl)-1*H*-indole-3-carboxylate	$C_{23}H_{21}FN_2O_2$	376.1587	
5F-AKB-48 5F-APINACA *N*-(Adamantan-1-yl)-1-(5-fluoropentyl)-1*H*-indazole-3-carboxamide	$C_{23}H_{30}FN_3O$	383.2373	

Chapter 4

4F-ABINACA 4F-ABUTINACA N-(4-fluorobutyl)-APINACA *N*-(Adamantan-1-yl)-1-(4-fluorobutyl)-1*H*-indazole-3-carboxamide	$C_{22}H_{28}FN_3O$	369.2216	
(−)-*trans*-Δ⁹-Tetrahydro-cannabinol Δ⁹-THC (6a*R*,10a*R*)-6,6,9-Trimethyl-3-pentyl-6a,7,8,10a-tetrahydro-6*H*-benzo[c]chromen-1-ol	$C_{21}H_{30}O_2$	314.2246	
Cannabidiol CBD 2-[(1*R*,6*R*)-6-Isopropenyl-3-methylcyclohex-2-en-1-yl]-5-pentylbenzene-1,3-diol	$C_{21}H_{30}O_2$	314.2246	
Cannabinol CBN 6,6,9-Trimethyl-3-pentyl-benzo[c]chromen-1-ol	$C_{21}H_{26}O_2$	310.1933	

METABOLITES

5F-ADB dimethylbutanoic acid 2-[[1-(5-Fluoropentyl)-1*H*-indazole-3-carbonyl]amino]-3,3-dimethylbutanoic acid	$C_{19}H_{26}FN_3O_3$	363.1958	

PB-22 N-pentanoic acid 3-[(8-Quinolinyloxy)carbonyl]-1*H*-indole-1-pentanoic acid	$C_{23}H_{20}N_2O_4$	388.1423	
5F-MDMB-PICA dimethylbutanoic acid 2-[[1-(5-Fluoropentyl)-1*H*-indole-3-carbonyl]amino]-3,3-dimethylbutanoic acid	$C_{20}H_{27}FN_2O_3$	362.2006	
MDMB-4en-PINACA dimethylbutanoic acid 2-[[1-(Pent-4-en-1-yl)-1*H*-indazole-3-carbonyl]amino]-3,3-dimethylbutanoic acid	$C_{19}H_{25}N_3O_3$	343.1896	
4F-MDMB-BINACA dimethylbutanoic acid 2-[[1-(4-Fluorobutyl)-1*H*-indazole-3-carbonyl]amino]-3,3-dimethylbutanoic acid	$C_{18}H_{24}FN_3O_3$	349.1802	

Chapter 4

161

4F-MDMB-BINACA N-(butanoic acid) dimethylbutanoic acid 2-[[1-(3-Carboxypropyl)-1*H*-indazole-3-carbonyl]amino]-3,3-dimethylbutanoic acid	$C_{18}H_{23}N_3O_5$	361.1638	
4F-MDMB-BICA dimethylbutanoic acid 2-[[1-(4-Fluorobutyl)-1*H*-indole-3-carbonyl]amino]-3,3-dimethylbutanoic acid	$C_{19}H_{25}FN_2O_3$	348.1849	
Cumyl-PeGaClone N-pentanoic acid 1,2-Dihydro-2-(2-phenylpropan-2-yl)-1-oxo-5*H*-pyrido[4,3-b]indole-5-pentanoic acid	$C_{25}H_{26}N_2O_3$	402.1943	
(−)-11-Nor-9-carboxy-Δ⁹-THC THC-COOH (6a*R*,10a*R*)-1-Hydroxy-6,6-dimethyl-3-pentyl-6a,7,8,10a-tetrahydrobenzo[c]chromene-9-carboxylic acid	$C_{21}H_{28}O_4$	344.1988	

ISTD			
(−)-*trans*-Δ⁹-THC-D₃	$C_{21}H_{27}D_3O_2$	317.2434	

Table S2. Detailed sampling parameters for the wastewater sampling device deployed in a German prison.

Sampling parameters for a prison	
Sample containers	12 sample containers (2 L capacity each)
Sampling interval	12 minutes (100 mL sampling volume) → 4 h composite samples in each sample container
Sampling time	48 hours (May 22, 2021 - May 24, 2021) (10 a.m. - 10 a.m.)

Table S3. Installation and deinstallation dates and times for PDMS rods placed at three different locations in a city district of Munich. Slightly different time periods with max. 3 h delay between the locations were covered.

Index	Installation date and time	Deinstallation date and time
September 21-24, 2021 (weekdays) Location 2	September 21, 2021 / 12.30 p.m.	September 24, 2021 / 1.30 p.m.
Location 3	September 21, 2021 / 2.30 p.m.	September 24, 2021 / 2.30 p.m.
Location 4	September 21, 2021 / 3.30 p.m.	September 24, 2021 / 3.00 p.m.
September 24-27, 2021 (weekend) Location 2	September 24, 2021 / 1.30 p.m.	September 27, 2021 / 10.30 a.m.

Figure S1. The optimized gradient program for the chromatographic separation of SCRAs in this study, Eluent A: water with 0.1% formic acid (UHPLC grade), Eluent B: acetonitrile with 0.1% formic acid (UHPLC grade).

Table S4. MRM parameters including the precursor ion (Q1) and the four most prominent product ions (Q3), declustering potential (DP), entrance potential (EP), collision cell entrance potential (CEP), collision energy (CE) and collision cell exit potential (CXP). The most prominent product ion is indicated for each analyte as underlined Q3 ion and the corresponding retention times are listed below the respective substance.

Analyte	Q1 m/z	Q3 m/z	DP in V	EP in V	CE in V	CXP in V
4F-MDMB-BINACA **4.84 min**	364.2	<u>219.0</u>	45	10	33	12
	364.2	304.1	45	10	21	16
	364.2	145.0	45	10	55	16
	364.2	116.9	45	10	71	14
4F-MDMB-BINACA dimethylbutanoic acid **2.97 min**	350.1	<u>219.0</u>	76	10	31	10
	350.1	304.0	76	10	19	16
	350.1	145.0	76	10	51	10
	350.1	89.9	76	10	79	12
4F-MDMB-BINACA N-(butanoic acid) dimethylbutanoic acid **1.21 min**	362.1	<u>316.2</u>	96	10	19	16
	362.1	231.1	96	10	27	14
	362.1	145.0	96	10	45	10
	362.1	213.0	96	10	37	16
5F-ADB **5.49 min**	378.2	<u>318.1</u>	45	10	21	16
	378.2	233.1	45	10	31	12
	378.2	145.0	45	10	59	16
	378.2	213.1	45	10	41	10
5F-ADB dimethylbutanoic acid **3.58 min**	364.1	<u>233.1</u>	45	10	29	12
	364.1	318.0	45	10	19	16
	364.1	145.0	45	10	55	16
	364.1	213.1	45	10	39	12
5F-AMB **4.79 min**	364.1	<u>233.0</u>	61	10	29	12
	364.1	304.1	61	10	21	14
	364.1	144.9	61	10	53	16
	364.1	213.0	61	10	37	12

Chapter 4

Analyte	Q1 m/z	Q3 m/z	DP in V	EP in V	CE in V	CXP in V
5F-MDMB-P7AICA **3.21 min**	378.1	<u>318.1</u>	40	10	39	16
	378.1	145.0	40	10	55	16
	378.1	298.2	40	10	41	14
	378.1	131.1	40	10	63	14
MDMB-4en-PINACA **5.91 min**	358.2	<u>213.2</u>	61	10	29	14
	358.2	298.2	61	10	21	26
	358.2	145.0	61	10	55	6
	358.2	171.0	61	10	53	8
MDMB-4en-PINACA dimethylbutanoic acid **3.95 min**	344.1	<u>213.1</u>	76	10	29	10
	344.1	298.1	76	10	19	16
	344.1	145.0	76	10	51	6
	344.1	171.0	76	10	45	22
ADB-4en-PINACA **3.04 min**	343.1	<u>213.0</u>	56	10	33	10
	343.1	298.1	56	10	19	16
	343.1	326.2	56	10	13	14
	343.1	145.1	56	10	53	4
5F-MDMB-PICA **4.85 min**	377.1	<u>232.1</u>	56	10	21	12
	377.1	144.1	56	10	53	16
	377.1	116.0	56	10	73	12
	377.1	88.9	56	10	103	10
5F-MDMB-PICA dimethylbutanoic acid **3.21 min**	363.1	<u>232.0</u>	66	10	19	12
	363.1	144.0	66	10	51	16
	363.1	116.0	66	10	69	12
	363.1	88.9	66	10	103	16
4F-MDMB-BICA **4.23 min**	363.1	<u>218.2</u>	66	10	19	12
	363.1	144.0	66	10	51	16
	363.1	115.8	66	10	69	14

Chapter 4

Analyte	Q1 m/z	Q3 m/z	DP in V	EP in V	CE in V	CXP in V
continued	363.1	89.1	66	10	99	22
4F-MDMB-BICA dimethylbutanoic acid 2.60 min	349.0	<u>218.0</u>	86	10	21	14
	349.0	144.0	86	10	49	6
	349.0	115.8	86	10	71	14
	349.0	89.0	86	10	103	40
5F-ADBICA 2.45 min	362.1	<u>232.1</u>	66	10	29	10
	362.1	345.1	66	10	13	16
	362.1	144.1	66	10	55	6
	362.1	116.0	66	10	69	18
5F-EDMB-PINACA 6.15 min	392.1	<u>233.2</u>	21	10	35	20
	392.1	318.2	21	10	25	20
	392.1	145.0	21	10	53	14
	392.1	213.0	21	10	41	20
5F-EMB-PINACA 5.49 min	378.1	<u>304.2</u>	86	10	21	16
	378.1	232.9	86	10	33	12
	378.1	213.1	86	10	39	12
	378.1	332.0	86	10	17	6
5F-EMB-PICA 4.85 min	377.1	<u>232.0</u>	51	10	23	12
	377.1	144.1	51	10	53	16
	377.1	115.9	51	10	71	12
	377.1	89.0	51	10	105	10
Cumyl-PeGaClone 7.08 min	373.1	<u>255.1</u>	31	10	19	14
	373.1	167.0	31	10	65	20
	373.1	185.0	31	10	51	10
	373.1	90.9	31	10	79	10
5F-Cumyl-PeGaClone 6.01 min	391.2	<u>273.0</u>	41	10	17	14
	391.2	90.9	41	10	71	10

Analyte	Q1 m/z	Q3 m/z	DP in V	EP in V	CE in V	CXP in V
continued	391.2	167.1	41	10	69	18
	391.2	119.1	41	10	39	12
Cumyl-PeGaClone N-pentanoic acid 3.12 min	403.1	<u>285.1</u>	36	10	17	20
	403.1	267.0	36	10	41	16
	403.1	91.0	36	10	73	10
	403.1	185.1	36	10	51	10
5F-Cumyl-PICA 5.55 min	367.1	<u>249.1</u>	30	10	21	12
	367.1	206.1	30	10	35	12
	367.1	232.1	30	10	37	12
	367.1	91.0	30	10	73	10
5F-Cumyl-PINACA 6.19 min	368.2	<u>250.2</u>	45	10	15	14
	368.2	233.1	45	10	27	12
	368.2	144.9	45	10	55	16
	368.2	213.0	45	10	41	12
5F-Cumyl-P7AICA 3.81 min	368.2	<u>250.2</u>	45	10	19	14
	368.2	145.0	45	10	53	16
	368.2	118.9	45	10	43	12
	368.2	174.0	45	10	45	10
Cumyl-4CN-BINACA 4.69 min	361.2	<u>243.1</u>	20	10	15	16
	361.2	226.0	20	10	29	12
	361.2	145.0	20	10	55	16
	361.2	91.1	20	10	69	10
Cumyl-CBMICA 6.16 min	347.1	<u>229.0</u>	81	10	19	12
	347.1	118.0	81	10	41	10
	347.1	91.1	81	10	67	42
	347.1	186.0	81	10	31	8

Analyte	Q1 m/z	Q3 m/z	DP in V	EP in V	CE in V	CXP in V
Cumyl-CH-MeGaClone 8.06 min	399.1	<u>281.2</u>	71	10	19	14
	399.1	185.1	71	10	55	20
	399.1	167.1	71	10	71	18
	399.1	119.2	71	10	35	10
Cumyl-BC[2.2.1] HpMeGaClone 8.29 min	411.2	<u>293.3</u>	56	10	19	12
	411.2	185.1	56	10	57	16
	411.2	90.8	56	10	75	14
	411.2	166.9	56	10	71	18
Cumyl-BC[2.2.1] HpMINACA 8.46 min	388.2	<u>270.0</u>	91	10	15	14
	388.2	253.2	91	10	31	12
	388.2	145.1	91	10	55	16
	388.2	118.9	91	10	41	24
AB-CHMINACA 3.84 min	357.2	<u>312.2</u>	26	10	21	16
	357.2	340.0	26	10	13	18
	357.2	241.0	26	10	35	14
	357.2	145.0	26	10	53	16
ADB-CHMINACA 4.53 min	371.2	<u>241.1</u>	41	10	35	12
	371.2	354.1	41	10	13	20
	371.2	326.1	41	10	23	16
	371.2	144.9	41	10	53	16
AB-FUBINACA 2.62 min	369.1	<u>324.1</u>	26	10	21	16
	369.1	352.0	26	10	13	18
	369.1	253.0	26	10	33	12
	369.1	109.0	26	10	49	12
ADB-FUBINACA 3.25 min	383.1	<u>338.1</u>	31	10	21	16
	383.1	366.1	31	10	13	18
	383.1	253.1	31	10	33	12

Analyte	Q1 m/z	Q3 m/z	DP in V	EP in V	CE in V	CXP in V
continued	383.1	109.0	31	10	51	12
AMB-FUBINACA 5.35 min	384.1	<u>253.0</u>	30	10	31	14
	384.1	324.0	30	10	21	16
	384.1	108.9	30	10	49	12
	384.1	352.0	30	10	15	20
FUB-144 7.36 min	350.1	<u>125.0</u>	45	10	29	12
	350.1	109.0	45	10	39	12
	350.1	252.1	45	10	29	12
	350.1	82.8	45	10	99	10
MDMB-FUBICA 5.43 min	397.1	<u>252.0</u>	21	10	21	10
	397.1	108.9	21	10	45	28
	397.1	83.0	21	10	117	6
	397.1	89.0	21	10	117	12
5F-PB-22 5.73 min	377.1	<u>232.1</u>	51	10	19	12
	377.1	144.0	51	10	51	16
	377.1	116.0	51	10	73	12
	377.1	88.9	51	10	103	10
PB-22- N-pentanoic acid 2.92 min	389.1	<u>244.0</u>	56	10	19	12
	389.1	144.0	56	10	45	16
	389.1	116.0	56	10	73	14
	389.1	101.0	56	10	41	12
5F-AKB-48 7.79 min	384.1	<u>135.0</u>	66	10	27	14
	384.1	93.0	66	10	69	10
	384.1	79.0	66	10	77	8
	384.1	107.0	66	10	63	14
4F-A-BINACA 7.17 min	370.1	<u>135.0</u>	91	10	25	16
	370.1	93.0	91	10	65	14

Analyte	Q1 m/z	Q3 m/z	DP in V	EP in V	CE in V	CXP in V
continued	370.1	78.9	91	10	75	8
	370.1	107.1	91	10	55	8
MDMB-CHMCZCA **8.46 min**	435.1	<u>290.1</u>	76	10	21	14
	435.1	194.0	76	10	57	10
	435.1	166.0	76	10	73	18
	435.1	179.0	76	10	69	8
MDMB-CHMICA **6.73 min**	385.1	<u>240.0</u>	30	10	23	12
	385.1	144.0	30	10	51	6
	385.1	108.9	30	10	51	12
	385.1	116.0	30	10	75	12
EG-018 **9.70 min**	392.1	<u>155.1</u>	71	10	31	8
	392.1	126.9	71	10	73	14
	392.1	264.1	71	10	33	14
	392.1	77.0	71	10	117	8
JWH-018 **8.12 min**	342.1	<u>155.0</u>	80	10	31	8
	342.1	127.0	80	10	51	2
	342.1	214.1	80	10	31	10
	342.1	76.8	80	10	97	8
JWH-210 **9.12 min**	370.1	<u>183.0</u>	131	10	33	10
	370.1	214.2	131	10	33	14
	370.1	155.2	131	10	45	8
	370.1	153.0	131	10	55	14
MAM-2201 **7.62 min**	374.1	<u>169.0</u>	136	10	33	18
	374.1	141.0	136	10	49	6
	374.1	114.9	136	10	87	12
	374.1	232.0	136	10	33	12

Analyte	Q1 m/z	Q3 m/z	DP in V	EP in V	CE in V	CXP in V
Δ⁹-THC 7.75 min	315.1	<u>193.1</u>	66	10	31	22
	315.1	122.9	66	10	39	10
	315.1	91.0	66	10	65	10
	315.1	77.2	66	10	87	20
Δ⁹-THC-COOH 5.20 min	345.0	<u>327.0</u>	71	10	21	14
	345.0	299.1	71	10	27	14
	345.0	91.0	71	10	63	16
	345.0	267.2	71	10	11	14
CBN 7.61 min	311.1	<u>223.1</u>	81	10	27	10
	311.1	292.9	81	10	23	14
	311.1	194.9	81	10	35	16
	311.1	208.0	81	10	41	10
CBD 6.78 min	315.1	<u>193.1</u>	66	10	29	10
	315.1	259.2	66	10	25	14
	315.1	122.9	66	10	39	14
	315.1	135.2	66	10	25	8
Δ⁹-THC-D3 7.73 min	318.1	<u>196.0</u>	36	10	27	12
	318.1	262.2	36	10	27	4
	318.1	123.1	36	10	45	8

Chapter 4

Table S5. Selected cannabinoids and their human metabolites selected for the target screening LC-MS/MS method.

SCRAs and their selected human metabolites				
Group A	**Group B**	**Group C**	**Group D**	**Metabolites**
4F-MDMB-BICA	Cumyl-PeGaClone	AB-CHMINACA	5F-PB-22	4F-MDMB-BICA dimethylbutanoic acid
4F-MDMB-BINACA	5F-Cumyl-PeGaClone	ADB-CHMINACA	5F-AKB-48	4F-MDMB-BINACA dimethylbutanoic acid
5F-ADB	5F-Cumyl-PICA	MDMB-CHMICA	4F-ABINACA	4F-MDMB-BINACA N-(butanoic acid) dimethylbut. acid
5F-AMB	5F-Cumyl-PINACA	MDMB-CHMCZCA	EG-018	5F-ADB dimethylbutanoic acid
5F-MDMB-P7AICA	5F-Cumyl-P7AICA	AB-FUBINACA	JWH-018	MDMB-4en-PINACA dimethylbutanoic acid
MDMB-4en-PINACA	4CN-Cumyl-BINACA	ADB-FUBINACA	JWH-210	5F-MDMB-PICA dimethylbutanoic acid
ADB-4en-PINACA	Cumyl-CBMICA	AMB-FUBINACA	MAM-2201	Cumyl-PeGaClone N-pentanoic acid
5F-MDMB-PICA / 5F-EMB-PICA*	Cumyl-CH-MeGaClone	FUB-144		PB-22 N-pentanoic acid
5F-ADBICA	Cumyl-BC[2.2.1]HpMeGaClone	MDMB-FUBICA		
5F-EDMB-PINACA	Cumyl-BC[2.2.1]HpMINACA			
5F-EMB-PINACA	*5F-MDMB-PICA and 5F-EMB-PICA cannot be distinguished by the analytical method developed (identical ion transitions and identical retention time)			
Phytocannabinoids and their human metabolites				
Δ^9-Tetrahydrocannabinol (Δ^9-THC), Cannabidiol (CBD) and Cannabinol (CBN)			11-Nor-9-carboxy-Δ^9-tetrahydrocannabinol (THC-COOH)	

Table S6. Optimization of the re-extraction procedure for SCRAs from the PDMS rods (1 cm length) collected in the wastewater of the prison. Comparison of different extractants (isohexane/ethyl acetate (9/1, v/v) and methanol), and benefit of the repeated extraction (2nd extraction yield). The total area values given represent the sum of the signal areas from both extractions. They were compared to the corresponding SCRA areas obtained after liquid-liquid-extraction of the most concentrated liquid wastewater sample from the prison.

Substance	4F-MDMB-BINACA		MDMB-4en-PINACA		4F-MDMB-BICA		5F-MDMB-PICA/5F-EMB-PICA		MAM-2201		EG-018	
	Isohex/ EtOAc	MeOH	Isohex/ EtOAc	MeOH	Isohex/ EtOAc	MeOH	Isohex/ EtOAc	MeOH	Isohex/ EtOAc	MeOH	Isohex/ EtOAc	MeOH
Area 1. extract	**1.9e6**	7.8e5	**3.7e7**	1.4e7	**2.2e5**	1.2e5	**2.8e5**	1.8e5	**7.5e4**	3.7e4	**5.5e6**	1.6e6
Area 2. extract	6.1e5	4.1e5	1.1e7	7.7e6	5.4e4	4.0e4	8.0e4	5.9e4	2.7e4	1.9e4	2.0e6	7.0e5
2nd extraction yield	**32%**	53%	**30%**	55%	**25%**	33%	**29%**	33%	**36%**	51%	**36%**	44%
Superior solvent	Isohexane/ethyl acetate (9/1, v/v)											
Total area (PDMS)	2.5e6		4.8e7		2.7e5		3.6e5		1.0e5		7.5e6	
Area (LLE), most intense sample	3.4e6		1.3e7		6.3e5		9.0e4		/		/	

A) 4F-MDMB-BICA

B) 5F-MDMB-PICA / 5F-EMB-PICA
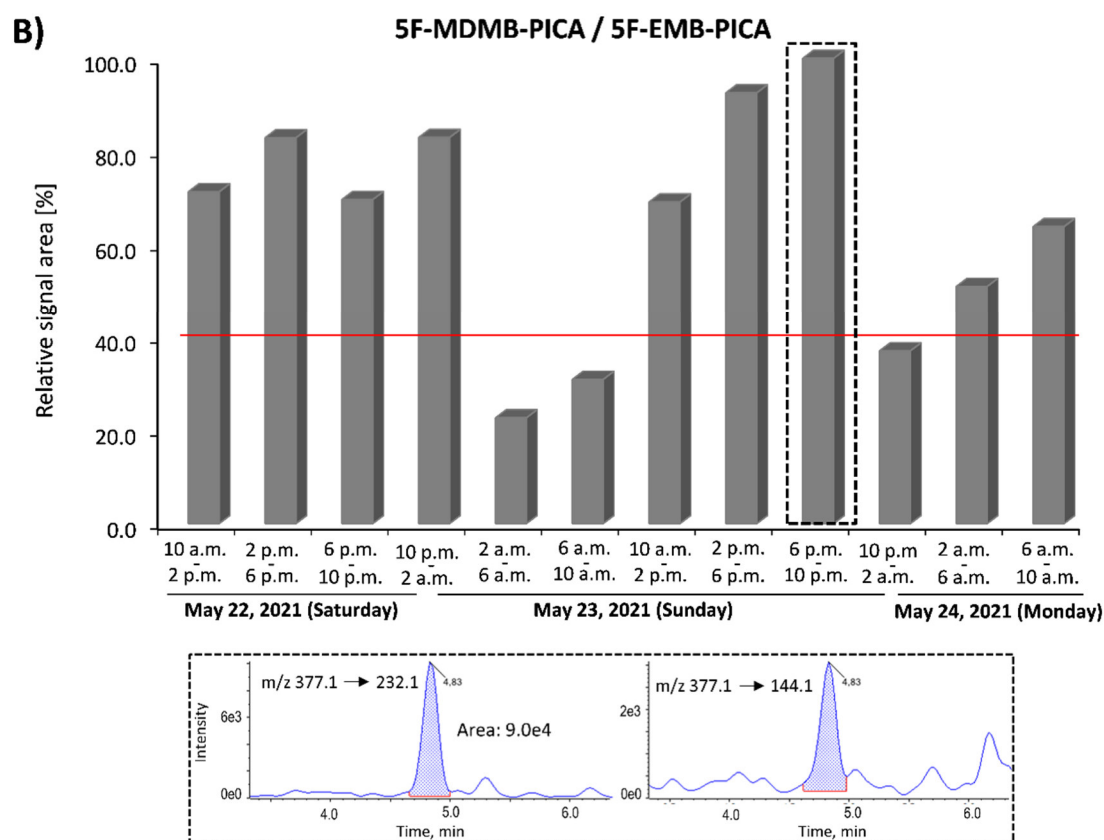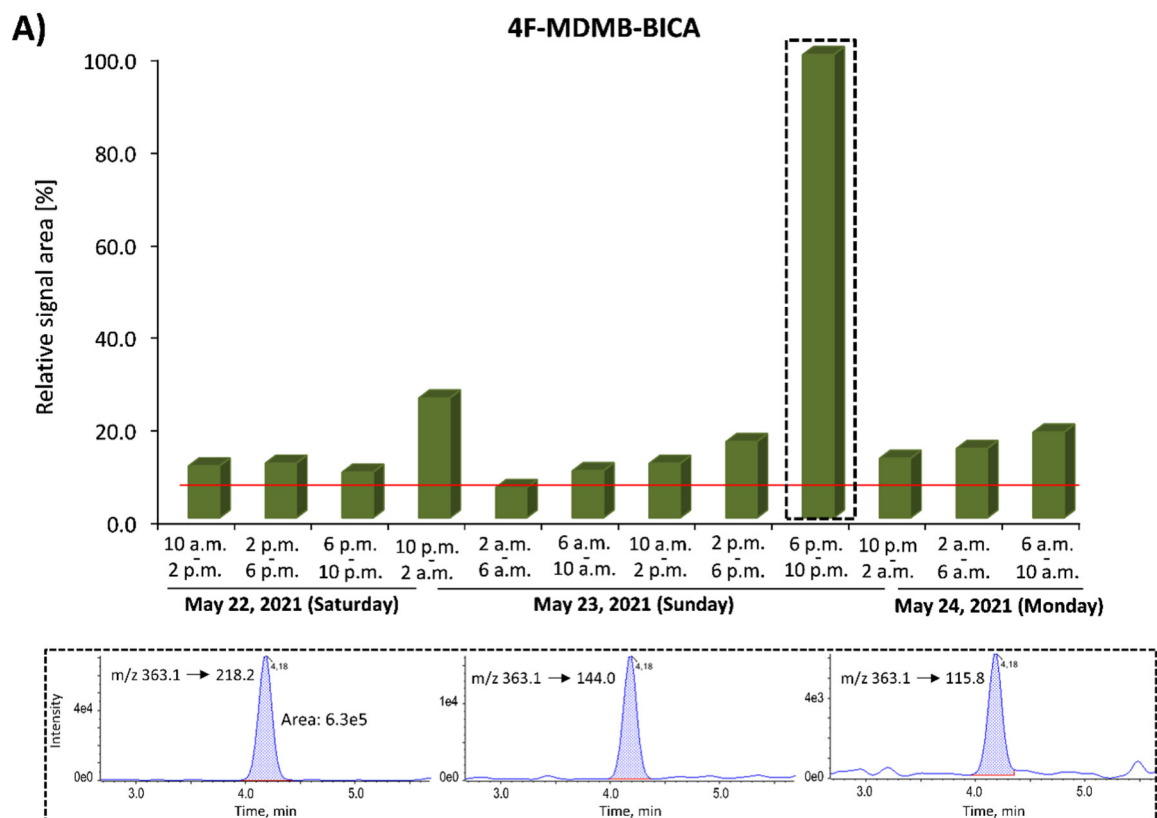
(continued)
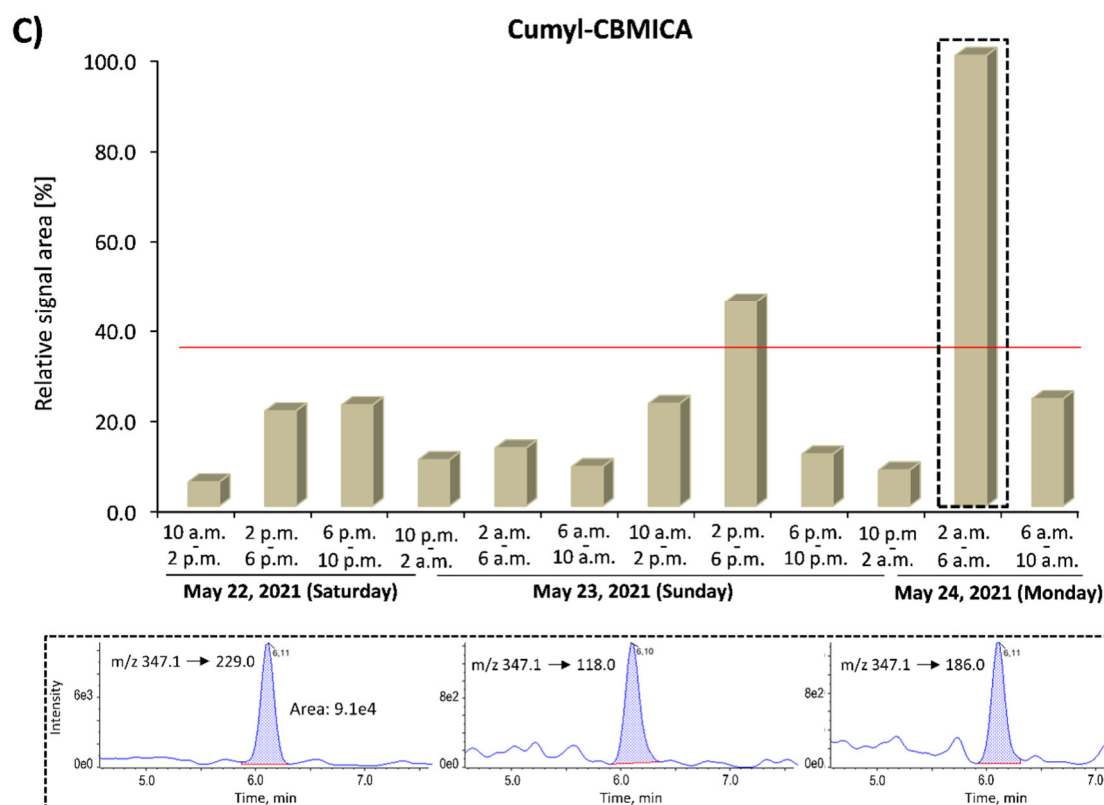
Figure S2. Generated time profiles for 4F-MDMB-BICA (A), 5F-MDMB/5F-EMB-PICA (B) and Cumyl-CBMICA (C, see below) prevalence patterns in the prison from May 22-24, 2021, with corresponding chromatograms for the most intense ion transitions for the samples indicated by dashed rectangles. The red line denotes the S/N ratio corresponding to 9/1 for the most intense ion transition, with S/N values calculated using Peak-To-Peak algorithm (Analyst® Software 1.6.2).
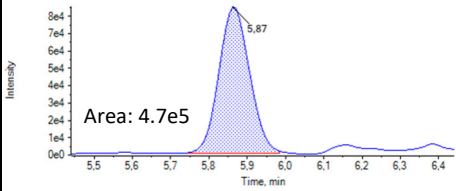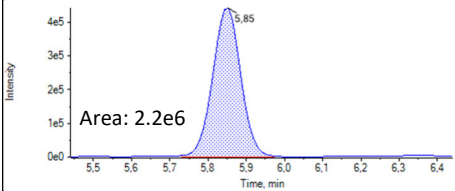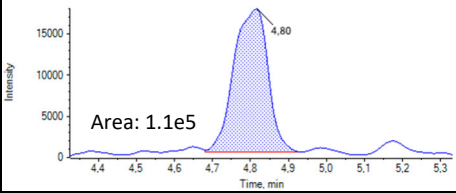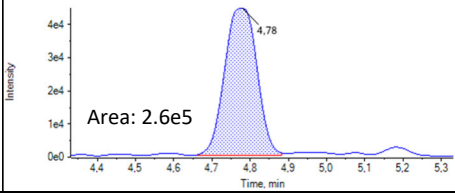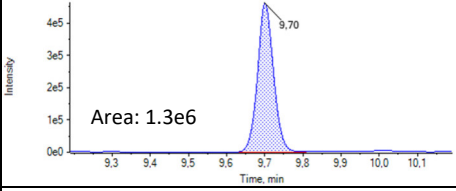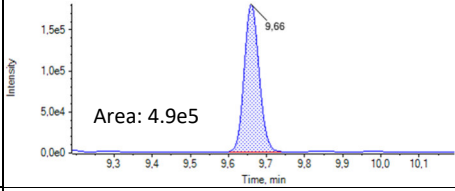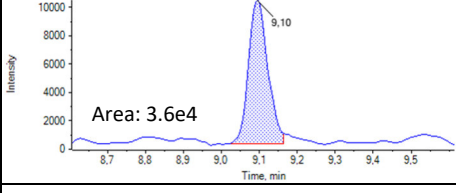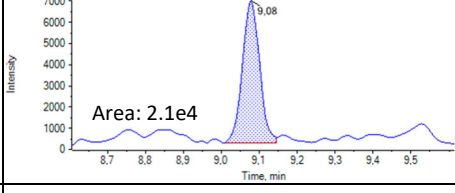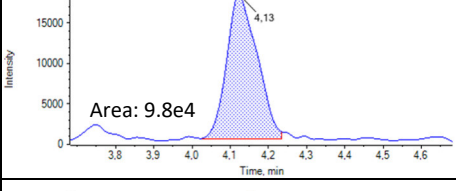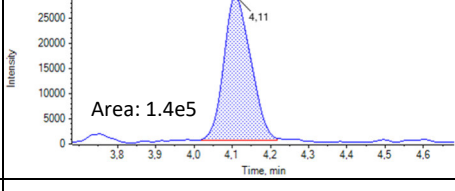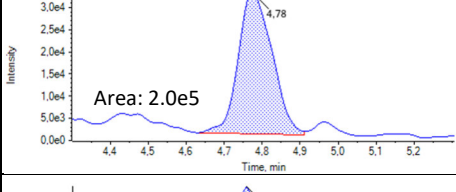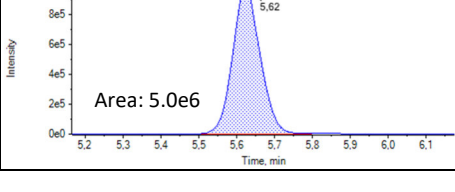
Table S7. Detection of different SCRAs and THC at three different locations within a city district of Munich. Installation (September 21, 2021) and deinstallation (September 24, 2021) time points for PDMS rods at each location are indicated correspondingly.

Cannabinoids (PDMS sampling in a city district)			
Sept 21, 2021 - Sept 24, 2021	Location 2 (M2) 12.30 p.m. - 1.30 p.m.	Location 3 (M3) 2.30 p.m. - 2.30 p.m.	Location 4 (M4) 3.30 p.m. - 3.00 p.m.
MDMB-4en-PINACA	+	+	+
5F-MDMB-PICA / 5F-EMB-PICA	+	+	+
EG-018	+	+	+
JWH-210	+	+	+
4F-MDMB-BICA	+	+	-
4F-MDMB-BINACA	+	-	-
5F-PB-22	+	-	-
THC	+	+	+
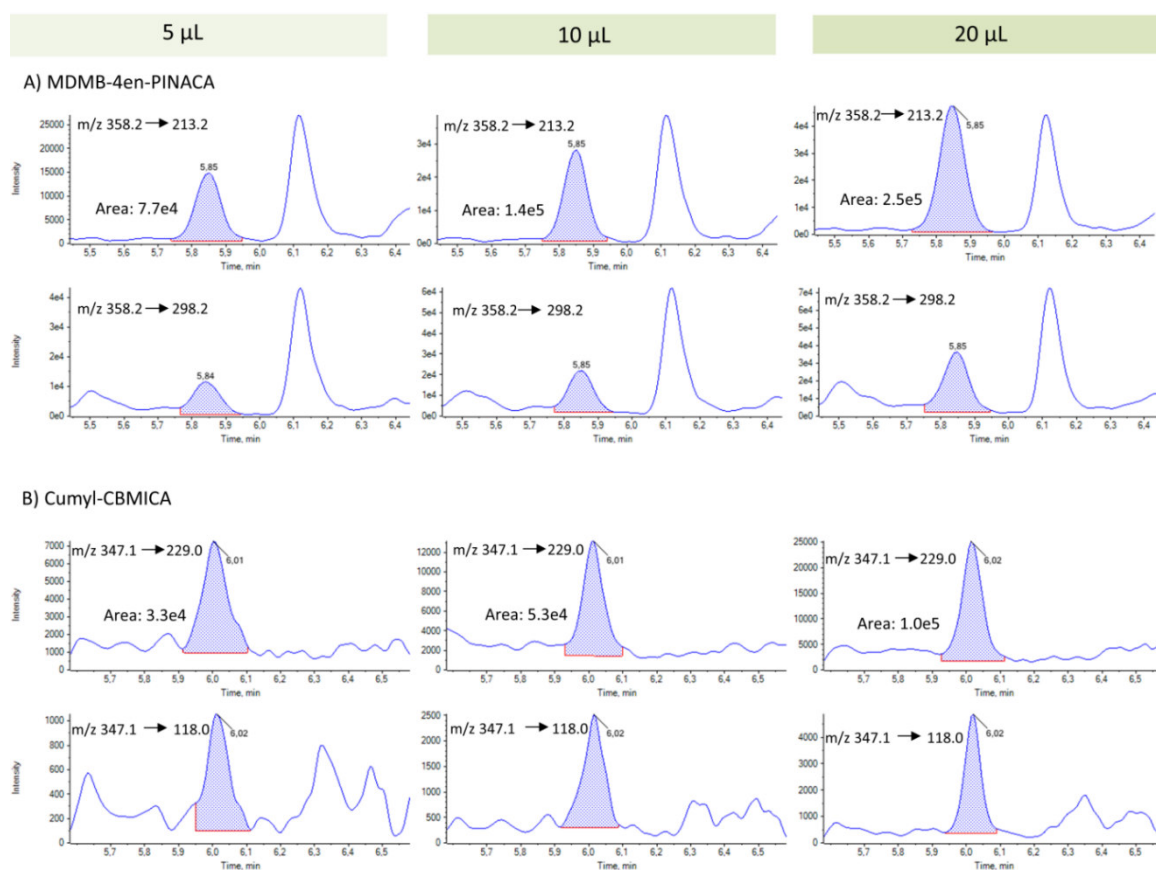
Figure S3. Authentic wastewater chromatograms for MDMB-4en-PINACA and Cumyl-CBMICA for increasing injection volumes from 5 µL to 20 µL. The two most intense ion transitions per substance with signal areas for the primary (most intense) ion transition are depicted.

Table S8. Semi-quantitative data, showing areas of the most intense ion generated after fragmentation (primary ion transition) for particular SCRAs, as detected at the two different locations (M2 and M3).

SCRAs (PDMS sampling)		
Sept 21 - Sept 24, 2021	Location 2 (M2) 12.30 p.m. - 1.30 p.m.	Location 3 (M3) 2.30 p.m. - 2.30 p.m.
MDMB-4en-PINACA	Area: 4.7e5	Area: 2.2e6
5F-MDMB-PICA / 5F-EMB-PICA	Area: 1.1e5	Area: 2.6e5
EG-018	Area: 1.3e6	Area: 4.9e5
JWH-210	Area: 3.6e4	Area: 2.1e4
4F-MDMB-BICA	Area: 9.8e4	Area: 1.4e5
4F-MDMB-BINACA	Area: 2.0e5	Not detected
5F-PB-22	Area: 5.0e6	Not detected

4.7 Unpublished data

Prison study: Comparison with conventional drugs

In addition to SCRAs, the liquid wastewater samples collected in the sewage system of the German prison investigated were screened for several conventional drugs. A list of the target conventional drugs screened (5.6 Supplementary Material, Table S2) as well as details on the wastewater sample preparation (5.2.2 Wastewater analysis) and the analytical detection method (5.2.5 Instrumentation and analytical conditions) can be found in Chapter 5.

The following compounds, most of which represent violation of the German Narcotics Act (German: Betäubungsmittelgesetz, BtMG), were detected in the analyzed wastewater samples by the LC-MS/MS analysis:

- ❖ Amphetamine
- ❖ Cocaine
- ❖ Methylphenidate
- ❖ Methadone and its metabolite 2-ethylidene-1,5-dimethyl-3,3-diphenylpyrrolidine (EDDP)
- ❖ Buprenorphine and its metabolite norbuprenorphine
- ❖ Tilidine and its metabolite nortilidine
- ❖ Tramadol* and its metabolite *O*-desmethyl-*cis*-tramadol
- ❖ Fentanyl
- ❖ Naloxone*

  *Substance not defined as an illicit drug according to the German Narcotics Act; metabolites are not included in the German Narcotics Act.

As previously shown, the acidification step of raw wastewater samples seemed to be vital for the recovery of SCRA metabolites using the sample procedure developed, while the parent SCRAs did not show significant differences in extraction yields for pH 7 and pH 2 (see 4.3.4 Assessment of SCRA use in a prison, Liquid wastewater samples). However, a significant adverse effect was observed for the recovery of conventional drugs when sample acidification was applied. Therefore, a single wastewater preparation procedure without sample acidification would allow for a simultaneous multi-analysis of conventional drugs and SCRAs, while SCRA metabolites need to be extracted using a separate preparation procedure.

The results obtained after the optimized liquid-liquid extraction (LLE) of conventional drugs from the wastewater samples of the prison are discussed in the following section, including the time profiles generated for individual substances. Conventional illicit drugs detected included two psychostimulants, amphetamine and cocaine. Amphetamine was detected during two individual 4-hour time intervals (Sunday: 2-6 p.m. and Monday: 2-6 a.m.) and cocaine during five individual 4-hour time intervals (Saturday: 10 a.m.-2 p.m; Sunday: 6-10 a.m., 10 a.m.-2 p.m., 2-6 p.m. and 6-10 p.m.) as shown in Figures S4A and S4C. The main metabolite of cocaine, benzoylecgonine, was not detected, possibly due to low concentrations in wastewater being below the detection limit. In contrast to the SCRAs detected, the prevalence of conventional illicit drugs was low. This was reflected in a low number of

conventional illicit drugs detected (two: amphetamine and cocaine), their low frequency of detection in different wastewater samples covering different time intervals, and their rather low amounts indicated by the signal areas close to the S/N ratio corresponding to 9/1 and 3/1 for the most and second most intense ion transition, respectively (red line in Figures S4A and S4C). Regular consumption of the substitution drugs methadone and buprenorphine in prison was evident from the pronounced occurrence of these substances in the wastewater samples examined. Particularly high amounts of methadone were detected, as even diluted wastewater samples were sufficient for the identification (cf. Figure S4D). After the LLE procedure, very high concentration ranges were reached, exceeding the saturation limit of the analytical detection method. The detection of metabolites EDDP and norbuprenorphine arising from the methadone and buprenorphine metabolism, respectively, indicated an active consumption of these two drugs. Both followed a trend similar like their parent substances. However, no consistent correlations could be observed between the relative area ratios of the corresponding metabolite to its parent substance for the different time intervals, showing that sometimes the metabolite and sometimes the parent substance dominated.

Based on the results of the wastewater analysis, there were notable differences in the trends of drug use in the prison investigated. It was clearly evident that the consumption of SCRAs was more prevalent than the consumption of conventional drugs. This was remarkable, since the typical single doses for SCRAs are much lower than those of the other drugs detected (apart from buprenorphine and fentanyl).

(continued)

B)

Methylphenidate

C)

Cocaine

(continued)

D)

Methadone and EDDP

E)

Buprenorphine and Norbuprenorphine

(continued)

F)

Fentanyl

G)

Naloxone

(continued)

H)

Tilidine and Nortilidine

I)
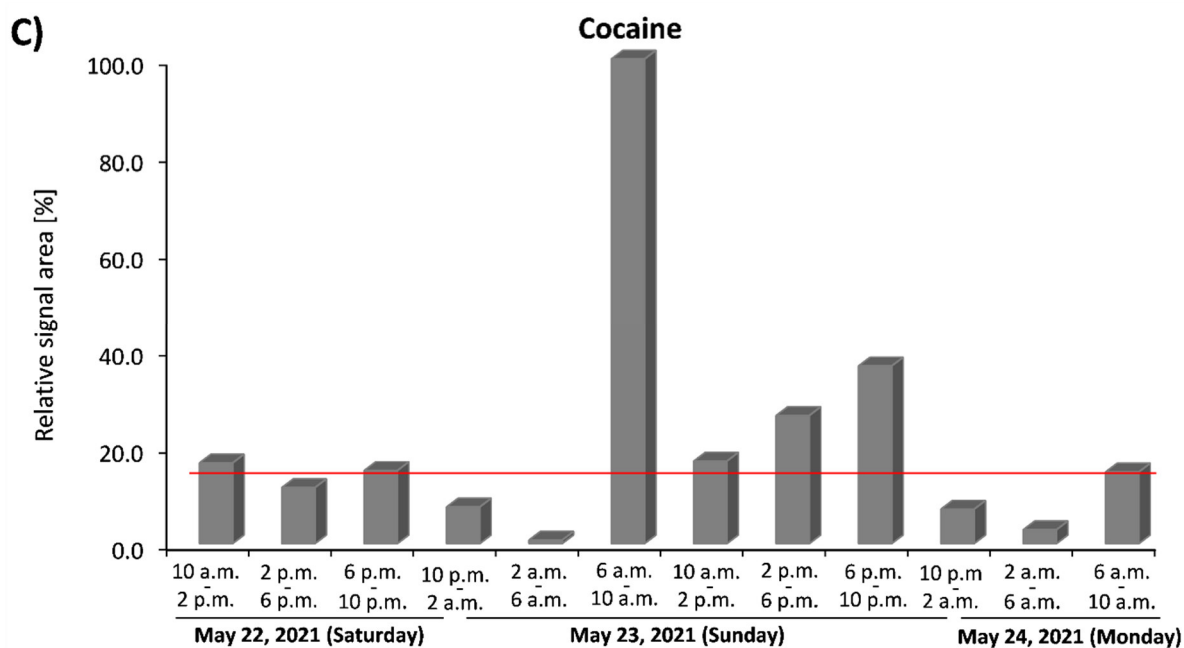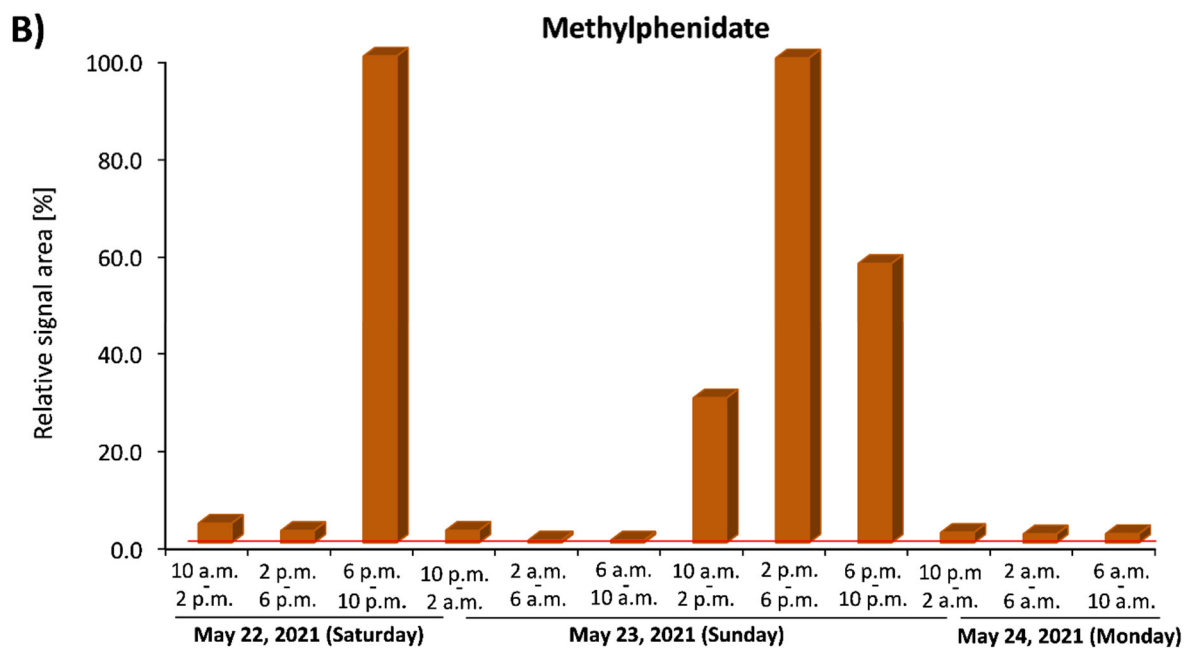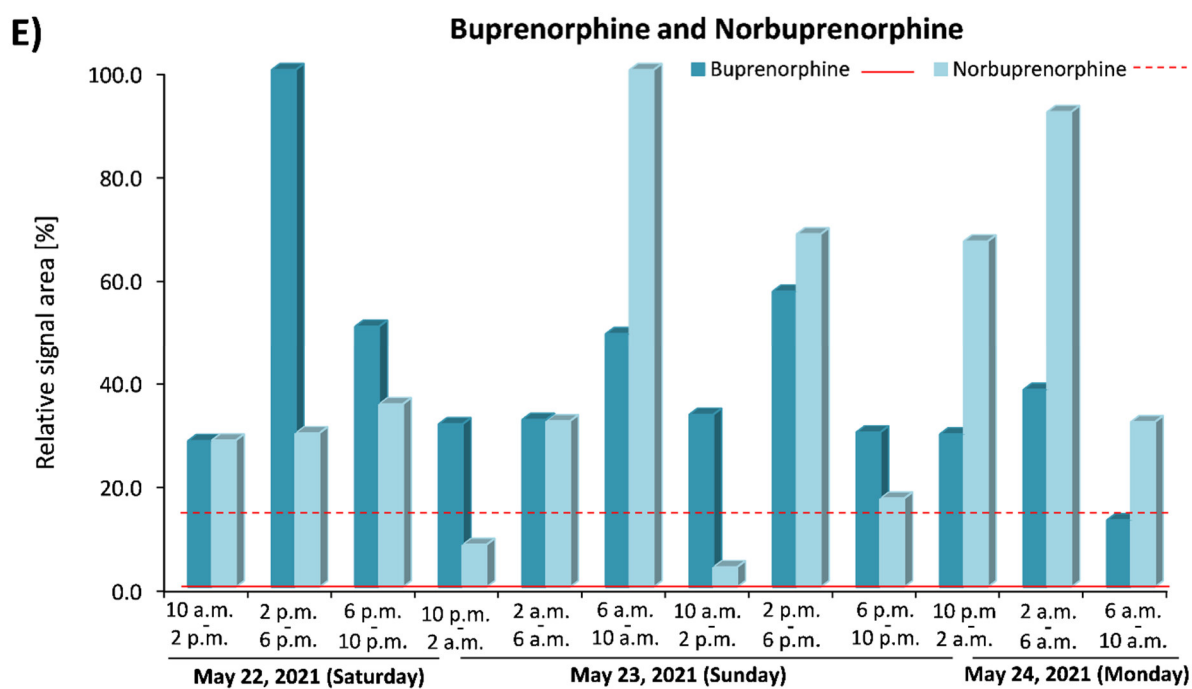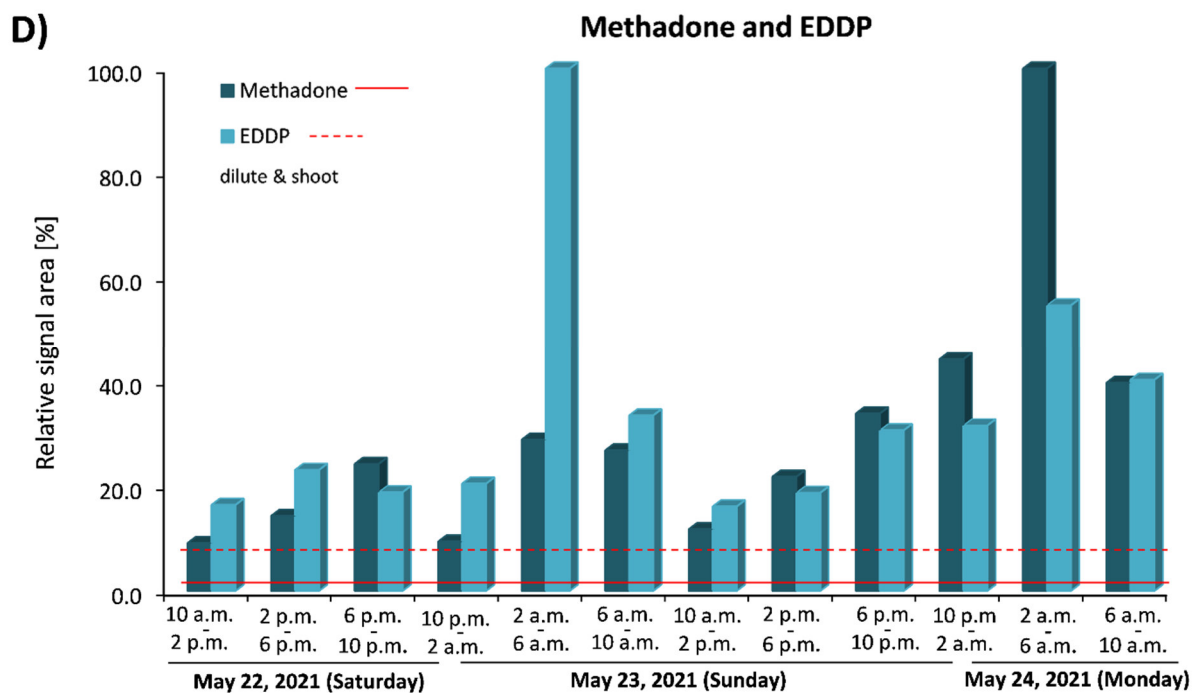
Tramadol and O-Desmethyl-cis-tramadol
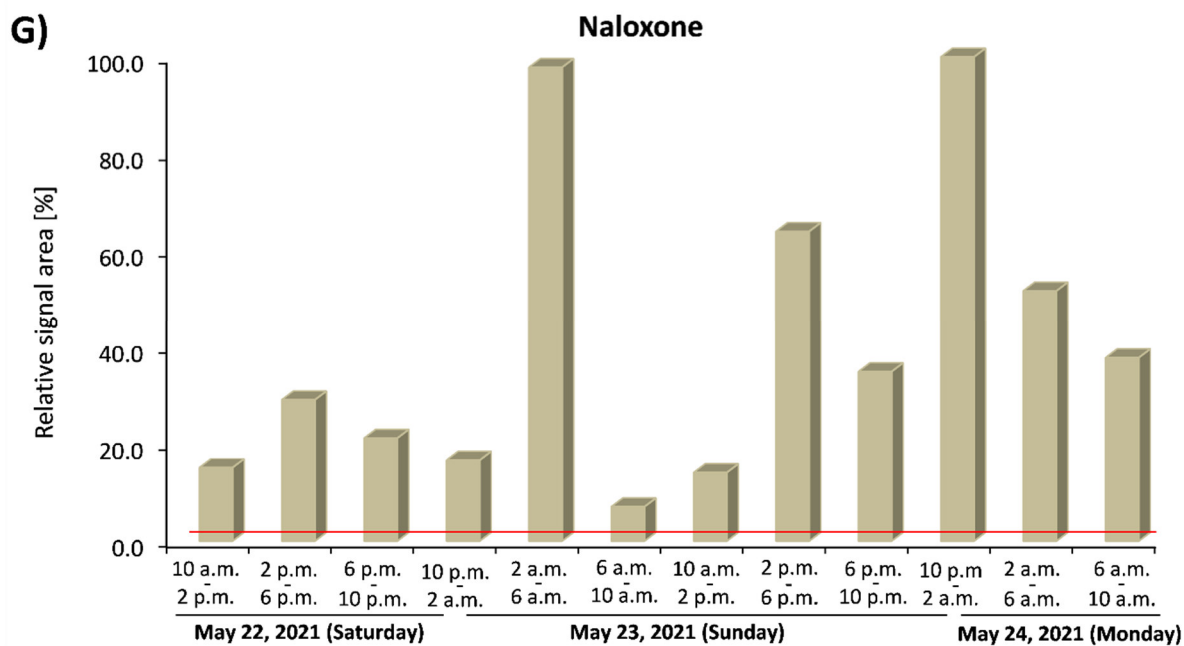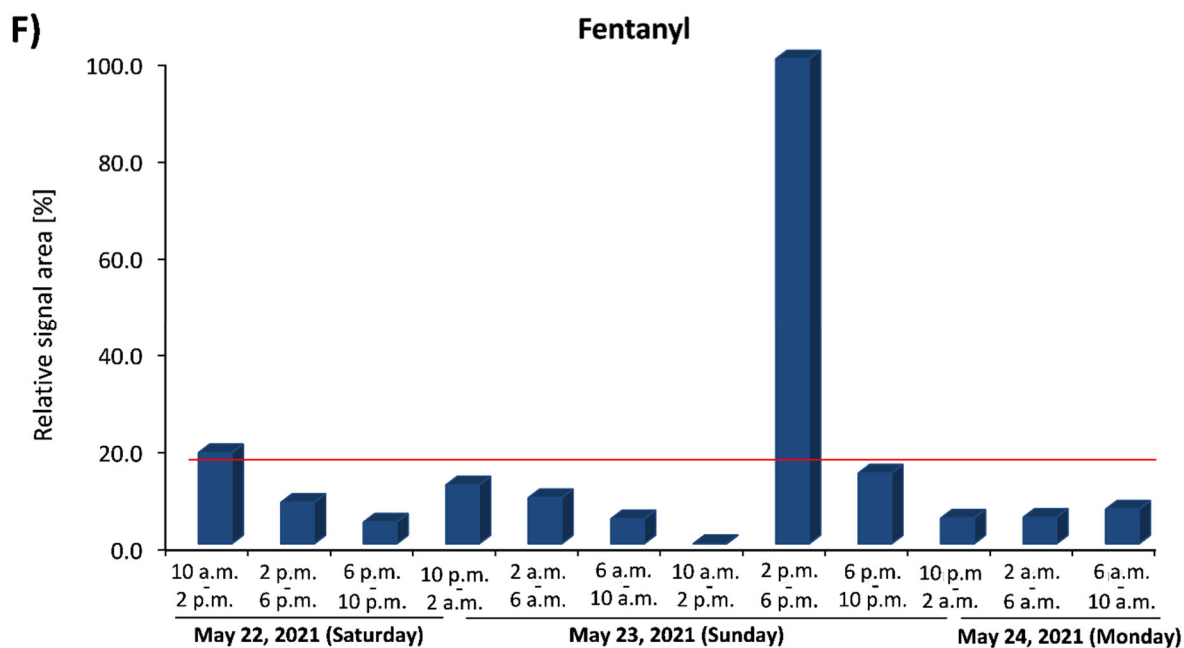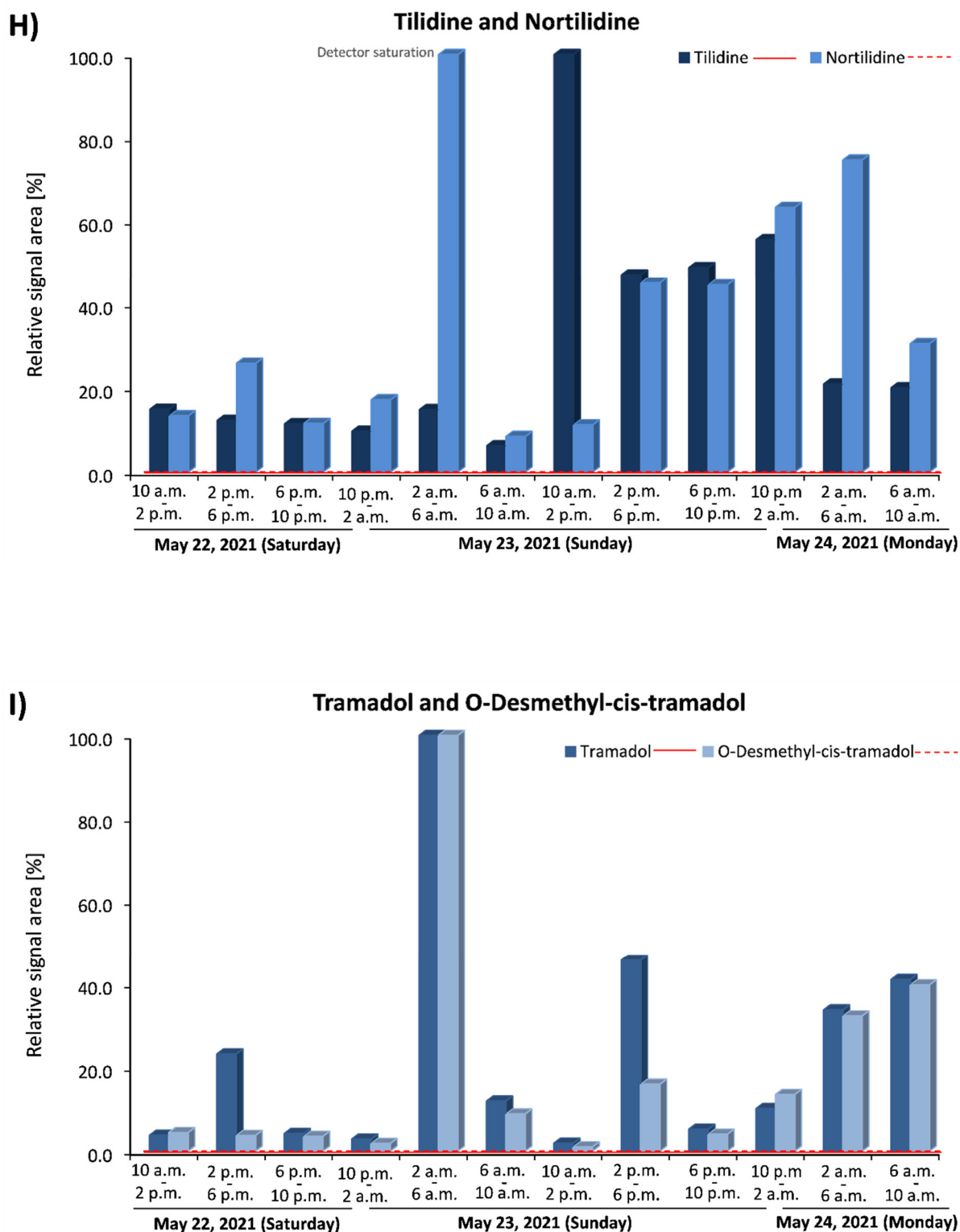
Figure S4. Time profiles for amphetamine (A), methylphenidate (B), cocaine (C), methadone and EDDP (D), buprenorphine and norbuprenorphine (E), fentanyl (F), naloxone (G), tilidine and nortilidine (H), and tramadol and *O*-desmethyl-*cis*-tramadol (I) detected in prison wastewater from May 22-24, 2021, each represented in relation to the most concentrated sample. S/N ratios of 9/1 and at least 3/1 for the most and second most intense ion transition, respectively, are indicated by the red line. The S/N values were calculated using Peak-To-Peak algorithm (Analyst® Software 1.6.2).

Chapter 5

Triangulation study

of police seizures, wastewater and hair analysis to assess SCRA and conventional drug use

Prevalence of synthetic cannabinoid receptor agonists use assessed by sewage monitoring via LC-MS/MS, Part B:

Triangulation of police seizures, wastewater and toxicological hair analysis
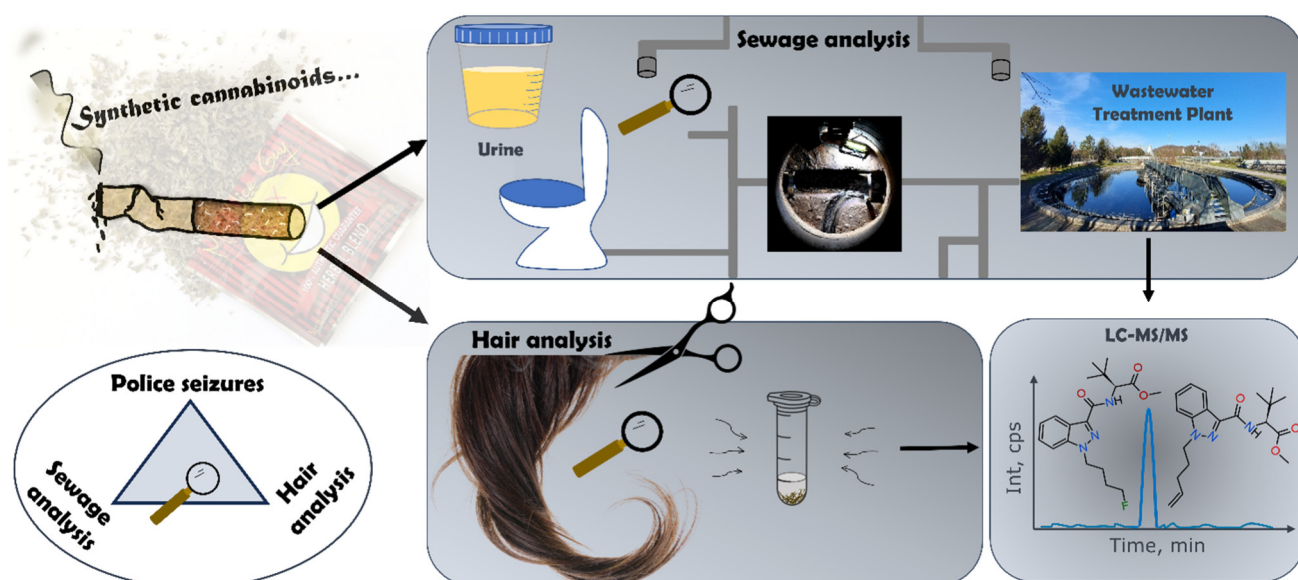
Hehet P, Scheufler F, Kunert N, Baumer C, Pütz M, Schäper J, Shehata O, Krause S, Wende M.
Manuscript for submission to *Forensic Chem.* **2024**.

Abstract

The structural variety and popularity of synthetic cannabinoid receptor agonists (SCRAs) has steadily increased over the last decade, while exact data on their prevalence and use are largely unknown. This study addresses the elucidation of this aspect by combining data originating from police seizures, wastewater and toxicological analysis. The toxicological analysis yielded specific information on the prevalence of SCRAs and conventional drugs in hair samples in Bavaria, Germany over 1.5 years (2021-2022), while wastewater analysis provided general trends concerning these drugs in community use over selected time periods in 2021 and 2022. A targeted and qualitative LC-MS/MS method was developed, regularly updated and employed to screen for 41 SCRAs and 8 of their metabolites in wastewater and hair samples. A total of 32 different SCRAs were found, including 32 SCRAs in hair samples, and 9 of these SCRAs in wastewater as well. The findings were triangulated with police seizures and indicated a widespread SCRA use in Bavaria over the investigated time period, with MDMB-4en-PINACA being the most frequently detected SCRA in 2021 and ADB-BUTINACA in 2022. Moreover, hair data analysis allowed for gaining comprehensive knowledge on SCRA use patterns. The collective studied included individuals presumably involved in criminal offences, with SCRAs detected in one third of the cases (35.2% prevalence). Young people under the age of 30 accounted for 60% of SCRA positive cases, and the vast majority of SCRA consumers appeared to be polydrug users, either inclined to additional use of cannabis, of other conventional drugs or mostly both. Widespread use of conventional drugs was confirmed by wastewater analysis as well, including a successful proof-of-concept of our newly introduced wastewater sampling approach with polydimethylsiloxane (PDMS) passive samplers to monitor multiple drug classes. Conclusively, results in this study strongly support the implementation of wastewater and hair analysis, using large screening panels of diverse drug classes to gather valuable prevalence data for illicit drug monitoring.

Keywords: synthetic cannabinoid receptor agonists (SCRAs, "Spice") · new psychoactive substances (NPS) · hair analysis · wastewater analysis · police seizures

5.1 Introduction

Synthetic cannabinoid receptor agonists (SCRAs) have established their own drug market with a variety of available products for different ways of consumption, such as herbal mixtures, pure powders or e-liquids for electronic cigarettes, all of which can contain a great chemical variety of SCRA compounds. To date, the European Union's (EU) Early Warning System (EWS) received reports of 245 new compounds of the SCRA class, which is a clear evidence of a highly diverse and dynamic SCRA drug market [1]. The dynamics is reflected by the mean annual emergence rate of new SCRA compounds in Europe with 10-11 compounds per year since 2016 rising to 15 (2021) and 24 compounds (2022) in the recent years [1]. Andrews et al. [2] analyzed structural changes of newly emerged SCRAs on the European market in correlation to key legislative responses and concluded that 20 out of 23 new compounds entering the drug market from June 2021 to July 2022 evaded the generic legislation introduced in May 2021 in China, one of the major source countries of SCRAs to the European market. A similar phenomenon was observed on the national level after enactment of the New Psychoactive Substances (NPS) Act in November 2016 in Germany, which was introduced as a generic control of NPS to strengthen the German drug legislation. After inclusion of indole, indazole and benzimidazole core structures in the NpSG, the response of the SCRAs market was the commencement of the tricyclic core scaffolds, i.e. carbazoles [3,4] and γ-carbolinones [4]. Variation of side chain moieties also served the purpose to bypass the NpSG, as shown by Pulver et al. [5] for Cumyl-BC[2.2.1]HpMINACA, Cumyl-BC[2.2.1]HpMICA, and Cumyl-BC[2.2.1]HpMeGaClone, all featuring a novel norbornyl methyl side chain. Nevertheless, the significance of SCRAs for drug policies is reflected in the number of intoxications, mass overdoses and fatalities related to their potency and use. One study in England [6] revealed one hundred sixty-five SCRA-related deaths within 2012-2019, with a lack of effective United Kingdom's (UK) legislation, limited knowledge on physiological risks of SCRA use and their interaction with other co-administered substances. These aspects were designated as important factors contributing to the deaths, which were found to prevail in socioeconomically deprived areas. "Spice"-related deaths in a study in Germany (Munich, Bavaria) revealed 41 different SCRAs among 98 fatalities (11.6% of all cases analyzed for SCRAs) within the period 2014-2020 [7]. These systematic reviews on fatal intoxication cases demonstrate and encourage the high importance of SCRA testing in routine analyses to shed more light on this topic and substantiate prevention.

Despite the usefulness in assessing adverse effects of SCRAs on public health, data from drug-related medical emergencies or deaths in medical facilities (post-mortem examinations) are not representative from a prevalence point of view. Therefore, common data sources for monitoring the illicit drug market and drug use can also include data of seizures of narcotics by police and customs, information of forensic toxicological examinations of human matrices (blood, urine, hair), data from rehabilitation programs as well as results of drug consumer surveys. Wastewater-based epidemiology (WBE) is a rapidly developing scientific approach for this application area, with potential to complement and extend the existing monitoring tools for estimation of illicit drug use by the significant advantage of providing near-time data and coverage of large populations in contrast to many of the other sources. One of the greatest advantages in comparison to the existing survey-based methods is the objective estimation of the market prevalence of illicit drugs, which is especially important for the SCRA prevalence

estimation. Due to the complete lack of awareness of most consumers regarding the specific SCRAs contained in products consumed, survey-studies cannot provide objective and comprehensive trends on SCRA use. Confiscation data, medical reports and toxicology data might only reflect a small portion of the population and a limited spectrum of SCRA products. Thus, combination and correlation of data gathered from different monitoring tools is a promising approach to complementarily estimate SCRA use at the population level.

When considering WBE, rather low SCRA concentrations are expected in wastewater, not only due to their low effective doses and distribution of consumers over many different compounds, but also due to their extensive metabolism resulting in low amounts of the remaining drug residues. This is confirmed by the scarce number of studies with positive results on SCRAs in wastewater, as exemplified in more detail in Part A of this study [8]. Forensic toxicology is an important tool for monitoring the types and extent of drug consumption in individual cases. Hair samples are increasingly gaining attention for this purpose due to some advantages over blood or urine, including a larger time window of detection, non-invasive sampling and long stability of target analytes in the keratine matrix. As SCRAs are extensively metabolized after consumption, mainly the parent compounds are detected in blood and hair, whereas urine analysis requires rather SCRA metabolites to be screened for [9-13]. While rapid elimination of drugs from blood, urine or oral fluid within hours or days often limits their toxicological confirmation, the long stability of drugs in hair implies a long detection window with the possibility to prove the chronic use. A segmental hair analysis allows for a more detailed retrospective record of an individual's SCRA use and consumption patterns. Increasing distance of hair segment from the hair root thereby corresponds to past periods of use. Several studies utilized hair analysis for SCRA investigations, predominantly using liquid chromatography-mass spectrometry (LC-MS) based methods [10,11,14-22] or alternatively gas chromatography-mass spectrometry (GC-MS) based methods [23-24]. In addition to SCRA monitoring, several LC-MS based methods encompassed a spectrum of NPS compounds belonging to different classes [25-26], even in combination with the conventional drugs of abuse in a single screening method [27]. However, SCRA and generally NPS screening procedures are usually not included in routine analyses in practice, thus lacking information on the prevalence of these compounds in the population. The dynamic nature of the SCRA market with relatively short commercial lifetime cycles for most compounds and the high diversity of these compounds have several implications for analytical method development. The need to provide an up-to-date analytical method for SCRAs in a timely manner, independent of the availability of reference material for quantitative analysis, encompassed by the uncertainty of interpretation of quantitative data for these novel compounds has led to the proposal of qualitative determination only of NPS in forensic toxicological casework [28]. Although targeted LC-MS/MS methods with triple quadrupole (QqQ) mass analyzers are limited to a targeted list of compounds, their sensitivity and selectivity addresses the requirement to detect low SCRA concentrations in complex matrices. The present work focussed on the most abundant SCRAs, as indicated by police and customs. Structure elucidation and analytical characterization of newly seized compounds used in this work have been performed on a nationwide level in the scope of the EU-projects ADEBAR and ADEBAR *plus* [29].

To assess the changing landscape of the SCRA drug market and corresponding consumption patterns in Bavaria, Germany, a comparative approach of wastewater analysis, forensic

toxicology and police seizures was performed over a 1.5 year period in 2021-2022. To the authors' best knowledge, this is first study combining wastewater and hair analysis to gain insight into illicit drug use, particularly SCRA use. So far, only one study utilized a similar approach by combining wastewater analysis and toxicological data (post-mortem blood samples) and investigated the appearance of NPS on a community scale [30]. Moreover, the approach in the present study was triangulated with analytical data of exhibits from police seizures. The inclusion of cannabis and other conventional drugs in the toxicological data analysis, among other data, allowed for gaining comprehensive knowledge on SCRA use patterns. Finally, we evaluated chronological changes within the SCRA drug market by monitoring increases or decreases of the predominant compounds with respect to their legal status to draw conclusions about the impact of legislative controls and law amendments.

5.2 Experimental

5.2.1 Chemicals and materials

All solvents, reagents and materials used were as described in Part A of this study [8]. Additional SCRAs (ADB-5Br-INACA, ADB-FUBIACA, BZO-4en-POXIZID and ADB-BUTINACA) for the updated analytical method were sourced and proceeded in an analogous way. More detailed information on these substances, such as their common synonyms, IUPAC names, molecular formulas, monoisotopic masses and chemical structures is given in the Supplementary Material (Table S1). At this point, it is important to note that the term ADB-BUTINACA refers to *N*-[1-amino-3,3-dimethyl-1-oxobutan-2-yl]-1-butyl-1*H*-indazole-3-carboxamide (cf. chemical structure in Table S1, Supplementary Material) in this study. Although the term ADB-BINACA would be consistent with the established semi-systematic nomenclature implemented by the European Monitoring Centre for Drugs and Drug Addiction (EMCDDA) in 2013, the name ADB-BINACA was first used in the scientific literature [31] for a chemically similar SCRA with a benzyl tail moiety instead of the butyl side chain (*N*-[1-amino-3,3-dimethyl-1-oxobutan-2-yl]-1-benzyl-1*H*-indazole-3-carboxamide). Since further official reports and scientific literature [32-34] used the name ADB-BUTINACA for the analogue with the 1-butyl substituent on the indazole ring, and the commercially available reference standard [35] applies to this name, we continued to use the term ADB-BUTINACA to differentiate the two compounds and avoid further confusion.

Reference standards of conventional drugs and their corresponding deuterated standards in methanol or acetonitrile were sourced from different companies (LGC Standards, Lipomed, and Sigma Aldrich). A detailed list of all compounds including information on the chemical drug class, suppliers of reference standards and solvents used for storage of the standards are provided in the Supplementary Material (Table S2). The concentration of standards amounted to 1 mg/mL, whilst the deuterated standards were delivered at a concentration level of 0.1 mg/mL. Standard and internal standard compounds were stored according to supplier recommendations at -18°C. High-purity solvents used as eluents and partially as extraction solvents for the analysis of the conventional drugs, including ultra LC-MS grade acetonitrile with 0.1% formic acid, ultra LC-MS grade water with 0.1% formic acid, ultra LC-MS grade water and methanol, were supplied by scienTEST-bioKEMIX GmbH (Wesel, Germany). Acetic acid (glacial), isohexane, acetone, ethyl acetate and isooctane were obtained from Merck KGaA

(Darmstadt, Germany) and sodium hydroxide (1 M solution) from Carl Roth GmbH + Co. KG (Karlsruhe, Germany), all as analytical reagent grade chemicals.

Materials for wastewater analysis were as given in Part A of this study [8]. The remaining required materials were related to hair analysis. For this purpose, safe-lock tubes of various volumes (2 mL, 5 mL) were supplied by Eppendorf AG (Hamburg, Germany), and 300 µL fixed insert glass vials with a screw top by Thermo Scientific (Langerwehe, Germany).

5.2.2 Wastewater analysis

Wastewater sampling

Wastewater sampling in a city district of Munich was performed in a similar way as in a prison, as described previously [8]. An automated wastewater sampling device was installed in a manhole of the sewer network at two different time periods, once during weekdays (Tuesday - Thursday; September 21-23, 2021) and once during the upcoming weekend (Friday - Sunday; September 24-26, 2021). For every time period, sampling was conducted over 48 h, yielding 12 individual 4-hour composite samples (cf. Table S3, Supplementary Material). In parallel, polydimethylsiloxane (PDMS) rods were mounted on the hose of the sampling device during the weekdays and during the upcoming weekend. In addition, two further locations in the city district were selected to install the PDMS rods for drug consumption monitoring during the weekdays period. All details regarding the installation and deinstallation dates and the exposure times for the PDMS rods in the sewage network of a city district in Munich can be found in Table S4 (Supplementary Material). A portion of each PDMS rod (2 cm length) was used for analysis. Wastewater sampling in the larger of the two wastewater treatment plants (WWTPs) in Munich (Gut Großlappen, with treated sewage pollution load corresponding to approximately 1.4 million inhabitants) was performed by PDMS rods placed in the influent wastewater after the mechanical treatment stage for different periods of time (Table S5, Supplementary Material). On the one hand, time intervals during weekdays compared to a weekend were examined, and on the other hand, different sampling periods during the upcoming weekdays were investigated. Only a small segment of the PDMS rod (1 cm length) was analyzed in the experiment performed in the WWTP in order to determine the detection capability when only small amounts of the solid phase adsorber (PDMS rod) are deployed.

Sample preparation

Liquid wastewater samples were treated according to the optimized procedure as described in our study performed in the sewage effluent of a prison [8]. Briefly, wastewater samples (10 mL) were acidified to a pH of 2-3 and subsequent extraction of SCRAs and their metabolites was achieved by a liquid-liquid extraction (LLE) procedure using an isohexane/ethyl acetate mixture (9/1, v/v). The extraction of the wastewater sample aliquot was performed two-fold, and the procedure was repeated in a separate experiment with additional 10 mL wastewater sample volume, resulting in a total wastewater volume of 20 mL. The extraction of conventional drugs was carried out in an analogous way, however the initial acidification step of wastewater was omitted.

Re-extraction of analytes from PDMS rods was achieved with an isohexane/ethyl acetate mixture (9/1, v/v) under shaking in a two-fold extraction procedure for a single rod. Depending on the length of the PDMS rod, either 1 mL (1 cm PDMS) or 1.5 mL extraction solvent volume (2 cm PDMS) were utilized. A more precise description of the extraction procedure can be

found in Part A of this study [8]. For conventional drugs, the optimized extraction procedure of the PDMS rods encompassed methanol instead of an isohexane/ethyl acetate mixture, while the other extraction conditions remained identical.

5.2.3 Hair analysis

Hair samples

Drug-free scalp hair for the analytical method development, calibration and quality control (QC) samples was provided by volunteers and analyzed for the target compounds prior to use. Authentic toxicology case samples were collected from male and female persons suspected of drug use on official authority order. The preferential anatomical collection site for hair was the posterior vertex region of the head. A hair strand was bundled with a string, cut close to the scalp with scissors and fixed on the string to a sheet of paper or wrapped in aluminium foil, indicating the scalp-near end. Alternative body hair samples (beard, arm, leg, pubic, axillary or chest hair) were used in small number of cases, when scalp hair was unavailable. Hair samples were wrapped and stored in aluminium foil at room temperature until analysis. Prior to analysis, sample characteristics such as hair color, length, anatomical collection site and cosmetic treatment were noted. When allowed by hair amount and length, segmentation into sections of 3 cm length was carried out, and each hair segment was analyzed and evaluated individually. Otherwise, the length of segments was adapted to the available length and amount of a hair sample.

Stock and working solutions

The working solution of all reference standards was prepared by combining and diluting their stock solutions (1 mg/mL) in methanol to a concentration of 1 ng/µL each. Further dilutions of this mixture in methanol yielded working solutions at lower concentration levels of 0.1 ng/µL and 0.01 ng/µL. Similarly, the working solution of internal standards was obtained by mixing and diluting stock solutions of all deuterated standards (0.1 mg/mL) in methanol to a concentration of 1 ng/µL each. This mixture was diluted to a concentration of 0.1 ng/µL for the final use. A detailed list of all reference standards and deuterated standards used for preparation of the working solutions is provided in the Supplementary Material (Table S2).

Sample preparation

Hair samples or segments were subjected to an external decontamination procedure including two sequential washing steps with isohexane and acetone, each step conducted for 30 sec by ultrasonication. After drying at room temperature, the samples were cut into small pieces of approximately 1 mm in length and weighed into a safe-lock tube (2 mL, polypropylene). In total, two different sample preparation procedures were carried out, one using an aliquot of 10 mg hair for analysis of the conventional drugs and SCRAs, the other using an aliquot of 20 mg hair for analysis of 11-nor-9-carboxy-Δ^9-tetrahydrocannabinol (THC-COOH), the major endogenously formed cannabis metabolite. The extraction of THC-COOH, based on alkaline digestion of hair matrix followed by an LLE was published recently by our group [36], and will hence not be detailed in this place. Hair sample preparation for the detection of conventional drugs and SCRAs was based on a methanolic extraction procedure that was derived from our initially established procedure used for GC-MS/MS analysis [37] as follows. A hair sample (10 mg) was weighed into a 2 mL safe-lock tube, provided with methanol (400 µL) and subsequently spiked with the internal standard working solution (100 µL, 0.1 ng/µL). The

methanolic extraction was conducted in an ultrasonic bath at 40°C for 1 h. After centrifugation at 13,000 rpm for 15 min, the residual extraction proceeded for approximately 18 h at room temperature. Following the extraction, a portion of the sample extract (200 µL) was transferred into a glass vial and further processed, while an equal aliquot of the extract was retained and kept at -18°C. The methanolic extract was evaporated to dryness under a gentle stream of nitrogen at 35°C and reconstituted in methanol (50 µL) and water (450 µL) for the LC-MS/MS analysis. Control samples including blanks with and without internal standard solution were prepared in an analogous way. Quality controls (0.4 and 4 ng/mg hair) and calibration samples (0.01, 0.02, 0.05, 0.1, 0.2, 0.5, 1.0, 2.0, 5.0, 10.0 and 20.0 ng/mg hair) were obtained by spiking samples of blank hair with appropriate volumes of the standard working solution at a suitable concentration level (cf. previous section) before the extraction.

In summary, a minimum quantity of 30 mg hair was required for analysis of a large panel of the most common drugs of abuse and NPS, including the chemical class of amphetamine-type stimulants, cocaine and its metabolites, opioids and related substances, phytocannabinoids and synthetic cannabinoids.

5.2.4 Seized sample analysis

Procedures of the seized sample analysis are not discussed in detail, since they followed well established protocols and are not relevant for the main scope of this study. Briefly, the extraction of SCRAs from seized material was performed using acetone and methanol for herbal blends and powders, respectively, with short extraction times. Analysis of the extracts was accomplished with our in-house GC-MS analytical method deployed in the context of the routine casework. Additional analysis of powders was performed with Fourier-transform infrared (FTIR) spectroscopy without further sample preparation.

5.2.5 Instrumentation and analytical conditions

The collected specimens were examined using our in-house validated LC-MS/MS methods. One method was used to screen each sample for conventional drugs of abuse and their metabolites. The second analytical method comprised of a large panel of SCRAs [8] and was continuously updated with new SCRAs, as applied in this follow-up study. Phytocannabinoids were successfully included in both methods. The third method specifically addresses THC-COOH, the main metabolite of cannabis in hair specimens, as published previously [36]. It is based on an LC-MS^3 analysis to meet the requirements of selective and sensitive detection of inherently low THC-COOH concentrations in hair.

All instrumental conditions applied to the analysis of authentic hair and wastewater samples using the SCRAs method were as described in Part A [8]. The ion transitions of new SCRAs included in the method and their optimized mass spectrometric parameters are given in Table S6 in the Supplementary Material. Analysis of conventional drugs was performed with the same analytical system, consisting of a Shimadzu LC Nexera X2 liquid chromatograph coupled to a QTRAP® 6500 (SCIEX, Darmstadt, Germany) triple stage quadrupole (QqQ) mass spectrometer. The chromatographic separation was performed on a Kinetex® Biphenyl (100 x 2.1 mm, 1.7 µm) analytical column in gradient elution mode at a constant flow of 0.5 mL/min, and the mobile phase consisted of UHPLC grade water with 0.1% formic acid (A) and UHPLC grade acetonitrile with 0.1% formic acid (B). The gradient program was following: 0 - 1.5 min 0% B; 1.5 - 9 min linear gradient to 50% B; 9 - 11 min linear gradient from 50% to 95% B; 11 -

13 min constantly 95% B. Subsequently, the system rapidly returned to the initial conditions (0% B; 100% A) which were held for 5 min (re-equilibration time) before injection of the next sample. Therefore, a total sample run amounted to 18 min for the set elution parameters. The autosampler and column temperatures were set to 6°C and 40°C, respectively, and the sample injection volume amounted to 5 µL. The electrospray interface was operated in positive mode (ESI+), and the following settings were used for the source: ion source voltage 4.5 kV, curtain gas 35 psi, nebulizer gas (GS1) and heater gas (GS2) both 65 psi, and TurboIonSpray® probe temperature 550°C.

Data acquisition was processed in Multiple Reaction Monitoring (MRM) mode using Analyst® Software 1.6.2, while the following data processing was performed with SCIEX OS® 2.0.1 Software.

5.3 Results and Discussion

5.3.1 Wastewater analysis

Assessment of SCRA use in a city district

After a protocol for wastewater sampling and analysis for SCRAs had been successfully established and tested on authentic samples, as shown in our previous study [8], the method was applied in this follow-up study to gain more detailed prevalence data from a major city. As absolute concentrations of the analytes have little significance, only signal areas were recorded, being sufficient for comparison of the methods or samples. In general, criteria for a positive analyte identification required a signal-to-noise (S/N) ratio of at least 3/1 for the two most intense ion transitions, as well as reproducible retention times and relative abundances of the diagnostic transitions as compared with a reference standard.

The wastewater sampling was performed in a smaller sewer network, belonging to a district of the city of Munich, Germany with a catchment area of about 25,000 inhabitants, during weekdays and a weekend in order to investigate possible differences in consumption patterns. Liquid wastewater sampling and enrichment on PDMS rods were used in parallel, as detailed in section 5.2.2. The more informative, time resolved liquid sampling will be discussed in detail. During the 48 h weekdays sampling period of September 21-23, 2021, several SCRAs were successfully detected in the collected liquid wastewater samples. These SCRAs were MDMB-4en-PINACA, 4F-MDMB-BICA, 5F-MDMB-PICA / 5F-EMB-PICA (not distinguishable, see [8]) and Cumyl-CBMICA. SCRA detections were assigned only to two time intervals: 6 - 10 p.m. on September 21, 2021 (Tuesday) with four SCRAs identified, and 10 a.m. - 2 p.m. on September 23, 2021 (Thursday) with two SCRAs detected. One striking feature is the appearance of the majority of the SCRAs detected in the time interval 6 - 10 p.m., which represents the time after the end of work, being the most plausible time for drug consumption during weekdays. MDMB-4en-PINACA and 4F-MDMB-BICA represented two SCRAs that were detected during both time intervals on two different weekdays, thus indicating their prevalent use.

Similar SCRAs were detected during the subsequent 48 h monitoring period on the weekend from September 24-26, 2021. Besides MDMB-4en-PINACA, 4F-MDMB-BICA and 5F-MDMB-PICA / 5F-EMB-PICA, the SCRAs 4F-MDMB-BINACA and Cumyl-BC[2.2.1]HpMINACA were detected as well. Representative chromatograms of some of the SCRAs detected are displayed in Figure 1. Cumyl-CBMICA, which was detected during the weekdays, was not detectable in

the samples from the following weekend. The detection of SCRAs during the weekend was referred to three time intervals: 2 - 6 p.m. and 6 - 10 p.m. on September 24, 2021 (Friday) with four SCRAs identified, and 2 - 6 p.m. on September 25, 2021 (Saturday) with one SCRA in the sewage system. An interesting trend was the high prevalence of SCRAs on Friday afternoon-evening (2 - 10 p.m.), which suggested pronounced consumption at the beginning of the weekend, presumably after the end of work on Friday. The presence of further SCRAs being below the analytical limit of detection during any time interval cannot be excluded. MDMB-4en-PINACA was present during the entire time period on Friday afternoon-evening, which indicated its high prevalence. This finding is in good agreement with frequent seizures of MDMB-4en-PINACA containing products in the city of Munich, as retrieved from our seizure data (cf. section 5.3.3). Furthermore, evidence of a certain prevalence of Cumyl-BC[2.2.1]HpMINACA, a relatively new SCRA at the time point of the study featuring a norbornyl methyl side chain, was gathered from the sample collected on Saturday. The substance consists of two regioisomers, which were observed in chromatograms in the form of two partially resolved signals.

The consumption trends disclosed by the liquid wastewater samples correlated with the results obtained by PDMS rods for the corresponding sampling period, as discussed in more detail in Part A [8].
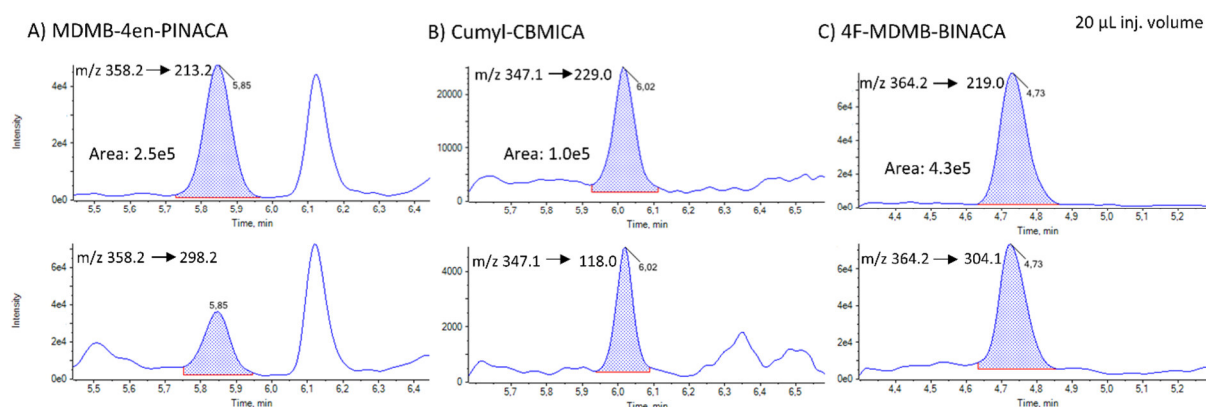
Figure 1. Representative chromatograms of SCRAs detected in the wastewater of a city district of Munich during September 21, 2021 (weekday, A and B) and September 24, 2021 (weekend, C), with both days representing the time interval 6 - 10 p.m. The two most intense ion transitions for each substance are displayed, measured using a 20 µL injection volume.

In contrast to the pronounced, but temporally distinctive SCRAs consumption pattern, phytocannabinoids (originating from *Cannabis sativa*) indicated rather higher prevalence with continuous detection of phytocannabinoids over the entire time frame of the wastewater sampling. Tetrahydrocannabinol (THC) and its metabolite THC-COOH were detected in all wastewater samples examined, both during weekdays (September 21-23, 2021; Figure 2A) and during the weekend (September 24-26, 2021; Figure 2B). Contrary to the signal patterns exhibited by SCRAs, significant patterns and differences between weekdays and weekend days for individual time intervals of cannabis use were not observed. However, it cannot be clarified whether higher prevalence of cannabis consumption, its pharmacokinetic profile or different analytical sensitivities when compared to SCRAs might have levelled out possible temporal differences. The phytocannabinoid THC and in one case its metabolite THC-COOH were detected by the passive sampling approach using PDMS rods as well.
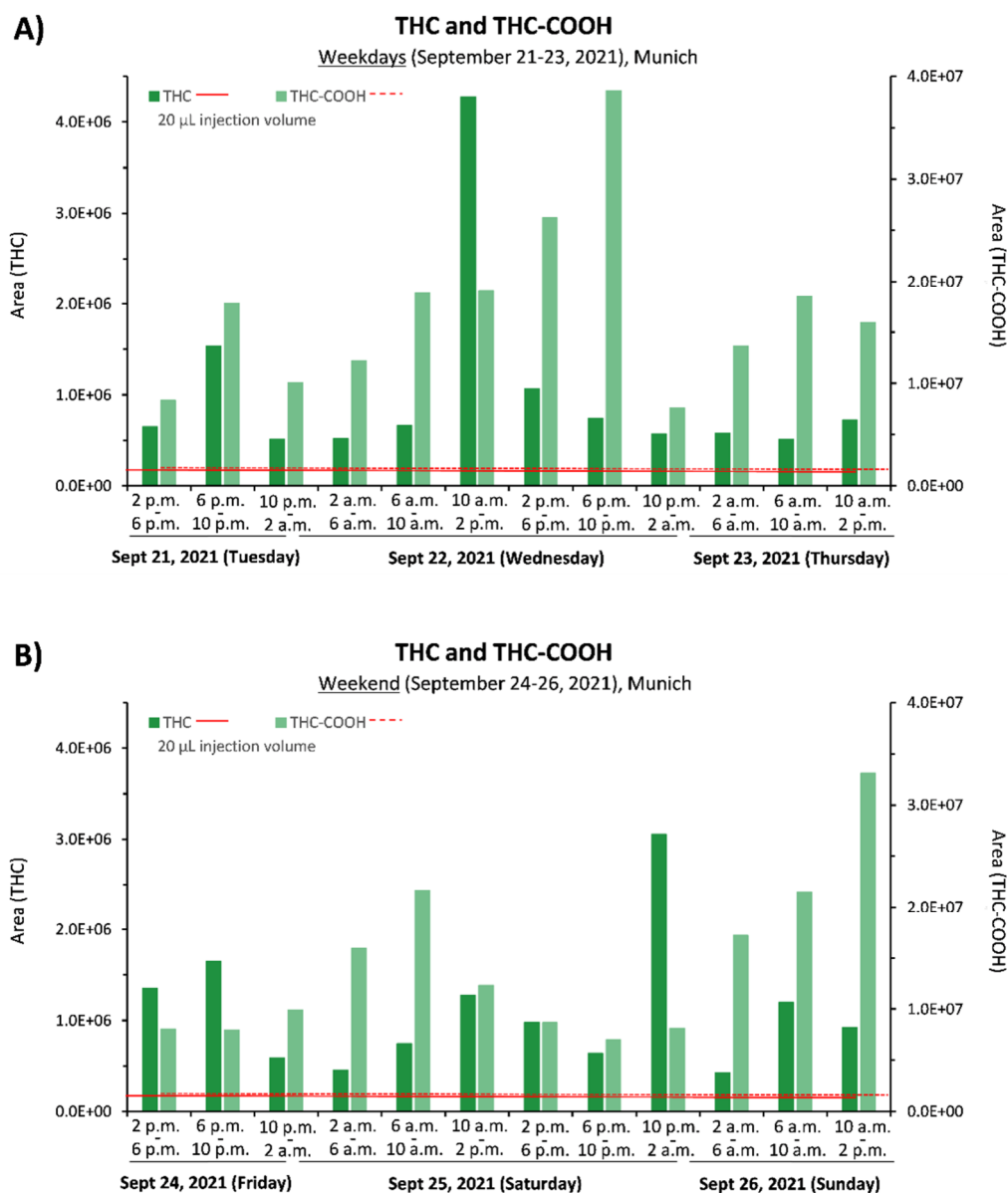
Figure 2. Prevalence of cannabis consumption reflected by tetrahydrocannabinol (THC) and its metabolite (THC-COOH), which were detected in wastewater samples collected in a city district of Munich during weekdays (A) and weekend (B) in September 2021. S/N ratios of 9/1 and 3/1 for the most and second most intense ion transition, respectively, are indicated by the solid (THC) and dotted red line (THC-COOH), as calculated using Peak-To-Peak algorithm (Analyst® Software 1.6.2). For THC-COOH, the ion transition 345.0 → 299.1 exhibited the best S/N ratio in wastewater matrix, and hence was used for the data evaluation shown.

Comparison with conventional drugs

Sampling and detection of conventional drugs in sewage water was possible by deployment of PDMS rods in sewers, analogously as previously conducted for SCRAs. At first, the best conditions for re-extraction of drugs from PDMS rods were determined. When comparing the extraction efficiencies for the isohexane/ethyl acetate mixture (9/1, v/v) and for methanol, the latter proved to be the better extraction solvent for several relevant conventional drugs, such as amphetamine, methamphetamine and MDMA (Table S7, Supplementary Material). In contrast, some other target analytes, such as cocaine and cocaethylene, were extracted more efficiently with the isohexane/ethyl acetate mixture (Table S7), analogously to the SCRAs.

Maintaining the same experimental approach as for SCRAs prevalence assessment [8], a second portion of PDMS rods (2 cm length) was deployed at the three different locations in a city district of Munich and analyzed for conventional drugs using methanol for re-extraction. Different results for the three locations during the time interval examined (September 21-24, 2021) were observed for several conventional drugs, too. Findings are shown in Table S8 (Supplementary Material), with main variations highlighted. A particularly interesting result is displayed in Figure 3. The sampling point at Location 3 is downstream of Location 4, so all substances observed at Location 4 were detected there as well. Additionally, heroin and acetylcodeine (one of several characteristic side alkaloids of illicitly manufactured heroin) were recorded. If different catchment areas and not temporal differences caused this observation, the spot of heroin entry into the sewage system must have been between Locations 3 and 4, as illustrated in the map below (Figure 3). As for the SCRAs, a small difference in the time period covered cannot be ruled out as a cause for this finding, but appears to be less likely.
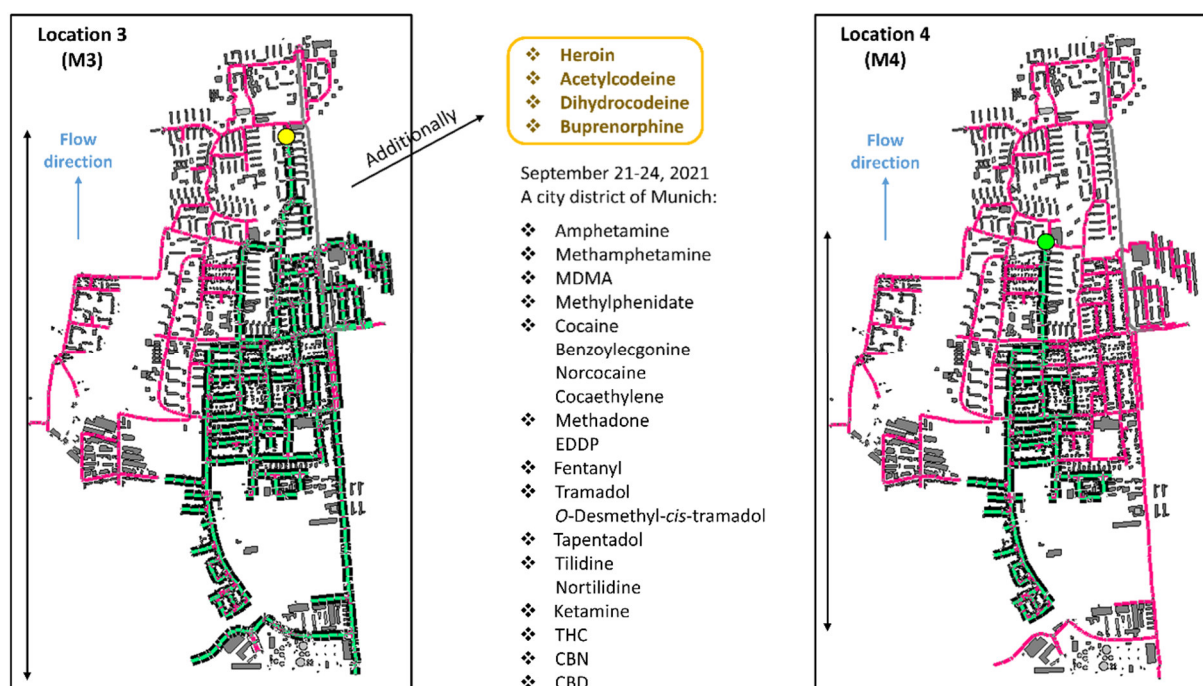
Figure 3. Maps of the city district showing the two PDMS sampling locations with their corresponding catchment areas each indicated in green. Conventional drugs identified at both locations during September 21-24, 2021 are displayed in black. Since Location 3 is downstream of Location 4, the additional conventional drugs detected at this location (indicated in yellow) can be attributed to the catchment area between these two locations.

The collected wastewater samples were investigated for the presence of conventional drugs as well. The wastewater samples collected at Location 2 during the period of September 21-23, 2021 (48 h, weekdays) resulted in the detection of methamphetamine, 3,4-methylene-dioxymethamphetamine (MDMA), methylphenidate, cocaine / benzoylecgonine / norcocaine / cocaethylene, codeine, dihydrocodeine, oxycodone, methadone / 2-ethylidene-1,5-dimethyl-3,3-diphenylpyrrolidine (EDDP), buprenorphine, naloxone, fentanyl, tramadol / *O*-desmethyl-*cis*-tramadol, tapentadol, tilidine / nortilidine, ketamine / norketamine, THC and cannabidiol (CBD). Cocaine and its metabolites norcocaine and cocaethylene were found in all

wastewater samples, indicating a substantial level of consumption. MDMA detection in more than 50% of all the wastewater samples examined indicated a prevalent use of ecstasy pills. Methamphetamine was a further conventional illicit drug identified in wastewater samples, but only in two of them. Interesting was the detection of ketamine, an arylcyclohexylamine derivative, that was present in all wastewater samples, while its metabolite norketamine was found in eight of the twelve samples. Synthetic opiods including methadone, buprenorphine, fentanyl, tramadol and tilidine were associated with a continuous use due to presence in all of the samples. Their active consumption was verified by the presence of corresponding metabolites, i.e. EDDP, nortilidine and *O*-desmethyl-*cis*-tramadol for methadone, tilidine and tramadol, respectively. The common use of cannabis was confirmed by the wastewater analysis as well as discussed in the previous section. Notable was also a high prevalence of CBD encountered in all of the investigated samples. This can originate from CBD contained in classic cannabis products (marijuana, hashish) or medical cannabis, as well as from commercial CBD products (CBD oil, CBD rich cannabis flowers, CBD e-liquids, etc.). An overview of all conventional drugs detected, their detection frequency and the corresponding time intervals is provided in Table S9 in the Supplementary Material. Although a direct comparison of the results with the data obtained by analysis of PDMS samples from the respective manhole (M2, Location 2) is difficult due to slightly different sampling periods (cf. Tables S3-S4, Supplementary Material), the findings gained with the both sampling approaches are generally in good agreement.

Compared to conventional drugs, SCRAs were detected in less wastewater samples. This does not necessarily indicate a lower degree of consumption, but can also be easily explained by much lower single effective doses of typical SCRAs compared to most other drugs (typically 10% or less). However, it has to be emphasized that the method applied can detect only a given set of targeted SCRAs. Prevalence of further SCRAs, which are not included in the analytical method, can be expected due to the dynamic nature of the SCRA drug market. Based on the findings presented, SCRAs seem to have established their own drug market, not only associated with more intensive patterns of use in certain niche settings and contexts like prisons [8], but also in a wider population.

Assessment of SCRA use by wide-district monitoring in WWTP

After the successful detection of several SCRAs in a city district of Munich comprising smaller catchment areas, the potential of the approach was exploited for a larger population covered by the main WWTP in the city (treated sewage pollution load corresponding to approximately 1.4 million inhabitants). This increased the potential number of consumers included, but also featured a potentially higher degree of dilution. Wastewater sampling was carried out during two time periods again, once including weekdays only (February 07-08, 2022) and once including weekdays combined with a weekend (February 04-08, 2022). During each time period, PDMS rods remained in sewage water for different sampling intervals, i.e. 1 h – 3 h – 21 h for the weekdays, and 1 h – 74 h – 95 h for the weekdays combined with the weekend. The analysis of PDMS rods gave satisfactory results and thus highlighted the significant value of large catchment areas when balanced against dilution, analyte desorption and matrix saturation effects during PDMS sampling. Multiple SCRAs and phytocannabinoids were successfully identified for different sampling intervals, as shown in Table 1. The substances detected match the previously discussed findings from a city district in Munich and from a

prison [8], but complemented the prevalence data by a further SCRA, AB-CHMINACA. All relevant phytocannabinoids, THC, cannabinol (CBN) and CBD, were also detected during almost all sampling periods.

The correlation between positive samples and longer sampling periods was remarkable, i.e. 21 h, 74 h and 95 h sampling intervals exhibited the highest number of findings. This observation implies that in most cases longer PDMS sampling periods rather mitigate the repercussions of desorption effects outlined earlier [8] by the benefit of longer sampling time. Only for EG-018 an opposite effect was observed. Therefore, sampling over longer periods of time, such as 4 days, appears to be well suited, at least for most of the SCRAs detected.

Table 1. Multiple SCRAs and phytocannabinoids identified in wastewater of the main WWTP in Munich during February 2022 using PDMS rods for influent wastewater sampling at different time intervals. The analysis was conducted with PDMS rods of 1 cm length for sampling and a 5 µL injection volume for LC-MS/MS.

Substance	Weekdays (Feb 07-08, 2022)			Weekdays + weekend (Feb 04-08, 2022)		
	1 h	3 h	21 h	1 h	74 h	95 h
MDMB-4en-PINACA			+		+	+
5F-MDMB-PICA / 5F-EMB-PICA			+		+	+
4F-MDMB-BICA		+	+		+	+
Cumyl-CBMICA			+			+
AB-CHMINACA		+				
EG-018				+		
JWH-210			+		+	+
THC		+	+		+	+
CBN		+	+		+	+
CBD	+	+	+	+	+	+

5.3.2 Hair analysis

In analogy to wastewater analysis, the three mandatory prerequisites for a positive SCRA identification in hair samples included a S/N ratio of at least 3/1 for two most intense diagnostic transitions, reproducible relative abundances of the diagnostic transitions and reproducible retention times relative to the corresponding reference standard. A representative UHPLC-MS/MS chromatogram of all SCRA reference standards covered by the updated analytical detection method is shown in Figure S1 (Supplementary Material), including target SCRA metabolites and phytocannabinoids.

Quantitative analysis of conventional drugs comprised 53 substances in total (cf. UHPLC-MS/MS chromatogram in Figure S2, Supplementary Material) including 13 deuterated standards. The most relevant substances for data evaluation in this study encompassed following drugs of abuse together with their metabolites: amphetamine (AMP), methamphetamine (mAMP), 3,4-methylenedioxy-amphetamine (MDA), 3,4-methylene-

dioxymethamphetamine (MDMA), cocaine (COC), benzoylecgonine (BE), norcocaine (NorCOC), cocaethylene (CE), heroin (HER), 6-monoacetylmorphine (6-MAM) and lysergic acid diethylamide (LSD). The presence of one of the listed drugs of abuse in one or multiple hair segments of a person was the requisite for a positive identification. Cannabis consumption was evaluated by quantitative determination of the main THC metabolite, THC-COOH, in a separate analytical method. Hence, the total number of conventional drugs screened for amounted to 41 substances.

5.3.2.1 Analyzed collective of authentic hair samples

In total, 398 cases (persons) were included in the analyzed sample collective, resulting in 676 hair segments. Whereas SCRAs screening was performed for all the cases (Collective 1, Table 2), an additional screening for SCRA metabolites encompassed a smaller portion of the collective with 152 cases (Collective 2, Table 2). Besides SCRAs, analysis of cannabis and other conventional drugs of abuse was performed in 370 cases (627 hair segments) to obtain a comprehensive picture of illicit drug consumption patterns and trends (Collective 3, Table 2). The age within the total sample collective ranged from 13 to 64 years, with a median age of 30 years (mean age = 32 years). The majority of the subjects were male (352 cases, 88.4%) and the remaining cases females (46 cases, 11.6%). The gender and age distribution with median and mean values were comparable for the three different collectives, i.e. groups examined (cf. Table 2).

Table 2. Characteristics of the analyzed sample collectives, including gender and age distribution. The corresponding positive cases are denoted for each collective in an analogous way. Additional information on SCRA positivity rate according to gender and polysubstance use (single vs. multiple SCRA consumption) is provided for the Collective 1 (SCRAs screening). Multiple SCRA consumption refers to at least two SCRAs present in hair segment(s) of a person.

Collective analyzed (∑ 398 cases)		Gender		Age			
		Male	Female	Age min [y]	Age max [y]	Age mean [y]	Age median [y]
Collective 1 (complete collective: SCRAs screening)							
Total	398 cases (676 hair segments)	352 cases	46 cases	13	64	32	30
SCRA positive	140 cases (226 hair segments)	127 cases	13 cases	15	60	30	28
SCRA positivity rate (Male and female sub-collective)		36.1%	28.3%				
Single SCRA consumption		68 cases (48.6%)					
Multiple SCRA consumption		72 cases (51.4%)					
Collective 2 (sub-collective: SCRAs + SCRA metabolites screening)							
Total	152 cases (284 hair segments)	132 cases	20 cases	17	58	32	30
SCRA positive	61 cases (105 hair segments)	54 cases	7 cases	17	58	31	29
SCRA metabolites positive	1 case (3 hair segments)	1 case	-	29		-	-
Collective 3 (sub-collective: SCRAs + Cannabis + Conventional drugs screening)							
Total	370 cases (627 hair segments)	328 cases	42 cases	13	64	32	29
Negative	42 cases (90 hair segments)	33 cases	9 cases	14	64	34	30
SCRA positive	134 cases (212 hair segments)	122 cases	12 cases	17	60	30	28
Cannabis positive	211 cases (354 hair segments)	194 cases	17 cases	13	60	30	27
Other conventional drugs positive	278 cases (454 hair segments)	250 cases	28 cases	16	62	31	29

5.3.2.2 Prevalence of SCRA use

When the hair amount and length allowed to, hair strands were analyzed in multiple segments and each hair segment was analyzed and evaluated individually. The developed method was applied to cases of individuals suspected of drug use who were involved in violations of the Narcotics Act, capital crimes and other criminal offences (murder, homicide, rape, theft, violence etc.), traffic offenses, intoxications or similar cases.

Of 398 cases / persons (676 hair segments) investigated, qualitative SCRA evaluation yielded 140 positive cases (226 positive hair segments) with minimum one SCRA detected. The positivity rate amounted to 35.2% SCRA positive cases. When normalizing positive results to gender, one in three males (36.1%) and one in four females (28.3%) were tested positive for SCRAs (Table 2), indicating no pronounced difference between genders. The age distribution of SCRA consumers was in the range between 15 and 60 years with a median age of 28 years (mean age = 30 years). The highest number of positive cases (45.7%) was present in the age group of 21-30 years, followed by the subsequent age group of 31-40 years (25.7%) (Figure 4A). Young people under 21 years and consumers above 41 years resembled significant portions of SCRA consumers as well (14.3% each). Figure 4B reveals the gender distribution for the different age groups with similar trends for males and females, particularly when higher variations for females are considered due to a lower total number of SCRA positive cases (13 females vs. 127 males). The high SCRA positivity rate among young people was in agreement with other studies, e.g. by Kutzler et al. [38], who reported the highest SCRA positivity rate for the youngest male sub-collective (16-25 years) investigated in their study. A comparatively large portion of young NPS users was also determined in the study of Larabi et al. [39] in France, with 11% of positive cases under an age of 20 years and 38% in the age group of 20-30 years. Low prices of SCRAs, their reputation of non-detectable and "legal" alternatives to conventional drugs, and their availability via the Internet might have specifically addressed the younger generation.

In 48.6% of the SCRA positive cases, only one SCRA was detected in hair segment(s) of the particular consumer (Table 2). In the remaining positive cases up to 19 different SCRAs were observed, but with decreasing percentage for increasing numbers of compounds detected. The aforementioned 19 different SCRAs including 2 of their metabolites were found only in one sample. Multiple SCRA detections in a hair sample can arise either from consumption of products containing several SCRAs or from frequent / regular consumption of various products, each containing a different SCRA. Both types of SCRA containing products have been encountered on the drug market, as confirmed by seized sample analysis in our laboratory. Even the use of different SCRAs in several batches of the same product was encountered frequently.

Chapter 5

A)

Age distribution of SCRA consumers

B)

Age and gender distribution of SCRA consumers
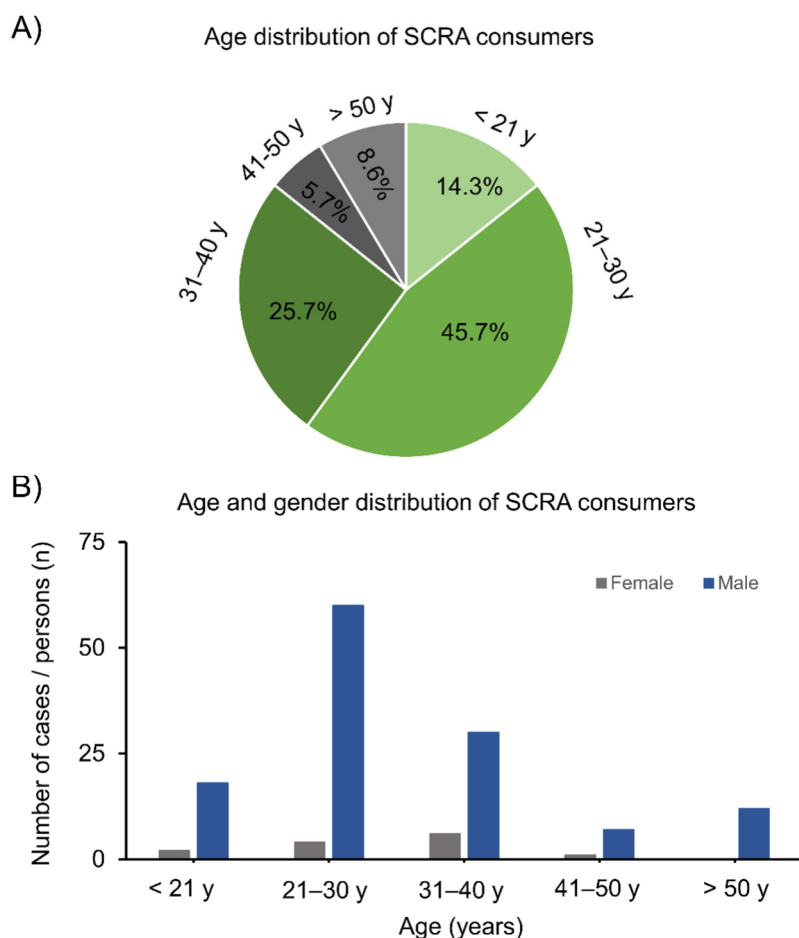
Figure 4. Age distribution of SCRA consumers (A), broken down by gender categories (B).

The diversity of SCRAs identified in hair samples reflects the domestic drug market scene. Within the time period investigated (February 2021 – July 2021, and 2022), a spectrum of 32 different SCRAs and 2 SCRA metabolites was detected in hair samples. The distribution of the different SCRAs over the 140 positive cases (226 SCRAs positive hair segments) is summarized in Figure 5. As previously stated, multiple compounds were often found in one case, and this must be considered for the following figures. MDMB-4en-PINACA (64 positive cases), ADB-BUTINACA (47 positive cases) and JWH-210 (41 positive cases) accounted for 49.7% of the most frequent SCRA detections, indicating three particularly prevalent compounds. The next most frequently detected compounds were 4F-MDMB-BICA (7.5%), 5F-ADB (4.2%), Cumyl-BC[2.2.1]HpMINACA (4.2%), 5F-MDMB-PICA / 5F-EMB-PICA (3.9%), ADB-5Br-INACA (2.9%) and Cumyl-CBMICA (2.9%), which in toto accounted for 25.8% of the most prevalent substances. The metabolites were not included in the present evaluation, since they seem to play a minor role in hair analysis (cf. section 5.3.2.3). The previously discussed trend of diverse SCRA products on the drug market is clearly reflected by our toxicological findings. Nevertheless, the presence of further SCRAs not included as target analytes in the analytical method cannot be excluded, and a single SCRA detection does not rule out the presence of further compounds, which might be below the analytical limit of detection. The most astonishing finding in our sample collective was the remarkably frequent detection of the naphthoylindole SCRA JWH-210. Alongside several other so-called JWH compounds, it played a major role on the German market more than a decade ago, until it was banned by the

national Narcotics Act in 2012. After MDMB-4en-PINACA and ADB-BUTINACA, JWH-210 was the third most commonly encountered SCRA in hair samples in this study (Figure 5), which was aligned with the results of Fels et al. [40] and Norman et al. [41] as recently as 2020, albeit with rather lower overall prevalence of JWH-210 in the latter study. Interestingly, on the international scale, the group of naphthoylindole SCRAs appeares to be rather characteristic for the German drug market, as concluded by Norman et al. [41].
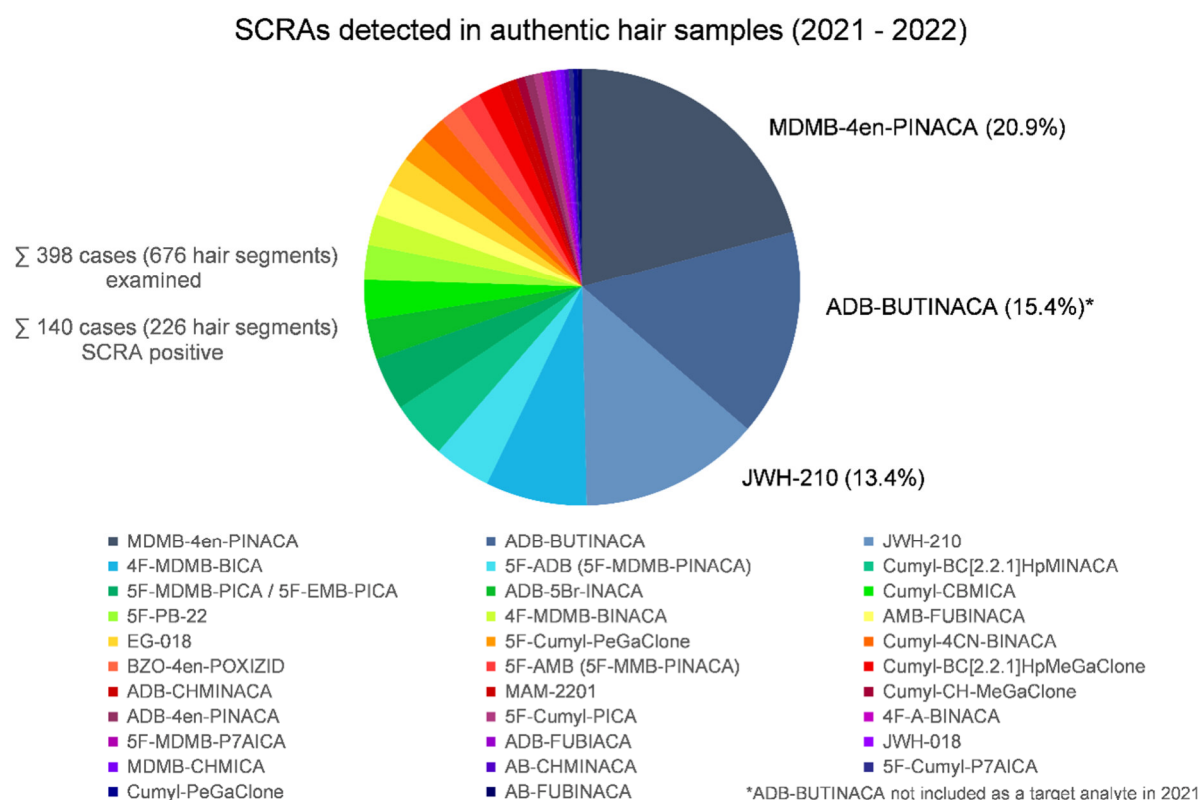
Figure 5. Distribution of SCRAs over persons who tested positive for at least one SCRA during the time period investigated, i.e. from February to July 2021 and during 2022. Overall, 32 different SCRAs were detected and a total of 306 SCRA detections were made across the 140 SCRA positive cases / persons. Note that total detections sum to greater than the total number of SCRA-positive persons since many persons tested positive for multiple SCRAs.

A direct comparison of the different studies regarding SCRAs prevalence is limited due to different analytical conditions (target compounds included, sensitivity, cut-off criteria), different populations (collective size, age and gender distribution) and different time periods. Furthermore, different geographical patterns worldwide can be expected, e.g. due to different supply chains and local trafficking groups, legislation or consumer preferences. For example, Norman et al. [41] noticed that not only SCRAs from the naphthoylindole family but also SCRAs exhibiting a γ-carbolinone core structure and/or a cumyl group were rather encountered in Germany than in the United Kingdom (UK) and the United States (US). Nevertheless, several of the most frequently detected SCRAs in the present work were in alignment with findings from other studies. The high prevalence of MDMB-4en-PINACA was reported in literature as well, as determined by means of both toxicological and environmental analysis in different

populations worldwide. These publications include SCRA prevalence data in prisons and wider populations from Germany, the UK and the US [41], wastewater analysis in China [42] and toxicological data on hair analysis in China [21]. A high prevalence of MDMB-4en-PINACA (42%) was also confirmed by the toxicology reports collected by United Nations Office on Drugs and Crime (UNODC) [43] in 2021 and up to October 2022. Further relevant SCRAs notified to UNODC were AB-PINACA, 4F-MDMB-BINACA and ADB-BUTINACA.

Not surprisingly, the SCRA positivity rate of 35% from our study, which refers to suspected individuals (mainly drug related offences), differs from several other studies, related to driving under influence of drugs (DUID) or abstinence tests. Data from German general population arising from DUID offenses, yielded SCRA prevalence of 10.8% based on a blood serum dataset of 2,539 samples between July 2018 and August 2020 [41]. For the latest period examined (2020), the data revealed a high positivity rate for 5F-MDMB-PICA and 4F-MDMB-BINACA, accompanied by the additional breakthrough of MDMB-4en-PINACA, 4F-MDMB-BICA and Cumyl-CBMICA, their prevalence being in the order they are listed. Kutzler et al. [38] achieved similar results for the most prevalent compounds when evaluating 5,097 hair samples in abstinence control between March 2020 and March 2021 throughout Germany, but with a lower positivity rate of 3.6%. Fels et al. [40] found a SCRA positivity rate of 7.3% in such a collective, but only of 0.3% for the residual designer drugs. Even higher prevalence of SCRAs (55%) than in our study was reported by Franz et al. [44] in the scope of drug abstinence testing during the time period 2012-2016. The high positivity rate was explained by a sample collective of individuals highly suspicious for SCRA use, thus resulting in specific requests to investigate SCRA use.

5.3.2.3 Detection of SCRA metabolites

Positivity rate for SCRA metabolites was very low in this study. Although a portion of about 40% of all hair samples was screened for SCRA metabolites, only one case gave a positive result for them. However, this finding matches other reports dealing with determination of SCRAs and their metabolites in hair samples, where the frequency and concentrations of parent compounds significantly exceeded the detection rate and concentrations of their corresponding metabolites in hair [11,21]. Drug consumption behavior (amount of drug, consumption route and consumption frequency), inter-individual variations in the metabolism profile and analytical method sensitivity might induce differences in the detection rate for metabolites in different studies.

5.3.2.4 Comparison of SCRAs and conventional drug use

To determine the extent and patterns of SCRA use in relation to conventional drugs including cannabis, screening and data evaluation for multiple drug categories was performed in each hair segment. Hair samples from 370 persons amounting to 627 hair segments were analyzed, of which 328 persons (537 hair segments) were positive for at least one conventional illicit drug (AMP, mAMP, MDA, MDMA, COC, BE, NorCOC, CE, HER, 6-MAM, and LSD), cannabis (THC-COOH) or SCRA. Cannabis was assessed separately from the remaining conventional drugs included in the data evaluation, as it is much closer related to SCRAs concerning pharmacological effects and expected consumption patterns. Concentrations above the lower limit of quantification (LLOQ) were considered as positive substance identification and

featured LLOQ of 0.1 pg/mg hair for THC-COOH [36] and 0.02 - 0.1 ng/mg hair for the conventional drugs included. The LLOQs of the individual conventional drugs are given in Table S10 in the Supplementary Material. SCRAs being found in toxicological samples were identified qualitatively pursuant to the criteria outlined in section 5.3.2.

SCRAs were detected in one third of the collective analyzed (36.2%), cannabis in half of the collective (57.0%) and the remaining conventional drugs in nearly two thirds of the total collective (75.1%), as shown in Figure 6A. Figure 6B illustrates the consumption patterns of the drugs investigated, i.e. the distribution of persons screened positive across the three categories (SCRAs, cannabis and the remaining conventional drugs) and the overlapping of categories for persons containing more than one substance. Among the collective examined (370 persons), 90 persons (24.3%) were positive for conventional drugs only, 24 (6.5%) for cannabis only, and 8 persons (2.2%) for SCRAs only. Interestingly, the majority of cannabis positive samples were either in combination with other conventional drugs (80 persons, 21.6%), SCRAs (18 persons, 4.9%) or both (89 persons, 24.1%), suggesting a low number of sole cannabis users. Therefore, the majority of subjects who used cannabis appear to be polydrug users inclined to the use of "harder drugs" or potent SCRAs. A similar trend was observed for SCRAs, where the consumers were almost equally distributed over additional cannabis (18 persons, 4.9%) or conventional drugs (19 persons, 5.1%) use. The vast majority of SCRA consumers (89 persons, 24.1%) have been engaged in both cannabis and other conventional drugs use as well. From the perspective of conventional drugs, consumers were almost equally distributed over exclusive conventional drugs use (24.3%), the combination of conventional drugs with cannabis (21.6%) and the combination of conventional drugs with both cannabis and SCRAs (24.1%). An interesting observation was the relatively low number of cannabis consumers also using SCRAs (6.5% vs. 4.9%), whereas a much higher share of SCRA users also consume cannabis (2.2% vs. 4.9%). Similarly, Salomone et al. [15] identified only 7.8% SCRA users among a collective of proven cannabis consumers.

Chapter 5
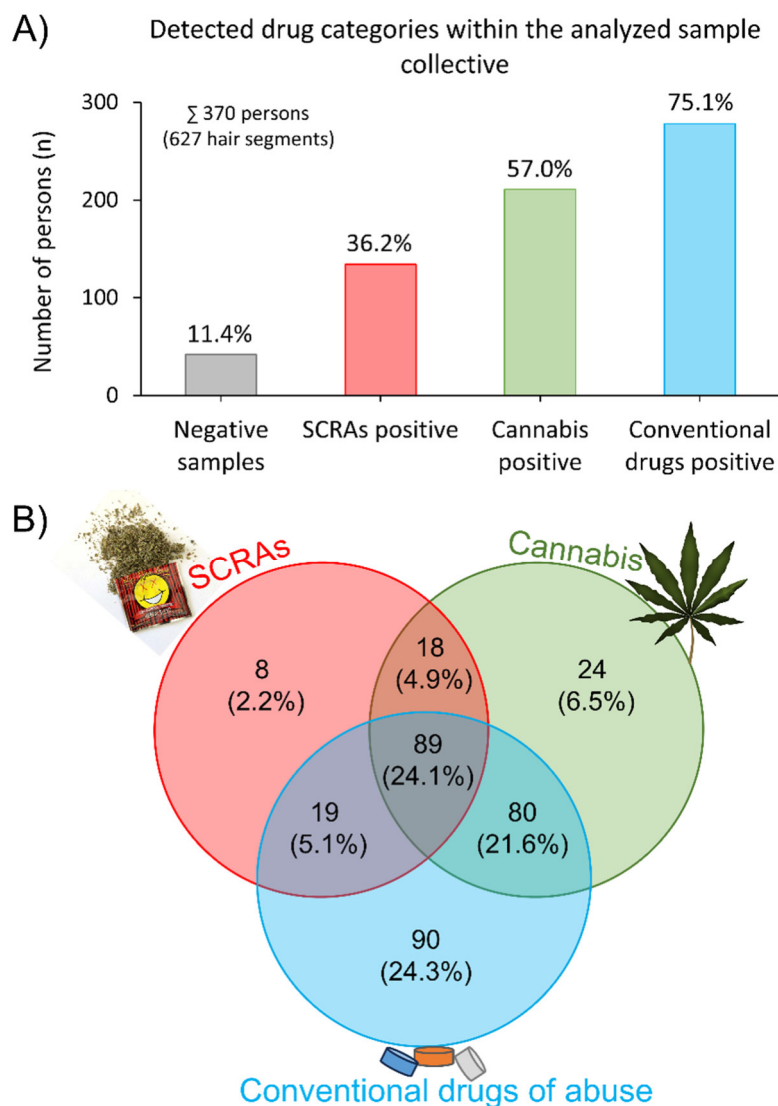
Figure 6. Prevalence of SCRAs (36.2%), cannabis (57.0%), and the remaining conventional drugs (75.1%) in the sample collective analyzed (n = 370 persons; 627 hair segments). The presence of at least one SCRA, THC-COOH, or one of the pre-defined conventional drugs in a hair segment was considered for positive evaluation and classification of the corresponding person into the respective category, with many persons screening positive for more than one category; negative sample collective (11.4%) is indicated accordingly (A). Distribution of persons screened positive across the three categories, particularly visualized for persons containing more than one substance (B). All percentages refer to the total number of persons analyzed, i.e. including persons tested negative.

Comparison of SCRA use in the context of cannabis and the remaining conventional drugs of abuse might help to better understand the consumption patterns, prevalence and spread of SCRAs on the market. So far, only few toxicological studies dealing with hair analysis were performed with this aim, most of them focusing on NPS in general. Adult patients admitted to hospitals in Paris and its suburbs from 2012–2017 were screened positive for NPS in 29% of the cases (141 patients) with 27 NPS identified in total, however the subclass of SCRAs was detected only in one case [39]. While exclusively NPS were found in 32% of patients, in more than half of the NPS cases (54%) at least two NPS mostly in combination with cocaine, amphetamines or opioids were encountered in the same hair segment. Similar findings arose from the study of Salomone et al. [45] from a population of nightclubs and festivals attendees

in the US. Among hair samples analyzed (n = 80), 57 samples tested positive for at least one drug, either conventional drug or NPS. The use of NPS was observed mainly in combination with conventional drugs (24 cases, 42.1% of the positive cases), while the rate of exclusive NPS use was relatively low (2 cases, 3.5%). The NPS detected included predominantly synthetic cathinones, whereas SCRAs were not detected in any of the hair samples. Further toxicological studies have reported low prevalence of SCRAs, including Adamowicz et al. [46] who found only UR-144 as sole SCRA in 7 out of 112 NPS positive cases in Poland by blood analysis during the three-year period 2012-2014. Besides other explanations (drug market situation, incomplete SCRAs coverage by the analytical screening method etc.), the very low concentrations and rapid metabolism of SCRAs can be expected as a major cause for such low prevalence rates. Ji et al. [47] developed a multi-analyte method used to analyze hair samples from 1,865 addicts in drug abstinence and the majority of 129 positive cases included conventional drugs, like mAMP and opioids, whereas SCRAs constituted only a small portion of drugs detected (2.7%) with only four positive cases. Conclusively, the scarce and lacking literature on SCRA consumption patterns and their co-use with conventional drugs prompts further research to shed light on these trends, as aimed with the present study.

5.3.2.5 Exclusive SCRA users and SCRA use among young population (< 21 years)

Exclusive SCRA use was observed in 8 cases, which are summarized in Table 3 in order to elucidate the demographic and consumption characteristics of this user group. Most of the SCRA only users have shown a tendency to use more than one SCRA and were in the age range between 25 and 35 years, males being overrepresented with 7 out of 8 cases. Interestingly, young people under 21 seem not to be exclusive SCRA users, but are rather tested positive for multidrug consumption. Table S11 provides an overview of the screening results for all SCRA positive cases with young people under the age of 21 (20 cases), showing demographic characteristics and segmental hair analysis with qualitative SCRA results (SCRAs identified) as well as quantitative results on cannabis and the remaining conventional drugs (licit and illicit) included in the analytical method. The consumption patterns of young SCRA users exhibited several remarkable details. Firstly, in the majority of cases (60%) more than one SCRA was identified in the SCRA use history. Secondly, use of multiple drugs belonging to different drug classes appeared to be a trend for young people under 21, with cannabis being the most prevalent drug among the conventional drugs screened. Out of 19 cases analyzed for cannabis, 84% of the cases tested positive. COC and MDMA were the second most frequently detected conventional drugs, each being encountered in 60% of the young population sub-collective analyzed (20 cases), followed by AMP (positivity rate of 55%). A summary of the positivity rates for all relevant conventional drugs is compiled in Table S12, Supplementary Material. Concentrations determined from the 31 hair samples (16 cases) positive for THC-COOH ranged from 0.12 to > 15 pg THC-COOH/mg hair, whereas COC, AMP and MDMA concentrations across the young population users were distributed from 0.11 to > 20 ng/mg, 0.06 to 2.6 ng/mg and 0.07 to 1.8 ng/mg hair, respectively. The determined drug concentrations allow to draw conclusions about the frequency of drug use, as based on our statistical data. The percentage of drug concentrations above our statistical median (50th percentile) was calculated for the particular drugs of abuse and indicated frequent or regular drug use (see Table S12, Supplementary Material). Cannabis headed the list again, with 75% of the positive cannabis samples being attributed to frequent or regular consumers. The corresponding

proportion for COC, MDMA and AMP was lower amounting to 58%, 33% and 18%, respectively.

When comparing the minimum age of SCRA consumers with the age trends in other drug categories (cf. section 5.3.2.1, Table 2), the cannabis user group exhibited the lowest age (13 years). The youngest subjects of conventional drugs and SCRA user groups were at an age of 16 and 17 years, respectively.

Table 3. Results of segmental hair analysis for samples screened positive for exclusive SCRA use (8 cases, 11 hair segments). Overview of sampling (sampling date and collection site) and segmentation characteristics (hair segment length examined), demographic characteristics of users (gender and age), as well as SCRAs detected. Segmental analysis was performed from proximal to distal segments, indicated by the increasing distance along the hair segments.

Exclusive SCRA use (positive cases / hair segments)					
Subject					SCRAs
Case	Sampling date	Gender	Age (y)	Collection site	Segment [cm]	Qualitative results
1	Apr 2021	M	49	Scalp	0 - 2.5	5F-Cumyl-PeGaClone
2	May 2021	M	53	Scalp	0 - 2	JWH-210
					2 - 5	JWH-210
3	Jun 2021	M	33	Scalp	0 - 2	-
					2 - 4	5F-AMB
					4 - 6	-
4	Feb 2022	M	35	Scalp	0 - 1.5	-
					1.5 - 3	MDMB-4en-PINACA JWH-210
					3 - 6	MDMB-4en-PINACA JWH-210 ADB-BUTINACA
5	Aug 2022	M	60	Scalp	0 - 1.5	Cumyl-BC[2.2.1]HpMeGaClone Cumyl-BC[2.2.1]HpMINACA
					1.5 - 4	-
6	Oct 2022	M	25	Scalp	0 - 4	Cumyl-BC[2.2.1]HpMeGaClone Cumyl-BC[2.2.1]HpMINACA
7	Oct 2022	F	35	Scalp	0 - 3	-
					3 - 6	5F-ADB
					6 - 9	JWH-210
8	Dec 2022	M	34	Scalp	0 - 1.5	-
					1.5 - 3.5	5F-MDMB-PICA / 5F-EMB-PICA

5.3.3 Correlation and complementarity of toxicological, wastewater and seizure data

Figure 7 shows the qualitative comparison of SCRA findings between toxicological data (hair samples) and wastewater samples during the investigated time period 2021-2022. While toxicological data comprise the period from February to July 2021 and the entire year 2022, wastewater data reflect snapshots from September 21-23, 2021; September 24-26, 2021 and February 04-08, 2022. The colors represent the relative frequency of SCRAs detection in wastewater (blue) and hair samples (orange). SCRAs detected in wastewater were plotted relative to each other with their frequency of occurrence during the three wastewater sampling campaigns. The highest frequency of occurrence is colored in dark blue and the lowest one in white. The prevalence of a specific SCRA in hair samples was calculated as the total number of persons screened positive for the SCRA in the collective analyzed (398 persons). Dark orange indicates the highest prevalence and white the lowest one. SCRAs listed in Figure 7 were the most prevalent compounds in hair samples, representing 75% of all SCRA detections across SCRA positive persons. Although the last three SCRAs did not meet this criterion, they were detected in municipal wastewater and were thus included in the list to be compared with their detection frequency in toxicological samples.

Wastewater analysis	SCRAs detected	Hair analysis
3	MDMB-4en-PINACA	64
n.a.	ADB-BUTINACA	47
1	JWH-210	41
3	4F-MDMB-BICA	23
1	Cumyl-BC[2.2.1]HpMINACA	13
0	5F-ADB (5F-MDMB-PINACA)	13
3	5F-MDMB-PICA / 5F-EMB-PICA	12
2	Cumyl-CBMICA	9
n.a.	ADB-5Br-INACA	9
1	4F-MDMB-BINACA	7
1	EG-018	7
1	AB-CHMINACA	1
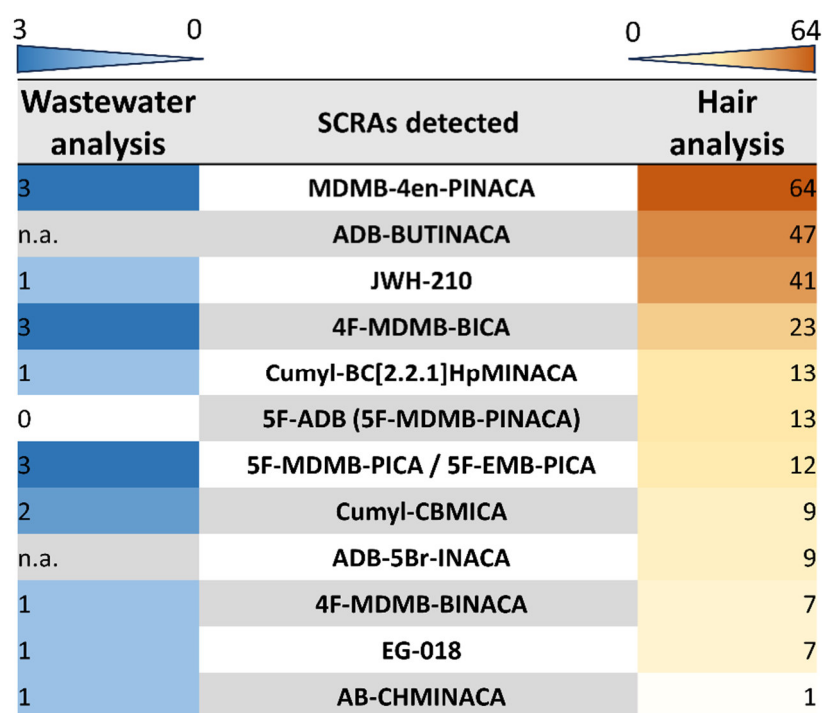
Figure 7. Heat map of SCRAs detected in wastewater and hair samples, plotted as relative frequency of occurrence during three wastewater sampling campaigns (blue) and in the hair sample collective analyzed, depicting the total number of positive persons for a specific SCRA (orange). n.a. = not analyzed; ADB-BUTINACA and ADB-5Br-INACA were not included in the targeted LC-MS/MS method for wastewater analysis during the investigated time periods; hair analysis data from February to July 2021 did not comprise these two SCRAs either.

In total, 32 different SCRAs were found in the toxicological hair samples (cf. Figure 5), 9 of these in wastewater as well, and hence 9 SCRAs overlapped in both matrices. Although only snapshots with three short time periods (max. 5 days) were included in the wastewater analysis, a remarkable number of SCRAs was identified. Their detection frequency during

different time periods suggested their widespread use, particularly for MDMB-4en-PINACA, 4F-MDMB-BICA and 5F-MDMB-PICA / 5F-EMB-PICA that were detected during each sampling campaign. The conclusion concords with the toxicological data, which reveal a significant SCRA prevalence with 35.2% SCRA positive cases. In spite of the limited and short wastewater sampling periods, the findings from wastewater correlate quite well with the most common SCRAs identified in hair samples. MDMB-4en-PINACA can be considered the most prevalent SCRA in the time period investigated, shown by both wastewater and toxicology data. A similar interference can be drawn for the SCRAs JWH-210 and 4F-MDMB-BICA. ADB-BUTINACA allows for limited conclusions only, since this analyte was not included in the targeted analytical method for wastewater analysis at that time. Minor deviations in the findings between wastewater and hair analysis, e.g. the absence of 5F-ADB in wastewater samples can be attributed to dilution effects, high metabolism rates or its infrequent use during the selected sampling periods.

The findings were also in good agreement with local market availability of SCRAs, as evident from seizures analyzed in our laboratory in the respective time frame. The heat map in Figure 8 illustrates that MDMB-4en-PINACA and ADB-BUTINACA accounted not only for the most frequent detections in the hair sample collective analyzed, but also for the highest portion of drug seizures. Moreover, MDMB-4en-PINACA dominated the scene in 2021, whereas ADB-BUTINACA peaked in the second half of 2022, evident in both toxicological findings and seizure data. Furthermore, the trend of increasing detection frequency of JWH-210 towards the end of 2022 was also mirrored by both data sources in an identical way. Finally, substances that were encountered less frequently in police seizures (e.g. Cumyl-CBMICA, 4F-MDMB-BINACA, EG-018, and AB-CHMINACA) were also rarely detected in toxicological cases (Figure 8).
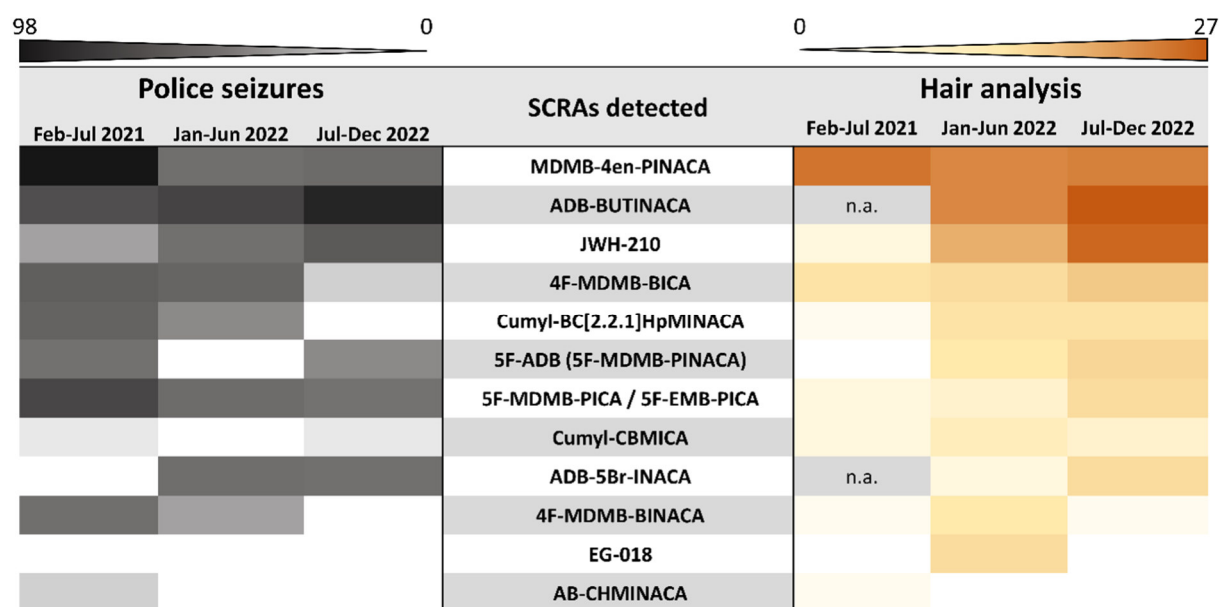
Figure 8. Prevalence of selected SCRAs between February 2021 and December 2022 in police seizures (left) compared to their frequency of occurrence in the hair sample collective analyzed in the corresponding period (right). The prevalence of a specific SCRA in the collective analyzed (398 persons) was calculated as the total number of persons screened positive for this SCRA.

The results demonstrate the complementarity of toxicological and wastewater data, which both provide a source of intelligence for the prevalence of SCRAs – either in a subset of drug

user population with resolved drug use profiles for individuals (hair analysis) or on a community level (wastewater analysis). In the wider sense, wastewater represents a diluted and pooled urine sample of a defined catchment area and additionally to the qualitative assessment of community SCRA use, this approach might be utilized to quantify the scale of SCRA use as average daily mass loads (mg/d/1000 people), as already being exemplified in several studies [48,49]. Furthermore, police seizures yield valuable information on the market availability of individual SCRAs and timely fluctuations of the market situation. Orthogonality of the approaches resulted in high overlap of findings, at least for the most abundant analytes, demonstrating the value of combining wastewater, toxicological and police seizure data. A trend in the use of SCRAs was evident from all three data sources, suggesting a notable population-scale SCRA use in the southeastern region of Germany (Bavaria). For future work, seizure data are still required to notice upcoming drug trends and enable updating of analyte panels for a broader survey using wastewater and toxicological analyses.

5.3.4 Impact of legislative controls on SCRAs market development

German drug legislation is based on two laws: The Narcotics Act (German: Betäubungs-mittelgesetz, BtMG) and a generic NPS Act (German: Neue-psychoaktive-Stoffe-Gesetz, NpSG). The BtMG sanctions a.o. possession and trade of a limited number of drugs contained in a very specific list of individual substances. The introduction of the generic NPS legislation (NpSG) in 2016, covering groups of substances as defined by structural features, complemented the BtMG and rendered a legal framework to control NPS. Whereas both laws lead to prosecution in the case of manufacturing, commercial distribution, import and export, the regulatory control of the NpSG does not sanction acquisition and possession of NPS intended for personal use. On the contrary, BtMG implies sanctions in any case and the level of penalties depends on the quantity of pure active compound seized. Since the very beginning, new SCRAs have continuously emerged on the drug market, containing structural features that appear to be selected or even specifically designed to bypass the existing legal controls. Legislative actions to cover new drugs often prompted the disappearance of these substances from the German drug market, which can also be observed in our data.

At the beginning of our study, JWH-210, 5F-MDMB-PICA, AMB-FUBINACA and AB-CHMINACA had been included in the BtMG for at least half a year, EG-018 and Cumyl-CBMICA in the NpSG. Figure 9 shows an extract of Figure 8, containing mainly SCRAs that were placed under legislation of the BtMG or NpSG during or close to the time interval covered by our study. As illustrated by Figure 9, the scheduling of 4F-MDMB-BINACA, MDMB-4en-PINACA and 4F-MDMB-BICA under the BtMG in January, May and November 2021, respectively, led to a decreased prevalence of these drugs thereafter. A similar effect can be observed for the coverage of Cumyl-BC[2.2.1]HpMINACA by the NpSG from July 2021 onwards. At the same time, the prevalence of ADB-BUTINACA significantly increased, until it was put under BtMG control in June 2023. For currently unknown reasons, JWH-210 showed a similar increase, although already being listed in the BtMG since 2012.
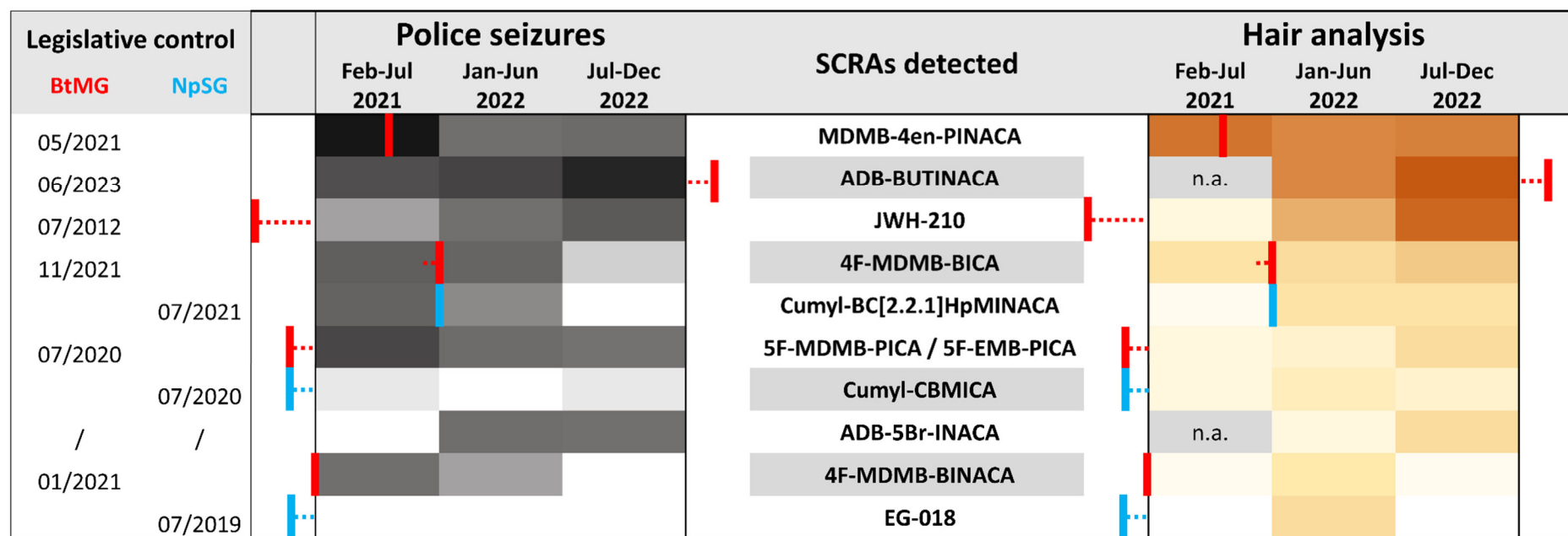
Figure 9. Prevalence of selected SCRAs with indicated time points of their legislative control in Germany, either by the BtMG or NpSG. The SCRAs shown include substances from Figure 8 that were placed under legislation of the BtMG or NpSG during or close to the time interval covered by our study, with the exception of JWH-210.

5.4 Conclusion

This study combined three different approaches - wastewater analysis, forensic toxicological hair analysis and police seizure data - to investigate the prevalence of SCRA use. Moreover, the wastewater and toxicological hair analyses were extended to conventional drugs of abuse to estimate the SCRA prevalence data in the context of common drugs consumption on a community level and on the level of individual SCRA users, respectively. A targeted LC-MS/MS screening method was used for delivering qualitative and semiquantitative information on SCRAs via wastewater and hair analyses. Cannabis and the remaining conventional drugs were determined either qualitatively (wastewater) or quantitatively (hair) using the same analytical methodology (LC-MS/MS).

After the successful application of the novel wastewater sampling approach using PDMS passive samplers to the effluent of a German prison and to a city district of Munich, Germany in our previous study, the potential of the methodology was exploited for assessment of a larger population covered by a WWTP in the city and extended to conventional drugs. Seven SCRAs were successfully detected in the WWTP samples, with remarkable correlation between increased detection rate and longer PDMS sampling time periods, up to 4 days. Similar experiments were conducted in the sewer network of a city district of Munich at several locations, allowing for a comparison between different catchment areas. In addition, wastewater sampling in the city district was performed with an automated pump-based liquid-sampling device. This sampling approach enabled high temporal resolution (4 h per individual sample) and revealed significant consumption patterns and differences during weekdays and the beginning of the weekend, showing specifically high prevalence of SCRAs consumption on Friday afternoon-evening (2 - 10 p.m.). Overall, SCRAs detected in wastewater of the city of Munich during selected time periods in September 2021 and February 2022 encompassed MDMB-4en-PINACA**,** 4F-MDMB-BINACA, 4F-MDMB-BICA**,** 5F-MDMB-PICA / 5F-EMB-PICA**,** Cumyl-CBMICA, Cumyl-BC[2.2.1]HpMINACA, AB-CHMINACA, EG-018, and JWH-210. Phytocannabinoids were identified as well, with THC and its metabolite THC-COOH being detected in all liquid wastewater samples examined, both during weekdays and weekend, indicating their rather high prevalence. Further conventional drugs were identified, and based on their detection frequency a substantial use of cocaine, MDMA, synthetic opioids (methadone, buprenorphine, fentanyl, tramadol and tilidine) and also of ketamine could be derived. From the analytical aspect, PDMS passive samplers have successfully demonstrated their applicability to extract additional drug classes besides SCRAs, including phyto-cannabinoids (THC, THC-COOH, CBN and CBD), amphetamine-type stimulants, cocaine and its metabolites, and a large panel of opioids. As shown in our previous study for SCRAs, the fast and flexible installation/deinstallation of PDMS passive samplers (PDMS rods) and selection of suitable sampling locations in the complex municipal sewage system allowed to assess spatial differences of conventional drugs use as well, with high local resolution.

Forensic toxicological analysis comprised hair samples from persons suspected of violations of the Narcotics Act and other criminal offences over a 1.5 year period during 2021-2022. The qualitative SCRA analysis of hair samples from 398 persons (676 hair segments) resulted in 140 SCRA positive persons (226 SCRA positive hair segments), yielding a positivity rate of 35.2% and a wide range of 32 individual SCRAs and 2 of their metabolites, with up to 19 different substances identified in a single sample. The most frequently detected SCRAs in hair

samples were MDMB-4en-PINACA, ADB-BUTINACA and JWH-210, which altogether constituted 49.7% of the SCRAs detected. Regarding the demographic characteristics of SCRA consumers, the median age was 28 years, with the highest number of positive cases (45.7%) in the age group of 21-30 years, and a significant portion of young people under the age of 21 (14.3%). When comparing SCRAs prevalence to that of cannabis (THC-COOH) and the remaining conventional drugs (AMP, mAMP, MDA, MDMA, COC, BE, NorCOC, CE, HER, 6-MAM, and LSD) within a slightly smaller sample collective (370 persons, 627 hair segments), SCRAs were detected in one third of the total collective (36.2%), cannabis in half of the collective (57.0%) and the remaining conventional drugs in nearly two thirds of the collective (75.1%). Most of the subjects investigated appeared to be conventional drug users only (24.3%) or polydrug users inclined to use of all three drug categories (24.1%), followed by co-users of cannabis and conventional drugs (21.6%). SCRA only use was recorded in 2.2% of the collective investigated. Interestingly, young people under 21 seemed not to be exclusive SCRA users, but rather tested positive for multiple drugs belonging to different drug classes, predominantly involving cannabis (84% of the young population sub-collective positive for cannabis).

Finally, the results of wastewater and hair analysis were triangulated with police seizure data from the same time period and region. A widespread use of SCRAs in Bavaria, Germany over the period 2021-2022 was evident from all the three data sources and the most dominant SCRA in 2021 was MDMB-4en-PINACA, which was successively replaced by ADB-BUTINACA in 2022. In general, scheduling of SCRAs under the Narcotics Act in Germany had an impact on their reduced local availability, as can be deduced from seizure and toxicological data.

Conclusively, the results suggest that SCRAs have entrenched on the drug market, and a significant prevalence of use is not confined to niche populations only, but has extended to wider populations as well. Wastewater and hair analysis have proven to be valuable tools for monitoring the dynamic nature of the SCRAs market, providing near real-time information and resolved individual consumption patterns, respectively. Additionally, our concept of combining prevalence data from three different perspectives and sources proved to be highly suitable for the assessment of the effectivity and sustainability of legislative scheduling of individual SCRAs. From the analytical point of view, an up-to-date analytical method is crucial to estimate the actual SCRA prevalence and gauge the market dynamics. Prospectively, SCRAs analysis should be included in routine screening methods not only for seized drugs, but also for wastewater and biological samples to shed more light on prevalence, persistence and changing patterns of this drug class. The combination of these different sources of information can be used to minimize public risk and propose appropriate legislative response measures.

5.5 References

[1]   European Monitoring Centre for Drugs and Drug Addiction. European Drug Report 2023: Trends and Developments. 2023; Luxembourg: Publications Office of the European Union. https://www.emcdda.europa.eu/publications/european-drug-report/2023_en. Accessed February 04, 2024. DOI: 10.2810/161905.

[2]   Andrews R, Jorge R, Christie R, Gallegos A. From JWH-018 to OXIZIDS: Structural evolution of synthetic cannabinoids in the European Union from 2008 to present day. *Drug Test Anal*. 2023;15(4):378-387. DOI:10.1002/dta.3422.

[3] Weber C, Pusch S, Schollmeyer D, Münster-Müller S, Pütz M, Opatz T. Characterization of the synthetic cannabinoid MDMB-CHMCZCA. *Beilstein J Org Chem.* 2016;12:2808-2815. DOI: 10.3762/bjoc.12.279.

[4] Angerer V, Mogler L, Steitz J-P, et al. Structural characterization and pharmacological evaluation of the new synthetic cannabinoid CUMYL-PEGACLONE. *Drug Test Anal*. 2018;10:597–603. DOI: 10.1002/dta.2237.

[5] Pulver B, Riedel J, Schönberger T, et al. Comprehensive structural characterisation of the newly emerged synthetic cannabimimetics Cumyl-BC[2.2.1]HpMeGaClone, Cumyl-BC[2.2.1]HpMINACA, and Cumyl-BC[2.2.1]HpMICA featuring a norbornyl methyl side chain. *Forensic Chem*. 2021;26:100371. DOI: 10.1016/j.forc.2021.100 371.

[6] Yoganathan P, Claridge H, Chester L, Englund A, Kalk NJ, Copeland CS. Synthetic Cannabinoid-Related Deaths in England, 2012-2019. *Cannabis Cannabinoid Res.* 2022;7(4):516-525. DOI: 10.1089/can.2020.0161.

[7] Groth O, Roider G, Angerer V, et al. "Spice"-related deaths in and around Munich, Germany: A retrospective look at the role of synthetic cannabinoid receptor agonists in our post-mortem cases over a seven-year period (2014-2020). *Int J Legal Med*. 2023;137(4):1059-1069. DOI: 10.1007/s00414-023-02995-2.

[8] Hehet P, Wende M, Shehata O, Krause S, Pütz M. Prevalence of synthetic cannabinoid receptor agonists use assessed by sewage monitoring via LC-MS/MS, Part A: Novel wastewater sampling approach applied in a prison and a major city. To be submitted to *Forensic Chem*.

[9] Knittel JL, Holler JM, Chmiel JD, et al. Analysis of Parent Synthetic Cannabinoids in Blood and Urinary Metabolites by Liquid Chromatography Tandem Mass Spectrometry. *J Anal Toxicol.* 2016;40(3):173-186. DOI: 10.1093/jat/bkv137.

[10] Cho B, Cho HS, Kim J, et al. Simultaneous determination of synthetic cannabinoids and their metabolites in human hair using LC-MS/MS and application to human hair. *Forensic Sci Int.* 2020;306:110058. DOI: 10.1016/j.forsciint.2019.110058.

[11] Shi Y, Zhou L, Li L, et al. Detection of a New Tert-Leucinate Synthetic Cannabinoid 5F-MDMB-PICA and Its Metabolites in Human Hair: Application to Authentic Cases. *Front Chem.* 2020;8:610312. DOI: 10.3389/fchem.2020.610312.

[12] Mogler L, Franz F, Rentsch D, et al. Detection of the recently emerged synthetic cannabinoid 5F-MDMB-PICA in 'legal high' products and human urine samples. *Drug Test Anal*. 2018;10(1):196-205. DOI: 10.1002/dta.2201.

[13] Minakata K, Yamagishi I, Nozawa H, et al. Sensitive identification and quantitation of parent forms of six synthetic cannabinoids in urine samples of human cadavers by liquid chromatography–tandem mass spectrometry. *Forensic Toxicol.* 2017;35:275-283. DOI: 10.1007/s11419-017-0354-0.

[14] Hutter M, Kneisel S, Auwärter V, Neukamm MA. Determination of 22 synthetic cannabinoids in human hair by liquid chromatography-tandem mass spectrometry. *J Chromatogr B.* 2012;903:95-101. DOI: 10.1016/j.jchromb.2012.07.002.

Chapter 5

[15]   Salomone A, Gerace E, D'Urso F, Di Corcia D, Vincenti M. Simultaneous analysis of several synthetic cannabinoids, THC, CBD and CBN, in hair by ultra-high performance liquid chromatography tandem mass spectrometry. Method validation and application to real samples. *J Mass Spectrom*. 2012;47(5):604-610. DOI: 10.1002/jms .2988.

[16]   Kim J, In S, Park Y, Park M, Kim E, Lee S. Deposition of JWH-018, JWH-073 and their metabolites in hair and effect of hair pigmentation*. Anal Bioanal Chem*. 2013;405(30):9769-78. DOI: 10.1007/s00216-013-7423-y.

[17]   Salomone A, Luciano C, Di Corcia D, Gerace E, Vincenti M. Hair analysis as a tool to evaluate the prevalence of synthetic cannabinoids in different populations of drug consumers. *Drug Test Anal*. 2014;6(1-2):126-134. DOI: 10.1002/dta.1556.

[18]   Gottardo R, Sorio D, Musile G, et al. Screening for synthetic cannabinoids in hair by using LC-QTOF MS: A new and powerful approach to study the penetration of these new psychoactive substances in the population. *Med Sci Law.* 2014;54(1):22-27. DOI: 10.1177/0025802413477396.

[19]   Kim J, Park Y, Park M, et al. Simultaneous determination of five naphthoylindole-based synthetic cannabinoids and metabolites and their deposition in human and rat hair*. J Pharm Biomed Anal*. 2015;102:162-175. DOI: 10.1016/j.jpba.2014.09.013.

[20]   Franz F, Jechle H, Angerer V, Pegoro M, Auwärter V, Neukamm MA. Synthetic cannabinoids in hair - Pragmatic approach for method updates, compound prevalences and concentration ranges in authentic hair samples. *Anal Chim Acta*. 2018;1006:61-73. DOI: 10.1016/j.aca.2017.12.029.

[21]   Liying Z, Min S, Baohua S, et al. Application of a UPLC-MS/MS method for quantitative analysis of 29 synthetic cannabinoids and their metabolites, such as ADB-BUTINACA and MDMB-4en-PINACA in human hair in real cases. *Forensic Sci Int.* 2022;331:111139.

[22]   Xu D, Ji J, Xiang P, Yan H, Zhang W, Shen M. Determination of 5 synthetic cannabinoids in hair by Segmental analysis using UHPLC-MS/MS and its application to eight polydrug abuse cases. *Forensic Sci Int.* 2023;346:111611. DOI: 10.1016/j.for sciint.2023.111611.

[23]   Wang Y, Pan Y, Yang H, Liu J, Wurita A, Hasegawa K. Quantification of MDMB-4en-PINACA and ADB-BUTINACA in human hair by gas chromatography-tandem mass spectrometry. *Forensic Toxicol*. 2022;40(2):340-348. DOI: 10.1007/s11419-022-00615-z.

[24]   Wang Y, Han L, Yi L, et al. Newly emerging synthetic cannabinoid ADB-4en-PINACA: its identification and quantification in an authentic human hair sample by GC-MS/MS*. Forensic Toxicol.* 2023;41(1):173-178. DOI: 10.1007/s11419-022-00643-9.

[25]   Boumba VA, Di Rago M, Peka M, Drummer OH, Gerostamoulos D. The analysis of 132 novel psychoactive substances in human hair using a single step extraction by tandem LC/MS. *Forensic Sci Int.* 2017;279:192-202. DOI: 10.1016/j.forsciint.2017.08. 031.

[26]   Nzekoue FK, Agostini M, Verboni M, et al. A comprehensive UHPLC-MS/MS screening method for the analysis of 98 New Psychoactive Substances and related
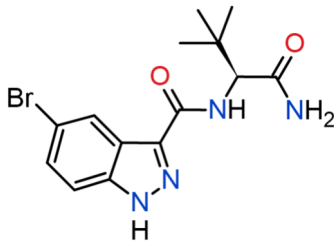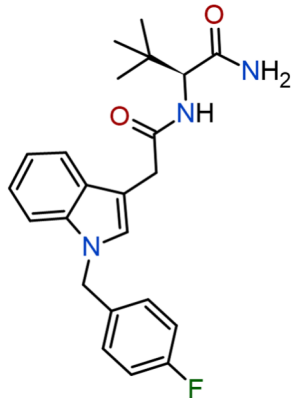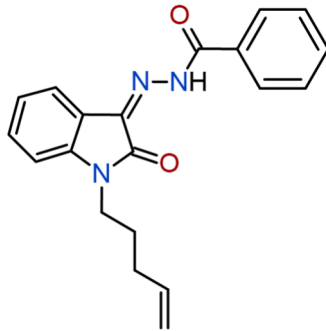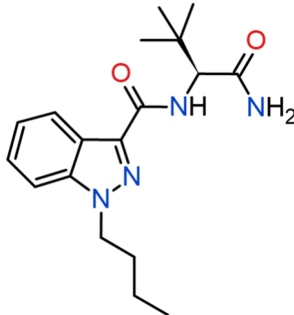
compounds in human hair. *J Pharm Biomed Anal.* 2021;205:114310. DOI: 10.1016/j.jpba.2021.114310.

[27] Mannocchi G, Di Trana A, Tini A, et al. Development and validation of fast UHPLC-MS/MS screening method for 87 NPS and 32 other drugs of abuse in hair and nails: application to real cases. *Anal Bioanal Chem*. 2020;412(21):5125-5145. DOI: 10.1007/s00216-020-02462-6.

[28] Gerostamoulos D, Elliott S, Walls HC, Peters FT, Lynch M, Drummer OH. To Measure or not to Measure? That is the NPS Question. *J Anal Toxicol.* 2016;40(4):318-320. DOI: 10.1093/jat/bkw013.

[29] Pulver B, Fischmann S, Westphal F, et al. The ADEBAR project: European and international provision of analytical data from structure elucidation and analytical characterization of NPS. *Drug Test Anal*. 2022;14:1491-1502. DOI:10.1002/dta.3280.

[30] Bade R, Stockham P, Painter B, et al. Investigating the appearance of new psychoactive substances in South Australia using wastewater and forensic data. *Drug Test Anal*. 2019;11(2):250-256. DOI: 10.1002/dta.2484.

[31] Qian Z, Hua Z, Liu C, Jia W. Four types of cannabimimetic indazole and indole derivatives, ADB-BINACA, AB-FUBICA, ADB-FUBICA, and AB-BICA, identified as new psychoactive substances. *Forensic Toxicol*. 2016;34:133-143. DOI: 10.1007/s11419-015-0297-2.

[32] Kronstrand R, Norman C, Vikingsson S, et al. The metabolism of the synthetic cannabinoids ADB-BUTINACA and ADB-4en-PINACA and their detection in forensic toxicology casework and infused papers seized in prisons. *Drug Test Anal.* 2022;14(4):634-652. DOI: 10.1002/dta.3203.

[33] World Health Organization, Expert Committee on Drug Dependence. Critical review report: ADB-BUTINACA. 2022. https://cdn.who.int/media/docs/default-source/controlled-substances/45th-ecdd/adb-butinaca_draft.pdf?sfvrsn=89c83ba5_1. Accessed January 30, 2024.

[34] Slovenian National Forensic Laboratory. Analytical Report ADB-BUTINACA (C18H26N4O2) 2-[(1-butyl-1H-indazol-3-yl)formamido]-3,3-dimethylbutanamide. 2019. https://www.policija.si/apps/nfl_response_web/0_Analytical_Reports_final/ADB-BUTINACA-ID-2082_report.pdf. Accessed January 30, 2024.

[35] Cayman Chemicals. ADB-BUTINACA reference material. Accessed January 30, 2024. https://www.caymanchem.com/product/29350/adb-butinaca.

[36] Hehet P, Franz T, Kunert N, Musshoff F. Fast and highly sensitive determination of tetrahydrocannabinol (THC) metabolites in hair using liquid chromatography-multistage mass spectrometry (LC-MS[3]). *Drug Test Anal*. 2022;14(9):1614-1622. DOI: 10.1002/dta.3330.

[37] Uhl M. Determination of drugs in hair using GC/MS/MS. *Forensic Sci Int.* 1997;84(1-3):281-294. DOI: 10.1016/s0379-0738(96)02072-5.

Chapter 5

[38]   Kutzler J, Polettini AE, Bleicher S, et al. Synthetic cannabinoids in hair-Prevalence of use in abstinence control programs for driver's license regranting in Germany. *Drug Test Anal*. 2023;1-14. DOI: 10.1002/dta.3578.

[39]   Larabi IA, Fabresse N, Etting I, et al. Prevalence of New Psychoactive Substances (NPS) and conventional drugs of abuse (DOA) in high risk populations from Paris (France) and its suburbs: A cross sectional study by hair testing (2012-2017). *Drug Alcohol Depend*. 2019;204:107508. DOI: 10.1016/j.drugalcdep.2019.06.011.

[40]   Fels H, Musshoff F, Graw M, DeVol D, Wagner T, Holzer A. Frequency of new psychoactive substances in hair and urine samples of individuals subject to drug testing in driving license regranting-A toxicological perspective. *Drug Test Anal*. 2023;15(8):919-926. DOI: 10.1002/dta.3533.

[41]   Norman C, Halter S, Haschimi B, et al. A transnational perspective on the evolution of the synthetic cannabinoid receptor agonists market: Comparing prison and general populations. *Drug Test Anal.* 2021;13(4):841-852. DOI: 10.1002/dta.3002.

[42]   Fan X, Zhang J, Fu X, et al. Analysis of synthetic cannabinoids in wastewater of major cities in China. *Sci Total Environ*. 2022;827:154267. DOI: 10.1016/j.scitotenv.2022.154267.

[43]   United Nations Office on Drugs and Crime (UNODC), Early Warning Advisory. Current NPS Threats, Volume V. 2022. https://www.unodc.org/documents/scientific/Current_NPS_Threats_V.pdf. Accessed January 25, 2024.

[44]   Franz F, Jechle H, Angerer V, Pegoro M, Auwärter V, Neukamm MA. Synthetic cannabinoids in hair - Pragmatic approach for method updates, compound prevalences and concentration ranges in authentic hair samples. *Anal Chim Acta.* 2018;1006:61-73. DOI: 10.1016/j.aca.2017.12.029.

[45]   Salomone A, Palamar JJ, Gerace E, Di Corcia D, Vincenti M. Hair Testing for Drugs of Abuse and New Psychoactive Substances in a High-Risk Population. *J Anal Toxicol.* 2017;41(5):376-381. DOI: 10.1093/jat/bkx020.

[46]   Adamowicz P, Gieroń J, Gil D, Lechowicz W, Skulska A, Tokarczyk B. The prevalence of new psychoactive substances in biological material - a three-year review of casework in Poland. *Drug Test Anal.* 2016;8(1):63-70. DOI: 10.1002/dta.1924.

[47]   Ji JJ, Xu D, Yan H, Xiang P, Shen M. LC-MS-MS Determination of 88 Psychotropic Drugs in 1,865 Hair Samples from Addicts in Drug Abstinence. *J Anal Toxicol*. 2023;47(1):52-58. DOI: 10.1093/jat/bkac024.

[48]   Diamanti K, Aalizadeh R, Alygizakis N, Galani A, Mardal M, Thomaidis NS. Wide-scope target and suspect screening methodologies to investigate the occurrence of new psychoactive substances in influent wastewater from Athens. *Sci Total Environ*. 2019;685:1058-1065. DOI: 10.1016/j.scitotenv.2019.06.173.

[49]   O'Rourke CE, Subedi B. Occurrence and Mass Loading of Synthetic Opioids, Synthetic Cathinones, and Synthetic Cannabinoids in Wastewater Treatment Plants in Four U.S. Communities. *Environ Sci Technol*. 2020;54(11):6661-6670. DOI: 10.1021/acs.est.0c00250.

5.6 Supplementary Material

Table S1. Semi-systematic and IUPAC names, common synonyms, molecular formulas, monoisotopic masses and chemical structures listed for additional target analytes, compared to Part A of this study.

Semi-systematic substance name / Synonyms / IUPAC name	Molecular formula	Monoisotopic mass [Da]	Chemical structure
ADB-5Br-INACA *N*-(1-Amino-3,3-dimethyl-1-oxobutan-2-yl)-5-bromo-1*H*-indazole-3-carboxamide	$C_{14}H_{17}BrN_4O_2$	353.0535	
ADB-FUBIACA ADB-FUBIATA AD-18 *N*-[1-Amino-3,3-dimethyl-1-oxobutan-2-yl]-1-[(4-fluorophenyl)methyl]-1*H*-indole-3-carboxamide	$C_{23}H_{26}FN_3O_2$	395.2009	
BZO-4en-POXIZID 4en-pentyl MDA-19 (Z)-*N'*-(2-Oxo-1-(pent-4-en-1-yl)indolin-3-ylidene)benzohydrazide	$C_{20}H_{19}N_3O_2$	333.1477	
ADB-BUTINACA ADB-BINACA *N*-[1-Amino-3,3-dimethyl-1-oxobutan-2-yl]-1-butyl-1*H*-indazole-3-carboxamide	$C_{18}H_{26}N_4O_2$	330.2056	

Chapter 5

221

Table S2. A detailed list of all target analytes assigned to conventional drugs, comprising information on the chemical drug class, suppliers of reference standards, and solvents used for storage of the standards.

Substance standard	Drug class	Supplier	Solvent
Amphetamine	Amphetamine-type stimulants	LGC Standards	MeOH
Methamphetamine	Amphetamine-type stimulants	LGC Standards	MeOH
3,4-Methylenedioxyamphetamine (MDA)	Amphetamine-type stimulants	LGC Standards	MeOH
3,4-Methylenedioxymethamphetamine (MDMA)	Amphetamine-type stimulants	Sigma Aldrich	MeOH
Ethylphenidate	Amphetamine-type stimulants	Sigma Aldrich	MeOH
Methylphenidate	Amphetamine-type stimulants	LGC Standards	MeOH
Methylendioxypyrovalerone (MDPV)	Amphetamine-type stimulants	LGC Standards	MeOH
Cocaine	Cocaine and metabolites	LGC Standards	ACN
Benzoylecgonine	Cocaine and metabolites	LGC Standards	MeOH
Norcocaine	Cocaine and metabolites	Sigma Aldrich	ACN
Cocaethylene	Cocaine and metabolites	LGC Standards	ACN
Lysergic acid diethylamide (LSD)	Hallucinogens	LGC Standards	ACN
N,N-Dimethyltryptamine (DMT)	Hallucinogens	Lipomed	MeOH
Heroin	Opioids and analgesics	LGC Standards	ACN
6-Monoacetylmorphine (6-MAM)	Opioids and analgesics	LGC Standards	ACN
Morphine	Opioids and analgesics	LGC Standards	MeOH
Acetylcodeine	Opioids and analgesics	LGC Standards	ACN
Codeine	Opioids and analgesics	Sigma Aldrich	MeOH
Dihydrocodeine	Opioids and analgesics	Sigma Aldrich	MeOH
Fentanyl	Opioids and analgesics	LGC Standards	MeOH
Methadone	Opioids and analgesics	LGC Standards	MeOH
2-Ethylidene-1,5-dimethyl-3,3-diphenylpyrrolidine (EDDP)	Opioids and analgesics	LGC Standards	MeOH
Buprenorphine	Opioids and analgesics	LGC Standards	MeOH
Norbuprenorphine	Opioids and analgesics	Lipomed	MeOH
Ketamine	Opioids and analgesics	LGC Standards	MeOH
Norketamine	Opioids and analgesics	Lipomed	MeOH
Methoxetamine	Opioids and analgesics	LGC Standards	MeOH
Oxycodone	Opioids and analgesics	LGC Standards	MeOH
Hydrocodone	Opioids and analgesics	LGC Standards	MeOH
Oxymorphone	Opioids and analgesics	LGC Standards	MeOH
Hydromorphone	Opioids and analgesics	LGC Standards	MeOH
Tramadol	Opioids and analgesics	LGC Standards	MeOH
O-Desmethyl-*cis*-tramadol	Opioids and analgesics	Sigma Aldrich	MeOH
Tilidine	Opioids and analgesics	Lipomed	MeOH
Nortilidine	Opioids and analgesics	LGC Standards	MeOH
Tapentadol	Opioids and analgesics	Lipomed	MeOH
Naloxone	Opioids and analgesics	LGC Standards	MeOH
Cannabinol (CBN)	Phytocannabinoids	LGC Standards	MeOH
Cannabidiol (CBD)	Phytocannabinoids	LGC Standards	MeOH
(−)-*trans*-Δ^9-tetrahydrocannabinol (Δ^9-THC)	Phytocannabinoids	LGC Standards	MeOH

	Internal standard			
Amphetamine-D5	Amphetamine-type stimulants	Sigma Aldrich	MeOH
Methamphetamine-D5	Amphetamine-type stimulants	LGC Standards	MeOH
MDMA-D5	Amphetamine-type stimulants	Sigma Aldrich	MeOH
Cocaine-D3	Cocaine and metabolites	LGC Standards	ACN
Benzoylecgonine-D3	Cocaine and metabolites	LGC Standards	MeOH
Heroin-D9	Opioids and analgesics	LGC Standards	ACN
MAM-D3	Opioids and analgesics	Sigma Aldrich	ACN
Morphine-D3	Opioids and analgesics	LGC Standards	MeOH
Dihydrocodeine-D6	Opioids and analgesics	LGC Standards	MeOH
Fentanyl-D5	Opioids and analgesics	LGC Standards	MeOH
Mathadone-D3	Opioids and analgesics	LGC Standards	MeOH
Tramadol-D6	Opioids and analgesics	LGC Standards	MeOH
(-)-Δ^9-THC-D3	Phytocannabinoids	Sigma Aldrich	MeOH

MeOH = methanol; ACN = acetonitrile

Table S3. Details of the programmed sampling parameters of the liquid sampling device.

Sampling parameters for a city district in Munich (Location 2)	
Sample containers	12 sample containers (1 L capacity each)
Sampling interval	12 minutes (50 mL sampling volume) → 4 h composite samples in each sample container
Sampling time	48 hours a) Sept 21, 2021 - Sept 23, 2021 (2 p.m. - 2 p.m.) b) Sept 24, 2021 - Sept 26, 2021 (2 p.m. - 2 p.m.)

Table S4. Installation and deinstallation dates and times for PDMS rods placed at three different locations in a city district of Munich.

Index	Installation date and time	Deinstallation date and time
September 21-24, 2021 (weekdays) Location 2	September 21, 2021 / 12.30 p.m.	September 24, 2021 / 1.30 p.m.
Location 3	September 21, 2021 / 2.30 p.m.	September 24, 2021 / 2.30 p.m.
Location 4	September 21, 2021 / 3.30 p.m.	September 24, 2021 / 3.00 p.m.
September 24-27, 2021 (weekend) Location 2	September 24, 2021 / 1.30 p.m.	September 27, 2021 / 10.30 a.m.

Chapter 5

Table S5. Installation and deinstallation dates and times for PDMS rods placed in the main WWTP in Munich for different periods of time.

Index	Installation date and time	Deinstallation date and time
Weekend 1h		February 04, 2022 / 11.30 a.m.
Weekend 74h	February 04, 2022 / 10.30 a.m.	February 07, 2022 / 12.30 p.m.
Weekend 95h		February 08, 2022 / 09.30 a.m.
Weekday 1h		February 07, 2022 / 1.30 p.m.
Weekday 3h	February 07, 2022 / 12.30 p.m.	February 07, 2022 / 3.30 p.m.
Weekday 21h		February 08, 2022 / 09.30 a.m.

Table S6. MRM parameters including the precursor ion (Q1) and the four most prominent product ions (Q3), declustering potential (DP), entrance potential (EP), collision cell entrance potential (CEP), collision energy (CE) and collision cell exit potential (CXP) for the newly added SCRAs of the analytical method. The most prominent product ion for each analyte is indicated as underlined Q3 ion, and the corresponding retention times are listed below the respective substance.

Analyte	Q1 m/z	Q3 m/z	DP in V	EP in V	CE in V	CXP in V
ADB-5Br-INACA (^{79}Br) 1.23 min	353.0	<u>308.0</u>	50	10	19	22
	353.0	336.1	50	10	11	14
	353.0	222.9	50	10	41	24
	353.0	240.0	50	10	29	20
ADB-5Br-INACA (^{81}Br) 1.23 min	355.0	<u>310.0</u>	71	10	23	4
	355.0	337.8	71	10	11	16
	355.0	224.8	71	10	39	26
	355.0	242.0	71	10	29	14
ADB-FUBIACA 3.13 min	396.1	<u>378.9</u>	66	10	13	26
	396.1	351.0	66	10	19	26
	396.1	238.1	66	10	33	20
	396.1	109.0	66	10	57	16
BZO-4en-POXIZID 5.54 min	334.1	<u>105.0</u>	101	10	21	14
	334.1	77.1	101	10	73	12
	334.1	51.0	101	10	113	22

continued	334.1	50.0	101	10	127	24
	331.1	<u>201.0</u>	26	10	33	10
ADB-BUTINACA 2.84 min	331.1	286.1	26	10	19	14
	331.1	314.1	26	10	13	18
	331.1	145.0	26	10	53	16

Chapter 5

Table S7. Optimization of the re-extraction procedure for conventional drugs from PDMS rods. Comparison of different extractants (isohexane/ethyl acetate (9/1, v/v) and methanol) for different representative substances, each conducted with one half of the PDMS rod (2 cm length). Compared area values indicate total areas after the two-fold extraction. All experiments were performed in duplicates during two different sampling periods (cf. PDMS 1 and PDMS 2).

Substance	Amphetamine				Methamphetamine				MDMA			
Sample	PDMS 1		PDMS 2		PDMS 1		PDMS 2		PDMS 1		PDMS 2	
Extraction solvent	Isohex/ EtOAc	MeOH	Isohex/ EtOAc	MeOH	Isohex/ EtOAc	MeOH	Isohex/ EtOAc	MeOH	Isohex/ EtOAc	MeOH	Isohex/ EtOAc	MeOH
Abs. recoveries (Area)	3.0e5	4.6e5	1.6e5	3.2e5	3.3e4	9.7e4	1.2e5	3.1e5	3.5e4	1.3e5	3.4e5	4.3e5
Rel. recoveries	65%	100%	50%	100%	34%	100%	39%	100%	27%	100%	79%	100%
Superior solvent	MeOH				MeOH				MeOH			
Substance	Cocaine				Norcocaine				Cocaethylene			
Sample	PDMS 1		PDMS 2		PDMS 1		PDMS 2		PDMS 1		PDMS 2	
Extraction solvent	Isohex/ EtOAc	MeOH	Isohex/ EtOAc	MeOH	Isohex/ EtOAc	MeOH	Isohex/ EtOAc	MeOH	Isohex/ EtOAc	MeOH	Isohex/ EtOAc	MeOH
Abs. recoveries (Area)	5.2e7	3.0e7	4.8e7	3.5e7	2.9e5	4.1e5	3.7e5	6.1e5	3.2e6	1.7e6	5.2e6	3.0e6
Rel. recoveries	100%	58%	100%	73%	71%	100%	61%	100%	100%	53%	100%	58%
Superior solvent	Isohex/EtOAc				MeOH				Isohex/EtOAc			

*PDMS 1 = PDMS sampling period from September 21-24, 2021 in Munich; PDMS 2 = PDMS sampling period from September 24-27, 2021 in Munich.

Table S8. Positive identifications of conventional drugs at three different locations within a city district of Munich, with installation (September 21, 2021) and deinstallation (September 24, 2021) time points for PDMS rods at each location.

Conventional drugs (PDMS sampling)			
Sept 21, 2021 - Sept 24, 2021	Location 2 (M2) 12.30 p.m. - 1.30 p.m.	Location 3 (M3) 2.30 p.m. - 2.30 p.m.	Location 4 (M4) 3.30 p.m. - 3.00 p.m.
Amphetamine	+	+	+
Methamphetamine	+	+	+
MDMA	+	+	+
Methylphenidate	+	+	+
Cocaine/Benzoylecgonine	+/+	+/+	+/+
Norcocaine/Cocaethylene	+/+	+/+	+/+
Methadone/EDDP	+/+	+/+	+/+
Buprenorphine	+	+	-
Fentanyl	+	+	+
Tramadol	+	+	+
O-Desmethyl-*cis*-tramadol	+	+	+
Tapentadol	+	+	+
Tilidine/Nortilidine	+/+	+/+	+/+
Ketamine	+	+	+
THC/CBN/CBD	+/+/+	+/+/+	+/+/+
Heroin	-	+	-
Acetylcodeine	-	+	-
Dihydrocodeine	-	+	-

Table S9. An overview of conventional drugs detected in a city district of Munich, their detection frequency and the corresponding time intervals. The wastewater samples were collected during the period of September 21-23, 2021 (48 h, weekdays).

Conventional drug (licit / illicit)	Detection frequency	Detection time interval
Methamphetamine	Sample 2	Sept 21, 2021: 6 - 10 p.m.
	Sample 7	Sept 22, 2021: 2 - 6 p.m.
MDMA	Samples 1 – 6	Sept 21, 2021 (2 p.m). - Sept 22, 2021 (2 p.m.)
	Sample 10	Sept 23, 2021: 2 - 6 a.m.
Methylphenidate	Samples 1 - 3	Sept, 21, 2021 (2 p.m.) - Sept 22, 2021 (2 a.m.)
	Samples 6 - 10	Sept 22, 2021 (10 a.m.) - Sept 23, 2021 (6 a.m.)
Cocaine Cocaethylene Norcocaine	All samples	Sept 21, 2021 (2 p.m.) - Sept 23, 2021 (2 p.m.)
Benzoylecgonine	Sample 1	Sept 21, 2021: 2 - 6 p.m.
	Sample 4	Sept 22, 2021: 2 - 6 a.m.
Codeine	All samples	Sept 21, 2021 (2 p.m.) - Sept 23, 2021 (2 p.m.)
Dihydrocodeine	Sample 5	Sept 22, 2021: 6 - 10 a.m.
	Sample 10	Sept 23, 2021: 2 - 6 a.m.
	Sample 12	Sept 23, 2021: 10 a.m. - 2 p.m.

Chapter 5

Oxycodone Methadone EDDP	All samples	Sept 21, 2021 (2 p.m.) - Sept 23, 2021 (2 p.m.)
Buprenorphine	Samples 1-6	Sept 21, 2021 (2 p.m.) - Sept 22, 2021 (2 p.m.)
	Samples 8-12	Sept 22, 2021 (6 p.m.) - Sept 23, 2021 (2 p.m.)
Naloxone Fentanyl Tramadol *O*-Desmethyl-*cis*-tramadol Tapentadol Tilidine Nortilidine	All samples	Sept 21, 2021 (2 p.m.) - Sept 23, 2021 (2 p.m.)
Ketamine	All samples	Sept 21, 2021 (2 p.m.) - Sept 23, 2021 (2 p.m.)
Norketamine	Samples 1-5	Sept 21, 2021 (2 p.m.) - Sept 22, 2021 (10 a.m.)
	Samples 9-11	Sept 22, 2021 (10 p.m.) - Sept 23, 2021 (10 a.m.)
THC CBD	All samples	Sept 21, 2021 (2 p.m.) - Sept 23, 2021 (2 p.m.)

Table S10. Lower limit of quantifications (LLOQs) of individual conventional drugs in hair, above which positive substance identification was assumed. The corresponding internal standard for quantification is indicated for each substance. The drugs of abuse listed were included in data evaluation for elucidation of SCRA user profiles.

Drug of abuse / Metabolite	Internal standard	LLOQ [ng/mg hair]
Amphetamine (AMP)	Amphetamine-D5	0.05
Methamphetamine (mAMP)	Methamphetamine-D5	0.05
3,4-Methylenedioxy-amphetamine (MDA)	MDMA-D5	0.05
3,4-Methylenedioxy-methamphetamine (MDMA)	MDMA-D5	0.05
Cocaine (COC)	Cocaine-D3	0.1
Benzoylecgonine (BE)	Benzoylecgonine-D3	0.05
Norcocaine (NorCOC)	Cocaine-D3	0.05
Cocaethylene (CE)	Cocaine-D3	0.05
Heroin (HER)	Heroin-D9	0.1
6-Monoacetylmorphine (6-MAM)	MAM-D3	0.1
Lysergic acid diethylamide (LSD)	Fentanyl-D5	0.02
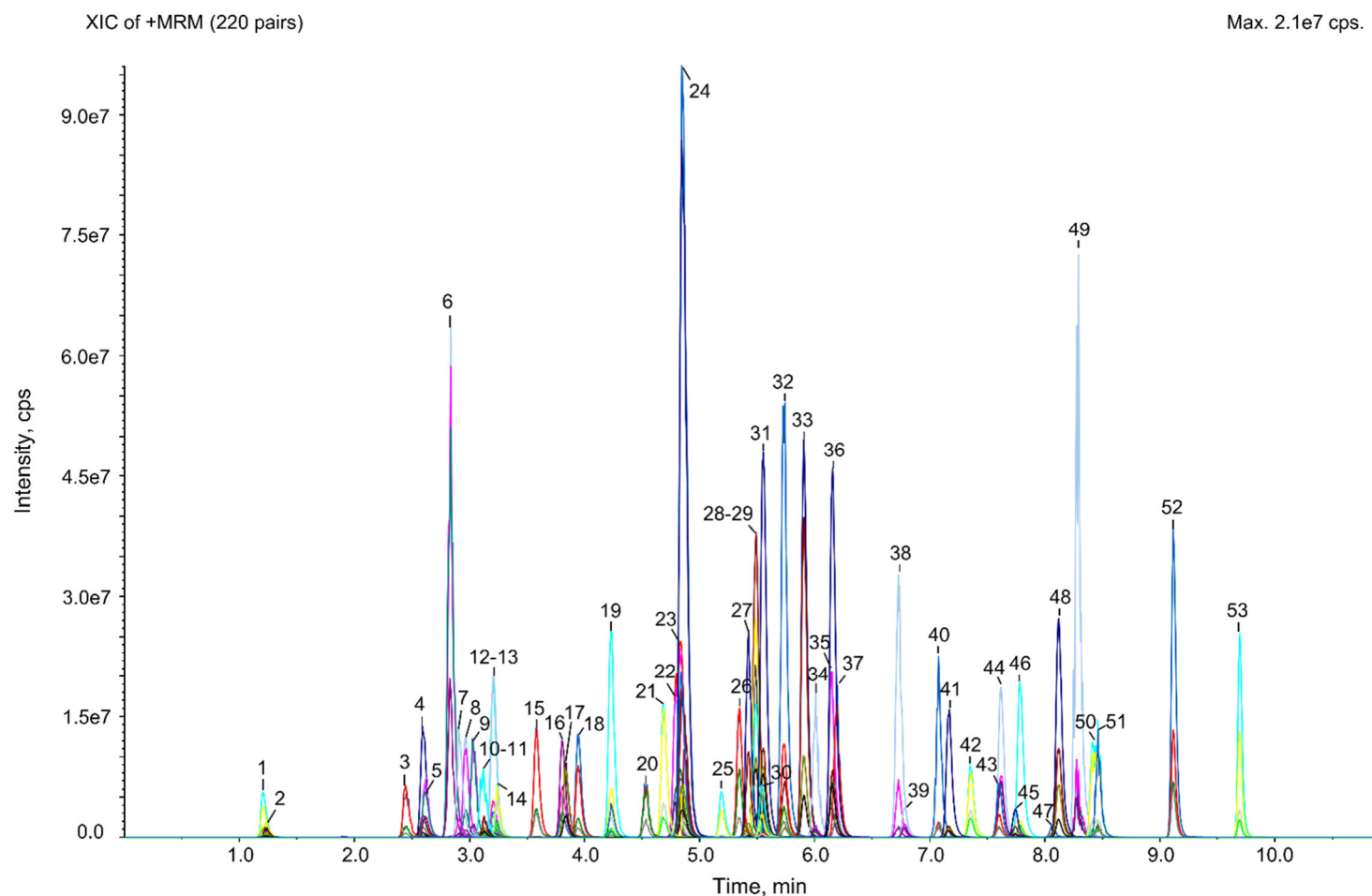
Figure S1. UHPLC-MS/MS chromatogram of all target SCRAs, phytocannabinoids and their selected human metabolites in acetonitrile/water (1/1, v/v) solution. 1: 4F-MDMB-BINACA N-(butanoic acid) dimethylbutanoic acid; 2: ADB-5Br-INACA; 3: 5F-ADBICA; 4: 4F-MDMB-BICA dimethylbutanoic acid; 5: AB-FUBINACA; 6: ADB-BINACA; 7: PB-22 N-pentanoic acid; 8: 4F-MDMB-BINACA dimethylbutanoic acid; 9: ADB-4en-PINACA; 10: Cumyl-PeGaClone N-pentanoic acid; 11: ADB-FUBIACA; 12: 5F-MDMB-PICA dimethylbutanoic acid; 13: 5F-MDMB-P7AICA; 14: ADB-FUBINACA; 15: 5F-ADB dimethylbutanoic acid; 16: 5F-Cumyl-P7AICA; 17: AB-CHMINACA; 18: MDMB-4en-PINACA dimethylbutanoic acid; 19: 4F-MDMB-BICA; 20: ADB-CHMINACA; 21: Cumyl-4CN-BINACA; 22: 5F-AMB; 23: 4F-MDMB-BINACA; 24: 5F-MDMB-PICA / 5F-EMB-PICA; 25: THC-COOH; 26: AMB-FUBINACA; 27: MDMB-FUBICA; 28: 5F-ADB; 29: 5F-EMB-PINACA; 30: BZO-4en-POXIZID; 31: 5F-Cumyl-PICA; 32: 5F-PB-22; 33: MDMB-4en-PINACA; 34: 5F-Cumyl-PeGaClone; 35: 5F-EDMB-PINACA; 36: Cumyl-CBMICA; 37: 5F-Cumyl-PINACA; 38: MDMB-CHMICA; 39: CBD; 40: Cumyl-PeGaClone; 41: 4F-ABINACA; 42: FUB-144; 43: CBN; 44: MAM-2201; 45: (-)-Δ^9-THC; 46: 5F-AKB-48; 47: Cumyl-CH-MeGaClone; 48: JWH-018; 49: Cumyl-BC[2.2.1]HpMeGaClone; 50: Cumyl-BC[2.2.1]HpMINACA; 51: MDMB-CHMCZCA; 52: JWH-210; 53: EG-018.
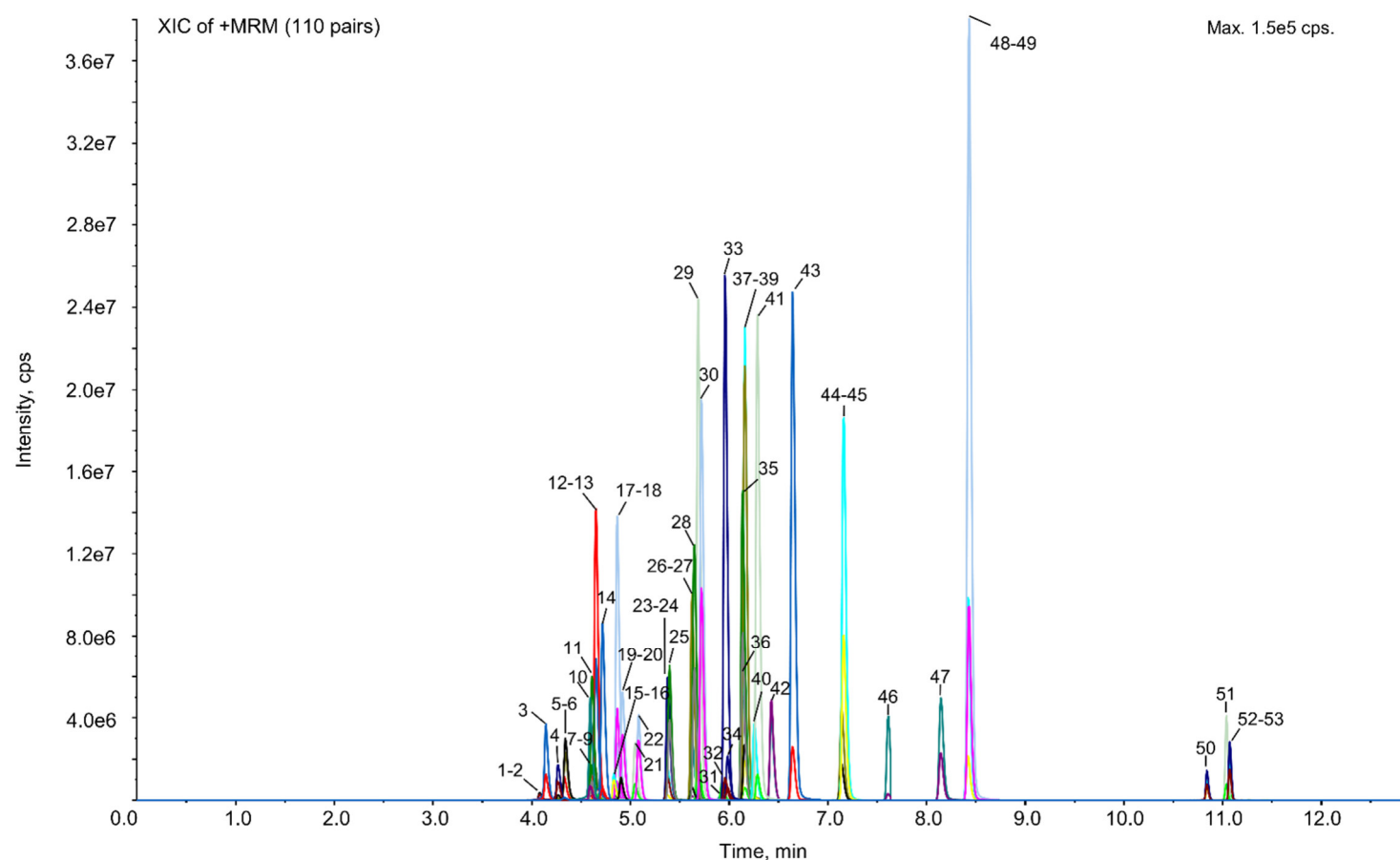
Figure S2. UHPLC-MS/MS chromatogram of hair spiked with all target analytes and deuterated standards at a concentration of 4 ng/mg hair (high QC). 1: Morphine-D3 (4.08 min); 2: Morphine (4.09 min); 3: Oxymorphone (4.15 min); 4: Hydromorphone (4.27 min); 5: Amphetamine-D5 (4.33 min); 6: Amphetamine (4.35 min); 7: Dihydrocodeine-D6 (4.60 min); 8: Dihydrocodeine (4.61 min); 9: Codeine (4.68 min); 10: Naloxone (4.60 min); 11: MDA (4.61 min); 12: Methamphetamine-D5 (4.65 min); 13: Methamphetamine (4.65 min); 14: *O*-Desmethyl-*cis*-tramadol (4.72 min); 15: MAM-D3 (4.83 min); 16: 6-MAM (4.84 min); 17: MDMA-D5 (4.86 min); 18: MDMA (4.87 min); 19: Oxycodone (4.91 min); 20: *N,N*-Dimethyltryptamine (4.92 min); 21: Hydrocodone (5.05 min); 22: Norketamine (5.09 min); 23: Benzoylecgonine-D3 (5.38 min); 24: Benzoylecgonine (5.38 min); 25: Ketamine (5.40 min); 26: Tramadol-D6 (5.62 min); 27: Tramadol (5.63 min); 28: Tapentadol (5.65 min); 29: Methylphenidate (5.69 min); 30: Methoxetamine (5.72 min); 31: Heroin-D9 (5.91 min); 32: Heroin (5.93 min); 33: Nortilidine (5.96 min); 34: Acetylcodeine (5.99 min); 35: Norcocaine (6.14 min); 36: MDPV (6.14 min); 37: Cocaine-D3 (6.16 min); 38: Cocaine (6.16 min); 39: Ethylphenidate (6.16 min); 40: Norbuprenorphine (6.26 min); 41: Tilidine (6.29 min); 42: LSD (6.43 min); 43: Cocaethylene (6.65 min); 44: Fentanyl-D5 (7.14 min); 45: Fentanyl (7.16 min); 46: Buprenorphine (7.61 min); 47: EDDP (8.15 min); 48: Methadone-D3 (8.42 min); 49: Methadone (8.43 min); 50: CBD (10.84 min); 51: CBN (11.04 min); 52: (-)-Δ⁹-THC-D3 (11.07 min); 53: (-)-Δ⁹-THC (11.08 min).

Table S11. Overview of the screening results for all SCRA positive cases with young people under the age of 21 (20 cases), showing demographic characteristics, qualitative SCRA results (SCRAs identified) and quantitative results on cannabis and remaining conventional drugs for segments examined.

Age < 21 years (SCRA positive cases)									
Subject						SCRAs	Conventional drugs of abuse	Cannabis	Other drugs
Case	Sampling date	Gender	Age (y)	Hair type	Segment [cm]	Qualitative results	[ng/mg]	THC-COOH [pg/mg]	[ng/mg]
								THC / CBD / CBN [ng/mg]	
1	Apr 2021	M	20	Scalp	0 - 3	-	AMP (0.31) MDMA (0.21)	8.40	-
								7.10 / - / 0.97	
					3 - 6	MDMB-4en-PINACA	AMP (0.86) MDMA (0.32)	8.20	KET (0.04)
								> 20.0 / 0.23 / 2.30	
					6 - 9	MDMB-4en-PINACA	AMP (1.40) MDMA (0.56)	7.90	KET (0.08)
								> 20.0 / 0.40 / 3.50	
2	Mar 2021	M	19	Scalp	0 - 3	MDMB-4en-PINACA 4F-MDMB-BINACA Cumyl-BC[2.2.1]-HpMINACA	COC (0.20) / BE (0.06)	10.00	COD (0.70) TRA (0.30) TIL (1.30) / NorTIL (1.10)
								10.0 / 1.70 / 0.70	
					3 - 6	MDMB-4en-PINACA 4F-MDMB-BINACA Cumyl-BC[2.2.1]-HpMINACA	COC (0.20) / BE (0.06)	11.00	COD (0.30) TRA (0.70) TIL (1.00) / NorTIL (0.70)
								15.0 / 3.60 / 0.90	
3	Apr 2021	M	17	Scalp	0 - 3.5	MDMB-4en-PINACA 4F-MDMB-BICA	MDMA (0.27)	11.00	-
								2.00 / 0.10 / 0.31	
4	Jun 2021	M	20	Scalp	0 - 3	-	-	3.80	-
								0.29 / 0.34 / -	

					3 - 6	MDMB-4en-PINACA 4F-MDMB-BICA	-	2.10	-
								0.50 / 0.57 / 0.11	
					6 - 11	MDMB-4en-PINACA 4F-MDMB-BICA	-	1.80	-
								0.43 / 0.52 / 0.14	
5	May 2021	M	18	Scalp	0 - 4	MDMB-4en-PINACA	AMP (0.57) MDMA (0.09) COC (> 20.0) / BE (8.50) / NorCOC (2.50) / CE (0.46)	1.20	TIL (0.02) / NorTIL (0.22) KET (1.50) / NorKET (0.04)
								0.41 / - / 0.12	
					4 - 8	-	AMP (0.10) COC (14.00) / BE (1.10) / NorCOC (0.35) / CE (0.21)	3.60	TIL (0.02) / NorTIL (0.21) KET (0.19) / NorKET (0.02)
								- / - / -	
6	Jun 2021	F	20	Scalp	0 - 3	MDMB-4en-PINACA	AMP (0.38) mAMP (0.75) COC (1.60) / BE (0.14) HER (0.48) / 6-MAM (2.10)	-	MOR (0.69) COD (0.20) AcCOD (0.25) HMOR (0.04) FEN (0.01) TRA (0.34) NorTIL (0.03)
								- / - / -	
					3 - 6	MDMB-4en-PINACA	AMP (0.45) mAMP (0.92) COC (4.10) / BE (0.53) HER (0.97) / 6-MAM (3.90)	0.12	MPD (0.05) MOR (0.48) COD (0.16) AcCOD (0.61) HMOR (0.03) FEN (0.01) TRA (0.08) NorTIL (0.02)
								0.21 / - / -	

					6 - 9	MDMB-4en-PINACA	AMP (0.82) mAMP (1.90) MDMA (0.07) COC (9.70) / BE (1.20) / NorCOC (0.06)	0.32	MPD (0.10) MOR (0.40) COD (0.14) AcCOD (1.20) HMOR (0.02) FEN (0.03) TRA (0.09) TIL (0.01) / NorTIL (0.01)
							HER (1.90) / 6-MAM (6.00)	0.53 / 0.14 / 0.23	
7	Aug 2021	M	18	Scalp	0 - 2.5	MDMB-4en-PINACA	AMP (0.06)	1.60	-
								0.66 / - / 0.18	
8	Jan 2022	M	20	Scalp	0 - 2.5	JWH-210 ADB-BUTINACA BZO-4en-POXIZID	COC (8.60) / BE (1.30) / NorCOC (0.12) / CE (0.26)	-	TIL (0.03) / NorTIL (0.24)
								- / - / -	
					2.5 - 5	JWH-210	mAMP (0.05) COC (> 20.0) / BE (3.30) / NorCOC (0.25) / CE (0.80)	-	TIL (0.04) / NorTIL (0.46)
								0.47 / - / -	
9	Apr 2022	M	20	Scalp	0 - 3	Cumyl-4CN-BINACA MDMB-4en-PINACA 4F-MDMB-BICA	AMP (0.16) MDMA (0.57)	3.00	-
								1.40 / - / 0.35	
					3 - 6	Cumyl-4CN-BINACA MDMB-4en-PINACA 4F-MDMB-BICA	AMP (0.22) MDMA (0.69)	1.70	TRA (0.06)
								2.00 / 0.11 / 0.60	
10	Aug 2022	M	15	Scalp	0 - 0.5	AMB-FUBINACA JWH-210	-	n.a. - / - / -	-
					0.5 - 1	AMB-FUBINACA JWH-210	mAMP (0.07)	n.a. - / - / -	-
					1 - 1.5	AMB-FUBINACA JWH-210	mAMP (0.09)	n.a. - / - / -	-

233

					1.5 - 2	AMB-FUBINACA JWH-210	mAMP (0.12)	n.a. / - / - / -	-
					2 - 2.5	AMB-FUBINACA JWH-210	mAMP (0.15)	n.a. / - / - / -	-
11	Sep 2022	M	19	Scalp	0 - 3.5	5F-MDMB-PICA / 5F-EMB-PICA	AMP (0.06) MDMA (0.08) COC (1.20) / BE (0.11)	14.00 / 0.27 / - / 0.18	COD (0.37) HCOD (0.03)
12	Sep 2022	M	18	Scalp	0 - 2.5	MDMB-4en-PINACA 4F-MDMB-BICA	COC (> 20.0) / BE (5.10) / NorCOC (0.82)	12.00 / 2.80 / 0.10 / 0.24	DHC (0.30) TRA (0.05) KET (0.09)
					2.5 - 5.5	MDMB-4en-PINACA 4F-MDMB-BICA	COC (> 20.0) / BE (4.30) / NorCOC (0.47)	9.00 / 3.70 / 0.12 / 0.36	DHC (0.07) TRA (0.32) / O-TRA (0.08) KET (0.18)
13	Sep 2022	M	18	Scalp	0 - 3	4F-MDMB-BICA ADB-BUTINACA JWH-210 MDMB-4en-PINACA	AMP (0.93) MDMA (0.76) COC (> 20.0) / BE (3.90)	15.00 / 19.00 / 3.60 / 3.80	KET (0.64) / NorKET (0.04)
					3 - 6	4F-MDMB-BICA ADB-BUTINACA JWH-210 MDMB-4en-PINACA	AMP (2.60) MDMA (1.80) COC (> 20.0) / BE (8.40) / CE (0.05) 6-MAM (0.25)	13.00 / > 20.0 / 6.10 / 6.30	KET (1.90) / NorKET (0.07)
14	Sep 2022	M	17	Scalp	0 - 3	MDMB-4en-PINACA 5F-ADB	AMP (0.31) MDMA (0.13) COC (3.30) / BE (0.32) / NorCOC (0.06)	- / - / - / -	-

15	Oct 2022	M	18	Scalp	0 - 2.5	JWH-210	-	1.40 0.57 / - / 0.10	-
					2.5 - 5.5	JWH-210	-	0.77 0.84 / - / 0.20	-
16	Nov 2022	M	19	Scalp	0 - 3	4F-MDMB-BICA	MDMA (0.31) 6-MAM (0.83)	8.80 0.71 / - / -	MOR (0.17) HCOD (0.06) OXY (0.33) TRA (0.13) TIL (0.64) / NorTIL (3.90)
					3 - 6	4F-MDMB-BICA ADB-BUTINACA	AMP (0.20) mAMP (0.08) MDMA (0.28) COC (0.11) HER (0.23) / 6-MAM (2.30)	6.80 1.20 / - / 0.12	MOR (0.21) AcCOD (0.22) HCOD (0.10) OXY (0.15) TRA (0.20) TIL (0.70) / NorTIL (3.30) KET (0.04)
17	Dec 2022	M	18	Scalp	0 - 3	JWH-210	COC (0.11)	5.70 2.10 / 0.16 / 0.20	TIL (0.12) / NorTIL (0.78)
					3 - 6	JWH-210	COC (0.15)	3.10 3.80 / 0.22 / 0.33	TIL (0.16) / NorTIL (0.61)
18	Dec 2022	F	17	Scalp	0 - 3	-	AMP (0.11) MDMA (0.09) COC (0.15)	- 0.42 / 0.17 / -	-
					3 - 6	MDMB-4en-PINACA	COC (0.31)	- 1.20 / 0.30 / 0.19	-

19	Dec 2022	M	18	Scalp	0 - 3.5	ADB-BUTINACA JWH-210	AMP (0.22) MDMA (0.31) COC (0.47)	8.50	TIL (0.02) / NorTIL (0.08) KET (0.02)
								7.20 / 0.22 / 0.73	
					3.5 - 7	ADB-BUTINACA JWH-210	AMP (0.58) MDMA (0.54) COC (1.30) / BE (0.80)	4.90	MPD (0.11) TIL (0.01) / NorTIL (0.07) KET (0.06)
								12.00 / 0.41 / 1.60	
20	Jan 2023	M	20	Scalp	0 - 3	ADB-BUTINACA JWH-210	MDMA (0.98)	0.40	MPD (0.05)
								0.13 / - / -	
					3 - 6	ADB-BUTINACA JWH-210	MDMA (1.20)	0.20	MPD (0.09)
								0.27 / - / -	

AMP = Amphetamine; mAMP = Methamphetamine; MDMA = 3,4-Methylenedioxymethamphetamine; MPD = Methylphenidate; COC = Cocaine; BE = Benzoylecgonine; NorCOC = Norcocaine; CE = Cocaethylene; HER = Heroin; 6-MAM = 6-Monoacetylmorphine; MOR = Morphine; COD = Codeine; AcCOD = Acetylcodeine; DHC = Dihydrocodeine; OXY = Oxycodone; HCOD = Hydrocodone; HMOR = Hydromorphone; FEN = Fentanyl; TRA = Tramadol; O-TRA = *O*-Desmethyl-*cis*-tramadol; TIL = Tilidine; NorTIL = Nortilidine; KET = Ketamine; NorKET = Norketamine; THC = Δ^9-Tetrahydrocannabinol; CBD = Cannabidiol; CBN = Cannabinol; n.a. = not analyzed.

Table S12. Summary of the positivity rates (prevalence) for cannabis (THC-COOH) and other conventional drugs, which were detected as co-substances among SCRA users under the age of 21. For persons tested positive, the proportion of frequent or regular drug users was calculated by means of statistical data from our laboratory.

Age < 21 years (SCRA positive cases)						
Substance	THC-COOH	AMP	mAMP	MDMA	COC+ BE + NorCOC + CE	HER + 6-MAM
Number of positive persons	16	11	4	12	12	3
Total number of persons	19	20				
Positivity rate (Positive persons) [%]	84	55	20	60	60	15
Frequent or regular use* [%]	75	18	25	33	58	67

*Correlation of concentration levels with frequency of drug use was based on statistical data of forensic hair samples examined in our laboratory. The results depicted include values above our statistical median concentration (> 50th percentile) for the particular drug of abuse, corresponding to frequent or regular drug use.

5.7 Unpublished data: Analytical challenges associated with SCRAs

5.7.1 Comparison of hair sample extraction procedures

The methanolic extraction has proven to be efficient for analysis of multiple drug classes in routine toxicological hair analysis using a single extraction step (5.2.3 and 5.3.2 Hair analysis). The spectrum of compounds ranged from relatively polar compounds such as morphine and amphetamine to hydrophobic SCRAs. However, the methanolic extraction might emerge suspicion whether the extraction efficiency is satisfying. Therefore, this aspect was tested for the diverse chemical class of SCRAs, using authentic hair samples from SCRA users. As shown in Figure S3, different SCRAs were readily extracted from hair matrix after 3 h (1 h sonication at 40°C + 2 h static extraction at room temperature), indicating that extended time periods up to 40 h do not increase the extraction yields. This was confirmed for chemically different SCRAs, ranging from 4F-MDMB-BINACA over Cumyl-BC[2.2.1]-HpMINACA to 5F-PB-22.
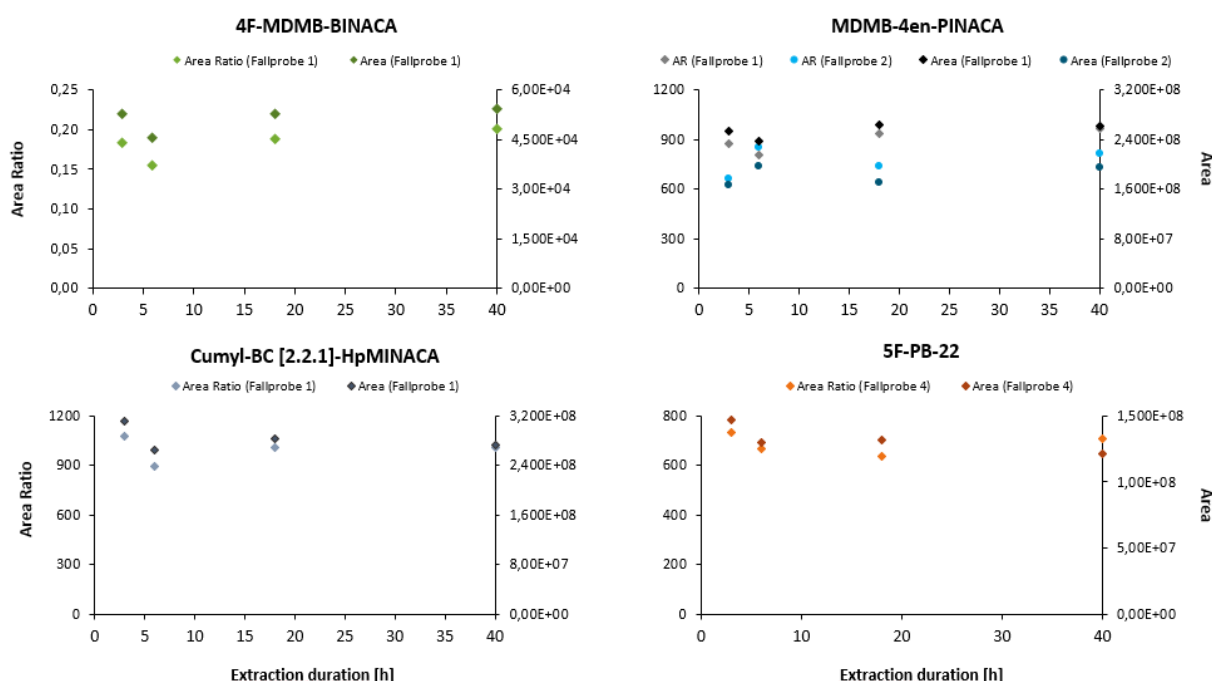
Figure S3. Variation of durations of the methanolic extraction (3 - 40 h) for different SCRAs from authentic hair samples. The extraction duration (x-axis) indicates 1 h sonication of hair samples at 40°C in combination with different durations of the static extraction at room temperature. Area Ratio (AR) = area of SCRA divided by the area of internal standard (THC-D3, 1 ng/mg hair).

Sample extraction procedure based on alkaline hair digestion with subsequent liquid-liquid extraction (Chapter 2) was tested as well, however the alkaline solution induced ester hydrolysis of SCRAs with an ester bond, as depicted exemplarily for MDMB-4en-PINACA in Figure S4. Since many toxicologically relevant SCRAs feature linked group with a terminal ester functionality (e.g. 'MDMB'-SCRAs), this hair sample extraction procedure is not recommended for the toxicological casework.
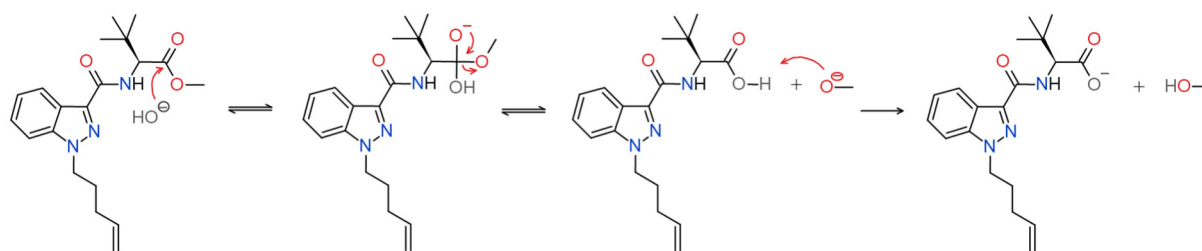
Figure S4. Ester hydrolysis of MDMB-4en-PINACA induced by the alkaline solution during the alkaline hair digestion step.

5.7.2 Analytical detection of SCRAs using LC-MS/MS

Due to high structural similarity of SCRAs, caution must be exercised during the development of analytical methods. Few examples are given below, showing molecular formulas, monoisotopic masses, and mass spectra of three isobaric SCRAs: 5F-MDMB-PICA, 5F-EMB-PICA and 5F-PB-22 (Table S13 and Figure S4). All three compounds feature identical mass spectra, so that only chromatographic separation offers a chance to distinguish these substances, when applying a targeted LC-MS/MS method. Another example comprises 4F-MDMB-BINACA and 5F-AMB, two isomers, whose structural differences are sufficient to yield partly different diagnostic fragment ions (Table S13 and Figure S5).

Table S13. Molecular formulas and monoisotopic masses of few isomeric and/or isobaric SCRA molecules and their corresponding protonated molecular ions.

Substance	Molecular formula	Monoisotopic mass [Da]	$[M+H]^+$ [Da]		
5F-MDMB-PICA	$C_{21}H_{29}FN_2O_3$	376.2162	377.2240	Isomers	Isobars
5F-EMB-PICA	$C_{21}H_{29}FN_2O_3$	376.2162	377.2240		
5F-PB-22	$C_{23}H_{21}FN_2O_2$	376.1587	377.1665		
4F-MDMB-BINACA	$C_{19}H_{26}FN_3O_3$	363.1958	364.2036	Isomers	
5F-AMB	$C_{19}H_{26}FN_3O_3$	363.1958	364.2036		

A) 5F-MDMB-PICA
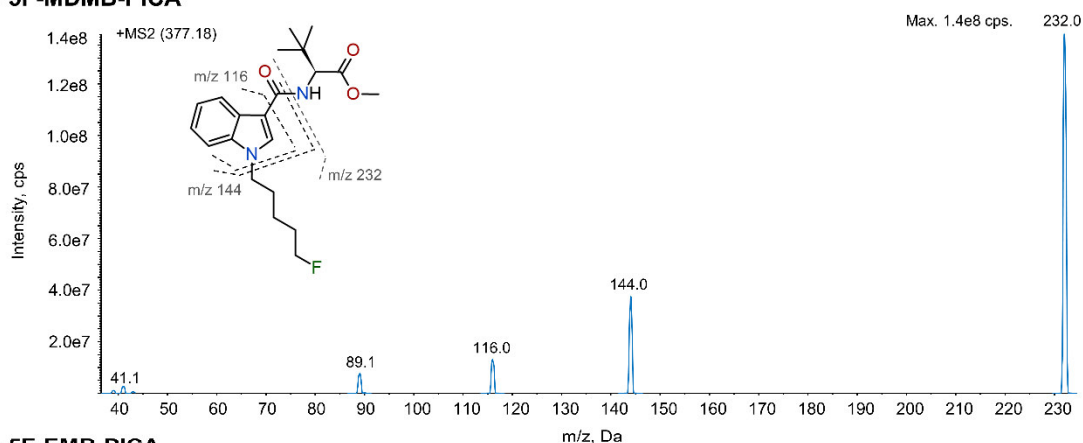
B) 5F-EMB-PICA
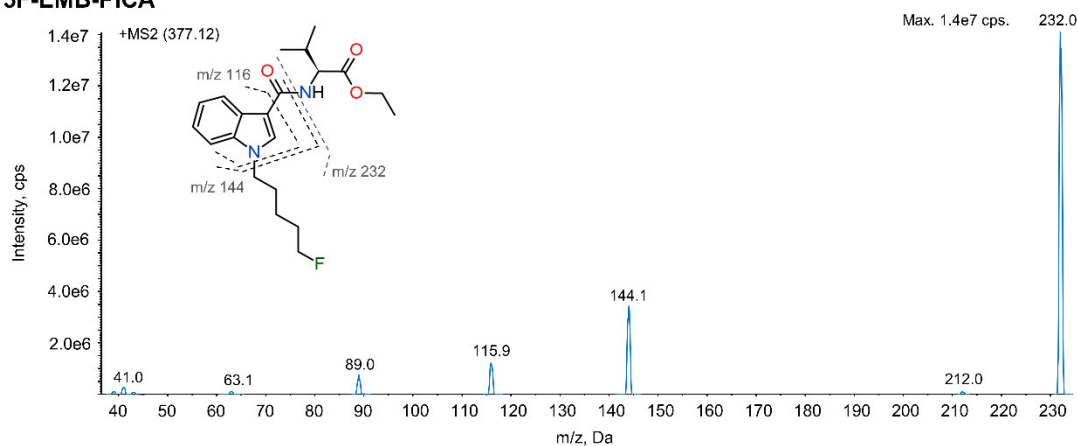
C) 5F-PB-22
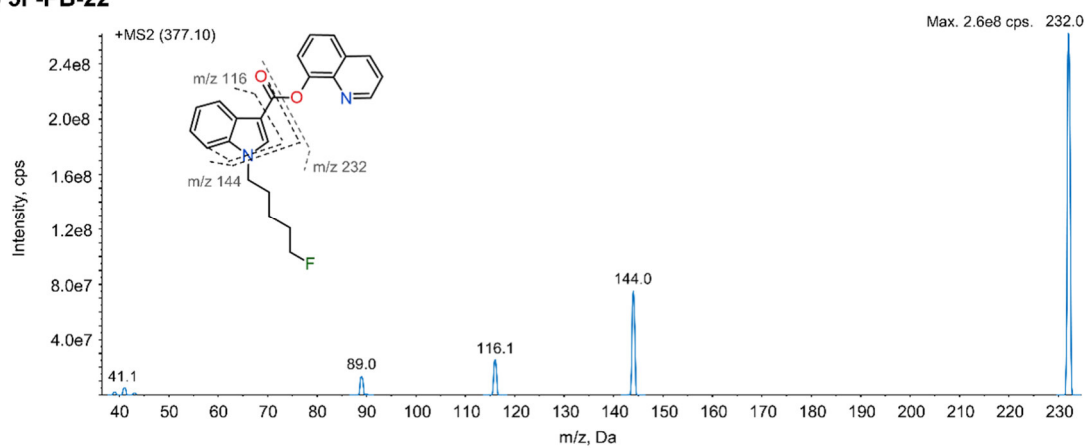
Figure S4. An example of three isobaric SCRAs, 5F-MDMB-PICA, 5F-EMB-PICA and 5F-PB-22, featuring identical fragmentation patterns and diagnostic ions by LC-MS/MS.
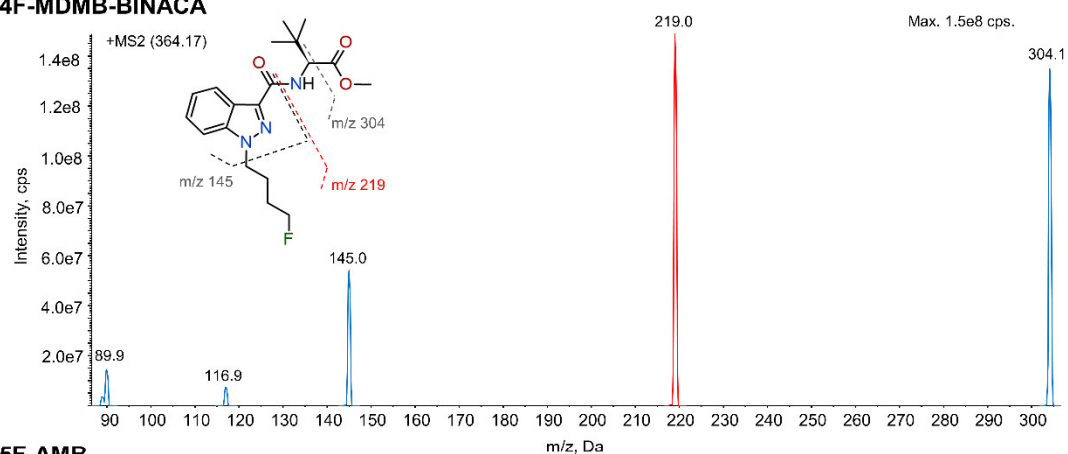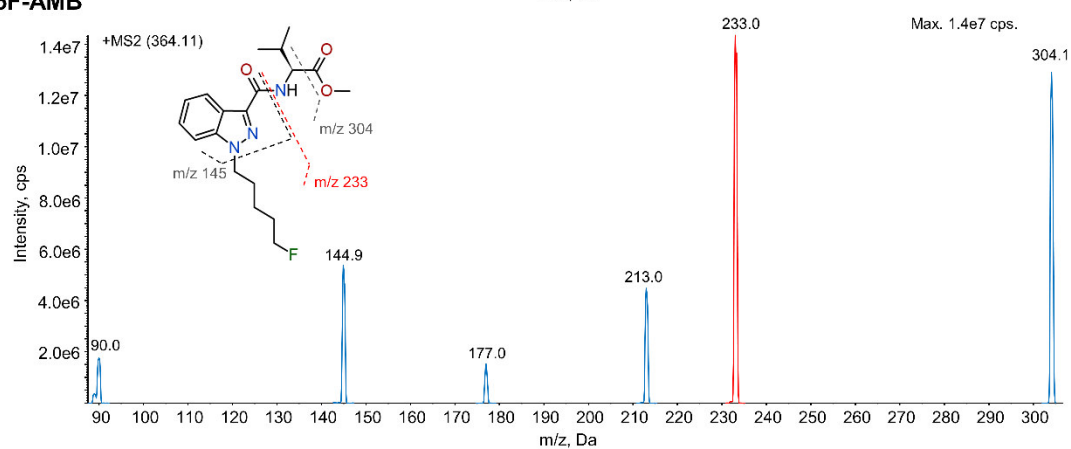
Figure S5. An example of two isomeric SCRAs (4F-MDMB-BINACA and 5F-AMB), whose structural differences are sufficient to yield partly different diagnostic fragment ions.

Chapter 6

Explosives analysis:

TATP

Determination of triacetone triperoxide (TATP) traces using passive samplers in combination with GC-MS and GC-PCI-MS/MS methods
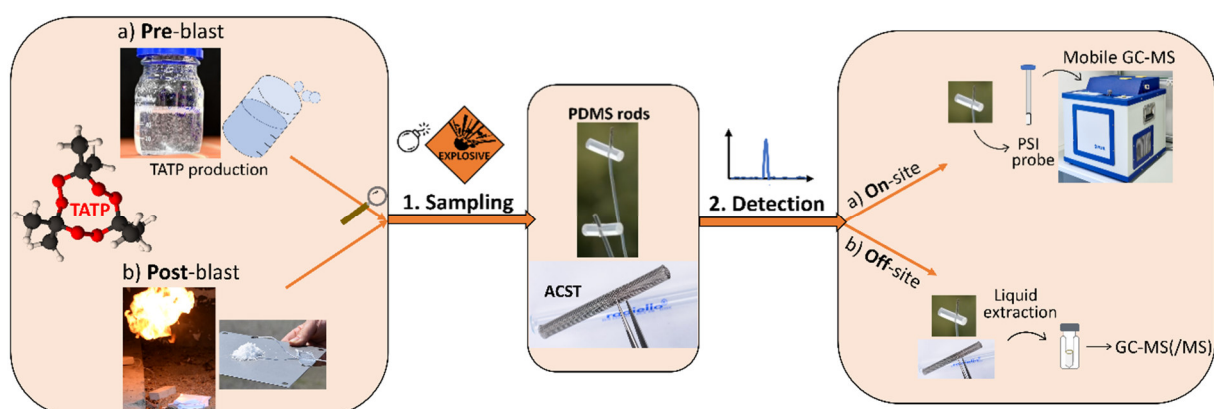
This chapter has been published as:

Abstract

The use of organic peroxides for the preparation of homemade explosives (HMEs) is common among terrorists due to inexpensive precursor chemicals and simple synthetic procedures. Triacetone triperoxide (TATP) is the most notable peroxide explosive, and has been deployed in several terrorist attacks as explosive filling of improvised explosive devices (IEDs). Forensic identification of TATP in pre-blast and post-blast residues, including on-site analysis, poses significant analytical challenges and induces demand for practicable and sensitive detection techniques. This work presents a concept suitable for laboratory and on-site identification of TATP residues in liquid samples (aqueous TATP synthetic waste) and in gas phase. It is based on TATP enrichment from the aqueous or gas phase using different types of passive samplers (polydimethylsiloxane (PDMS) sampling rods and activated carbon sampling tubes (ACST)) and subsequent identification of the explosive by gas chromatography-mass spectrometry (GC-MS) or GC with positive chemical ionization and tandem MS (GC-PCI-MS/MS) analytical techniques. Additionally, investigation of the stability of TATP in aqueous solutions and of the stability of enriched TATP in passive samplers under different storage conditions, as well as development of TATP re-extraction procedures from passive samplers have been performed in this study. The practical use of passive samplers was demonstrated during and after TATP production processes. Moreover, post-blast sampling of TATP under different conditions of controlled blasting events was investigated using the passive sampling concept.

Keywords: homemade explosives (HMEs); improvised explosive devices (IEDs); triacetone triperoxide (TATP); passive sampling; GC-PCI-MS/MS; post-blast residue

6.1 Introduction

The analysis and detection of peroxide-based homemade explosives (HMEs) has significantly gained importance in forensic investigations due to emergent terrorist attacks worldwide performed with this class of HMEs. Triacetone triperoxide (TATP) represents one of the most frequently encountered HMEs as a common component of improvised explosive devices (IEDs), used as primary explosive or as the main charge. Therefore, there is a great demand for law enforcement agencies (LEAs) to continuously develop and improve analytical techniques for the detection of HMEs, particularly TATP, at clandestine production sites, in synthesis waste or on evidence secured after an explosion (post-blast).

Sensitive trace detection of explosives requires efficient sampling techniques, which enable pre-concentration of target analytes on a sampling medium. For this purpose, passive and active sampling techniques, traditionally used for environmental monitoring of pollutants in air and aquatic systems, seemed well suited for monitoring of explosives. The few known applications of detection of explosives in the environment via passive sampling include mapping and tracking of unexploded ordnances in aquatic systems [1,2], vapor sampling of dinitrotoluene (DNT) and trinitrotoluene (TNT) in atmosphere and soil [3], or detection of buried explosives [4]. In general, the sampling medium (sorbent) is either exposed to the respective environment via assistance of a pump (active sampling), or operates in the purely diffusive mode (passive sampling). Besides applications in environmental monitoring, passive/active sampling was also utilised for forensic explosives monitoring. Different sorbent materials have been deployed, e.g. Tenax TA (polydiphenylphenylene oxide, PPPO) as vapor pre-concentrators of the plastic explosive tagging agents 4-nitrotoluene (4-NT) and 2,3-dimethyl-2,3-dinitrobutane (DMNB) [5], or in a micromechanical cantilever-based olfactory sensing system for 2,4-DNT [6]. Most recently, a passive sampling device consisting of Nomex (aromatic polyamide) coated with a PPPO film was selected as the winning design among six film-based sorbents that were evaluated for 15 explosives, including TATP [7]. Subsequently, the application of the passive sampler was successfully trialled in operationally relevant scenarios (room-scale exposures, baggage, vehicles, and shipping containers) for detection of bulk commercial and military explosives vapors, being successful for explosives with vapor pressures higher than that of TNT [8]. TATP and other peroxide explosives were tested only in small-scale arrangement in laboratory-scale trials.

Polydimethylsiloxane coated (PDMS) fibers have been reported as the most effective solid-phase microextraction (SPME) fibers for rapid field headspace analysis of explosives [9], also with special applications for the headspace-GC/MS detection of TATP traces in post-explosion debris [10,11]. Alternative post-blast sampling methods for TATP are based on liquid extraction of debris [12] or on surface swabbing [13]. In general, TATP exhibits one of the highest vapor pressures (6.7 Pa at 25°C, [14]) among explosives, favouring vapor sampling over the traditional extraction or swabbing sampling. Although the saturation equilibrium gas phase concentration of TATP corresponds to a ppb-level (600 µg/L), this value is typically not reached in practice, where diffusion processes limit the actual air concentration (estimated to 3.1 ng/L at the diffusion equilibrium state) to ppt-concentration levels of TATP [14]. These challenges prompt an ongoing research for vapor phase sampling of TATP, inducing continuous development of novel sampling techniques, such as planar SPME (PSPME) with direct ion mobility spectrometry (IMS) analysis in both, active (less than 5 sec sampling) and

passive sampling modes (within 30 sec sampling) [15]. The sorbent consisted of a PDMS coated activated glass fiber filter. Liquid phase sampling using PDMS rods was initially described for sampling of organic micropollutants by Pawliszyn et al. [16], later applied to explosives [17,18], but still lacking investigation of liquid phase sampling for peroxide explosives. Therefore, the applicability of PDMS samplers for aqueous phase sampling of TATP was one of the objectives addressed in the present study.

Activated charcoal sorbents have been traditionally used in environmental monitoring [19,20] for volatile organic compounds (VOCs) or in forensic analysis for extraction of accelerants from fire debris [21] or from the surface of hands of suspected arsonists [22]. In the context of explosives, activated charcoal has been used as an adsorbent for TATP and HMTD in a training aid for explosive detection dogs [23], however not for sampling purposes, to the best of our knowledge. Hence, this represents a novel approach for gas phase sampling and detection of explosives, particularly for TATP in this study.

Analytical techniques and devices for the detection of trace quantities of TATP are provided in several comprehensive overviews [24-29], with current detection capabilities ranging from colorimetric sensor arrays, fluorescence based sensors, luminescence sensors, optoelectronic sensors, electrochemical molecular-imprinted polymer (MIP) sensors, biosensors, surface-enhanced Raman spectroscopy (SERS), IMS, electrospray ionization (ESI)-IMS, to mass spectrometric (MS) methods, such as selected-ion flow tube mass spectrometry (SIFT-MS), desorption ESI-MS, gas chromatography-MS (GC-MS) and liquid chromatography-MS (LC-MS). Few studies also demonstrated the ability to directly integrate field sampling techniques (passive or active sampler formats) with an on-site detection equipment for explosives. Fan et al. [15] presented a PSPME sampling procedure with subsequent IMS analysis, and McEneff et al. [7] integrated passive sampling based on PPPO sorbent with IMS and a vehicle-mounted thermal desorption (TD)-MS instrument.

The aim of this work was to develop sampling methods for liquid and gas phase detection of TATP based on passive sampling using polydimethylsiloxane (PDMS) and activated charcoal as sorbent materials, in combination with subsequent GC-MS analysis. As a prerequisite, different key parameters, such as stability of TATP in aqueous phase, retention behaviour of TATP on passive samplers under different storage conditions, development of optimized extraction protocols and preliminary uptake kinetics experiments in gas phase were systematically investigated in laboratory based studies. The study focused also on the ability of direct (without sample preparation) or indirect (with simple sample preparation) integration of passive samplers with different mobile and stationary GC-MS based detection techniques. The overarching aim was to investigate the performance and suitability of passive samplers in different operational environments, including exposures during and after a TATP production process (pre-blast detection) as well as after controlled explosions of TATP under various conditions (post-blast detection).

6.2 Experimental

6.2.1. Reagents and materials

Triacetone triperoxide (TATP) standard was purchased from AccuStandard Inc. (New Haven, USA) as 0.1 mg/mL solution in acetonitrile. Solid TATP for post-blast experiments was obtained by in-house synthesis. The internal standard (ISTD), ^{13}C-TATP, was synthesized and provided

by the Joint Research Centre of the European Commission (Ispra, Italy) at a concentration of 30 µg/mL in methanol. Acetonitrile and methanol, both supplied by LGC Standards (Wesel, Germany), were used for serial dilutions of the standard and internal standard, respectively. Acetone, isohexane, ethyl acetate and carbon disulfide were purchased from Merck KGaA (Darmstadt, Germany), all as analytical reagent grade chemicals. Helium (99.999% purity, Westfalen, Münster, Germany) and ammonia (99.98% purity, Westfalen, Münster, Germany) were used as a carrier gas in GC and as a chemical ionization reagent gas in MS, respectively. Round polydimethylsiloxane (PDMS) cord (LUX & CO. Bergwerks- und Industriebedarf GmbH, Cologne, Germany) was provided by the Federal Criminal Police Office (Wiesbaden, Germany), activated charcoal sampling tubes (ACST) (Sigma-Aldrich, St. Louis, United States) by the Joint Research Centre of the European Commission (Ispra, Italy), and SPME fibers were supplied by Merck (Darmstadt, Germany). The round PDMS cord was cut to small rods of the desired length before use (mostly 1 cm or 2 cm). The cutting occurred with a scalpel and a digital caliper gauge in order to achieve a constant and reproducible size of each piece. The physical size of the PDMS rods was determined by the digital caliper gauge during cutting. All above mentioned samplers were deployed as passive samplers, whereas activated charcoal ORBO sorbent tubes (Orbo 32 Small, Product Code 20267-U, Sigma Aldrich, St. Louis, United States) and Tenax TA (polydiphenylphenylene oxide, Product Code 25055, Sigma Aldrich, St. Louis, United States) filled stainless steel tubes were used as active samplers in this study.

6.2.2. Passive samplers and TATP extraction procedures

6.2.2.1 Polydimethylsiloxane (PDMS) rods

The extraction procedure for TATP from PDMS rods was based on our previous studies dealing with drugs extraction from wastewater [30]. A PDMS rod (1 cm length; Figure 1, middle) was placed in a glass vial (1.5 mL volume capacity), followed by addition of isohexane/ethyl acetate mixture (1 mL, 9/1, v/v) and ^{13}C-TATP as internal standard (18 µL, 0.25 µg/mL). For longer PDMS rods (2 cm length), larger extraction solvent mixture volumes were used (1.5 mL). The extraction was performed using a vertical shaker (VV3, VWR International GmbH, Ismaning, Germany) at medium intensity level for 15 minutes. The liquid phase was transferred to a separate vial and a second extraction step of the PDMS rod was carried out in analogous way, using 1 mL of the organic extraction mixture for 1 cm PDMS rods, and 0.75 mL for 2 cm rods. The combined extract of the two extraction steps was evaporated to a volume of approximately 50 µL at 35°C under a gentle stream of nitrogen, and quantitatively analyzed by GC-PCI-MS/MS, as described in section 6.2.6.1.

6.2.2.2 Activated charcoal sampling tubes (ACST)

Extraction of TATP from ACST (Figure 1, left) proceeded in an analogous way as described for PDMS rods, but using larger extraction volumes. A mixture of isohexane/ethyl acetate (2 mL, 9/1, v/v) was added to the ACST adsorbent together with ^{13}C-TATP (18 µL, 0.25 µg/mL) and placed in a transport glass tube provided by the supplier. Extraction (second extraction with 1 mL of the solvent mixture), concentration to a volume of approximately 50 µL, and analysis were conducted as described above.

An alternative method encompassed extraction with carbon disulfide (2 mL) by shaking for 30 minutes using a tube rotator (Stuart Variable Speed Rotator SB3, Scientifica Panzeri, Sesto San

Giovanni, Italy). The resulting extract was then injected into the GC-MS system and quantified for TATP (cf. section 6.2.6.3).

6.2.2.3 Solid-phase microextraction (SPME) fibers

SPME fibers (85 µm, carboxene/PDMS, or 100 µm, PDMS; both 1 cm length; Figure 1, right) were attached to a SPME holder and thermally desorbed in a headspace GC-MS, as described later (section 6.2.6.2).

Figure 1. Passive samplers used in the present study, including activated carbon sampling tubes (ACST), polydimethylsiloxane (PDMS) rods (here: attached to a length of wire), and solid-phase microextraction (SPME) fibers (from left to right).

6.2.2.4 Liquid-liquid extraction (LLE) in aqueous samples

For the examination of TATP stability in aqueous phase (cf. section 6.2.3.1), the spiked water samples (500 µL) were extracted with ethyl acetate (250 µL) by agitation for 30 seconds using a vortex mixer. The organic phase (162 µL) was transferred to a glass vial with a 200 µL-glass insert, and ^{13}C-TATP (18 µL, 0.25 µg/mL) was added as ISTD before analysis with a resulting end concentration of 25 ng/mL. The procedure described was simple and sufficient to compare spiked concentrations of TATP for investigation of stability profiles in water. Few modifications in the LLE were made for aqueous samples originating from non-spiked, real TATP synthesis waste collected after controlled TATP productions. To a portion of aqueous TATP synthesis waste (10 mL) was added ISTD (^{13}C-TATP, 18 µL, 0.25 µg/mL), followed by addition of isohexane (1.5 mL) and agitation for 30 seconds using a vortex mixer. The organic phase (1.1 mL) was transferred to a glass vial and the extraction procedure repeated using 0.75 mL of the extraction solvent. The collected organic phases were combined, evaporated to an end volume of approximately 50 µL at 35°C under a gentle stream of nitrogen and analyzed by GC-PCI-MS/MS.

6.2.3. Liquid phase sampling

6.2.3.1 TATP stability in aqueous phase

Stability of TATP in water was investigated using laboratory scale experiments at ambient temperature (20°C-25°C), under light exclusion (storage in a box wrapped with aluminum foil in a closed cupboard), and at the original pH of the distilled water used (pH 7). The experiments were conducted in two different environments, once allowing for continuous air exchange (non-sealed containers) and once without continuous air exchange (sealed containers). Three separate replicates (n = 3) were prepared for each assay. Samples were

prepared as follows: a stock solution of TATP in acetonitrile (18 µL, 100 µg/mL) was diluted with 18 mL of distilled water to a concentration of 100 ng/mL. After standing for 1 hour, it was aliquoted in glass vials (1.5 mL volume capacity), which were filled to their maximum in order to minimize the gas phase. Each vial was assigned to one sampling time point and the initial sampling was undertaken. Samples were collected over a period of 11 days with increasing sampling intervals in the course of the experiment (0 h, 4 h, 15 h, 24 h, subsequently every 24 h at the 2nd, 3rd, 4th, 5th, 8th and 11th day), each from a new vial. After the corresponding samples were taken (500 µL), LLE was performed as described in previous section and GC-PCI-MS/MS analysis was carried out without further concentration steps to prevent any possible loss of the volatile TATP.

6.2.3.2 TATP sampling from aqueous phase

A saturated TATP solution in acetone was 100-fold diluted with acetone, a small portion (0.5 mL) of which was further diluted in 0.5 L of tap water, yielding a test solution for the subsequent comparison experiments. Different conditions were investigated for TATP sampling in aqueous phase using PDMS rods, including static enrichment as well as dynamic enrichment using a horizontal shaker, with varying time intervals for both sampling modes. All experiments were performed in triplicate. For the static conditions, PDMS rods (1 cm and 2 cm length) were mounted on a metal wire and fully immersed in 0.5 L of the aforementioned aqueous TATP solution in a sealed glass container (0.5 L volume capacity). The experiments were performed at ambient temperature for three different sampling periods (6 h, 12 h and 24 h), each sampling period in a separate test solution and container. Investigation of dynamic conditions was performed in an analogous way, but agitating the samples with a horizontal shaker (HS250 Basic, IKA Labortechnik) at a motion frequency of 240/min and shortening sampling periods to 1 h, 2 h and 3 h. After the particular sampling period, the PDMS rods were recovered from the containers, dried on a paper towel and extracted as described above (cf. section 6.2.2.1).

To assess the extraction efficiency of TATP from PDMS rods using isohexane/ethyl acetate (9/1, v/v), multiple extractions were examined. Several PDMS rods were mounted on metal wires, immersed in 0.5 L of the aqueous TATP test solution in a sealed 0.5 L glass container and shaken for 1 hour in the dynamic mode, as described before. Afterwards, a portion of the dried PDMS rods (3 x 1 cm and 3 x 2 cm) was subjected to three consecutive extraction steps using equal extraction volumes for each step (1 mL for 1 cm length, and 1.5 mL for 2 cm). The individual extracts of each sample were investigated separately. A small amount (162 µL) was taken from each extract as a backup sample before evaporation and the ISTD (18 µL, 0.25 µg/mL of ^{13}C-TATP) was added to the residual volumes, which were then evaporated to approximately 50 µL at 35°C under a gentle stream of nitrogen and analyzed by GC-PCI-MS/MS.

For the direct comparison of two orthogonal methods (direct analysis of PDMS rods via mobile GC-MS vs. LLE with subsequent laboratory-based (stationary) GC-PCI-MS/MS), different dilutions of aqueous TATP synthesis waste, including negative control samples, were prepared. Therefore, two identical portions (10 mL each) of the diluted TATP synthesis waste were taken from each sample, one for LLE extraction and one for enrichment of TATP using a PDMS rod, according to optimized extraction procedures. The PDMS rod (1 cm length) was directly inserted into the Prepless Sample Introduction (PSI) probe of the thermal desorption

unit of the mobile GC-MS (cf. section 6.2.6.5) and analyzed. The second set of experiments was conducted analogously, but featured extensively diluted TATP synthesis waste samples, larger portions of sample (200 mL) and longer extraction period (16 h, dynamic mode) for PDMS extraction of TATP.

6.2.4 Gas phase sampling

6.2.4.1 TATP sampling from gas phase

A test solution was prepared by diluting 200 µL of synthesis waste from an in-house TATP synthesis (saturated solution in acetone/water mix, additionally 10-fold diluted with acetone) and 20 mL of distilled water to a concentration level of 0.42 µg/mL (quantified by GC-PCI-MS/MS after LLE according to section 6.2.2.4).

For determination of the passive uptake of TATP in PDMS from the gas phase, several test solutions were prepared, deposited in a petri dish and placed at the bottom of 60 L polyethylene high-density (PE-HD) barrels (one dish per barrel), which were sealed with close fitting lids. Before placing the lids, PDMS passive samplers (1 cm length, n = 2) were positioned at the inner side of the barrel lids, using a metal wire and adhesive tape to reach the end position in the middle of the lids, approximately 7 cm below. The barrels were kept under a constant ambient temperature (19 - 21°C) in a controlled environment. PDMS rods were recovered after 0.5 hours up to 5 days, including following sampling time periods: 0.5 h, 1 h, 2 h, 6 h, 12 h, 24 h, 48 h, 72 h and 120 h (5 days). To avoid any artefacts, every barrel corresponded to a specific sampling period and was hence opened only once. In a second set of otherwise identical experiments, TATP solutions were first let to equilibrate for 10 h in individual closed barrels. Then, all passive samplers (PDMS, ACST and SPME, n = 1) were mounted in each barrel, by exchanging the lids against a second set of lids with pre-mounted samplers. In that way, the time for exchanging the lids and hence the air exchange during the lid opening was kept to a minimum. Time periods examined were 1 h, 3 h, 4 h, 10 h, 27 h and 98 h (approximately 4 days), besides for SPME with the maximum sampling period of up to 4 h. Additionally, the performance of all the three passive samplers was investigated at the 10-fold lower concentration level of the TATP aqueous waste solution (0.042 µg/mL) for the shortest sampling period (1 h). In all the experimental setups (Figure S1, Supplementary Material), each sampling time period was investigated in a separate container. An additional experiment with blank water was performed as a negative control. Recovered samplers were extracted with isohexane/ethyl acetate as described previously, and analyzed by GC-PCI-MS/MS (ACST and PDMS rods) or directly by headspace GC-MS (SPME fibers).

6.2.4.2 Determination of TATP uptake rate for ACST passive samplers

A constant and monitored concentration of TATP in the gas phase was required to determine the uptake rate of TATP for ACST passive samplers. Therefore, an air sampling method with a constant TATP concentration in the vapor phase was established as follows: small quantities of solid TATP (100 mg) were placed in an exposure chamber (1 m^3 volume, 1 m x 0.8 m x 1.3 m; Figure 2, A) to obtain defined concentrations of gaseous TATP at controlled relative humidity and temperature. TATP was weighed into a vial which was then sealed with parafilm, having three small holes punched with the tip of a glass pipette. The chamber was set to dynamic mode until equilibrium between TATP evaporation and extraction of chamber air was reached.

Dynamic mode in this setup was achieved by connecting the chamber to a pump (KNF N810FT.18 vacuum pump), which extracted air at a flow rate of 8.2 L/min from the chamber, resulting in an air exchange rate of 0.492 h^{-1}. The establishment of a stable (steady-state) concentration of TATP in vapor phase when switching the chamber from static to dynamic mode was monitored in various time intervals (Figure S2, Supplementary Material). The present TATP concentration inside the chamber was determined by active sampling of chamber air on Tenax TA filled stainless steel tubes, followed by thermal desorption and analysis with GC-MS. Four samples (two 1 L and two 2 L) were collected from the chamber. Afterwards, ACST integrated into a diffusive body (Radiello passive sampler; Figure 2, B), thus eliminating variations due to convection effects, were exposed to the TATP atmosphere in the chamber for 950 min and the uptake rate was estimated based on six replicates (n = 6).

Figure 2. Experimental setup of the dynamic chamber mode to ensure a constant TATP concentration inside the chamber (A); Radiello passive sampler consisting of ACST integrated in a diffusive body for quantification of TATP amounts in air (B).

6.2.4.3 TATP sampling during and after a TATP synthesis

During TATP synthesis

A TATP synthesis, yielding four smaller batches (approximately 10 g each) and one larger batch (approximately 60 g), was performed in a laboratory of the Explosive Ordnance Disposal (EOD) unit of the Bavarian State Criminal Police Office. The suitability of passive samplers for TATP gas phase detection was investigated during the production process, using both ACST (without diffusive body) and PDMS rods (1 cm). Passive samplers were installed on different locations inside (Figure S3, Supplementary Material) and outside the production room, before the synthesis was carried out. Passive samplers located inside the production room were deployed shortly before the beginning of production and sampled the air atmosphere for 24 h, whereas passive samplers outside the production room were installed for 5 h during the last phase of the production process. Moreover, the two producers' laboratory coats were collected shortly after the completed TATP production and placed in a sealed polyethylene bag together with three passive samplers, which sampled the gas phase for 0.5 h (PDMS) and 15 h (PDMS and ACST). The samplers were extracted with isohexane/ethyl acetate (see 6.2.2.1 and 6.2.2.2) and subjected to quantitative GC-PCI-MS/MS analysis.

After TATP synthesis

ACST inclusive diffusion bodies were installed in TATP containing indoor environments to assess their suitability under real world conditions. In the laboratory and storage bunker of the EOD team of the Polícia de Segurança Pública in Portugal, multiple passive samplers were installed after several TATP productions. The last TATP production and storage of greater TATP amounts (2 kg) had been four months prior to the experiment. The samplers were deployed for 7 days, extracted using carbon disulfide (cf. section 6.2.2.2) and quantified by GC-MS.

6.2.4.4 Detection of TATP in post-blast samples

Solid TATP was synthesized and distributed into smaller (8 x 5 g) or larger portions (1 x 10 g and 1 x 25 g), referring to moist weight. Four smaller portions as well as the large portions were dried for approximately 3 days by standing at room temperature (average temperature of 20°C), either on two individual steel plates (2 x 5 g) or on filter papers (residual portions) and the dry weights were determined. The weight loss amounted to 45% and 36% of the initial weight for smaller and larger TATP portions, respectively. The moist portions were used with residual moisture, 2 h after vacuum filtration. The prepared portions of moist and dry TATP were deposited on individual steel plates (4 x 5 g, 1 x 25 g) and folded cotton laboratory coats (4 x 5 g, 1 x 10 g), and ignited by remote using electric ignition pills. The moist TATP samples deflagrated completely with considerable flame but little noise. In contrast, the dried samples showed typical detonation with a sharp bang. The substrate materials were collected individually, placed in gas-tight aluminum-covered bags together with passive samplers (one PDMS rod and one ACST per sample) and sealed with aluminum tape. Longer PDMS rods (2 cm length) were deployed in this experiment. Part of the samples was secured immediately after the explosion, another part after 1 h waiting time being kept in an indoor environment at summer temperatures (19 - 22°C, 45% humidity). The samplers were exposed within the bags for 98 hours, then extracted and analyzed with GC-PCI-MS/MS as detailed before. Up to nine and twelve extracts were analyzed for PDMS rods and ACST, respectively.

6.2.5. (Short-term) stability studies of TATP in passive samplers (PDMS rods and ORBO activated charcoal tubes)

For subsequent stability studies, PDMS rods were enriched with TATP from aqueous solutions, ACST with TATP from a vapor phase. Experiments for each passive sampler were performed in duplicate (n = 2).

a) PDMS rods

Several PDMS rods (1 cm length) were placed in a diluted aqueous TATP synthesis waste solution (0.5 L) and hence enriched with TATP in the dynamic mode, using the horizontal shaker for 1 hour. The PDMS rods were dried shortly with a paper towel and subsequently exposed to various conditions that may influence the stability of TATP enriched in the PDMS material. These included storage of PDMS rods in sealed glass containers (without air exchange), with and without light exclusion, as well as storage in non-sealed glass containers (with air exchange enabled) without light exclusion. All experiments were performed at ambient temperature. Samples were collected over a period of 48 h with increasing sampling intervals in the course of the experiment (0 h, 1 h, 5 h, 14 h, 24 h and 48 h). The PDMS rods were extracted and analyzed by GC-PCI-MS/MS as mentioned before. In an analogous way, a

further set of PDMS rods was enriched with only 10% of the initial TATP concentration level in aqueous solution, and processed as described above.

b) Activated charcoal ORBO tubes

Ten 1 L air samples were taken from the chamber (dynamic mode) at flow rate of 150 mL/min, delivered by a flow sample pump (SKC Pocket Pump, Model, 210-1002, SKC Ltd., Dorset, UK). The exact flow rate was determined with a Bios Defender 520 M primary air flow calibrator (Bios International Corp., NJ, United States). All activated charcoal sorbents (Figure S4, Supplementary Material) were stored at ambient temperature, under light exclusion and without air exchange (sealed glass vials). Pairs of the tubes (n = 2) were extracted and analyzed after 1 h, 5 h, 8 h, 23 h and 30 h storage time. Both parts of the charcoal tube (sampling and control) were separately transferred into glass vials and each extracted with 2 mL of carbon disulfide. The vials were capped and shaken for 30 minutes. Extracts were then injected into the GC-MS system and quantified against an external calibration curve as later described (section 6.2.6.3).

6.2.6. Instrumentation and analytical methods

6.2.6.1 GC-PCI-MS/MS

GC-PCI-MS/MS analysis was performed with a TRACE GC Ultra gas chromatograph (Thermo Fisher Scientific) coupled to a TSQ triple stage quadrupole mass spectrometer. All analyses were performed using a PTV splitless injection of 2 µL sample volume, that was evaporated in the following manner: injection temperature of 50°C was held constant for 0.2 min, then increased to 280°C at 14.5°C/sec and maintained at 280°C for 8 min. Chromatographic separation was achieved by a fused-silica capillary column (30 m x 0.25 mm i.d., 0.25 µm film thickness; TG-5MS, Thermo Scientific), whereby the GC system was run with the following temperature program: the initial temperature of 80°C was held for 1.8 min, followed by a temperature ramp of 35°C/min to a final temperature of 300°C, which was then held for 5 min. Helium was used as the carrier gas with a flow rate of 1.2 mL/min. Analyte ionization was achieved on the one hand by electron ionization (EI) and on the other hand by positive ion chemical ionization (PCI) with ammonia reagent gas at a flow rate of 2.2 mL/min. All experiments were conducted using a 70 eV source, with an emission current of 70 µA, and a source operating temperature of 180°C. The transfer line was operated at 250°C.

Collision-induced dissociation (CID) experiments on TATP and ^{13}C-TATP were performed using the adduct ions m/z 240 [TATP-NH$_4$]$^+$ and m/z 243 [^{13}C-TATP-NH$_4$]$^+$, respectively, isolated in the first quadrupole and subsequently subjected to CID. The optimized product ion spectra were generated at increasing CID voltages ranging from 0 - 25 eV in increments of 5 eV. The mass spectrometer was operated in selected reaction monitoring mode (SRM), selecting two product ions of the fragmentation reaction, as shown in Table 1. Analysis of TATP by PCI using ammonia reagent gas was already reported in the literature [31], however CID produced extremely low abundance product ions without m/z 223 [TATP+H]$^+$ being observed. We were able to successfully detect the product ion m/z 223, and additionally, an analogous product ion was formed by the isotopically labelled ISTD (^{13}C-TATP) as well (cf. Table 1).

System operation and data processing were controlled by Thermo Xcalibur 2.1 software. Quantification was based on a calibration curve with solvent standards at 0, 5, 10, 50, 100, 500, 1000, 5000 and 10 000 ng/mL concentration levels of TATP, and a constant concentration

of ISTD at each calibration point (25 ng/mL). The gradually increasing concentration ratios of TATP to ^{13}C-TATP were plotted versus the detected signal area ratios of the isotopologues (TATP/^{13}C-TATP).

Table 1. Used SRM and MS/MS parameters for TATP and ^{13}C-TATP including the precursor ion and both prominent product ions, together with optimized collision energies.

Compound	Precursor Ion m/z	Product Ion m/z	Collision Energy [eV]
TATP	240.1	43.1	15
		223.1	5
^{13}C-TATP	243.1	44.1	15
		226.1	5

6.2.6.2 Headspace GC-MS

The Single Quadrupole GC-MS system consisted of a capillary gas chromatograph (TRACE GC Ultra, Thermo Fisher Scientific) linked to a mass spectrometer (DSQ II, Thermo Fisher Scientific) with a 70 eV electron ionization source. GC oven conditions were as follows: initial oven temperature of 40°C held for 2 min, followed by a heating program to 250°C at 10°C/min, with a 1 min final isotherm. Transfer line temperature was maintained at 250°C. The mass spectrometer scanned from m/z 26 to 300 in Full Scan Mode. The system was operated at a source temperature of 200°C with helium as the carrier gas at a flow rate of 1.0 mL/min. Splitless PTV injections were done using a splitless time of 1 min. After headspace-sampling with SPME fibers (see section 6.2.2.3), the fiber was introduced into the GC-MS system and heated to 200°C resulting in desorption of volatiles which were then transferred to the analytical column (30 m x 0.25 mm i.d., 0.25 μm film thickness; ZebronTM ZB-SemiVolatiles, Phenomenex).

6.2.6.3 GC-MS

GC-MS analyses were carried out on an Agilent 7890A gas chromatograph coupled to an Agilent 5975C mass spectrometer (Agilent Technologies, Santa Clara, United States). All analyses were performed using a pulsed splitless injection of 1 μL sample until 0.75 min, followed by a split flow of 50 mL/min. Helium was used as the carrier gas with a column flow rate of 1.5 mL/min. The capillary column was an Agilent J&W HP-5ms Ultra Inert containing (5%-phenyl)-methylpolysiloxane (30 m x 0.25 mm i.d., 1.0 μm film thickness). The oven temperature started at 60°C for 10 min, and then increased at a rate of 10°C/min up to 150°C, which was held for 20 min, and in a final step increased up to 320°C at a rate of 40°C/min and remained at this temperature for 10 min. The MS interface was maintained at 320°C, while the source temperature was set to 300°C. The solvent delay was set to 9 min, and the acquisitions were made in selected ion monitoring (SIM) scan mode with the following selected ions: m/z 43, m/z 58, m/z 75, m/z 89, m/z 101, m/z 117 and m/z 222. Detection was performed in the electron impact ionization mode at 70 eV electron energy, and quantification was based on an external calibration curve (0, 20, 50, 100 and 500 ng/mL TATP standards prepared in acetonitrile).

6.2.6.4 Thermal Desorption (TD)-GC-MS

Tenax TA filled stainless steel tubes were thermally desorbed on a Perkin Elmer TurboMatrix 650 Thermal Desorber (Perkin Elmer, Waltham, United States), coupled to an Agilent 7890A gas chromatograph and an Agilent 5975C mass spectrometer (Agilent, Santa Clara, United States). The stainless-steel tubes were heated at 280˚C to displace the organic vapors (primary desorption), which were then concentrated using a secondary sorbent (Tenax TA) and a cold trap in order to be finally desorbed at 300°C (secondary desorption) and passed to the GC-MS. The thermal desorber was connected to the GC-separation column through a fused silica transfer line, heated at 220˚C. Instrumental settings of the thermal desorber are summarized in Table S1 (Supplementary Material). All other settings of the GC-MS system were the same as described under 6.2.6.3.

6.2.6.5 Mobile GC-MS

The field-portable Griffin 450TM GC-MS, specialized on mobile applications and on-site analysis, was equipped with a Low-Thermal Mass GC (LTM-GC) split/splitless inlet as a thermal desorption unit using PSI (Prepless Sample Introduction), an analytical column (30 m x 0.25 mm i.d., 0.25 μm film thickness; DB-5-MS) and a cylindrical ion trap (CIT) mass analyzer. Thermal desorption of volatiles sampled with PDMS rods was performed at 200°C injector temperature, using 1 min splitless injection time. The GC oven program was held at the initial oven temperature of 50°C for 1 min, then increased at 50°C/min to 300°C and held for 2 min at the final temperature. Therefore, the run time lasted a total of 8 min. Transfer line temperature was maintained at 280°C. The mass spectrometer operated in electron ionization mode with source temperature at 200°C. The scan range comprised m/z 40 to 425 in Full Scan Mode.

6.3 Results and Discussion

6.3.1. Liquid phase sampling

All analyses regarding liquid phase sampling are summarized in Table S2 (Supplementary Material), including relevant experimental parameters for each sample set, number of sample replicates (n), mean values, standard deviation (SD) and relative standard deviation (RSD). The last three parameters are provided when applicable, i.e. for at least two replicate samples (n = 2 and n = 3). The data allow to conclude that the method precision was very good with RSD < 15% for the majority of the values.

6.3.1.1 TATP stability and sampling in aqueous phase

The stability of TATP in distilled water is presented in Figure 3A, plotting the actual concentration relative to the starting concentration of TATP. The stability profiles highly varied depending on the possibility of passive air exchange, i.e. open vs. closed containers. TATP remained stable under the applied experimental conditions over the investigated period of eleven days in closed containers without significant degradation. This proves a high stability of TATP against chemical transformation processes in water, such as chemical hydrolysis (cf. Figure 3A, closed container). In contrast, a significant substance loss could be observed in open containers. The initial TATP concentration was decaying rapidly, as reflected in the relatively short half-life period of approximately 1.5 days. Eventually, after five days TATP was not

detectable anymore in the aqueous solution in open container, while the initial TATP concentration was preserved in closed containers and exhibited a constant plateau. The possibility of air exchange as the only difference between the two assays indicated that evaporation or sublimation was the most plausible cause for the observed loss of TATP. Since earlier findings proved solid TATP to be prone to sublimation [14], this effect is not surprising for the investigated liquid phase.

The fact that TATP remained stable in contained aqueous solutions offered the possibility for its successful detection in water samples, calling for the development of an extraction protocol. Solid phase extraction of water samples with PDMS rods has shown to be robust, matrix tolerant and highly sensitive [16,30], and therefore appeared to be a promising approach. A procedure for TATP sampling in aqueous phase using PDMS rods was optimized with respect to sampling mode (static or dynamic mode), sampling time and amount of PDMS material deployed. All three parameters had a significant impact on the TATP amounts adsorbed to PDMS. Enrichment in dynamic mode using a shaker led to a more effective sampling rate and yielded a substantial increase of TATP enriched in PDMS material, when compared to the static mode without agitation (Figure 3B). Sampling over 24 hours in static mode was nearly equivalent to 1 hour of sampling in dynamic mode. Hence, the sampling time can be effectively reduced by mechanic agitation, overcoming diffusive transport of TATP molecules as the rate determining step. Moreover, gas bubbles on the surface of PDMS rods could be observed in static mode during all the examined time periods (6 h, 12 h and 24 h). This gas layer reduces the contact surface between liquid and solid phase, and can thus be expected to have a negative effect on TATP enrichment in this sampling mode. Another interesting trend to be seen in Figure 3B is the influence of PDMS rod length – and hence surface – on the amount of TATP adsorbed. This relation can be considered as proportional in the small range investigated, under consideration of the standard deviations. As for the shorter PDMS rods, a proportional time dependence of the adsorption was observed for the 2 cm rods as well (Figure 3B).

Figure 3C depicts the results of a validation study on the extraction efficiency from PDMS rods using isohexane/ethyl acetate (9/1, v/v). In order to ensure a proper comparison and assessment of the absolute recoveries from single extraction steps, the ISTD was introduced at the stage after the performed individual extractions. The extraction efficiency of the first relative to the second extraction step was determined to be greater than 80%, in particular 87.6% and 81.3% for 1 cm and 2 cm PDMS length, respectively. Accordingly, the second extraction yielded additional 12.4% (1 cm PDMS) and 18.7% (2 cm PDMS), whereas the relative TATP amounts remaining in the third extract were negligible. The extraction efficiencies determined for both, 1 cm and 2 cm PDMS lengths, proved to be satisfactory, implying an optimized extraction procedure for both PDMS lengths using isohexane/ethyl acetate (9/1, v/v). The ratio of absolute concentrations detected (ratio of 1.96 for the 2 cm vs. 1 cm extract) confirmed the previously identified trend of TATP amounts being directly proportional to the sorbent material amount.

A) Stability of TATP in **water**

◆ without air exchange (closed container)   ◆ with air exchange (open container)

B) TATP enrichment from aqueous samples using **PDMS rods**

Static enrichment   Dynamic enrichment (shaker)

C) Multiple **extraction** of TATP from PDMS rods using isohexane/ethyl acetate (9/1, v/v)

Extraction

1 cm PDMS   2 cm PDMS
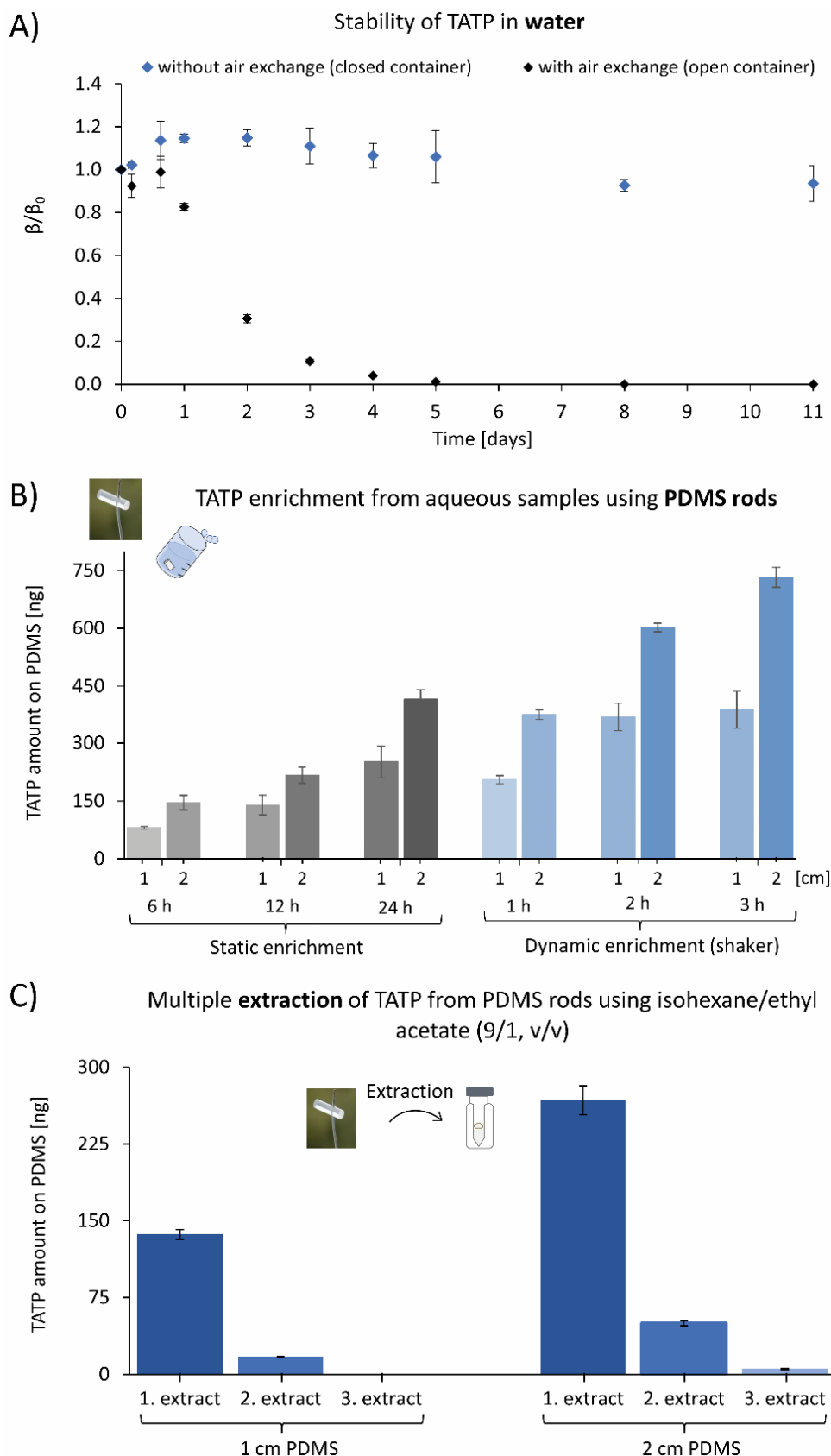
Figure 3. Stability profile of TATP in distilled water, showing concentrations relative to initial conditions (ß/ß$_0$) during 11 days (n = 3), in closed and in open containers (A); TATP sampling in aqueous phase using PDMS rods and sampling procedure optimization with respect to sampling mode (static and dynamic), sampling time, and amount of PDMS material deployed (1 cm and 2 cm length; n = 3) (B); Examination of the extraction efficiency using isohexane/ethyl acetate (9/1, v/v) for TATP extraction from PDMS rods (1 cm and 2 cm length), displaying recovered TATP concentration for three consecutive extracts (n = 3) (C).

6.3.1.2 Comparison of LLE and PDMS sampling in combination with stationary and mobile GC-MS based techniques

Following the basic studies in well-defined distilled and tap water solutions, more realistic experiments with TATP synthesis waste samples in different dilutions were carried out. Therefore, two different techniques for TATP extraction from its aqueous synthesis waste, LLE and PDMS rod extraction, were comparatively examined in combination with two different analytical systems, laboratory-based (stationary) GC-PCI-MS/MS and mobile thermal desorption GC-MS analysis with PSI probe, respectively. Several negative control samples of simulated aqueous waste without TATP were also included in the study, but did not yield signals by either of the two analytical techniques, confirming the selectivity of both methods. Both approaches yielded positive TATP identification in several samples actually containing TATP with coincident detection patterns, as shown in Figure 4, proving that both approaches are suitable for liquid phase sampling and analysis of TATP. However, LLE combined with GC-PCI-MS/MS analysis demonstrated superior sensitivity over PDMS rod sampling coupled to direct analysis via mobile GC-MS, as can be seen for the last two samples in Figure 4. A second set of experiments was conducted with stronger dilution of the waste samples, where the sensitivity of PDMS/mobile GC-MS approach was insufficient for a positive TATP identification in all the samples investigated, even despite larger sample volume (200 mL) and longer extraction time (16 h, dynamic mode). The direct introduction of PDMS rods into the PSI probe of the thermal desorption unit in the portable GC-MS system (PSI probe) enabled analysis without additional need of extraction, providing near-real-time response. However, the benefits of a less time-consuming and laborious on-site analysis must be balanced against an expected lower sensitivity in comparison to the more selective and sophisticated laboratory-based systems, as observed in the second set of experiments. Afterwards, comparative studies of LLE vs. PDMS extraction of the samples obtained were undertaken with the more sensitive GC-PCI-MS/MS system. Interestingly, the detected quantities enriched by LLE (10 mL sample volume, 30 sec extraction) were nearly identical to those obtained by PDMS sampling using larger sample volumes (200 mL) and longer extraction duration (16 h, dynamic mode) (Figure S5, Supplementary Material). In this context, the LLE technique proved to be more suitable than PDMS sampling for GC-PCI-MS/MS analysis due to significantly reduced time and sample consumption, yet yielding comparable analytical results.
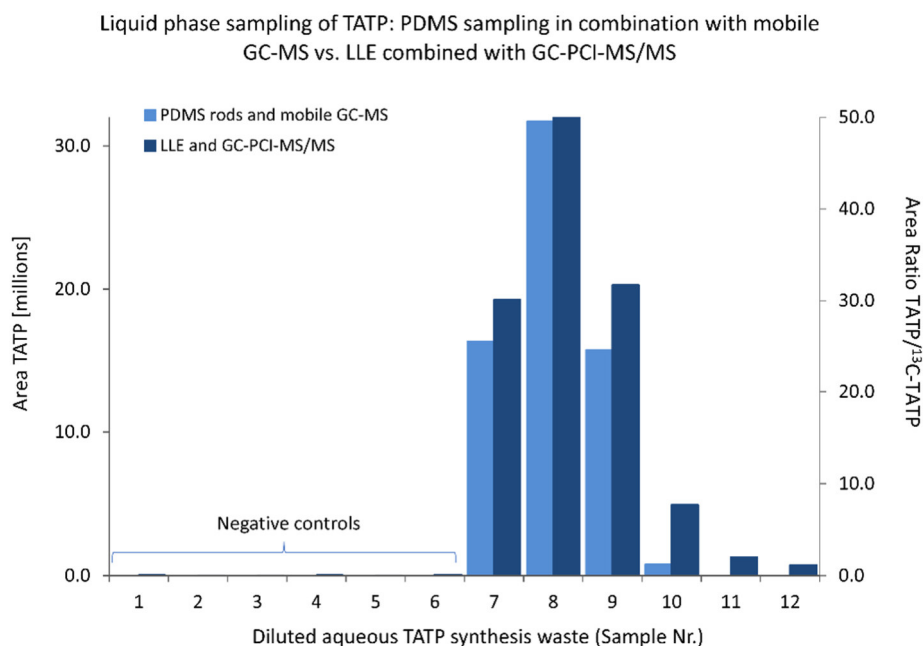
Figure 4. TATP detection in diluted aqueous TATP synthesis waste samples (Samples 7 – 12, 10 mL portions analyzed) and negative controls (Samples 1 – 6), once using PDMS rods and mobile GC-MS analysis and once LLE in combination with GC-PCI-MS/MS analysis.

6.3.2. Gas phase sampling

All analyses regarding gas phase sampling are compiled in Table S3 (Supplementary Material), including relevant experimental parameters for each sample set, number of sample replicates (n), mean values, standard deviation (SD) and relative standard deviation (RSD). The last three parameters are provided when applicable, i.e. for at least two replicate samples (n = 2 and n = 3). In general, the method precision was very good with RSD < 15% for the majority of the values obtained by analyses in combination with GC-PCI-MS/MS. Few significantly higher RSD values were observed for the experiment regarding monitoring of TATP concentration when switching from static to dynamic chamber mode (active sampling in combination with TD-GC-MS method, cf. section 6.2.4.2). This can be attributed to the intrinsically higher and not always reproducible background of Tenax TA during the thermal desorption process.

Compared to liquid phase sampling, TATP passive sampling in gas phase enables a much broader spectrum of passive sampler formats and sorbents to use. Consequently, gas phase sampling was evaluated for three different types of passive samplers, PDMS rods, ACST and SPME fibers. The gas phase above two portions of 20 mL of aqueous TATP synthesis waste with different concentration levels (0.042 and 0.42 µg/mL) was sampled in a total volume of 60 L gas phase (60 L PE-HD barrels). At the lower concentration level, positive identification of TATP was achieved by ACST and PDMS sampling in combination with GC-PCI-MS/MS analysis. By using SPME fiber sampling and subsequent headspace GC-MS analysis, no TATP could be detected for the investigated sampling period of 1 hour. The mass chromatograms obtained after PDMS and ACST sampling under these conditions are shown in Figure 5A and B, respectively, encompassing the TATP quantifier ion transition (m/z 240 → m/z 43) as well as the corresponding ion transition for the internal standard (^{13}C-TATP, m/z 243 → m/z 44). TATP exhibited two distinctive signals between 3.7 and 3.8 minutes retention time (Figure 5) that can be attributed to two separable conformers existent at room temperature as reported in

previous studies [32,33]. The displayed chromatograms show high signal-to-noise ratios (S/N) with values of S/N = 3905 and S/N = 9985 for PDMS and ACST, respectively, implying that significantly lower concentration levels can also be successfully detected. As the last step during sample preparation yielded different volumes of the extracts, comparable are only the concentrations and not the absolute areas. The concentrations are expressed as TATP/ISTD signal area ratios which are independent of fluctuations during sample preparation, since ISTD compensates for these accordingly. As indicated by the greater quantities of TATP sampled per unit time on the ACST sampler, its performance exceeds that of the PDMS passive sampler, in the particular case by factor of approximately 26.
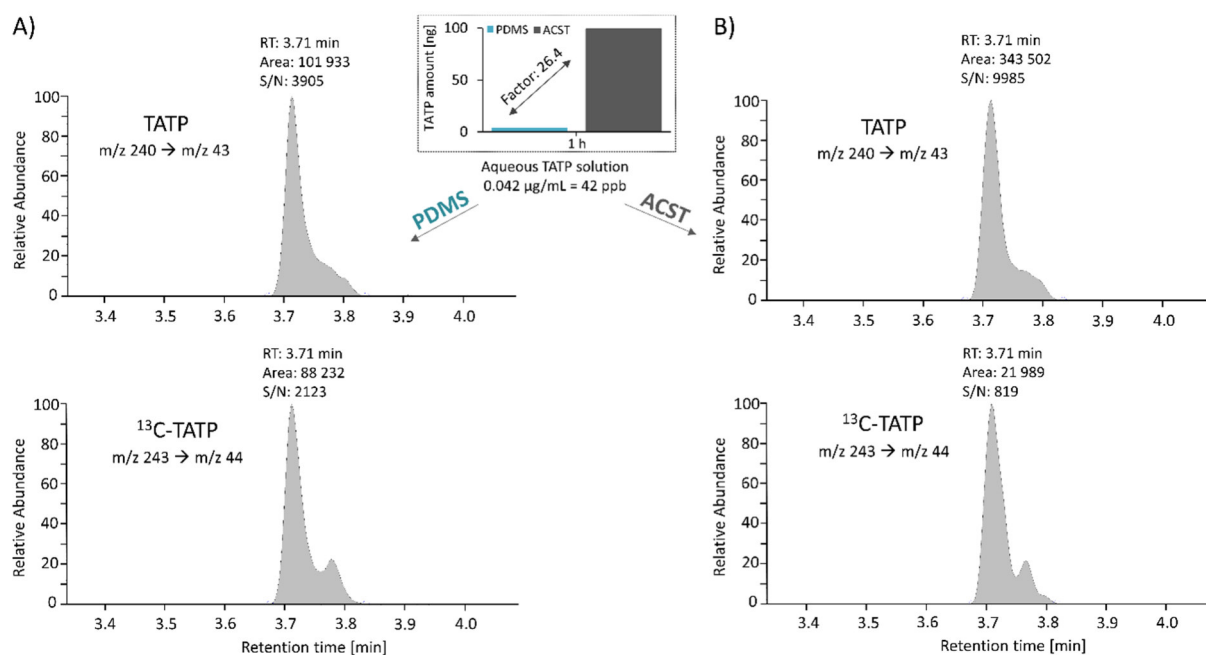
Figure 5. PDMS rod (A) and ACST (B) gas phase sampling of aqueous TATP synthesis waste (concentration level of 0.042 µg/mL) for 1 hour, encompassing the quantifier ion transition for TATP (above) and the corresponding ion transition for the internal standard ^{13}C-TATP (below).

In another series of experiments, a possible time dependency of TATP adsorption was probed for ACST, PDMS and SPME. A set of barrels with each containing 20 mL of the aqueous TATP solution at 0.42 µg/mL was prepared, one for each time interval to be tested. After a saturation time of 10 hours, the samplers were mounted, subjected to the gas phase and recovered after different time intervals. As expected, the higher concentration level of the aqueous TATP solution (0.42 µg/mL) gave a clearly positive result for PDMS rod and for ACST sampling in the gas phase, but it was also sufficient for the detection of TATP in the gas phase after 1 hour sampling with SPME fibers in combination with subsequent thermal desorption in the GC-MS system. Although a certain tendency towards increasing signal areas with increasing sampling intervals (1 h, 3 h and 4 h) existed also for SPME fibers (cf. Table S2, Supplementary Material), no unequivocal quantitative conclusions could be drawn. The experiment was repeated at 3 hours sampling time with two different fibers, PDMS material with 100 µm film thickness vs. mixed sorbent material consisting of carboxene/PDMS with 80 µm thickness, giving better results for the latter (cf. Table S4, Supplementary Material). The study revealed a pronounced time dependency of TATP sampling for ACST and PDMS samplers. ACST gave a good correlation between the increase in TATP amounts and the

sampling periods. The curve featured a sharp increase within the first 4 hours and continued with a lesser slope, i.e. lower sampling rate (Figure 6A) until the end of the experiment. In contrast, the initial growth in TATP concentration sampled on PDMS rods was followed by a decay, starting after 10 h in both of the experiments conducted (Figure 6B). The effect was rather unexpected for a closed system with constant or rather increasing TATP concentration in the gas phase. TATP decomposition can be excluded (cf. section 6.3.4) as well as loss of TATP from the sealed system, so more likely the adsorption-desorption equilibrium seemed to be shifted towards desorption from the PDMS phase after 10 hours. One possible explanation might be a competition between the PDMS sorbent phase with PE material of the barrel, which had a much higher surface. In order to shed more light on the effect observed, the experiment was repeated with PDMS rods in duplicate and without pre-saturation of the barrels. As depicted in Figure 6B, this resulted in slower adsorption kinetics with longer time needed to reach the adsorption maximum (24 h) when compared to the experiment with pre-saturation of the gas phase (10 h), but confirmed the general effect of TATP loss from PDMS starting after 10 h in both of the experiments. The difference in absolute TATP quantities sampled on PDMS might be explained by the slightly different experimental setups, where the greater number and different types of passive samplers in the pre-saturation experiment might act competitively, and thus lead to decreased amounts of TATP sampled on the PDMS phase.

Conclusively, ACST has shown superior overall performance in direct comparison with PDMS rods and SPME fibers for gas phase sampling of TATP. The continuous increase of the TATP sampled on ACST in the course of time, even after several days, and its much higher sampling capacity satisfied all requirements of a passive sampler for practical application in casework.
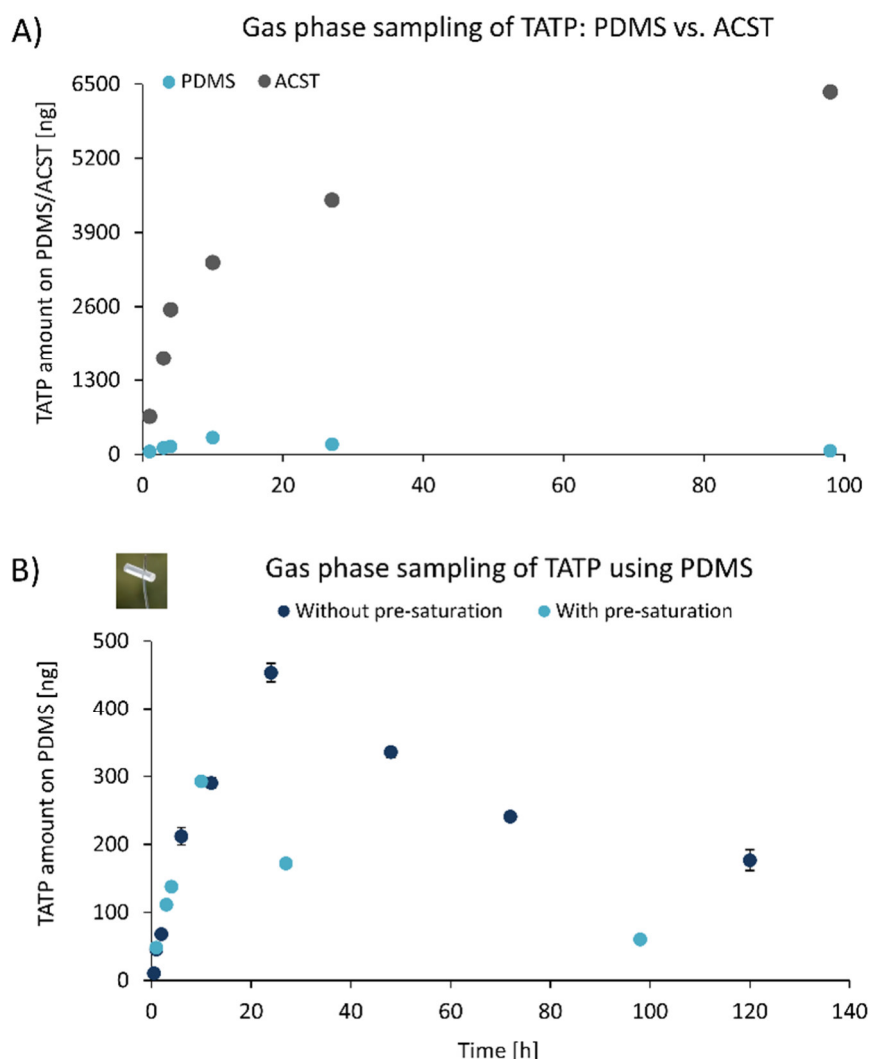
Figure 6. Gas phase sampling over diluted aqueous TATP synthesis waste (concentration level of 0.42 μg/mL) during 98 hours, using ACST (gray dots, n = 1) and PDMS rods (turquoise dots, n = 1), with pre-saturation of the gas phase for 10 hours (A). Enlarged view on PDMS curve (turquoise dots), together with the results of the second set of experiments over 120 hours, however without pre-saturation of the gas phase (dark blue dots, n = 2) (B).

6.3.3. Determination of TATP uptake rate for ACST

The uptake rate for TATP was not available from the manufacturer of the Radiello passive sampling devices (ACST integrated in a diffusive body). It was therefore determined indirectly by setting a known TATP concentration inside the chamber in dynamic mode in six replicate experiments. One of the required parameters to determine the uptake rate was the concentration of TATP inside the chamber. This concentration was determined by sampling chamber air on Tenax tubes, followed by thermal desorption and GC-MS analysis (see section 6.2.6.4), resulting in average concentration of 28.0 ± 0.29 μg/m³. From the concentration of TATP inside the chamber, the volume diffused to ACST was calculated, which referenced to the sampling time (950 min), yielded the uptake rate of approximately 40 mL/min according to the formula below. The measured and calculated values are given in Table 2.

$$c\,(TATP\ in\ chamber) = \frac{m\,(TATP\ adsorbed\ on\ ACST)}{V\,(diffused\ to\ ACST)}$$

$$V \ (diffused \ to \ ACST) = \frac{m \ (TATP \ adsorbed \ on \ ACST)}{c \ (TATP \ in \ chamber)}$$

$$Uptake \ rate = \frac{V \ (diffused \ to \ ACST)}{sampling \ time}$$

Table 2. Determination of the TATP uptake rate for ACST with integrated diffusive body, showing average values of six replicate measurements.

Replicate	Abs. TATP amount on ACST [µg]	c (TATP) in chamber [mg/m^3]	Volume diffused [mL]	Exposure time [min]	Uptake rate [mL/min]
n = 6	1.03	28	36654.4	950	38.6 SD = 2.7 (7.1%)

6.3.4. Stability of TATP on passive samplers

In order to elucidate TATP retention behavior on the sorbent phase of passive samplers after the sampling procedure, particularly regarding the adsorption maximum observed for PDMS, a systematic study with variation of the two main parameters, light and air exposure, was performed. Accordingly, multiple PDMS rods were enriched by exposure to an aqueous TATP solution, dried, and stored under different conditions before analysis. The TATP adsorbed on PDMS during storage at ambient temperature in sealed glass containers (without air exchange) and with light exclusion can be regarded as stable over a time period of 48 hours, since the initial concentration was maintained (cf. Figure 7, left; black dots). Light did not have a negative impact on the stability of TATP in PDMS, as confirmed by the constant concentration maintained during the examined time interval of 48 hours (Figure 7, left; orange dots). Consequently, light exposure can be deemed as a non-critical factor during transport or storage of PDMS rods containing TATP. In contrast to the barrel experiments, no significant degree of desorption seems to have occurred either. This might be attributed to the substantially lower surface, or to a possibly lower adsorption of TATP on glass, compared to PE. Exposure to air, i.e. the possibility of active air exchange, however, has shown to be an important factor not only during, but also after sampling of TATP using PDMS rods. The rods containing TATP suffered rapid loss of concentration, which was completed after 24 hours (Figure 7, left; blue dots). As the sealed containers had contained air as well, an oxidation by atmospheric oxygen seems less likely a reason for the decline of TATP than desorption effects. Stability of TATP in PDMS rods at tenfold lower concentration level (Figure S6, Supplementary Material) followed identical trends under the storage conditions described, indicating that the concentration level does not affect the stability of TATP adsorbed to PDMS material. The observed depletion of TATP from PDMS was in accordance with the study of Simon et al. [34], who investigated the mechanism and effect of PDMS on TATP volatilization, concluding that the enthalpy of volatilization for TATP in PDMS (25.7 kJ/mol) is lower than that for the bulk material (84.8 kJ/moL), so that it is easier for TATP to enter the atmosphere from the polymer

than from the bulk material. The study also revealed that the TATP volatilization from PDMS exhibited temperature dependence in a similar way as the sublimation from crystalline TATP. The stability studies for ORBO tubes filled with activated charcoal were performed after enrichment of the samplers in the gas phase. In accordance with the results for the PDMS rods, the stability profile of TATP on activated charcoal at ambient temperature, without active air exchange and under light exclusion exhibited a constant plateau over a period of 30 hours (Figure 7, right), suggesting equally high stability of TATP adsorbed on activated charcoal, the same sorbent used in the ACST passive sampling tubes.
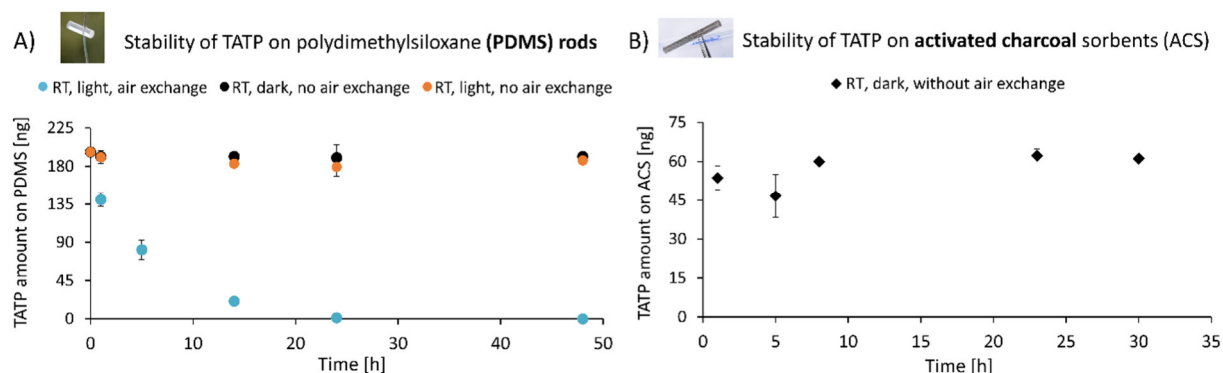
Figure 7. Stability profiles of TATP on PDMS rods (A, n = 2) and activated charcoal (B, n = 2) over 48 hours and 30 hours, respectively, during storage at ambient temperature under different conditions: open glass containers (air exchange) and under light conditions is represented by turquoise dots (PDMS, A), all other without air exchange (sealed glass containers), either with light exclusion (PDMS: black dots, and activated charcoal: black rhombus) or without light exclusion (PDMS: orange dots).

6.3.5. Application studies for gas phase sampling

6.3.5.1 TATP sampling during and after a TATP synthesis

With the suitability of the passive samplers established on laboratory-scale trials, the methodology developed was further applied to real case scenarios. Passive samplers were mounted on different locations of TATP containing environments to investigate their suitability under real conditions. The first scenario was the surveillance of the production of approximately 100 g of TATP (Figure 8, PDMS rods and ACST employed), the second was the assessment of a production location about 4 months after a production and storage of approximately 2 kg of TATP (Figure 9, only ACTS employed). As shown in Figure 8, TATP was successfully detected during the synthesis at different locations inside the production room (fume hood, cupboard, door; 24 h sampling), but also outside the synthesis laboratory (5 h sampling), including two locations in the producer's office as well as one location in the hallway, approximately at 14 m longitudinal distance from the production room. It should be noted at this point that the entrance door of the production room was opened for certain periods of time during the production. As to be expected, the TATP signal detected was decreasing with increasing distances relative to the location of the solid TATP (fume hood). Although the trend of relative quantities determined at different locations was similar for PDMS rods (Figure 8A) and ACST (Figure 8B), the absolute quantities sampled by ACST significantly exceeded those sampled by PDMS rods, suggesting enhanced performance of ACST. This is displayed in Figure 8C for the most distant location outside the production room.

Moreover, gas phase sampling of the two producers' laboratory coats shortly after the TATP production resulted in positive TATP identification, even after only 0.5 hours sampling with a PDMS rod (Figure 8D). This finding suggests suitability of the passive samplers for gas phase sampling of clothes of persons being suspected of handling or producing TATP. The concentrations measured for ACST and PDMS were surprisingly similar (cf. 15 h sampling, Figure 8D), which might result from saturation effects or from sublimation controlled adsorption kinetics.

In general, deployment of multiple sets of duplicate samplers at different locations is recommended, particularly for larger spaces, to assure the widest coverage of the monitored area and to minimize possible negative effects on detection due to specific airflow dynamics and patterns. Furthermore, it is advisable to place the samplers at rather lower heights, since TATP vapors have shown the tendency to accumulate at the floor level, which was demonstrated by Fischer et al. [35] in a double T-shaped chamber with highest TATP concentration measured below the sample source.
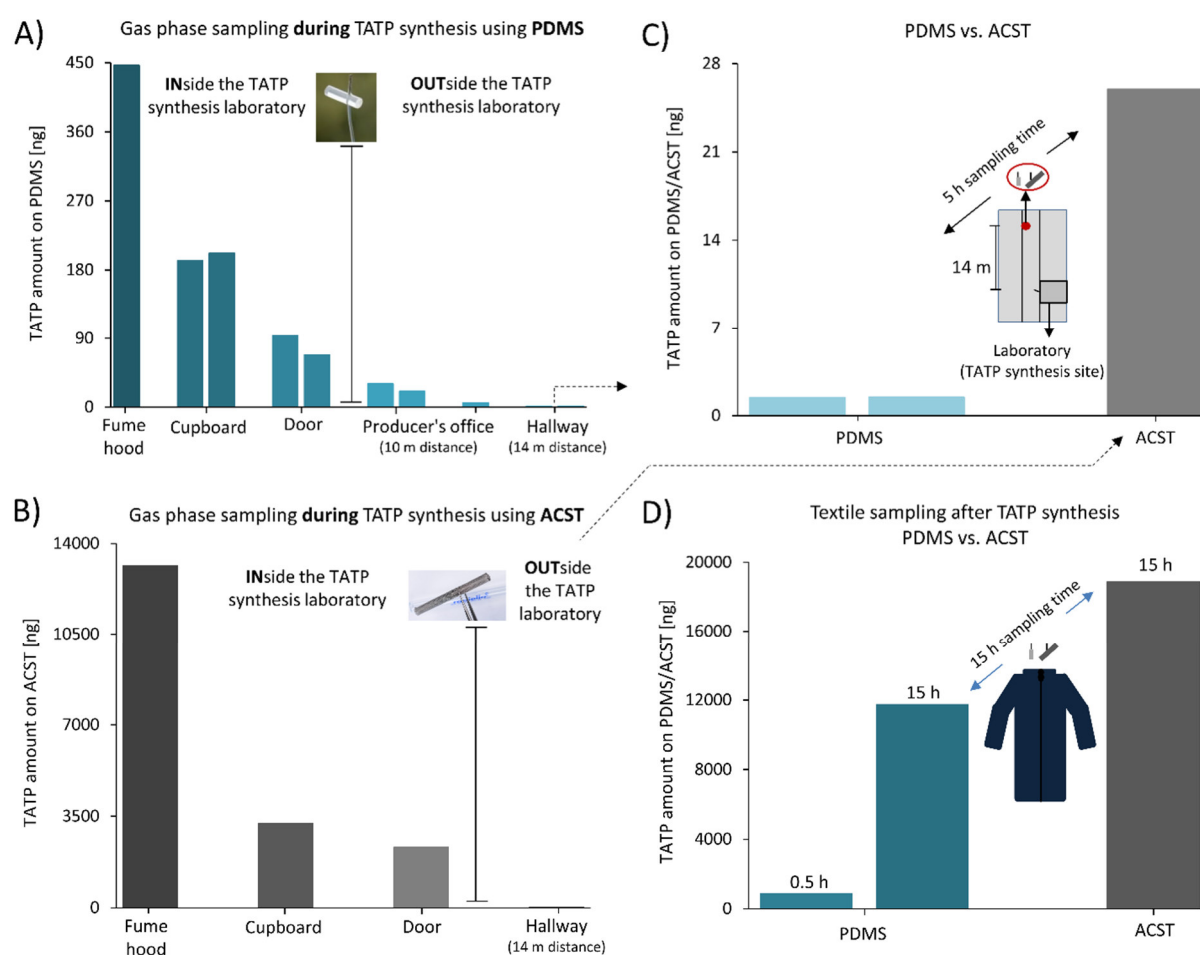
Figure 8. Gas phase sampling during an ongoing TATP production with passive samplers at different locations inside, but also outside the production room, once using PDMS rods (A, n = 1 or n = 2 as indicated by individual bars for specific locations) and once using ACST (B, n = 1). Displayed are the re-extracted TATP concentrations after GC-PCI-MS/MS analysis for each passive sampler, with enlarged display of PDMS and ACST sampled at the most distant location outside the production room (C). Gas phase sampling of laboratory coats, worn by the two chemists producing TATP, which were collected after the performed TATP synthesis, is shown as well (D, n = 1).

Interestingly, detection of TATP was possible even a long time after a completed TATP production and removal of the explosive from the production site. Successful TATP identification with ACST integrated in the diffusive body (Radiello passive sampler, 7 days sampling) was demonstrated 4 months after the last production and storage of 2 kilograms of TATP in a Portuguese EOD lab. Individual location sites of ACST with the absolute amounts adsorbed and calculated initial TATP concentrations in air, based on the previously determined TATP uptake rate (40 mL/min), can be found in Figure 9. Quantitative results (indicated in Figure 9) were plausible, since higher concentrations were detected inside (refrigerator) or close to past storage locations (storage cabinet).
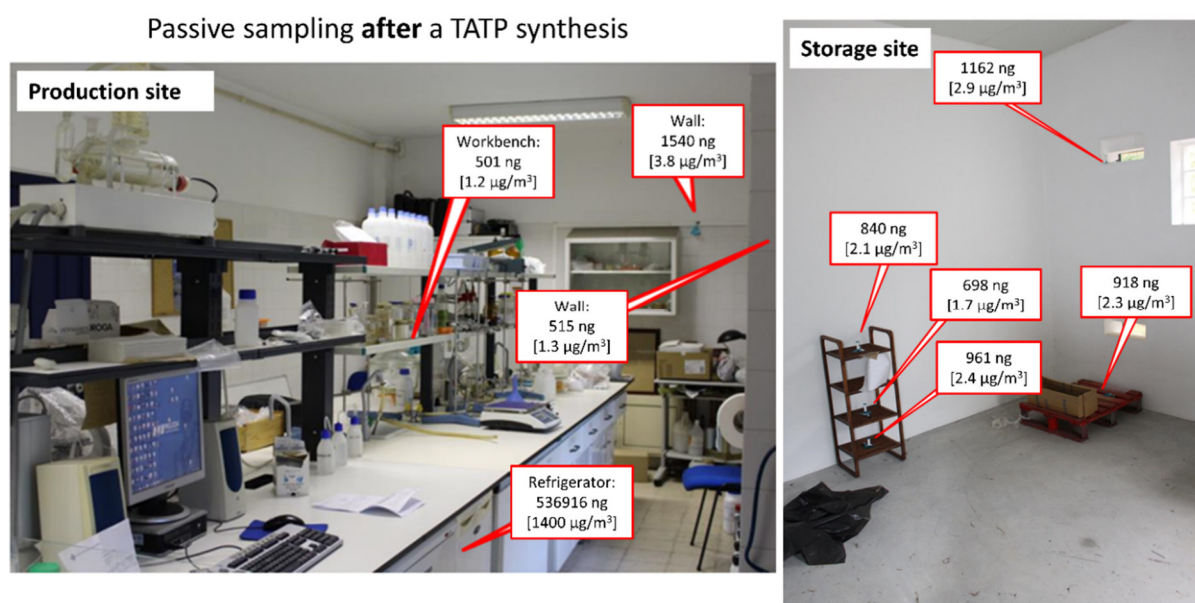
Figure 9. Individual location sites of ACST integrated in the diffusive body (Radiello passive sampler) with the absolute amount of TATP adsorbed, together with the calculated initial concentrations in air, based on the previously estimated TATP uptake rate (40 mL/min).

6.3.5.2 Post-blast samples

After passive sampling gave excellent results for the detection of TATP production residues, the suitability of this sampling protocol for post-blast residues was investigated. This was carried out by remote ignition of 5 – 25 g amounts of moist or dry TATP on different materials, followed by sampling with ACST and PDMS rods, and analyzing the residues. Due to the great effort associated with blast experiments and the considerable amount of parameters and conditions to be varied, each experiment was conducted only once (n = 1). The reproducibility of single explosions is difficult to be maintained and cannot be guaranteed due to several factors, such as possible differences during ignition, impact of external conditions, e.g. wind, on the ignition event as well as on the residues, inhomogeneous explosive material, or non-reproducible distribution of the solid explosive over the substrate material surface. However, the experiments conducted are not intended to quantitate the impact of the individual factors, but rather to show scale and scope of the methodology. Still, some tendencies were observed and certain conclusions could be drawn. When comparing the two substrate materials investigated, steel plates and folded cotton laboratory coats, TATP residues could be detected for both materials after a blasting event, but significantly more for the textile (Figure 10). This

finding appears to be reasonable due to the larger and rougher textile surface, achieved by numerous layers of individual fibers, offering adhesive areas for TATP particles and presumably slowing loss by sublimation before sampling. As soil can be considered as a further appropriate substrate material for TATP detection, samples of soil around the centre of explosion were also collected, exhibiting successfully detected TATP by gas phase sampling (Figure 10). To probe the influence of residual moisture, a part of the TATP samples was used right after filtration, another part after three days of drying. Both types of TATP gave very different reactions upon ignition - deflagration for the moist material, detonation for the dry one. Whereas the deflagration was a fast combustion reaction featured by a considerable flame formation, the detonation propagated supersonically through a shock wave. No residual solid TATP was observed after any of the explosions, but few drops of liquid for the moist TATP on the steel plates. While giving positive identification of TATP in both cases, higher amounts of TATP were generally detected after blasting of moist TATP in comparison to dry TATP, and the effect was observed for both substrate materials, steel and textile (cf. Figure 10). Although the dry TATP samples had a lower mass in comparison to the moist TATP samples (ca. 55% or 64% of the initial weight left) due to evaporation of water, as well as sublimation of TATP during the drying process, this effect alone cannot explain the mostly huge differences. To address the possible loss of TATP by post-blast sublimation, some experiments were repeated with a time interval of 1 hour between explosion and sampling. As expected, the results indicated that the time elapsed after a TATP explosion might be a decisive point for a successful analytical detection. The samples collected at the later time point exhibited lower amounts in comparison to the samples collected immediately. This trend was consistently reflected in both substrate materials, with exception of the dry TATP sampled on textile, where the quantities detected were almost equal.

The amount of TATP deployed for explosion might also play an important role for the post-blast analysis of residues. The relation observed was inverse, showing that greater TATP amounts, both for steel (2.9 g vs. 16.0 g dry TATP on steel plates) and for textile (3.0 g vs. 6.4 g dry TATP), led to lower amounts detected (see Figure 10). This might be explained by a more quantitative conversion of TATP when greater amounts used, a higher energy release leading to enhanced sublimation, or a wider local spreading of residues due to a higher pressure. All the general trends observed in this study were pursued by PDMS rods and ACST consistently, as shown for the sampling on steel plates (Figure S7, Supplementary Material).

It has to be mentioned that for most of the above experiments the first extracts of the samplers were highly concentrated and led to detector saturation, preventing any direct comparison. Therefore, the samplers were extracted several times consecutively until delivering suitable extracts for analysis. As this required different numbers of extractions for several samples, not all of the samples can be directly compared to each other. Direct quantitative comparison of the performance of the two types of passive samplers is shown in Figure S8 (Supplementary Material), representing the ninth extraction (direct injection of corresponding supernatants) for PDMS rods and ACST for post-blast samples of textile under different conditions. All the samples investigated exhibited a drastically higher sampling capacity and overall enhanced sampling performance of ACST in comparison to PDMS rods. Nevertheless, first extracts of PDMS samplers were still sufficient for unambiguous detection of TATP. As samplers and substrates were both confined in gas-tight aluminum bags with possibly close contact, the effects observed can be regarded as the combination of gas phase

and surface sampling. Further experiments regarding assessment and comparison of gas phase and surface post-blast sampling are aimed to be scrutinized in a follow-up study. Moreover, aspects to be investigated in the next step represent longer post-blast sampling periods and the effect of larger TATP amounts. However, the enhanced performance of ACST in comparison to PDMS rods was in good accordance between the single setups (Figure S8) as well as with findings from the previous gas phase sampling experiments (cf. sections 6.3.2 and 6.3.5.1).
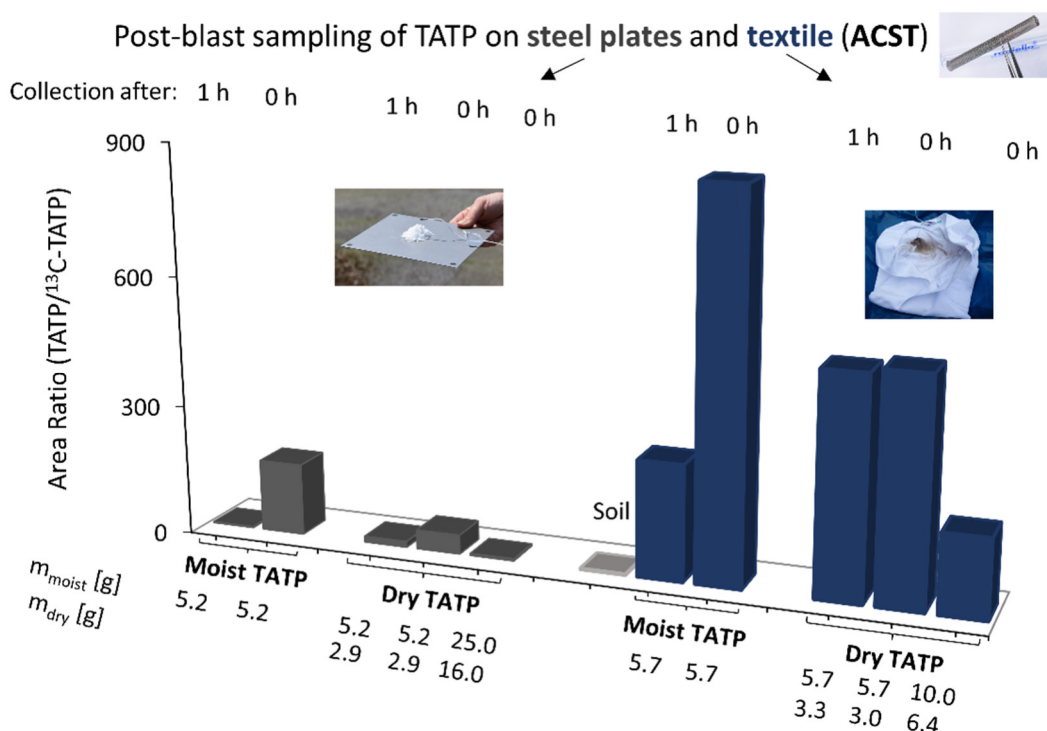
Figure 10. Results of post-blast sampling of moist and dry TATP on steel plates (grey) as well as on textile (blue), with collection of the substrate material either immediately or 1 hour post-blast. TATP sampling using ACST was followed by semi-quantitative GC-PCI-MS/MS analysis, enabling relative comparison of different conditions by plotting area ratios of TATP vs. its internal standard ^{13}C-TATP.

6.4 Conclusion

A new strategy for trace detection of the homemade explosive TATP from synthesis waste and for post-blast applications was developed. It is based on different passive samplers (polydimethylsiloxane (PDMS) rods and activated charcoal sampling tubes (ACST)) for TATP enrichment and detection in aqueous and gas phase. The optimized procedures were successfully applied to several operational scenarios. Interesting insights have been gained, not only regarding the remarkable stability of TATP in aqueous phase (min. 11 days in sealed containers), but also of TATP adsorbed on passive samplers. TATP residues were successfully extracted from authentic aqueous TATP synthesis waste samples using two independent enrichment strategies, LLE and PDMS sampling rods. The positive impact of mechanical agitation (shaking), longer sampling times and larger surface of PDMS material, reflected in greater amounts of PDMS deployed, were detailed yielding an optimized PDMS enrichment strategy for liquid phase sampling. For gas phase sampling of TATP from synthesis waste, ACST

have shown superior performance in direct comparison with PDMS rods and SPME fibers, and hence are recommended for this application field. The continuous increase of TATP sampled on ACST in the course of time, in contrast to PDMS rods, and its much higher sampling capacity satisfied the requirements for practical application in casework. The implementation of passive samplers was successfully combined with several different GC-MS based analytical methods for TATP identification, including a stationary and quantitative GC-MS method, as well as a field-portable GC-MS system with direct thermal desorption analysis of the PDMS rods for fast and on-site analysis. Furthermore, an internal standard quantification method using ^{13}C-labelled TATP was successfully developed and tested for a highly sensitive GC-PCI-MS/MS system, compatible with passive sampler enrichment and conventional LLE.

Finally, the developed methodology was successfully demonstrated for several authentic scenarios, thus enabling TATP monitoring for forensic applications. Passive sampling with PDMS rods and particularly ACST gave excellent results for the detection of TATP production residues in ambient air, not only in the course of TATP synthesis but also several months after a completed production. The methodology also proved to be suitable for the detection of residual TATP traces after a blasting event. The influence of substrate material, sampling time point after blasting and residual moisture of the explosive were probed for ACST and for PDMS samplers and showed distinctive trends, while giving positive identification of TATP in all cases. The described application experiments in operational environments clearly demonstrated the value of the method for the sensitive and reliable detection of TATP from synthesis waste, production sites and post blast evidence. Being cost-effective, easy to use and without any requirements for technically trained personal, the passive samplers presented in this study represent suitable and promising sampling techniques for law enforcement agencies, allowing for follow up analysis on-site or in a forensic laboratory. The passive sampling approach offers several advantages over active sampling, including reduced size and signature, flexible deployment, even at remote areas, without demand for electricity or maintenance, thus enabling autonomous and cost-effective analyte collection over longer periods of time.

6.5 References

[1]   Warren JK, Vlahos P, Smith R, Tobias C. Investigation of a new passive sampler for the detection of munitions compounds in marine and freshwater systems. *Environ Toxicol Chem.* 2018;37:1990-1997. DOI: 10.1002/etc.4143.

[2]   Estoppey N, Mathieu J, Diez EG, et al. Monitoring of explosive residues in lake-bottom water using Polar Organic Chemical Integrative Sampler (POCIS) and chemcatcher: determination of transfer kinetics through Polyethersulfone (PES) membrane is crucial. *Environ Pollut.* 2019;252:767-776. DOI: 10.1016/j.envpol. 2019.04.087.

[3]   Acevedo D, Padilla I, Torres PM, Torres A, Anaya AA. Vapor sampling of ERCs for environmental assessment in atmospheric and soil settings. In: *Proceedings of SPIE, Detection and Remediation Technologies for Mines and Minelike Targets XII.* 2007; 6553. DOI: 10.1117/12.719642.

[4]   Baez B, Correa SN, Hernandez-Rivera SP. Transport of explosives II: use of headspace-SPME/GC μ-ECD and TEEM GC/MS for detection of TNT vapors from sand buried samples. In: *Proceedings of SPIE, Detection and Remediation Technologies for Mines and Minelike Targets X*. 2005;5794. DOI: 10.1117/12.602446.

[5]   Gruznov VM, Baldin MN, Efimenko AP, Maksimov EM, Naumenko II, Pronin VG. Rapid gas-chromatographic determination of marking agents added to the industrial plastic explosives in air. *J Anal Chem*. 2015;70:207-212. DOI: 10.1134/S10619348 14120053.

[6]   Chae M-S, Kim J, Yoo YK, Kang JY, Lee JH, Hwang KS. A Micro-Preconcentrator Combined Olfactory Sensing System with a Micromechanical Cantilever Sensor for Detecting 2,4-Dinitrotoluene Gas Vapor. *Sensors.* 2015;15:18167-18177. DOI: 10.3390/s150818167.

[7]   McEneff GL, Murphy B, Webb T, et al. Sorbent Film-Coated Passive Samplers for Explosives Vapour Detection Part A: Materials Optimisation and Integration with Analytical Technologies. *Sci Rep*. 2018;8:5815. DOI: 10.1038/s41598-018-24244-y.

[8]   McEneff GL, Richardson A, Webb T, et al. Sorbent Film-Coated Passive Samplers for Explosives Vapour Detection Part B: Deployment in Semi-Operational Environments and Alternative Applications. *Sci Rep*. 2018;8:5816. DOI: 10.1038/s41598-018-24245-x.

[9]   Lorenzo N, Wan T, Harper RJ, et al. Laboratory and field experiments used to identify *Canis lupus* var. *familiaris* active odor signature chemicals from drugs, explosives, and humans. *Anal Bioanal Chem.* 2003;376:1212–1224. DOI: 10.1007/s00216-003-2018-7.

[10]   Muller D, Levy A, Shelef R, Abramovich-Bar S, Sonenfeld D, Tamiri T. Improved method for the detection of TATP after explosion. *J Forensic Sci.* 2004;49:935-938.

[11]   Kende A, Lebics F, Eke Z, Torkos K. Trace level triacetone-triperoxide identification with SPME-GC-MS in model systems. *Microchim Acta.* 2008;163:335-338. DOI: 10.1007/s00604-008-0001-x.

[12]   Xu X, van de Craats AM, Kok EM, de Bruyn PCAM. Trace Analysis of Peroxide Explosives by High Performance Liquid Chromatography-Atmospheric Pressure Chemical Ionization-Tandem Mass Spectrometry (HPLC-APCI-MS/MS) for Forensic Applications. *J Forensic Sci*. 2004;49:1230-1236.

[13]   Romolo FS, Cassioli L, Grossi S, Cinelli G, Russo MV. Surface-sampling and analysis of TATP by swabbing and gas chromatography/mass spectrometry. *Forensic Sci Int*. 2013;224:96-100. DOI: 10.1016/j.forsciint.2012.11.005.

[14]   Härtel MAC, Klapötke TM, Stiasny B, Stierstorfer J. Gas-phase Concentration of Triacetone Triperoxide and Diacetone Diperoxide (DADP). *Propellants Explos Pyrotech.* 2017;42:623-634. DOI: 10.1002/prep.201700034.

[15]   Fan W, Young M, Canino J, Smith J, Oxley J, Almirall JR. Fast detection of triacetone triperoxide (TATP) from headspace using planar solid-phase microextraction (PSPME) coupled to an IMS detector. *Anal Bioanal Chem*. 2012;403:401–408. DOI: s00216-012-5878-x.

[16]   Montero L, Popp P, Paschke A, Pawliszyn J. Polydimethylsiloxane rod extraction, a novel technique for the determination of organic micropollutants in water samples by thermal desorption-capillary gas chromatography-mass spectrometry. *J Chrom A*. 2004;1025:17-26. DOI: 10.1016/j.chroma2003.08.058.

[17]   Schramm S, Vailhen D, Bridoux MC. Use of experimental design in the investigation of stir bar sorptive extraction followed by ultra-high-performance liquid chromatography–tandem mass spectrometry for the analysis of explosives in water samples. *J Chrom A*. 2016;1433:24-33. DOI: 10.1016/j.chroma.2016.01.011.

[18]   Gaurav, Malik AK, Rai PK. Development of a new SPME–HPLC–UV method for the analysis of nitro explosives on reverse phase amide column and application to analysis of aqueous samples. *J Hazard Mater.* 2009;172:1652-1658, DOI: 10.1016/ j.jhazmat. 2009.08.039.

[19]   Olansandan TA, Matsushita H, A passive sampler–GC/ECD method for analyzing 18 volatile organohalogen compounds in indoor and outdoor air and its application to a survey on indoor pollution in Shizuoka, Japan. *Talanta.* 1999;50:851-863. DOI: 10.1016/S0039-9140(99)00166-6.

[20]   Huang C, Tong L, Dai X, Xiao H. Evaluation and Application of a Passive Air Sampler for Atmospheric Volatile Organic Compounds. *Aerosol Air Qual Res.* 2018;18:3047-3055. DOI: 10.4209/aaqr.2018.03.0096.

[21]   Newman RT, Dietz WR, Lothridge K. The use of activated charcoal strips for fire debris extractions by passive diffusion. Part 1: The effects of time, temperature, strip size, and sample concentration. *J Forensic Sci.* 1996;41:361-370.

[22]   Muller D, Levy A, Shelef R. A New Method for the Detection of Ignitable Liquid Residues on Arsonist Suspects Hands. *Fire Technol.* 2014;50:393–402. DOI: 10.1007/ s10694-012-0275-8.

[23]   Wilhelm I, Bikelytė G, Wittek M, Härtel MAC, Röseling D, Klapötke TM, Phlegmatization of TATP and HMTD with Activated Charcoal as Training Aid for Explosive Detection Dogs. *Propellants Explos Pyrotech.* 2022;47:e202100057. DOI: 10.1002/prep.202100057.

[24]   Strobel R, Czarnopys G. Analysis and detection of explosives and explosives residues. In: Daeid NN, Houck MM, ed. *Interpol's Forensic Science Review 2010.* Boca Raton, Florida:CRC Press;2010:453-523.

[25]   Klapec DJ, Czarnopys G. Analysis and detection of explosives and explosives residues review: 2010 to 2013. In: *17th Interpol International Forensic Science Managers Symposium,* Lyon 8th-10th October 2013, Review Papers. 2013;280-435.

[26]   Klapec DJ, Czarnopys G. Analysis and detection of explosives and explosives residues review: 2013 to 2016. In: *18th Interpol International Forensic Science Managers Symposium,* Lyon 11th-13th October 2016, Review Papers. 2016;194-261.

[27]   Klapec DJ, Czarnopys G, Pannuto J. Interpol review of detection and characterization of explosives and explosives residues 2016-2019. *Forensic Sci Int Synerg.* 2020;2:670-700. DOI: 10.1016/j.fsisyn.2020.01.020.

Chapter 6

[28]   Klapec DJ, Czarnopys G, Pannuto J. Interpol review of the analysis and detection of explosives and explosive residues. *Forensic Sci Int Synerg.* 2023;6:100298. DOI: 10.1016/j.fsisyn.2022.100298.

[29]   To KC, Ben-Jaber S, Parkin IP. Recent Developments in the Field of Explosive Trace Detection. *ACS Nano.* 2020;14:10804-10833. DOI: 10.1021/acsnano.0c01579.

[30]   Hehet P, Wende M, Shehata O, Krause S, Pütz M. Prevalence of synthetic cannabinoid receptor agonists use assessed by sewage monitoring via LC-MS/MS, Part A: Novel wastewater sampling approach using polydimethylsiloxane (PDMS) passive samplers. Manuscript in preparation.

[31]   Sigman ME, Clark CD, Fidler R, Geiger CL, Clausen CA. Analysis of triacetone triperoxide by gas chromatography/mass spectrometry and gas chromatography/ tandem mass spectrometry by electron and chemical ionization. *Rapid Commun Mass Spectrom.* 2006;20:2851-28577. DOI: 10.1002/rcm.2678.

[32]   Denekamp C, Gottlieb L, Tamiri T, Tsoglin A, Shilav R, Kapon M. Two Separable Conformers of TATP and Analogues Exist at Room Temperature. *Org Lett.* 2005;7: 2461-2464. DOI: 10.1021/ol050801c.

[33]   Haroune N, Crowson A, Campbell B. Characterisation of triacetone triperoxide (TATP) conformers using LC-NMR. *Sci Justice.* 2011;51:50-56. DOI: 10.1016/j.scijus. 2010.09.002.

[34]   Simon AG, Van Arsdale K, Wagner J, Barrow J. Effects of polydimethylsiloxane (PDMS) on triacetone triperoxide (TATP) volatilization. *Forensic Chem.* 2022;28: 100413. DOI: 10.1016/j.forc.2022.100413.

[35]   Fischer C, Pohl T, Weber K, Vogel A, van Haren G, Schweikert W. TATP stand-off detection with open path: FTIR techniques. In: *Proceedings of SPIE, Optics and Photonics for Counterterrorism, Crime Fighting, and Defence VIII.* 2012;8546. DOI: 10.1117/12.974592.

Chapter 6

6.6 Supplementary Material
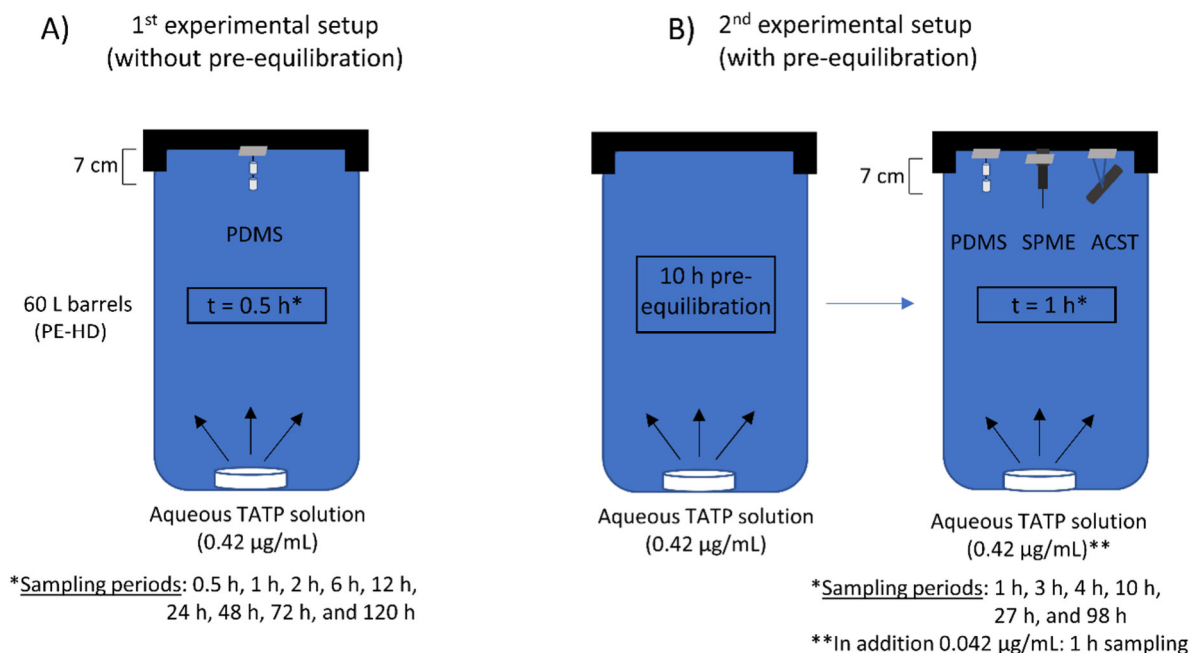
Figure S1. Experimental setups for diffusive gas phase sampling of TATP from aqueous solutions using different passive air samplers. First experimental setup (A) featured PDMS rods for gas phase sampling of an aqueous TATP solution at a concentration level of 0.42 µg/mL TATP, without pre-equilibration of the gas phase. The second experimental setup (B) was similar, however with 10 h pre-equilibration time, and included three different passive samplers (PDMS rods, SPME fibers and ACST). Additionally, a lower concentration level of aqueous TATP solution (0.042 µg/mL) was investigated in a separate experiment after 1 h sampling. Sample collection occurred in individual barrels at different sampling periods, which are indicated accordingly. For a blank control sample (24 h sampling period) the TATP solution addition was omitted.
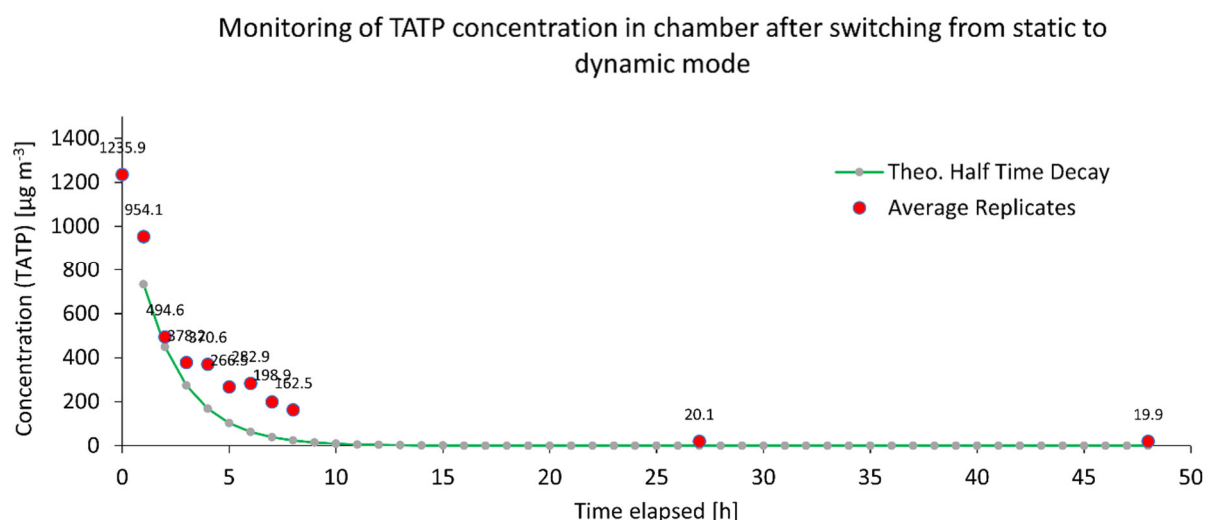
Figure S2. TATP vapor phase concentration over time after switching the chamber from static to dynamic mode. The graph includes the average of the two replicate measurements (n = 2) at each time interval (red dots) and the theoretical half time decline curve (green line). The concentration decline followed an almost exponential trend. The deviation from the theoretical dilution function of gas phase concentration might be due to the remobilization of TATP adsorbed to the chamber walls into the air.

After 48 h, the TATP concentration in the chamber reached a stable (steady-state) concentration of approximately 20 µg/m^3.
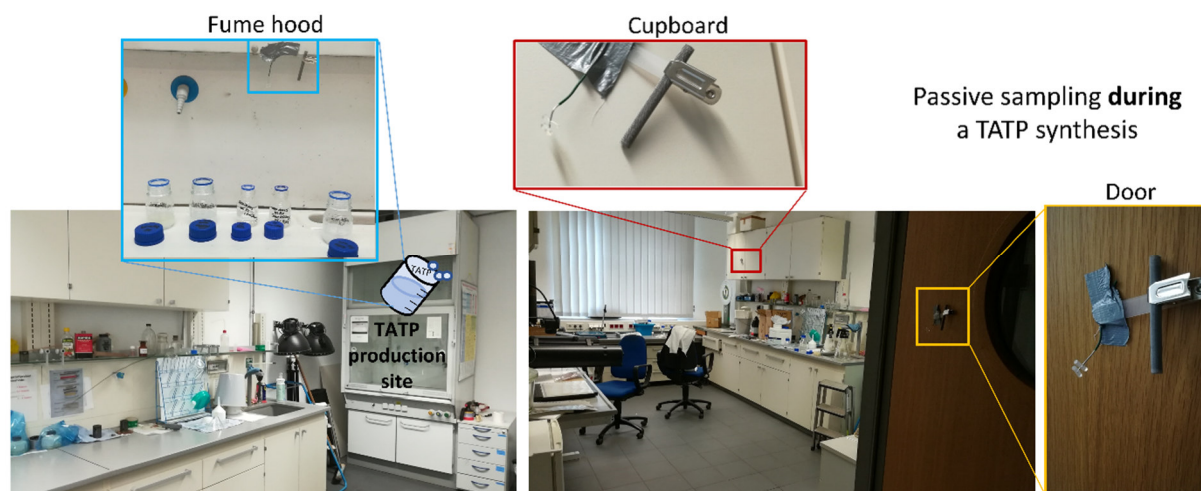
Figure S3. The locations of passive samplers (PDMS rods and ACST) inside the production laboratory included the fume hood where TATP was synthesized, the surface of a cupboard door in the room, and the inner surface of the entrance door.

Next to the locations inside the production room (Figure S3), few locations outside the production site were monitored as well. The positions comprised of two different locations in the producer's office at a distance of approximately 10 m longitudinally from the production room, and a location at the wall in the hallway, approximately 14 m longitudinally away from the production site.
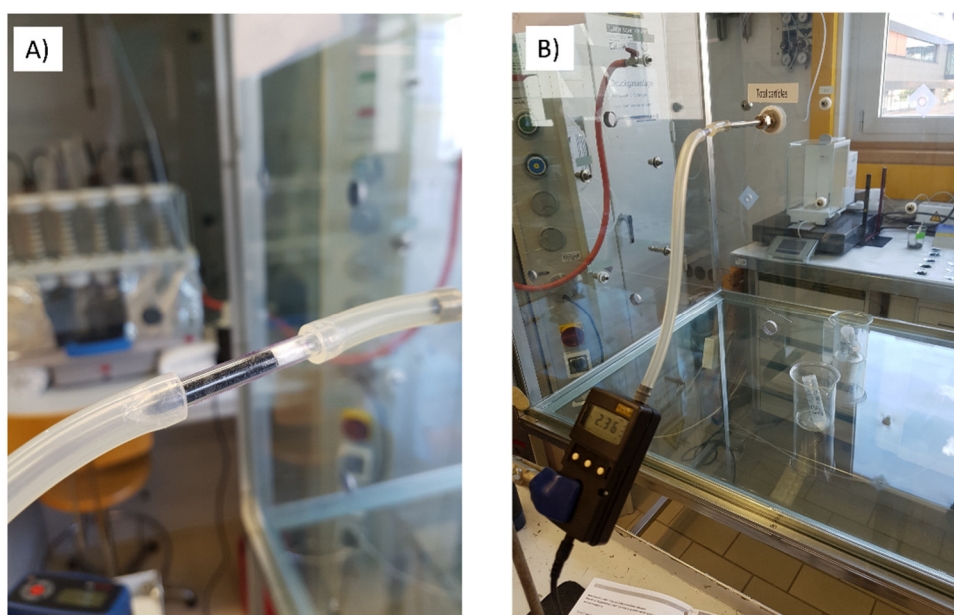
Figure S4. Activated charcoal sorbents (ORBO tubes) used for the (short-term) stability study of TATP adsorbed on activated charcoal (A). Experimental setup for the enrichment of the sorbents with TATP from vapor phase inside the chamber, using the dynamic mode.

Table S1. Instrumental settings of the Thermal Desorber.

Temperature Settings	[˚C]	Time Settings	[min]	Split Flow Rates	[mL/min]
Valve	250	Purge	1	Inlet Split	71
Transfer Line	220	Primary Desorption	10	Outlet Split	30
Primary Desorption	280	Trap Hold	2	Desorption Flow	21
Cold Trap	-30			Column Flow	1.5
Secondary Desorption	300				
Heating Rate [˚C/s]	99				

Table S2. Summary of analyses performed for liquid phase sampling, including relevant experimental parameters for each sample set, number of sample replicates (n), mean values, standard deviation (SD) and relative standard deviation (RSD). The last three parameters are provided when applicable, i.e. for at least two replicate samples (n = 2 and n = 3). The corresponding units of the mean values, SD and RSD are indicated individually for each analysis.

Liquid phase sampling				
Analysis	Replicates (n)	Mean	Standard deviation (SD)	Relative standard deviation (RSD)
1. TATP stability in aqueous phase **a) without air exchange**	(n)	[Relative conc. ratio]	[Relative conc. ratio]	[%]
t = 0 d	3	1.00	0.00	0.0
t = 0.2 d	3	1.02	0.01	1.4
t = 0.6 d	3	1.14	0.09	7.8
t = 1 d	3	1.15	0.02	1.8
t = 2 d	3	1.15	0.04	3.3
t = 3 d	3	1.11	0.08	7.5
t = 4 d	3	1.07	0.06	5.4
t = 5 d	3	1.06	0.12	11.5
t = 8 d	3	0.93	0.03	2.9
t = 11 d	3	0.94	0.08	8.9
b) with air exchange				
t = 0 d	3	1.00	0.00	0.0
t = 0.2 d	3	0.92	0.05	5.7
t = 0.6 d	3	0.99	0.07	7.4
t = 1 d	3	0.83	0.02	1.9
t = 2 d	3	0.31	0.02	6.3
t = 3 d	3	0.11	0.01	10.1
t = 4 d	3	0.04	0.01	14.8
t = 5 d	3	< LOD	/	/
t = 8 d	3	< LOD	/	/
t = 11 d	3	< LOD	/	/

2. TATP sampling from aqueous phase (PDMS) a) Static enrichment		(n)	[ng]	[ng]	[%]
6 h	1 cm	3	80.6	3.6	4.4
	2 cm	3	145.6	19.3	13.2
12 h	1 cm	3	139.2	25.9	18.6
	2 cm	3	216.6	21.1	9.8
24 h	1 cm	3	251.4	41.4	16.5
	2 cm	3	415.1	26.2	6.3
b) Dynamic enrichment					
1 h	1 cm	3	205.4	10.8	5.3
	2 cm	3	376.1	12.6	3.4
2 h	1 cm	3	369.8	35.6	9.6
	2 cm	3	602.2	11.4	1.9
3 h	1 cm	3	388.9	48.2	12.4
	2 cm	3	732.4	25.7	3.5
3. Multiple extraction of TATP from PDMS rods using isohexane /ethyl acetate (9/1, v/v)		(n)	[ng]	[ng]	[%]
1. extract	1 cm	3	136.7	4.6	3.4
2. extract		3	16.9	0.5	2.7
3. extract		3	< LOD	/	/
1. extract	2 cm	3	267.6	14.0	5.2
2. extract		3	50.0	2.3	4.7
3. extract		3	5.1	0.7	13.5

4. PDMS rods: mobile GC-MS vs. LLE - GC-PCI-MS/MS	1 / 1	12 samples, each investigated by the two different analytical methods in parallel (n = 1 for each method)
5. LLE vs. PDMS sampling combined with GC-PCI-MS/MS	1 / 1	12 samples, each investigated using two different sampling procedures in parallel (n = 1 for each sampling procedure)
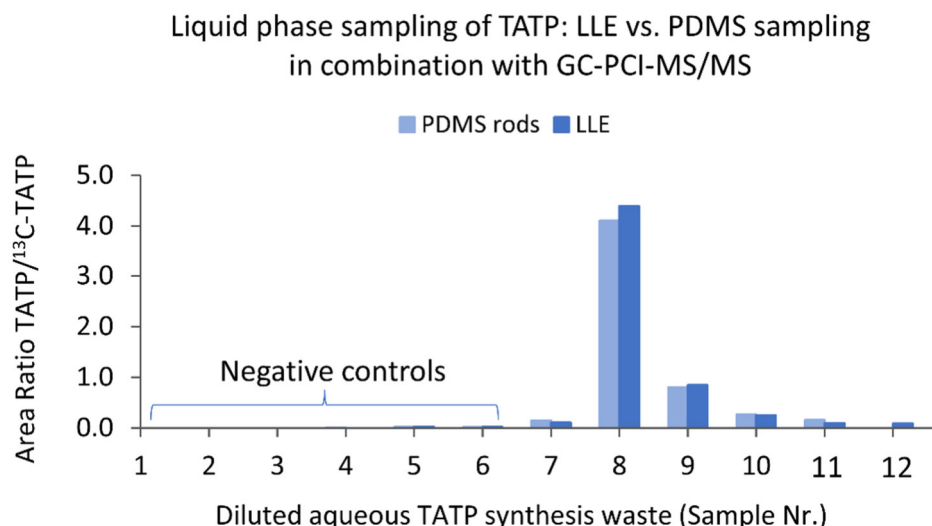
Figure S5. TATP detection in diluted aqueous TATP synthesis waste samples (Samples 7 - 12) and negative control samples (Samples 1 – 6), enriched either by LLE (10 mL sample volume) or by PDMS rods using larger sample volumes (200 mL). Both approaches were aimed for GC-PCI-MS/MS analysis.

Table S3. Summary of analyses performed for gas phase sampling, including relevant experimental parameters and/or description of each sample set, number of sample replicates (n), mean values, standard deviation (SD) and relative standard deviation (RSD). The last three parameters are provided when applicable, i.e. for at least two replicate samples (n = 2 and n = 3). The corresponding units of the mean values, SD and RSD are indicated individually for each analysis.

Gas phase sampling		
Analysis	Replicates (n)	Comment
1. PDMS vs. ACST vs. SPME (high concentration)	(n) PDMS/ACST/ SPME	Comparison of the performance of all the three passive samplers (n = 1 each) using TATP aqueous waste solution at a concentration level of 0.42 µg/mL
t = 1 h	1 / 1 / 1	PDMS / ACST / SPME*
t = 3 h	1 / 1 / 1	PDMS / ACST / SPME*
t = 4 h	1 / 1 / 1	PDMS / ACST / SPME
t = 10 h	1 / 1	PDMS / ACST
t = 27 h	1 / 1	PDMS / ACST
t = 98 h	1 / 1	PDMS / ACST
2. PDMS vs. ACST vs. SPME (low concentration)	(n) PDMS/ACST/ SPME	Comparison of the performance of all the three passive samplers (n = 1 each) at the 10-fold lower concentration level of the TATP aqueous waste solution (0.042 µg/mL)
t = 1 h	1 / 1 / 1	PDMS / ACST / SPME
3. PDMS vs. ACST vs. SPME, negative control		
t = 27 h	1 / 1 / 1	PDMS / ACST / SPME

*Additional sampling was performed for t = 1 h and t = 3 h in order to test the reproducibility and compare different SPME fiber materials, respectively. The corresponding PDMS and ACST data from this data set are not shown.

Analysis	Replicates (n)	Mean	Standard deviation (SD)	Relative standard deviation (RSD)
4. Gas phase sampling of TATP using PDMS rods (without pre-saturation; conc. level: 2.6 µg/mL)	(n)	[ng]	[ng]	[%]
t = 0.5 h	2	10.6	0.9	8.8
t = 1 h	2	45.4	6.9	15.2
t = 2 h	2	68.3	3.0	4.4
t = 6 h	2	212.1	13.1	6.2
t = 12 h	2	290.5	8.2	2.8
t = 24 h	2	453.8	13.5	3.0
t = 48 h	2	335.7	8.0	2.4
t = 72 h	2	240.9	5.8	2.4
t = 120 h	2	176.9	15.3	8.6
5. Monitoring of TATP concentration when switching from static to dynamic chamber mode	(n)	[µg/m^3]	[µg/m^3]	[%]
t = 0 h	2	1235.9	174.0	14.1
t = 1 h	2	954.1	195.3	20.5
t = 2 h	2	494.6	96.0	19.4
t = 3 h	2	378.2	17.4	4.6
t = 4 h	2	370.6	92.0	24.8
t = 5 h	2	266.5	122.7	46.0
t = 6 h	2	282.9	9.0	3.2
t = 7 h	2	198.9	85.2	42.8
t = 8 h	2	162.5	65.1	40.1
t = 27 h	2	20.1	1.5	7.5
t = 48 h	2	19.9	0.5	2.5
6. Determination of TATP uptake rate for ACST	(n)	[mL/min]	[mL/min]	[%]
	6	38.6	2.7	7.1
7. Stability of TATP on PDMS rods **a) high concentration** **RT, light, air exchange**	(n)	[ng]	[ng]	[%]
t = 0 h	2	196.8	5.5	2.8
t = 1 h	2	140.4	8.1	5.8
t = 5 h	2	81.2	11.5	14.2
t = 14 h	2	20.9	1.9	9.2
t = 24 h	2	< LOD	/	/
t = 48 h	2	< LOD	/	/
RT, light, no air exchange				
t = 0 h	2	196.8	5.5	2.8
t = 1 h	2	190.8	7.5	3.9
t = 14 h	2	183.2	4.8	2.6
t = 24 h	2	179.5	10.9	6.0
t = 48 h	2	187.0	2.6	1.4
RT, dark, no air exchange				

Chapter 6

t = 0 h	2	196.8	5.5	2.8
t = 1 h	2	191.2	0.6	0.3
t = 14 h	2	191.7	2.1	1.1
t = 24 h	2	190.3	15.0	7.9
t = 48 h	2	191.7	1.3	0.7
b) low concentration **RT, light, air exchange**				
t = 0 h	2	19.9	0.9	4.6
t = 1 h	2	15.6	0.3	1.8
t = 5 h	2	5.8	1.5	25.7
t = 14 h	2	< LOD	/	/
t = 24 h	2	< LOD	/	/
t = 48 h	2	< LOD	/	/
RT, dark, no air exchange				
t = 0 h	2	19.9	0.9	4.6
t = 1 h	2	19.8	0.1	0.3
t = 14 h	2	17.9	0.4	2.5
t = 24 h	2	18.8	0.3	1.4
t = 48 h	2	19.6	1.7	8.6
8. Stability of TATP on **act. charcoal sorbents** **RT, dark, no air exchange**	(n)	[ng]	[ng]	[%]
t = 1 h	2	53.7	4.6	8.5
t = 5 h	2	46.6	8.4	17.9
t = 8 h	2	60.0	0.2	0.4
t = 23 h	2	62.3	2.5	4.0
t = 30 h	2	61.2	0.6	1.0
Application studies for gas phase sampling				
9. TATP sampling during **a TATP synthesis** **a) PDMS**	(n)	[ng]	[ng]	[%]
Fume hood (115 cm, distance from the produced TATP)	1			
Cupboard	2	196.9	6.8	3.4
Door	2	80.9	17.7	21.9
Producer's office	2	25.5	6.9	27.1
Producer's office	1			
Hallway	2	1.4	0.01	0.9
b) ACST				
Fume hood (115 cm, distance from the produced TATP)	1	ACST deployed together with PDMS rods, one of each passive sampler per sampling site		
Cupboard	1			
Door	1			
Hallway	1			
c) Textile sampling **PDMS vs. ACST**				
PDMS 0.5 h	1			
PDMS 15 h	1	PDMS and ACST deployed in parallel		
ACST 15 h	1			

Analysis	Replicates (n)	Comment		
10. TATP sampling after a TATP synthesis ACST incl. diffusive body	(n)	TATP amount on ACST [ng]	Uptake rate [mL/min]	TATP concentration in air [µg/m³]
a) Production site				
Workbench	1	501	40	1.2
Wall (next to storage cabinet)	1	1540	40	3.8
Wall	1	515	40	1.3
Refrigerator	1	536916	40	1400
b) Storage site				
Shelf 1	1	840	40	2.1
Shelf 2	1	698	40	1.7
Shelf 3	1	961	40	2.4
Pallet	1	918	40	2.3
Window	1	1162	40	2.9
11. Post-blast sampling ACST and PDMS* Steel plates vs. textile	(n) ACST/PDMS	TATP type	TATP amount [g]	Sample collection time point after explosion [h]
Steel plates as substrate materials	1 / 1	Moist	5.2	1
	1 / 1	Moist	5.2	0
	1 / 1	Dry	2.9	1
	1 / 1	Dry	2.9	0
	1 / 1	Dry	16.0	0
Soil sample	1 / 1	Moist	2 x 5.7	1 / 0.5**
		Soil collected around the centre of two consecutive explosions using folded cotton laboratory coat as substrate; each explosion included one coat		
Folded cotton laboratory coats as substrate materials	1 / 1	Moist	5.7	1
	1 / 1	Moist	5.7	0
	1 / 1	Dry	3.3	1
	1 / 1	Dry	3.0	0
	1 / 1	Dry	6.4	0

* PDMS rods deployed together with ACST, one of each passive sampler per sample investigated

** The interval between the two consecutive explosions amounted to 0.5 h. Soil collection occurred 0.5 h after the second explosion, i.e. 1 h after the first explosion.

Table S4. Gas phase sampling of TATP using two different SPME fiber materials (PDMS material with 100 µm film thickness and mixed sorbent material consisting of carboxene/PDMS with 80 µm thickness) over different sampling periods. The resulting signal areas of the two most prominent TATP ions (m/z 43 and m/z 58) after GC-MS analysis of the fibers are given.

SPME fiber material	Sampling time [h]	TATP signal area m/z 43	TATP signal area m/z 58
Carboxene/PDMS (80 µm thickness)	1	1 989 200	180 873
	1	2 101 528	205 726
	3	4 788 426	414 598
	4	3 585 379	303 162
PDMS (100 µm thickness)	3	467 506	44 188
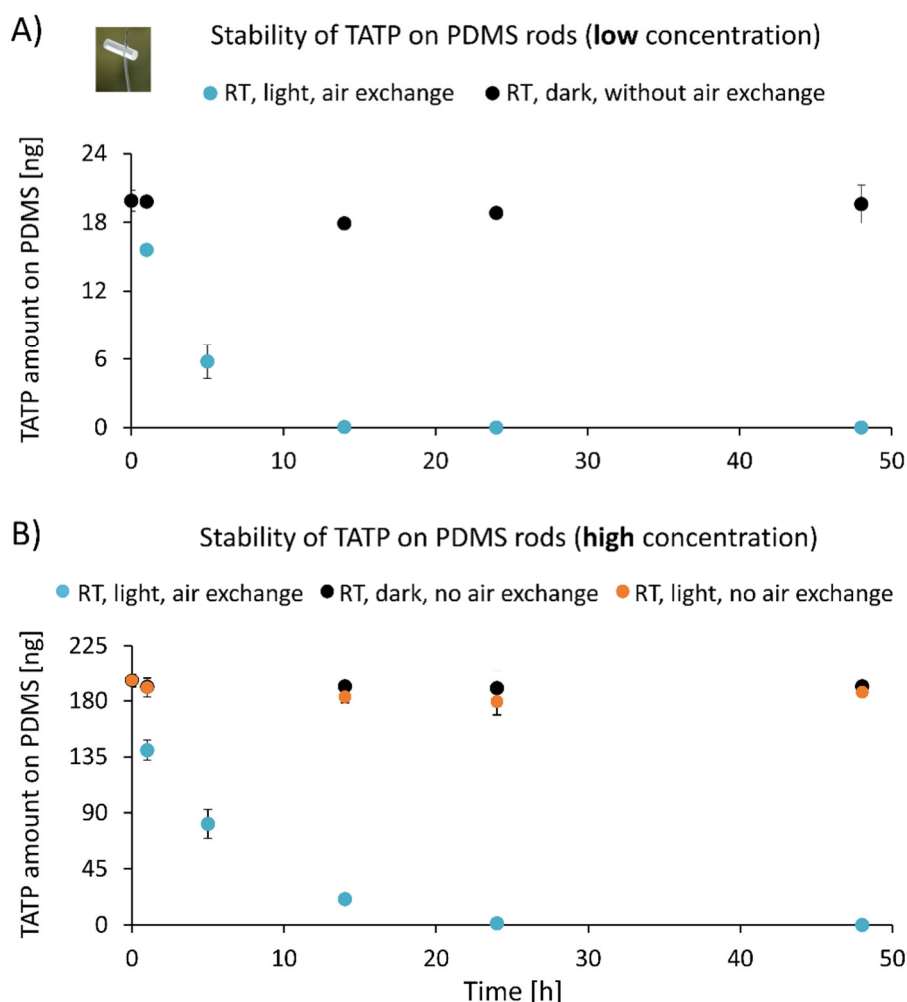
Figure S6. Stability profiles of TATP on PDMS over 48 hours at low (A) and tenfold higher (B) concentration level of adsorbed TATP, during storage at ambient temperature under different conditions: open glass containers (air exchange) and under light conditions are represented by turquoise dots, all other without air exchange (sealed glass containers), either with light exclusion (black dots) or without light exclusion (orange dots). All analyses were performed in duplicate (n = 2).
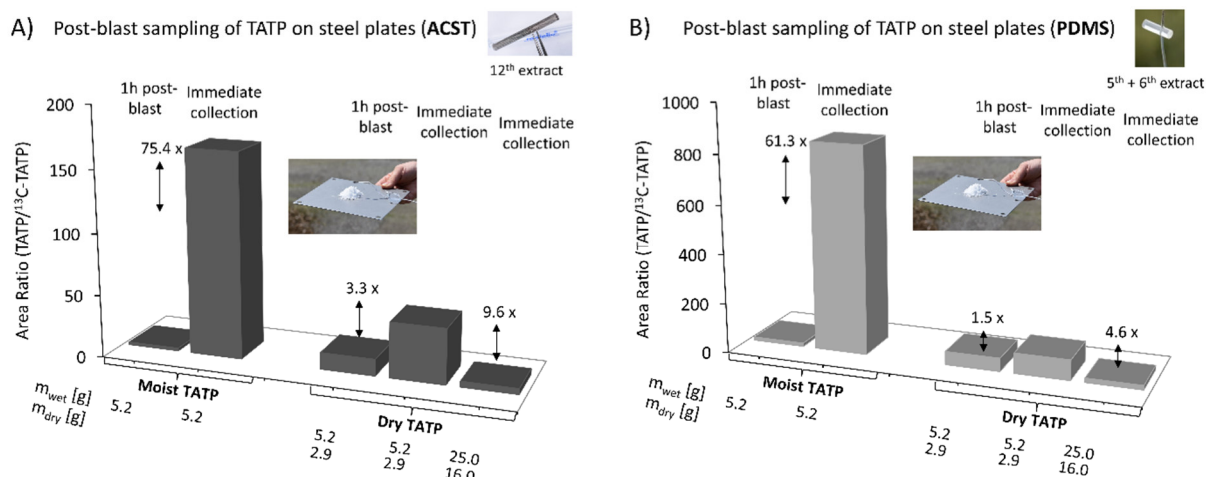
Figure S7. Post-blast sampling of steel substrates using ACST (A) and PDMS rods (B) in parallel, one of each passive sampler deployed per substrate. Although a direct quantitative comparison is limited due to different extracts of passive samplers (12th extract for ACST, and combined 5th and 6th extracts shown for PDMS rods), all the general trends observed for different conditions were pursued by ACST and PDMS rods consistently.
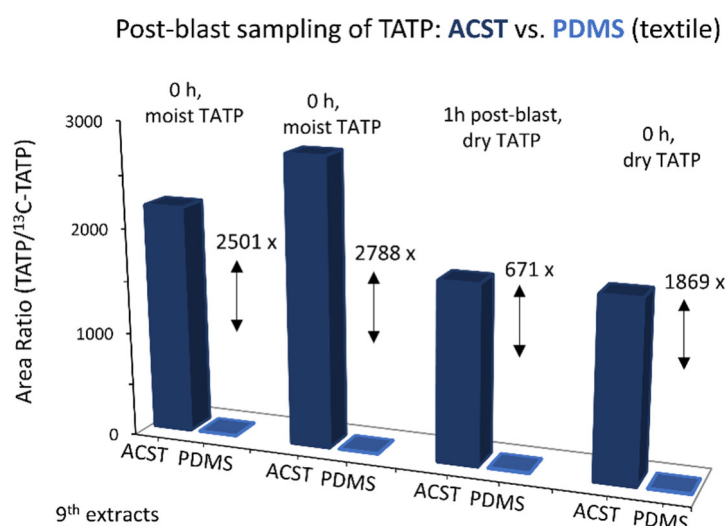
Figure S8. Direct quantitative comparison of the performance of the two passive samplers, representing ninth extractions (direct injection of corresponding supernatants) for PDMS rods and ACST that sampled post-blast samples of textile under different conditions.

Summary and Conclusion

III. Summary and Conclusion

The relevance of forensic science in the criminal justice framework is undisputable. Thus, it is crucial to continuously develop and improve the technological tools used in forensic science for sound evidence gathering. The field of forensic drugs and explosives analysis is highly dynamic since the methodologies must keep pace not only with the general technological progress, but also with emerging trends such as continuous development of the illicit drug market with new potent psychoactive substances, or the continuous need for novel proactive approaches and concepts to reduce terrorist threats with homemade explosives.

In this thesis new approaches, strategies and methods were developed for qualitative and/or quantitative detection and identification of trace amounts of illicit drugs and explosives in complex media. The focus regarding illicit drugs was directed to biogenic and synthetic cannabinoids, and for explosives to the homemade explosive TATP. Media investigated comprised hair and sewage, and various pre-blast and post-blast matrices regarding explosives. The most important outcome of the work is deductively summarized below.

Chapter 2. Forensic toxicology - Hair analysis

Femtogram level detection of a cannabis metabolite as a proof of active cannabis consumption

LC-based methods increasingly gain significance in forensic and toxicology laboratories. However, establishing an unambiguous proof of active cannabis consumption via hair analysis is still challenging regarding sensitivity and effort. Therefore, a fast, simple, highly sensitive and reliable LC-MS^3 routine method was developed for identification and quantitative determination of the major cannabis consumption marker via hair analysis, with the limit of quantification (LOQ) reaching 0.1 pg/mg hair. The target consumption marker included 11-nor-9-carboxy-Δ^9-THC (THC-COOH), which is one of the major endogenously formed metabolites of the psychoactive cannabinoid tetrahydrocannabinol (THC) in blood. After alkaline digestion of hair, two sample processing procedures were compared: solid-phase extraction (SPE) and liquid-liquid extraction (LLE). Sample preparation by LLE was optimized and proved satisfactory for successful validation of the procedure, yielding significant advantages over SPE, such as less laborious, costly and time-consuming steps. A significant analytical detection improvement was introduced by the multistage fragmentation (MS^3) using a linear ion trap (LIT), which led to both enhanced sensitivity and selectivity when compared to the commonly used MS^2 acquisition mode. Ion collection in the LIT for a certain time period (250 ms) resulted in an enhanced sensitivity, and the additional fragmentation step in the MS^3 acquisition mode yielded a consecutive fragmentation cascade and thus improved selectivity. Hence, the final method encompassed the optimized LLE workup in combination with the LC-MS^3 analytical detection. The method developed was fully validated for the following parameters: selectivity, linearity, limit of detection (LOD), LOQ, precision, accuracy, processed sample stability, matrix effect and recovery. The method showed satisfactory results for the majority of the validation parameters and hence proved to be suitable for application to authentic hair samples. Finally, the method was successfully applied to numerous different authentic toxicology case samples and resulted in the detection of THC-

COOH in concentrations ranging from 0.1 to > 15 pg/mg hair. The successful establishment of the method in the routine casework demonstrated its suitability, robustness and very good performance, proving superior over the current standard methods relying on time-consuming derivatization procedures in combination with GC-MS/MS analysis. Key features of the method developed are illustrated in Figure 1.
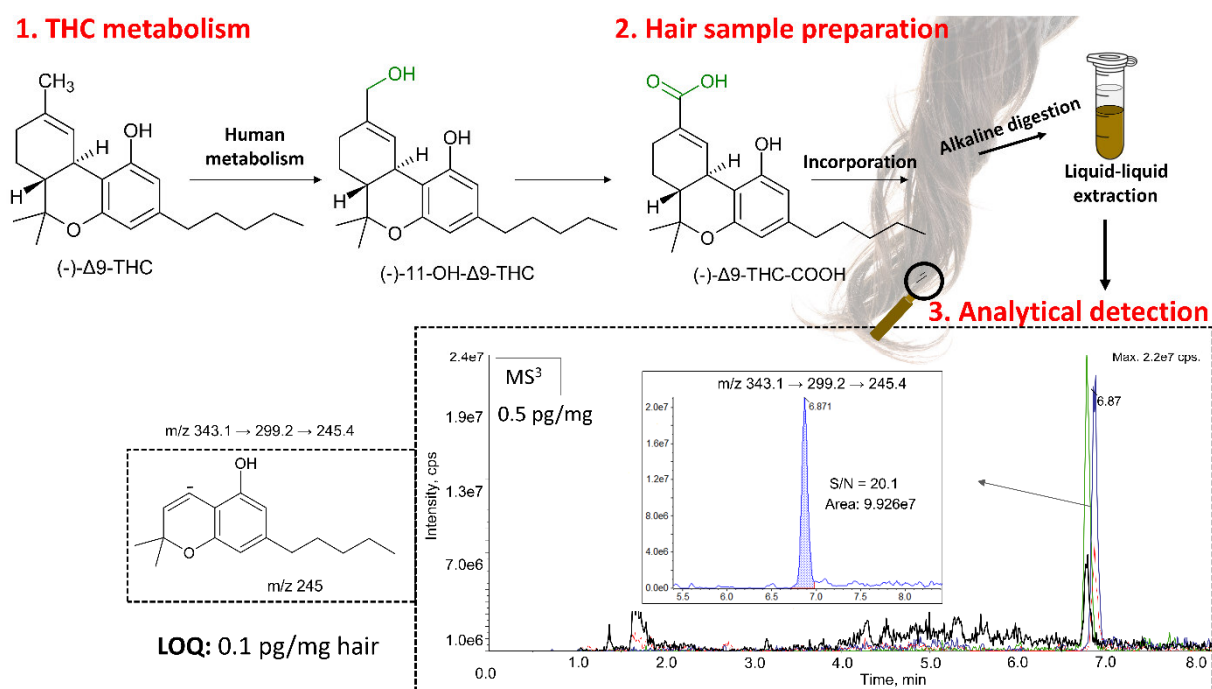

Figure 1. Summary of the LC-MS^3 method developed for the quantitative determination of the major cannabis consumption marker, THC-COOH, via hair analysis.

Chapters 3 and 4. Sewage analysis

Showcasing the potential of sewage analysis to track the prevalence of illicit drugs

This section represents the development and application of different analytical tools for monitoring illicit drug use by wastewater analysis. The study focused on the prevalence of new psychoactive substances (NPS) use, with synthetic cannabinoid receptor agonists (SCRAs), the most prevalent sub-class of NPS encountered in Europe, in the spotlight. In the first step, the fate of SCRAs in sewage was investigated using wastewater effluent and activated sludge (95/5, w/w) as inoculum for laboratory scale die-away experiments of six representative SCRAs and two of their human metabolites. The SCRAs examined comprised the most common, chemically diverse sub-classes with indole (5F-PB-22, PB-22 pentanoic acid), indazole (AMB-FUBINACA, 5F-ADB, 5F-ADB dimethylbutanoic acid), carbazole (MDMB-CHMCZCA, EG-018), and γ-carboline (Cumyl-PeGaClone) chemical core structures (Figure 2). In order to distinguish biological and physico-chemical degradation processes, an active and an inactive assay were prepared for each substance. While the active assay included microbial activity conditions, the inactive assay was sterilized with sodium azide in order to suppress the bioactivity. The degradation processes were monitored by an LC-MS/MS analytical method, which was successfully validated in terms of the linearity of calibration, instrumental limit of detection (ILOD), instrumental limit of quantification (ILOQ), filtration recovery, matrix effect, and precision. All validation parameters were satisfactory for the SCRAs examined, apart from low recoveries of the two most non-polar substances, MDMB-CHMCZCA and EG-018. Filtration was found to reduce the recovery of these cannabinoids, where up to 89% analyte loss was suffered, so in authentic wastewater samples both the dissolved and the particulate fraction must be considered for analysis to maximize recoveries of SCRAs. Finally, the results of the stability study disclosed that the majority of examined SCRAs, with exception of the selected human metabolites, was recalcitrant to biodegradation over a period of 29 days (Figure 3). Similar transformation kinetics in both assays indicated that the stability of SCRAs was rather influenced by physico-chemical properties like sorption and hydrolysis and not by biodegradation. Overall, the stability data indicated parent SCRAs as suitable biomarkers in a sewer network, where the typical residence times of analytes can be expected to be less than 10 hours. This finding served as a starting point for the implementation of a wastewater analysis study on the prevalence of SCRAs.
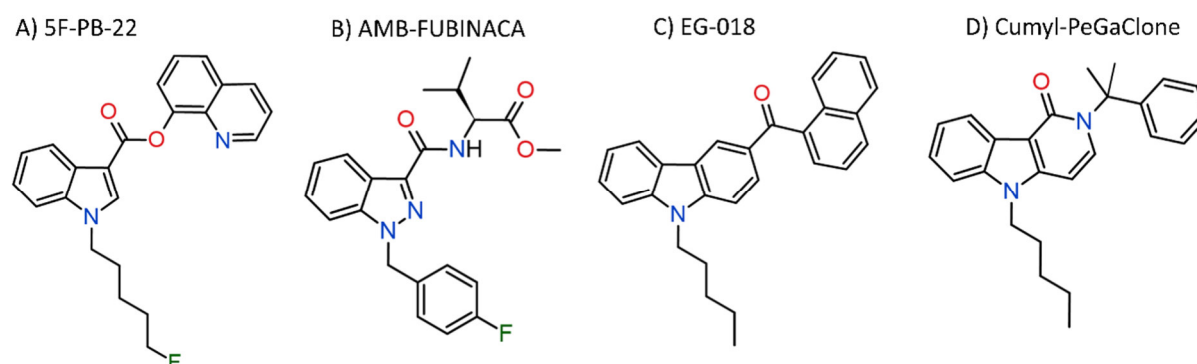
Figure 2. Chemical structures of some representative SCRAs, investigated for their stability in sewage water.
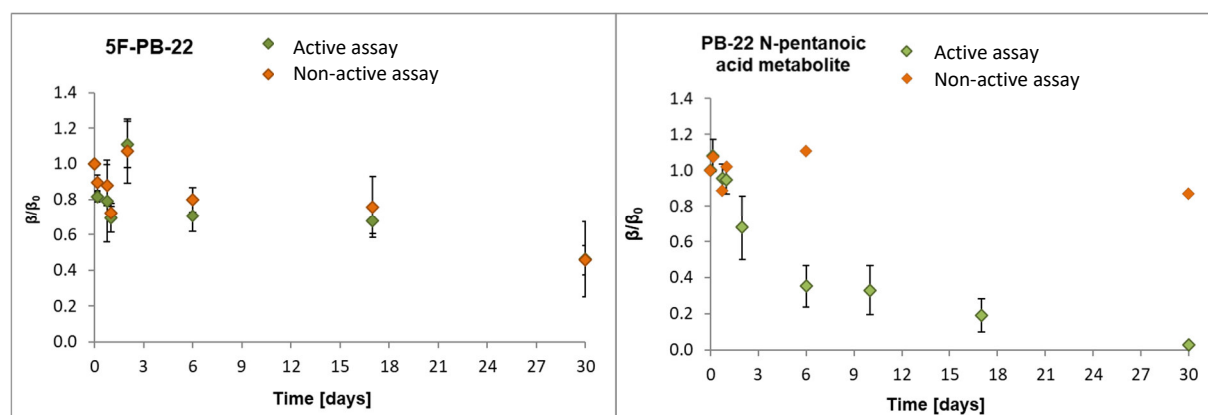
Figure 3. Stability profiles of 5F-PB-22 (left) and its human metabolite PB-22 N-pentanoic acid (right) showing concentrations relative to t_0 (β/β_0) during 29 days. LC-MS/MS analysis including active assay (indicated in green) and non-active assay (indicated in orange).
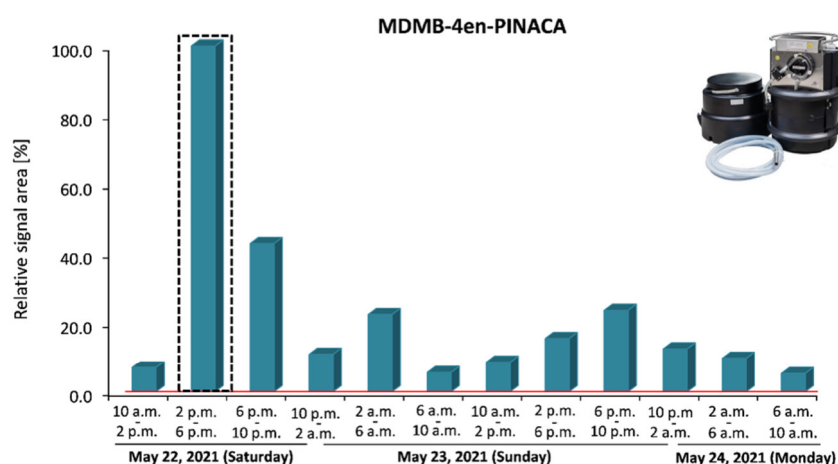
Afterwards, sampling protocols, analytical procedures and a detection method for wastewater analysis of SCRAs were developed and optimized. Two different wastewater sampling approaches were compared and assessed in terms of their advantages and disadvantages. On the one hand, the traditional approach comprised time-resolved liquid sampling with an automatized sampling device and subsequent liquid-liquid extraction (LLE), and on the other hand, a time-averaged passive sampling with novel solid phase samplers was introduced. The passive sampling approach comprised polydimethylsiloxane (PDMS) rods as solid phase adsorbers that were directly deployed in wastewater to allow for the extraction of the illicit drugs. After sampling, the target analytes were re-extracted in the laboratory.

Whereas the traditional liquid sampling approach was technically more demanding and time-consuming, the novel passive sampling approach based on PDMS was simple, fast to use and yielded summarized parameters over several days. The practical application of both sampling approaches and analytical methods developed was probed by analysis of wastewater samples of two different populations in Germany: a prison population and a population of a Munich city district. Both sampling approaches and subsequent LC-MS/MS analyses provided valuable snapshots of the drug consumption patterns in the respective populations during selected time periods investigated in 2021. Several SCRAs, including MDMB-4en-PINACA, 4F-MDMB-BINACA, 4F-MDMB-BICA, 5F-MDMB-PICA/5F-EMB-PICA, Cumyl-CBMICA, 5F-PB-22, EG-018, MAM-2201 and JWH-210, were detected in real sewage water of the selected populations. The wastewater analysis highlighted a significant SCRA use in the prison examined and the findings were in accordance with drugs seized from this prison in a correlated time frame. In addition, prevalence of the most abundant SCRAs in prison correlated with the SCRAs detected in the general population. When comparing the two sampling approaches, liquid wastewater sampling additionally allowed for timely resolved data. This data exhibited remarkable time profiles for several analytes, a phenomenon that was especially pronounced in the prison investigated, e.g. for MDMB-4en-PINACA (cf. Figure 4A). Nevertheless, both PDMS and liquid sampling revealed comparable results on SCRA consumption patterns in the different populations, validating the suitability of the PDMS sampling approach. Offering numerous advantages, such as simple and straightforward handling, low consumables costs and fast installation/deinstallation, even by not technically educated staff, without requirements for
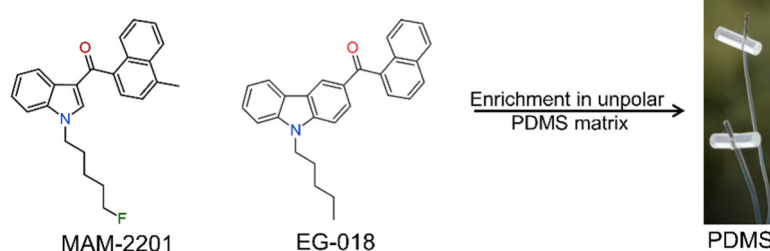
more complex sampling devices, the newly introduced PDMS sampling approach (Figure 4B) represents a very promising monitoring tool for illicit drug use via wastewater epidemiology. Time-weighted average data over max. 4 days have been examined in this study, however even longer sampling intervals are conceivable.

Moving from a small prison population to a major city population implied a larger and more complex sewer system, increased water flows and larger catchment areas. Hence, the selection of relevant manholes as sampling locations was based on a computational sewer network model, which provided geo-referenced locations of manholes, hydraulically directed graph with interconnections among buildings, sewers and manholes, and data about wastewater flow and the catchment areas connected to each manhole. This strategy allowed for geographical differences in drug consumption patterns to be easily investigated, as demonstrated for three different catchment areas in the city district of Munich with a different SCRA pattern at different locations.


Figure 4. Time profile for MDMB-4en-PINACA detected in a German prison after liquid wastewater sampling from May 22-24, 2021 (A); Newly introduced PDMS wastewater sampling approach, with PDMS rods acting as solid phase adsorbers of unpolar illicit drugs (B).

Chapter 5. Wastewater, hair and seized sample analysis

Consumption patterns and prevalence of SCRA and conventional drugs abuse revealed by triangulation of different data sources

A novel approach based on combination of wastewater analysis, hair analysis and police seizure data was used to assess the prevalence and the changing landscape of the SCRA drug market and consumption patterns. Moreover, the approach included a wide panel of conventional drugs of abuse, i.e. phytocannabinoids (THC, THC-COOH, CBN and CBD), amphetamine-type stimulants, cocaine and its metabolites, and a large panel of opioids, to obtain a broader context of the SCRA prevalence data both on a community level (wastewater analysis) and on the level of individual users (hair analysis). The toxicological hair analysis allowed for a comprehensive SCRA user profiling, with valuable insights gained into demographic characteristics of users (age and gender) and polydrug use regarding different drug categories analyzed (SCRAs, cannabis, and other conventional drugs of abuse). The study was performed in Bavaria, Germany over a 1.5 year period in 2021-2022. Specimens were analyzed for 41 markers of conventional drugs of abuse and 41 SCRAs / 8 SCRA metabolites, either qualitatively (wastewater) or quantitatively (hair) using a targeted LC-MS/MS analytical method.

After the successful proof-of-concept of the newly introduced polydimethylsiloxane (PDMS) passive sampling approach for wastewater monitoring (cf. Chapters 3 and 4), the methodology was extended to a wastewater treatment plant (WWTP) in the city and a larger panel of illicit drugs. The analysis of PDMS rods yielded promising results: seven SCRAs and all relevant phytocannabinoids were detected in the WWTP. Moreover, the findings correlated with the SCRAs detected in a randomly chosen district of the city, where wastewater sampling was conducted additionally with a liquid sampling device. The high temporal resolution (4 h per individual sample) of this sampling approach disclosed remarkable consumption patterns between weekdays and the beginning of the weekend, showing high prevalence of SCRAs on Friday afternoon-evening (2 - 10 p.m.). In total, nine SCRAs were identified via wastewater analysis in the city of Munich during selected time periods in September 2021 (city district) and February 2022 (WWTP): MDMB-4en-PINACA, 4F-MDMB-BINACA, 4F-MDMB-BICA, 5F-MDMB-PICA/5F-EMB-PICA, Cumyl-CBMICA, Cumyl-BC[2.2.1]HpMINACA, AB-CHMINACA, EG-018, and JWH-210. Noteworthy was also the identification of phytocannabinoids THC and its metabolite THC-COOH in all of the liquid wastewater samples examined, both during weekdays and weekend, which suggested their rather high prevalence. Furthermore, a significant use of cocaine, MDMA, opioids (methadone, buprenorphine, fentanyl, tramadol and tilidine) and ketamine was deduced from their high detection frequencies in liquid wastewater samples. Similar sampling experiments were simultaneously conducted with PDMS at several locations in the sewer network of the city district of Munich, allowing for a comparison between different catchment areas. PDMS passive samplers successfully demonstrated their applicability to extract conventional drugs of abuse, allowing to assess spatial differences of illicit drug use with high local resolution (Figure 5).
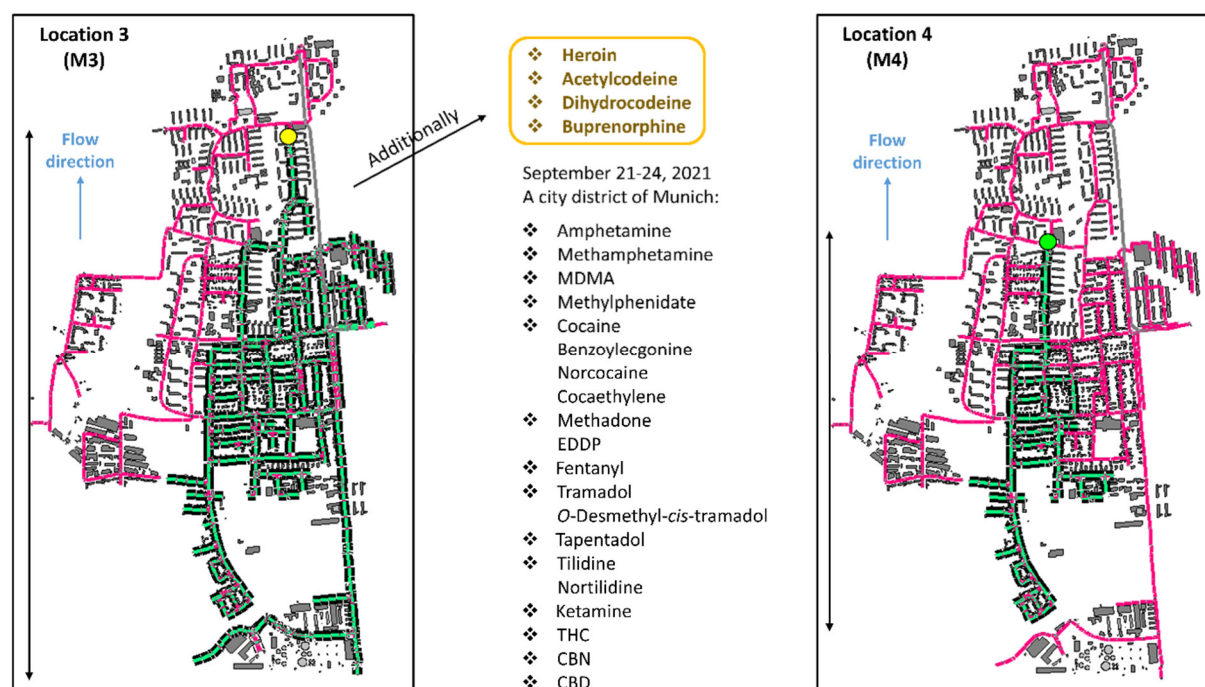
Figure 5. Successful extraction of conventional drugs of abuse using PDMS sampling approach in the sewer network of a city district of Munich, allowing to assess spatial differences of illicit drug use with high local resolution.

Forensic toxicological analysis provided information on SCRA prevalence in hair samples from persons suspected of violations of the Narcotics Act and other criminal offences during 2021-2022. A total of 676 hair segments from 398 persons were qualitatively analyzed for SCRAs and resulted in a positivity rate of 35.2%. A wide range of 32 SCRAs and 2 of their metabolites was observed across the SCRA-positive sub-collective, with up to 19 different substances found in a single hair sample. The most prevalent compounds were MDMB-4en-PINACA, ADB-BUTINACA and JWH-210, which altogether constituted approximately 50% of the SCRA detections (Figure 6A). Demographic characteristics of consumers indicated high SCRA prevalence among young people, with the median age of 28 years across users and the majority of positive cases was categorized in the age group of 21-30 years (45.7%). Normalization of positive results to gender yielded no significant differences - one in three males (36.1%) and one in four females (28.3%) screening positive for a SCRA. Evaluation and determination of the extent and patterns of SCRA use in relation to cannabis and other conventional drugs was performed within a slightly smaller sample collective (370 persons, 627 hair segments). SCRAs were detected in one third of the collective analyzed (36.2%), cannabis in half of the collective (57.0%), and the remaining conventional drugs in nearly two thirds of the total collective (75.1%). In total, 90 persons (24.3%) were positive for conventional drugs only, 24 (6.5%) for cannabis only, and 8 persons (2.2%) for SCRAs only. The majority of SCRA consumers appeared to be polydrug users, showing additional use of cannabis (18 persons, 4.9%), other conventional drugs (19 persons, 5.1%) or combination of both (89 persons, 24.1%). Figure 6B depicts the distribution of persons tested positive across the three drug categories.

Hair analysis: Application to authentic cases
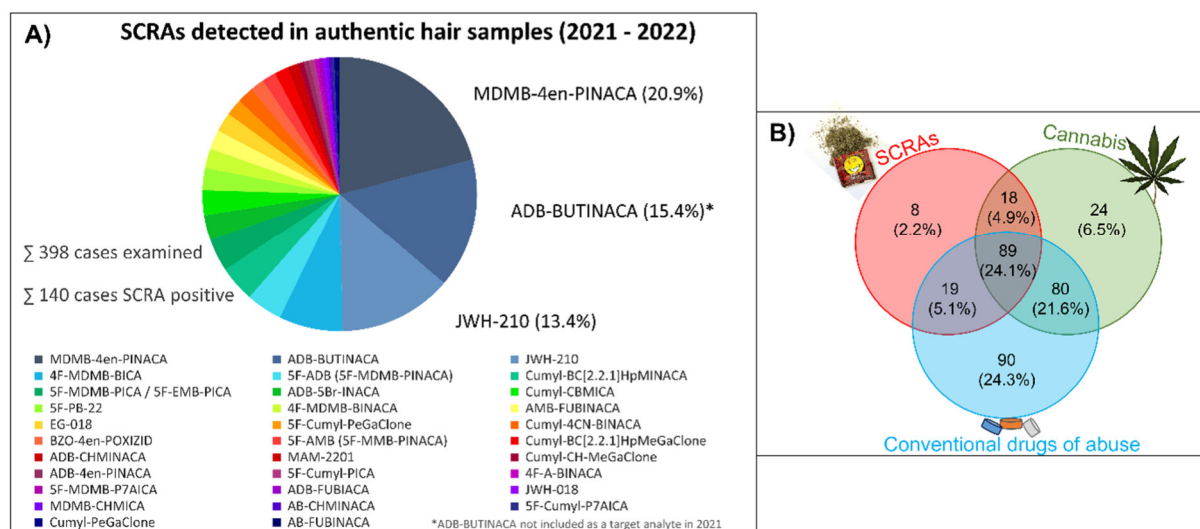
Figure 6. A wide range of 32 SCRAs inclusive 2 of their metabolites observed across the SCRA-positive sub-collective during 2021-2022 (A); Distribution of persons tested positive across the three drug categories, particularly visualized for the drug co-use (B).

The findings from the toxicological and wastewater analyses reflected the domestic SCRA market well, as evident from the evaluation of local seizures. Triangulation of the data illustrated that MDMB-4en-PINACA was the most prevalent SCRA in the time period investigated, primarily in 2021, together with JWH-210 and 4F-MDMB-BICA. Furthermore, high portion of seizures and frequent detections in hair samples indicated widespread use of ADB-BUTINACA in 2022. The chronological change of the SCRA drug market correlated with the national legislative controls and legal status of the SCRAs. Scheduling of MDMB-4en-PINACA under the national Narcotics Law (BtMG) in May 2021 led to decreased prevalence of this compound, and a successive replacement with ADB-BUTINACA peaked in the second half of 2022, until this substance was banned by the BtMG in June 2023 as well (Figure 7).

In summary, the combination of toxicological hair analysis, wastewater analysis and police seizures proved to be a valuable tool to monitor the use and prevalence of SCRAs. The results in the investigated collective and on the community level suggested a notable population-scale SCRA use in the southeastern region of Germany (Bavaria), where SCRAs do not appear to be "niche drugs" anymore. Prospectively, seizure data are required to notice upcoming trends and update analytical methods for wastewater and toxicological analyses to keep pace with newly emerging SCRA analogs.
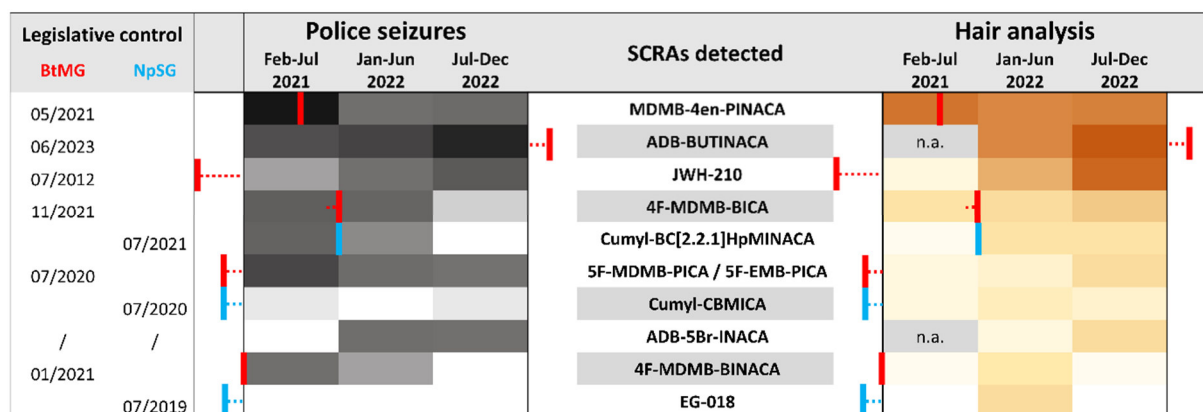
Figure 7. Prevalence of selected SCRAs according to police seizures (left) and hair analysis data (right) with indicated time point of their legislative control in Germany, either by the national Narcotics Act (BtMG, red line) or the New Psychoactive Substances Act (NpSG, blue line).

Chapter 6. Explosives analysis: TATP

## New detection methodology for production sites and post-blast residues of the "terrorist explosive" TATP

Triacetone triperoxide (TATP) is a typical home-made explosive (HME), that has been used in a number of terrorist attacks all over the world in the past years. The identification of TATP in remaining synthesis waste residues or in the gas phase of a room or area can provide evidence for a past synthesis or handling with explosives (e.g. storage room) at this locality. Localities often provide linkages to persons so that ultimately the explosive is linked to a crime suspect. In post-blast scenarios, identifying the cause of the explosion and the explosive used becomes the pivot of the investigation in order to be able to reconstruct the crime. In the optimum case, the combination of pre- and post-blast analysis can link a suspect and a bomb manufacturing site to an explosion site.

In this work, a new strategy for the enrichment and detection of TATP from aqueous and gas phase has been developed and successfully applied during and after a controlled TATP synthesis (pre-blast), as well as after controlled blastings (post-blast), enabling identification of TATP traces for forensic applications. The methodology developed relies on different passive samplers, polydimethylsiloxane (PDMS) rods and activated carbon sampling tubes (ACST), for TATP enrichment from different media (aqueous and gas phase) in combination with subsequent GC-MS based analytical detection (Figure 8). For liquid sampling, the initial assessment of stability of TATP in aqueous phase revealed its remarkable stability over at least 11 days in sealed containers. A successful extraction from the aqueous waste of a TATP synthesis was achieved using two independent enrichment strategies, liquid-liquid extraction (LLE) and PDMS sampling rods. The PDMS extraction strategy was optimized concerning sampling times, mechanical agitation (shaking) and length of PDMS rods deployed. For gas phase sampling, a systematic study on TATP uptake kinetics in the gas phase above TATP solutions included evaluation of three different passive samplers, PDMS, ACST and the traditionally used solid-phase microextraction (SPME) fibers. Moreover, gas phase monitoring of TATP was successfully performed during a TATP synthesis with the newly introduced PDMS

Summary

rods and the ACST passive samplers, even at some distance outside the production room. Even gas phase analysis of the laboratory coats worn during the synthesis gave a positive result, with successful TATP detection after only 0.5 h sampling using a PDMS rod. For all gas phase experiments, ACST have shown superior performance due to their significantly higher sampling capacity without showing the negative desorption effects after prolonged time observed for PDMS. Hence, ACST are recommended for gas phase sampling of TATP, PDMS for liquid phase sampling.

The passive sampling concept was successfully implemented and combined with several different GC-MS based analytical methods, encompassing a stationary and a field-portable GC-MS system. The field-portable GC-MS system with direct thermal desorption analysis has shown to deliver fast and on-site detection of TATP from PDMS sampling rods, but to the price of a lower sensitivity. In addition, a laboratory-based, highly sensitive and quantitative GC-PCI-MS/MS method for analysis of liquid extracts, either originating from passive samplers or from conventional extraction procedures, has been established. Besides the excellent results for the identification of TATP production sites, the GC-MS/MS methodology also proved suitable for the trace detection of TATP remnants after a blasting event. Moist or dry TATP (3 – 25 g) was initiated remotely under different conditions and the gas phase of the residues was analyzed. The different parameters included two different substrate materials (textile and steel), variation of the time point of sample collection after blast (immediate vs. 1 h) and the residual moisture of the explosive (moist vs. dry TATP). TATP traces were evidenced for all the investigated parameters, however with distinctive trends, underlining the need for a prompt on-site sampling, followed by sensitive GC-MS/MS detection in a laboratory. The successful application of the developed methodology in realistic operational scenarios clearly demonstrated its value for forensic casework. The passive samplers allow for fast, simple, cost-effective, unsuspicious and autonomous on-site sampling without requirements for technically trained personal, and thus represent a very promising and perspective approach for law enforcement agencies.
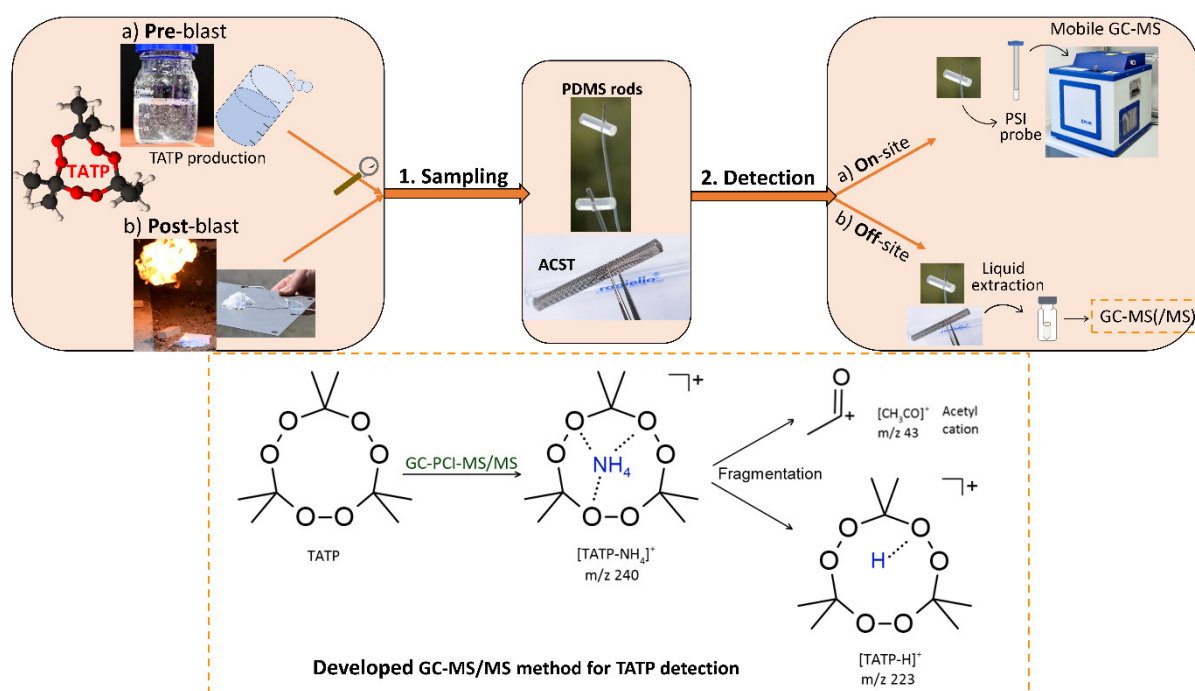
Figure 8. The enrichment and trace detection of TATP from aqueous and gas phase, with applications in realistic pre-blast (TATP production sites) and post-blast (blasting events) operational scenarios. The sensitive analytical detection is based on a GC-PCI-MS/MS method.

IV. Outlook

The work in this dissertation provided methodological developments for forensic analysis of drugs and explosives, and allowed for relevant application studies, partly even implemented in the routine casework. Nevertheless, the initial developments and findings opened a space for further follow-up studies.

Sewage analysis

Despite relating to a separated drug market, SCRAs in prison examined correlated well with the SCRAs detected in the wider population, with considerable prevalence in both populations. However, the relatively short periods of monitoring duration in these prevalence studies allow limited conclusions only. Further wastewater analyses comprising greater number of prisons and cities as well as a longer timeframe to estimate correlations of SCRA prevalence in prisons and general populations would shed light on NPS use and consumption patterns on a large scale.

The presented analytical methodologies feature targeted analyte screenings, meaning that only selected target analytes, which mostly relied on analytical data from police and customs seizures, were included in the analytical method. While being very selective and sensitive, the number of targets for a single analysis is somewhat limited and must constantly be updated over time. To keep pace with the dynamic NPS market, approaches and methodologies for non-targeted monitoring and NPS-suspect search using high-resolution mass spectrometry (HRMS) set-up should be also elaborated to disclose new and unknown SCRAs entering the drug market, thus representing an early warning system based on wastewater analysis. Finally, quantitative methodologies for comparative WBE of SCRAs and conventional drugs use should be performed in order to gain further insights into SCRA use patterns. Further studies regarding standardization and validation of the PDMS rods approach are recommended, particularly if designated for quantitative analysis.

Explosives analysis: TATP

Post-blast investigations of TATP using the methodology developed merit further examinations and a follow-up study. Based on the initial proof-of-principle study, two parameters should be pursued in more detail: longer delays after an explosion, before sampling of evidence, and the effect of larger TATP amounts (i.e., kg amounts). These parameters play a particularly important role for the operational use. Another interesting question is whether gas phase and surface post-blast sampling of an evidence yields similar or rather distinctive results.

V. Anhang

Veröffentlichte Arbeiten

Als Erstautorin in international anerkannten wissenschaftlichen Zeitschriften mit Peer-Review

- ❖ **P. Hehet*,** N. Köke*, D. Zahn, T. Frömel, T. Rößler, T. P. Knepper, M. Pütz. Synthetic cannabinoid receptor agonists and their human metabolites in sewage water: Stability assessment and identification of transformation products. *Drug Test. Anal.* **2021**; 13:1758-1767. *geteilte Erstautorenschaft

- ❖ **P. Hehet*,** T. Franz*, N. Kunert, F. Musshoff. Fast and highly sensitive determination of tetrahydrocannabinol (THC) metabolites in hair using liquid chromatography-multistage mass spectrometry (LC-MS^3). *Drug Test. Anal.* **2022**;14:1614-1622. *geteilte Erstautorenschaft

- ❖ **P. Hehet,** M. Pütz, B. Kämmerer, G. Umlauf, O. Geiss, J. G. Nunes Caetano, K. Karaghiosoff, M. Wende. Determination of triacetone triperoxide (TATP) traces using passive samplers in combination with GC-MS and GC-PCI-MS/MS methods. *Forensic Sci. Int.* **2023**;348:111673.

- ❖ **P. Hehet,** M. Wende, O. Shehata, S. Krause, M. Pütz. Prevalence of synthetic cannabinoid receptor agonists use assessed by sewage monitoring via LC-MS/MS, Part A: Novel wastewater sampling approach applied in a prison and a capital city. To be submitted to *Forensic Chem.* **2024.**

- ❖ **P. Hehet**, F. Scheufler, N. Kunert, C. Baumer, M. Pütz, J. Schäper, O. Shehata, S. Krause, M. Wende. Prevalence of synthetic cannabinoid receptor agonists use assessed by sewage monitoring via LC-MS/MS, Part B: Triangulation of wastewater, toxicological hair and police seizure data. To be submitted to *Forensic Chem.* **2024.**

Vorträge / Konferenzbeiträge: Vorträge

- ❖ **P. Hehet**. Determination of drugs and their metabolites via hair analysis. Vortrag im Rahmen der Vorlesung *„Strukturaufklärung und Spurenanalytik"*. **2018**, 16.10.2018, Hochschule Fresenius, Institute for Analytical Research, Idstein, Deutschland.

- ❖ **P. Hehet**. Moderne Massenspektrometrie – Chancen und Herausforderungen. *Symposium fachübergreifender moderner Analytik*. **2019**, 22.07.2019, Holzkirchen (HEXAL AG), Deutschland.

- ❖ **P. Hehet** (on behalf of SYSTEM consortium). Presentation of the Project SYSTEM – Synergy of integrated Sensors and Technologies for urban sEcured environment. *Security of Explosives pan-European Specialists Network (EXERTER) Virtual Conference*. **2020**, 05.11.2020, online.

- ❖ **P. Hehet**, T. Franz, N. Kunert, F. Mußhoff. Fast and highly sensitive determination of 11-nor-9-carboxy-Δ9-tetrahydrocannabinol in hair using liquid-chromatography-multistage mass spectrometry (LC-MS^3). *XXII. Symposium der Gesellschaft für Toxikologische und Forensische Chemie (GTFCh)*. **2021**, 15.04. - 17.04.2021, online.

- ❖ **P. Hehet,** N. Kunert, C. Baumer, F. Scheufler**.** Detektion von synthetischen Cannabinoiden in Haaren*. 43. Symposium der Arbeitsgruppe "Toxikologie" der Kommission Kriminalwissenschaft und -technik / Erkennungsdienst (KKWT / ED).* **2021**, 16.09.2021, Tutzing, Deutschland.

- ❖ **P. Hehet** / M. Pütz**.** EU-Projekt SYSTEM. *43. Symposium der Arbeitsgruppe "Toxikologie" der Kommission Kriminalwissenschaft und -technik / Erkennungsdienst (KKWT / ED).* **2021**, 16.09.2021, Tutzing, Deutschland.

- ❖ **P. Hehet** / P. Olejnik. Project SYSTEM: Detection of home-made explosive production (TATP). *Community of European Research and Innovation for Security - Fight against Crime and Terrorism (CERIS-FCT) Workshop: Explosives (DG HOME)*. **2021**, 19.10.2021, online.

- ❖ **P. Hehet**. Prevalence of new psychoactive substances (NPSs) use assessed by wastewater analysis: Synthetic cannabinoid receptor agonists (SCRAs). *EU Project SYSTEM Workshop for Law Enforcement Agencies*. **2022**, 11.02.2022, online.

- ❖ **P. Hehet**, M. Pütz, G. Umlauf, O. Geiss, J. G. Nunes Caetano, K. Karaghiosoff, M. Wende. Determination of triacetone triperoxide (TATP) using passive samplers in combination with GC-MS and GC-PCI-MS/MS methods. *9th European Academy of Forensic Science (EAFS) Conference*. **2022**, 30.05. – 03.06.2022, Stockholm, Schweden.

- ❖ **P. Hehet** / M. Pütz. Project SYSTEM: Detection strategies. *CHEMTEC Specialist Meeting Technology*. **2022**, 19.09. – 21.09.2022, Niederlande.

- ❖ **P. Hehet**, B. Kämmerer, M. Wende. Neue Nachweismethode zur Spurendetektion von TATP mittels GC-PCI-MS/MS: Anwendungen in pre-blast und post-blast Szenarien. *Symposium der Arbeitsgruppe "Sprengstoff" der Kommission Kriminalwissenschaft und -technik / Erkennungsdienst (KKWT / ED).* **2023**, 23.05. – 25.05.2023, Forensisches Institut Zürich, Schweiz.

- ❖ **P. Hehet,** M. Pütz, N. Kunert, F. Scheufler, C. Baumer, O. Shehata, S. Krause, M. Wende. Results of a multi-site prevalence study on synthetic cannabinoid receptor agonists (SCRAs) in sewage systems: Correlation with hair analysis and seizure data. *60th Annual meeting of The International Association of Forensic Toxicologists (TIAFT).* **2023**, 27.08. – 31.08.2023, Rom, Italien.

- ❖ **P. Hehet.** Neue analytische Methoden zur Identifizierung von Drogen und improvisierten Sprengstoffen in forensischen Beweismitteln. *VI. Symposium über fachübergreifende moderne Analytik.* **2023**, 13.10.2023, Schule für ABC-Abwehr und Gesetzliche Schutzaufgaben, Sonthofen, Deutschland**.**

- ❖ **P. Hehet.** TATP-Spurenanalytik im Rahmen des EU-Projektes „SYSTEM". *Internationales Symposium 2023 für Sprengstoffermittelnde und Entschärfende unkonventioneller Spreng- und Brandvorrichtungen.* **2023**, 28.11. – 30.11.2023, Deutschland.

Konferenzbeiträge: Poster

- ❖ **P. Hehet***, N. Köke*, T. Frömel, D. Zahn, M. Pütz, T. P. Knepper. Stability test of selected synthetic cannabinoids and some of their human metabolites in sewage water and identification of transformation products. *8. Late Summer Workshop der Wasserchemischen Gesellschaft.* **2019**, 22.09. – 25.09.2019, Haltern am See, Deutschland. *geteilte Erstautorenschaft

- ❖ **P. Hehet**, N. Köke, T. P. Knepper, M. Pütz. Biotransformation of synthetic cannabinoids and some of their human metabolites in sewage system. *XXI. Symposium der Gesellschaft für Toxikologische und Forensische Chemie (GTFCh).* **2019**, 11.04. – 13.04.2019, Mosbach, Deutschland.

- ❖ **P. Hehet**, M. Wende, M. Pütz, C. Baumer, M. Uhl, F. Scheufler. Comparative study of wastewater and hair analysis to assess synthetic cannabinoid receptor agonists (SCRA) use. *Society of Hair Testing (SoHT) - Italian Group of Forensic Toxicologists (GTFI) Joint Meeting*. **2022**, 08.06. – 10.06.2022, Verona, Italien.

Zeitschriftenbeiträge

- ❖ **P. Hehet.** Expertenseminar „Illegale Rauschgiftlabore" in Holland: Doktorandin am SG 201 stellt Kernstück ihrer Arbeit in der Praxis vor. *LKA-Spiegel* (Das Magazin des Bay. Landeskriminalamtes). **2023**, 1:18-19.

- ❖ **P. Hehet**. Entwicklung neuer Nachweismethoden für Sprengstoffe – „Sprengen für die Wissenschaft". *LKA Jahresbericht 2022.* **2023**, S. 54.

Auszeichnungen

- ❖ Award for best Poster Presentation to Petra Hehet at the Annual Meeting of the Society of Hair Testing, Verona, **2022** (Prof. Dr. Donata Favretto, President SoHT):
  P. Hehet, M. Wende, M. Pütz, C. Baumer, M. Uhl, F. Scheufler. Comparative study of wastewater and hair analysis to assess synthetic cannabinoid receptor agonists (SCRA) use.

"*The important thing is not to stop questioning.*

Curiosity has its own reason for existing."

Albert Einstein